

K.A. Gschneidner, Jr.,
J.-C.G. Bünzli and V.K. Pecharsky
Editors



HANDBOOK ON THE
PHYSICS AND CHEMISTRY OF

RARE EARTHS

Volume 35



HANDBOOK ON THE PHYSICS AND CHEMISTRY
OF RARE EARTHS
VOLUME 35

HANDBOOK ON THE PHYSICS AND CHEMISTRY
OF RARE EARTHS

Advisory Editorial Board

G. ADACHI, *Kobe, Japan*

W.J. EVANS, *Irvine, USA*

S.M. KAUZLARICH, *Davis, USA*

G.H. LANDER, *Karlsruhe, Germany*

M.F. REID, *Christchurch, New Zealand*

Editor Emeritus

LeRoy EYRING, *Tempe, USA*

HANDBOOK ON THE PHYSICS AND CHEMISTRY OF

RARE EARTHS

VOLUME 35

EDITORS

Karl A. GSCHNEIDNER, Jr.

*Ames Laboratory–US DOE, and
Department of Materials Science and Engineering
Iowa State University
Ames, Iowa 50011-3020
USA*

Jean-Claude G. BÜNZLI

*Swiss Federal Institute of Technology
Institute of Molecular & Biological Chemistry
BCH 1402
CH-1015 Lausanne
Switzerland*

Vitalij K. PECHARSKY

*Ames Laboratory–US DOE, and
Department of Materials Science and Engineering
Iowa State University
Ames, Iowa 50011-3020
USA*

2005



ELSEVIER
NORTH
HOLLAND

AMSTERDAM, BOSTON, HEIDELBERG, LONDON, NEW YORK, OXFORD,
PARIS, SAN DIEGO, SAN FRANCISCO, SINGAPORE, SYDNEY, TOKYO

ELSEVIER B.V.
Radarweg 29
P.O. Box 211, 1000 AE Amsterdam
The Netherlands

ELSEVIER Inc.
525 B Street, Suite 1900
San Diego, CA 92101-4495
USA

ELSEVIER Ltd
The Boulevard, Langford Lane
Kidlington, Oxford OX5 1GB
UK

ELSEVIER Ltd
84 Theobalds Road
London WC1X 8RR
UK

© 2005 Elsevier B.V. All rights reserved.

This work is protected under copyright by Elsevier B.V., and the following terms and conditions apply to its use:

Photocopying

Single photocopies of single chapters may be made for personal use as allowed by national copyright laws. Permission of the Publisher and payment of a fee is required for all other photocopying, including multiple or systematic copying, copying for advertising or promotional purposes, resale, and all forms of document delivery. Special rates are available for educational institutions that wish to make photocopies for non-profit educational classroom use.

Permissions may be sought directly from Elsevier's Rights Department in Oxford, UK: phone (+44) 1865 843830, fax (+44) 1865 853333, e-mail: permissions@elsevier.com. Requests may also be completed on-line via the Elsevier homepage (<http://www.elsevier.com/locate/permissions>).

In the USA, users may clear permissions and make payments through the Copyright Clearance Center, Inc., 222 Rosewood Drive, Danvers, MA 01923, USA; phone: (+1) (978) 7508400, fax: (+1) (978) 7504744, and in the UK through the Copyright Licensing Agency Rapid Clearance Service (CLARCS), 90 Tottenham Court Road, London W1P 0LP, UK; phone: (+44) 20 7631 5555; fax: (+44) 20 7631 5500. Other countries may have a local reprographic rights agency for payments.

Derivative Works

Tables of contents may be reproduced for internal circulation, but permission of the Publisher is required for external resale or distribution of such material. Permission of the Publisher is required for all other derivative works, including compilations and translations.

Electronic Storage or Usage

Permission of the Publisher is required to store or use electronically any material contained in this work, including any chapter or part of a chapter.

Except as outlined above, no part of this work may be reproduced, stored in a retrieval system or transmitted in any form or by any means, electronic, mechanical, photocopying, recording or otherwise, without prior written permission of the Publisher. Address permissions requests to: Elsevier's Rights Department, at the fax and e-mail addresses noted above.

Notice

No responsibility is assumed by the Publisher for any injury and/or damage to persons or property as a matter of products liability, negligence or otherwise, or from any use or operation of any methods, products, instructions or ideas contained in the material herein. Because of rapid advances in the medical sciences, in particular, independent verification of diagnoses and drug dosages should be made.

First edition 2005

Library of Congress Cataloging in Publication Data

A catalog record is available from the Library of Congress.

British Library Cataloguing in Publication Data

A catalogue record is available from the British Library.

ISBN: 0-444-52028-7

ISBN: 0-444-85022-8 (series)

ISSN: 0168-1273

© The paper used in this publication meets the requirements of ANSI/NISO Z39.48-1992 (Permanence of Paper).
Printed in The Netherlands.

PREFACE

Karl A. GSCHNEIDNER Jr., Jean-Claude G. BÜNZLI, and Vitalij K. PECHARSKY

These elements perplex us in our rearches [sic], baffle us in our speculations, and haunt us in our very dreams. They stretch like an unknown sea before us – mocking, mystifying, and murmuring strange revelations and possibilities.

Sir William Crookes (February 16, 1887)

In keeping with the tradition of the *Handbook on the Physics and Chemistry of Rare Earths* volume 35 covers a wide diversity of topics involving the rare earth elements. The topics range from solid oxides for advanced, energy efficient electrical power generation (Chapter 223); to the oxo-selenate members of the vast family of complex oxo-anions (Chapter 224); to organic beta-diketonate complexes (Chapter 225); to the utilization of organic complexes for molecular recognition and sensing (Chapter 226).

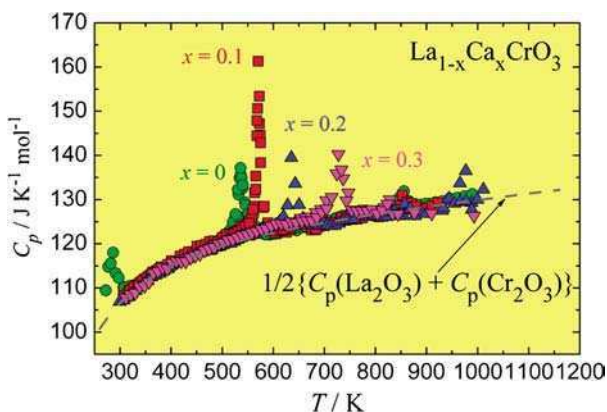
In addition, the volume contains an abbreviated subject index of the 226 chapters published to date, which is located immediately after the **Contents of Volumes 1–34**.

Chapter 223. Rare-earth Materials for Solid Oxide Fuels (SOFC)

by Natsuko Sakai, Katsuhiko Yamaji, Teruhisa Horita, Yue Ping Xiong and Harumi Yokokawa

National Institute of Advanced Industrial Science and Technology, Tsukuba, Japan

Fuel cell technology has the potential to transform the electrical power generation as we know it today to a much more energy efficient and environmentally friendly technology in the early 21st century. There are several different kinds of fuel cells which can be readily classified by the electrolyte material utilized to convert the energy produced by a chemical reaction to electric energy. The hydrogen fuel cell to power automobiles, which today receives lots of exposure in the popular press, is one of them. Another is the solid oxide fuel cell (SOFC) technology for large scale electrical power generation (hundreds of kilo watts). Sakai and co-workers discuss the role of the rare oxide base materials in high temperature SOFC. A single cell of a SOFC power generator consists of a dense metal oxide electrolyte with a porous anode on one side and a porous cathode on the other side. Oxygen gas is reduced to the oxide ion at the cathode/electrolyte interface, and the oxide ion diffuses to the anode/electrolyte interface. The oxidation of the fuel (H₂ or CO) by the oxide ion results in the emission of electrons, which pass through an external circuit performing useful electric work before returning to the cathode.



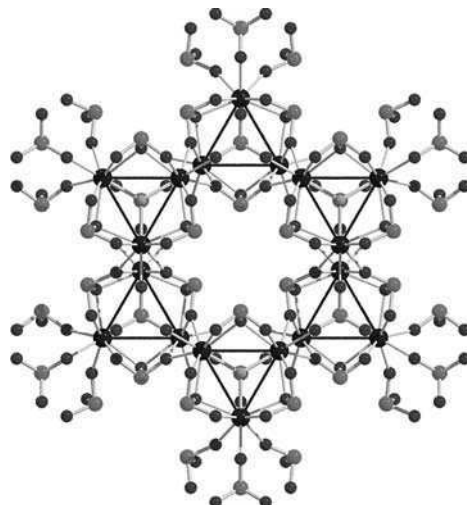
Many of the SOFC components – the electrolyte, anode, cathode and interconnects – consist of rare earth oxide materials. These include yttria stabilized zirconia, R_2O_3 -ceria, rare earth-alkaline earth manganites, and rare earth cobaltites, chromates and titanates. These complex rare earth metal oxides have good chemical stability at the severe SOFC operating conditions, exhibit high ionic or mixed ionic conductivity, good catalytic activity, the flexibility of changing the chemical composition and/or the ratio of component binary oxides, and can crystallize in a variety of structures, such as the fluoride, spinel and perovskite.

Chapter 224. Oxo-selenates of Rare Earth Elements

by Mathias S. Wickleder and Carl von Ossietzky

Universität Oldenburg, Oldenburg, Germany

Oxygen containing compounds is one of the largest groups of rare earth compounds, second to rare earth metal-organic materials. Familiar oxo-compounds include the natural occurring mineral families – silicates, phosphates and carbonates, and the derived families – nitrates, sulfates, perchlorates, manganites, ferrites, chromites, cobaltites, titanates, etc. Complex oxo-anions have attracted considerable attention in recent years because they can be used as precursors for preparing rare earth catalytic materials with large surface areas, non-centrosymmetric compounds for non-linear optical properties, electronic and magnetic materials, high temperature superconductors, etc. Wickleder's review focuses on one particular family of oxo-compounds, which is not well known, but has been studied extensively in the past few years because of their rich structural chemistry, complex thermal behaviors and dual oxidation states {selenites [or oxo-selenate (IV)] and selenates [or oxo-selenate (VI)]}. The oxo-selenate (IV) ion is much more stable than the oxo-selenate (VI), which is just the opposite of the stability of their isomorphous cousins the sulfate and the sulfite ions. Because of this reversal of stability there are more oxo-selenite (IV) compounds, and one can use the thermal decomposition of the oxo-selenate (VI) to prepare oxo-selenate (IV) compounds. In

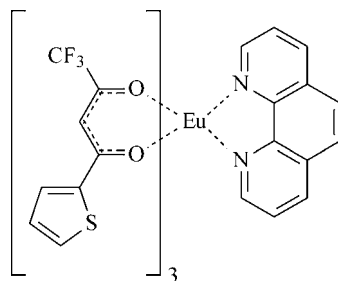


addition to the IV and VI oxidation states, a few of the mixed valent oxo-selenated (IV/VI) compounds are known, but much remains to be discovered.

The emphasis of this chapter is on the crystallography and crystal chemistry of these oxo-selenates. The structural description includes the important characteristic features – coordination numbers, geometry, connectivity of polyhedra and bond lengths. The SeO_4^{2-} anion has the ideal tetrahedral symmetry, while the SeO_3^{2-} anion has a pyramidal shape due to its lone electron pair at the selenium atom. The former is a strong oxidizer. In addition to the crystallography of this family of oxo-anions, some information exists on the vibrational spectra and thermal behaviors.

Chapter 225. Rare-earth Beta-diketonates
by Koen Binnemans
Catholic University of Leuven, Leuven, Belgium

The rare earth β -diketonates were first prepared at the end of the 19th century, more than 100 years ago by one of the pioneers of rare earth research, G. Urbain. The β -diketonate complexes are one of the most extensively investigated rare earth coordination compounds. This popularity is due to the fact that they are easily synthesized, readily available from commercial sources, and have many applications. Binnemans points out that there have been four periods of active research: the late 1950s–early 1960s, the mid 1960s, the 1970s–1985, which he calls the Golden Years of β -diketonate research, and the 1990s. In the first period these compounds were studied as extractants for the solvent–solvent extraction processes used to separate the individual rare earth elements. In the 1960s they were studied for their potential as laser materials, i.e. chelate lasers and liquid lasers. In the Golden Years, the β -diketonates were used as NMR shift reagents. The latest period of active research focused on their electroluminescent



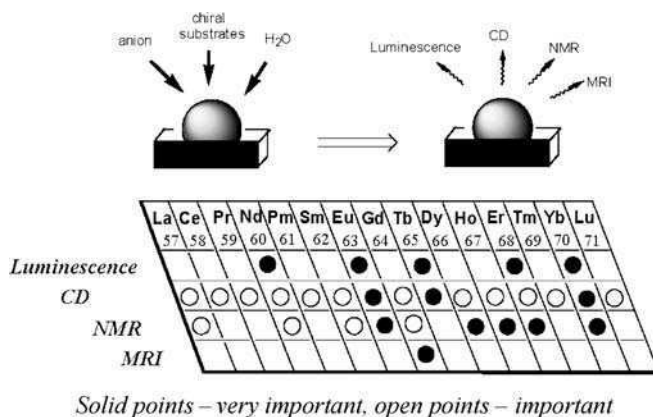
properties for organic light emitting diodes, their high vapor pressures as volatile reagents for chemical deposition, and their utilization as catalysts for organic reactions.

There are three main types of rare earth β -diketonates: the tris complexes, the Lewis base adducts of the tris complexes, and tetrakis complexes. The tris complexes have three β -diketonate ligands for each rare earth ion, i.e. $R(\beta\text{-diketonate})_3$. The Lewis base adducts are formed by reaction with water or other organic Lewis bases. The tetrakis complexes have four β -diketonate ligands around rare earth ion and have the general formula $[R(\beta\text{-diketonate})_4]^-$.

The rare earth β -diketonates are excellent compounds to test theoretical models in the field of spectroscopy, however, many applications are unlikely because these compounds have low thermal stability and may decompose during the construction of the devices. There are, however, some uses where photochemical stability is not a problem, such as fingerprint analysis or fluorimetric analysis. Their volatility has application as reagents for chemical vapor deposition, while their mild Lewis acidity has been utilized in Diels–Alder reactions. With passing of the Golden Age, one of the major applications – NMR shift reagents – has been reduced to a small fraction of its peak usage due to the development of high-field NMR spectrometers. Still, today there are a number of specialty applications for NMR shift reagents, such as the enantiomeric purity of chiral compounds, also see the next paragraph (Chapter 226) by Shinoda and co-workers.

Chapter 226. Molecular Recognition and Sensing via Rare Earth Complexes
by Satoshi Shinoda, Hiroyuki Miyake and Hiroshi Tsukube
Osaka City University, Osaka, Japan

Molecular recognition is one of the important areas of molecular-based biology, biomaterials, chemistry, medicine, and physics. When a lanthanide containing receptor binds with a given substrate, specific interactions may occur in the inner and/or outer coordination sphere(s). By monitoring these resultant interactions precise information about the substrate can be obtained. Since the lanthanide cations properties vary in a systematic manner as a function of their atomic number, i.e. radius, electron transfer ability, Lewis acidity, light-emitting efficiency and magnetic properties, one can select the most suitable lanthanide and use it in a tailor-made synthesis of a functional compound. Furthermore, the trivalent lanthanide ions have a similar ionic radii and coordination geometry to those of the Ca^{2+} cation, they can be



substituted for Ca^{2+} in many compounds and living organs, and thus are of great interest in biological studies.

In this chapter Shinoda, Miyake and Tsukube have summarized the recent advances in the chemistry of rare earth complexes in molecular recognition and sensing technology. The main techniques are luminescence, circular dichroism (CD), nuclear magnetic resonance (NMR) and magnetic resonance imaging (MRI), see above figure. Luminescence studies of both the intensity and splitting patterns of the emission signals give information about the microenvironments around the excited lanthanide ion. CD gives deep insights into the ligand condensation geometry, stereochemistry, electronic state and other environment-dependent parameters. NMR is a useful paramagnetic biological probe which gives angular and distance information on amino acids, nucleotides, and proteins. MRI, which is a specialized branch of NMR, has received much attention for the last 30 years as a medical imaging technology. Currently MRI contrast agents have been found to exhibit a high sensitivity toward external stimuli such as pH, P_{O_2} and intracellular concentrations of specific analytes. Since lanthanide complexes are widely used as labeling agents in gene and protein science and technology, new compounds are anticipated to play an important role as smart materials in chemistry, biology, medicine and related technologies of the next generation.

This page intentionally left blank

CONTENTS

Preface v

Contents xi

Contents of Volumes 1–34 xiii

Index of Contents of Volumes 1–35 xxiii

223. Natsuko Sakai, Katsuhiko Yamaji, Teruhisa Horita, Yue Ping Xiong and Harumi Yokokawa
Rare-earth materials for Solid Oxide Fuel Cells (SOFC) 1

224. Mathias S. Wickleder
Oxo-selenates of rare earth elements 45

225. Koen Binnemans
Rare-earth beta-diketonates 107

226. Satoshi Shinoda, Hiroyuki Miyake and Hiroshi Tsukube
Molecular recognition and sensing via rare earth complexes 273

Author index 337

Subject index 377

This page intentionally left blank

CONTENTS OF VOLUMES 1–34

VOLUME 1: Metals

1978, 1st repr. 1982, 2nd repr. 1991; ISBN 0-444-85020-1

1. Z.B. Goldschmidt, *Atomic properties (free atom)* 1
 2. B.J. Beaudry and K.A. Gschneidner Jr, *Preparation and basic properties of the rare earth metals* 173
 3. S.H. Liu, *Electronic structure of rare earth metals* 233
 4. D.C. Koskenmaki and K.A. Gschneidner Jr, *Cerium* 337
 5. L.J. Sundström, *Low temperature heat capacity of the rare earth metals* 379
 6. K.A. McEwen, *Magnetic and transport properties of the rare earths* 411
 7. S.K. Sinha, *Magnetic structures and inelastic neutron scattering: metals, alloys and compounds* 489
 8. T.E. Scott, *Elastic and mechanical properties* 591
 9. A. Jayaraman, *High pressure studies: metals, alloys and compounds* 707
 10. C. Probst and J. Wittig, *Superconductivity: metals, alloys and compounds* 749
 11. M.B. Maple, L.E. DeLong and B.C. Sales, *Kondo effect: alloys and compounds* 797
 12. M.P. Dariel, *Diffusion in rare earth metals* 847
- Subject index 877

VOLUME 2: Alloys and intermetallics

1979, 1st repr. 1982, 2nd repr. 1991; ISBN 0-444-85021-X

13. A. Iandelli and A. Palenzona, *Crystal chemistry of intermetallic compounds* 1
 14. H.R. Kirchmayr and C.A. Poldy, *Magnetic properties of intermetallic compounds of rare earth metals* 55
 15. A.E. Clark, *Magnetostrictive RFe_2 intermetallic compounds* 231
 16. J.J. Rhyne, *Amorphous magnetic rare earth alloys* 259
 17. P. Fulde, *Crystal fields* 295
 18. R.G. Barnes, *NMR, EPR and Mössbauer effect: metals, alloys and compounds* 387
 19. P. Wachter, *Europium chalcogenides: EuO, EuS, EuSe and EuTe* 507
 20. A. Jayaraman, *Valence changes in compounds* 575
- Subject index 613

VOLUME 3: Non-metallic compounds – I

1979, 1st repr. 1984; ISBN 0-444-85215-8

21. L.A. Haskin and T.P. Paster, *Geochemistry and mineralogy of the rare earths* 1
 22. J.E. Powell, *Separation chemistry* 81
 23. C.K. Jørgensen, *Theoretical chemistry of rare earths* 111
 24. W.T. Carnall, *The absorption and fluorescence spectra of rare earth ions in solution* 171
 25. L.C. Thompson, *Complexes* 209
 26. G.G. Libowitz and A.J. Maeland, *Hydrides* 299
 27. L. Eyring, *The binary rare earth oxides* 337
 28. D.J.M. Sevan and E. Summerville, *Mixed rare earth oxides* 401
 29. C.P. Khattak and F.F.Y. Wang, *Perovskites and garnets* 525
 30. L.H. Brixner, J.R. Barkley and W. Jeitschko, *Rare earth molybdates (VI)* 609
- Subject index 655

VOLUME 4: Non-metallic compounds – II

1979, 1st repr. 1984; ISBN 0-444-85216-6

31. J. Flahaut, *Sulfides, selenides and tellurides* 1
32. J.M. Haschke, *Halides* 89
33. F. Hulliger, *Rare earth pnictides* 153
34. G. Blasse, *Chemistry and physics of R-activated phosphors* 237
35. M.J. Weber, *Rare earth lasers* 275
36. F.K. Fong, *Nonradiative processes of rare-earth ions in crystals* 317
- 37A. J.W. O’Laughlin, *Chemical spectrophotometric and polarographic methods* 341
- 37B. S.R. Taylor, *Trace element analysis of rare earth elements by spark source mass spectroscopy* 359
- 37C. R.J. Conzemius, *Analysis of rare earth matrices by spark source mass spectrometry* 377
- 37D. E.L. DeKalb and V.A. Fassel, *Optical atomic emission and absorption methods* 405
- 37E. A.P. D’Silva and V.A. Fassel, *X-ray excited optical luminescence of the rare earths* 441
- 37F. F.W.V. Boynton, *Neutron activation analysis* 457
- 37G. S. Schuhmann and J.A. Philpotts, *Mass-spectrometric stable-isotope dilution analysis for lanthanides in geochemical materials* 471
38. J. Reuben and G.A. Elgavish, *Shift reagents and NMR of paramagnetic lanthanide complexes* 483
39. J. Reuben, *Bioinorganic chemistry: lanthanides as probes in systems of biological interest* 515
40. T.J. Haley, *Toxicity* 553
- Subject index 587

VOLUME 5

1982, 1st repr. 1984; ISBN 0-444-86375-3

41. M. Gasgnier, *Rare earth alloys and compounds as thin films* 1
42. E. Gratz and M.J. Zuckermann, *Transport properties (electrical resistivity, thermoelectric power thermal conductivity) of rare earth intermetallic compounds* 117
43. F.P. Netzer and E. Bertel, *Adsorption and catalysis on rare earth surfaces* 217
44. C. Boulesteix, *Defects and phase transformation near room temperature in rare earth sesquioxides* 321
45. O. Greis and J.M. Haschke, *Rare earth fluorides* 387
46. C.A. Morrison and R.P. Leavitt, *Spectroscopic properties of triply ionized lanthanides in transparent host crystals* 461
- Subject index 693

VOLUME 6

1984; ISBN 0-444-86592-6

47. K.H.J. Buschow, *Hydrogen absorption in intermetallic compounds* 1
48. E. Parthé and B. Chabot, *Crystal structures and crystal chemistry of ternary rare earth–transition metal borides, silicides and homologues* 113
49. P. Rogl, *Phase equilibria in ternary and higher order systems with rare earth elements and boron* 335
50. H.B. Kagan and J.L. Namy, *Preparation of divalent ytterbium and samarium derivatives and their use in organic chemistry* 525
- Subject index 567

VOLUME 7

1984; ISBN 0-444-86851-8

51. P. Rogl, *Phase equilibria in ternary and higher order systems with rare earth elements and silicon* 1
52. K.H.J. Buschow, *Amorphous alloys* 265
53. H. Schumann and W. Genthe, *Organometallic compounds of the rare earths* 446
- Subject index 573

VOLUME 8

1986; ISBN 0-444-86971-9

54. K.A. Gschneidner Jr and F.W. Calderwood, *Intra rare earth binary alloys: phase relationships, lattice parameters and systematics* 1
55. X. Gao, *Polarographic analysis of the rare earths* 163
56. M. Leskelä and L. Niinistö, *Inorganic complex compounds I* 203
57. J.R. Long, *Implications in organic synthesis* 335
- Errata 375
- Subject index 379

VOLUME 9

1987; ISBN 0-444-87045-8

58. R. Reisfeld and C.K. Jørgensen, *Excited state phenomena in vitreous materials* 1
59. L. Niinistö and M. Leskelä, *Inorganic complex compounds II* 91
60. J.-C.G. Bünzli, *Complexes with synthetic ionophores* 321
61. Zhiquan Shen and Jun Ouyang, *Rare earth coordination catalysis in stereospecific polymerization* 395
- Errata 429
- Subject index 431

VOLUME 10: High energy spectroscopy

1988; ISBN 0-444-87063-6

62. Y. Baer and W.-D. Schneider, *High-energy spectroscopy of lanthanide materials – An overview* 1
63. M. Campagna and F.U. Hillebrecht, *f-electron hybridization and dynamical screening of core holes in intermetallic compounds* 75
64. O. Gunnarsson and K. Schönhammer, *Many-body formulation of spectra of mixed valence systems* 103
65. A.J. Freeman, B.I. Min and M.R. Norman, *Local density supercell theory of photoemission and inverse photoemission spectra* 165
66. D.W. Lynch and J.H. Weaver, *Photoemission of Ce and its compounds* 231
67. S. Hüfner, *Photoemission in chalcogenides* 301
68. J.F. Herbst and J.W. Wilkins, *Calculation of 4f excitation energies in the metals and relevance to mixed valence systems* 321
69. B. Johansson and N. Mårtensson, *Thermodynamic aspects of 4f levels in metals and compounds* 361
70. F.U. Hillebrecht and M. Campagna, *Bremsstrahlung isochromat spectroscopy of alloys and mixed valent compounds* 425
71. J. Röhrler, *X-ray absorption and emission spectra* 453
72. F.P. Netzer and J.A.D. Matthew, *Inelastic electron scattering measurements* 547
- Subject index 601

VOLUME 11: Two-hundred-year impact of rare earths on science

1988; ISBN 0-444-87080-6

- H.J. Svec, *Prologue* 1
73. F. Szabadváry, *The history of the discovery and separation of the rare earths* 33
74. B.R. Judd, *Atomic theory and optical spectroscopy* 81
75. C.K. Jørgensen, *Influence of rare earths on chemical understanding and classification* 197
76. J.J. Rhyne, *Highlights from the exotic phenomena of lanthanide magnetism* 293
77. B. Bleaney, *Magnetic resonance spectroscopy and hyperfine interactions* 323
78. K.A. Gschneidner Jr and A.H. Daane, *Physical metallurgy* 409
79. S.R. Taylor and S.M. McLennan, *The significance of the rare earths in geochemistry and cosmochemistry* 485
- Errata 579
- Subject index 581

VOLUME 12

1989; ISBN 0-444-87105-5

80. J.S. Abell, *Preparation and crystal growth of rare earth elements and intermetallic compounds* 1
 81. Z. Fisk and J.P. Remeika, *Growth of single crystals from molten metal fluxes* 53
 82. E. Burzo and H.R. Kirchmayr, *Physical properties of $R_2Fe_{14}B$ -based alloys* 71
 83. A. Szytuła and J. Leciejewicz, *Magnetic properties of ternary intermetallic compounds of the RT_2X_2 type* 133
 84. H. Maletta and W. Zinn, *Spin glasses* 213
 85. J. van Zytveld, *Liquid metals and alloys* 357
 86. M.S. Chandrasekharaiah and K.A. Gingerich, *Thermodynamic properties of gaseous species* 409
 87. W.M. Yen, *Laser spectroscopy* 433
 Subject index 479

VOLUME 13

1990; ISBN 0-444-88547-1

88. E.I. Gladyshevsky, O.I. Bodak and V.K. Pecharsky, *Phase equilibria and crystal chemistry in ternary rare earth systems with metallic elements* 1
 89. A.A. Eliseev and G.M. Kuzmichyeva, *Phase equilibrium and crystal chemistry in ternary rare earth systems with chalcogenide elements* 191
 90. N. Kimizuka, E. Takayama-Muromachi and K. Siratori, *The systems R_2O_3 – M_2O_3 – $M'O$* 283
 91. R.S. Houk, *Elemental analysis by atomic emission and mass spectrometry with inductively coupled plasmas* 385
 92. P.H. Brown, A.H. Rathjen, R.D. Graham and D.E. Tribe, *Rare earth elements in biological systems* 423
 Errata 453
 Subject index 455

VOLUME 14

1991; ISBN 0-444-88743-1

93. R. Osborn, S.W. Lovesey, A.D. Taylor and E. Balcar, *Intermultiplet transitions using neutron spectroscopy* 1
 94. E. Dormann, *NMR in intermetallic compounds* 63
 95. E. Zirngiebl and G. Güntherodt, *Light scattering in intermetallic compounds* 163
 96. P. Thalmeier and B. Lüthi, *The electron–phonon interaction in intermetallic compounds* 225
 97. N. Grewe and F. Steglich, *Heavy fermions* 343
 Subject index 475

VOLUME 15

1991; ISBN 0-444-88966-3

98. J.G. Sereni, *Low-temperature behaviour of cerium compounds* 1
 99. G.-y. Adachi, N. Imanaka and Zhang Fuzhong, *Rare earth carbides* 61
 100. A. Simon, Hj. Mattausch, G.J. Miller, W. Bauhofer and R.K. Kremer, *Metal-rich halides* 191
 101. R.M. Almeida, *Fluoride glasses* 287
 102. K.L. Nash and J.C. Sullivan, *Kinetics of complexation and redox reactions of the lanthanides in aqueous solutions* 347
 103. E.N. Rizkalla and G.R. Choppin, *Hydration and hydrolysis of lanthanides* 393
 104. L.M. Vallarino, *Macrocyclic complexes of the lanthanide(III) yttrium(III) and dioxouranium(VI) ions from metal-templated syntheses* 443
 Errata 513
 Subject index 515

MASTER INDEX, Vols. 1–15

1993; ISBN 0-444-89965-0

VOLUME 16

1993; ISBN 0-444-89782-8

105. M. Loewenhaupt and K.H. Fischer, *Valence-fluctuation and heavy-fermion 4f systems* 1
 106. I.A. Smirnov and V.S. Oskotski, *Thermal conductivity of rare earth compounds* 107
 107. M.A. Subramanian and A.W. Sleight, *Rare earths pyrochlores* 225
 108. R. Miyawaki and I. Nakai, *Crystal structures of rare earth minerals* 249
 109. D.R. Chopra, *Appearance potential spectroscopy of lanthanides and their intermetallics* 519
 Author index 547
 Subject index 579

VOLUME 17: Lanthanides/Actinides: Physics – I

1993; ISBN 0-444-81502-3

110. M.R. Norman and D.D. Koelling, *Electronic structure, Fermi surfaces, and superconductivity in f electron metals* 1
 111. S.H. Liu, *Phenomenological approach to heavy-fermion systems* 87
 112. B. Johansson and M.S.S. Brooks, *Theory of cohesion in rare earths and actinides* 149
 113. U. Benedict and W.B. Holzapfel, *High-pressure studies – Structural aspects* 245
 114. O. Vogt and K. Mattenberger, *Magnetic measurements on rare earth and actinide mononictides and monochalcogenides* 301
 115. J.M. Fournier and E. Gratz, *Transport properties of rare earth and actinide intermetallics* 409
 116. W. Potzel, G.M. Kalvius and J. Gal, *Mössbauer studies on electronic structure of intermetallic compounds* 539
 117. G.H. Lander, *Neutron elastic scattering from actinides and anomalous lanthanides* 635
 Author index 711
 Subject index 753

VOLUME 18: Lanthanides/Actinides: Chemistry

1994; ISBN 0-444-81724-7

118. G.T. Seaborg, *Origin of the actinide concept* 1
 119. K. Balasubramanian, *Relativistic effects and electronic structure of lanthanide and actinide molecules* 29
 120. J.V. Beitz, *Similarities and differences in trivalent lanthanide- and actinide-ion solution absorption spectra and luminescence studies* 159
 121. K.L. Nash, *Separation chemistry for lanthanides and trivalent actinides* 197
 122. L.R. Morss, *Comparative thermochemical and oxidation – reduction properties of lanthanides and actinides* 239
 123. J.W. Ward and J.M. Haschke, *Comparison of 4f and 5f element hydride properties* 293
 124. H.A. Eick, *Lanthanide and actinide halides* 365
 125. R.G. Haire and L. Eyring, *Comparisons of the binary oxides* 413
 126. S.A. Kinkad, K.D. Abney and T.A. O'Donnell, *f-element speciation in strongly acidic media: lanthanide and mid-actinide metals, oxides, fluorides and oxide fluorides in superacids* 507
 127. E.N. Rizkalla and G.R. Choppin, *Lanthanides and actinides hydration and hydrolysis* 529
 128. G.R. Choppin and E.N. Rizkalla, *Solution chemistry of actinides and lanthanides* 559
 129. J.R. Duffield, D.M. Taylor and D.R. Williams, *The biochemistry of the f-elements* 591
 Author index 623
 Subject index 659

VOLUME 19: Lanthanides/Actinides: Physics – II

1994; ISBN 0-444-82015-9

130. E. Holland-Moritz and G.H. Lander, *Neutron inelastic scattering from actinides and anomalous lanthanides* 1
131. G. Aeppli and C. Broholm, *Magnetic correlations in heavy-fermion systems: neutron scattering from single crystals* 123
132. P. Wachter, *Intermediate valence and heavy fermions* 177
133. J.D. Thompson and J.M. Lawrence, *High pressure studies – Physical properties of anomalous Ce, Yb and U compounds* 383
134. C. Colinet and A. Pasturel, *Thermodynamic properties of metallic systems* 479
Author index 649
Subject index 693

VOLUME 20

1995; ISBN 0-444-82014-0

135. Y. Ōnuki and A. Hasegawa, *Fermi surfaces of intermetallic compounds* 1
136. M. Gasgnier, *The intricate world of rare earth thin films: metals, alloys, intermetallics, chemical compounds, . . .* 105
137. P. Vajda, *Hydrogen in rare-earth metals, including RH_{2+x} phases* 207
138. D. Gignoux and D. Schmitt, *Magnetic properties of intermetallic compounds* 293
Author index 425
Subject index 457

VOLUME 21

1995; ISBN 0-444-82178-3

139. R.G. Bautista, *Separation chemistry* 1
140. B.W. Hinton, *Corrosion prevention and control* 29
141. N.E. Ryan, *High-temperature corrosion protection* 93
142. T. Sakai, M. Matsuoka and C. Iwakura, *Rare earth intermetallics for metal–hydrogen batteries* 133
143. G.-y. Adachi and N. Imanaka, *Chemical sensors* 179
144. D. Garcia and M. Faucher, *Crystal field in non-metallic (rare earth) compounds* 263
145. J.-C.G. Bünzli and A. Milicic-Tang, *Solvation and anion interaction in organic solvents* 305
146. V. Bhagavathy, T. Prasada Rao and A.D. Damodaran, *Trace determination of lanthanides in high-purity rare-earth oxides* 367
Author index 385
Subject index 411

VOLUME 22

1996; ISBN 0-444-82288-7

147. C.P. Flynn and M.B. Salamon, *Synthesis and properties of single-crystal nanostructures* 1
148. Z.S. Shan and D.J. Sellmyer, *Nanoscale rare earth–transition metal multilayers: magnetic structure and properties* 81
149. W. Suski, *The $ThMn_{12}$ -type compounds of rare earths and actinides: structure, magnetic and related properties* 143
150. L.K. Aminov, B.Z. Malkin and M.A. Teplov, *Magnetic properties of nonmetallic lanthanide compounds* 295
151. F. Auzel, *Coherent emission in rare-earth materials* 507
152. M. Dolg and H. Stoll, *Electronic structure calculations for molecules containing lanthanide atoms* 607
Author index 731
Subject index 777

VOLUME 23

1996; ISBN 0-444-82507-X

153. J.H. Forsberg, *NMR studies of paramagnetic lanthanide complexes and shift reagents* 1
 154. N. Sabbatini, M. Guardigli and I. Manet, *Antenna effect in encapsulation complexes of lanthanide ions* 69
 155. C. Görller-Walrand and K. Binnemans, *Rationalization of crystal-field parametrization* 121
 156. Yu. Kuz'ma and S. Chykhrij, *Phosphides* 285
 157. S. Boghosian and G.N. Papatheodorou, *Halide vapors and vapor complexes* 435
 158. R.H. Byrne and E.R. Sholkovitz, *Marine chemistry and geochemistry of the lanthanides* 497
 Author index 595
 Subject index 631

VOLUME 24

1997; ISBN 0-444-82607-6

159. P.A. Dowben, D.N. McIlroy and Dongqi Li, *Surface magnetism of the lanthanides* 1
 160. P.G. McCormick, *Mechanical alloying and mechanically induced chemical reactions* 47
 161. A. Inoue, *Amorphous, quasicrystalline and nanocrystalline alloys in Al- and Mg-based systems* 83
 162. B. Elschner and A. Loidl, *Electron-spin resonance on localized magnetic moments in metals* 221
 163. N.H. Duc, *Intersublattice exchange coupling in the lanthanide–transition metal intermetallics* 339
 164. R.V. Skolozdra, *Stannides of rare-earth and transition metals* 399
 Author index 519
 Subject index 559

VOLUME 25

1998; ISBN 0-444-82871-0

165. H. Nagai, *Rare earths in steels* 1
 166. R. Marchand, *Ternary and higher order nitride materials* 51
 167. C. Görller-Walrand and K. Binnemans, *Spectral intensities of f - f transitions* 101
 168. G. Bombieri and G. Paolucci, *Organometallic π complexes of the f -elements* 265
 Author index 415
 Subject index 459

VOLUME 26

1999; ISBN 0-444-50815-1

169. D.F. McMorro, D. Gibbs and J. Bohr, *X-ray scattering studies of lanthanide magnetism* 1
 170. A.M. Tishin, Yu.I. Spichkin and J. Bohr, *Static and dynamic stresses* 87
 171. N.H. Duc and T. Goto, *Itinerant electron metamagnetism of Co sublattice in the lanthanide–cobalt intermetallics* 177
 172. A.J. Arko, P.S. Riseborough, A.B. Andrews, J.J. Joyce, A.N. Tahvildar-Zadeh and M. Jarrell, *Photoelectron spectroscopy in heavy fermion systems: Emphasis on single crystals* 265
 Author index 383
 Subject index 405

VOLUME 27

1999; ISBN 0-444-50342-0

173. P.S. Salamakha, O.L. Sologub and O.I. Bodak, *Ternary rare-earth–germanium systems* 1
 174. P.S. Salamakha, *Crystal structures and crystal chemistry of ternary rare-earth germanides* 225
 175. B. Ya. Kotur and E. Gratz, *Scandium alloy systems and intermetallics* 339
 Author index 535
 Subject index 553

VOLUME 28

2000; ISBN 0-444-50346-3

176. J.-P. Connerade and R.C. Karnatak, *Electronic excitation in atomic species* 1
 177. G. Meyer and M.S. Wickleder, *Simple and complex halides* 53
 178. R.V. Kumar and H. Iwahara, *Solid electrolytes* 131
 179. A. Halperin, *Activated thermoluminescence (TL) dosimeters and related radiation detectors* 187
 180. K.L. Nash and M.P. Jensen, *Analytical separations of the lanthanides: basic chemistry and methods* 311
 Author index 373
 Subject index 401

VOLUME 29: The role of rare earths in catalysis

2000; ISBN 0-444-50472-9

- P. Maestro, *Foreword* 1
 181. V. Paul-Boncour, L. Hilaire and A. Percheron-Guégan, *The metals and alloys in catalysis* 5
 182. H. Imamura, *The metals and alloys (prepared utilizing liquid ammonia solutions) in catalysis II* 45
 183. M.A. Ulla and E.A. Lombardo, *The mixed oxides* 75
 184. J. Kašpar, M. Graziani and P. Fornasiero, *Ceria-containing three-way catalysts* 159
 185. A. Corma and J.M. López Nieto, *The use of rare-earth-containing zeolite catalysts* 269
 186. S. Kobayashi, *Triflates* 315
 Author index 377
 Subject index 409

VOLUME 30: High-Temperature Superconductors – I

2000; ISBN 0-444-50528-8

187. M.B. Maple, *High-temperature superconductivity in layered cuprates: overview* 1
 188. B. Raveau, C. Michel and M. Hervieu, *Crystal chemistry of superconducting rare-earth cuprates* 31
 189. Y. Shiohara and E.A. Goodilin, *Single-crystal growth for science and technology* 67
 190. P. Karen and A. Kjekshus, *Phase diagrams and thermodynamic properties* 229
 191. B. Elschner and A. Loidl, *Electron paramagnetic resonance in cuprate superconductors and in parent compounds* 375
 192. A.A. Manuel, *Positron annihilation in high-temperature superconductors* 417
 193. W.E. Pickett and I.I. Mazin, *$R\text{Ba}_2\text{Cu}_3\text{O}_7$ compounds: electronic theory and physical properties* 453
 194. U. Staub and L. Soderholm, *Electronic 4f state splittings in cuprates* 491
 Author index 547
 Subject index 621

VOLUME 31: High-Temperature Superconductors – II

2001; ISBN 0-444-50719-1

195. E. Kaldis, *Oxygen nonstoichiometry and lattice effects in $\text{YBa}_2\text{Cu}_3\text{O}_x$. Phase transitions, structural distortions and phase separation* 1
 196. H.W. Weber, *Flux pinning* 187
 197. C.C. Almasan and M.B. Maple, *Magnetoresistance and Hall effect* 251
 198. T.E. Mason, *Neutron scattering studies of spin fluctuations in high-temperature superconductors* 281
 199. J.W. Lynn and S. Skanthakumar, *Neutron scattering studies of lanthanide magnetic ordering* 315
 200. P.M. Allenspach and M.B. Maple, *Heat capacity* 351
 201. M. Schabel and Z.-X. Shen, *Angle-resolved photoemission studies of untwinned yttrium barium copper oxide* 391
 202. D.N. Basov and T. Timusk, *Infrared properties of high- T_c superconductors: an experimental overview* 437
 203. S.L. Cooper, *Electronic and magnetic Raman scattering studies of the high- T_c cuprates* 509

204. H. Sugawara, T. Hasegawa and K. Kitazawa, *Characterization of cuprate superconductors using tunneling spectra and scanning tunneling microscopy* 563
 Author index 609
 Subject index 677

VOLUME 32

2001; ISBN 0-444-50762-0

205. N.H. Duc, *Giant magnetostriction in lanthanide–transition metal thin films* 1
 206. G.M. Kalvius, D.R. Noakes and O. Hartmann, *μ SR studies of rare-earth and actinide magnetic materials* 55
 207. Rainer Pöttgen, Dirk Johrendt and Dirk Kußmann, *Structure–property relations of ternary equiatomic YbTX intermetallics* 453
 208. Kurima Kobayashi and Satoshi Hirose, *Permanent magnets* 515
 209. I.G. Vasilyeva, *Polysulfides* 567
 210. Dennis K.P. Ng, Jianzhuang Jiang, Kuninobu Kasuga and Kenichi Machida, *Half-sandwich tetrapyrrole complexes of rare earths and actinides* 611
 Author index 655
 Subject index 733

VOLUME 33

2003; ISBN 0-444-51323-X

211. Brian C. Sales, *Filled skutterudites* 1
 212. Oksana L. Sologub and Petro S. Salamakha, *Rare earth – antimony systems* 35
 213. R.J.M. Konings and A. Kovács, *Thermodynamic properties of the lanthanide(III) halides* 147
 214. John B. Goodenough, *Rare earth – manganese perovskites* 249
 215. Claude Piquet and Carlos F.G.C. Geraldes, *Paramagnetic NMR lanthanide induced shifts for extracting solution structures* 353
 216. Isabelle Billard, *Lanthanide and actinide solution chemistry as studied by time-resolved emission spectroscopy* 465
 217. Thomas Tröster, *Optical studies of non-metallic compounds under pressure* 515
 Author index 591
 Subject index 637

VOLUME 34

2004; ISBN 0-444-51587-9

218. Yaroslav M. Kalychak, Vasyl' I. Zaremba, Rainer Pöttgen, Mar'yana Lukachuk and Rolf-Dieter Hoffman, *Rare earth–transition metal–indides* 1
 219. P. Thalmeier and G. Zwicknagl, *Unconventional superconductivity and magnetism in lanthanide and actinide intermetallic compounds* 135
 220. James P. Riehl and Gilles Muller, *Circularly polarized luminescence spectroscopy from lanthanide systems* 289
 221. Oliver Guillou and Carole Daignebonne, *Lanthanide-containing coordination polymers* 359
 222. Makoto Komiyama, *Cutting DNA and RNA* 405
 Author index 455
 Subject index 493

This page intentionally left blank

INDEX OF CONTENTS OF VOLUMES 1–35

- 4*f* levels, thermodynamic aspects **10**, ch. 69, p. 361
4*f* state splittings in cuprates **30**, ch. 194, p. 491
- absorption spectra of ions in solution **3**, ch. 24,
p. 171; **18**, ch. 120, p. 150
- actinide concept, origin of **18**, ch. 118, p. 1
- activated phosphors **4**, ch. 34, p. 237
- activated thermoluminescence **28**, ch. 179, p. 187
- amorphous alloys **7**, ch. 52, p. 265
- Al- and Mg-based **24**, ch. 161, p. 83
 - magnetic **2**, ch. 16, p. 259
- anion interaction in organic solvents **21**, ch. 145,
p. 305
- antimony alloy systems **33**, ch. 212, p. 35
- atomic properties (free atom) **1**, ch. 1, p. 1
- atomic theory **11**, ch. 74, p. 81
- beta-diketonates **35**, ch. 225, p. 107
- biochemistry **18**, ch. 129, p. 591
- bioinorganic chemistry **4**, ch. 39, p. 515
- biological systems **13**, ch. 92, p. 423
- carbides **15**, ch. 99, p. 61
- catalysis **29**, foreword, p. 1
- ceria-containing three-way **29**, ch. 184, p. 159
 - metals and alloys **29**, ch. 181, p. 5
 - metals and alloys in liquid ammonia solutions **29**,
ch. 182, p. 45
 - mixed oxides **29**, ch. 183, p. 75
 - zeolites **29**, ch. 185, p. 269
- cerium **1**, ch. 4, p. 337
- cerium compounds, low-temperature behavior **15**,
ch. 98, p. 1
- chalcogenides, magnetic measurements on mono-
17, ch. 114, p. 301
- chemical analysis by
- atomic emission with inductively coupled plasmas
13, ch. 91, p. 385
 - mass spectrometry, *see* spectroscopy, mass
 - neutron activation **4**, ch. 37E, p. 457
 - optical absorption **4**, ch. 37D, p. 405
 - optical atomic emission **4**, ch. 37D, p. 405
 - polarography **4**, ch. 37A, p. 341; **8**, ch. 55, p. 163
 - spectrophotometry **4**, ch. 37A, p. 341
 - trace determination in high-purity oxides **21**,
ch. 146, p. 367
 - X-ray excited optical luminescence **4**, ch. 37E,
p. 441
- chemical sensors **21**, ch. 143, p. 179
- chemical understanding and classification **11**,
ch. 75, p. 197
- chirality sensing **35**, ch. 226, p. 273
- coherent emission **22**, ch. 151, p. 507
- cohesion, theory of **17**, ch. 112, p. 149
- complexes **3**, ch. 25, p. 209
- antenna effect **23**, ch. 154, p. 69
 - beta-diketonates **35**, ch. 225, p. 107
 - half-sandwich tetrapyrrole **32**, ch. 210, p. 611
 - macrocycles **15**, ch. 104, p. 443
 - molecular recognition in **35**, ch. 226, p. 273
 - organometallic π type **25**, ch. 168, p. 265
 - sensing in **35**, ch. 226, p. 273
 - with synthetic ionophores **9**, ch. 60, p. 321
- coordination catalysis in stereospecific
polymerization **9**, ch. 61, p. 395
- coordination in organic solvents **21**, ch. 145, p. 305
- coordination polymers **34**, ch. 221, p. 359
- corrosion prevention and control **21**, ch. 140, p. 29
- corrosion protection **21**, ch. 141, p. 93
- cosmochemistry **11**, ch. 79, p. 485
- crystal chemistry
- of intermetallic compounds **2**, ch. 13, p. 1
 - of ternary germanides **27**, ch. 174, p. 225
 - of ternary systems with chalcogenides **13**, ch. 89,
p. 191
 - of ternary systems with metallic elements **13**,
ch. 88, p. 1
 - of ternary transition metal borides **6**, ch. 48, p. 113
 - of ternary transition metal silicides **6**, ch. 48,
p. 113
 - of ThMn₁₂-type compounds **22**, ch. 149, p. 143
- crystal field **2**, ch. 17, p. 295

- in non-metallic compounds **21**, ch. 144, p. 263
- crystal field parametrization, rationalization of **23**, ch. 155, p. 121
- crystal structures, *see* crystal chemistry
- cuprates
 - angle-resolved photoemission **31**, ch. 201, p. 391
 - crystal chemistry **30**, ch. 188, p. 31
 - electronic $4f$ state splittings **30**, ch. 194, p. 491
 - electron paramagnetic resonance **30**, ch. 191, p. 375
 - electronic theory **30**, ch. 193, p. 453
 - flux pinning **31**, ch. 196, p. 187
 - Hall effect **31**, ch. 197, p. 251
 - heat capacity **31**, ch. 200, p. 351
 - infrared properties **31**, ch. 202, p. 437
 - magnetoresistance **31**, ch. 197, p. 251
 - magnetic ordering **31**, ch. 199, p. 315
 - oxygen nonstoichiometry **31**, ch. 195, p. 1
 - phase equilibria **30**, ch. 190, p. 229
 - phase transitions **31**, ch. 195, p. 1
 - positron annihilation **30**, ch. 192, p. 417
 - Raman scattering **31**, ch. 203, p. 509
 - spin fluctuations **31**, ch. 198, p. 281
 - superconductivity overview **30**, ch. 187, p. 1
 - single-crystal, growth of **30**, ch. 189, p. 67
 - tunneling spectra **31**, ch. 204, p. 563
- diffusion in metals **1**, ch. 12, p. 847
- divalent samarium derivatives in organic chemistry **6**, ch. 50, p. 525
- divalent ytterbium derivatives in organic chemistry **6**, ch. 50, p. 525
- DNA, cutting of **34**, ch. 222, p. 405
- dynamical screening of core holes in intermetallic compounds **10**, ch. 63, p. 75
- elastic and mechanical properties of metals **1**, ch. 8, p. 591
- electron paramagnetic resonance, *see* EPR
- electronic excitation in atomic species **28**, ch. 176, p. 1
- electronic structure
 - calculations for molecules **22**, ch. 152, p. 607
 - of metals **1**, ch. 3, p. 233; **17**, ch. 110, p. 1
- electronic theory of cuprates **30**, ch. 193, p. 453
- electron–phonon interaction in intermetallic compounds **14**, ch. 96, p. 225
- electron–spin resonance, *see* EPR
- emission spectra **10**, ch. 71, p. 453
- EPR **2**, ch. 18, p. 387; **24**, ch. 162, p. 221; **30**, ch. 191, p. 375
- europium chalcogenides **2**, ch. 19, p. 507
- exchange coupling in transition metal intermetallics **24**, ch. 163, p. 339
- excited state phenomena in vitreous materials **9**, ch. 58, p. 1
- f*-electron hybridization in intermetallic compounds **10**, ch. 63, p. 75
- f*-element speciation in strongly acidic media (superacids) **18**, ch. 126, p. 507
- Fermi surfaces
 - of intermetallic compounds **20**, ch. 135, p. 1
 - of metals **17**, ch. 110, p. 1
- fluorescence spectra of ions in solution **3**, ch. 24, p. 171
- fluoride glasses **15**, ch. 101, p. 287
- fluorides **5**, ch. 45, p. 387
- flux pinning in cuprates **31**, ch. 196, p. 187
- garnets **3**, ch. 29, p. 525
- geochemistry **3**, ch. 21, p. 1; **11**, ch. 79, p. 485; **23**, ch. 158, p. 497
- germanium, ternary systems **27**, ch. 173, p. 1
- halides **4**, ch. 32, p. 89; **18**, ch. 124, p. 365
 - metal-rich **15**, ch. 100, p. 191
 - simple and complex **28**, ch. 177, p. 53
 - thermodynamic properties **33**, ch. 213, p. 147
 - vapors and vapor complexes **23**, ch. 157, p. 435
- Hall effect in cuprates **31**, ch. 197, p. 251
- heat capacity
 - of cuprates **31**, ch. 200, p. 351
 - of metals **1**, ch. 5, p. 379
- heavy fermions **14**, ch. 97, p. 343; **16**, ch. 105, p. 1; **19**, ch. 132, p. 177
 - phenomenological approach **17**, ch. 111, p. 87
 - photoelectron spectroscopy **26**, ch. 172, p. 265
- high pressure studies **1**, ch. 9, p. 707
 - anomalous Ce, Yb and U compounds **19**, ch. 133, p. 383
 - optical studies of non-metallic compounds **33**, ch. 217, p. 515
 - structural aspects **17**, ch. 113, p. 245
- high temperature superconductors, *see* cuprates
- history of the discovery and separation **11**, ch. 73, p. 33
- Hund, F. **14**, dedication, p. ix
- hydration **15**, ch. 103, p. 393; **18**, ch. 127, p. 529
- hydrides **3**, ch. 26, p. 299; **18**, ch. 123, p. 293
- hydrogen absorption in intermetallic compounds **6**, ch. 47, p. 1

- hydrogen in metals, including RH_{2+x} phases **20**,
ch. 137, p. 207
- hydrolysis **15**, ch. 103, p. 393; **18**, ch. 127, p. 529
- hyperfine interactions **11**, ch. 77, p. 323
- inelastic electron scattering **10**, ch. 72, p. 547
- infrared properties of cuprates **31**, ch. 202, p. 437
- inorganic complex compounds **8**, ch. 56, p. 203; **9**,
ch. 59, p. 91
- intermediate valence **19**, ch. 132, p. 177
- itinerant electron metamagnetism in cobalt
intermetallics **26**, ch. 171, p. 177
- kinetics of complexation in aqueous solutions **15**,
ch. 102, p. 347
- Kondo effect **1**, ch. 11, p. 797
- lanthanide-induced shifts **4**, ch. 38, p. 483; **23**,
ch. 153, p. 1; **33**, ch. 215, p. 353
- laser spectroscopy **12**, ch. 87, p. 433
- lasers **4**, ch. 35, p. 275
- light scattering in intermetallic compounds **14**,
ch. 95, p. 163
- liquid metals and alloys **12**, ch. 85, p. 357
- LIS, *see* lanthanide-induced shifts
- luminescence studies of ions **18**, ch. 120, p. 150
- luminescence spectra of ions in solution **3**, ch. 24,
p. 171
- μ SR studies of magnetic materials **32**, ch. 206, p. 55
- magnetic and transport properties of metals **1**, ch. 6,
p. 411
- magnetic correlations in heavy-fermion systems **19**,
ch. 131, p. 123
- magnetic properties
- of intermetallic compounds **2**, ch. 14, p. 55; **20**,
ch. 138, p. 293
 - of nonmetallic compounds **22**, ch. 150, p. 295
 - of ternary RT_2X_2 type intermetallic compounds
12, ch. 83, p. 133
 - of $ThMn_{12}$ -type compounds **22**, ch. 149, p. 143
- magnetic structures **1**, ch. 7, p. 489
- magnetism **34**, ch. 219, p. 135
- exotic phenomena **11**, ch. 76, p. 293
 - surface **24**, ch. 159, p. 1
- magnetoresistance in cuprates **31**, ch. 197, p. 251
- magnetostriction
- RFe_2 **2**, ch. 15, p. 231
 - transition metal thin films **32**, ch. 205, p. 1
- marine chemistry **23**, ch. 158, p. 497
- mechanical alloying **24**, ch. 160, p. 47
- mechanically induced chemical reactions **24**,
ch. 160, p. 47
- metal–hydrogen batteries **21**, ch. 142, p. 133
- mineralogy **3**, ch. 21, p. 1
- minerals, crystal structures **16**, ch. 108, p. 249
- mixed valence systems
- bremsstrahlung isochromat spectroscopy **10**,
ch. 70, p. 425
 - calculation of $4f$ excitation energies **10**, ch. 68,
p. 321
 - many-body formulation of spectra **10**, ch. 64,
p. 103
- molecular recognition **35**, ch. 226, p. 273
- molybdates (VI) **3**, ch. 30, p. 609
- Mössbauer effect **2**, ch. 18, p. 387
- of intermetallic compounds **17**, ch. 116, p. 539
- nanostructures
- Al- and Mg-based systems **24**, ch. 161, p. 83
 - properties **22**, ch. 147, p. 1
 - synthesis **22**, ch. 147, p. 1
 - transition metal multilayers **22**, ch. 148, p. 81
- neutron scattering
- elastic **17**, ch. 117, p. 635
 - inelastic **1**, ch. 7, p. 489
 - intermultiple transitions **14**, ch. 93, p. 1
 - inelastic of anomalous lanthanides **19**, ch. 130, p. 1
 - in heavy-fermion systems **19**, ch. 131, p. 123
 - of magnetic ordering in cuprates **31**, ch. 199,
p. 315
 - of spin fluctuations in cuprates **31**, ch. 198, p. 281
- nitride materials, ternary and higher order **24**,
ch. 166, p. 51
- NMR **2**, ch. 18, p. 387
- in intermetallic compounds **14**, ch. 94, p. 63
 - lanthanide induced shifts for extracting solution
structures **33**, ch. 215, p. 353
 - of complexes **23**, ch. 153, p. 1
 - of paramagnetic complexes **4**, ch. 38, p. 483
 - solution structure by paramagnetic NMR analysis
33, ch. 215, p. 353
- nonradiative processes in crystals **4**, ch. 36, p. 317
- nuclear magnetic resonance, *see* NMR
- organic synthesis **8**, ch. 57, p. 335
- organometallic compounds **7**, ch. 53, p. 446
- oxidation–reduction properties **18**, ch. 122, p. 239
- oxides
- binary **3**, ch. 27, p. 337; **18**, ch. 125, p. 413
 - mixed **3**, ch. 28, p. 401
 - sesqui, defects in **5**, ch. 44, p. 321
 - sesqui, phase transformation in **5**, ch. 44, p. 321

- ternary systems, R_2O_3 – M_2O_3 – $M'O$ **13**, ch. 90, p. 283
- oxo-selenates **35**, ch. 224, p. 45
- oxygen nonstoichiometry and lattice effect in $YBa_2Cu_3O_x$ **31**, ch. 195, p. 1
- permanent magnets **32**, ch. 208, p. 515
- perovskites **3**, ch. 29, p. 525
 - manganese **33**, ch. 214, p. 249
- phase equilibria
 - in cuprates **30**, ch. 190, p. 229
 - in ternary systems with boron **6**, ch. 49, p. 335
 - in ternary systems with chalcogenides **13**, ch. 89, p. 191
 - in ternary systems with metallic elements **13**, ch. 88, p. 1
 - in ternary systems with silicon **7**, ch. 51, p. 1
 - intra rare earth binary alloys **8**, ch. 54, p. 1
- phase transitions, structural distortions and phase separation in $YBa_2Cu_3O_x$ **31**, ch. 195, p. 1
- phosphides **23**, ch. 156, p. 285
- photoemission
 - angle-resolved studies of untwinned $YBa_2Cu_3O_x$ **31**, ch. 201, p. 391
 - in chalcogenides **10**, ch. 67, p. 301
 - inverse spectra, local density supercell theory **10**, ch. 65, p. 165
 - of Ce and its compounds **10**, ch. 66, p. 231
 - spectra, local density supercell theory **10**, ch. 65, p. 165
- physical metallurgy **11**, ch. 78, p. 409
- physical properties
 - of cuprates **30**, ch. 193, p. 453
 - of metals **1**, ch. 2, p. 173
 - of $R_2Fe_{14}B$ -based alloys **12**, ch. 82, p. 71
- pnictides **4**, ch. 33, p. 153
 - magnetic measurements on mono- **17**, ch. 114, p. 301
- positron annihilation in high-temperature superconductors **30**, ch. 192, p. 417
- preparation and purification of metals **1**, ch. 2, p. 173
- pyrochlores **16**, ch. 107, p. 225
- quasicrystalline, Al- and Mg-based systems **24**, ch. 161, p. 83
- Raman scattering of cuprates **31**, ch. 203, p. 509
- redox reactions in aqueous solutions **15**, ch. 102, p. 347
- relativistic effects and electronic structure **18**, ch. 119, p. 29
- RNA, cutting of **34**, ch. 222, p. 405
- scandium alloy systems and intermetallics **27**, ch. 175, p. 339
- scanning tunneling microscopy of cuprates **31**, ch. 204, p. 563
- selenates **35**, ch. 224, p. 45
- selenides **4**, ch. 31, p. 1
- selenites **35**, ch. 224, p. 45
- separation chemistry **3**, ch. 22, p. 81; **18**, ch. 121, p. 197; **21**, ch. 139, p. 1
 - analytical, basic chemistry and methods **28**, ch. 180, p. 311
- shift reagents **4**, ch. 38, p. 483; **23**, ch. 153, p. 1; **33**, ch. 215, p. 353; **35**, ch. 225, p. 107
- single crystals
 - growth from molten metal fluxes **12**, ch. 81, p. 53
 - growth of cuprates **30**, ch. 189, p. 67
 - growth of metals and intermetallic compounds **12**, ch. 80, p. 1
- skutterudites, filled **33**, ch. 211, p. 1
- solid electrolytes **28**, ch. 178, p. 131; **35**, ch. 223, p. 1
- solid oxide fuel cells (SOFC) **35**, ch. 223, p. 1
- solution chemistry **15**, ch. 103, p. 393; **18**, ch. 127, p. 529; **18**, ch. 128, p. 559; **21**, ch. 145, p. 305
- solvation in organic solvents **21**, ch. 145, p. 305
- spectral intensities of f - f transitions **24**, ch. 167, p. 101
- spectroscopic properties in transparent crystals **5**, ch. 46, p. 461
- spectroscopy
 - appearance potential **16**, ch. 109, p. 519
 - bremsstrahlung isochromat **10**, ch. 70, p. 425
 - circularly polarized luminescence **34**, ch. 220, p. 289
 - high-energy **10**, ch. 62, p. 1
 - magnetic resonance **11**, ch. 77, p. 323
 - mass
 - spark source matrices **4**, ch. 37C, p. 377
 - spark source trace element analysis **4**, ch. 37B, p. 359
 - stable-isotope dilution analysis **4**, ch. 37G, p. 471
 - with inductively coupled plasmas analysis **13**, ch. 91, p. 385
 - optical **11**, ch. 74, p. 81
 - photoelectron in heavy fermion systems **26**, ch. 172, p. 265
 - time-resolved emission in solution chemistry **33**, ch. 216, p. 465
- Spedding, F. H., **11**, prologue, p. 1

- spin glasses **12**, ch. 84, p. 213
- stannides, transition metal ternary systems **24**,
ch. 164, p. 399
- steels **25**, ch. 165, p. 1
- stresses, static and dynamic **26**, ch. 170, p. 87
- sulfides **4**, ch. 31, p. 1
- poly **32**, ch. 209, p. 567
- superconductivity **1**, ch. 10, p. 749; **34**, ch. 219,
p. 135, also *see* cuprates
- in metals **17**, ch. 110, p. 1
- high-temperature layered cuprates: overview **30**,
ch. 187, p. 1
- surfaces
- adsorption on **5**, ch. 43, p. 217
- catalysis on **5**, ch. 43, p. 217
- systematics, intra rare earth binary alloys **8**, ch. 54,
p. 1
- tellurides **4**, ch. 31, p. 1
- ternary equiatomic YbTX intermetallics **32**, ch. 207,
p. 453
- theoretical chemistry **3**, ch. 23, p. 111
- thermal conductivity of compounds **16**, ch. 106,
p. 107
- thermochemical properties **18**, ch. 122, p. 239
- of cuprates **30**, ch. 190, p. 229
- of gaseous species **12**, ch. 86, p. 409
- of metallic systems **19**, ch. 134, p. 479
- thin films **5**, ch. 41, p. 1; **20**, ch. 136, p. 105
- toxicity **4**, ch. 40, p. 553
- transition metal indides **34**, ch. 218, p. 1
- transport properties of intermetallics **5**, ch. 42,
p. 117; **17**, ch. 115, p. 409
- triflates **29**, ch. 186, p. 315
- tunneling spectra of cuprates **31**, ch. 204, p. 563
- unconventional superconductivity and magnetism
34, ch. 219, p. 135
- valence fluctuations **2**, ch. 20, p. 575; **16**, ch. 105,
p. 1
- X-ray absorption spectra **10**, ch. 71, p. 453
- X-ray scattering **26**, ch. 169, p. 1

This page intentionally left blank

Chapter 223

RARE-EARTH MATERIALS FOR SOLID OXIDE FUEL CELLS (SOFC)

Natsuko SAKAI, Katsuhiko YAMAJI, Teruhisa HORITA, Yue Ping XIONG and Harumi YOKOKAWA

National Institute of Advanced Industrial Science and Technology, Higashi 1-1-1, Tsukuba, Ibaraki 305-8565, Japan

E-mail: n-sakai@aist.go.jp

Contents

List of symbols	1	3.3. Ionic conductivity and transport number of electrolytes	21
List of acronyms	2	3.4. Electron/hole conductivity of the anode, cathode and interconnect	23
1. Introduction	3	3.5. Mechanical strength of the electrolyte and interconnect	29
2. Overview of the SOFC materials	9	3.6. Thermal expansion matching with other SOFC components	30
2.1. Electrolytes	9	3.7. Chemical stability, compatibility with other cell component	36
2.2. Anodes	14	Summary	40
2.3. Cathodes	15	References	40
2.4. Interconnects	16		
3. Key issues in SOFC materials design	17		
3.1. Materials and preparation cost	18		
3.2. Processing simplicity	18		

List of symbols

a, b, x, y	fractional atomic coordinates
α	thermal diffusivity
C_0	oxygen concentration at the surface
C_p	molar heat capacity
$C_{p,n}$	molar heat capacity estimated by Neumann–Kopp’s theory
D_O	oxygen self diffusivity
D_{O^*}	oxygen isotope diffusivity
D_V	oxygen vacancy diffusivity
δ	molar oxygen deficiency
E	ideal electric potential

$\Delta E_{\text{electrolyte}}$	electric potential in electrolyte
$\varepsilon_{\text{electrolyte}}$	efficiency of the electrolyte
F	Faraday's constant
ΔG	Gibb's free energy change in the redox reaction
ΔH	enthalpy change in the redox reaction
η	ideal efficiency
j_{O_2}	oxygen flux through the interconnect
$J_{\text{O}_2, \text{electrolyte}}$	oxygen flux through the electrolytes
$J_{\text{O}^{2-}}^{\text{surf}}$	oxide ion flux determined by surface exchange rate
J_{ext}	electrical flux in the external circuit
k_s	surface exchange rate constant
K_{ox}	equilibrium constant of oxygen defect formation
L	thickness of the electrolyte or interconnect plate
λ	thermal conductivity
λ_0	thermal conductivity of dense material
μ_{O_2}	chemical potential of oxygen molecule
n	number of electron in the redox reaction
v_m	molar volume
p	partial pressure
p_{O_2}	partial pressure of oxygen
π	relative porosity
r	correlation factor
R	gas constant
ρ	density
ΔS	entropy change in the redox reaction
σ	electrical conductivity
$\sigma_{\text{O}^{2-}}$	oxide ion conductivity
σ_e	electron conductivity
σ_h	hole conductivity
T	temperature
V_{O}	oxygen vacancy in the lattice
z	sample thickness

List of acronyms

APU	auxiliary power unit
FCEV	fuel cell electric vehicle
GDC	gadolinium doped ceria
JPY	Japanese yen
MCFC	molten carbonate fuel cell
METI	ministry of economy, trade and industry
MOLB	mono block layer built

LSCF	lanthanum strontium cobalt ferrite, $(\text{La,Sr})(\text{Co,Fe})\text{O}_3$
LSGM	lanthanum gallate (LaGaO_3) with the substitution of strontium and magnesium $(\text{La,Sr})(\text{Ga,Mg})\text{O}_x$
LSGMC	lanthanum gallate (LaGaO_3) with the substitution of strontium, magnesium and cobalt $(\text{La,Sr})(\text{Ga,Mg,Co})\text{O}_x$
LSM	lanthanum strontium manganite $(\text{La,Sr})\text{MnO}_3$
PAFC	phosphoric acid fuel cell
PEFC	polymer electrolyte fuel cell/proton exchange membrane fuel cell
PNNL	Pacific Northwest National Laboratory
RDC	rare earth doped ceria
ScSZ	scandia stabilized zirconia
SOFC	solid oxide fuel cell
YSZ	yttria stabilized zirconia

1. Introduction

The world trend of research and development for fuel cell was largely changed from the beginning of 21st century. The research and development concerning fuel cell technology was drastically accelerated in Japan in the beginning of this century. The Japanese national strategy concerning fuel cell and hydrogen utilization was reported by the Agency of Natural Resources and Energy in 2002, and it encouraged the rapid introduction of the fuel cell electric vehicle (FCEV) using a polymer electrolyte fuel cell (PEFC) with pure hydrogen as fuel. This national report predicted that a strong collaboration is inevitable among developers, universities, public research institutes and governmental organizations to accelerate the introduction of fuel cells in the real world. Moreover, the fuel cell project team is organized by the Ministry of Economy, Trade and Industry (METI), the Ministry of the Environment, and the Ministry of Land, Infrastructure and Transport, which indicates that the development of fuel cells including the enactment of legal controls and the preparation of infrastructures is supported under the collaboration of these three ministries. Many campaigns for the enlightenment about fuel cell vehicles have been made by governments, and the automobile companies. The Japanese governmental budget concerning fuel cells and hydrogen technologies of METI in FY 2004 is 32.9 billion JPY (ca. \$300 million US). In the United States, the president proposed \$1.7 billion of research funding over five years for the FreedomCAR and the Hydrogen fuel initiative (Williams and Strakey, 2003).

Most of the fuel cells concerning these projects or initiatives are polymer electrolyte fuel cells (PEFCs), which consist of proton conductive organic membrane with platinum electrodes and operates at around 80 °C. PEFC has an excellent durability in fast start-up and shut-down conditions, and a higher energy conversion efficiency than conventional engines. However, only very high purity hydrogen can be used as the fuel of PEFC, because the platinum electrodes are rapidly disintegrated by the sulfur or carbon monoxide in the fuel or the

ambient atmosphere. Furthermore, platinum is the common electrode material which raises the fabrication cost of PEFC.

There are many types of fuel cells which are categorized by their electrolyte materials in [table 1](#). The component materials, operation conditions, and usage are quite different among each type of fuel cell. However, the principle of power generation is the same, that is, the Gibbs energy change due to the fuel oxidation is converted to electrical energy according to the following equation:

$$\Delta G = nFE, \quad (1)$$

where the ideal efficiency

$$\eta = \Delta G/\Delta H = (\Delta H - T\Delta S)/\Delta H. \quad (2)$$

The ideal potential corresponds to the open circuit voltage if the electrolyte is an ideal ionic conductor.

As we can see from the above equations, a larger ideal efficiency is obtained at lower temperatures, however, it is impossible to obtain the ideal efficiency in the general fuel cell operation. In the actual fuel cell operation, the Ohmic resistance of the materials and some slow chemical reactions at electrolyte/electrode interfaces cause energy losses, and hence the actual efficiency is much lower than the ideal efficiency. Since such efficiency losses decrease with increasing temperature, the high temperature fuel cells (SOFC, MCFC) have advantages in the energy conversion efficiency. Their actual efficiencies are comparable to PEFC when hydrogen is used as fuel, and much higher than PEFC when methane or a hydrocarbon fuel is used.

The single cell of a solid oxide fuel cell (SOFC) consists of a dense metal oxide electrolyte with a porous anode and cathode on each side. Oxygen gas is dissociated and reduced to the oxide ion on cathode/electrolyte interface, and the oxide ion diffuses to the interface of anode/electrolyte. The oxidation of fuel (H_2 , CO) is governed by the reaction of the oxide ion accompanied with the emission of electrons. These electrons pass through the external circuit and reduce the oxygen gas at the cathode/electrolyte interface. The power generation mechanism of SOFC with an oxide ion conducting electrolyte is shown in [Fig. 1](#). Since the SOFC operates at the highest temperature of all the fuel cells, it cannot be used in the rapid start-up or shut-down modes which are required as a power generation units of vehicles. However, the high temperature operation of SOFC makes possible internal reforming and power generation of hydrocarbon fuels and water directly fed to the cell stacks, which results in a high efficiency. The high temperature exhaust gas of SOFC can be utilized in other energy conversion devices such as gas turbines, engines, boilers etc. which will raise the total efficiency. The most of components are also made of metal or metal oxides which have high durability even at high temperatures. Hence, SOFC is expected to be used as power generation devices in electric power plants, large buildings, remote places, etc.

Many of the complex metal oxides containing rare earths are used as SOFC materials. The main reason is that the rare earth containing oxides have relatively good chemical stability which withstands the severe SOFC operating conditions. Another reason is the compositional

Table 1
Type of fuel cells categorized by electrolyte materials

	Polymer electrolyte PEFC	Phosphoric acid PAFC	Molten carbonate MCFC	Solid oxide SOFC
Electrolyte	Organic polymer	Phosphoric acid solution	Molten carbonate (NaCl, KCl, LiCl, etc.)	Oxide ion conducting ceramics (YSZ, LSGM, etc.)
Conductive ion in electrolytes	Proton (H ⁺)	Proton (H ⁺)	Carbonate ion (CO ₃ ²⁻)	Oxide ion (O ²⁻)
Operation temperature	70–90 °C	200 °C	600–650 °C	800–1000 °C
Possible fuels for power generation	High purity H ₂ ; CO should be under 10 ppm	H ₂ ; CO should be under several %	H ₂ ; CO; internal reforming of CH ₄ is possible	H ₂ , CO; internal reforming of CH ₄ is easy
Actual efficiency (HHV) using methane (CH ₄)	30–40%	36–42%	45–60%	45–65%
Scale and use	Several kW Automobile, stationary	Several 100 kW Distributed power generation for industry	Several 100 kW Large scale power generation plant	Several kW–100 kW Distributed power generation for industry and stationary APU for automobile
R&D status	Fundamental research– system evaluation	System evaluation– marketing	Fundamental research– system evaluation– marketing	Fundamental research– system evaluation

Table 2a
Candidate materials for SOFC electrolyte and anode

Material	Advantages	Problems	R&D status and remarks
Electrolyte			
Y ₂ O ₃ -ZrO ₂ (YSZ)	High mechanical strength High chemical stability Fine, sinterable powder is commercially available Easy thin film preparation	Relatively lower ionic conductivity (0.13 S cm ⁻¹ at 1000 °C) Conductivity gradually degraded in long term operation	100 kW class system (Siemens Westinghouse) 10 kW class system (Mitsubishi Heavy Ind.) kW class system (TOTO Ltd., Sulzer Ltd. Acumentrics Co.)
Sc ₂ O ₃ -ZrO ₂ (ScSZ)	Higher ionic conductivity than YSZ (0.3 S cm ⁻¹ at 1000 °C)	High cost of scandium	1 kW class module (Toho Gas/SSMC/Nippon Shokubai)
(La, Sr)(Ga, Mg, Co)O ₃ (LSGMCo)	Higher ionic conductivity than YSZ (0.2–0.5 S cm ⁻¹ at 1000 °C)	High temperature (~1500 °C) is needed for sintering High reactivity with other components Gallium vaporization on anode side at high temperatures	1 kW class module (Mitsubishi Materials/KEPCO)
M ₂ O ₃ -CeO ₂ (ceria) (M = Gd, Sm, etc.)	Higher ionic conductivity than YSZ (0.32 S cm ⁻¹ at 1000 °C) Low activation energy	Mixed conduction of oxide ion and electron causes undesirable efficiency loss Isothermal lattice expansion is observed at fuel side	Single cell/several stack (Imperial College/CERES Co.)
Anode			
Ni-YSZ (Ni-ScSZ, Ni-LSGMCo, Ni-ceria)	Most popular material High catalytic activity	Poor stability against carbon deposition Degradation is observed by nickel sintering in long term operation	Used in most SOFC stacks and modules in field tests Addition of ruthenium (Ru), CeO ₂ etc. is applied to improve catalytic activity

Table 2b
Candidate materials for SOFC cathode

Material	Advantages	Problems	R&D status and remarks
Cathode			
(La, Sr)MnO ₃ (LSM)	Most popular material Good chemical stability Thermal expansion matches with YSZ	La ₂ Zr ₂ O ₇ formed at the interface between YSZ and LSM may degrade the electrode performance	Applicable for high temperature SOFC (~1000 °C) Adopted in most SOFC stacks with YSZ electrolyte
(La, Sr) _{1-y} MnO ₃	Lower reactivity with YSZ	Manganese diffusion into YSZ is observed Thermal treatment above 1200 °C may degrade the electrode performance	
SmCoO ₃	High catalytic activity	High thermal expansion High reactivity with YSZ forming La ₂ Zr ₂ O ₇	Adopted in SOFCs with LSGM electrolyte Suitable for lower temperature operation (~700 °C)
(La, Sr)(Co, Fe)O ₃ (LSCF)	High catalytic activity Mixed conductor (hole and oxide ion)	High reactivity with YSZ forming La ₂ Zr ₂ O ₇	Suitable for lower temperature operation (~700 °C)

Table 2c
Candidate materials for SOFC interconnect

Material	Advantages	Problems	R&D status and remarks
Interconnect (La, Ca)(Cr, M)CrO ₃ (M = transition metals, Al)	Good sinterability at lower temperature Thin film preparation is possible High electronic conductivity	Lower conductivity at fuel side Oxide ion conductivity is generated in fuel side, causing efficiency loss by oxygen permeation Isothermal lattice expansion is observed at fuel side High reactivity with cathode materials Poor thermal conductivity	Adopted in tubular type SOFC stacks (Siemens Westinghouse) (TOTO Ltd.)
(La, Sr)(Cr, M)CrO ₃ (M = transition metals, Al)	Good sinterability Relatively good chemical stability Lesser isothermal expansion in fuel side	High temperature is needed for sintering Poor thermal conductivity Thin film preparation is difficult	Adopted in planar type SOFC stacks (Mitsubishi Heavy Industry)
(M, M')TiO ₃ (M = alkaline earths, M' = rare earths)	Good sinterability Lesser isothermal expansion in fuel side	Lower conductivity in air	Adopted in tubular type SOFC stacks (Mitsubishi Heavy Industry)
Alloys: Fe-Cr alloy, Cr-based alloy	Good thermal conductivity Good mechanical strength	Oxide scale is formed on both air and fuel side Chromium is vaporized and precipitated at the electrode/electrolyte interface	Adopted in planar type SOFC stacks operated below 800 °C (Mitsubishi Materials Co./KEPCO)

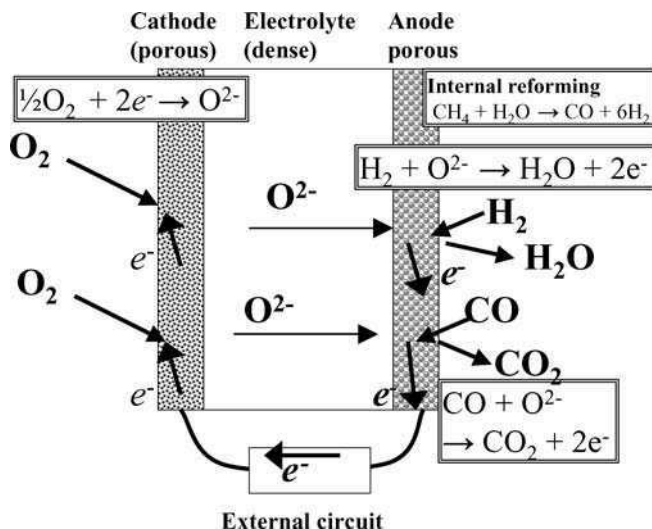


Fig. 1. Schematic view of the power generation of a SOFC single cell with an oxide ion conducting electrolyte.

flexibility in rare earth containing oxides: the complex oxides consist of rare earth and transition metals or alkaline earth metals exhibit a variety of structures such as spinel, brownmillerite, perovskite or fluorite structures; and they exhibit high ionic or mixed ionic conductivity (oxide ion, hole, proton, electron); or interesting catalytic activity which is important for fuel cell power generation.

The materials considered as candidates in SOFC stack developments are summarized in [table 2](#), where it is seen that the most of materials contain rare earths. Although many review papers have reported the material chemistry in SOFCs, in the present paper we are reporting on the current status of research and development of rare-earth containing materials for the state-of-the art SOFCs.

2. Overview of the SOFC materials

2.1. Electrolytes

The electrolyte is the most important component in fuel cells. The oxide ions or protons diffuse in the electrolyte according to the chemical potential. The electrolyte material should have high ionic conductivity and high transport number of the ion. In SOFC, oxide ion conducting metal oxides are generally used. The oxide ion conductivities of some candidate materials for SOFC electrolytes are shown in [Fig. 2](#). Yttria stabilized zirconia (YSZ) is the classic material of SOFC electrolytes. YSZ has a fluorite type structure, and it has a high mechanical strength and excellent chemical stability over a wide range of oxygen potentials at high temperatures. However, its oxide ion conductivity is ca. 0.13 S cm^{-1} at $T = 1000^\circ\text{C}$, and it is not

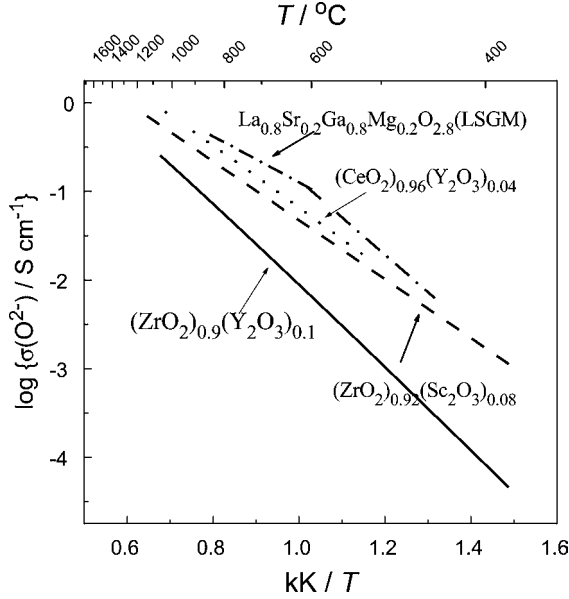


Fig. 2. Total conductivities of popular SOFC electrolytes as functions of temperature.

as high as those of electrolytes in other types of fuel cells. Hence, the conventional SOFCs with YSZ electrolyte are generally operated at 1000 °C, and stable power generation has been already produced by several hundreds kW stacks by Siemens Westinghouse Power Corporation (George and Casanova, 2003) in the US and by several tens kW stacks in a project in Japan sponsored by the New Energy Development Organization (NEDO), Japan (Fujii, 2003).

Although it needs high temperatures for SOFC operation, the external heat is not necessary in the steady state operation of large size cell stacks, because the stack temperature can be maintained by Joule heat generated by the $T \Delta S$ term in the equation (2).

The SOFC stacks consist of all oxide materials for obtaining high durability at high temperatures. However, the material selection is quite severe for conventional high temperature SOFCs. Since the electrolyte and interconnects are exposed to a large oxygen partial pressure gradient at $T = 1000$ °C, all metals other than precious metals will be degraded, so that perovskite type oxides having high electronic conductivity are used as interconnects.

Although there are many restrictions for materials for high temperature SOFCs, their designs are rich in variety as shown in fig. 3. The vertical stripe type tubular SOFC (fig. 3a) was adopted by Siemens Westinghouse Co. USA (George and Casanova, 2003) and TOTO Co in Japan (Takeuchi et al., 2003), and the segment type in series was adopted by Mitsubishi Heavy Industry, Japan (Konishi et al., 2002). In tubular SOFCs, a thin electrolyte film is fabricated on a porous electrode & substrate. Interconnect is attached a part of electrolyte, which is used to connect single cells in series. High dimensional stability and durability are expected for tubular SOFCs. However, their power generation performances are relatively low because of

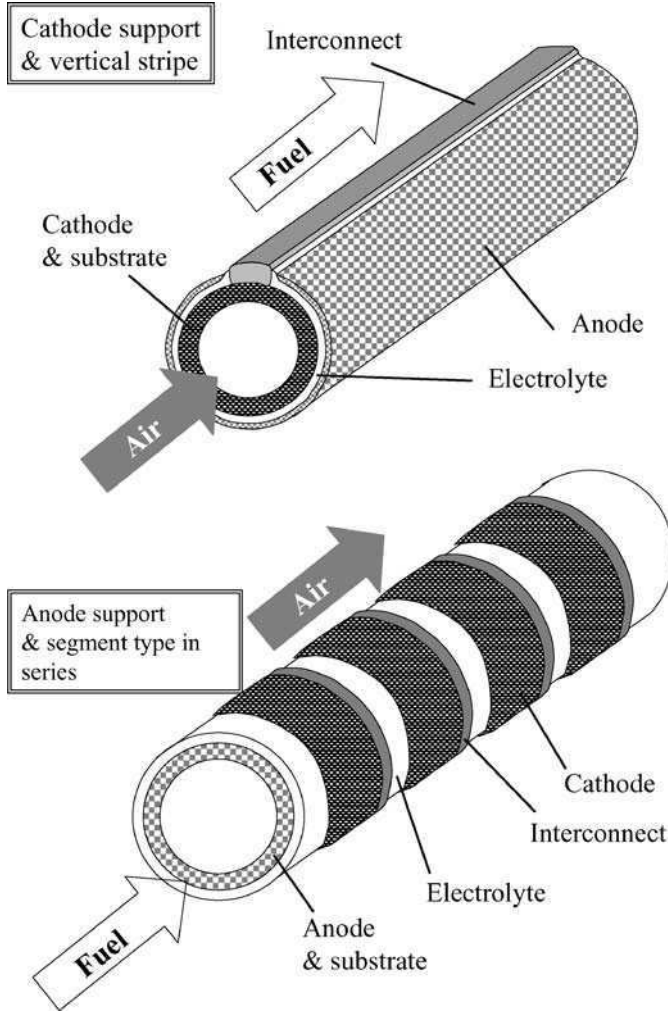


Fig. 3a. Schematic view of SOFC cell design: tubular type.

a long current path in the cell, which cause a large Ohmic resistance. In the planar SOFC design (fig. 3b), the current path is perpendicular to cell components, which reduces the Ohmic resistance. However, side sealing is necessary to obtain sufficient gas tightness. The gas leak causes fuel combustion without generating electricity, which results in an efficiency loss and undesirable inhomogeneous heat generation in the cells. It should be noted that the flat plate of cell components may bend under their own weight in a large stack. Furthermore, the reaction between SOFC components and sealant always causes severe problems. Hence, a high ceramic technology is required to fabricate planar SOFC stacks, which has been realized by

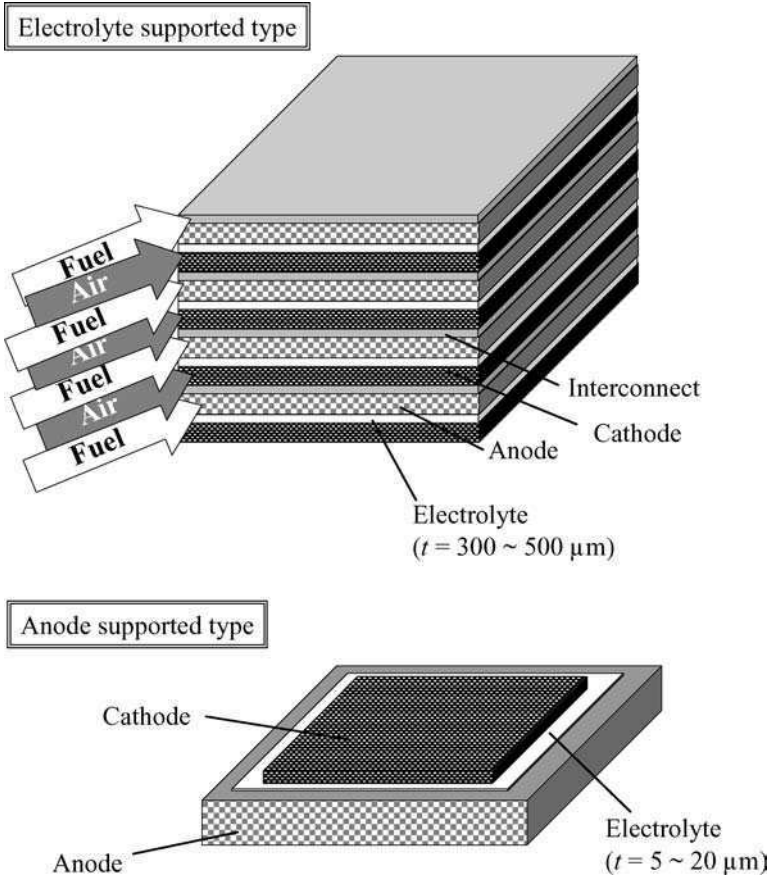


Fig. 3b. Schematic view of SOFC cell design: planar type.

the collaboration of Chubu Electric Power Company and Mitsubishi Heavy Industry, Kobe as the MOLB (mono block layer built) type SOFC (Nakanishi et al., 2003). These SOFCs are called conventional type SOFCs, which operate at 900 to 1000 °C.

An anode supported type SOFC was recently proposed as a design which can operate at lower temperatures <900 °C. An extremely high power density, over 1 W/cm², was reported for a single cell by Visco et al. (1999) at Lawrence Berkeley National Laboratory, and University of California in US, and now the stack developments are promoted by Pacific Northwest National Laboratory (PNNL) and Delphi Co. for auxiliary power unit in heavy duty mobiles (Mukerjee et al., 2003). In an anode supported SOFC, a thin, dense electrolyte film (thickness ~10 μm) is prepared on a porous composite substrate of nickel metal and yttria stabilized zirconia (YSZ) as the anode, and the porous cathode is attached to the dense electrolyte. The thin electrolyte and planar cell stack decreases the Ohmic loss, and results in a high power

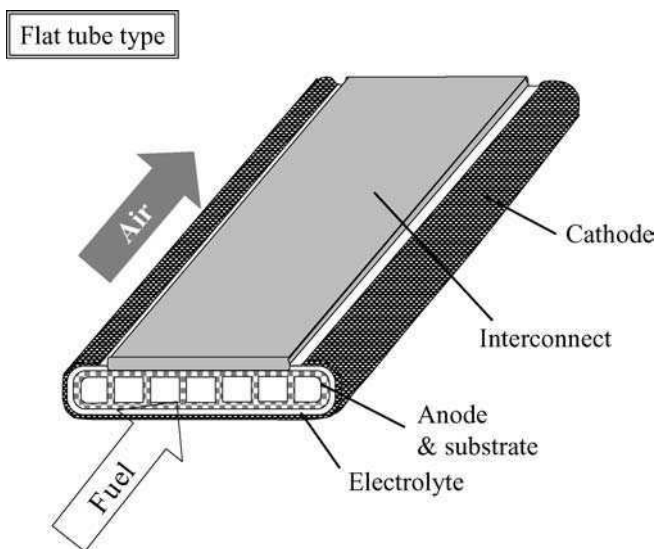


Fig. 3c. Schematic view of SOFC cell design: flat tube type.

density. It has been suggested that the operation temperature of the anode supported SOFCs can be lowered to 700 °C, which make it possible to use ferritic steels as interconnects for cost reduction.

The gas sealing at the side of anode substrate is a serious problems in the anode supported type SOFCs as well as in the conventional planar type SOFCs. The lower operation temperature makes it difficult to select an appropriate sealing agent. Moreover, a large oxide ion flux through the thin electrolyte may cause a rise of oxygen partial pressure in the anode side. The degradation and dimensional instability on start-up and shutdown of the anode supported type cell stacks due to the oxidation of the nickel component in the anode substrate.

As you can suppose, the most important factor required in a SOFC material is the durability and mechanical strength to withstand a large temperature and oxygen potential change because of the fast start-up and shut-down. The high oxide ionic conductivity is also important factor, however, it can not be the first priority. Ytria stabilized zirconia (YSZ) is a remarkable material concerning durability and mechanical properties, and its processing technology to fabricate thin dense films etc. is well established. In the anode-supported type SOFC, a thin film of YSZ is utilized to reduce the Ohmic loss of the electrolyte which makes it possible to operate at lower temperatures.

An alternative approach to reduce the operating temperature is to use new electrolyte materials such as scandium doped zirconia (ScSZ), and rare earth doped ceria (RDC) which have the fluorite type structure, or lanthanum gallate based oxides such as $(La,Sr)(Ga,Mg)O_3$ (LSGM) with perovskite structure, all of which have higher ionic conductivities than YSZ. An 1 kW class SOFC stack with $(La,Sr)(Ga,Mg,Co)O_3$ electrolyte was demonstrated by the collaboration of Mitsubishi Materials Corp. and The Kansai Electric Power Co., Inc. in 2001,

which was the first report that proved the power generation by SOFC with an electrolyte other than YSZ (Yamada et al., 2003). In 2003, another 1 kW SOFC stack with the ScSZ electrolyte was demonstrated by the collaboration of Toho Gas Co. Ltd./Sumitomo Precision Products Co. Ltd./Nippon Shokubai Co. Ltd.

The flat tube design (fig. 3c) was proposed to improve the sealing problems in the anode supported planar SOFCs without losing its high performance. The 1 kW SOFC stack of flat-type design was recently demonstrated by Kyocera Co. Japan in 2004.

On the other hand, there are few reports about SOFC stacks, which employ rare earth doped ceria electrolytes, although a high power density has been reported for single cell test (Steele, 2000; Bance et al., 2004). The rare earth doped ceria exhibits isothermal expansion in a reducing atmosphere due to the reduction of cerium ion from tetravalent (Ce^{4+}) to trivalent state (Ce^{3+}) accompanying the formation of oxygen vacancies, which results in the warping or destruction of the electrolyte plate. The formation of trivalent cerium ion also causes a decrease of oxide ion transport number, which reduces the efficiency of the cell.

The proton conducting oxides such as $\text{Ba}(\text{Ce},\text{M})\text{O}_{3-\delta}$ were investigated by some researchers as alternative electrolyte materials, however these materials have some problems in chemical stability in humid or CO_2 containing atmospheres.

Incidentally, the high potentials of new electrolyte materials such as ScSZ (Yamamoto et al., 1989), LSGM (Ishihara et al., 1994), $\text{Ba}(\text{Ce},\text{M})\text{O}_{3-\delta}$ (Iwahara et al., 1981) were first pointed out by Japanese researchers, which indicates that the Japanese research activity concerning solid state ionics is at a high level.

2.2. Anodes

Ni-YSZ cermet (a ceramic and metal composite), which has a high catalytic activity, is the most popular anode material. The improvement of Ni-YSZ anode was tried by adding gadolinium doped ceria ($\text{Ce}_{1-x}\text{Gd}_x\text{O}_{2-\delta}$) (Joeger and Gauckler, 2001) or by adopting a $\text{NiCe}_{1-x}\text{Gd}_x\text{O}_{2-\delta}$ cermet (Marina et al., 1999). A decrease of the anode overpotential was observed in both cases. Originally, the combination of nickel and ceria was often employed as a catalyst for methane reforming or combustion (Wang et al., 2001). Since internal reforming power generation is popular in SOFCs in which methane or hydrocarbons are generally fed to the cell with an excess amount of steam, both reforming and power generation occur simultaneously on the anode, thus the application of ceria-based materials for anode is reasonable. The internal reforming & power generation is a simple system. The heat required for reforming is supplied by Joule heat during the power generation, which results in a high thermal efficiency. However, steam/carbon ratio is set around two or three to avoid undesirable carbon deposition; hence steam control technology is a most important part in SOFC development. Reducing the amount of steam is being intensively investigated as an advanced development of SOFC. This would result in the highest efficiency if the hydrocarbon fuel is oxidized by oxygen flux through the electrolyte, however, the carbon deposition by thermal decomposition of hydrocarbons is observed in the actual operation, which degrades nickel. To reduce the carbon deposition, a thin film electrolyte with higher ionic conductive material, or a highly catalytic active anode have been investigated. Ukai et al. reported that a stable operation with

97% CH₄ + 3% H₂O over 200 hours attained in a single cell by using the ScSZ electrolyte and the Ni-ScSZ anode (Ukai et al., 2001). Gorte et al. reported a carbon resistive anode material (Cu-CeO₂-YSZ) for direct oxidation power generation of hydrocarbon fuels (Gorte et al., 2002).

When ceria oxides are used in anode materials in combination with zirconia-based electrolytes, the calcination temperatures should be set as low as possible to prevent the formation of ceria-zirconia solid solutions which have a lower oxide ion conductivity. The detailed properties of those solid solutions are discussed in section 3.7 concerning the chemical stability of SOFC materials.

In the anode supported SOFCs, the nickel component in Ni-YSZ anode is degraded by oxidation because of frequent start-up and shut-down operations due to the incompleteness of gas sealing. To improve the redox stability, new types of anode materials have been reported, such as La_{1-x}Sr_xCr_{1-y}RuO_{3-δ} (Sauvet and Fouletier, 2002) or (La,Sr)(Ti,Ce)O₃ (Marina and Pedersen, 2002), however, their catalytic activity is not sufficient. The anode atmosphere in SOFC is strongly reducing at high temperature, and there are only a few oxides that can stably exist under these conditions. Hence the control of the catalytic activity of complex oxides is extremely complicated, and more investigations are needed.

2.3. Cathodes

The cathode reaction in SOFC includes the dissolution and reduction of the oxygen molecule, and the reaction is restricted at the triple phase boundary of the gaseous oxygen molecule/oxygen vacancy in electrolyte/electron from electrode. Hence, the cathode material has both high electrical conductivity and catalytic activity for oxygen reduction. The most popular cathode material is an alkaline earth doped lanthanum manganite, (La, Ca)MnO₃ or (La, Sr)MnO₃ which have high chemical stability in oxidizing atmosphere at high temperatures. Lanthanum manganites have high electronic (hole) conductivity, and the transport number of the electron hole is quite high. However, the optimization of electrode/electrolyte interface is always a key issue to determine the cell performance.

As shown in the electrolyte section 2.1, the operation temperature of SOFC may be lowered from 1000 °C to 600–700 °C. With decreasing temperature, the increase of reaction resistance due to the reduction of the electrochemical reaction rate is more significant than that of Ohmic resistance, and the reaction resistance at the cathode tends to be larger than at the anode. Hence, the improvement of catalytic activity for oxygen reduction reaction is more important for cathode materials. In connection with the improvement of electrolyte materials, the development of highly catalytic active cathode materials is focused on oxide materials, such as lanthanum cobaltite based oxides. Strontium doped lanthanum cobaltite, (La, Sr)CoO₃ is a classic material which has both high electronic conductivity and catalytic activity. However, it can not be used as the cathode in conventional SOFCs operating at 1000 °C, because it reacts with YSZ electrolyte forming La₂Zr₂O₇ layer at the interface, which results in an increase of the overpotential. Lowering the operation temperature may suppress the formation of La₂Zr₂O₇ and make it possible use cobaltite based materials as the cathodes. Actually in the SOFCs which operate at 600–700 °C, (Sm, Sr)CoO₃ (Ishihara et al., 1997), (Ba, La)CoO₃

(Ishihara et al., 2002), (La, Sr)(Fe, Co)O₃ (Hartley et al., 2000) etc. are used as cathode materials. Some rare-earth cobaltite materials have a significant amount of oxygen vacancies, and exhibit mixed conduction of an electron (or a hole) and the oxide ion, which can expand the reaction area of the cathode reaction (which requires the triple interface of gaseous oxygen molecule/oxygen vacancy/electron) and reduce the reaction overpotential.

2.4. Interconnects

Interconnect material holds a unique position in fuel cell components. It does not contribute to power generation, however, it connects SOFC single cells in series to obtain high voltage and power. In solid oxide fuel cells (SOFC), the size of single cell is rather small compared to those of other type of fuel cells because the brittleness of ceramic component makes it difficult to fabricate larger size cells. Hence the importance of material design for SOFC interconnect is much larger than for other types of fuel cells. The interconnects are exposed in a large gradient of the oxygen potential ($p(\text{O}_2) = 21.3 \text{ kPa}$ on the air side, and 10^{-13} Pa on the fuel side at 1000°C) at high temperatures. In such severe conditions, the interconnect materials should retain sufficient electronic conductivity and mechanical strength, and have a high chemical compatibility with other cell components such as electrodes or sealing materials. Moreover, the thermal expansion matching with electrolyte materials is also required. It should be noted that alloys can not be adopted for SOFC interconnects because all metal components except precious metals will be oxidized. A large number of publications have been devoted to interconnect materials, however, no consensus has been reached on which material is the best for SOFC interconnects. This is in striking contrast to the situation for SOFC electrolyte, in which yttria-substituted zirconia has both good (ionic) conductivity, remarkable chemical stability and mechanical strength. Substituted lanthanum chromites presently are still the best candidate materials for interconnects of high temperature SOFCs which work at $T \sim 1000^\circ\text{C}$, unless a complete new and superior material is found as a major breakthrough. The lanthanum chromite based interconnects are already utilized in the tubular SOFC stacks with several hundred kW class stacks in Siemens Westinghouse Corporation in USA, several ten kW class stacks in TOTO Ltd., Japan; and in the planar SOFC stacks in Mitsubishi Heavy Industry Co. in Japan. Lanthanum chromite (LaCrO₃) is one of the most stable perovskite-type oxides having a melting point above 2600 K. A high hole conductivity is obtained by the substitution of alkaline earth metals such as strontium, calcium, and magnesium. The substitution of alkaline earth metal causes the oxidation of chromium ion from the Cr³⁺ to the Cr⁴⁺ state, and the tetravalent chromium ion is the main carrier of hole conduction. However, the tetravalent chromium ion is not stable in the reducing atmosphere, and it will be reduced to the trivalent chromium ion (Cr³⁺) accompanying the formation of oxygen vacancies. The reduction of tetravalent chromium ion results in a decrease of the hole conductivity, and the formation of oxygen vacancies results in the generation of the isothermal expansion and oxide ion conduction which may cause a serious problems in cell operation. The details of these phenomena are explained in the later sections in this paper.

In tubular type SOFC, the interconnects cover a part of the electrode substrate as thin films with thickness of several ten micrometers. Sakai et al. have found that calcium substituted

lanthanum chromites have good sinterability (Sakai et al. 1990a, 1990c, 1993a), and similar compositions have been adopted for interconnects in some tubular SOFCs. The isothermal expansion of calcium substituted lanthanum chromites is quite large, and it may reach about 0.7%. Such an expansion causes the bending of the interconnect plate and mechanical stresses at the interfaces between the interconnects and other cell components. However, it is thought that the thin, round-shape of interconnects may alleviate the mechanical stress in the tubular SOFC stacks.

The isothermal expansion can be suppressed by the substitution of a small amount of strontium, and the transition metals such as Co, Ni, V, Mn, Ti etc. These compositions are generally used for planar type SOFC stacks, in which interconnects should be dense flat plates.

The alternative oxide interconnects have been proposed for the 10 kW class tubular SOFC stacks by Mitsubishi Heavy Industry/Electric Power Development Co., Japan (Konishi et al., 2002). The material is based on strontium titanates with the substitution of alkaline earths and rare earths, $(M, M')TiO_3$ ($M = Ca, Sr, Ba$) ($M' = La, Sm, Pr, Gd, Nd, Y, Er, etc.$) (Miyachi et al., 1999; Nishi et al., 1999).

On the other hand, the alloy interconnects have been used for the developers of SOFCs which operate at lower temperatures. Chromium based alloys proposed by Plansee Co. can be used at the temperatures lower than 900 °C. The high chemical stability is maintained by the dispersion of Y_2O_3 particles in Cr95%–Fe5% by a mechanical alloying process (Batawi et al., 1999).

To reduce the fabrication costs, the possibility of using ferritic steels for SOFC interconnects operated at $T = 700\text{--}800$ °C has recently been considered. The formation of an oxide scale is inevitable for alloy interconnects at both the air and the fuel sides during SOFC operation. Even in the reducing atmosphere at fuel side, the surface of alloy is oxidized due to the presence of water vapor. Hence, the durability of these alloy interconnects depends on the electrical conductivity of the oxide scales formed during the operation time.

The vaporization of chromium components from alloy is also a serious problem. It is widely known that the chromium-containing vapor is transported to the triple phase boundary at cathode side and precipitates as Cr_2O_3 , which seriously damages the cathode activity (Taniguchi et al., 1995). Such chromium poisoning effect is significant for the case of lanthanum manganite cathode/YSZ electrolyte, in which the active area for cathode reaction is restricted in the vicinity of triple phase boundary. Matsuzaki et al. reported that the chromium poisoning can be suppressed if they adopted the combination of lanthanum cobaltite cathode/rare earth doped ceria electrolyte, in which the active area extends around the triple phase boundary (Matsuzaki and Yasuda, 2001).

3. Key issues in SOFC materials design

As discussed in the section 2, many materials have been considered as candidates for SOFC components. This is because the operation condition of SOFC is very severe so that many factors need to be considered for choosing various materials. The major requirements for SOFC materials are follows:

- (a) Low cost in preparation.
- (b) Processing simplicity (good sinterability, thin film fabrication etc.).
- (c) High oxide ion conductivity, and high ionic transport number (for electrolyte).
- (d) High electron/hole conductivity (for anode, cathode and interconnect).
- (e) High mechanical strength (for electrolyte and interconnect).
- (f) Thermal expansion matching.
- (g) Good chemical stability at high temperatures (for all components).

In this section, we discuss each of issues.

3.1. *Materials and preparation cost*

The SOFC is expected to be used as a distributed power generation (DG) device in an energy network, so that the fabrication and power generation costs should be competitive with those of conventional power generation devices. The cost-reduction in the cell and stack fabrication is the most important target for realization of SOFCs in DG market.

In PEFCs or PAFCs, the most of important cost problem is using platinum as electrodes. The SOFC should have an advantage because it operates at high temperatures at which no precious metals are required for activating the electrochemical reactions. Nevertheless, Itoh et al. suggested that the materials preparation cost shares a large part (~60%) of the total cost of the SOFC stack (Itoh et al., 1994). The price of rare earths are relatively higher than other components, which will have an effect on the materials cost. In zirconia based electrolytes, the amount of rare earths is around 20 mol% in $\text{RO}_{1.5}$, which is not a significant problem. The application of thin-film electrolytes will also decrease the rare earth amount. However, for other types of electrolytes such as ceria or lanthanum gallates, the amount of rare earth reaches over 50 mol%. Moreover, in lanthanum gallate based electrolytes, the high cost of gallium makes the matter worse. The rare earth with low purity such as lanthanum concentrate have been tried instead of pure rare earths to reduce the cost, however it resulted in the significant degradation of chemical stability or oxide ion conductivity, which was not acceptable. Hence the preferred way to reduce the cost is to reduce the total amount of rare earth by using thin films.

Similar problems are also encountered for cathodes and interconnects which are complex oxides of rare earths and transition metals. For the cathode supported tubular type SOFCs, the cost of lanthanum manganite cathode is very important because it is a large fraction of the total cell capacity.

3.2. *Processing simplicity*

Needless to say, the all oxide materials in SOFC are initially synthesized as powders by mixing of constituent metals or metal oxides and subsequently calcination. The difficulty of synthesis depends on the number of elements, the activities of starting oxides and the chemical stability of products. The dense polycrystalline body required for electrolyte or interconnect are prepared by sintering the powder compacts. There are many complicated factors which control the sinterability of the powders.

Most of fluorite-type oxide ion conductors, such as YSZ, ScSZ, or rare earth doped ceria (RDC) contain only two metal components, which is profitable for preparation of homogeneous powders at relatively low temperatures. Actually, fine, homogenous powders are available in the commercial market. The dense polycrystalline bodies of YSZ and ScSZ can be easily obtained by the sintering at $T = 1400\text{--}1500\text{ }^{\circ}\text{C}$ in air. The conventional RDC powder requires higher temperatures above $1500\text{ }^{\circ}\text{C}$, however, the using of nano-sized powder can lower the sintering temperature. The shrinkage behavior of the powder compact is important in the cell fabrication, and it can be controlled in some degree by the particle size distribution, or by addition of a slight amount of sintering aids. The film fabrication is also easy for YSZ or ScSZ, by casting a slurry of ceramic powders and organic solvents onto a substrate and sintering in air. This is a much more inexpensive method than dry processes such as plasma spraying or chemical vapor deposition technique. It is also possible to prepare these thin films on porous electrode substrates (lanthanum manganite or NiO-YSZ cermets) by a co-sintering process, which effectively reduces the fabrication cost.

On the other hand, perovskite type oxide ion conductors, such as lanthanum gallate based oxides, consist of four or more metal elements, which makes the synthesis more difficult than for zirconia or ceria based materials. The most popular compositions of lanthanum gallate electrolytes are: $(\text{La}, \text{Sr})(\text{Ga}, \text{Mg})\text{O}_{3-\delta}$ (LSGM) and $(\text{La}, \text{Sr})(\text{Ga}, \text{Mg}, \text{Co})\text{O}_{3-\delta}$ (LSGMC); and their phase relations are somewhat complicated. The perovskite phase is the main phase if $(\text{La} + \text{Sr})$ and $(\text{Ga} + \text{Mg} + \text{Co})$ ratio is ideally unity. However, the formation of a variety of secondary phases is caused by a slight deviations from the stoichiometry. In the La (or Sr) excess condition, LaSrGaO_4 often precipitates as a secondary phase, and $\text{SrLaGa}_3\text{O}_7$ or Ga_2O_3 precipitates in Ga excess condition. Preparation temperature also affects on the phase relations. Even though the single phase of perovskite LSGM was prepared by the sintering at 1773 K , these secondary phases can be precipitated in the subsequent annealing at lower temperatures, i.e., 1273 K (Stevenson et al., 1998). Hence, the thin film fabrication of LSGM is more difficult than YSZ or RDC, although the result of many trials have been reported (Matsuda et al., 2003).

In lanthanum chromite interconnects, the improvement of sinterability was one of the big issues. The alkaline-earth doped lanthanum chromites usually have poor sinterability in air because of the high vapor pressure of the chromium component (Anderson, 1978; Group and Anderson, 1976). The main species of the vaporized phase consists of hexavalent chromium, CrO_3 (g) which exists in oxidizing atmospheres at high temperatures. The mass transport is dominated by vaporization and condensation of chromium components via gaseous phases, which does not result any grain growth or particle joining. In order to lower the vapor pressure of the chromium component and obtain dense polycrystalline bodies, the sintering atmosphere was controlled by a reducing atmosphere (Group and Anderson, 1976), or by using Cr_2O_3 /lanthanum chromite/ Cr_2O_3 sandwiches (Tai and Lessing, 1991). An alternative approach for lowering the CrO_3 vapor pressure is by precipitating secondary phases, which form stable compounds with chromium. It is well known that a small amount of CaO precipitate reacts with CrO_3 , and drastically improves the densification of $(\text{La}, \text{Ca})\text{CrO}_3$ in air (Sakai et al., 1990a, 1990c; Yokokawa et al., 1991a, 1991b). The CaO precipitation is possible if the molar ratio of $(\text{La} + \text{Ca})/\text{Cr}$ is slightly higher than unity, and calcium content is

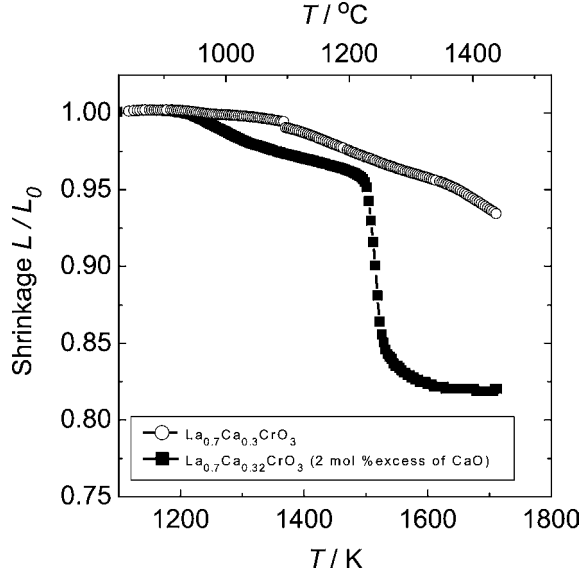


Fig. 4. The sintering shrinkage of powder compacts of calcium substituted lanthanum chromites.

more than 15 mol% of lanthanum. The secondary phase exists as a melt of calcium oxychromate, $\text{Ca}_a(\text{CrO}_4)_b$, in air, and enhances the densification by a liquid sintering mechanism, at $T > 1050^\circ\text{C}$ (Sakai et al., 1993a, 1993b; Mori et al., 1991). The liquid phase formation results in good sinterability even at $T = 1300^\circ\text{C}$. The shrinkage curve of $\text{La}_{0.7}\text{Ca}_{0.3}\text{CrO}_3$ with 2 mol% CaO excess is shown in fig. 4. The shrinkage occurs in two stages. In the first stage at 1000 to 1100 °C is due to the particle rearrangements, and in the second stage a drastic shrinkage at 1250 °C is due to rapid grain growth and the elimination of pores with assistance of the liquid calcium chromate $\text{Ca}_a(\text{CrO}_4)_b$.

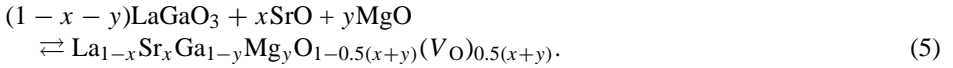
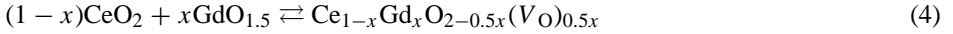
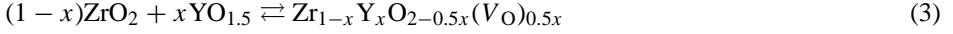
Liquid phase sintering was also observed for $(\text{La}, \text{Ca})(\text{Cr}, \text{Co})\text{O}_3$ (Koc and Anderson, 1990, 1992a, 1992b) and $(\text{La}, \text{Ca})(\text{Cr}, \text{Ni})\text{O}_3$ (Christie et al., 1994). Hence the liquid phase formation seems to be a common phenomenon for calcium substitute lanthanum chromites. However, it also has an affect on the chemical stability of the sintered polycrystals, which will be discussed in the section 3.5.

For strontium-doped lanthanum chromites, the precipitation of SrO is not possible, because strontium ions are more stable in the perovskite structure than the lanthanum ions. Lanthanum oxide, La_2O_3 , is often precipitated instead of SrO. This causes the disintegration of sintered specimens at ambient temperatures by the volume change associated with the formation of lanthanum hydroxide, $\text{La}(\text{OH})_3$, due to the reaction of La_2O_3 with the water vapor in the air (Meadowcroft, 1969; Sakai et al., 1990a). The substitution of transition metals such as zinc (Hayashi et al., 1988), cobalt (Zhou et al., 1996), or vanadium (Larsen et al., 1997) have been used to improve the sintering of strontium substituted lanthanum chromite. The substitution of strontium and transition metals is often utilized for interconnects of the planar type

SOFCs. However, a sintering temperature above 1500 °C is required. Thus these lanthanum chromites can not be co-sintered with electrodes, because such a high temperature treatment may degrade the electrode activity.

3.3. Ionic conductivity and transport number of electrolytes

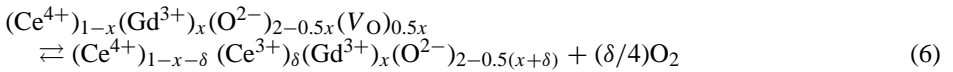
Most of the electrolytes used in the SOFC stacks are oxide ion conductors. Oxygen vacancies are formed by the substitution of rare earths or alkaline earths, and oxide ions in the lattice diffuse via vacancies.



The oxygen vacancy (V_O) concentration increases with the amount of substituted elements (x or y). However, the oxide ion conductivities of substituted zirconia and ceria exhibit a maximum in a certain value of x , i.e., ca. 8 mol% Y_2O_3 in YSZ, 10 mol% R_2O_3 in RDC. It is thought that the mobility of the oxide ion decreases by the interaction of oxygen vacancies and cations in heavily substituted compositions. This phenomenon is typical for fluorite-type oxide ion conductors.

As shown in [fig. 2](#), the oxide ion conductivity ($\sigma_{\text{O}^{2-}}$) of YSZ is around 0.13 S cm^{-1} at 1000 °C, and the conductivity of alternative electrolytes such as ScSZ, LSGM or GDC are significantly higher, i.e., 0.3 S cm^{-1} , at the same temperature. The activation energy of GDC is lower than those of YSZ or LSGM, therefore GDC exhibits a higher conductivity than the other electrolytes at lower temperatures.

However, the oxide ion transport number also needs to be evaluated as well as the conductivity when the materials are considered as SOFC electrolytes. As already pointed out in the [section 2.1](#), the reduction of cerium ion in RDC occurs in a reducing atmosphere, for example:



As a result, trivalent cerium ion (Ce^{3+}) can act as the electron carrier in RDC in reducing atmosphere which decreases the transport number of oxide ion. Hence, it is important to determine the electron/hole conductivity as well as total conductivity. The electron and hole conductivity can be determined separately from oxide ion conductivity by using the ion blocking method with a modified Hebb–Wagner’s cell. The oxygen partial pressure dependences of the ionic and the electron/hole conductivities are compared for YSZ ([Park and Blumental, 1989](#)), GDC ([Xiong et al., 2004](#)), and LSGM ([Yamaji et al., 1997](#); [Kim and Yoo, 2001](#)) and as a function of the oxygen partial pressure in [fig. 5](#) from the data at 1273 K. In the SOFC operating condition ($p(\text{O}_2) = 10^4$ to 10^{-13} Pa at 1273 K), the transport number of oxide ion is greater than 99% for YSZ, above 98% for LSGM, however, it is less than 50% for GDC at $p(\text{O}_2) = 10^{-13}$ Pa.

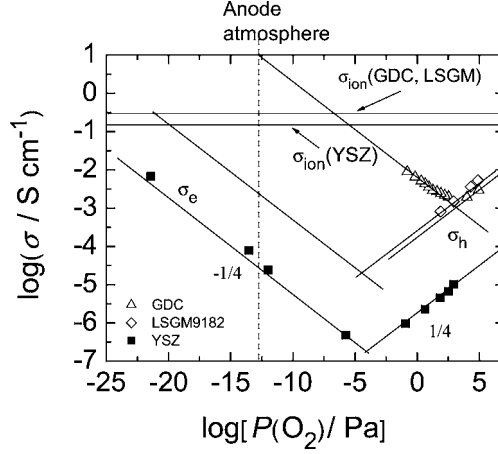


Fig. 5. The electronic and hole conductivity of $Zr_{0.85}Y_{0.15}O_{1.925}$ (Park and Blumental, 1989), $La_{0.9}Sr_{0.1}Ga_{0.8}Mg_{0.2}O_{2.85}$ (LSGM9182), (Yamaji et al., 1997; Kim and Yoo, 2001) and $Ce_{0.8}Gd_{0.2}O_{1.9}$ (GDC), (Xiong et al., 2004) measured by the ion blocking method at 1273 K.

Hence it can be concluded that the RDC is a mixed conductor of electrons and the oxide ions. If both electrons and oxide ions diffuse in the solids, it results in the oxygen permeation without power generation, which lower the efficiency of the electrolyte. The efficiency of the electrolytes can be evaluated as follows:

$$\varepsilon_{\text{electrolyte}} = \frac{J_{\text{ext}} \times \Delta E_{\text{electrolyte}}}{J_{O^{2-}, \text{ electrolyte}} \times \frac{RT}{4F} \ln \frac{p_{O_2}^I}{p_{O_2}^{II}}} \quad (7)$$

Choudhury and Pedeson (1970) estimated $\Delta E_{\text{electrolyte}}$, $J_{O^{2-}, \text{ electrolyte}}$, J_{ext} as follows:

$$\Delta E_{\text{electrolyte}} = -\frac{RT}{2F} \int_{p_{O_2}^I}^{p_{O_2}^{II}} \frac{\sigma_{O^{2-}}}{r\sigma_e - \sigma_{O^{2-}}} d \ln p_{O_2}, \quad (8)$$

$$J_{O^{2-}, \text{ electrolyte}} = -\frac{rRT}{2FL} \int_{p_{O_2}^I}^{p_{O_2}^{II}} \frac{\sigma_e \sigma_{O^{2-}}}{r\sigma_e - \sigma_{O^{2-}}} d \ln p_{O_2}, \quad (9)$$

$$J_{\text{ext}} = \left(1 + \frac{1}{r}\right) J_{O^{2-}} \quad (10)$$

Fig. 6 shows the calculated efficiency of YSZ, LSGM, and GDC films with thickness of $50 \mu\text{m}$ as a function of temperature under a current density of $I = 300 \text{ mA/cm}^2$. The efficiency

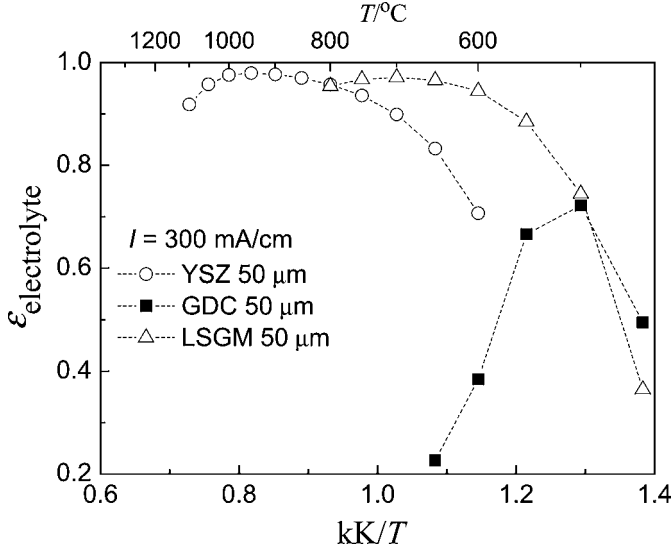


Fig. 6. The temperature dependence of energy conversion factor (ε) of $\text{Zr}_{0.85}\text{Y}_{0.15}\text{O}_{1.925}$ (YSZ), $\text{La}_{0.9}\text{Sr}_{0.1}\text{Ga}_{0.8}\text{Mg}_{0.2}\text{O}_{2.85}$ (LSGM9182) and $\text{Ce}_{0.8}\text{Gd}_{0.2}\text{O}_{1.9}$ (GDC) films with a thickness of $50\ \mu\text{m}$ at current density $300\ \text{mA cm}^{-2}$.

of each electrolyte has a maximum at a certain temperature. In temperature regions higher than the maximum, the efficiency decreases because of the increase of oxygen permeation without generating power. In temperature regions lower than the maximum, the efficiency also decreases due the decrease of oxide ion conductivity. The maximum efficiency reaches $\varepsilon = 0.98$ at $T = 950\ ^\circ\text{C}$ for YSZ. The maximum efficiency of LSGM reaches $\varepsilon = 0.97$ at $T = 700\ ^\circ\text{C}$, which indicates this electrolyte is suitable for the operation at lower temperatures than the case of YSZ. In contrast with those electrolytes, the maximum efficiency of GDC does not exceed $\varepsilon = 0.7$. Such a low efficiency is due to the mixed conduction of electron and oxide ion in fuel atmosphere as can be expected from the data presented in fig. 6.

3.4. Electron/hole conductivity of the anode, cathode and interconnect

At the interface of cathode/electrolyte, the adsorbed gaseous oxygen molecules (O_2) are dissociated and reduced to oxide ion (O^{2-}) and diffuse into the electrolyte: For reduction of oxygen molecules, electrons are supplied by the cathodes. Hence, the cathode material in principle should be a good electron (or hole) conductor. Since metal components can not be used in the SOFC cathode atmosphere, the perovskite oxides such as $(\text{La},\text{Sr})\text{MnO}_3$ or $(\text{La},\text{Sr})\text{CoO}_3$ are generally used. The electrical conductivity (σ) of $\text{La}_{0.8}\text{Sr}_{0.2}\text{MnO}_3$ is $141\ \text{S cm}^{-1}$ at $1273\ \text{K}$ (Kuo et al., 1990). $(\text{La},\text{Sr})\text{CoO}_3$ exhibits much a higher electrical conductivity, for example, $\sigma = 1338\ \text{S cm}^{-1}$ for $\text{La}_{0.5}\text{Sr}_{0.5}\text{CoO}_3$ at $T = 1273\ \text{K}$ (Petrov et al., 1995), however, it can not be used as the cathode material at this temperature because of its high reactivity with

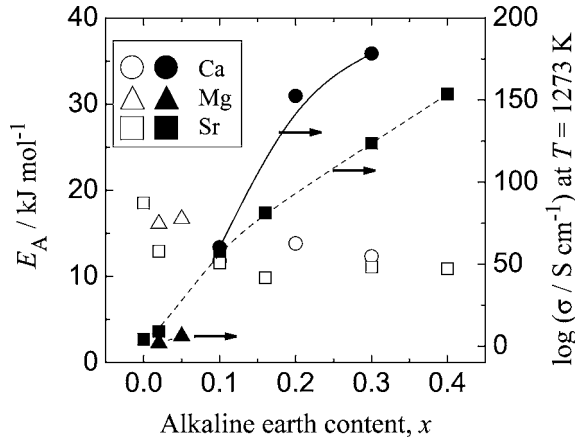
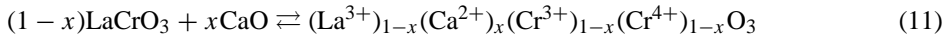


Fig. 7. The electrical conductivity (closed symbols) at $T = 1273$ K and activation energy (open symbols) of alkaline earth substituted lanthanum chromites: $\text{LaCr}_{1-x}\text{Mg}_x\text{O}_3$ (Anderson and Sparlin, 1984); $\text{La}_{1-x}\text{Sr}_x\text{CrO}_3$ (Karim and Aldred, 1979); $\text{La}_{1-x}\text{Ca}_x\text{CrO}_3$ (Yasuda and Hikita, 1993).

YSZ forming $\text{La}_2\text{Zr}_2\text{O}_7$. The electrical conductivity of these perovskite type oxides exhibit a metallic temperature dependence, which indicates that the electron is delocalized around transition metal ions.

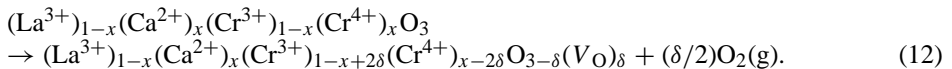
The SOFC anodes are the porous composites of nickel metal and electrolyte materials. The high electrical conductivity of the anode is maintained by the metal component, so that its volume fraction should be set above 50%. It is important to keep the anode atmosphere in a reducing condition to prevent the oxidation of nickel.

Concerning the interconnects, alkaline earth substituted lanthanum chromites are electronic hole conductor in an oxidizing atmosphere, and their total conductivity (σ) increases linearly with the alkaline earth content as shown in fig. 7 for $\text{LaCr}_{1-x}\text{Mg}_x\text{O}_3$ (Anderson and Sparlin, 1984), $\text{La}_{1-x}\text{Sr}_x\text{CrO}_3$ (Karim and Aldred, 1979), and $\text{La}_{1-x}\text{Ca}_x\text{CrO}_3$ (Yasuda and Hikita, 1993). This is simply understood because the hole carrier is Cr^{4+} ion which is generated to maintain charge neutrality by the substitution of alkaline earths ion M^{2+} . This reaction can be expressed for calcium substituted lanthanum chromites as:



Although the substituted lanthanum chromites exhibit a semi-conductive temperature dependence, their activation energies are quite low (10–20 kJ mol^{-1}).

However, it should be noted that the conductivities significantly decrease in reducing atmospheres. This is caused by the reduction of Cr^{4+} to Cr^{3+} accompanying the formation of oxygen deficiency (δ). This reaction for calcium substituted lanthanum chromites is given by the following equation:



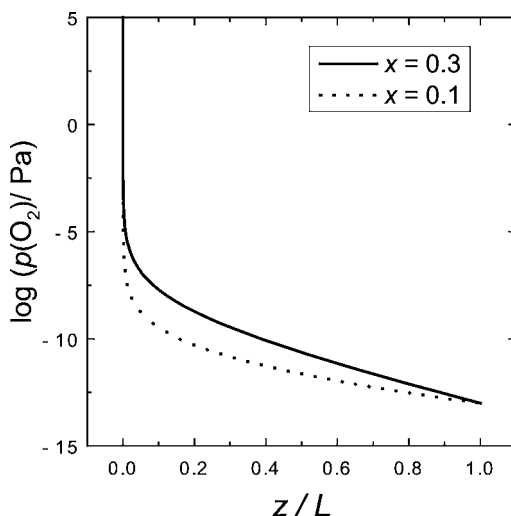


Fig. 8. The calculated oxygen partial pressure at 1273 K in a dense plate of $\text{La}_{1-x}\text{Ca}_x\text{CrO}_{3-\delta}$ ($x = 0.1, 0.3$) with thickness z . The oxygen pressure was fixed at $p(\text{O}_2) = 213 \text{ kPa}$ at $z = 0$ and $p(\text{O}_2) = 10^{-13} \text{ Pa}$ at $z = L$. $D_V = 10^{-9} \text{ m}^2 \text{ s}^{-1}$.

In a strongly reducing atmosphere, it will be reduced to $\text{La}_{1-x}\text{Ca}_x\text{CrO}_{3-0.5x}$, which has a comparable conductivity to that of non-substituted LaCrO_3 , ca. $\sigma = 1 \text{ S cm}^{-1}$ at $T = 1273 \text{ K}$. For the case of $\text{La}_{0.7}\text{Ca}_{0.3}\text{CrO}_{2.85}$, it corresponds to $p(\text{O}_2) = 10^{-18} \text{ Pa}$. Since the oxygen partial pressure $p(\text{O}_2)$ ranges from 10^{-13} to 10^{-11} Pa in the fuel atmosphere in a SOFC operation at $T = 1273 \text{ K}$, the decrease of conductivity should always be taken into account.

Based on the model considered by van Van Hassel et al. (1993), the distribution of oxygen partial pressure, $p(\text{O}_2)$, in a dense plate of $\text{La}_{1-x}\text{Ca}_x\text{CrO}_{3-\delta}$ ($x = 0.1, 0.3$) can be calculated as a function of normalized thickness z/L as shown in fig. 8. The oxygen partial pressure is fixed to 213 kPa at $z/L = 0$ and 10^{-13} Pa at $z/L = 1$. The oxygen potentials in a dense interconnect plate are very low in most parts of the plate, and a steep gradient is observed in the vicinity of the surface exposed to the oxidizing atmosphere ($z/L = 0$). As a result, the oxygen potential in the plate is low for the most part, and a large gradient is observed in the vicinity of the surface facing the oxidizing atmosphere. As the oxygen potential decreases from $x = 0-L$, the content of tetravalent chromium ion (Cr^{4+}) decreased and the content of oxygen vacancy increased, which leads to a decrease of hole conductivity (σ_h) and an increase of oxide ion conductivity (σ_{O_2-}). Fig. 9 shows the hole and oxide ion conductivities of the dense plate of $\text{La}_{1-x}\text{Ca}_x\text{CrO}_{3-\delta}$ ($x = 0.1, 0.3$) under the same condition as for fig. 8. The hole conductivity gradually decreased in the dense plate and this tendency is more significant for the sample with the higher amount of calcium substitution. On the other hand, the oxide ion conductivity steeply increased from 10^{-6} S m^{-1} to 10 S m^{-1} . The increase of oxide ion conductivity should result in the oxygen permeation which occurs even through a completely dense plate. This

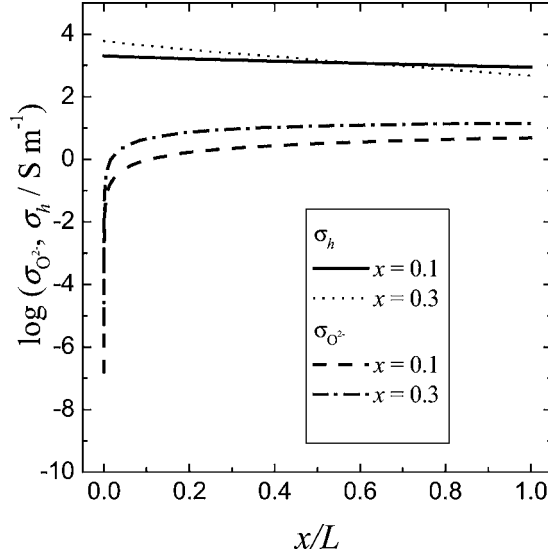


Fig. 9. The hole and oxide ion conductivity of $\text{La}_{1-x}\text{Ca}_x\text{CrO}_{3-\delta}$ ($x = 0.1, 0.3$) as a function of sample thickness z/L , $T = 1273$ K, $p(\text{O}_2) = 213$ kPa at $z = 0$, 10^{-13} Pa at $z = L$.

oxygen permeation through the interconnect plate will cause the fuel oxidation (combustion) without generating electric power, which lowers the cell efficiency.

The flux of oxygen permeation ($J_{\text{O}^{2-}}$) through a dense plate of oxide interconnect with thickness L can be expressed by using the defect model described by van Van Hassel et al. (1993).

$$J_{\text{O}^{2-}} = \frac{1}{4FL} \int_{p_{\text{O}_2}(z=0)}^{p_{\text{O}_2}(z=L)} \frac{\sigma_{\text{O}^{2-}} \cdot \sigma_{\text{h}}}{\sigma_{\text{O}^{2-}} + \sigma_{\text{h}}} d\mu_{\text{O}_2} \quad (13)$$

Since the hole conductivity (σ_{h}) is much larger than oxide ion conductivity ($\sigma_{\text{O}^{2-}}$), eq. (13) can be re-written as follows at a constant temperature:

$$J_{\text{O}^{2-}} = \frac{RT}{4FL} \int_{p_{\text{O}_2}(z=0)}^{p_{\text{O}_2}(z=L)} \sigma_{\text{O}^{2-}} d \ln p(\text{O}_2). \quad (14)$$

The oxide ion conductivity can be calculated from the Nernst–Einstein theory:

$$\sigma_{\text{O}^{2-}} = \frac{4F^2(3-\delta)D_{\text{O}}}{RTv_{\text{m}}} = \frac{4F^2\delta D_{\text{V}}}{RTv_{\text{m}}}. \quad (15)$$

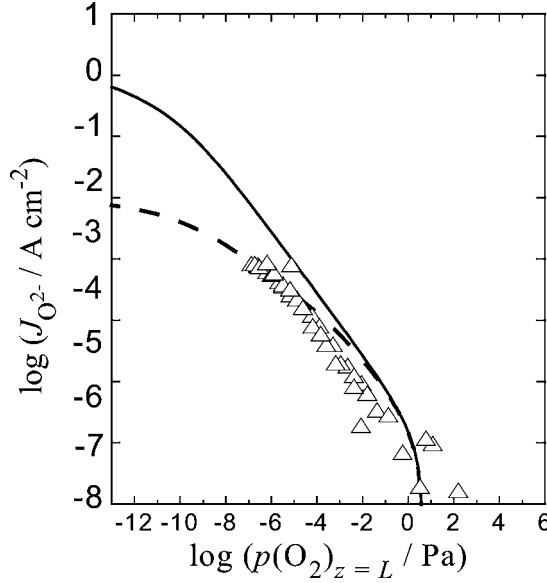


Fig. 10. The oxygen permeation flux ($J_{O_2^-}$) through $\text{La}_{0.9}\text{Ca}_{0.1}\text{CrO}_{3-\delta}$ as a function of oxygen potential at reducing side. Thickness: 1 mm. $T = 1273$ K. Solid line: derived from the diffusion limited mechanism ($D_V = 10^{-9} \text{ m}^2 \text{ s}^{-1}$). Dashed line: derived from the surface reaction limited mechanism ($k = 10^{-12} \text{ m s}^{-1}$). Triangles: experimental data measured by a blocking method.

If we assume that there is no interaction between the defect species and ions, the defect equilibrium in $\text{La}_{1-x}\text{Ca}_x\text{CrO}_{3-\delta}$ can be expressed as follows:

$$K_{\text{ox}} = \frac{(1-x+2\delta)^2\delta}{(3-\delta)(x-2\delta)^2} (p_{\text{O}_2})^{1/2}. \quad (16)$$

The calculated oxygen permeation is shown as a solid line in [fig. 10](#) for $\text{La}_{0.9}\text{Ca}_{0.1}\text{CrO}_3$, and in [fig. 11](#) for $\text{La}_{0.76}\text{Ca}_{0.25}\text{CrO}_{3-\delta}$. The parameters used in the calculation are estimated from experimental results, and are listed in [table 3](#). The calculated oxygen permeation of $\text{La}_{0.75}\text{Ca}_{0.25}\text{CrO}_3$ flux reaches $J_{O_2^-} = 2 \text{ A cm}^{-2}$ for a 1 mm thick plate. Since the current density in SOFC power generation is normally $0.3\text{--}1 \text{ A cm}^{-2}$, the oxygen permeation flux of 2 A cm^{-2} should have canceled out the power generation. However, as a practical matter, the SOFCs with (La, Ca)CrO₃ interconnects do work with a stable power output, which is not consistent with the estimated oxygen permeation flux.

Hence it was important to find a better measurement and evaluation for the oxygen permeation flux through lanthanum chromites. The oxygen permeation flux can also be determined experimentally by a blocking method for $\text{La}_{1-x}\text{Ca}_x\text{CrO}_{3-\delta}$ ([Sakai et al., 1996, 1999](#)). The experimental values are also plotted as symbols in [fig. 10](#) and [fig. 11](#), and they are in good agreement with the calculated values (solid line) except at the low $p(\text{O}_2)$ range. This deviation is thought to be due to the oxygen redox reaction at the surface becoming the rate-determining

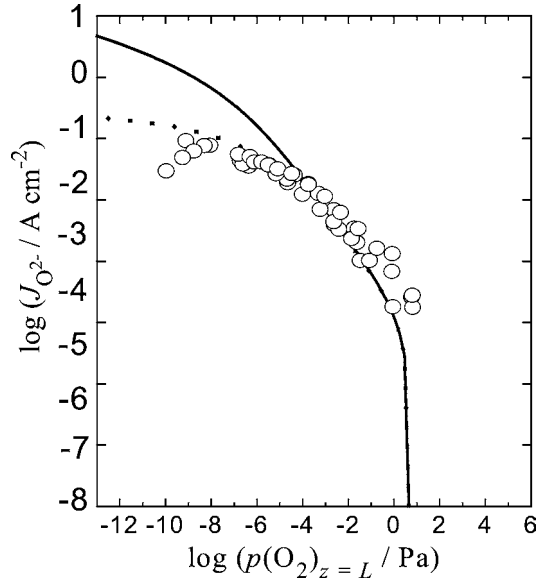


Fig. 11. The oxygen permeation flux ($J_{O^{2-}}$) through $\text{La}_{0.75}\text{Ca}_{0.25}\text{CrO}_{3-\delta}$ as a function of oxygen potential at reducing side. Thickness: 1 mm. $T = 1273$ K. Solid line: derived from the diffusion limited mechanism ($D_V = 10^{-9} \text{ m}^2 \text{ s}^{-1}$). Dashed line: derived from the surface reaction limited mechanism ($k = 10^{-9} \text{ m s}^{-1}$). Circles: experimental data measured by a blocking method.

Table 3

Parameters used in calculation of oxygen permeation and conductivities through dense interconnect plate

Temperature, T	1273 K
Thickness of interconnect plate, L	1 mm
Molar fraction of calcium, x	0.1 and 0.25
Defect equilibrium constant, K_{ox}	$1 \times 10^{-8} \text{ bar}^{0.5}$ (for $x = 0.1$) $9 \times 10^{-8} \text{ bar}^{0.5}$ ($x = 0.25$)
Molar volume of $\text{La}_{1-x}\text{Ca}_x\text{CrO}_{3-\delta}$, v_m	$3.4 \times 10^{-5} \text{ m}^3 \text{ mol}^{-1}$
Oxygen vacancy diffusivity, D_V	$1.7 \times 10^{-9} \text{ m}^2 \text{ s}^{-1}$

step, and this suggests that the permeation flux depends only on the oxygen potential gap between the surface and gaseous phase, not on the sample thickness.

The effect of this surface reaction can be estimated by using the theoretical procedure described by Bouwnmeester et al. (1994). They assumed that the surface reaction is the rate determining step, and that it linearly depends on the oxygen potential gradient in the vicinity of the surface. The oxygen permeation flux at surface ($J_{O^{2-}}^{\text{surf}}$) can be modeled as:

$$J_{O^{2-}}^{\text{surf}} = -4Fj_{O_2} = \frac{1}{4}k_s C_0 \frac{4F \Delta \mu_{O_2}}{RT}. \quad (17)$$

There are several reports about the surface reaction constant (k_s) of $\text{La}_{R1-xR}\text{Ca}_x\text{CrO}_{3-\delta}$. Yasuda and Hikita (1994) determined the chemical diffusion coefficients and surface reaction constants by using the electrical conductivity relaxation. They obtained relatively high reaction constants (k_s) from 10^{-5} to 10^{-6} m s^{-1} in the $p(\text{O}_2)$ range from 10^{-5} to 10^{-12} Pa at 1273 K. On the other hand, the surface reaction rate constants which were determined by $^{18}\text{O}_2$ tracer diffusion exhibit lower values from 10^{-9} m s^{-1} in air to 10^{-8} m s^{-1} in $\text{H}_2\text{-CO}_2$ mixtures (Sakai et al., 2000a). It must be noted that the chemical diffusion coefficient and surface reaction constant are not independently determined in either method. Hence the large discrepancy among the k_s values is related to the large difference in chemical diffusion coefficient between these two experimental methods, which is due to the difference of chemical potential gradient.

The effect of surface reaction on the oxygen permeation flux was examined for $\text{La}_{0.9}\text{Ca}_{0.1}\text{CrO}_{3-\delta}$ and $\text{La}_{0.75}\text{Ca}_{0.25}\text{CrO}_{3-\delta}$, and the results are summarized in fig. 10 and fig. 11 as dashed lines. When k_s is fixed to 10^{-12} m s^{-1} for $\text{La}_{0.9}\text{Ca}_{0.1}\text{CrO}_{3-\delta}$ and 10^{-9} m s^{-1} for $\text{La}_{0.75}\text{Ca}_{0.25}\text{CrO}_{3-\delta}$, the estimated data are in good agreement with experimental data. Hence, if the oxygen permeation is fully surface reaction limited, k_s should have been lower than 10^{-9} m s^{-1} for the whole $p(\text{O}_2)$ range.

Since the permeation flux is controlled by the surface reaction, the extrapolated oxygen permeation flux at a $p(\text{O}_2)$ gradient from 10^4 to 10^{-13} Pa at $T = 1273\text{K}$ is about 0.03 A cm^{-2} for 1 mm thick plate of $\text{La}_{0.75}\text{Ca}_{0.25}\text{CrO}_{3-\delta}$. The efficiency loss by the permeation is less than several per cent even for the general tubular cell design using thin interconnect of calcium substituted lanthanum chromite (Sakai et al., 2004). However, the permeation loss will be significant for new cell designs such as flat tubes having thin interconnects with high surface area.

3.5. Mechanical strength of the electrolyte and interconnect

The mechanical properties of lanthanum chromites are important and are influenced by many factors, such as lattice defects, grain size, second phase at grain boundary or a triple point in polycrystals. Generally, the mechanical strength greatly depends on the sintering temperature with the sample sintered at higher temperature exhibiting better mechanical strengths.

The zirconium oxides partially stabilized by magnesium or yttrium substitution are well known as the materials having an extremely high bending strength, >1500 MPa (Tsukuma and Shimada, 1985). These materials consist of a mixture of the cubic and tetragonal structures, and the stress is relieved by the phase transition of the tetragonal phase to the monoclinic phase. However, the ionic conductivity of those partially stabilized zirconia is not high because of the lower rare earth content.

The three-point bending strength of the 8 mol% Y_2O_3 substituted ZrO_2 as the SOFC electrolyte ranges from 250 MPa (Mori et al., 1994) for the samples prepared by conventional sintering, to 400 MPa for the samples prepared by a spark plasma sintering (SPS) technique (Takeuchi et al., 2002) at room temperature. Since the particle size of the conventional sintering body is about 10–20 μm and that of SPS sintering body is less than 1 μm , which indicates that the mechanical strength strongly depends on the particle size of the sintered bodies. The

suppression of grain growth is possible by using special sintering methods such as SPS or hot isostatic pressing, however, it also raises the fabrication costs. The suppression of grain growth is also possible by mixing Al_2O_3 powder, etc., however, the addition of a large amount of Al_2O_3 also causes a decrease of ionic conductivity.

The three-point bending strength of LSGM at room temperature ranges from 110 to 160 MPa (Drennan et al., 1997; Sammes et al., 1998; Yasuda et al., 2000), which are considerably lower than those of YSZ. The addition of Al_2O_3 to $\text{La}_{0.9}\text{Sr}_{0.1}\text{Ga}_{0.8}\text{Mg}_{0.2}\text{O}_{2.85}$ raised the bending strength to 300 MPa at room temperature for 7.5 wt% Al_2O_3 (Yasuda et al., 2000). However, the ionic conductivity decreased by one order of magnitude.

In contrast the bending strength values reported for YSZ or LSGM, there is a large scatter of the mechanical strength data of rare earth doped ceria. Ballon et al. (1998), reported that the modulus of rupture of the gadolinium doped ceria ranges from 110 to 222 MPa at room temperature, which are comparable with LSGM. However, Sameshima et al. (1999), reported the flexural strength of $\text{Ce}_{0.8}\text{Sm}_{0.2}\text{O}_{1.9}$ as 68.4 ± 15 MPa which is extremely low.

Concerning the lanthanum chromites as SOFC interconnects, there was no significant difference in fracture strength of $\text{La}_{0.7}\text{Ca}_{0.3}\text{CrO}_3$ (256 MPa for the sample sintered at $T = 1700^\circ\text{C}$) and $\text{La}_{0.7}\text{Sr}_{0.3}\text{CrO}_3$ (234 MPa) for the same sintering condition (Sammes and Ratonaraj, 1994). However, it should be noted that at high temperature, the *in situ* mechanical strength decreased to ca. 50 MPa for $\text{La}_{1-x}\text{Sr}_x\text{Cr}_{1-y}\text{Co}_y\text{O}_3$ (Sammes and Ratonaraj, 1995). A survey of the mechanical strengths in a reducing atmosphere shows a much more complicated situation. The *in situ* mechanical strength of $\text{La}_{1-x}\text{Ca}_x\text{CrO}_3$ (Armstrong et al., 1996) and $\text{La}_{1-x}\text{Sr}_x\text{Cr}_{1-y}\text{Co}_y\text{O}_3$ (Sammes and Ratonaraj, 1992) is drastically degraded in a reducing atmosphere at high temperature, whereas $\text{La}_{1-x}\text{Sr}_x\text{CrO}_3$ remained a sufficient strength. This fact strongly suggests that the amount and the distribution state of secondary phases at grain boundary or triple point in the polycrystals will affect on the strength in reducing atmospheres.

3.6. Thermal expansion matching with other SOFC components

In an SOFC operation, the materials are exposed to a large temperature change from room temperature to 1000°C . A temperature distribution is also expected due to the inhomogeneous fuel reforming and combustion in the cell. Unfortunately, the thermal conduction in SOFC materials is low. The thermal diffusivity of oxide materials at high temperatures can be measured by a laser flash method. The temperature dependence of thermal diffusivity (α) is shown in fig. 12 for $\text{La}_{1-x}\text{Ca}_x\text{CrO}_{3-\delta}$ (Sakai et al., 1990b), LaMnO_3 (Kobayashi et al., 1993), and YSZ (Hasselmann et al., 1987). The thermal conductivity of LaMnO_3 has a minimum around $T = 700$ K (423°C), which corresponds to a phase transition. Although LaCrO_3 also has a phase transition around $T = 540$ K, no minimum was observed in its thermal diffusivity. A possible reason for the absence of this peak in LaCrO_3 data may be the sparse sampling in the measurements. The thermal conductivity (λ) can be calculated from the thermal diffusivity, the heat capacity (C_p), and the density (ρ) of the oxides using the following equation:

$$\lambda = \frac{C_p \rho \alpha}{v_m}, \quad (18)$$

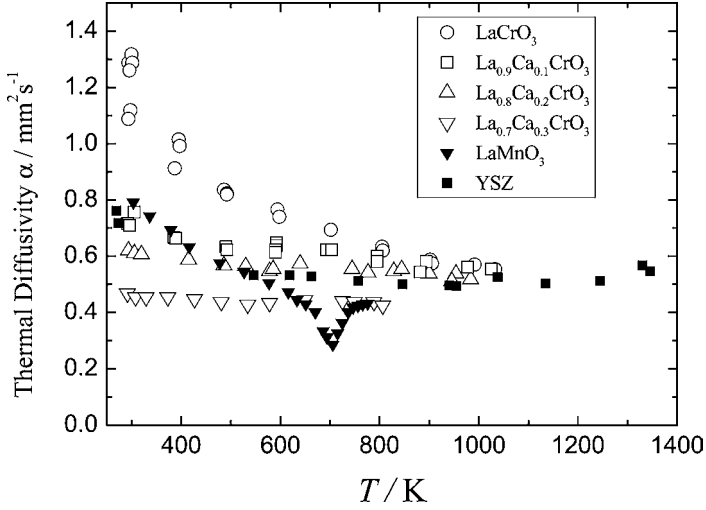


Fig. 12. The thermal diffusivity of some SOFC materials: LaCrO_3 (Sakai and Stølen, 1995), $\text{La}_{1-x}\text{Ca}_x\text{CrO}_3$ (Sakai et al., 1996), LaMnO_3 (Kobayashi et al., 1993), and YSZ (Hasselmann et al., 1987).

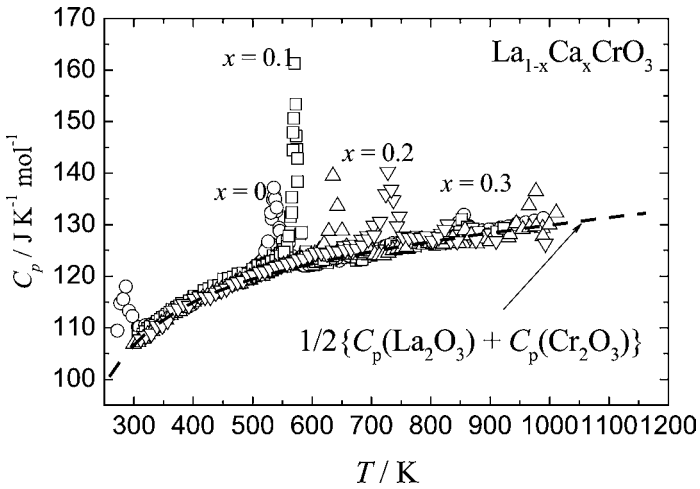


Fig. 13. The molar heat capacity of $\text{La}_{1-x}\text{Ca}_x\text{CrO}_3$ measured by an adiabatic method: The dashed line is the sum of the heat capacities of La_2O_3 and Cr_2O_3 divided by two.

The temperature dependences of the heat capacities are shown in fig. 13 for LaCrO_3 (Sakai and Stølen, 1995), and $\text{La}_{1-x}\text{Ca}_x\text{CrO}_{3-\delta}$ (Sakai and Stølen, 1996), which were measured by an adiabatic calorimetry technique. The peaks found in the intermediate temperatures are due to the phase transition from orthorhombic structure (low temperature) to rhombohedral

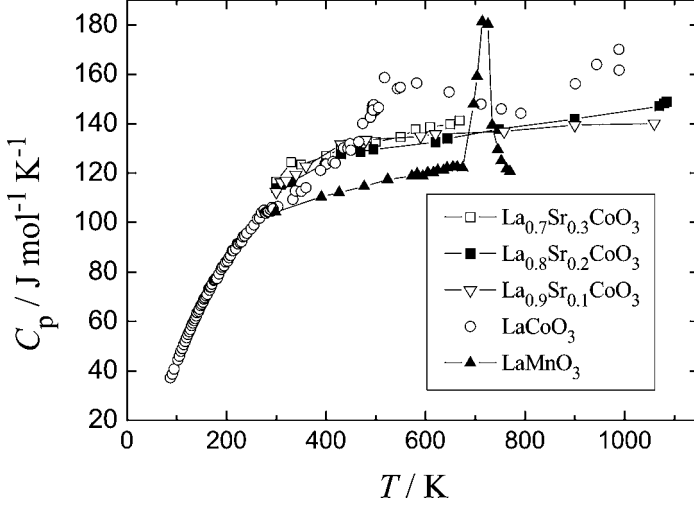


Fig. 14. The molar heat capacity of LaCoO_3 (Horinouchi et al., 1981), $\text{La}_{1-x}\text{Sr}_x\text{CoO}_3$ (Barkhatova, et al., 1990), and LaMnO_3 (Kobayashi et al., 1993).

structure (high temperature). The small peak found at $T = 300$ K for LaCrO_3 corresponds to the magnetic phase transition from antiferromagnetism to paramagnetism. The dashed line of fig. 13 is the sum of the heat capacities ($C_{p,n}$) calculated from the constituent binary oxides, lanthanum oxide (La_2O_3) and chromium oxide, divided by two, i.e.,

$$C_{p,n}(\text{LaCrO}_3) = 1/2C_p(\text{La}_2\text{O}_3) + 1/2C_p(\text{Cr}_2\text{O}_3). \quad (19)$$

The absolute values and temperature dependence of the calculated heat capacity ($C_{p,n}$) agree well with the actual heat capacity of LaCrO_3 , which indicates that the heat capacity of those oxides can be estimated by Neumann-Kopp's theory. The heat capacity data of LaMnO_3 (Kobayashi et al., 1993), LaCoO_3 (Horinouchi et al., 1981), and $\text{La}_{1-x}\text{Sr}_x\text{CoO}_3$ (Barkhatova, et al., 1990) measured by a laser flash method are shown in fig. 14. The heat capacities of LaMnO_3 and $\text{La}_{1-x}\text{Sr}_x\text{CoO}_3$ show peaks due to the phase transition from orthorhombic to rhombohedral structure, however, the heat capacity of LaCoO_3 shows complicated temperature dependence due to the magnetic phase transitions.

The thermal conductivities of LaMnO_3 (Kobayashi et al., 1993), $\text{La}_{1-x}\text{Ca}_x\text{CrO}_{3-\delta}$ (Sakai et al., 1996), and YSZ (Fitzsimmons, 1964; Hasselman et al., 1987) are shown in fig. 15. The conductivities (by extrapolations) of these oxide materials seems to approach $2 \text{ W K}^{-1} \text{ m}^{-1}$ at $T = 1273$ K except for YSZ which is about 15% smaller. For $\text{La}_{1-x}\text{Ca}_x\text{CrO}_{3-\delta}$, the conductivity data were corrected for sample porosity (π) by using the equation suggested by Maxwell (1904):

$$\frac{\lambda}{\lambda_0} = \frac{1 - \pi}{1 + 0.5\pi}. \quad (20)$$

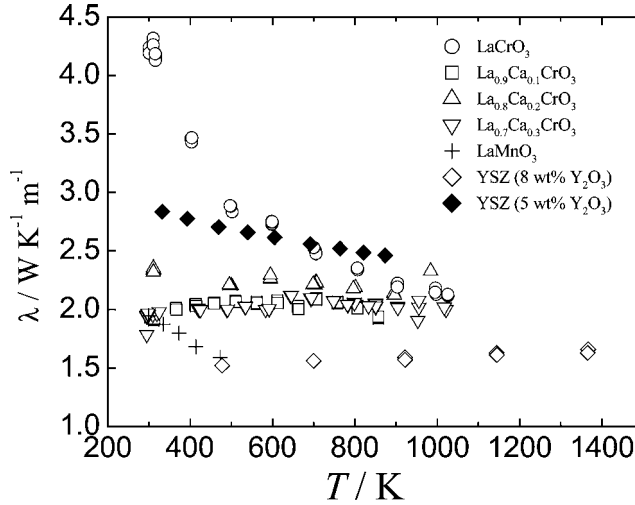


Fig. 15. The thermal conductivity of $\text{La}_{1-x}\text{Ca}_x\text{CrO}_3$ (Sakai et al., 1996), LaMnO_3 (Kobayashi et al., 1993), and YSZ (Fitzsimmons, 1964; Hasselman et al., 1987).

Table 4
Mean free path of phonons in $\text{La}_{1-x}\text{Ca}_x\text{CrO}_3$ calculated from the thermal conductivity and heat capacity

Ca content, x	T (K)	C_p per volume ($\text{MJ K}^{-1} \text{m}^{-3}$)	Thermal conductivity ($\text{W K}^{-1} \text{m}^{-1}$)	Mean free path (pm)
0	300	31.117	4.276	823
0	967	36.416	2.142	353
0.1	304	30.069	2.143	419
0.2	309	30.901	1.956	380
0.3	301	30.768	1.935	377

The thermal conductivity of pure LaCrO_3 linearly depends on the inverse temperature, which indicates that the main carrier of thermal conduction are phonons. The phonon tends to be scattered in the solids by heavy metal ions such as lanthanum (La^{3+}) in the lattice. Moreover, the alkaline earth or rare-earth substitution causes the decrease of thermal conductivity at room temperatures, which indicates that the phonon is also scattered by the substituted cations which randomly occupied the lattice. As a result, the thermal conductivity of calcium substituted samples showed no dependence on temperature. The length of mean free path of phonon (l) can be calculated from thermal conductivity, molar volume (V_m), molar heat capacity (C_p) and velocity of the sound (u) as follows:

$$l = \frac{3\lambda v_m}{C_p u}. \quad (21)$$

The estimated length of the mean free path in $\text{La}_{1-x}\text{Ca}_x\text{CrO}_{3-\delta}$ is shown in table 4, and they are ranged round 300 pm ($= 3 \text{ \AA}$) which is shorter than their lattice parameters. This indicates

that the phonon is mainly scattered by the heavy lanthanum ion which randomly occupies the lattice. Such a low thermal conductivity easily causes a large temperature distribution during the operation of the SOFCs.

Hence, the thermal stress caused by expansion mismatch with other SOFC components is a severe problem in the SOFC interconnects. In the planar SOFCs, the expansion mismatch between the dense electrolyte and the interconnect can easily cause the destruction of the whole cell, and results in the rapid degradation of the SOFC stack.

The thermal expansion coefficients of YSZ (Nielsen and Leipold, 1964), ScSZ (Yamamoto et al., 1995), and LSGM (Yasuda et al., 2000) ranges from $(10.4 \text{ to } 10.7) \times 10^{-6} \text{ K}^{-1}$ (from room temperature to 1000°C in air), and they do not depend on the oxygen partial pressure. The thermal expansion coefficients of $\text{Ce}_{0.8}\text{M}_{0.2}\text{O}_{1.9}$ ($\text{M} = \text{La}, \text{Sm}$) is $(11.4 \text{ to } 11.8) \times 10^{-6} \text{ K}^{-1}$ in air (Sameshima et al., 1999). However, in a reducing atmosphere, the reduction of tetravalent cerium ion to trivalent state causes an additional expansion, the so called isothermal expansion. Hence if ceria is heated to high temperature in a reducing atmosphere, it results in a larger thermal expansion coefficient. Yasuda and Hishinuma (1997) reported that linear isothermal expansion of $\text{Ce}_{0.8}\text{Gd}_{0.2}\text{O}_{1.9}$ reaches 1.5% composed to the length in air at 800°C , and it can not alleviate by changing the gadolinium content. Such an uncontrollable isothermal expansion would cause a serious problem in utilization of this material as SOFC electrolyte.

Concerning interconnect materials, pure LaCrO_3 has an averaged thermal expansion coefficient $\beta = (8.6 \text{ to } 9.4) \times 10^{-6} \text{ K}^{-1}$ (from room temperature to 1000°C in air) which is significantly lower than that of YSZ electrolyte ($10.6 \times 10^{-6} \text{ K}^{-1}$) or lanthanum strontium manganite ($10.7\text{--}11.1 \times 10^{-6} \text{ K}^{-1}$). Furthermore, LaCrO_3 has an anomaly in the thermal expansion due to the phase transition from the low temperature orthorhombic phase to the high temperature rhombohedral phase at $T = 563 \text{ K}$ (290°C). However, thermal expansion behavior and phase transition temperature can be easily controlled by substituting a variety of alkaline earths and transition metals. Figs. 16a and 16b show the effect of substitution on thermal expansion coefficient in air (Sakai et al., 1990c; Hayashi et al., 1988; Koc and Anderson, 1992b; Hofer and Kock, 1993; Yasuda et al., 2001). In most cases, the thermal expansion coefficient changes monotonically with composition. The thermal expansion coefficients of YSZ are also shown in fig. 16a for comparison. Concerning the anomalies of phase transition, the transition temperature can be lowered by strontium substitution, increase with calcium substitution. However, the anomaly is alleviate in heavily substituted samples, such as $\text{La}_{0.7}\text{Ca}_{0.3}\text{CrO}_3$, which is probably due to microscopic sample inhomogeneity.

The isothermal expansion due to oxygen vacancy formation is also significant for substituted lanthanum chromites, which is observed in reducing atmospheres as well as rare earth substituted ceria as already discussed in the previous paragraph. The effect of oxygen vacancy formation on expansion behavior was checked by Yasuda et al. by measuring the thermal expansion coefficient in different atmospheres (Yasuda et al., 2001). The results are shown in table 5 along with our data for $\text{Ce}_{0.8}\text{Y}_{0.2}\text{O}_{1.9}$. The anomalously high thermal expansion coefficients on heating in $\text{H}_2\text{--N}_2$ atmosphere are due to oxygen vacancy formation. This work indicates that the isothermal expansion is large for alkaline earth doped lanthanum chromites, $\text{La}_{1-x}\text{M}_x\text{CrO}_{3-\delta}$ ($\text{M} = \text{Ca}, \text{Sr}$). However, in contrast with the case of ceria, the isothermal

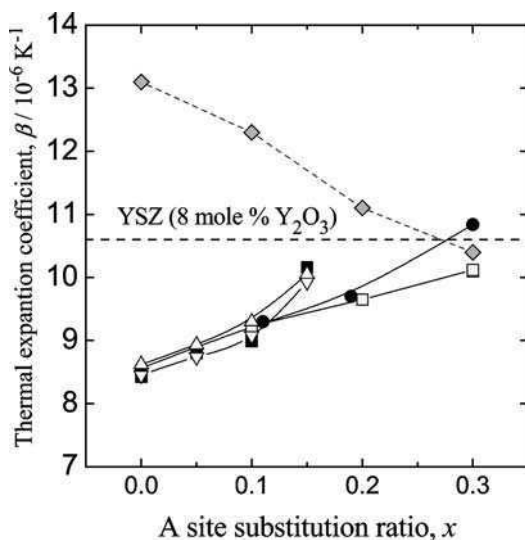


Fig. 16a. The thermal expansion coefficient as functions substitution ratio: (\square) $\text{La}_{1-x}\text{Sr}_x\text{CrO}_3$ (Yasuda et al., 2001), (\bullet) $\text{La}_{1-x}\text{Ca}_x\text{CrO}_3$ (Sakai et al., 1990c), (\blacklozenge) $\text{La}_{1-x}\text{Ca}_x\text{Cr}_{0.9}\text{Co}_{0.1}\text{O}_3$ (Koc and Anderson, 1992a, 1992b), (\blacksquare) $\text{La}_{1-x}\text{Sr}_x\text{Cr}_{0.95}\text{Zn}_{0.05}\text{O}_3$ (Hayashi et al., 1988), (∇) $\text{La}_{1-x}\text{Sr}_x\text{Cr}_{0.95}\text{Cu}_{0.05}\text{O}_3$ (Hayashi et al., 1988), (\triangle) $\text{La}_{1-x}\text{Sr}_x\text{Cr}_{0.95}\text{Cu}_{0.10}\text{O}_3$ (Hayashi et al., 1988).

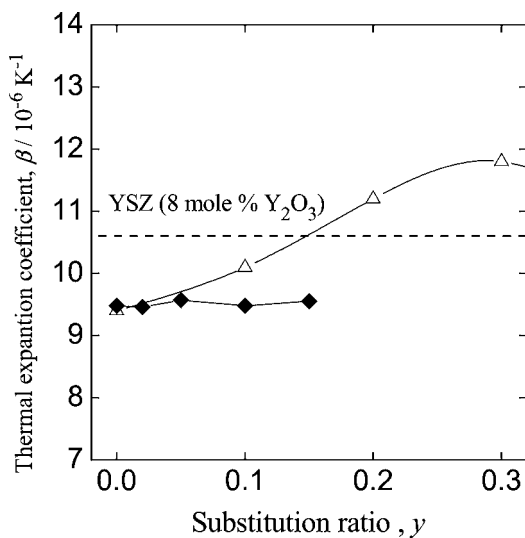


Fig. 16b. The thermal expansion coefficient as functions of substitution ratio: (\triangle) $\text{LaCr}_{1-y}\text{Mg}_y\text{O}_3$ (Koc and Anderson, 1992a, 1992b), (\blacklozenge) $\text{LaCr}_{1-y}\text{Ni}_y\text{O}_3$ (Hofer and Kock, 1993).

Table 5
Averaged thermal expansion coefficient from room temperature to 1273 K in air and reducing atmosphere

Composition	Atmosphere	β (10^{-6} K^{-1})	Ref.
$\text{Ce}_{0.8}\text{Y}_{0.2}\text{O}_{1.9}$	Air	12.16	This paper
	Ar-1% H_2 -1% H_2O	15.18	
$\text{La}_{0.9}\text{Sr}_{0.1}\text{CrO}_3$	Air	9.23	Yasuda et al., 2001
	1% H_2 -99% N_2	10.34	
$\text{La}_{0.7}\text{Sr}_{0.3}\text{CrO}_3$	Air	10.1	Yasuda et al., 2001
	1% H_2 -99% N_2	16.9	
$\text{La}_{0.96}\text{Sr}_{0.04}\text{Cr}_{0.87}\text{Al}_{0.11}\text{Co}_{0.02}\text{O}_3$	Air	9.4	Yasuda et al., 2001
	1% H_2 -99% N_2	9.87	

expansion of lanthanum chromites can be suppressed by the substitution of chromium by transition metals or aluminum.

3.7. Chemical stability, compatibility with other cell component

Since SOFCs should operate for more than several years when it is utilized as a distribution power generation unit, the durability of materials is strictly required. Each candidate material is expected to have a sufficient chemical stability. However, in some combinations of materials, the interfaces of two materials are not stable with respect to each other, so that the interdiffusion of metal ions and the formation of secondary phases are observed. It is well known that lanthanum cobaltite, LaCoO_3 , and stoichiometric lanthanum manganite, LaMnO_3 , react with YSZ during the cell fabrication process or under the operating conditions, and as a result the lanthanum zirconate, $\text{La}_2\text{Zr}_2\text{O}_7$, forms. This phase has the pyrochlore structure and has a low electrical conductivity. The precipitation of $\text{La}_2\text{Zr}_2\text{O}_7$ at the triple phase boundary may cause the degradation of cathode performance. The lanthanum manganite with excess manganese, $\text{LaMn}_{1+x}\text{O}_3$, is reported to have a lower reactivity with YSZ. The possibility of forming secondary phase can be evaluated by making thermodynamic calculations. Yokokawa et al. suggested that the local chemical equilibrium is maintained at the interface at temperatures around 1000 °C, and evaluated the interface stability of lanthanum manganite cathode/YSZ electrolyte (Yokokawa et al., 1990, 1991a, 1991b). They calculated that $\text{La}_2\text{Zr}_2\text{O}_7$ would form at the YSZ/lanthanum perovskite oxide interfaces by estimating the thermodynamic functions of the complex oxides. They also predicted that the reaction at the interface of YSZ and lanthanum manganite with excess manganese is suppressed, however, the diffusion of manganese into YSZ occurs simultaneously. The manganese component in YSZ diffuses rapidly via the grain boundary, and it affects the oxide ion conductivity and oxygen transport number of YSZ (Kawada et al., 1992). It should be noted that the formation and disappearance of $\text{La}_2\text{Zr}_2\text{O}_7$ precipitates depends the oxygen potential at the interface which is affected by the electrochemical reaction overpotential (Yokokawa et al., 1994).

For lanthanum cobaltites, the formation of $\text{La}_2\text{Zr}_2\text{O}_7$ can not suppressed except by lowering the temperature. Hence, rare earth doped ceria is often introduced as the interlayer be-

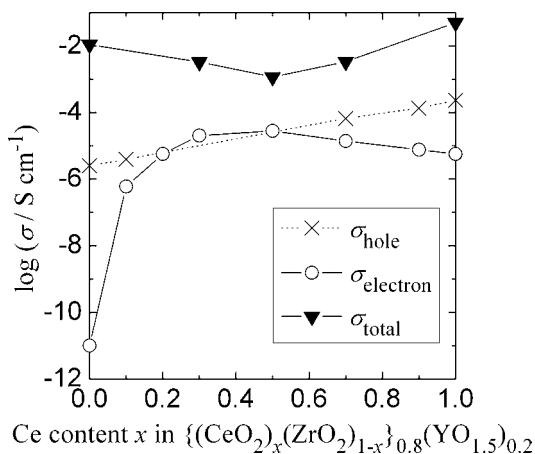


Fig. 17. The conductivity of $\{(\text{CeO}_2)_x(\text{ZrO}_2)_{1-x}\}_{0.8}(\text{YO}_{1.5})_{0.2}$ at $T = 1073$ K in air as a function of cerium content (x). The electron conductivity is extrapolated from the data obtained in a reducing atmosphere.

tween YSZ and lanthanum cobaltite to prevent the reaction. Rare earth substituted ceria is often used as the interlayer or additives at cathodes, and it raise the electrochemical performance of the cathodes. However, when the mixture of ceria and yttria powder was calcined at the temperatures above 1200°C , the formation of a ceria–zirconia–yttria solid solution is observed (Sakai et al., 2001). The ceria-zirconia-rare earth oxide solid solution has lower ionic conductivity than YSZ or rare earth substituted ceria, however, the electronic conductivity is rather enhanced (Xiong et al., 2001). Fig. 17 shows the total conductivity, and extrapolated electron conductivity of $\{(\text{CeO}_2)_x(\text{ZrO}_2)_{1-x}\}_{0.8}(\text{YO}_{1.5})_{0.2}$ solid solution at $T = 1073$ K, $p(\text{O}_2) = 0.1$ MPa as a function of cerium content (x). The electron conductivity seems to have a maximum at $x = 0.5$ whereas the ionic conductivity shows the minimum at the same composition.

Although the decrease of ionic conductivity is not desirable for SOFC electrolytes, the increase of electronic conductivity in ceria–zirconia–yttria solid solution may result in an interesting change of the oxygen transport properties on the surface of the oxides. Fig. 18 shows the oxygen isotope diffusivity (D_{O}^*) and surface exchange rate (k) of $\{(\text{CeO}_2)_x(\text{ZrO}_2)_{1-x}\}_{0.8}(\text{YO}_{1.5})_{0.2}$ at $T = 700^\circ\text{C}$ in $p(\text{O}_2) = 21.3$ kPa. It should be noted that the compositional dependence of the oxygen surface exchange coefficient (k) is somewhat similar to that observed for the electron conductivity (fig. 17). The increase of oxygen surface exchange rate may result in the increase of the oxygen permeation flux in the solids, which would be a positive affect on the electrochemical performance.

Although the formation of $\text{La}_2\text{Zr}_2\text{O}_7$ or of ceria-zirconia solid solutions are serious problems, the diffusion of a transition metal is rather small in fluorite type electrolytes. However, in perovskite-type electrolytes such as LSGM, the interdiffusion of such transition metals from electrodes is very significant. Zhang et al. (1999) reported that the interfacial resistance increased significantly when $\text{Ni-Ce}_{0.8}\text{Sm}_{0.2}\text{O}_{1.9}$ anode was calcined on a LSGM electrolyte

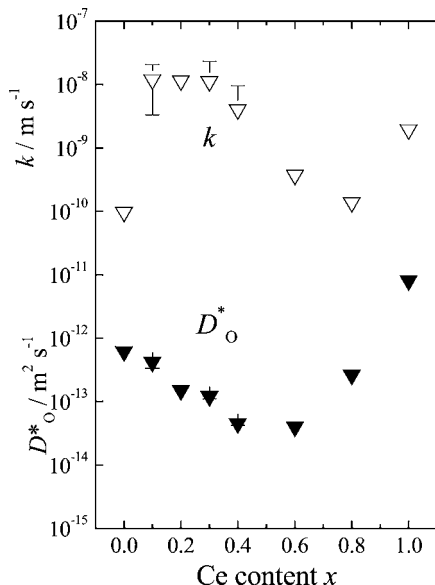


Fig. 18. The oxygen isotope diffusivity (D_{O}^*) and surface exchange rate constant (k) of $\{(\text{CeO}_2)_x(\text{ZrO}_2)_{1-x}\}_{0.8}(\text{YO}_{1.5})_{0.2}$ at $T = 973 \text{ K}$ in $p(\text{O}_2) = 213 \text{ kPa}$.

above $T = 1350 \text{ }^\circ\text{C}$. This degradation is caused by the nickel diffusion from the anode into the LSGM electrolyte. The fast diffusion of cobalt and iron components also occurs at the interface of the LSGM electrolyte and the $(\text{La}, \text{Sr})(\text{Co}, \text{Fe})\text{O}_3$ cathode, and a part of the diffusion is governed by the grain boundaries of the LSGM polycrystalline bodies (Sakai et al., unpublished data). Such diffusions of transition metals cause a significant decrease of the transport number of oxide ion in LSGM. This fact indicates that LSGM can not be co-sintered with electrodes, because high temperatures $>1723 \text{ K}$ are needed to obtain dense LSGM polycrystalline bodies.

SOFC interconnects are exposed to a large gradient of oxygen potential at high temperature. The chemical stability of dense alkaline earth substituted lanthanum chromites were evaluated under simulated SOFC operation condition at $1000 \text{ }^\circ\text{C}$, flowing $97\% \text{ H}_2 + 3\% \text{ H}_2\text{O}$ on one side and dry air on opposite side, and passing an electric current of $I = 300 \text{ mA cm}^{-2}$ (Sakai et al., 1993b). For $(\text{La}, \text{Ca})\text{CrO}_3$ polycrystals, the precipitation of $\text{Ca}_a(\text{CrO}_4)_b$ melt is observed on air side, and CaO and CaCr_2O_4 is observed on fuel side of the sample after the treatment for 200 h. The precipitation is more significant for heavily doped $(\text{La}, \text{Ca})\text{CrO}_3$ sintered at low temperatures around $1300 \text{ }^\circ\text{C}$. $\text{Ca}_a(\text{CrO}_4)_b$ liquid phase acts as the sintering aid for $(\text{La}, \text{Ca})\text{CrO}_3$. However, $\text{Ca}_a(\text{CrO}_4)_b$ remains at the grain boundary of the sintered specimens and is squeezed out to surface during the stability test. At fuel side, $\text{Ca}_a(\text{CrO}_4)_b$ is reduced and decomposed to CaO and CaCr_2O_4 . The low electrical conductivity of these two phases will affect the total cell performance (Yasuda and Hishinuma, 1995). Furthermore, the calcium oxide may react with Ni-YSZ anode forming CaZrO_3 . $(\text{La}, \text{Ca})\text{CrO}_3$ sintered at

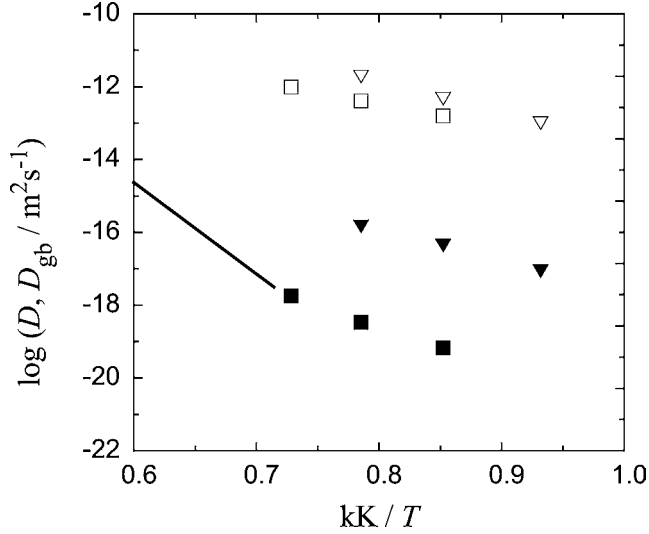


Fig. 19. The temperature dependence of the diffusivity in lanthanum chromites: Closed symbols and line represent bulk diffusivity (D_{bulk}) and open symbols represent grain boundary diffusivity (D_{gb}). (■, □) ^{40}Ca in $\text{La}_{0.75}\text{Ca}_{0.25}\text{CrO}_3$ (Horita et al., 1998). (▼, ▽) ^{18}O in $\text{La}_{0.8}\text{Ca}_{0.2}\text{CrO}_3$ (Sakai et al., 2000a, 2000b), (—) La^{3+} in LaCrO_3 (Akashi et al., 1998).

1873 K exhibited much less precipitation, because most of the $\text{Ca}_a(\text{CrO}_4)_b$ is converted into CaO at high temperature sintering. For $(\text{La},\text{Sr})\text{CrO}_3$ and $(\text{La},\text{Sr})(\text{Cr},\text{Co})\text{O}_3$, the precipitation of SrO and Cr_2O_3 is observed, however, the amounts of the precipitates were much smaller than those observed for $(\text{La},\text{Ca})\text{CrO}_3$. The amount of $\text{Ca}_a(\text{CrO}_4)_b$ should be suppressed to the minimum value, which results in a sintering improvement. A recent paper reports that the strict control of the compositions in the preparations can result in the smaller amount of $\text{Ca}_a(\text{CrO}_4)_b$ precipitation in $(\text{La},\text{Ca})\text{CrO}_3$, and as a result exhibits a reasonable chemical stability.

In order to follow such degradation behaviors, the strontium and calcium diffusivities in $\text{La}_{1-x}\text{Ca}_x\text{CrO}_{3-\delta}$ were determined by using tracer diffusion techniques and secondary ion mass spectrometry analysis (SIMS) (Horita et al., 1998). The temperature dependences of the diffusivities in lanthanum chromites are plotted in fig. 19 for ^{44}Ca in $\text{La}_{1-x}\text{Ca}_x\text{CrO}_{3-\delta}$ (Horita et al., 1998), La^{3+} in LaCrO_3 (Akashi et al., 1998), and ^{18}O in $\text{La}_{1-x}\text{Ca}_x\text{CrO}_{3-\delta}$ (Sakai et al., 2000a, 2000b). It should be emphasized that fast diffusion along grain boundary is observed in oxidizing atmosphere at 800 to 1000 °C, and that the grain boundary diffusivity (D_{gb}) is 10^4 – 10^5 times higher than bulk diffusivity. Although the relative surface area of grain boundary is small, the calculated flux of calcium component via grain boundary becomes 10–100 times larger than that through bulk (Sakai et al., 2000c), and it agrees with the precipitation rate of $\text{Ca}_a(\text{CrO}_4)_b$ secondary phase on the surface. The fast cation diffu-

sion along grain boundary is also observed for the case of the interface reaction between the (La,Ca)CrO₃ interconnect/(La,Sr)MnO₃ cathode (Nishiyama et al., 1996).

Summary

In this paper, we have shown that rare earths are used in most of the candidate materials for SOFCs. However, it should also be noted that most of the SOFC materials are complex oxides of rare earths and other metals. The oxide ion conductivities of zirconia or ceria are controlled by rare earths substitutions, however, the electrical conductivity or catalytic activity are rather controlled by transition metals or alkaline earths.

The most important problem of rare earths is their high costs. The reduction in the cost of lanthanum or samarium would lead to a reduction of the total fabrication cost of the SOFC cell stacks. The possibility of using rare earth mixtures as an alternative of pure lanthanum have been tried, however, it resulted in the degradation of the performance of the SOFC.

Another issue for SOFC material research is to increase the available thermodynamic data for rare-earth containing complex oxides. Although there has been intensive researches on the binary oxides, there is a paucity of data for complex oxides such as the perovskites, and the fluorite oxides with some substitutions. Most of the SOFC materials are complex oxides with several metal components which have been reported in the past twenty years. However, it is a matter of regret that there are only a few reports concerning calorimetric studies of these materials. Fundamental research on these advanced materials is necessary especially from the viewpoint of evaluating chemical stability and durability of the SOFC components.

References

- Akashi, T., Nanko, M., Maruyama, T., Shiraishi, Y., Tanabe, J., 1998. *J. Electrochem. Soc.* **145** (6), 2090.
- Anderson, H.U., 1978. In: Paulmor III, H., Davis, R.F., Hare, T.M. (Eds.), *Processing of Crystalline Ceramics*. Plenum Press, New York, USA.
- Anderson, H.U., Sparlin, D.M., 1984. DOE/ER/10598-5.
- Armstrong, T.R., Stevenson, J.W., Pederson, L.R., Raney, P.E., 1996. *J. Electrochem. Soc.* **143** (9), 2919.
- Ballon, O., Sammes, N.M., Staniforth, J., 1998. *J. Power Sources* **75**, 116.
- Bance, P., Brandon, N.P., Girvan, B., Holbeche, P., O'Dea, S., Steele, B.C.H., 2004. *J. Power Sources* **131**, 86.
- Barkhatova, L.Yu., Klimenko, A.N., Konochuk, O.F., Petrov, A.N., Sergeev, S.V., 1990. *Russ. J. Phys. Chem.* **64** (11), 1670.
- Batawi, E., Glatz, W., Kraussler, W., Jaonusek, M., Doggwiler, B., Diethelm, R., 1999. In: Singhal, S.C., Dokiya, M. (Eds.), *Solid Oxide Fuel Cells VI*, vol. **PV99-19**. The Electrochemical Society, Pennington, NJ, USA, p. 731.
- Bouwnmeester, H.J.M., Kruidhof, H., Burggraaf, A.J., 1994. *Solid State Ionics* **72**, 185.
- Choudhury, N.S., Pedeson, J.W., 1970. *J. Electrochem. Soc.* **117**, 1384.
- Christie, G.M., Middleton, P.H., Steele, B.C.H., 1994. *J. Eur. Ceram. Soc.* **14**, 163.
- Drennan, J., Zeizko, V., Hay, D., Ciacchi, F.T., Rajendran, S., Badwal, S.P.S., 1997. *J. Mater. Sci.* **7**, 9.
- Fitzsimmons, E.S., Gen. Elec. Co. Aircraft Nuclear Propulsion Dept., DC-61-6-4, 1.
- Fujii, H., 2003. In: Singhal, S.C., Dokiya, M. (Eds.), *Solid Oxide Fuel Cells VIIIP*, vol. **V2003-07**. The Electrochemical Society, Pennington, NJ, USA, p. 9.
- George, R., Casanova, A., 2003. Abstracts of 2003 Fuel Cell Seminar, Miami, FL, USA, November 3–7, p. 895.

- Gorte, R.J., Kim, H., Vohs, J.M., 2002. *J. Power Sources* **106**, 10.
- Group, L., Anderson, H.U., 1976. *J. Am. Ceram. Soc.* **59** (9–10), 439.
- Hartley, A., Sahibzada, M., Weston, M., Metcarfe, L.S., Mantzavinos, D., 2000. *Catalysis Today* **55**, 197.
- Hasselmann, D.P.H., Johnson, L.F., Bentsen, L.D., Syed, R., Lee, H.L., Swain, M.V., 1987. *Am. Ceram. Soc. Bull.* **66** (5), 799.
- Hayashi, S., Fukaya, K., Saito, H., 1988. *J. Mater. Sci. Lett.* **7**, 457.
- Hofer, H.E., Kock, W.F., 1993. *J. Electrochem. Soc.* **140** (10), 2889.
- Horinouchi, K., Takahashi, Y., Fueki, K., 1981. *Yogyo-Kyokai-Shi* **89** (2), 104.
- Horita, T., Sakai, N., Kawada, T., Yokokawa, H., Dokiya, M., 1998. *J. Am. Ceram. Soc.* **81** (2), 315.
- Ishihara, T., Matsuda, H., Takita, Y., 1994. *J. Am. Chem. Soc.* **116**, 3801.
- Ishihara, T., Honda, M., Shibayama, T., Minami, H., Nishiguchi, H., Takita, Y., 1997. *J. Electrochem. Soc.* **145** (9), 3177.
- Ishihara, T., Fukui, S., Nishiguchi, H., Takita, Y., 2002. *Solid State Ionics* **152–153**, 619.
- Itoh, H., Mori, M., Mori, N., Abe, T., 1994. *J. Power Sources* **49**, 315.
- Iwahara, H., Esaka, T., Uchida, H., Maeda, N., 1981. *Solid State Ionics* **3/4**, 359.
- Joeger, M., Gauckler, L.G., 2001. In: Yokokawa, H., Singhal, S.C. (Eds.), *Solid Oxide Fuel Cells VII*, vol. **PV2001-16**. The Electrochemical Society, Pennington, NJ, USA, p. 662.
- Karim, D.P., Aldred, A.T., 1979. *Phys. Rev. B* **20** (6), 2255.
- Kawada, T., Sakai, N., Yokokawa, H., Dokiya, M., 1992. *Solid State Ionics* **53–56**, 418.
- Kim, J.-H., Yoo, H.I., 2001. *Solid State Ionics* **140**, 105.
- Kobayashi, H., Satoh, H., Kamegashira, N., 1993. *J. Alloys and Compounds* **192**, 93.
- Koc, R., Anderson, H.U., 1990. *Ceram. Trans.* **12**, 659.
- Koc, R., Anderson, H.U., 1992a. *J. Eur. Ceram. Soc.* **9**, 285.
- Koc, R., Anderson, H.U., 1992b. *J. Mater. Sci. Lett.* **11**, 1191.
- Konishi, K., Iritani, J., Kougami, K., Komiyama, N., Kabata, T., Hisatome, N., Nagata, K., Ikeda, K., 2002. In: Huijismans, J. (Ed.), *Proc. fifth European SOFC Forum, The European Fuel Cell Forum, Oberrohrdorf, Switzerland*, p. 439.
- Kuo, J., Kuo, H., Anderson, H.U., Sparlin, D.M., 1990. *J. Solid State Chem.* **87**, 55.
- Larsen, P.H., Hendriksen, P.V., Mogensen, M., 1997. *J. Thermal Analysis* **49**, 1263.
- Marina, O., Bagger, C., Primdahl, S., Mogensen, M., 1999. *Solid State Ionics* **123**, 199.
- Marina, O., Pedersen, L., 2002. In: Huijismans, J. (Ed.), *Proc. fifth European SOFC Forum, The European Fuel Cell Forum, Oberrohrdorf, Switzerland*, p. 481.
- Matsuda, M., Ohara, O., Murata, K., Ohara, S., Fukui, T., Miyake, M., 2003. *Electrochem. Solid State Lett.* **6** (7), A140.
- Matsuzaki, Y., Yasuda, I., 2001. *J. Electrochem. Soc.* **148** (2), A126.
- Maxwell, J.C., 1904. *Treatise on Electricity and Magnetism*. Clarendon Press, Oxford. Quoted by Parrot, J.E., Stuckes, A.D., in: *Thermal Conductivity of Solids*, Goldsmid, H.J. (Ed.). Applied Physics Series, Pion, London, UK.
- Meadowcroft, D.B., 1969. *Brit. J. Appl. Phys. (J. Phys. D)* **2** (2), 1225.
- Miyachi, M., Yamamoto, H., Tsuru, Y., 1999. *Jpn. Pat. No. 11-86887*.
- Mori, M., Sakai, N., Kawada, T., Yokokawa, H., Dokiya, M., 1991. *Denki Kagaku* **59** (4), 314.
- Mori, M., Abe, T., Itoh, H., Yamamoto, O., Takeda, T., Kawahara, T., 1994. *Solid State Ionics* **74** (3–4), 157.
- Mukerjee, S., Shaffer, S., Zizelman, J., Chick, L., Meinhardt, K., Sprengle, V., Weil, S., Paxton, D., Deibler, J., 2003. Abstracts of 2003 Fuel Cell Seminar, Miami, FL, USA, November 3–7, 2003, p. 852.
- Nakanishi, A., Hattori, M., Sasaki, Y., Miyamoto, H., Aiki, H., Takenobu, K., Nishiura, M., 2003. In: Singhal, S.C., Dokiya, M. (Eds.), *Solid Oxide Fuel Cells VIII*, vol. **PV2003-07**. The Electrochemical Society, Pennington, NJ, USA, p. 53.
- Nielsen, T.H., Leipold, M.H., 1964. *J. Am. Ceram. Soc.* **47** (3), 155.
- Nishi, T., Murakami, N., Yamamoto, H., 1999. *Jpn. Pat. No. 11-54137*.
- Nishiyama, H., Aizawa, M., Yokokawa, H., Horita, T., Sakai, N., Dokiya, M., Kawada, T., 1996. *J. Electrochem. Soc.* **143** (7), 2332.
- Park, J.-H., Blumental, R.N., 1989. *J. Am. Ceram. Soc.* **72** (8), 1485.
- Petrov, A.N., Kononchuk, O.F., Andreev, A.V., Cherepanov, V.A., Kofstad, P., 1995. *Solid State Ionics* **90**, 189.
- Sakai, N., Kawada, T., Yokokawa, H., Dokiya, M., Iwata, T., 1990a. *J. Mater. Sci.* **25**, 4531.
- Sakai, N., Kawada, T., Yokokawa, H., Dokiya, M., 1990b. *Proceedings of the 11th Symposium on Thermophysical Properties*, Tokyo, November 1990, p. 208.

- Sakai, N., Kawada, T., Yokokawa, H., Dokiya, M., Iwata, T., 1990c. *Solid State Ionics* **40/41**, 394.
- Sakai, N., Kawada, T., Yokokawa, H., Dokiya, M., Kojima, I., 1993a. *J. Am. Ceram. Soc.* **76**.
- Sakai, N., Kawada, T., Yokokawa, H., Dokiya, M., 1993b. In: Badwal, S.P.S., Bannister, M.M., Hannink, R.H.J. (Eds.), *Science and Technology of Zirconia V*. The Australian Ceramic Society, The Technomic Publication Co. Inc., Australia, p. 764.
- Sakai, N., Stølen, S., 1995. *J. Chem. Thermodyn.* **27**, 493.
- Sakai, N., Horita, T., Yokokawa, H., Dokiya, M., 1996. *Solid State Ionics* **86-88**, 1273.
- Sakai, N., Stølen, S., 1996. *J. Chem. Thermodyn.* **28**, 421.
- Sakai, N., Yamaji, K., Horita, T., Yokokawa, H., Kawada, T., Dokiya, M., Hiwatashi, K., Ueno, A., Aizawa, M., 1999. *J. Electrochem. Soc.* **146** (4), 1341.
- Sakai, N., Yamaji, K., Horita, T., Yokokawa, H., Kawada, T., Dokiya, M., 2000a. *J. Electrochem. Soc.* **147** (9), 3178.
- Sakai, N., Yamaji, K., Horita, T., Yokokawa, H., Kawada, T., Dokiya, M., 2000b. *J. Electrochem. Soc.* **147** (9), 3078.
- Sakai, N., Yamaji, K., Horita, T., Negishi, H., Yokokawa, H., 2000c. *Solid State Ionics* **135**, 469.
- Sakai, N., Hashimoto, T., Katsube, T., Yamaji, K., Negishi, H., Horita, T., Yokokawa, H., Xiong, Y.P., Nakagawa, M., Takahashi, Y., 2001. *Solid State Ionics* **143**, 151.
- Sakai, N., Yamaji, K., Horita, T., Yokokawa, H., 2004. *Int. J. Appl. Ceram. Tech.* **1** (1), 23.
- Sameshima, S., Ishikawa, T., Kawanami, M., Hirata, Y., 1999. *Mat. Chem. and Phys.* **61**, 31.
- Sammes, N.M., Ratnaraj, R., 1992. *J. Mater. Sci. Lett.* **11**, 1191.
- Sammes, N., Ratonaraj, R., 1994. *J. Mater. Sci.* **29**, 4319.
- Sammes, N., Ratonaraj, R., 1995. *J. Mater. Sci.* **30**, 4523.
- Sammes, N.M., Keppeler, F.M., Nafe, H., Fldinger, F., 1998. *J. Am. Ceram. Soc.* **81**, 3104.
- Sauvet, A.-L., Fouletier, J., 2002. *Electrochimica Acta* **106**, 10.
- Steele, B.C.H., 2000. *Solid State Ionics* **129**, 95.
- Stevenson, J.W., Armstrong, T.R., Pederson, L.R., Li, J., Lewinsohn, C.A., Baskaran, S., 1998. *Solid State Ionics* **113-115**, 571.
- Tai, L.W., Lessing, P.A., 1991. *J. Am. Ceram. Soc.* **74** (1), 155.
- Takeuchi, T., Kondoh, I., Tamari, N., Balakrishnan, N., Nomura, K., Kageyama, H., Takeda, Y., 2002. *J. Electrochem. Soc.* **149** (4), A455.
- Takeuchi, H., Ueno, A., Kuroishi, M., Aikawa, S., Abe, T., 2003. In: Singhal, S.C., Dokiya, M. (Eds.), *Solid Oxide Fuel Cells VIII*, vol. **PV2003-07**. The Electrochemical Society, Pennington, NJ, USA, p. 70.
- Taniguchi, S., Kadowaki, M., Kawamura, H., Yasuo, T., Akiyama, Y., Miyake, Y., Saitoh, T., 1995. *J. Power Sources* **55**, 73.
- Tsukuma, K., Shimada, M., 1985. *Am. Ceram. Soc. Bull.* **64**.
- Ukai, Y., Mizutani, Y., Kume, Y., Yamamoto, O., 2001. In: Yokokawa, H., Singhal, S.C. (Eds.), *Solid Oxide Fuel Cells VII*, vol. **PV2001-16**. The Electrochemical Society, Pennington, NJ, USA, p. 375.
- Van Hassel, B.A., Kawada, T., Sakai, N., Yokokawa, H., Dokiya, M., 1993. *Solid State Ionics* **66**, 41.
- Visco, S., Jacobson, C.P., De Jonghe, L.C., 1999. In: Dokiya, M., Singhal, S.C. (Eds.), *Solid Oxide Fuel Cells VI*, vol. **PV99-19**. The Electrochemical Society, Pennington, NJ, USA, p. 861.
- Wang, J.B., Tai, Y.R., Dow, W.-P., Huang, T.-J., 2001. *Appl. Catalysis A. General* **218**, 69.
- Williams, M.C., Strakey, J.P., 2003. In: Singhal, S.C., Dokiya, M. (Eds.), *Solid Oxide Fuel Cells VIII*, vol. **PV2003-07**. The Electrochemical Society, Pennington, NJ, USA, p. 3.
- Xiong, Y.P., Yamaji, K., Horita, T., Sakai, N., Negishi, H., Yokokawa, H., 2001. *J. Electrochem. Soc.* **148** (2), E489.
- Xiong, Y., Yamaji, K., Horita, T., Sakai, N., Yokokawa, H., 2004. *J. Electrochem. Soc.* **151** (5), A407.
- Yamada, T., Chitose, N., Akikusa, J., Murakami, N., Akubay, T., Miyazawa, T., Adachi, K., Hasegawa, A., Yamada, M., Hoshino, K., Hosoi, K., Komada, N., Yoshida, H., Kawano, M., Sasaki, T., Inagaki, T., Miura, K., Ishihara, T., Takita, Y., 2003. In: Singhal, S.C., Dokiya, M. (Eds.), *Solid Oxide Fuel Cells VIII*, vol. **PV2003-07**. The Electrochemical Society, Pennington, NJ, USA, p. 113.
- Yamaji, K., Horita, T., Ishikawa, M., Sakai, N., Yokokawa, H., Dokiya, M., 1997. In: Stimming, U., Singhal, S.C., Tagawa, H., Lehnart, W. (Eds.), *Solid Oxide Fuel Cells V*, vol. **PV97-18**. The Electrochemical Society, Pennington, NJ, p. 1041.
- Yamamoto, O., Takeda, Y., Kanno, R., Kohno, K., Kamiharai, T., 1989. *J. Mater. Sci. Letters* **8**, 198.
- Yamamoto, O., Arati, Y., Takeda, Y., Imanishi, N., Mizutani, Y., Kawai, M., Nakamura, Y., 1995. *Solid State Ionics* **79**, 137.
- Yasuda, I., Hikita, T., 1993. *J. Electrochem. Soc.* **140** (6), 1699.
- Yasuda, I., Hikita, T., 1994. *J. Electrochem. Soc.* **141** (5), 1269.

- Yasuda, T., Hishinuma, M., 1995. *Solid State Ionics* **80**, 141.
- Yasuda, I., Hishinuma, M., 1997. In: Ramanarayanan, T.A., Worrell, W.L., Tuller, H.L., Khandkar, A.C., Mogensen, M., Gopel, W. (Eds.), *Ionic and Mixed Conducting Ceramics III*, vol. **PV97-24**. The Electrochemical Society, Pennington, NJ, USA, p. 178.
- Yasuda, I., Matsuzaki, Y., Tamakawa, T., Koyama, T., 2000. *Solid State Ionics* **135**, 381.
- Yasuda, I., Ogiwara, T., Yakabe, T., 2001. In: Yokokawa, H., Singhal, S.C. (Eds.), *Solid Oxide Fuel Cells VII*, vol. **PV2001-16**. The Electrochemical Society, Pennington, NJ, USA, p. 783.
- Yokokawa, H., Sakai, N., Kawada, T., Dokiya, M., 1990. *Denki Kagaku* **58**, 161.
- Yokokawa, H., Sakai, N., Kawada, T., Dokiya, M., 1991a. *J. Electrochem. Soc.* **138** (4), 1018.
- Yokokawa, H., Sakai, N., Kawada, T., Dokiya, M., 1991b. *J. Electrochem. Soc.* **138**, 2719.
- Yokokawa, H., Horita, T., Sakai, N., Kawada, T., Dokiya, M., 1994. In: Bossell, U. (Ed.), *Proc. First European Solid Oxide Fuel Cell Forum*, 3–7 October 1994, Lucerne, Switzerland, p. 425.
- Zhang, X., Ohara, S., Maric, R., Mukai, K., Fukui, T., Yoshida, H., Nishimura, M., Inagaki, T., Miura, K., 1999. *J. Power Sources* **83**, 170.
- Zhou, H.B., Taira, H., Takagi, H., Tomono, K., 1996. *J. Soc. Mat. Sci. Jpn.* **45** (6), 13.

This page intentionally left blank

Chapter 224

OXO-SELENATES OF RARE EARTH ELEMENTS

Mathias S. WICKLEDER

*Institut für Reine und Angewandte Chemie, Carl von Ossietzky Universität Oldenburg,
D-26111 Oldenburg, Germany*

Contents

1. Introduction	45	3.1.3. SeO ₂ -rich and SeO ₂ -poor oxo-selenates(IV)	72
1.1. Nomenclature and scope	45	3.1.4. Oxo-selenate(IV)-hydrates and acidic oxo-selenates(IV)	73
1.2. Some generalities on SeO ₄ ²⁻ and SeO ₃ ²⁻	47	3.2. Anionic derivatives of oxo-selenates(IV)	77
2. Oxo-selenates(VI)	48	3.2.1. General remarks and syntheses	77
2.1. Binary oxo-selenates(VI)	48	3.2.2. Halide-oxo-selenates(IV)	81
2.1.1. Anhydrous oxo-selenates(VI)	48	3.2.3. Oxide-halide oxo-selenates(IV)	84
2.1.2. Oxo-selenate(VI)-hydrates	49	3.2.4. Derivatives with complex anions	88
2.1.3. Acidic oxo-selenates(VI)	55	3.3. Cationic derivatives of selenates(IV)	88
2.2. Ternary oxo-selenates(VI)	57	3.3.1. Alkali metal containing oxo-selenates(IV)	88
2.2.1. Anhydrous ternary oxo-selenates(VI)	57	3.3.2. Transition metal containing oxo-selenates(IV)	91
2.2.2. Hydrates of ternary oxo-selenates(VI)	59	3.4. Properties of oxo-selenates(IV)	94
2.3. Properties of oxo-selenates(VI)	61	3.4.1. Thermal behaviour of oxo-selenates(IV)	94
2.3.1. Thermal behaviour of oxo-selenates(VI)	61	3.4.2. Vibrational spectra of oxo-selenates(IV)	96
2.3.2. Vibrational spectra of oxo-selenates(VI)	63	3.4.3. Thermochemical investigations of oxo-selenates(IV)	97
2.3.3. Miscellaneous	65	4. Mixed-valent oxo-selenates(VI/IV)	99
3. Oxo-selenates(IV)	65	Acknowledgements	102
3.1. Binary oxo-selenates(IV)	65	References	102
3.1.1. Syntheses	65		
3.1.2. The oxo-selenates(IV) R ₂ (SeO ₃) ₃	67		

1. Introduction

1.1. Nomenclature and scope

The most important sources of rare earth elements in nature are silicates, phosphates and carbonates. They have low solubilities and are chemically quite inert. Therefore, especially

silicates and phosphates, play an important role as storage materials in nuclear waste management (McCarthy et al., 1978; Boatner et al., 1980; Petek et al., 1982) and are well investigated (Felsche, 1973; Wickleder, 2002a). There are other fields in which complex oxo-anions were also of great importance in rare earth chemistry. For example in the early days of lanthanide separation the crucial process was the fractional crystallization of ternary nitrates or sulfates (Prandtl, 1938). And even the break-through in rare earth separation techniques, the development of liquid–liquid extraction and chromatographic methods, is based on rare earth compounds with complex anions, in this case for example tributylphosphates and polycarboxylates (Bock, 1950). Also, more recently, compounds of the rare earth elements containing complex oxo-anions have attracted considerable attention for several reasons. One point of current interest is the thermal behaviour of the rare earth compounds and their potential as precursors for the preparation of lanthanide oxides with large surfaces for catalytic purposes (Brezeanu et al., 1999). Namely, the thermally labile nitrates and perchlorates are suitable candidates. Another point of recent research is the development of new non-centrosymmetric compounds and the investigation of their non-linear optical (NLO) properties (Vigdorichik and Malinovskii, 1990, 1995; Held et al., 2000).

With respect to all of these specific aspects and the large variety of complex anions, the number of respective rare earth compounds is huge. A review that tries to cover the whole area comprehensively necessarily may not be very detailed. Several of such reviews have been published within the last decades and they provide an excellent view over this still growing field (Gmelin, 1980–1984; Wickleder, 2002a). This handbook offers also several chapters with a substantial amount of information concerning complex rare-earth based compounds (Thompson, 1979; Leskelä and Niinistö, 1986; Niinistö and Leskelä, 1987). Therefore, in the present chapter we will restrict ourselves to a part of the whole area, i.e. the oxo-selenates of rare earth elements. On one hand this allows us to cover necessary details without being beyond the scope of this review. On the other hand the family of rare earth oxo-selenates has grown remarkably over the last few years as a result of their rich structural chemistry and complex thermal behaviour. Nevertheless, our knowledge is still incomplete and interesting areas of the field have not been investigated at all. To name only one: oxo-selenates of lanthanides in the lower valent state are not known, even for the typical divalent rare earth ions Eu^{2+} and Yb^{2+} . Owing to the unique properties of divalent lanthanides on one hand and the need of new host lattices for these ions on the other hand, the investigation of their crystal chemistry seems to be challenging.

Generally, oxo-selenates can be classified according to the oxidation state of the selenium atom as oxo-selenates(IV), and oxo-selenates(VI). Besides this systematically correct naming, chemists usually use the terms *selenites* instead of oxo-selenates(IV), and *selenates* instead of oxo-selenates(VI). Therefore, both nomenclatures will be used in parallel throughout this text. Compared to the respective sulfur species, the oxo-selenate(IV) ion is very stable so that numerous compounds with this anion have been prepared. Furthermore, the thermal decomposition of oxo-selenates(VI) leads usually to oxo-selenates(IV), again in contrast to the findings for the decomposition of sulfates. This is especially true for rare earth oxo-selenates(VI), so that thermolysis might be a synthetic route for the preparation of rare earth oxo-selenates(IV).

Consequently, we will start with the description of oxo-selenates(VI) in the first part of this chapter, and then move on to the major part of the article which is dedicated to oxo-selenates(IV). The oxo-selenate(VI) section provides the description of various binary compounds in the first part (section 2.1), and will discuss the respective ternary phases in the second part (section 2.2). Among the properties of oxo-selenates(VI) (section 2.3), the thermal behaviour turns out to be the best investigated one. The oxo-selenate(IV) section also starts with the binary species (section 3.1). These are the best investigated oxo-selenates so far, so that more details can be given, for example on synthesis (section 3.1.1) of the $R_2(SeO_3)_3$ type compounds (section 3.1.2) which are completely known. Subsequent sections are devoted to the anionic (section 3.2) and cationic (section 3.3) derivatives of oxo-selenates(IV) and finally, properties of oxo-selenates(IV) will be discussed. The last section summarizes our present knowledge of mixed-valent oxo-selenates(IV/VI) which, unfortunately, remains limited.

Most of the sections contain structural data. The structural details are supported by a number of tables summarizing important crystallographic information. Only those data that have been obtained reliably, usually by X-ray single crystal diffraction or high quality X-ray powder diffraction, are considered. For some compounds the structure determinations has been carried out several times. In these cases the tables will contain all data for comparison.

The structure descriptions will emphasize important characteristic features like coordination numbers and geometry, connection of polyhedra and selected bond distances. One of the most helpful tools to symbolize the connectivity within a structure is the formalism of *Niggli*. This system allows the specification of the mutual adjunction of atoms or atom groups, and of the dimensionality of the structure that results from the linkage. For example the *Niggli* formula ${}^3_{\infty}[Ce(SeO_4)_{8/4}]$ means, that one cerium atom is surrounded by eight SeO_4^{2-} groups, and these are attached to four cerium atoms forming an infinite three-dimensional network. For selected compounds the structural description is supported by appropriate figures. For convenience of the reader they all have been drawn in the same style: the SeO_4^{2-} ions are always represented as polyhedra (tetrahedra); the bonds within SeO_3^{2-} or $Se_2O_5^{2-}$ groups are emphasized as dark-grey lines; the trivalent rare earth ions are black, additional cations or anions are usually shown as white spheres.

Most of the properties of oxo-selenates that have been investigated so far represent vibrational spectroscopy and thermal behaviour, and only occasionally other types of measurements have been performed. The most interesting ones among the latter are thermochemical measurements in the systems R_2O_3/SeO_2 or $R_2O_3/RCI_3/SeO_2$ including the development of phase diagrams. The discussion of these findings will also be supported by a number of tables providing the most important data.

1.2. Some generalities on SeO_4^{2-} and SeO_3^{2-}

The anions SeO_4^{2-} and SeO_3^{2-} are isomorphous with their respective sulfur analogues. The selenate group shows ideal tetrahedral symmetry (point group T_d) with four identical distances $Se^{VI}-O$ of about 1.64 Å. The free selenite ion has a pyramidal shape (C_{3v} symmetry) owing to the lone electron pair at the selenium atom. Thus, the SeO_3^{2-} ion can be treated as a *pseudo*-tetrahedral anion and the lone electron pair often acts as an invisible ligand within

the crystal structures of selenites. This observation is called the stereochemical activity of the lone electron pair and it will turn out as one of the most striking structural features of rare earth oxo-selenates(IV). The distances $\text{Se}^{\text{IV}}\text{-O}$ within the SeO_3^{2-} ion are about 1.73 Å and the angles O-Se-O are 103° . Due to the different coordination modes of selenate and selenite ions the ideal symmetry is usually severely distorted in the salts of these anions. This is also reflected by the distances Se-O that may vary by about ± 0.1 Å depending of the coordination of the oxygen atoms. By the same orders of magnitude, the bond lengths increase if hydrogen atoms are attached to the oxygen atoms, forming HSeO_4^- and HSeO_3^- ions, respectively. Thus, inspection of the distances Se-O and the coordination of the oxygen atoms usually allows to distinguish between HSeO_4^- and SeO_4^{2-} as well as between HSeO_3^- and SeO_3^{2-} , respectively, even if hydrogen atoms could not be located.

In contrast with the findings for sulfur, the tetravalent state is much more stable for selenium. The reduction potential of the couple $\text{SeO}_4^{2-}/\text{SeO}_3^{2-}$ is only 0.03 V in alkaline solution while the respective value is 0.12 V for the couple $\text{SO}_4^{2-}/\text{SO}_3^{2-}$. Therefore, the selenite ion is much less reducing than the sulfite ions and, in turn, selenates are strong oxidizers (Bard and Parsons, 1985).

Common routes for the synthesis of selenates and selenites are the reactions of oxides or carbonates with H_2SeO_4 and H_2SeO_3 , respectively. Selenic acid, H_2SeO_4 , is most conveniently obtained from SeO_2 and H_2O_2 (Brauer, 1975). The disadvantage of this procedure is, that one usually obtains hydrates or, at higher acid concentrations, hydrogenselenates or hydrogenselenites. Because both oxides SeO_3 and SeO_2 are solids under ambient conditions, solid state reactions with the respective metal oxides are an alternative route to prepare the anhydrous compounds. This method works especially well for SeO_2 that has a melting point of 340°C , while for SeO_3 (m.p. 118°C) the low decomposition temperature of 185°C ($\text{SeO}_3 \rightarrow \text{SeO}_2 + 1/2\text{O}_2$) may cause some difficulties.

Finally, I would like to mention some safety aspects. Selenium compounds are poisonous and it is strongly recommended to work always in a well ventilated hood, and one should especially avoid swallowing the powder dust of selenium compounds. Oxo-selenates decompose at high temperatures what should be taken into account if reactions are carried out in closed systems. Oxo-selenates(VI) and in particular selenic acid, H_2SeO_4 , are very strong oxidizers. This should be carefully considered throughout the preparative work, especially if oxidizable components are involved in the reactions.

2. Oxo-selenates(VI)

2.1. Binary oxo-selenates(VI)

2.1.1. Anhydrous oxo-selenates(VI)

Selenates of the rare earth elements are usually obtained from reactions of the respective oxides with selenic acid. In most cases, this procedure does not lead to the anhydrous compounds but to hydrates, $\text{R}_2(\text{SeO}_4)_3 \cdot x\text{H}_2\text{O}$. Accordingly, the anhydrous species are poorly investigated. The only exceptions are $\text{Sc}_2(\text{SeO}_4)_3$, $\text{Yb}_2(\text{SeO}_4)_3$, and $\text{Ce}(\text{SeO}_4)_2$ that have been obtained

even from aqueous solutions under special conditions: $\text{Sc}_2(\text{SeO}_4)_3$ crystallizes if the pH value is carefully adjusted by adding LiOH to the solution (Valkonen, 1978a) and single crystals of $\text{Yb}_2(\text{SeO}_4)_3$ grow if the temperature is kept at 90 °C (Iskhakova and Ovanisyan, 1995). According to X-ray single crystal determinations, $\text{Sc}_2(\text{SeO}_4)_3$ and $\text{Yb}_2(\text{SeO}_4)_3$ are isotypic and have monoclinic symmetry (the structures have been described with different settings of space group $P2_1/c$, see table 1). The selenates show the R^{3+} ions in octahedral coordination of oxygen atoms that belong to six monodentate SeO_4^{2-} groups. The SeO_4^{2-} ions are coordinated by four R^{3+} ions as might be expressed by the formulation $\text{R}(\text{SeO}_4)_{6/4}$ ($\equiv \text{R}_2(\text{SeO}_4)_3$) according to Niggli's formalism. The crystal structure can be seen as a three-dimensional network of $[\text{RO}_6]$ octahedra and $[\text{SeO}_4]$ tetrahedra connected via all vertices. This connectivity motive of polyhedra is also known for the respective sulfates, $\text{Sc}_2(\text{SO}_4)_3$ and $\text{Yb}_2(\text{SO}_4)_3$, but the symmetries are higher for the latter, $R\bar{3}$ and $Pbcn$, respectively (Wickleder, 2000a). However, as can be seen from the lattice parameters given in table 1, the deviations from the orthorhombic symmetry are only small for $\text{Sc}_2(\text{SeO}_4)_3$ (when transformed to $P2_1/n$) and $\text{Yb}_2(\text{SeO}_4)_3$, and phase transitions might occur. This has been shown for $\text{Er}_2(\text{SeO}_4)_3$ by means of temperature dependent powder diffraction experiments (Krügermann and Wickleder, 2004): when $\text{Er}_2(\text{SeO}_4)_3$ is prepared by dehydration of $\text{Er}_2(\text{SeO}_4)_3 \cdot 8\text{H}_2\text{O}$, it forms in the trigonal-rhombohedral modification of $\text{Sc}_2(\text{SO}_4)_3$ and transforms at higher temperatures to the orthorhombic structure of $\text{Er}_2(\text{SO}_4)_3$ (see section 2.3.1). As can be seen from fig. 1, in the two modifications the connectivity of the polyhedra remains the same and only their orientation with respect to each other changes.

Another interesting feature of the crystal structures is that they can be seen as analogues of simple A_2B_3 type compounds with complex anions: if the tetrahedral anions are regarded as spheres, the trigonal-rhombohedral structure of $\text{Er}_2(\text{SeO}_4)_3$ adopts the Al_2O_3 structure and the orthorhombic $\text{Er}_2(\text{SeO}_4)_3$ modification as well as the monoclinic forms of $\text{Sc}_2(\text{SeO}_4)_3$ and $\text{Yb}_2(\text{SeO}_4)_3$ are the complex variant of Rh_2S_3 . $\text{Ce}(\text{SeO}_4)_2$ has been obtained in form of yellow single crystals (Iskhakova et al., 1990c). The orthorhombic compound is isotypic with $\text{Ce}(\text{SO}_4)_2$ and contains Ce^{4+} ions in coordination of eight monodentate selenate ions with typical bond lengths Ce–O ranging from 2.28 to 2.42 Å. The $[\text{CeO}_8]$ polyhedra are square antiprisms and they are linked with the SeO_4^{2-} tetrahedra to a three-dimensional structure as may be formulated by $\infty^3[\text{Ce}(\text{SeO}_4)_{8/4}]$.

2.1.2. Oxo-selenate(VI)-hydrates

Due to their easy accessibility, hydrates of rare earth selenates have been studied much more intensively than the anhydrous derivatives, and selenate hydrates $\text{R}_2(\text{SeO}_4)_3 \cdot x\text{H}_2\text{O}$ with x ranging from 1 to 12 have been reported (Nabar and Paralkar, 1976a; Giolito and Giesbrecht, 1969; Petrov et al., 1969, 1970; Rosso and Perret, 1970; Hájek et al., 1979; Smolyakova et al., 1973; Suponitskii et al., 1969; Gupta et al., 1982). However, sufficient characterizations have not been undertaken in any case, and only hydrates with $x = 4, 5, 8, 9,$ and 12 can be seen to exist without any doubt with respect to structure determinations. Among the hydrates the composition $\text{R}_2(\text{SeO}_4)_3 \cdot 8\text{H}_2\text{O}$ is the most investigated one, probably because it crystallizes preferably from aqueous solutions. Depending on the size of R^{3+} , the octahydrates are known to occur in two slightly different monoclinic mod-

Table 1
Crystallographic data of binary oxo-selenates(VI)

Compound	Space group	Lattice parameters					Reference	
		a (Å)	b (Å)	c (Å)	α (deg)	β (deg)		γ (deg)
Sc ₂ (SeO ₄) ₃	<i>P2₁/c</i>	8.899(2)	9.212(2)	15.179(3)		124.83(2)	Valkonen, 1978a	
Yb ₂ (SeO ₄) ₃	<i>P2₁/n</i>	9.220(2)	9.521(2)	12.886(3)		91.04(1)	Iskhakova and Ovanisyan, 1995	
Ce(SeO ₄) ₂	<i>Pbca</i>	9.748(2)	9.174(1)	13.740(3)			Iskhakova et al., 1990c	
La ₂ (SeO ₄) ₃ ·12H ₂ O	<i>C2/c</i>	10.670(2)	20.390(6)	10.740(2)		110.12(2)	Karvinen and Niinistö, 1986	
Nd ₂ (SeO ₄) ₃ ·8H ₂ O-I	<i>C2/c</i>	7.102(1)	13.992(2)	18.253(3)		99.84(2)	Krügermann, 2002	
Sm ₂ (SeO ₄) ₃ ·8H ₂ O-I	<i>C2/c</i>	7.014(1)	13.878(1)	18.121(2)		99.40(1)	Ovanisyan et al., 1988a	
Sm ₂ (SeO ₄) ₃ ·8H ₂ O-I	<i>C2/c</i>	7.0218(7)	13.898(2)	18.154(2)		99.357(8)	Krügermann, 2002	
Eu ₂ (SeO ₄) ₃ ·8H ₂ O-I	<i>C2/c</i>	7.004(1)	13.889(2)	18.167(3)		99.37(2)	Krügermann, 2002	
Gd ₂ (SeO ₄) ₃ ·8H ₂ O-I	<i>C2/c</i>	7.007(1)	13.868(3)	18.146(3)		99.14(2)	Krügermann, 2002	
Tb ₂ (SeO ₄) ₃ ·8H ₂ O-I	<i>C2/c</i>	6.972(2)	13.824(2)	18.104(4)		99.10(3)	Krügermann, 2002	
Ho ₂ (SeO ₄) ₃ ·8H ₂ O-II	<i>C2/c</i>	13.763(2)	6.8964(8)	18.646(2)		101.96(2)	Krügermann, 2002	
Er ₂ (SeO ₄) ₃ ·8H ₂ O-II	<i>C2/c</i>	13.728(2)	6.8751(7)	18.602(3)		101.85(2)	Krügermann and Wickleder, 2004	
Yb ₂ (SeO ₄) ₃ ·8H ₂ O-II	<i>C2/c</i>	13.704(6)	6.831(3)	18.507(7)		101.90(3)	Hiltunen and Niinistö, 1976	
Yb ₂ (SeO ₄) ₃ ·8H ₂ O-II	<i>C2/c</i>	13.751(2)	6.8544(9)	18.549(2)		101.80(2)	Krügermann, 2002	
Y ₂ (SeO ₄) ₃ ·8H ₂ O-II	<i>C2/c</i>	13.772(2)	6.883(1)	18.650(2)		101.84(2)	Krügermann, 2002	
Sc ₂ (SeO ₄) ₃ ·5H ₂ O-I	<i>P1</i>	11.225(4)	11.804(3)	5.766(2)	91.30(4)	100.10(2)	89.03(7)	Valkonen et al., 1975
Sc ₂ (SeO ₄) ₃ ·5H ₂ O-I	<i>P$\bar{1}$</i>	5.789(1)	11.239(1)	11.851(1)	89.12(1)	88.81(1)	79.84(1)	Krügermann, 2002
Sc ₂ (SeO ₄) ₃ ·5H ₂ O-II	<i>P$\bar{1}$</i>	9.109(1)	10.631(1)	17.286(2)	72.21(1)	79.84(1)	89.87(1)	Krügermann, 2002
La ₂ (SeO ₄) ₃ ·5H ₂ O	<i>P2₁/a</i>	9.879(1)	14.199(2)	10.761(1)		92.78(2)	Krügermann, 2002	
Ce ₂ (SeO ₄) ₃ ·5H ₂ O	<i>P2₁/a</i>	9.820(3)	14.050(5)	10.690(5)		92.00(4)	Aslanov et al., 1973	
Ce ₂ (SeO ₄) ₃ ·5H ₂ O	<i>P2₁/c</i>	10.722(2)	14.101(2)	9.876(1)		93.18(2)	Krügermann, 2002	
Pr ₂ (SeO ₄) ₃ ·5H ₂ O	<i>P2₁/c</i>	10.659(2)	14.046(4)	9.851(2)		93.02(2)	Krügermann, 2002	
Pr ₂ (SeO ₄) ₃ ·4H ₂ O-I	<i>P2₁/n</i>	13.367(2)	7.404(1)	13.670(2)		92.11(2)	Iskhakova and Makarevich, 1996	
Gd ₂ (SeO ₄) ₃ ·4H ₂ O-II	<i>P$\bar{1}$</i>	6.947(1)	9.317(2)	10.882(2)	94.81(2)	106.88(2)	99.33(2)	Krügermann, 2002
La(HSeO ₄) ₃	<i>P6₃/m</i>	9.717(1)		6.1698(8)				Göhausen and Wickleder, 2001
Gd(HSeO ₄)(SeO ₄)	<i>Pbca</i>	9.204(1)	13.516(2)	10.040(1)				Göhausen and Wickleder, 2001
Eu(HSeO ₄)(SeO ₄)	<i>Pbca</i>	9.232(5)	13.514(6)	10.061(4)				Iskhakova et al., 1991
Nd(HSeO ₄)(Se ₂ O ₇)	<i>Pna2₁</i>	11.275(2)	6.1836(7)	12.281(2)				Wickleder, 2001
ScH(SeO ₄) ₂ ·2H ₂ O	<i>C2/m</i>	8.708(5)	5.632(4)	9.105(9)		101.64(7)		Valkonen, 1978b
(H ₅ O ₂)Sc(SeO ₄) ₂	<i>C2/m</i>	8.6835(8)	5.6139(6)	9.080(1)		101.75(2)		Krügermann, 2002
H ₃ OCE ^{III} Ce ^{IV} (SeO ₄) ₄	<i>Cc</i>	12.297(2)	16.267(2)	9.295(1)		129.51(1)		Iskhakova and Tursina, 1989

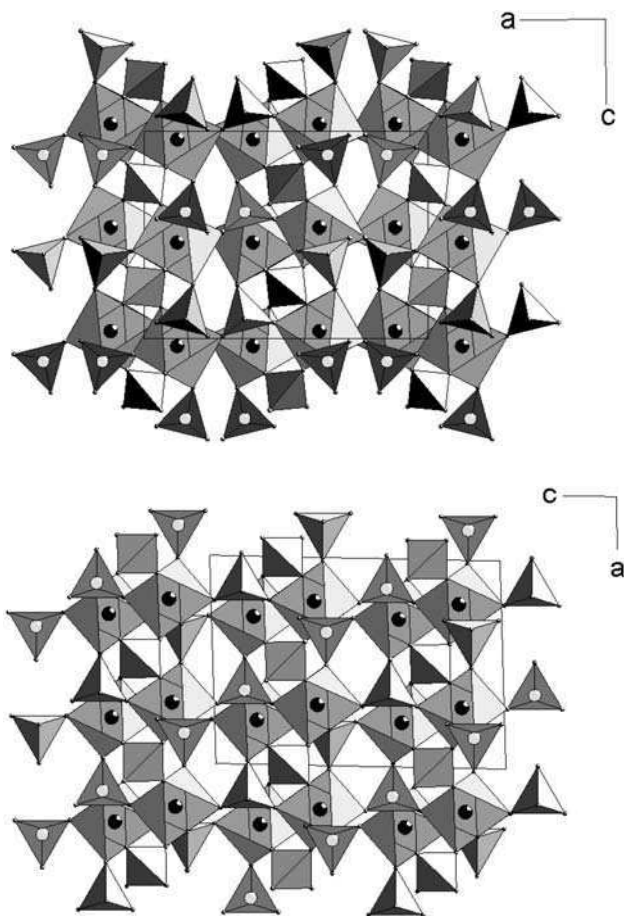


Fig. 1. Crystal structures of the trigonal-rhombohedral (bottom) and the orthorhombic modification (top) of $\text{Er}_2(\text{SeO}_4)_3$. Note, that in both forms the connectivity of $[\text{ErO}_8]$ octahedra (light grey) and SeO_4^{2-} tetrahedra (dark grey) remains the same.

ifications (table 1), which should be named $\text{R}_2(\text{SeO}_4)_3 \cdot 8\text{H}_2\text{O}$ -I and $\text{R}_2(\text{SeO}_4)_3 \cdot 8\text{H}_2\text{O}$ -II, respectively (Hiltunen and Niinistö, 1976; Ovanisyan et al., 1988a; Krügermann, 2002; Krügermann and Wickleder, 2004). Modification I has been observed for the larger rare earth elements $\text{R} = \text{Nd-Tb}$, modification II for $\text{R} = \text{Ho-Yb}$, and Y. In both structures the R^{3+} ions are in eightfold coordination of oxygen atoms that belong to four monodentate SeO_4^{2-} ions and four H_2O molecules. The $[\text{RO}_8]$ polyhedra are distorted dodecahedra and are linked by the selenate groups into two-dimensional layers according to $\infty^2[\text{R}(\text{H}_2\text{O})_{4/1}(\text{Se}(1)\text{O}_4)_{3/3}(\text{Se}(2)\text{O}_4)_{1/2}]$. This means that two crystallographically different selenate ions are present in the ratio of 3:1: $\text{Se}(1)\text{O}_4^{2-}$ is coordinated by three R^{3+} ions while

$\text{Se}(2)\text{O}_4^{2-}$ has only two R^{3+} neighbours. The non-coordinating vertices of the tetrahedra act as acceptors in hydrogen bonds that hold the sheets together. The donors for the hydrogen bonds are water molecules. The difference in the two modifications of the octahydrates is mainly in the arrangement of the layers with respect to each other, as can be seen from fig. 2.

There is one example of a highly hydrated rare earth selenate: $\text{La}_2(\text{SeO}_4)_3 \cdot 12\text{H}_2\text{O}$. It has been obtained from an aqueous solution when the crystallization was carried out at 0°C (Karvinen and Niinistö, 1986). In contrast to the octahydrates, only half of the twelve independent H_2O molecules are bonded to La^{3+} ions while the remaining half are crystal water molecules. The coordination number of La^{3+} is eight and it arises from five monodentate selenate ions and three water molecules. One part of the SeO_4^{2-} ions connects four La^{3+} with each other, a second one only three. This leads to infinite chains running along the c-axis of the monoclinic unit cell. The chains can be formulated according to $\infty^1[\text{La}(\text{H}_2\text{O})_{3/1}(\text{Se}(1)\text{O}_4)_{2/4}(\text{Se}(2)\text{O}_4)_{3/3}]$. The crystal water molecules are fixed in between these chains via hydrogen bonds, wherein the non-coordinating oxygen atoms of $\text{Se}(2)\text{O}_4^{2-}$ are the acceptors.

Crystal structure determinations are available for the pentahydrates $\text{R}_2(\text{SeO}_4)_3 \cdot 5\text{H}_2\text{O}$ ($\text{R} = \text{La}, \text{Ce}, \text{Pr}$) (Aslanov et al., 1973; Krügermann, 2002), and two modifications of $\text{Sc}_2(\text{SeO}_4)_3 \cdot 5\text{H}_2\text{O}$ (Valkonen et al., 1975; Krügermann, 2002) (table 1). The hydrates of the larger lanthanides are isotypic with each other and contain two crystallographically different R^{3+} ions in the structure that are coordinated by nine and eight oxygen atoms, respectively. The selenate groups are highly connecting due to their partly chelating coordination modes, leading to a three-dimensional network. Only four H_2O molecules are bonded to R^{3+} ions, the fifth resides in empty cavities of the structure.

For $\text{Sc}_2(\text{SeO}_4)_3 \cdot 5\text{H}_2\text{O}$ two modifications are known. $\text{Sc}_2(\text{SeO}_4)_3 \cdot 5\text{H}_2\text{O}$ -I has been reported for the first time some thirty years ago and the non-centrosymmetric space group $P1$ had been given (Valkonen et al., 1975). As it has been shown recently, however, the correct space group is in fact $P\bar{1}$ (Krügermann, 2002). In the crystal structure of $\text{Sc}_2(\text{SeO}_4)_3 \cdot 5\text{H}_2\text{O}$ -I three different Sc^{3+} ions are present. Two of those are located on the special sites $1f$ and $1d$ of that space group, respectively. They are coordinated by four monodentate selenate ions and two H_2O molecules. The third occupies a general position and has three H_2O and just as many SeO_4^{2-} ligands. The linkage of the Sc^{3+} ions via selenate groups leads to a three-dimensional network. This is in contrast to the crystal structure of $\text{Sc}_2(\text{SeO}_4)_3 \cdot 5\text{H}_2\text{O}$ -II, which is also triclinic (space group $P\bar{1}$) but contains only two crystallographically different Sc^{3+} ions. Both of them are octahedrally coordinated by oxygen atoms. For $\text{Sc}(1)^{3+}$, these atoms belong to six monodentate selenate groups that are further coordinated to three $\text{Sc}(1)^{3+}$ ions yielding *anionic* sheets according to $\infty^2[\text{Sc}(1)(\text{SeO}_4)_{6/3}]^-$. The second scandium ion, $\text{Sc}(2)^{3+}$, is surrounded by three SeO_4^{2-} ions and three H_2O molecules. Again, the SeO_4^{2-} groups are linked to three $\text{Sc}(2)^{3+}$ ions leading to *cationic* layers according to $\infty^2[\text{Sc}(2)(\text{H}_2\text{O})_{3/1}(\text{SeO}_4)_{3/3}]^+$. Cationic and anionic layers alternate along $[001]$. The remaining two H_2O molecules are located between these layers. Fig. 3 compares the two modifications of $\text{Sc}_2(\text{SeO}_4)_3 \cdot 5\text{H}_2\text{O}$.

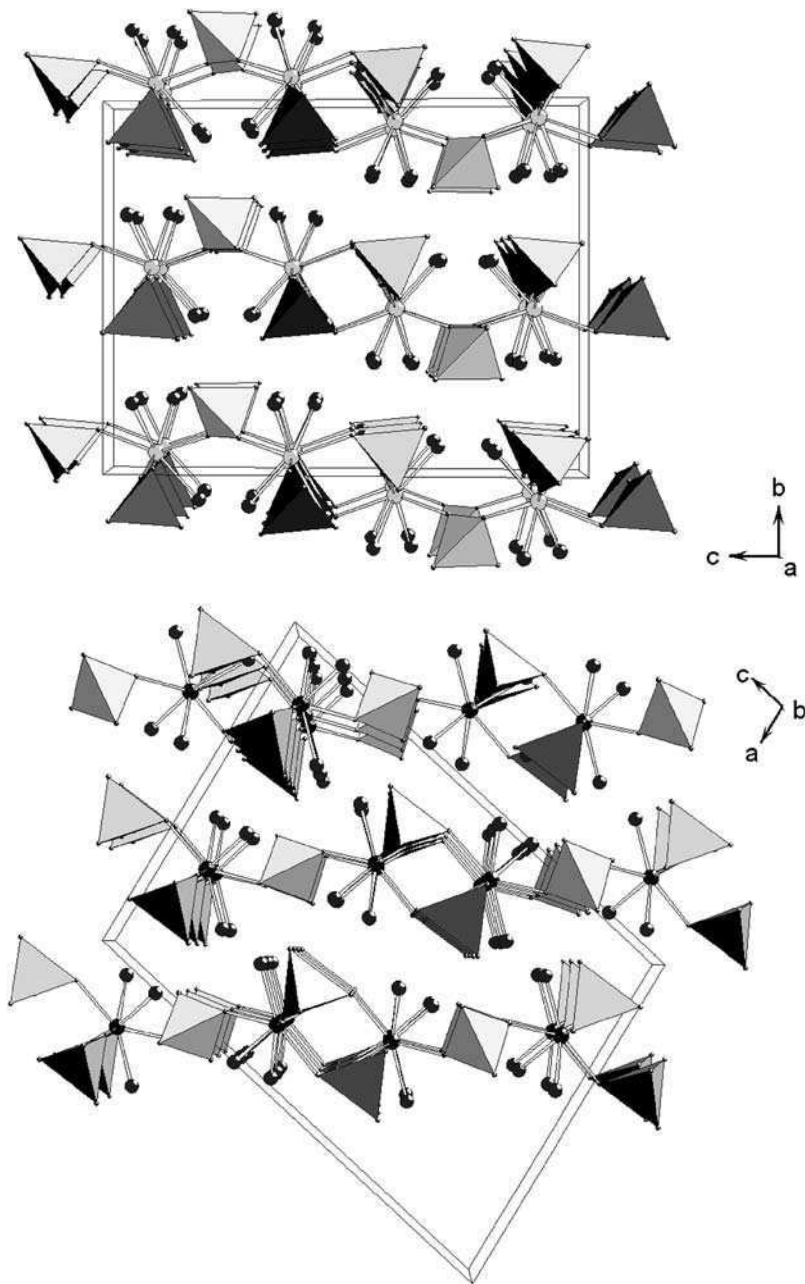


Fig. 2. Stacking of the layers $\infty^2[\text{R}(\text{H}_2\text{O})_{4/1}(\text{Se}(1)\text{O}_4)_{3/3}(\text{Se}(2)\text{O}_4)_{1/2}]$ in $\text{R}_2(\text{SeO}_4)_3 \cdot 8\text{H}_2\text{O}$ -I (top: R = Nd–Tb) and $\text{R}_2(\text{SeO}_4)_3 \cdot 8\text{H}_2\text{O}$ -II (bottom: R = Ho–Yb, Y).

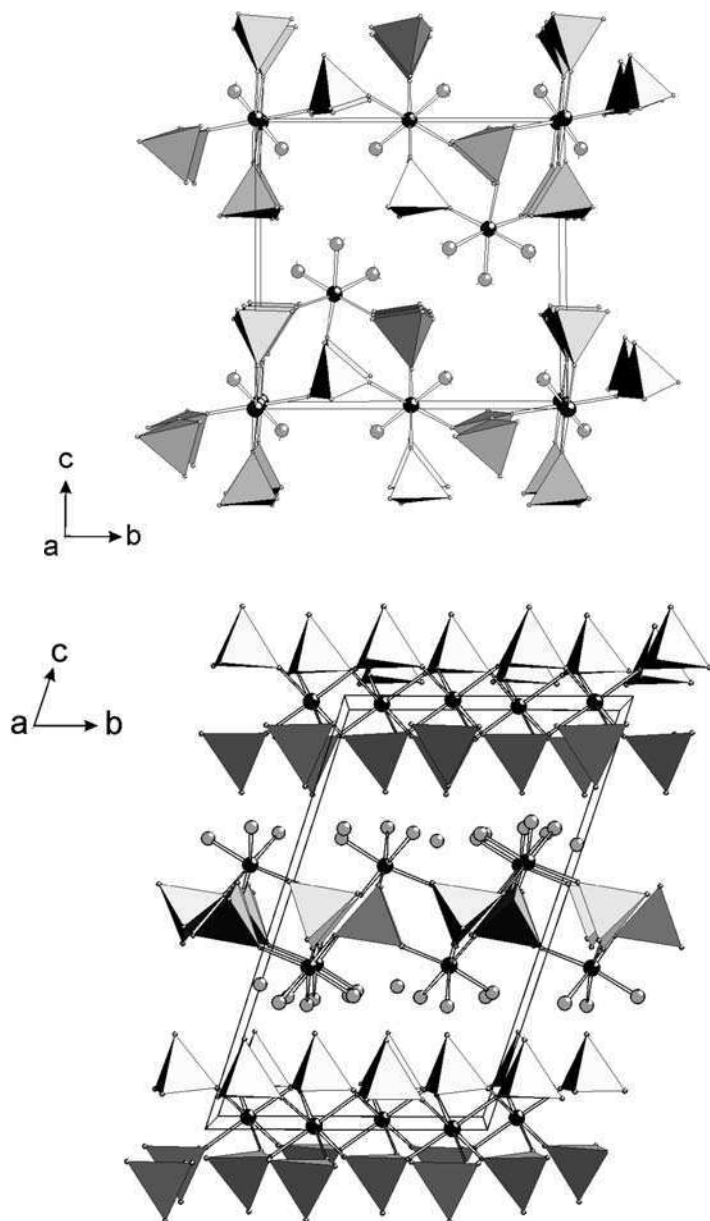


Fig. 3. Crystal structures of the two modifications of $\text{Sc}_2(\text{SeO}_4)_3 \cdot 5\text{H}_2\text{O}$. In modification I (above) all of the H_2O molecules are coordinated to Sc^{3+} ions, while in modification II (below) some of them are situated between the cationic and anionic layers of the composition ${}_{\infty}^2[\text{Sc}(2)(\text{H}_2\text{O})_{3/1}(\text{SeO}_4)_{3/3}]^+$ and ${}_{\infty}^2[\text{Sc}(1)(\text{SeO}_4)_{6/3}]^-$, respectively.

The selenate hydrates with the lowest water content that have been structurally characterized are $\text{Pr}_2(\text{SeO}_4)_3 \cdot 4\text{H}_2\text{O}$ (Iskhakova and Makarevich, 1996) and $\text{Gd}_2(\text{SeO}_4)_3 \cdot 4\text{H}_2\text{O}$ (Krügermann, 2002). They have different crystal structures, as can be predicted from the much different ionic radii of Pr^{3+} and Gd^{3+} . Consequently, the two forms should be named again as modification I and II, respectively. The praseodymium compound shows the Pr^{3+} ion in eightfold coordination of oxygen atoms that belong to two H_2O molecules and five SeO_4^{2-} ions. One of the selenate groups acts as chelating ligand. The selenate ions are surrounded by four and three Pr^{3+} ions, respectively, resulting in a three-dimensional structure, which can be described by ${}^3_{\infty}[\text{Pr}(\text{H}_2\text{O})_{2/1}(\text{Se}(1)\text{O}_4)_{3/3}(\text{Se}(2)\text{O}_4)_{2/4}]$. According to the smaller size of Gd^{3+} compared to Pr^{3+} , the structure of $\text{Gd}_2(\text{SeO}_4)_3 \cdot 4\text{H}_2\text{O}$ is different and coordination numbers of only eight and seven, respectively, are found for the cations. For $\text{Gd}(1)^{3+}$, a square antiprismatic $[\text{GdO}_8]$ polyhedron is found due to the coordination of five monodentate selenate ions and three H_2O molecules. The seven oxygen atoms coordinating $\text{Gd}(2)^{3+}$ are provided by six SeO_4^{2-} groups and one water molecule, and the coordination polyhedron is a monocapped trigonal prism. Two of the three crystallographically different SeO_4^{2-} ions link four Gd^{3+} ions with each other, and the third is attached to three Gd^{3+} ions. Furthermore, significant hydrogen bonding is observed in the crystal structure.

2.1.3. Acidic oxo-selenates(VI)

Hydrogen selenates of the rare earth elements can be obtained by the reaction of sesquioxides and concentrated selenic acid. However, the high viscosity of the acid complicates the growth of single crystals so that only for one compound, $\text{La}(\text{HSeO}_4)_3$, a structure determination has been performed (Göhausen and Wickleder, 2001). It shows the La^{3+} ion in tricapped-trigonal-prismatic coordination of oxygen atoms that belong to nine monodentate HSeO_4^- ions. Each hydrogen selenate group connects three La^{3+} ions with each other according to the formulation ${}^3_{\infty}[\text{La}(\text{HSeO}_4)_{9/3}]$. In this way, rods are formed that are running along the c-axis of the hexagonal unit cell (fig. 4). Linkage of the rods occurs in the hexagonal plane and leads to channels that are also running in c-direction and provide enough space for the hydrogen atoms. If the complex anions are regarded as spheres, the UCl_3 structure can be extracted as the parent structure of $\text{La}(\text{HSeO}_4)_3$.

The isotopic hydrogen-selenate-selenates $\text{Gd}(\text{HSeO}_4)(\text{SeO}_4)$ and $\text{Eu}(\text{HSeO}_4)(\text{SeO}_4)$ are formed in the reaction of the respective oxides with diluted selenic acid (70%) (Iskhakova et al., 1991; Göhausen and Wickleder, 2001). They contain the R^{3+} ions in eightfold coordination of oxygen atoms which belong to four selenate and four hydrogen-selenate groups. Each of the anions is attached to four R^{3+} ions leading to a three-dimensional structure. The hydrogen atom of the HSeO_4^- group is involved in an asymmetric bifurcated hydrogen bond. It is worthwhile to mention, that in contrast to $\text{La}(\text{HSeO}_4)_3$, the OH group of the hydrogen selenate ion is coordinated to a metal ion in the structure of the hydrogen selenate-selenates.

A unique acidic selenate is the mixed hydrogen selenate-diselenate $\text{Nd}(\text{HSeO}_4)(\text{Se}_2\text{O}_7)$ (Wickleder, 2001). It is the only diselenate of the rare earth elements so far. In the crystal structure, Nd^{3+} is surrounded by six $\text{Se}_2\text{O}_7^{2-}$ and three HSeO_4^- ions. The anions are monodentate and tricapped trigonal prisms $[\text{NdO}_9]$ are formed. These are linked to chains in di-

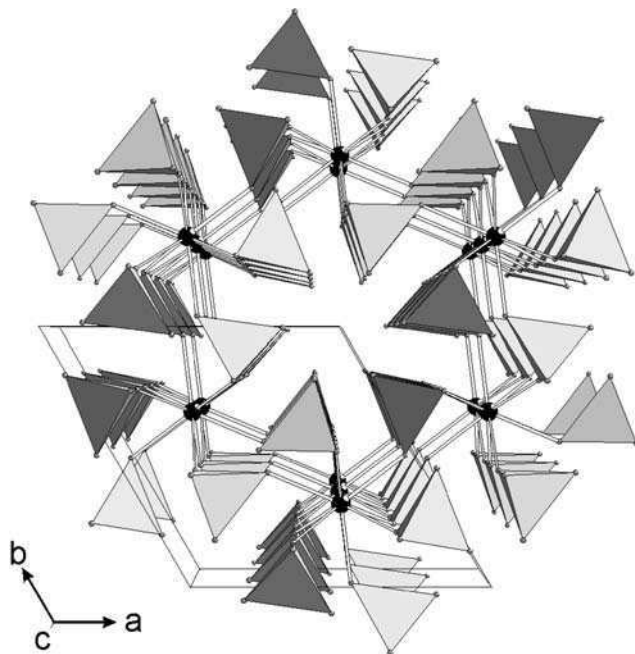


Fig. 4. Perspective view of the crystal structure of $\text{La}(\text{HSeO}_4)_3$ along $[001]$. The vertices of the tetrahedra pointing towards the channels are the OH groups of the anions.

rection of the b-axis that are connected further by HSeO_4^- groups in $[001]$, and $\text{Se}_2\text{O}_7^{2-}$ ions in $[100]$ directions. The $\text{Se}_2\text{O}_7^{2-}$ ion shows an angle Se–O–Se of 124° and the distances Se–O to the bridging oxygen atom are 1.78 and 1.79 Å, respectively.

The acidic scandium selenate $\text{ScH}(\text{SeO}_4)_2 \cdot 2\text{H}_2\text{O}$ has been reported long time ago (Valkonen, 1978b). The compound has been obtained from the treatment of Sc_2O_3 with a 20% solution of selenic acid but the structure determination allowed no decision where the hydrogen atom is placed. A reinvestigation of the crystal structure recently showed that the compound contains H_5O_2^+ ions and should preferably be formulated as $(\text{H}_5\text{O}_2)\text{Sc}(\text{SeO}_4)_2$ (Krügermann, 2002). The H_5O_2^+ ions are located between anionic layers of the composition ${}_\infty^2[\text{Sc}(\text{SeO}_4)_{6/3}]^-$ that arise from the connection of $[\text{ScO}_6]$ octahedra and selenate tetrahedra (fig. 5). The bond length of 2.47 Å between the two symmetrically related oxygen atoms of the H_5O_2^+ ion hints at a strong hydrogen bond.

For the element cerium, the mixed valent acidic selenate $(\text{H}_3\text{O})\text{Ce}_2(\text{SeO}_4)_4$ has been described (Iskhakova and Tursina, 1989). The assignment of the different oxidation states of cerium can be done by inspection of the Ce–O distances. Both species, Ce^{3+} and Ce^{4+} , are eightfold coordinated by oxygen atoms. The distances for Ce^{3+} range from 2.41 to 2.55 Å while the respective values for Ce^{4+} are found to lie between 2.25 and 2.41 Å. In the three-

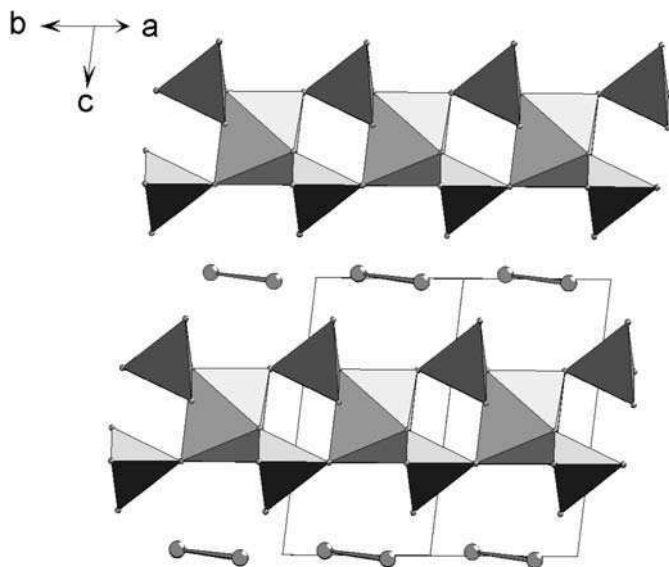


Fig. 5. Crystal structure of $(\text{H}_5\text{O}_2)\text{Sc}(\text{SeO}_4)_2$. The H_5O_2^+ ions are drawn as dumbbells; the distance between the oxygen atoms within the H_5O_2^+ ion is 2.47 Å.

dimensional structure, the selenate groups are connected with the $[\text{CeO}_8]$ polyhedra via vertices and the H_3O^+ ions reside in empty holes of the lattice.

2.2. Ternary oxo-selenates(VI)

2.2.1. Anhydrous ternary oxo-selenates(VI)

Similarly to the binary species, the ternary selenates are frequently obtained as hydrates. They can be easily dehydrated (see section 2.3.1), leading to powder samples of the respective anhydrous selenates. Single crystals could be obtained if the crystallizations are carried out under careful adjustment of concentration, pH value, and temperature. However, the exact influence of these parameters is not known, and in all of the studies reported so far, the crystallization of anhydrous selenates seems to occur accidentally rather than by design. A second route, which necessarily would lead to anhydrous compounds, is the solid state reaction of the respective binary selenates. Unfortunately the decomposition temperature of selenates is quite low (especially when compared with the respective sulfates that can be obtained by solid state reactions), so that frequently *selenites* are obtained instead of the desired products. For these reasons structure determinations of anhydrous ternary selenates are quite rare and much work remains to be done. The few examples of carefully characterized selenates containing alkali metal ions and rare earth ions in a ratio of 1:1 are $\text{KPr}(\text{SeO}_4)_2$, $\text{KDy}(\text{SeO}_4)_2$, and $\text{NaPr}(\text{SeO}_4)_2$ (table 2) (Iskhakova et al., 1990a, 1990b; Ovanisyan and Iskhakova, 1989).

Table 2
Crystallographic data of ternary oxo-selenates(VI)

Compound	Space group	Lattice parameters						Reference
		a (Å)	b (Å)	c (Å)	α (deg)	β (deg)	γ (deg)	
KPr(SeO ₄) ₂	<i>P2</i> ₁ / <i>c</i>	8.823(1)	7.371(1)	11.139(1)		91.33(1)		Iskhakova et al., 1990a
KDy(SeO ₄) ₂	<i>Pna</i> 2 ₁	27.470(2)	5.657(1)	8.989(1)				Iskhakova et al., 1990b
NaPr(SeO ₄) ₂	<i>P</i> $\bar{1}$	6.639(1)	7.118(1)	7.361(1)	99.16(2)	96.93(2)	89.77(3)	Ovanisyan and Iskhakova, 1989
(NH ₄) ₃ Sc(SeO ₄) ₃	<i>R</i> 3	15.567(5)		9.871(3)				Valkonen and Niinistö, 1978
Na _{3,68} Dy _{1,44} (SeO ₄) ₄	<i>I4</i> ₁ / <i>a</i>	10.655(1)		12.290(1)				Ovanisyan et al., 1988b
KEr(SeO ₄) ₂ ·H ₂ O	<i>P</i> $\bar{1}$	5.676(8)	8.611(9)	9.298(8)	108.7(1)	84.1(1)	106.2(1)	Ovanisyan and Iskhakova, 1988
NaLa(SeO ₄) ₂ ·2H ₂ O	<i>P2</i> ₁ / <i>c</i>	11.421(2)	7.135(2)	11.178(2)		107.5(1)		Ovanisyan et al., 1986
NaLa(SeO ₄) ₂ ·2H ₂ O	<i>P2</i> ₁ / <i>c</i>	11.195(2)	7.147(1)	22.253(4)		101.24(2)		Krügermann, 2002
NaCe(SeO ₄) ₂ ·2H ₂ O	<i>P2</i> ₁ / <i>c</i>	11.210(2)	7.1225(9)	22.245(4)		101.54(2)		Krügermann, 2002
NaSm(SeO ₄) ₂ ·2H ₂ O	<i>P2</i> ₁ / <i>c</i>	11.077(2)	7.0353(7)	21.992(2)		101.85(2)		Krügermann, 2002
RbNd(SeO ₄) ₂ ·3H ₂ O	<i>P</i> $\bar{1}$	5.843(1)	7.021(3)	13.261(1)	91.50(4)	95.33(2)	106.76(2)	Gasanov et al., 1985
CsNd(SeO ₄) ₂ ·4H ₂ O	<i>P2</i> ₁ / <i>c</i>	6.850(3)	19.479(5)	8.974(4)		94.80(3)		Ovanisyan et al., 1987a
RbCe(SeO ₄) ₂ ·5H ₂ O	<i>P2</i> ₁ / <i>c</i>	7.200(2)	8.723(1)	19.258(6)		90.88(2)		Ovanisyan et al., 1987b
(NH ₄)Pr(SeO ₄) ₂ ·5H ₂ O	<i>Pccn</i>	7.019(1)	9.865(2)	17.497(2)				Iskhakova, 1995
NaEr(HSeO ₄) ₂ (SeO ₄)·5H ₂ O	<i>Pn</i>	11.158(2)	5.7615(7)	11.389(1)		98.47(2)		Krügermann, 2002

In the crystal structure of $\text{KPr}(\text{SeO}_4)_2$, a ninefold coordination of Pr^{3+} by oxygen atoms is observed. These are provided by five monodentate and two chelating selenate groups. Crystallographically, two selenate ions can be distinguished and they connect three and four Pr^{3+} ions with each other as can be expressed by $\infty^2[\text{Pr}(\text{Se}(1)\text{O}_4)_{3/3}(\text{Se}(2)\text{O}_4)_{4/4}]^-$. In this way, layers are formed that are held together by K^+ ions. The same coordination of the Pr^{3+} ion is found in $\text{NaPr}(\text{SeO}_4)_2$. Nevertheless, the connection of the polyhedra leads in this case to a three-dimensional network that incorporates the Na^+ ions. If the R^{3+} radius is lowered, a new structure is formed as can be seen from the non-centrosymmetric crystal structure of $\text{KDy}(\text{SeO}_4)_2$. The coordination number of Dy^{3+} is eight and it arises from six monodentate and one chelating selenate groups. The linkage of the $[\text{DyO}_8]$ polyhedra and selenate tetrahedra occurs in a way that an open framework is built providing large holes for the incorporation of the K^+ ions.

A different R^{3+}/A^+ ratio is found in the trigonal-rhombohedral crystal structure of $(\text{NH}_4)_3\text{Sc}(\text{SeO}_4)_3$ (Valkonen and Niinistö, 1978). In the crystal structure the Sc^{3+} ions are in sixfold coordination of oxygen atoms and the $[\text{ScO}_6]$ octahedra are linked by selenate ions to one-dimensional anionic chains according to $\infty^1[\text{Sc}(\text{SeO}_4)_{6/2}]^{3-}$. Connection of the chains and charge compensation is achieved by the NH_4^+ ions that are seven and eightfold coordinated, respectively. There is one report on a non-stoichiometric selenate, $\text{Na}_{3.68}\text{Dy}_{1.44}(\text{SeO}_4)_4$. It is said to have a mixed occupation of the cationic sites by Dy^{3+} and Na^+ in the tetragonal crystal structure but the compound needs further characterization (Ovanisyan et al., 1988b).

2.2.2. Hydrates of ternary oxo-selenates(VI)

The hydrates of ternary selenates are usually obtained upon evaporation of a solution of rare earth oxides and, for example, the carbonates of the desired second component. Although there is little challenge in the synthesis, the number of structurally characterized compounds is very limited (table 2), and the exact composition is often not known. This is especially true for the water content, which is difficult to determine accurately by means of most often used thermoanalytical investigations and IR spectroscopy (Ionashiro and Giolito, 1980, 1982a, 1982b; Nabar and Paralkar, 1980; Nabar and Ajgaonkar, 1981a, 1981b, 1982a, 1982b, 1985). Therefore, there are a number of different, and sometimes contradictory, reports. What remains certain is, that in most cases the compounds contain the R^{3+} and A^+ cations in an 1:1 molar ratio, and the water content of the selenates $\text{AR}(\text{SeO}_4)_2 \cdot x\text{H}_2\text{O}$ seems to vary from $x = 0.5$ to $x = 5$. The hydrate with the lowest water content that has been structurally investigated so far is $\text{KEr}(\text{SeO}_4)_2 \cdot \text{H}_2\text{O}$ (Ovanisyan and Iskhakova, 1988). It consists of anionic chains according to $\infty^1[\text{Er}(\text{SeO}_4)_{6/3}(\text{H}_2\text{O})_{1/1}]^-$ that run along the a-axis of the triclinic unit cell. One of the six selenate ions that are coordinated to Er^{3+} acts as chelating ligand so that a coordination number of eight is realized for the cation. The chains are connected with each other by the ninefold coordinated potassium ions.

The dihydrate $\text{NaLa}(\text{SeO}_4)_2 \cdot 2\text{H}_2\text{O}$ has been first reported in 1986 by Ovanisyan et al. (1986). According to this investigation, the La^{3+} ions are in ninefold coordination of five monodentate and one chelating SeO_4^{2-} groups and two water molecules. The linkage of the

polyhedra leads to a three-dimensional network. Unfortunately, the structure determination suffers from some unusually large displacement parameters that could not be explained satisfactory. It was only recently shown that the problem was caused by a superstructure leading to a doubled c-axis (Krügermann, 2002). However, the crystallographically correct model does not change the structural features of the compound. The dihydrates $\text{NaR}(\text{SeO}_4)_2 \cdot 2\text{H}_2\text{O}$ ($\text{R} = \text{Ce}, \text{Sm}$) have been found to be isotypic (Krügermann, 2002).

In the triclinic crystal structure of the trihydrate $\text{RbNd}(\text{SeO}_4)_2 \cdot 3\text{H}_2\text{O}$ the Nd^{3+} ions are eightfold coordinated by three H_2O molecules and five monodentate selenate ions (Gasanol et al., 1985). The latter are surrounded by two and three Nd^{3+} ions, respectively, leading to anionic layers of the composition $\infty^2[\text{Nd}(\text{SeO}_4)_{3/3}(\text{SeO}_4)_{2/2}(\text{H}_2\text{O})_3]^-$ which are held together by the Rb^+ ions.

The coordination polyhedron around Nd^{3+} in the crystal structure of $\text{CsNd}(\text{SeO}_4)_2 \cdot 4\text{H}_2\text{O}$ is a tricapped trigonal prism (Ovanisyan et al., 1987a). Besides three H_2O molecules, six of the nine oxygen atoms belong to two chelating and two monodentate selenate ions. The chelating ions are monodentate to neighboring Nd^{3+} ions and vice versa, so that each anion is coordinated to two rare earth ions as may be expressed by the formulation $\infty^2[\text{Nd}(\text{SeO}_4)_{4/2}(\text{H}_2\text{O})_3]^-$, indicating that layers are formed. These are strongly corrugated and their stacking in b-direction of the monoclinic unit cell leads to voids which are filled by either the Cs^+ ions or the remaining H_2O molecules that are not bonded to Nd^{3+} ions. This water molecule is, however, attached to the Cs^+ ion that has a total coordination number of 13 in sum. According to their X-ray powder diffraction pattern, the selenates $\text{CsR}(\text{SeO}_4)_2 \cdot 4\text{H}_2\text{O}$ with $\text{R} = \text{La}, \text{Ce}, \text{Pr}, \text{Sm}$ are isotypic with the neodymium compound (Nabar and Ajsaonkar, 1985).

The highest content of water is observed in the pentahydrates $\text{RbCe}(\text{SeO}_4)_2 \cdot 5\text{H}_2\text{O}$ and $(\text{NH}_4)\text{Pr}(\text{SeO}_4)_2 \cdot 5\text{H}_2\text{O}$ (Ovanisyan et al., 1987b; Iskhakova, 1995). Interestingly, no pentahydrates have been found for the respective ternary sulfates so far. Despite the similar ionic radii of Rb^+ and NH_4^+ and as well of Ce^{3+} and Pr^{3+} , the two selenates have different crystal structures. In both, the R^{3+} ions are in ninefold coordination of oxygen atoms from five H_2O molecules and four monodentate selenate ions. But while in the ammonium compound infinite $\infty^1[\text{Pr}(\text{SeO}_4)_{4/2}(\text{H}_2\text{O})_5]^-$ chains are formed, the linkage of the polyhedra leads to $\infty^2[\text{Ce}(\text{SeO}_4)_{4/2}(\text{H}_2\text{O})_5]^-$ layers in the rubidium compound (fig. 6). Note, that the coordination of the selenate groups is the same in both structures.

Besides these ternary selenates, there is one example for a ternary selenate-hydrogenselenate. In $\text{NaEr}(\text{HSeO}_4)_2(\text{SeO}_4) \cdot 5\text{H}_2\text{O}$, the H_2O molecules are exclusively coordinated to Er^{3+} ions that have additionally two SeO_4^{2-} ions and one HSeO_4^- group as ligands (CN 8). Na^+ is surrounded by four selenate and two hydrogenselenate ions which act as monodentate ligands. The linkage of the coordination polyhedra leads to a three-dimensional structure (Krügermann, 2002).

Some additional reports on ternary rare earth selenates with alkaline earth metals have been published. These compounds are said to have compositions $\text{MgR}_2(\text{SeO}_4)_4 \cdot x\text{H}_2\text{O}$ ($x = 6-21$) and $\text{CaR}_2(\text{SeO}_4)_4 \cdot x\text{H}_2\text{O}$ ($x = 6-16$) but only thermoanalytical investigations have been performed (see section 2.3.1) (de Ávila Agostini et al., 1990a, 1990b).

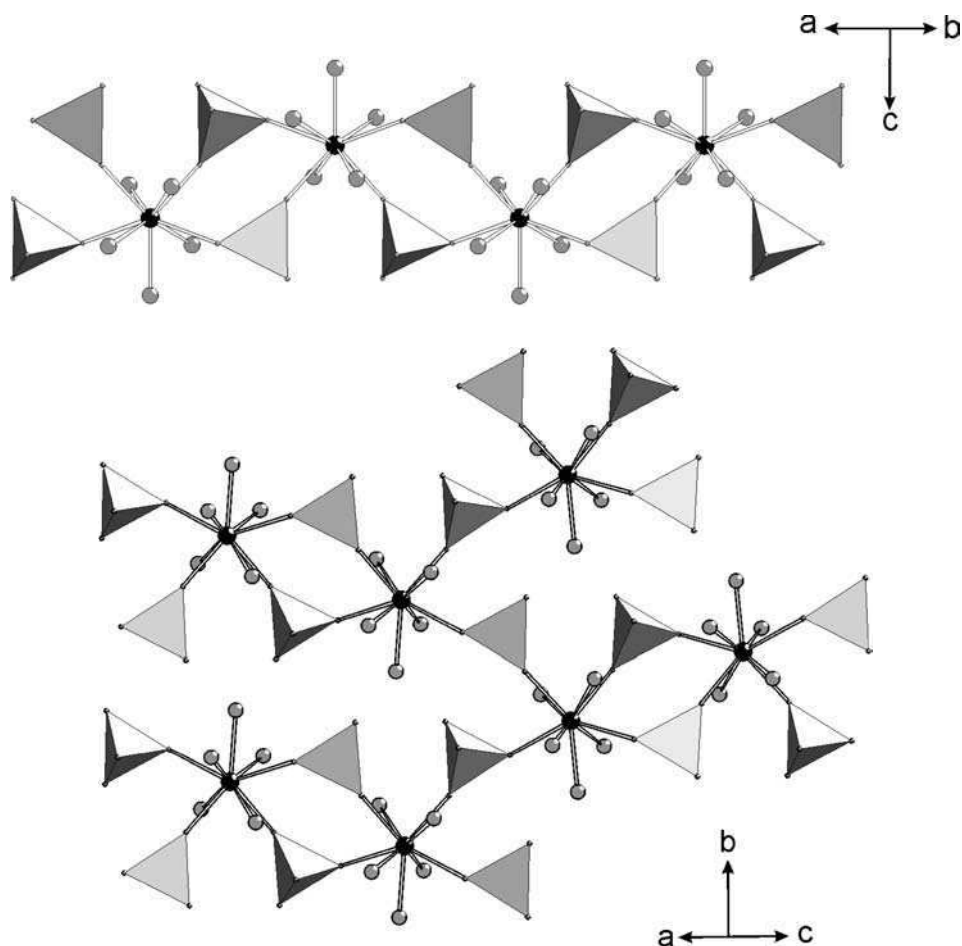


Fig. 6. Chains of the composition $\infty^1[\text{Pr}(\text{SeO}_4)_{4/2}(\text{H}_2\text{O})_5]^-$ (top) and $\infty^2[\text{Ce}(\text{SeO}_4)_{4/2}(\text{H}_2\text{O})_5]^-$ layers (bottom) in the ternary oxo-selenate(VI) pentahydrates $(\text{NH}_4)\text{Pr}(\text{SeO}_4)_2 \cdot 5\text{H}_2\text{O}$ and $\text{RbCe}(\text{SeO}_4)_2 \cdot 5\text{H}_2\text{O}$.

2.3. Properties of oxo-selenates(VI)

2.3.1. Thermal behaviour of oxo-selenates(VI)

Investigations of the thermal behaviour of the selenate hydrates $\text{R}_2(\text{SeO}_4)_3 \cdot x\text{H}_2\text{O}$ were carried out for various compositions mainly by differential thermal analysis (DTA) and thermogravimetric measurements (TG) (Nabar and Paralkar, 1976b; Hájek et al., 1979; Barfiwala and Ajsaonkar, 1995). The decomposition starts in the temperature range between 100 and 200 °C with the loss of water yielding the respective anhydrous selenates. The dehydration often occurs in more than one step with lower hydrates as intermediates. Thus, heating of $\text{La}_2(\text{SeO}_4)_3 \cdot 12\text{H}_2\text{O}$ leads to an octahydrate in a first step (Karvinen and Niinistö,

Table 3
Thermal decomposition of binary oxo-selenate-hydrates

Reaction	Temperature range	Comments
1. $R_2(SeO_4)_3 \cdot xH_2O \rightarrow R_2(SeO_4)_3 + xH_2O \uparrow$	100–200 °C	Reactions 1–3 not well resolved in DTA/TG experiments
2. $R_2(SeO_4)_3 \rightarrow R_2(SeO_3)_3 + 3/2O_2 \uparrow$	650–750 °C	
3. $R_2(SeO_3)_3 \rightarrow R_2O(SeO_3)_2 + SeO_2$	730–800 °C	
4. $R_2O(SeO_3)_2 \rightarrow R_2O_2(SeO_3) + SeO_2$	750–850°	
5. $R_2O_2(SeO_3) \rightarrow R_2O_3 + SeO_2$	900–1100 °C	Tb ₄ O ₇ for R = Tb Pr ₆ O ₁₁ for R = Pr as final oxides

1986). For $Er_2(SeO_4)_3 \cdot 8H_2O$, a trihydrate has been assumed as intermediate (Krügermann and Wickleder, 2004), by analogy to the decomposition of $Er_2(SO_4)_3 \cdot 8H_2O$. On the other hand, the decomposition of anhydrous selenates is different when compared to sulfates. While the latter form oxide sulfates at high temperatures, the selenates decompose to the respective selenites, $R_2(SeO_3)_3$, in a first step. The different behaviour can be attributed to higher stability of the oxidation state IV for selenium compared to sulfur. The formation of $R_2(SeO_3)_3$ is usually observed around 700 °C. Upon further heating the selenites successively lose SeO_2 forming $R_2O(SeO_3)_2$, $R_2O_2(SeO_3)$, and finally, R_2O_3 (see section 3.4.1). The intermediate $R_2O(SeO_3)_2$ is not seen in any case because the thermal effects of formation of $R_2(SeO_3)_3$, $R_2O(SeO_3)_2$, and $R_2O_2(SeO_3)$ occur in a narrow temperature range and are not well resolved in the DTA/TG investigations (table 3). The resolution is not only dependent on the specific rare earth element, but also on the experimental conditions like heating rates, gas atmosphere and the sensitivity of the measuring device. For $Er_2(SeO_4)_3 \cdot 8H_2O$ the decomposition has been also monitored by means of temperature dependent XRD (fig. 7) (Krügermann and Wickleder, 2004). In these investigations, the formation of $Er_2(SeO_4)_3$, $Er_2(SeO_3)_3$, $Er_2O_2(SeO_3)$, and Er_2O_3 was established. Furthermore, a phase transition of $Er_2(SeO_4)_3$ has been observed (see section 2.1.1).

Investigations on the decomposition characteristics of rare earth selenates have been also done in large number for ternary hydrates, even for those that were not characterized structurally. Most of the investigated selenates have the composition $AR(SeO_4)_2 \cdot xH_2O$ and A is an alkali metal ion (Nabar and Paralkar, 1980; Giolito and Ionashiro, 1981, 1988a, 1988b; Ionashiro and Giolito, 1980, 1982a, 1988; Nabar and Ajgaonkar, 1981a, 1981b, 1982a, 1985; Cruz et al., 1990; Spirandeli Crespi et al., 1994). Selenates that are richer in A are also mentioned, for example, $Na_3R(SeO_4)_3 \cdot H_2O$ and $K_3R(SeO_4)_3 \cdot xH_2O$ (Nabar and Khandekar, 1984; Nabar and Naik, 1998) and, moreover, the decomposition of ternary compounds containing alkaline earth metal ions like Mg^{2+} and Ca^{2+} has been described. The compounds $MgR_2(SeO_4)_4 \cdot xH_2O$ ($x = 6–21$) and $CaR_2(SeO_4)_4 \cdot xH_2O$ ($x = 6–16$) were obtained from aqueous solutions of the binary selenates for nearly whole lanthanide series (de Ávila Agostini et al., 1990a, 1990b). According to all of these investigations, it is very likely that the first step of the thermal decomposition is the dehydration. Depending on the water content, this step can be split more or less significantly, indicating the formation of lower hydrates.

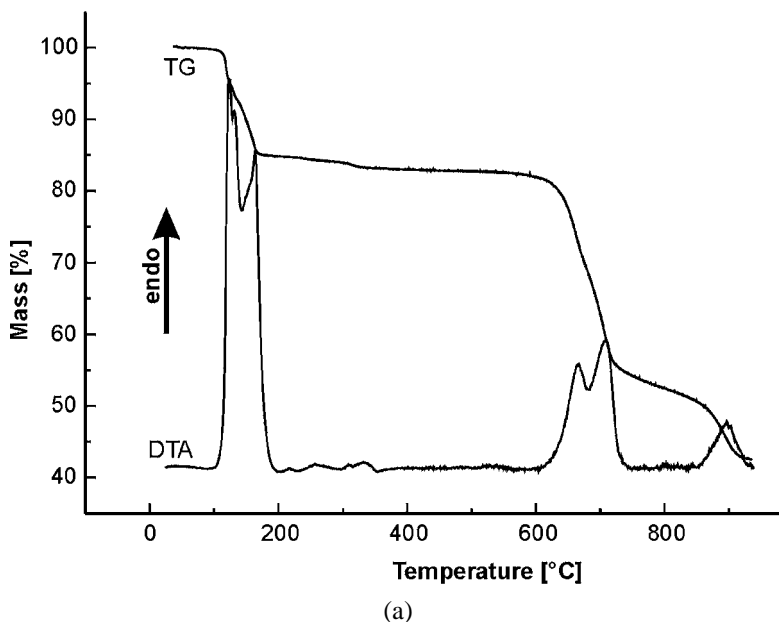


Fig. 7. DTA/TG investigation (a) and temperature dependent XRD (b, see next page) for the thermal decomposition of $\text{Er}_2(\text{SeO}_4)_3 \cdot 8\text{H}_2\text{O}$.

The anhydrous double selenates that are formed in this reaction remain stable up to about 600°C . Their decompositions seem to be quite complicated and the reports are somewhat contradictory. The most likely scenario is that first binary selenates $\text{R}_2(\text{SeO}_4)_3$ and A_2SeO_4 (or ASeO_4 for $\text{A} = \text{Mg}, \text{Ca}$) are formed. The selenates $\text{R}_2(\text{SeO}_4)_3$ then decompose according to the mechanism discussed above (table 3), which means the formation of $\text{R}_2\text{O}(\text{SeO}_3)_2$, $\text{R}_2\text{O}_2(\text{SeO}_3)$, and R_2O_3 , while the alkali and alkaline earth selenates do not decompose due to their higher stability. Other reports suggest that alkali selenates also decompose to yield respective oxides. It seems, that certainty can only be achieved by careful characterization of all intermediates, preferably by X-ray diffraction methods.

2.3.2. Vibrational spectra of oxo-selenates(VI)

Besides thermal analysis, vibrational spectroscopy has been the most frequent method for the characterization of rare earth selenates (Giolito and Giesbrecht, 1969; Petrov et al., 1969, 1970; Hájek et al., 1979; Gupta et al., 1982). It was especially helpful if other methods for the structure determination were not available. In all the compounds that have been measured, the SeO_4^{2-} ions show significant deviations from the ideal tetrahedral symmetry. Therefore, usually more than the expected four vibrations are found in infrared (IR) and Raman spectra, respectively. Furthermore, a factor group splitting cannot be neglected in any case. A large number of data has been collected, so that a reliable range for the expected vibration energies can be given (table 4). The symmetric stretching vibration ν_1 (symmetry species A_1 for T_d

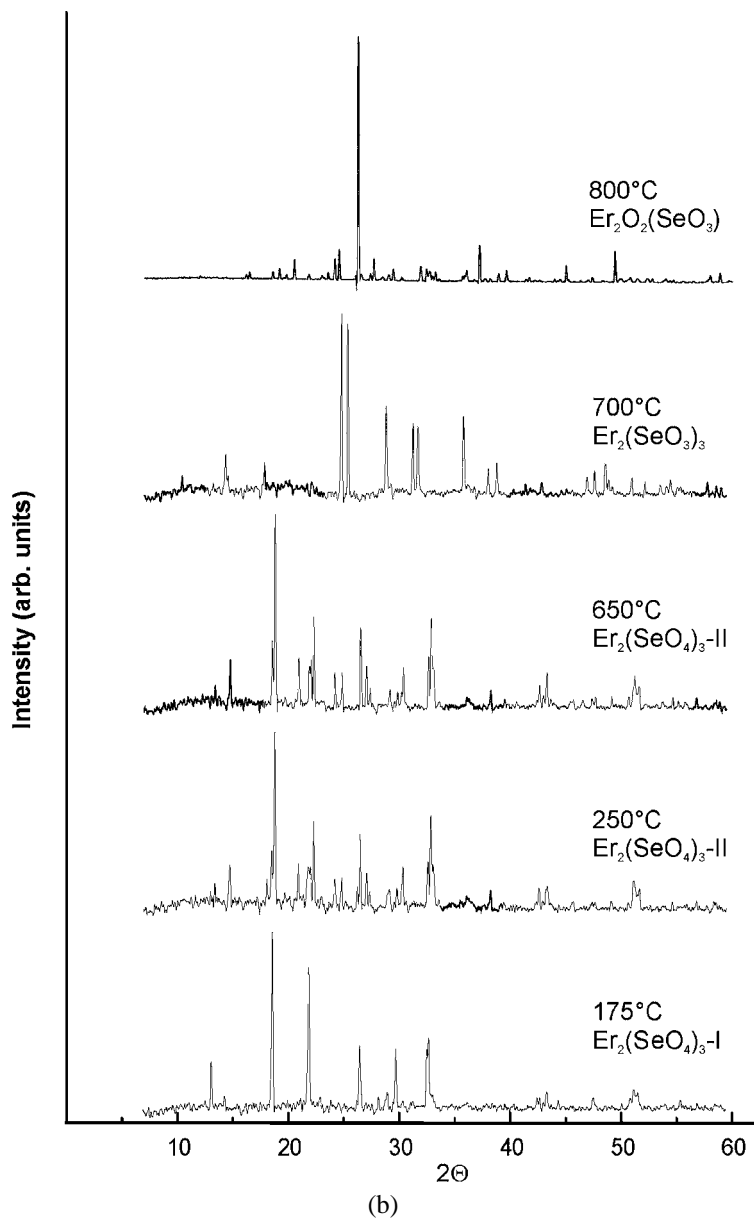


Fig. 7. (Continued).

Table 4
Typical vibration energy ranges (cm^{-1}) of the SeO_4^{2-} ion in rare earth oxo-selenates(VI)

Vibration mode	ν_1 (A_1)	ν_2 (E)	ν_3 (F_2)	ν_4 (F_2)
Description	Symm. stretching	Symm. bending	Asymm. stretching	Asymm. bending
Range	830–850	320–340	850–950	350–440

symmetry) occurs in the narrow range from 830 up to 850 cm^{-1} and also the symmetric bending mode ν_2 (E for T_d symmetry) is always found around $330 \pm 10 \text{ cm}^{-1}$. A more prominent splitting and a wider range for the frequencies is found for the asymmetric stretching and bending modes ν_3 and ν_4 , respectively (both F_2 species for T_d symmetry). For ν_3 , values from 850 to 950 cm^{-1} have been reported, while ν_4 ranges from 350 to 440 cm^{-1} .

2.3.3. Miscellaneous

Occasionally, other properties of rare earth selenates have been investigated. In some cases solubilities have been determined, and also heats of formation were measured. All these investigations have been performed some thirty years ago and no further improvement has been made up to date, so that referring to the Gmelin handbook (1980–1984) shall be sufficient here.

Three more recent reports are dealing with magnetochemical investigations of the rare earth selenate octahydrates $R_2(\text{SeO}_4)_3 \cdot 8\text{H}_2\text{O}$ with $R = \text{Yb, Dy, Pr}$ (Neogy and Nandy, 1982, 1983; Nandi and Neogy, 1988). In particular, the authors explain the observed finding in terms of crystal field splitting, and were able to fit their data quite reasonable assuming a crystal field with D_4 symmetry, although this is not in accordance with the R^{3+} site symmetry (C_1) found in the structure determination.

3. Oxo-selenates(IV)

3.1. Binary oxo-selenates(IV)

3.1.1. Syntheses

Due to the high stability of the oxidation state IV for selenium, oxo-selenates(IV) (selenites), of the rare earth elements are much better investigated than the respective oxo-sulfates(IV) (sulfites). Furthermore, SeO_2 is a solid at room temperature and its melting point of 340 °C allows typical solid state reactions, so that anhydrous lanthanide selenites are, in contrast to the respective selenates, known quite well. Typical fusion reactions of the oxides R_2O_3 and SeO_2 are carried out in sealed glass or even quartz glass ampoules. If single crystals are desired, an appropriate flux should be added. These are usually the alkali metal chlorides ACl ($A = \text{Li–Cs}$) but also LiF has been shown to work well. In the latter case, however, it is advisable to use a metal container (gold, Monel) for the reaction to avoid side reactions of the fluoride melt with the glass ampoule. The reaction temperature must be chosen with respect to the melting point of the flux and is usually around 800 °C. It should be mentioned that the flux sometimes takes part in the reaction, and formations of halide-selenites are observed. If no

Table 5
Synthetic routes to the binary rare earth oxo-selenates(IV) $R_2(SeO_3)_3$

Reaction	Conditions	Comments
$R_2O_3 + 3SeO_2 \rightarrow R_2(SeO_3)_3$ (solid state)	Quartz glass or metal ampoule (Au, Monel); flux (NaCl, LiF, CsBr) needed for single crystal growth; $T = 500\text{--}850\text{ }^\circ\text{C}$	Formation of side products (halide-selenites) possible if flux is used; at lower temperatures and SeO_2 excess the formation of diselenites is observed
$R_2O_3 + 3SeO_2 \rightarrow R_2(SeO_3)_3$ (hydrothermal)	Teflon lined steel autoclave; $T = 180\text{--}200\text{ }^\circ\text{C}$	Rare earth nitrates may serve as initial compounds; formation of hydrates possible; at low pH hydrogenselenites may form
$R_2(SeO_4)_3 \rightarrow R_2(SeO_3)_3 + 3/2O_2 \uparrow$	Quartz glass or metal ampoule (Au, Monel); flux (NaCl, LiF) needed for single crystals; $T = 800\text{--}850^\circ$	Formation of side products (halide-selenites) possible if flux is used; take care to avoid over-pressure!
$R_2O_3 + H_2SeO_3 \rightarrow R_2(SeO_3)_3 \cdot 3H_2O$	Glass beaker; $T \sim 100\text{ }^\circ\text{C}$	H_2O content of the product varies; acid selenites and diselenites may form; usually no single crystals due to low solubility of the selenite-hydrates

flux is added, in most cases only powder samples are obtained. Depending on the R_2O_3/SeO_2 ratio and, more important, on the reaction temperature, different products may form. At low temperatures they are richer in SeO_2 , in accordance with the formation of $Se_2O_5^{2-}$ groups, while at higher temperatures SeO_3^{2-} is the dominant anion. Several systems R_2O_3/SeO_2 have been investigated thermochemically in great detail, as will be shown in section 3.4.3. As discussed in section 2.3.1, the thermal decomposition of the selenates $R_2(SeO_4)_3$ can be used to prepare anhydrous selenites. The thermal decomposition reaction usually leads to powder samples of $R_2(SeO_3)_3$ but single crystals could be obtained if the reaction is carried out in the presence of a flux. For the synthesis of single crystals of $La_2(SeO_3)_3$, hydrothermal conditions have been successfully applied. Finally, selenites can be obtained in the reaction of rare earth oxides and selenious acid but this reaction is not advisable because it often leads to undefined hydrates of low solubility. Another drawback of the reactions in aqueous solutions is that, depending on the conditions like pH value, concentration and temperatures, different species, such as H_2SeO_3 , $HSeO_3^-$, SeO_3^{2-} and $Se_2O_5^{2-}$ exist, so that a great number of compounds can form. Thus, careful adjustment and monitoring of these parameters is necessary to synthesize the desired compound in such a way. The different preparative routes are summarized in table 5 using sesquiselenites, $R_2(SeO_3)_3$, as the example which are the best known group among the binary oxo-selenates(IV) so far.

3.1.2. The oxo-selenates(IV) $R_2(SeO_3)_3$

According to structural investigations on single crystals, five different structure types have been found for anhydrous rare earth selenites, depending on the radius of the R^{3+} ion. $La_2(SeO_3)_3$ and $Ce_2(SeO_3)_3$ crystallize isotypically in the orthorhombic system and contain tenfold coordinated R^{3+} ions and two crystallographically different selenite groups (Wickleder, 2000a; Harrison, 2000; Krügermann, 2002; Wontcheu, 2004). The distances R–O range from 2.48 to 2.80 Å. The oxygen atoms belong to seven SeO_3^{2-} ions with three of them being chelating ligands. According to ${}^3[R(Se(1)O_3)_2/4(Se(2)O_3)_5/5]$, the selenite ions are four and fivefold coordinated by R^{3+} ions. The $Se(1)O_3^{2-}$ groups connect the R^{3+} ions into sheets parallel to the (010) plane that are linked in the [010] direction via $Se(2)O_3^{2-}$ ions. The three-dimensional network provides empty space for the lone pairs of the selenium atoms (fig. 8, left). For the smaller lanthanide ions $R = Pr, Nd$ a new structure type is found that is, however, closely related to $La_2(SeO_3)_3$ (Krügermann and Wickleder, 2002a; Krügermann, 2002; Wontcheu, 2004). Compared to the structure of the latter, the unit cell of the selenites $R_2(SeO_3)_3$ ($R = Pr, Nd$) has a volume that is three times as high as the respective volume of the lanthanum compound. Six crystallographically different R^{3+} and nine different SeO_3^{2-} ions are present in the structure. The coordination number for all of the R^{3+} ions is nine and is achieved by the monodentate coordination of five and the chelating coordination of two SeO_3^{2-} groups. Six of the anions link five R^{3+} ions with each other, the remaining three connect only four. As can be seen from fig. 8, that compares this structure with the one found for $R = La, Ce$, the difference is small and arises mainly from tilting of the anions in the structures of $R_2(SeO_3)_3$ ($R = Pr, Nd$). These minor changes in the structure seem to be the reason that a phase transition of the one phase into the other can be observed by

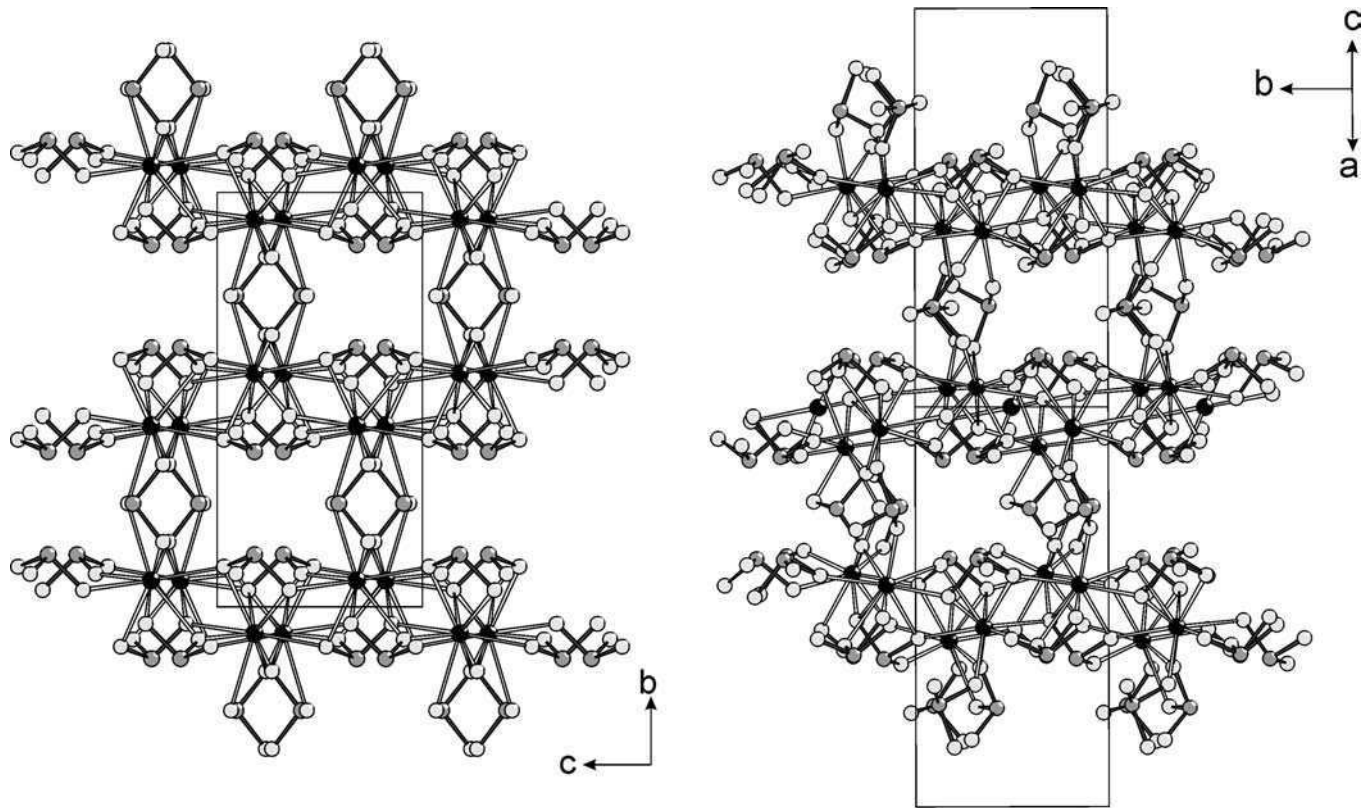


Fig. 8. Comparison of the crystal structures of $\text{R}_2(\text{SeO}_3)_3$ -I and -II for the examples of $\text{La}_2(\text{SeO}_3)_3$ (left) and $\text{Nd}_2(\text{SeO}_3)_3$ (right).

X-ray single crystal diffraction experiments at high temperatures. According to these observations, the orthorhombic modification should be named $R_2(\text{SeO}_3)_3$ -I, and the monoclinic one $R_2(\text{SeO}_3)_3$ -II. The phase transition can be also seen by means of temperature dependent X-ray powder diffraction, and for $\text{Nd}_2(\text{SeO}_3)_3$ it has been monitored also by differential scanning calorimetry (DSC) measurements (see section 3.4.3).

For $R = \text{Sm}$, a new structure type emerges, which shall be named as modification III. It is triclinic and shows two crystallographically different samarium ions, $\text{Sm}(1)^{3+}$ and $\text{Sm}(2)^{3+}$, in eight and ninefold coordination of oxygen atoms, respectively (Krügermann, 2002; Wontcheu, 2004). The latter belong to six SeO_3^{2-} groups for $\text{Sm}(1)^{3+}$ and seven selenite ions for $\text{Sm}(2)^{3+}$, with two of the ligands being chelating in both cases. The linkage of the polyhedra leads to a three-dimensional network, and again the accumulation of lone electron pairs in empty voids of the structure is observed. A very similar and also triclinic structure is adopted by the selenites of the heavy lanthanides $R = \text{Eu-Lu}$, as can be seen also by the comparable lattice parameters (table 6). Nevertheless, there are significant differences, especially in the coordination numbers, so that this modification is named $R_2(\text{SeO}_3)_3$ -IV. The compounds contain two crystallographically different R^{3+} ions and three crystallographically different SeO_3^{2-} groups (Krügermann and Wickleder, 2002b; Krügermann, 2002; Wontcheu, 2004). $R(1)^{3+}$ is coordinated by three $\text{Se}(2)\text{O}_3^{2-}$ and two $\text{Se}(3)\text{O}_3^{2-}$ groups and one $\text{Se}(1)\text{O}_3^{2-}$ ion. Because the latter acts as a chelating ligand, a coordination number of seven results. The coordination polyhedron can be seen as a pentagonal bipyramide. $R(2)^{3+}$ is surrounded by oxygen atoms of three $\text{Se}(1)\text{O}_3^{2-}$, two $\text{Se}(3)\text{O}_3^{2-}$ and one $\text{Se}(2)\text{O}_3^{2-}$ groups, respectively. Two selenite ions ($1 \times \text{Se}(2)\text{O}_3^{2-}$, $1 \times \text{Se}(3)\text{O}_3^{2-}$) are attached in a chelating way leading to a coordination number of eight. Each of the three crystallographically different selenite groups is attached to four R^{3+} ions in a way that all oxygen atoms of a selenite ion are monodentate and two of them are additionally chelating. The linkage of the R^{3+} polyhedra and the selenite ions leads to rectangular channels along $[01\bar{1}]$ providing enough space to incorporate the lone pairs (fig. 9).

For the smallest rare earth ion, Sc^{3+} , another structure type, modification V, occurs (Wontcheu and Schleid, 2003a). In the hexagonal crystal structure, the Sc^{3+} ion is in octahedral coordination of oxygen atoms that belong to six monodentate SeO_3^{2-} ions. The latter are surrounded by four Sc^{3+} ions leading to a three-dimensional network according to the formulation $\infty^3[\text{Sc}(\text{SeO}_3)_{6/4}]$. As can be seen from fig. 10, the linkage of Sc^{3+} ions and selenite groups occurs in a way that hexagonal channels are formed in the c-direction. Within these channels, lone electron pairs of the selenium atoms are located. A special feature of the structure arises if the complex anions are regarded as spherical anions Z^{2-} : the resulting lattice Sc_2Z_3 ($= \text{Sc}_{2/3}\text{Z}$) can be interpreted as cation deficient variety of the NiAs structure.

In one case, $\text{Ce}(\text{SeO}_3)_2$, the structure of the tetravalent rare earth selenite has been reported (Delage et al., 1986). Orange single crystals could be obtained by the reaction of CeO_2 with excess SeO_2 in a silica tube. In the crystal structure, the Ce^{4+} ions are coordinated by eight oxygen atoms that belong to six monodentate and one chelating SeO_3^{2-} groups. The two crystallographically different selenite ions are attached to four and three Ce^{4+} ions, respectively, and a three-dimensional network $\infty^3[\text{Ce}(\text{Se}(1)\text{O}_3)_{3/3}(\text{Se}(2)\text{O}_3)_{4/4}]$ is formed. Although the

Table 6
Crystallographic data of oxo-selenites in the systems R_2O_3/SeO_2

Compound	Space group	Lattice parameters						Reference
		a (Å)	b (Å)	c (Å)	α (deg)	β (deg)	γ (deg)	
$La_2(SeO_3)_3$	<i>Pnma</i>	8.467(3)	14.286(1)	7.1003(2)				Wickleder, 2000b; Harrison, 2000
$Ce_2(SeO_3)_3$	<i>Pnma</i>	8.3923(3)	14.211(1)	7.0458(2)				Wontcheu, 2004
$Pr_2(SeO_3)_3$	<i>P2₁/n</i>	16.883(4)	7.079(2)	21.746(5)		102.13(2)		Wontcheu, 2004
$Nd_2(SeO_3)_3$	<i>P2₁/n</i>	16.853(2)	7.057(1)	21.583(3)		102.11(1)		Wontcheu, 2004; Krügermann and Wickleder, 2002a
$Sm_2(SeO_3)_3$	<i>P$\bar{1}$</i>	6.990(2)	7.932(2)	9.109(2)	70.20(2)	75.36(2)	63.53(2)	Wontcheu, 2004
$Eu_2(SeO_3)_3$	<i>P$\bar{1}$</i>	7.1264(4)	8.1285(4)	9.1152(6)	71.372(2)	70.075(2)	65.652(2)	Krügermann, 2002; Wontcheu, 2004
$Gd_2(SeO_3)_3$	<i>P$\bar{1}$</i>	7.1052(5)	8.1087(7)	9.0673(8)	71.364(4)	70.168(4)	65.747(4)	Krügermann, 2002; Wontcheu, 2004
$Tb_2(SeO_3)_3$	<i>P$\bar{1}$</i>	7.0620(3)	8.0629(4)	9.0406(5)	71.476(2)	70.084(2)	65.896(2)	Krügermann, 2002; Wontcheu, 2004
$Dy_2(SeO_3)_3$	<i>P$\bar{1}$</i>	7.0308(1)	8.0410(2)	9.0096(2)	71.383(1)	70.095(1)	65.903(1)	Wontcheu, 2004
$Ho_2(SeO_3)_3$	<i>P$\bar{1}$</i>	7.0079(3)	8.0204(4)	8.9769(4)	71.370(2)	70.098(2)	65.935(2)	Wontcheu, 2004
$Er_2(SeO_3)_3$	<i>P$\bar{1}$</i>	6.982(1)	8.006(1)	8.950(1)	71.38(1)	70.13(1)	65.87(1)	Krügermann and Wickleder, 2002b; Wontcheu, 2004
$Tm_2(SeO_3)_3$	<i>P$\bar{1}$</i>	6.9461(3)	7.9658(4)	8.9196(5)	71.480(2)	70.223(2)	65.964(2)	Wontcheu, 2004
$Yb_2(SeO_3)_3$	<i>P$\bar{1}$</i>	6.9179(1)	7.9393(1)	8.9001(2)	71.455(1)	70.293(1)	65.038(1)	Krügermann, 2002; Wontcheu, 2004
$Lu_2(SeO_3)_3$	<i>P$\bar{1}$</i>	6.9022(2)	7.9341(2)	8.8726(2)	71.413(1)	70.325(1)	65.985(1)	Wontcheu, 2004
$Y_2(SeO_3)_3$	<i>P$\bar{1}$</i>	6.9934(5)	8.0248(6)	8.9882(8)	71.332(3)	69.916(3)	65.770(4)	Krügermann, 2002; Wontcheu, 2004
$Sc_2(SeO_3)_3$	<i>P6₃/m</i>	8.1428(5)		7.6456(4)				Wontcheu and Schleid, 2003a
$Ce(SeO_3)_2$	<i>P2₁/n</i>	7.008(1)	10.587(2)	7.262(1)		107.00(1)		Delage et al., 1986
$Sm_2(Se_2O_5)_2(SeO_3)$	<i>P2₁/c</i>	10.036(2)	10.225(2)	12.873(2)		112.29(2)		Wickleder, 2005a
$Sm_2O(SeO_3)_2$	<i>P4₂/ncm</i>	10.751(2)		5.2635(7)				Wontcheu, 2004
$Eu_2O(SeO_3)_2$	<i>P4₂/ncm</i>	10.7405(7)		5.2577(3)				Wontcheu, 2004
$Gd_2O(SeO_3)_2$	<i>P4₂/ncm</i>	10.6873(6)		5.2503(2)				Wontcheu, 2004
$Tb_2O(SeO_3)_2$	<i>P4₂/ncm</i>	10.646(1)		5.2156(3)				Wontcheu and Schleid, 2002a
$Dy_2O(SeO_3)_2$	<i>P4₂/ncm</i>	10.6007(4)		5.2000(2)				Wontcheu, 2004
$Ho_2O(SeO_3)_2$	<i>P4₂/ncm</i>	10.5570(3)		5.1880(1)				Wontcheu, 2004
$Er_2O(SeO_3)_2$	<i>P4₂/ncm</i>	10.5220(6)		5.1735(2)				Wontcheu, 2004
$Tm_2O(SeO_3)_2$	<i>P4₂/ncm</i>	10.4887(5)		5.1425(4)				Wontcheu, 2004

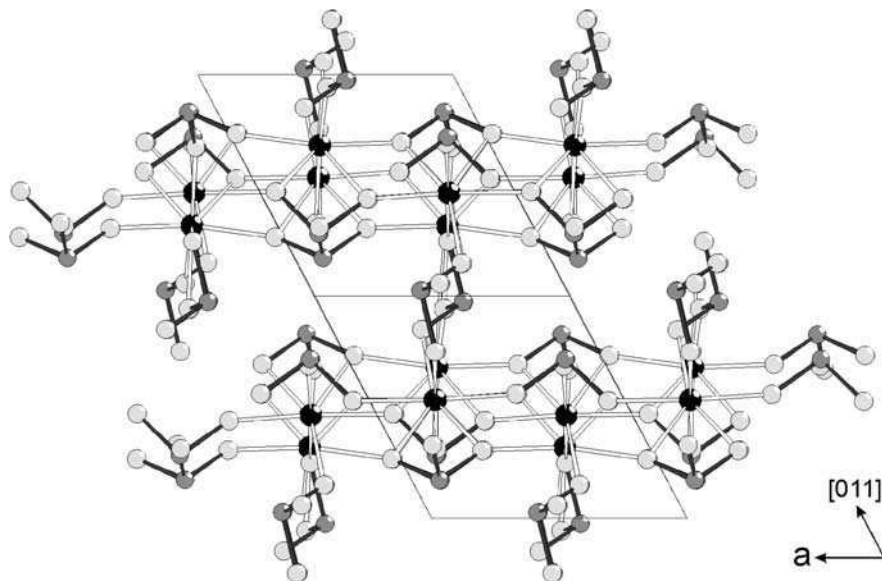


Fig. 9. Projection of the crystal structure of the oxo-selenates(IV) $R_2(\text{SeO}_3)_3$ -IV ($R = \text{Tb-Lu}$).

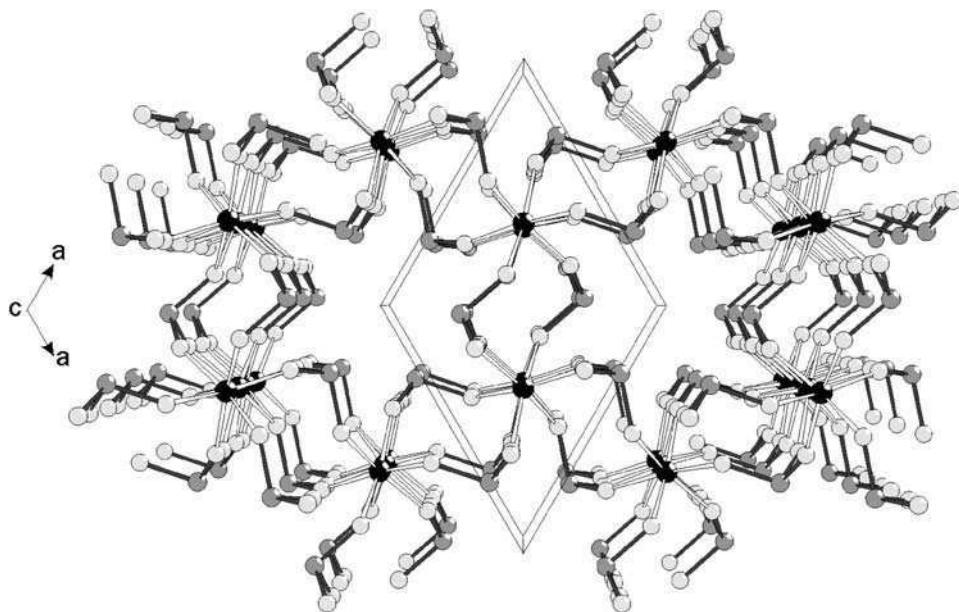


Fig. 10. Perspective view of the $\text{Sc}_2(\text{SeO}_3)_3$ crystal structure along $[001]$. The linkage of Sc^{3+} ions and SeO_3^{2-} groups leads to channels that incorporate lone electron pairs of the selenium atoms.

lone pair activity is not so prominent in the structure compared to the findings for the trivalent lanthanides, the need of space for the lone pairs is still obvious.

3.1.3. *SeO₂-rich and SeO₂-poor oxo-selenates(IV)*

As mentioned above, the reaction of R_2O_3 with SeO_2 can also lead to selenites of other compositions than $R_2Se_3O_9$ ($= R_2(SeO_3)_3$). A higher SeO_2 content is observed for $R_2Se_5O_{13}$, $R_2Se_4O_{11}$, and $R_2Se_{3.5}O_{10}$; low SeO_2 concentrations are found for $R_2Se_2O_7$, $R_2Se_{1.5}O_6$ and R_2SeO_5 (Oppermann and Zhang-Preße, 2001; Oppermann et al., 2002a; Zhang-Preße and Oppermann, 2002; Castro et al., 1994; de Pedro et al., 1994, 1995; Leskelä and Hölsä, 1985; Niinistö et al., 1980; Karvinen et al., 1987; Wildner, 1994). Unfortunately not all of these phases have been structurally characterized but it seems clear that the uptake of additional SeO_2 is achieved by the formation of diselenite groups, $Se_2O_5^{2-}$, whereas the loss of SeO_2 forces the formation of oxide-selenites (table 6). For $Sm_2Se_5O_{13}$ this assumption has been proved by X-ray single crystal diffraction, and it has been shown that both $Se_2O_5^{2-}$ and SeO_3^{2-} ions are present in the structure (Wickleder, 2005a). Therefore, the compound should be written as $Sm_2(Se_2O_5)_2(SeO_3)$. The two crystallographically different samarium ions, $Sm(1)^{3+}$, and $Sm(2)^{3+}$, are surrounded by eight and nine oxygen atoms, respectively. For $Sm(1)^{3+}$ the latter belong to four $Se_2O_5^{2-}$ and two SeO_3^{2-} groups that are partly coordinated in a chelating way. $Sm(2)^{3+}$ is coordinated by four $Se_2O_5^{2-}$ and three SeO_3^{2-} ions, respectively. The most striking feature of the crystal structure is that the linkage of the polyhedra occurs only in two dimensions. The layers formed are stacked parallel to the (011) plane, and the lone

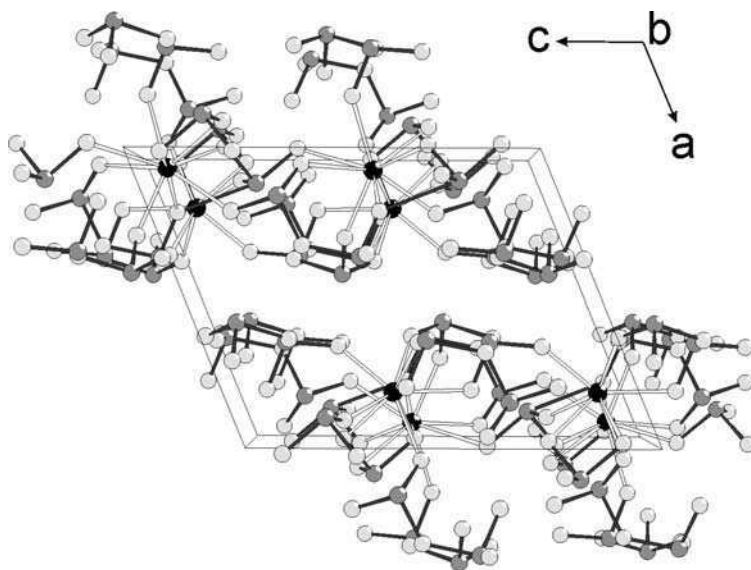


Fig. 11. Perspective representation of the layered structure of $Sm_2(Se_2O_5)_2(SeO_3)$.

Table 7
Observed compounds in the systems R_2O_3/SeO_2 and their structure

Compound	Structure	Example	Comment
$R_2Se_5O_{13}$	$R_2(Se_2O_5)_2(SeO_3)$	R = Sm	Not observed in thermochemical and DTA investigations
$R_2Se_4O_{11}$	$R_2(Se_2O_5)(SeO_3)_2$	No structure determined	Observed in thermochemical and DTA investigations
$R_2Se_{3.5}O_{10}$	$R_2(Se_2O_5)_{0.5}(SeO_3)_{2.5}$	No structure determined	Observed in thermochemical investigations
$R_2Se_3O_9$	$R_2(SeO_3)_3$	Whole series of R	Observed in thermochemical and DTA investigations; five structure types (I–V)
$R_2Se_2O_7$	$R_2(SeO_3)_2O$	R = Sm–Tm	Compounds isotypic throughout the series
$R_2Se_2O_5$	$R_2(SeO_3)_2O_2$	No structure determined	Observed in thermochemical and DTA investigations
$R_2Se_{1.5}O_6$	$R_2(SeO_3)_{1.5}O_{1.5}$	No structure determined	Observed in thermochemical and DTA investigations

electron pairs are obviously arranged between these layers (fig. 11). According to the findings for $Sm_2Se_5O_{13}$, it is likely that the selenites $R_2Se_4O_{11}$ and $R_2Se_{3.5}O_{10}$ are also diselenite-selenites that can be formulated as $R_2(Se_2O_5)(SeO_3)_2$ and $R_2(Se_2O_5)_{0.5}(SeO_3)_{2.5}$, respectively (table 7).

For the three phases on the SeO_2 -poor side of the system R_2O_3/SeO_2 , $R_2Se_2O_7$, $R_2Se_{1.5}O_6$ and R_2SeO_5 , a structural investigation has been first reported for the example of $Tb_2Se_2O_7$ (Wontcheu and Schleid, 2002a) and subsequently for the series $R_2Se_2O_7$ with R = Sm–Tm (Wontcheu, 2004). Single crystals have been obtained according to the equation $2R_2O_3 + RBr_3 + 2SeO_2 \rightarrow R_2O(SeO_3)_2 + 3ROBr$ when CsBr was used as a flux. The oxide-bromides forming in the reaction have been detected by XRD. In the case of R = Tb, Tb_4O_7 was the initial oxide and metallic Tb has been added to achieve reduction to Tb^{3+} . It turned out clearly that these compounds have to be described as oxide-selenites and the formula should be given as $R_2O(SeO_3)_2$. The tetragonal structure consists of oxide-centered tetrahedra that are linked to chains according to ${}_{\infty}^1[OR_{4/2}]^{4+}$. These are oriented along the c-axis of the tetragonal unit cell and connected by the SeO_3^{2-} ions (fig. 12).

The oxide ion within the tetrahedron shows a short bond length of about 2.25 Å to the R^{3+} ions and the R–R distances within the tetrahedron are about 3.70 Å. Further coordination by selenite groups provides a coordination number of eight for the Tb^{3+} ions. In the direction of the ${}_{\infty}^1[OR_{4/2}]^{4+}$ chains, distinct channels are formed incorporating lone pairs of the selenium atoms (fig. 12). With respect to the observations for $R_2Se_2O_7$, it can be assumed that also the compositions $R_2Se_{1.5}O_6$ and R_2SeO_5 have to be formulated as oxide-selenites according to $R_2O_{1.5}(SeO_3)_{1.5}$ and $R_2O_2(SeO_3)$, respectively. Table 7 summarizes the phases in the systems R_2O_3/SeO_2 and their potential structure.

3.1.4. Oxo-selenate(IV)-hydrates and acidic oxo-selenates(IV)

The hydrous rare earth selenites $R_2(SeO_3)_3 \cdot xH_2O$ were prepared nearly thirty years ago and various values for x have been reported (Petrov et al., 1973; Savchenko et al., 1968; Giolito and Giesbrecht, 1967). As can be seen from table 17 (see section 3.4.3), for the sys-

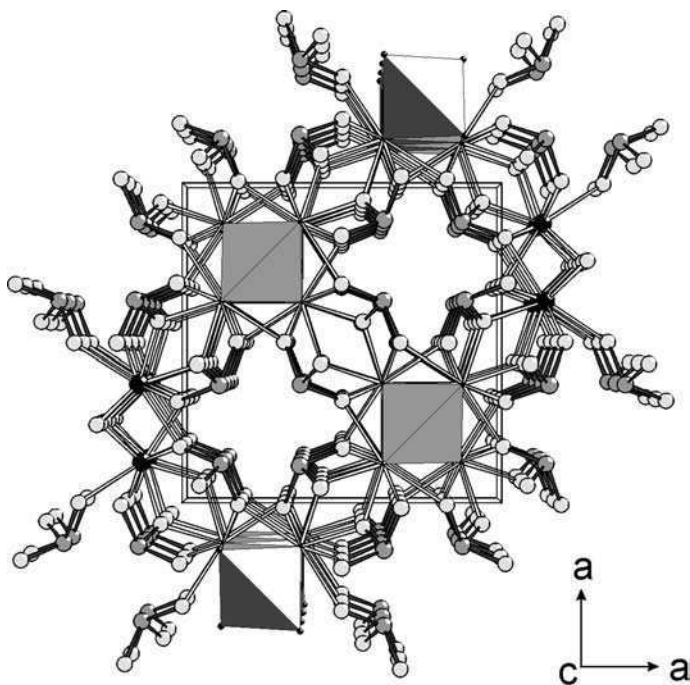


Fig. 12. The tetragonal crystal structure of the oxide-selenites $R_2O(SeO_3)_2$. ($R = Sm-Tm$) viewed along $[001]$. The oxide ions are the centers of tetrahedra of metal ions (shown as polyhedra) that are edge-connected to chains according to $\infty^1[OR_4/2]^{4+}$.

tem $Nd_2O_3-SeO_2-H_2O$, the tetrahydrate $Nd_2(SeO_3)_3 \cdot 4H_2O$ has been found to be the stable hydrate (Gospodinov and Stancheva, 2003). The tetrahydrate has also been shown to be the only stable hydrate in the system $Tm_2O_3-SeO_2-H_2O$ (Gospodinov and Stancheva, 2001). Unfortunately, only X-ray powder diffraction and IR measurements have been performed, so that details of the crystal structures are not known.

The same investigations of the solubility isotherms show the existence of the acidic selenites $R(HSeO_3)(SeO_3) \cdot 2H_2O$ ($M = Nd, Tm$) at higher SeO_2 concentrations (see section 3.4.3). The neodymium compound and its samarium analogue have been obtained in single crystalline form (Koskenlinna et al., 1994; de Pedro et al., 1994). The crystal structure consist of layers according to $\infty^2[R(SeO_3)_{4/4}(HSeO_3)_{2/2}(H_2O)_{1/1}]$ with the R^{3+} ions in eightfold coordination of oxygen atoms, because one of the selenite ions acts as chelating ligand. Only two oxygen atoms of the $HSeO_3^-$ ions are involved in the linkage of the R^{3+} ions, while the OH group of the anion is oriented towards the empty space between the layers. It is involved in hydrogen bonding that keeps the layers together. Furthermore, the non-coordinated H_2O molecules of the compound are part of the hydrogen bonding system. The layers are stacked in $[001]$ direction (fig. 13). The respective anhydrous species, $R(HSeO_3)(SeO_3)$, have been reported for $R = La$ and Pr (Morris et al., 1992a;

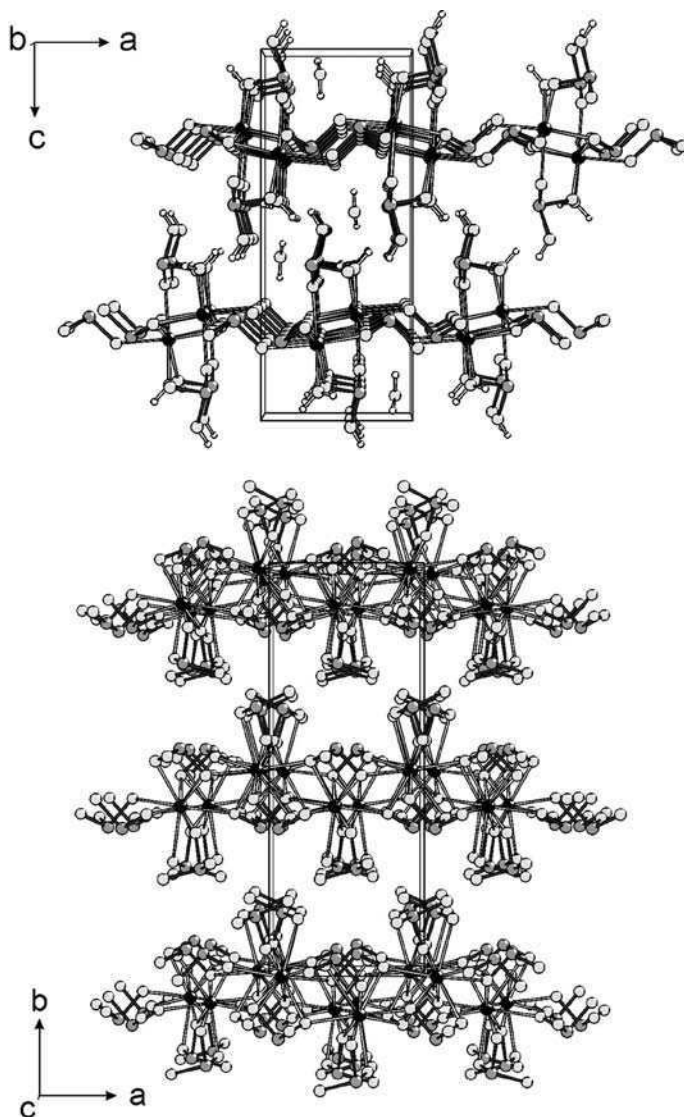


Fig. 13. Layered structures of the acidic oxo-selenates(IV) $R(\text{HSeO}_3)(\text{SeO}_3) \cdot 2\text{H}_2\text{O}$ (top) and $R(\text{HSeO}_3)(\text{SeO}_3)$ (bottom) shown for the examples of $\text{Sm}(\text{HSeO}_3)(\text{SeO}_3) \cdot 2\text{H}_2\text{O}$ and $\text{Pr}(\text{HSeO}_3)(\text{SeO}_3)$, respectively.

Castro et al., 1994). The isotopic compounds also have layered structures which have to be formulated as to $\infty^2[\text{R}(\text{SeO}_3)_{5/5}(\text{HSeO}_3)_{2/2}]$. Owing to the chelating coordination of three anions, the coordination number of the R^{3+} ions is ten. The layers are stacked along the c -axis and are held together by hydrogen bonding (fig. 13, bottom).

Table 8
Observed compounds in the systems $R_2O_3/SeO_2/H_2O$

Compound	Ratio of binary components	Comment
$R_2(SeO_3)_3 \cdot xH_2O$	$R_2O_3 \cdot 3SeO_2 \cdot xH_2O$	Values $x = 0.5-5$ reported; most certain $x = 4$ (see table 6)
$R_2(HSeO_3)_2(SeO_3)_2$ = $R(HSeO_3)(SeO_3)$ ¹⁾	$R_2O_3 \cdot 4SeO_2 \cdot H_2O$	Structure known for $R = La, Pr$
$R_2(HSeO_3)_2(SeO_3)_2 \cdot 4H_2O$ = $R(HSeO_3)(SeO_3) \cdot 2H_2O$	$R_2O_3 \cdot 4SeO_2 \cdot 5H_2O$	Structure known for $R = Nd, Sm$
$R_2(HSeO_3)_6$ = $R(HSeO_3)_3$	$R_2O_3 \cdot 6SeO_2 \cdot 3H_2O$	Structure known for $R = Sc$
$R_2(Se_2O_5)_3(H_2SeO_3)_2 \cdot 2H_2O$	$R_2O_3 \cdot 8SeO_2 \cdot 4H_2O$	Structure known for $R = Nd$
$R_2(Se_2O_5)_2(HSeO_3)_2(H_2SeO_3)_2$ = $R(Se_2O_5)(HSeO_3)(H_2SeO_3)$	$R_2O_3 \cdot 8SeO_2 \cdot 3H_2O$	Structure known for $R = Pr$

¹⁾Some of the formulae have been doubled to avoid fractional numbers for the ratios.

For the system $Nd_2O_3-SeO_2-H_2O$, the hydrogenselenite $Nd(HSeO_3)_3$ has been shown to be the stable compound if the SeO_2 concentration is further increased (see also section 3.4.3) (Gospodinov and Stancheva, 2003). The structure of this compound is not known, and the same is true for other members of the rare earth series of this composition. The only exception is $Sc(HSeO_3)_3$ that has been obtained from strongly acidic solutions (Valkonen and Leskelä, 1978). According to ${}^3_\infty[Sc(HSeO_3)_{6/2}]$, the crystal structure can be described as a three-dimensional network of $[ScO_6]$ octahedra and selenite groups. Due to the small radius of Sc^{3+} , it can be assumed that hydrogen selenites of the larger rare earth elements will have different structures. On the SeO_2 rich side of the system $Nd_2O_3-SeO_2-H_2O$, the complex diselenite $Nd_2(Se_2O_5)_3(H_2SeO_3) \cdot 2H_2O$ forms (Stancheva et al., 1998). It contains two crystallographically different Nd^{3+} ions, both in ninefold coordination of oxygen atoms. $Nd(1)^{3+}$ is surrounded by seven $Se_2O_5^{2-}$ groups of which two are attached in a chelating way. $Nd(2)^{3+}$ has two chelating and two monodentate $Se_2O_5^{2-}$ neighbours and, furthermore, two H_2O and one H_2SeO_3 ligands. The coordination polyhedra are linked to sheets which are stacked in c-direction and held together by hydrogen bonds with the acid and the water molecules as donors (fig. 14).

A compound that is even richer in SeO_2 has been investigated for praseodymium. Its formula is given as $PrH_3(Se_2O_5)(SeO_3)_2$ (Koskenlinna and Valkonen, 1977), but a detailed inspection of the distances $Se-O$ reveals that it should actually be formulated according to $Pr(Se_2O_5)(HSeO_3)(H_2SeO_3)$. Various anions have different functionalities in the structure. The diselenite and hydrogenselenite groups link the Pr^{3+} ions to double chains that are connected via hydrogen bonds of the H_2SeO_3 molecules. These are only monodentate to the Pr^{3+} ions which are in ninefold coordination of oxygen atoms.

All phases that have been found in the systems $R_2O_3/SeO_2/H_2O$ are summarized in table 8. The same table gives the ratio of the binary components in these phases. There might be other compositions that exist under special conditions and that have not been detected yet, and considering limited knowledge even for the established phases, systematic structural investigations are highly desirable.

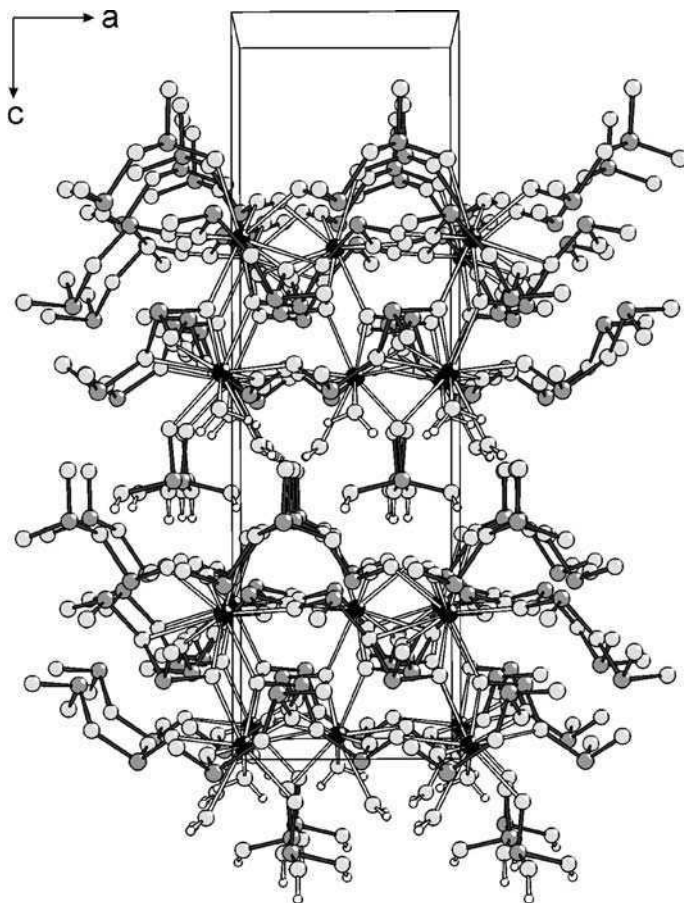


Fig. 14. Crystal structure of the SeO_2 -rich acidic selenite $\text{Nd}_2(\text{Se}_2\text{O}_5)_3(\text{H}_2\text{SeO}_3)\cdot 2\text{H}_2\text{O}$. The H_2SeO_3 molecules are involved in hydrogen bonds that keep the layered structure together.

3.2. Anionic derivatives of oxo-selenates(IV)

3.2.1. General remarks and syntheses

As anionic derivatives of selenates(IV), those compounds shall be considered in which some of the selenite (or diselenite) anions are replaced by halide ions (section 3.2.2) or even by complex anions (section 3.2.3). In a strict sense, the oxide-selenites mentioned in section 3.1 are anionic derivatives of selenates(IV) with SeO_3^{2-} groups replaced by oxide ions. However, they belong to the *binary* system $\text{R}_2\text{O}_3/\text{SeO}_2$ and that's why they were discussed in that context and not within this section. On the other hand, the oxide-halides will be discussed here because they are members of the *ternary* systems $\text{R}_2\text{O}_3/\text{RX}_3/\text{SeO}_2$ (see section 3.2.2).

Thermochemical investigations of the systems ROCl/SeO_2 ($\text{R} = \text{Sm}, \text{Yb}$) and $\text{SmOBr}/\text{SeO}_2$ revealed the formation of various halide-selenates(IV) (see section 3.4). They have the com-

Table 9
Observed compounds in the systems $R_2O_3/RX_3/SeO_2$ ($X = F, Cl, Br$)

Compound	Ratio of binary components	Comment
$R(Se_3O_7)X$ ($= R_3Se_9O_{21}X_3$) ¹⁾	$R_2O_3 \cdot RX_3 \cdot 9SeO_2$	Thermochemically observed for $R = Sm, Yb$; $X = Cl, Br$; no structure known
$R(Se_2O_5)X$ ($= R_3Se_6O_{15}X_3$)	$R_2O_3 \cdot RX_3 \cdot 6SeO_2$	Thermochemically observed for $R = Sm, Yb$; $X = Cl, Br$; no structure known
$R(SeO_3)X$ ($= R_3Se_3O_9X_3$)	$R_2O_3 \cdot RX_3 \cdot 3SeO_2$	Thermochemically observed for $R = Sm, Yb$; $X = Cl, Br$; single crystals for $R = Nd, Er, Ho$ with $X = Cl$, and $R = La$; $X = F$
$R_3(SeO_3)_4X$ ($= R_9Se_{12}O_{36}X_3$)	$4R_2O_3 \cdot RX_3 \cdot 12SeO_2$	Single crystals for $R = Pr-Dy$; $X = F$
$R_2O(SeO_3)X_2$ ($= R_6Se_3O_{12}X_6$)	$2R_2O_3 \cdot 2RX_3 \cdot 3SeO_2$	Thermochemically observed for $R = Yb$ (only for $X = Cl$); no structure known
$R_3O_2(SeO_3)_2X$ ($= R_9Se_6O_{24}X_3$)	$4R_2O_3 \cdot RX_3 \cdot 6SeO_2$	Structure known for $R = Tb, Dy, Er$; $X = Cl$
$R_4O_3(SeO_3)_2X_2$ ($= R_{12}Se_6O_{27}X_6$)	$4R_2O_3 \cdot 2RX_3 \cdot 6SeO_2$	Structure known for $R = Yb, Tb, Er$; $X = Cl$
$R_5O_4(SeO_3)_2X_3$	$2R_2O_3 \cdot RX_3 \cdot 2SeO_2$	Structure known for $R = Tb$; $X = Cl$, and $R = Gd$; $X = Br$
$R_9O_8(SeO_3)_4X_3$	$4R_2O_3 \cdot RX_3 \cdot 4SeO_2$	Structure known for $R = Pr, Nd, Sm, Gd$; $X = Cl$, and $R = La, Pr$; $X = Br$

¹⁾In some cases multiples of the sum formulae were chosen to allow integer numbers for the ratios.

position RSe_3O_7X ($= ROX \cdot 3SeO_2$), RSe_2O_5X ($= ROX \cdot 2SeO_2$), $RSeO_3X$ ($= ROX \cdot SeO_2$) for $R = Sm$ and $X = Cl, Br$ (Oppermann et al., 2002b, 2003). The same compositions have been found in the ytterbium system but additionally the $YbOCl$ rich phase $Yb_2SeO_4Cl_2$ ($2YbOCl \cdot SeO_2$) is observed (Schmidt et al., 2004), that has obviously to be interpreted as an oxide-chloride-selenite. Other oxide-halide-selenites, exhibiting a wide range of compositions, have been prepared and structurally characterized. Interestingly, these compounds have not been found in the respective phase diagrams. Moreover, several compounds have been prepared in the respective fluoride systems. Table 9 summarizes the compounds that have been found in the systems $R_2O_3/RX_3/SeO_2$ to date. The known structural chemistry of the compounds will be discussed in the following way, first for the halide-selenites (section 3.2.2), and then for the oxide-halide-selenites (section 3.2.3). Details of the thermochemical investigations can be found in section 3.4. A few examples of oxo-selenate(IV) derivatives with complex anions are given in section 3.2.4.

The syntheses of halide-oxo-selenates(IV) and oxide-halide-oxo-selenates(IV) are very similar to those described for the binary oxo-selenates(IV) (see section 3.1.1). The reactions are carried out in silica ampoules or metal tubes, especially when fluorides are involved. The trihalides, RX_3 ($X = F, Cl, Br$), or the respective oxide-halides, ROX , of the rare earth elements may serve as the halide source. Usually a flux should be added if single crystals are needed, and it is most convenient to use an alkali metal halide containing the desired anion for that purpose. In one case, $ErClSeO_3$, the synthesis has also been shown to work hydrothermally (Berdonosov et al., 2003). It is remarkable that iodides cannot be prepared in this way because I^- reduces SeO_3^{2-} under the reaction conditions and both, elemental iodine and selenium are produced. The routes described so far for the growths of single crystals of the compounds under discussion are given in table 10, crystallographic data can be found in table 11.

Table 10
Synthetic routes for single crystal growth of selected anionic oxo-selenate(IV) derivatives

Reaction	Conditions	Comments
$R_2O_3 + RCl_3 + 3SeO_2 \rightarrow RCl(SeO_3)$	Silica ampoule; excess RCl_3 advisable; $T = 830^\circ C$	
$R_2O_3 + ROCl + 2SeO_2 \rightarrow R_3O_2Cl(SeO_3)_2$	Silica ampoule; CsCl flux; $T = 850^\circ C$	Flux can be removed by washing
$3R_2O_3 + ROCl + RCl_3 + 4SeO_2 \rightarrow 2R_4O_3Cl_2(SeO_3)_2$	Silica ampoule; CsCl flux; $T = 850^\circ C$	Flux can be removed by washing
$3R_2O_3 + 3ROX + RX_3 + 4SeO_2 \rightarrow 2R_5O_4X_3(SeO_3)_2$	Silica ampoule; CsX flux; $T = 830^\circ C$	X = Cl, Br; flux can be removed by washing
$7R_2O_3 + 3ROX + RX_3 + 8SeO_2 \rightarrow 2R_9O_8X_3(SeO_3)_4$	Silica ampoule; CsX flux; $T = 850^\circ C$	X = Cl, Br; flux can be removed by washing
$2R_2O_3 + RCl_3 + 6SeO_2 + 3CsCl \rightarrow 3CsRCl_2(SeO_3) + R_2(SeO_3)_3$	Silica ampoule; $T = 830^\circ C$	To date only for R = Tm; both products identified by XRD
$ROF + SeO_2 \rightarrow RF(SeO_3)$	Silica jacketed gold ampoule; LiF flux	To date only for R = La; ratio ROF/LiF max. 1:2
$4R_2O_3 + RF_3 + 12SeO_2 \rightarrow 3R_3F(SeO_3)_4$	Silica jacketed gold ampoule; NaCl flux	Single crystals of poor quality
$2R_2(SeO_4)_3 + 5LiF \rightarrow R_3F(SeO_3)_4 + LiRF_4 + 2Li_2SeO_3 + 3O_2 \uparrow$	Silica jacketed gold ampoule	High quality single crystals; formation of $LiRF_4$ proved by XRD; formation of Li_2SeO_3 not certain; take care to avoid over-pressure explosion!

Table 11
Crystallographic data of anionic oxo-selenate(IV) derivatives

Compound	Space group	Lattice parameters					Reference
		a (Å)	b (Å)	c (Å)	α (deg)	β (deg)	
LaF(SeO ₃)	<i>P</i> 2 ₁ / <i>c</i>	18.198(3)	7.1575(8)	8.464(1)		96.89	Wickleder, 2000b
Gd ₃ F(SeO ₃) ₄	<i>P</i> 6 ₃ <i>mc</i>	10.443(1)		6.9432(2)			Göhausen and Wickleder, 2000
Dy ₃ F(SeO ₃) ₄	<i>P</i> 6 ₃ <i>mc</i>	10.360(1)		6.8647(7)			Krügermann and Wickleder, 2002b
Nd ₃ F(SeO ₃) ₄	<i>P</i> 6 ₃ <i>mc</i>	10.515(1)		712.11(4)			Krügermann, 2002
Sm ₃ F(SeO ₃) ₄	<i>P</i> 6 ₃ <i>mc</i>	10.474(1)		7.0224(7)			Krügermann, 2002
NdCl(SeO ₃)	<i>Pnma</i>	11.153(2)	5.3519(6)	13.568(1)			Wickleder, 2002b
HoCl(SeO ₃)	<i>Pnma</i>	7.209(1)	6.926(1)	8.769(2)			Wickleder, 2003
ErCl(SeO ₃)	<i>Pnma</i>	7.218(1)	6.922(1)	8.743(1)			Wickleder, 2002b
Tb ₃ O ₂ Cl(SeO ₃) ₂	<i>Pnma</i>	5.3516(4)	15.3051(9)	10.8172(7)			Wontcheu and Schleid, 2005
Dy ₃ O ₂ Cl(SeO ₃) ₂	<i>Pnma</i>	5.33381(2)	15.2104(7)	10.7656(4)			Wontcheu, 2004
Er ₃ O ₂ Cl(SeO ₃) ₂	<i>C</i> 2/ <i>c</i>	14.9823(6)	11.0203(5)	5.4795(3)		105.51(5)	Wontcheu, 2004
Er ₄ O ₃ Cl ₂ (SeO ₃) ₂	<i>P</i> 1̄	8.6164(2)	11.7056(3)	12.0842(3)	67.666(1)	77.833(1)	85.270(1) Wontcheu, 2004
Yb ₄ O ₃ Cl ₂ (SeO ₃) ₂	<i>P</i> 1̄	8.5388(1)	11.4590(2)	11.9547(2)	68.132(1)	77.113(1)	85.747(1) Wontcheu and Schleid, 2004a
Tb ₅ O ₄ Cl ₃ (SeO ₃) ₂	<i>C</i> 2/ <i>m</i>	12.2913(4)	5.4617(4)	9.7879(7)		90.485(6)	Wontcheu and Schleid, 2005
Gd ₅ O ₄ Br ₃ (SeO ₃) ₂	<i>C</i> 2/ <i>m</i>	12.437(1)	5.4991(4)	10.0529(9)		91.869(3)	Wontcheu, 2004
La ₉ O ₈ Br ₃ (SeO ₃) ₄	<i>P</i> 1̄	7.1172(3)	9.1956(4)	9.9658(5)	99.856(2)	94.938(2)	95.840(2) Wontcheu, 2004
Pr ₉ O ₈ Br ₃ (SeO ₃) ₄	<i>P</i> 1̄	7.0035(4)	9.0609(6)	9.8591(7)	99.623(3)	95.076(2)	95.874(3) Wontcheu, 2004
Pr ₉ O ₈ Cl ₃ (SeO ₃) ₄	<i>P</i> 1̄	7.0012(1)	9.0163(2)	9.6688(2)	99.787(1)	94.979(1)	95.901(1) Wontcheu, 2004
Nd ₉ O ₈ Cl ₃ (SeO ₃) ₄	<i>P</i> 1̄	6.9630(2)	8.9680(3)	9.6387(3)	99.528(2)	95.176(2)	95.893(2) Wontcheu, 2004
Sm ₉ O ₈ Cl ₃ (SeO ₃) ₄	<i>P</i> 1̄	6.8870(1)	8.8879(2)	9.5909(2)	98.674(1)	95.419(1)	96.031(1) Wontcheu, 2004
Gd ₉ O ₈ Cl ₃ (SeO ₃) ₄	<i>P</i> 1̄	6.8017(5)	8.8286(7)	9.6018(8)	97.241(6)	95.539(6)	96.265(1) Wontcheu and Schleid, 2003b
Y(Se ₂ O ₅)NO ₃ ·3H ₂ O	<i>P</i> 2 ₁ 2 ₁ 2 ₁	6.216(1)	7.100(2)	20.689(6)			Valkonen and Ylinen, 1979
(H ₃ O)Nd(SeO ₃)(HSeO ₃)(ClO ₄)	<i>P</i> 2 ₁	5.659(1)0	19.186(2)	7.187(1)		104.98(2)	Wickleder 2005a, 2005b

As far as anionic oxo-selenate(IV) derivatives containing other complex anions like NO_3^- are known, they have been prepared from aqueous solution due to the thermal lability of the compounds. No systematic investigations have been undertaken to elucidate the influence of parameters like concentrations, pH value, and temperature. On the other hand, with respect to the absence of a center of symmetry in the compounds known so far, a careful investigation of such systems seems to be worthwhile.

3.2.2. Halide-oxo-selenates(IV)

Powder samples of the chloride-selenites $\text{RCl}(\text{SeO}_3)$ have been prepared for $\text{R} = \text{La}-\text{Yb}$ and Y by solid state reactions of the oxide halides ROCl and SeO_2 . The powder patterns of the compounds could be indexed in the tetragonal ($\text{R} = \text{La}-\text{Eu}$) or orthorhombic system ($\text{R} = \text{Gd}-\text{Yb}$ and Y), respectively (Shabalin et al., 2003). Recent single crystal investigations confirmed the orthorhombic symmetry for the chloride-selenites of the smaller rare earth elements, but also revealed orthorhombic symmetry for the respective compounds of the larger lanthanides. The crystal structure determinations have been carried out for $\text{NdCl}(\text{SeO}_3)$ and $\text{ErCl}(\text{SeO}_3)$ (Wickleder, 2002b), and subsequently, for $\text{HoCl}(\text{SeO}_3)$ (Wickleder, 2003). The single crystals have been obtained in the reactions of the oxides R_2O_3 and chlorides RCl_3 with SeO_2 at 830°C in silica tubes. In the crystal structure of $\text{NdCl}(\text{SeO}_3)$, two crystallographically different neodymium ions, $\text{Nd}(1)^{3+}$ and $\text{Nd}(2)^{3+}$, are present, both of them located in the special site $4c$ of space group $Pnma$ (table 11). $\text{Nd}(1)^{3+}$ is coordinated by eight oxygen atoms and one Cl^- ion. The coordination polyhedron can be described as a distorted tricapped trigonal prism. Within the prism, the bond lengths $\text{Nd}(1)-\text{O}$ range from 2.38 to 2.50 Å, the distances to the capping oxygen atoms and the chloride cap are 2.86 ($2\times$) and 2.90 Å, respectively. The $[\text{Nd}(1)\text{O}_8\text{Cl}]$ polyhedra are connected via common *cis*-edges to *zig-zag* chains along the *b* axis. $\text{Nd}(2)^{3+}$ is surrounded by four oxygen atoms and just as many chloride ions forming a distorted square antiprism with typical bond lengths of about 2.40 Å for $\text{Nd}-\text{O}$ and between 2.79 and 3.05 Å for $\text{Nd}-\text{Cl}$. Similar to the $[\text{Nd}(1)\text{O}_8\text{Cl}]$ prisms, the $[\text{Nd}(2)\text{Cl}_4\text{O}_4]$ polyhedra are linked to *zig-zag* chains in the *b*-direction via common *cis*-edges. The different chains are connected by edges of oxygen atoms in the *a*-, as well as by triangular faces in the *c*-directions. The eight oxygen atoms of the $\text{Nd}(1)$ polyhedron belong to six selenite groups, two of them being attached in a chelating manner whereas the four oxygen atoms of $[\text{Nd}(2)\text{O}_4\text{Cl}_4]$ are donated by four monodentate selenite ions. When viewed along the $[010]$ direction the stereochemical activity of the lone pair of the *pseudo*-tetrahedral SeO_3^{2-} ion is obvious (fig. 15).

$\text{ErCl}(\text{SeO}_3)$ is isotopic with the recently described chloride tellurite $\text{HoCl}(\text{TeO}_3)$ (Meyer and Schleid, 2002). In the crystal structure of $\text{ErCl}(\text{SeO}_3)$ the Er^{3+} ion is coordinated by five oxygen atoms with distances $\text{Er}-\text{O}$ ranging from 2.19 to 2.36 Å and two chloride ligands at 2.70 and 2.73 Å, respectively. The polyhedron $[\text{ErO}_5\text{Cl}_2]$ is best regarded as a pentagonal bipyramid with one oxygen atom and a chloride ion at the apices. The polyhedra are linked via opposite edges in the *c*-direction to yield infinite chains that are connected via chloride ions to a three-dimensional network. The oxygen atoms within the $[\text{ErO}_5\text{Cl}_2]$ polyhedron belong to three monodentate and one chelating SeO_3^{2-} ions. The lower coordination number of Er^{3+} in $\text{ErCl}(\text{SeO}_3)$ compared to Nd^{3+} in $\text{NdCl}(\text{SeO}_3)$ leads also to a smaller coordination

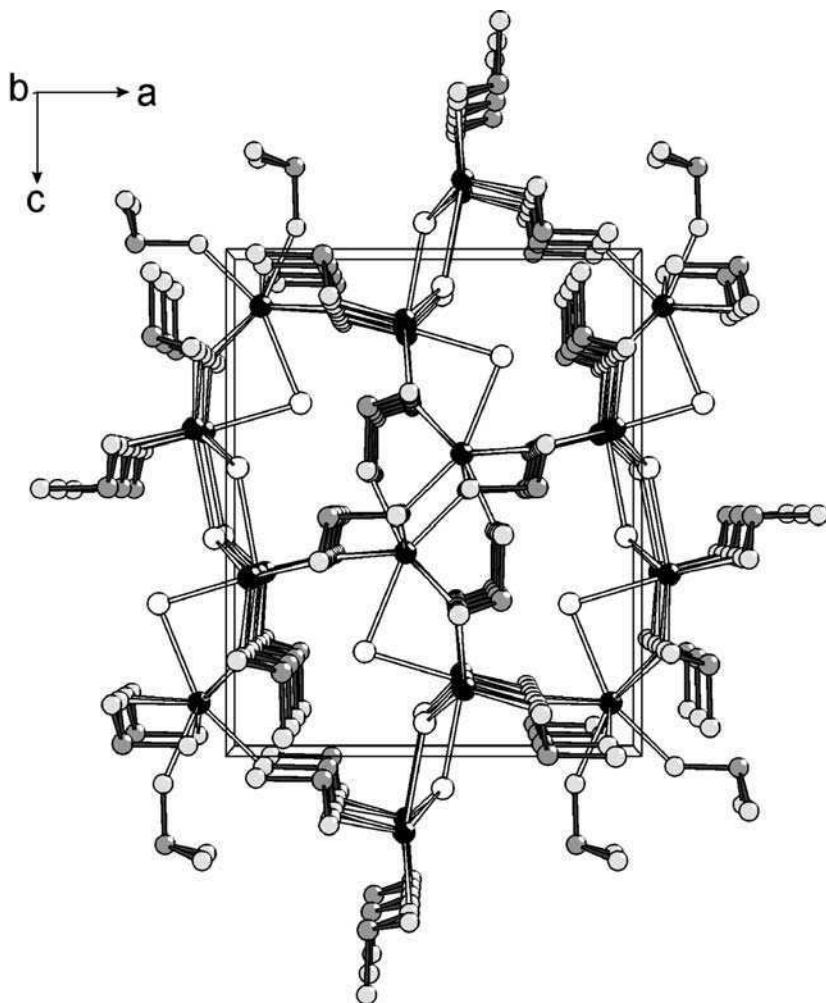


Fig. 15. Perspective view of the crystal structure of $\text{NdCl}(\text{SeO}_3)$ along $[010]$.

number of the anions. In $\text{NdCl}(\text{SeO}_3)$, the Cl^- ions are connected to three and two Nd^{3+} ions, the selenite groups are bonded to five metal ions. In the erbium compound, there is only one two-coordinated chloride ion and the SeO_3^{2-} group is connected to only four Er^{3+} ions. The holmium selenite $\text{HoCl}(\text{SeO}_3)$ adopts the structure of the erbium compound (Wickleder, 2003).

The fluoride systems $\text{R}_2\text{O}_3 \cdot \text{RF}_3 \cdot \text{SeO}_2$ have not been investigated thermochemically, but some fluoride derivatives of rare earth oxo-selenates(IV) have been prepared. They have the composition RFSeO_3 ($= \text{R}_2\text{O}_3 \cdot \text{RF}_3 \cdot 3\text{SeO}_2$) and $\text{R}_3\text{F}(\text{SeO}_3)_4$ ($= 4\text{R}_2\text{O}_3 \cdot \text{RF}_3 \cdot 12\text{SeO}_2$), re-

spectively. The synthesis of these phases is more complicated compared to the respective chlorides due to the high melting points of the trifluorides, RF_3 . The problem can be solved by the use of an appropriate flux, and LiF works quite well. In fact, LiF can also be the F^- source in the reaction, so that fluoride-selenites can be produced from LiF, R_2O_3 , and SeO_2 . Also, the decomposition of the selenates, $\text{R}_2(\text{SeO}_4)_3$, in the presence of LiF is a convenient route to obtain single crystals of these compounds (Wickleder, 2000a; Göhause and Wickleder, 2000; Krügermann and Wickleder, 2002b; Krügermann, 2002). Owing to the aggressive nature of LiF melts, the reactions have to be carried out in metal ampoules, preferably in gold tubes.

The composition $\text{RF}(\text{SeO}_3)$ has been observed only for $\text{R} = \text{La}$ (Wickleder, 2000a). The crystal structure of $\text{LaF}(\text{SeO}_3)$ contains three crystallographically different La^{3+} and SeO_3^{2-} ions, respectively. $\text{La}(1)^{3+}$ is surrounded by four F^- ions and six oxygen ligands. The latter belong to four monodentate and one chelating selenite groups, leading to a coordination number of 11. $\text{La}(2)^{3+}$ has also a coordination number of 11, and in addition to seven fluoride ions, two chelating SeO_3^{2-} groups are attached to this ion. In contrast, $\text{La}(3)^{3+}$ is exclusively surrounded by oxygen atoms and coordination is the same as that of the La^{3+} ions in $\text{La}_2(\text{SeO}_3)_3$. Furthermore, in accordance with the findings for $\text{La}_2(\text{SeO}_3)_3$, in $\text{LaF}(\text{SeO}_3)$, the La^{3+} ions are linked to layers that are connected in the [100] direction by SeO_3^{2-} groups. The main difference between the two compounds is that the connection within the sheets occurs also via fluoride ions in $\text{LaF}(\text{SeO}_3)$. It is worthwhile to mention that the structure $\text{LaF}(\text{SeO}_3)$ is very similar to that of $\text{La}_2(\text{SeO}_3)_3$, as can be seen easily by comparing figs. 16 and 8.

The fluoride selenites $\text{R}_3\text{F}(\text{SeO}_3)_4$ with a lower F^- content were obtained for $\text{R} = \text{Nd}$, Sm , Gd and Dy (Göhause and Wickleder, 2000; Krügermann and Wickleder, 2002b; Krügermann, 2002). They are not known for the smaller rare earth elements. The crystal structures of the isotopic compounds contain R^{3+} ions in triangular formation caused by the selenite group $\text{Se}(1)\text{O}_3^{2-}$ which acts as a μ_3 -ligand, as well as by a $\mu_3\text{-F}^-$ ion capping the triangle on the opposite side (fig. 17). Each edge of the ring is bridged by one oxygen atom of the independent selenite group, $\text{Se}(2)\text{O}_3^{2-}$. The remaining oxygen atoms of this selenite ion belong also to the coordination sphere of the R^{3+} ions of the ring. The coordination sphere of the three M^{3+} ions is completed by three $\text{Se}(1)\text{O}_3^{2-}$ and six $\text{Se}(2)\text{O}_3^{2-}$ ligands, so that the building unit $[\text{M}_3\text{F}(\text{Se}(1)\text{O}_3)_4(\text{Se}(2)\text{O}_3)_9]$ results. These fragments are stacked with the same orientation along the c-axis of the hexagonal unit cell leading to the non-centrosymmetry of the crystal structure (space group $P6_3mc$, table 11). The linkage of the fragments is performed by both selenite groups. The capping $\text{Se}(1)\text{O}_3^{2-}$ group connects one ring to three others so that each oxygen atom of the anion is bidentate bridging while $\text{Se}(2)\text{O}_3^{2-}$ links two other triangles in a way that all oxygen atoms of the group are monodentate and two of them are additionally chelating ligands. The connectivity can be written as $[\text{M}_3\text{F}(\text{Se}(1)\text{O}_3)_{4/4}(\text{Se}(2)\text{O}_3)_{9/3}]$. The influence of the lone pairs of the ψ^1 -tetrahedral anion is even more prominent than found for the other selenites. The lone pair of the $\text{Se}(1)\text{O}_3^{2-}$ ion is oriented along the c-axis towards the fluoride ion so that a very long distance Se-F of 3.69 Å results. The lone pairs of the $\text{Se}(2)\text{O}_3^{2-}$ ions are incorporated in channels which are running parallel to the [001] direction. The diameter of these channels is 6.63 Å with respect to opposite selenium atoms.

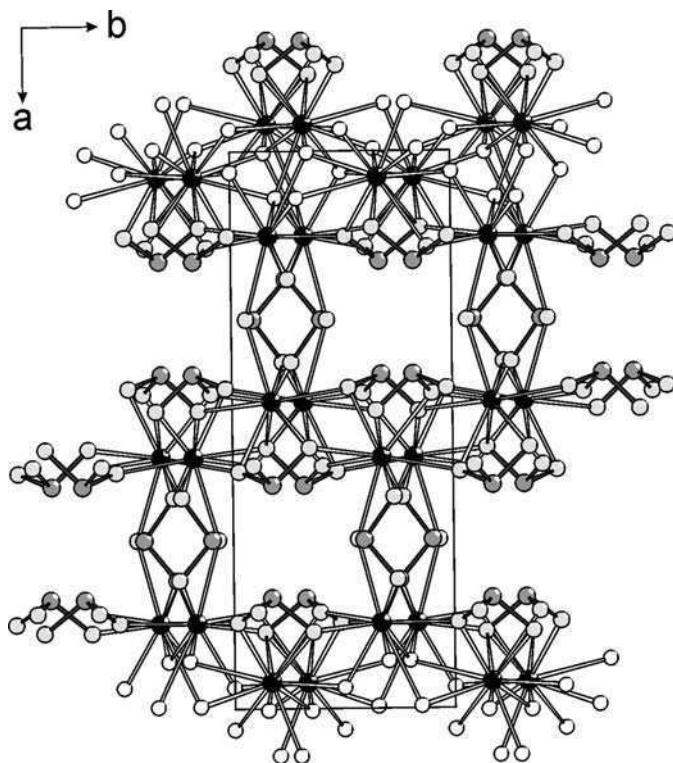


Fig. 16. Projection of the crystal structure of $\text{LaF}(\text{SeO}_3)$ on (001). The relationship of this compound with $\text{La}_2(\text{SeO}_3)_3$ is obvious by comparison with fig. 8.

3.2.3. Oxide-halide oxo-selenates(IV)

If the concentration of R_2O_3 in the systems $\text{R}_2\text{O}_3 \cdot \text{RCl}_3 \cdot \text{SeO}_2$ increases, the formation of oxide-chloride-selenites is observed. A common feature of their crystal structures is that the oxide ions are located in tetrahedra formed by the metal ions. Depending on the composition, the $[\text{OR}_4]$ tetrahedra exhibit different degrees of condensation. For example, in the crystal structure of $\text{Tb}_3\text{O}_2\text{Cl}(\text{SeO}_3)_2$, which was produced in the reaction of SeO_2 , Tb_4O_7 and Tb in a TbCl_3 melt, the oxide-centered Tb tetrahedra, $[\text{OTb}_4]$, are connected by *trans* edges to chains ${}^1_\infty[\text{OTb}_4/2]$ along the a-axis that are further linked to strands according to ${}^1_\infty[\text{Tb}(1)_{3/3}\text{Tb}(2)_{2/1}\text{O}_4/2]$ (Wontcheu and Schleid, 2002b; Wontcheu, 2004; Wontcheu and Schleid, 2005). The strands are arranged along the a-direction leading to *pseudo*-hexagonal channels which incorporate the lone pairs of the selenite ions (fig. 18). Both of the crystallographically different Tb^{3+} ions are in eightfold coordination. $\text{Tb}(1)^{3+}$ has two Cl^- ions and six oxygen atoms as ligands while $\text{Tb}(2)^{3+}$ is surrounded by one Cl^- ion and seven oxygen atoms.

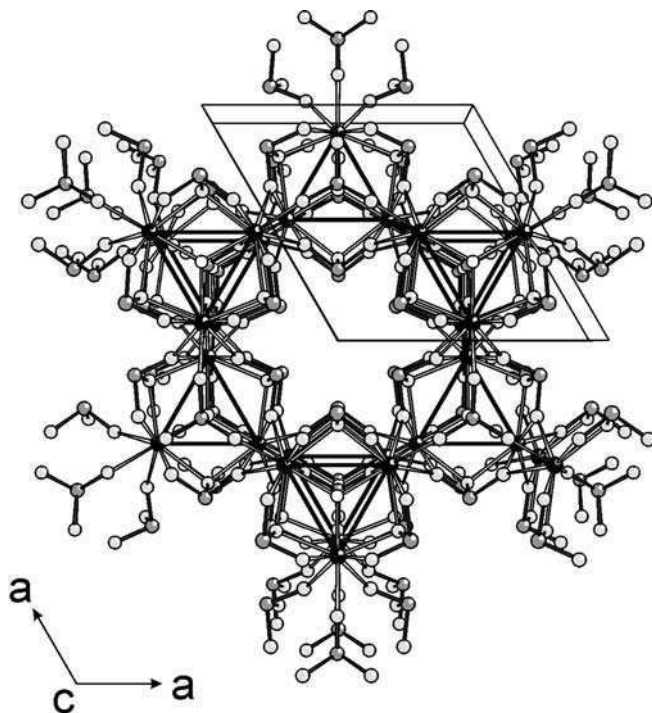


Fig. 17. Perspective view of the non-centrosymmetric crystal structure of the fluoride-selenites $R_3F(SeO_3)_4$ ($R = Nd, Sm, Gd, Dy$) along $[001]$. The connection of the R^{3+} ions to R_3 triangles is emphasized by black lines. The lone electron pairs of the selenium atoms are located in the hexagonal channels that are formed along the c -axis.

The compound is comparable to that of $Cu_3ErO_2Cl(SeO_3)_2$ which is isotypic with the mineral francisite, $Cu_3BiO_2Cl(SeO_3)_2$. In this compound open channels are also formed in order to incorporate the lone electron pairs (Berrigan and Gatehouse, 1996). In contrast to the terbium compound, the chloride ions are also located in these channels without being attached to the cations. Thus, the eightfold coordination of Er^{3+} arises only from oxygen ligands. The composition $R_3O_2Cl(SeO_3)_2$ has also been obtained for $R = Dy$ and Er (Wontcheu, 2004). While the dysprosium compound is isotypic with its respective terbium analogue, $Er_3O_2Cl(SeO_3)_2$ shows a different structure type (table 11). The formation of double chains $\infty^1[Er(1)_{3/3}Er(2)_{2/1}O_{4/2}]$ is exactly the same as observed in $Tb_3O_2Cl(SeO_3)_2$ but the coordination number of one of the two crystallographically different Er^{3+} ions is only seven, as might be expected from the smaller radius of Er^{3+} compared to Tb^{3+} .

A higher degree of condensation of $[OR_4]$ tetrahedra is observed for the composition $R_4O_3Cl_2(SeO_3)_2$ that is known for $R = Er, Yb$ by single crystal investigations (Wontcheu, 2004; Wontcheu and Schleid, 2004a). Six tetrahedra are connected to $[O_6R_{12}]$ units that are further linked via two *trans*-edges and four vertices into layers according to $\infty^2[O_{6/1}R_{4/1}R_{8/2}]$. The layers are connected by weak interactions with the selenium atoms of the anions. For the

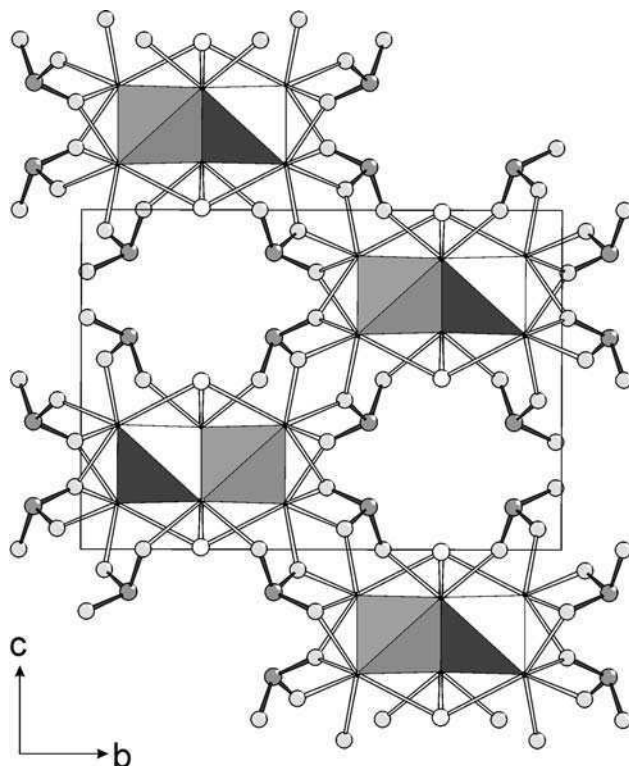


Fig. 18. Projection of the crystal structure of $\text{Tb}_3\text{O}_2\text{Cl}(\text{SeO}_3)_2$ on (100). Similarly to $\text{Tb}_2\text{O}(\text{SeO}_3)_2$ (see fig. 12), oxide-centered $[\text{OTb}_4]$ tetrahedra are condensed into chains. In this case even double chains form due to the high oxide content.

eight crystallographically different R^{3+} ions, coordination numbers of eight ($5\times$) and seven ($3\times$) are found. Three of the R^{3+} ions are exclusively coordinated by oxygen atoms, the remaining five also have Cl^- ligands.

At even higher oxide contents, the $[\text{OR}_4]$ condensation increases further as can be shown for the compounds $\text{R}_5\text{O}_4\text{X}_3(\text{SeO}_3)_2$ that have been confirmed for $\text{R} = \text{Gd}$, $\text{X} = \text{Br}$, and $\text{R} = \text{Tb}$, $\text{X} = \text{Cl}$ (Wontcheu, 2004; Wontcheu and Schleid, 2005). In these crystal structures the same double chains ${}^1_\infty[\text{R}(1)_{3/3}\text{R}(2)_{2/1}\text{O}_{4/2}]$ as in the selenites $\text{R}_3\text{O}_2\text{Cl}(\text{SeO}_3)_2$ ($\text{R} = \text{Tb}$, Dy , Er) are observed but in the present case these are further connected via common vertices to yield layers of the composition ${}^2_\infty[\text{O}_4\text{R}_5]$. The coordination numbers of the three crystallographically different R^{3+} ions are six ($1\times$) and eight ($2\times$), respectively. The SeO_3^{2-} ions are coordinated to the R^{3+} ions in a way that the lone electron pairs of the selenium atoms are located in the space between the layers. Again, the X^- ions are involved in the connection of the layers.

The highest degree of condensation of $[\text{OR}_4]$ tetrahedra is exhibited in the compounds $\text{R}_9\text{O}_8\text{X}_3(\text{SeO}_3)_4$. This composition has been investigated for most of the lighter lanthanides

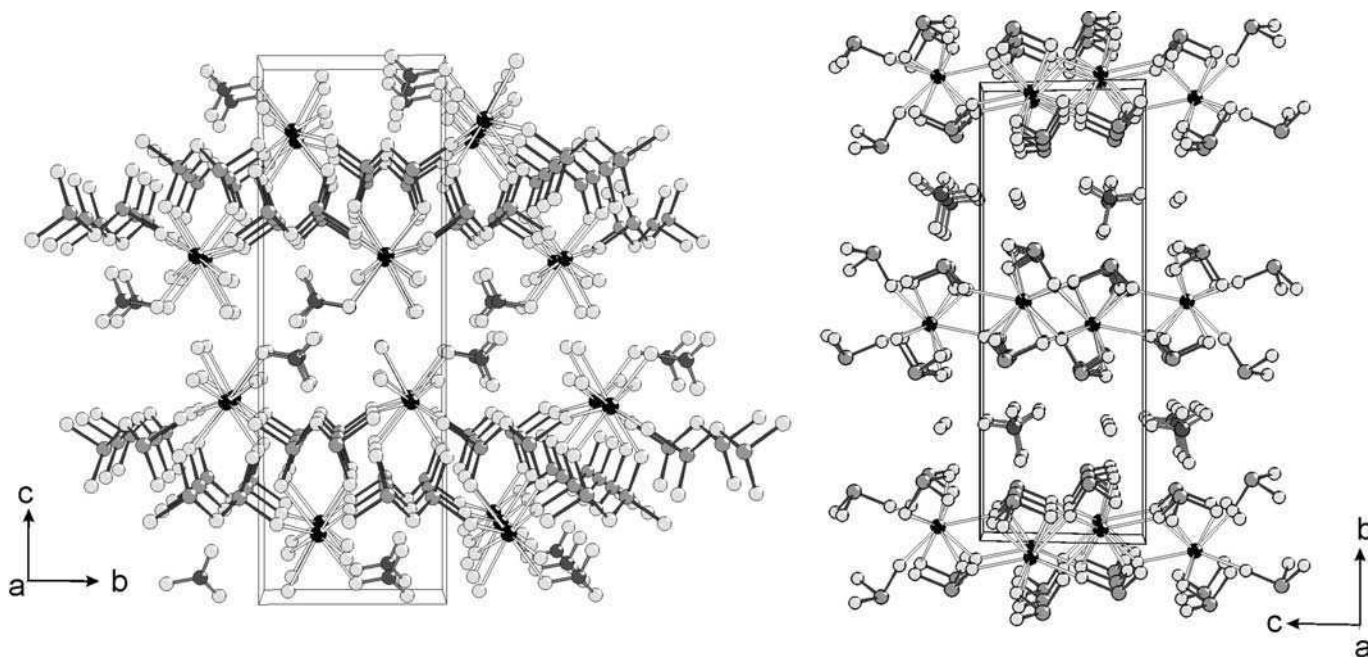


Fig. 19. The layered structures of the selenite-nitrates $R(\text{Se}_2\text{O}_5)(\text{NO}_3)\cdot 3\text{H}_2\text{O}$ ($R = \text{Pr-Lu, Y}$) (left) and the unique selenite-perchlorate $(\text{H}_3\text{O})\text{Nd}(\text{SeO}_3)(\text{HSeO}_3)(\text{ClO}_4)$ (right). In the latter, the ClO_4^- ions are not coordinated to Nd^{3+} ions but reside between the layers of the composition $\infty_2[\text{Nd}(\text{HSeO}_3)_{4/4}(\text{SeO}_3)_{3/3}]$.

with $X = \text{Cl}, \text{Br}$ (table 11) (Wontcheu and Schleid, 2003b; Wontcheu, 2004). The condensation of the tetrahedra occurs again via edges and vertices and leads to layers of the composition $\infty^2[\text{O}_8\text{R}_9]$. These are stacked in the direction of the c -axis of the triclinic unit cell. According to the large ionic radii of the light rare earth elements, the observed coordination numbers for R^{3+} are eight or even nine, and the bond lengths fall into the expected ranges.

3.2.4. Derivatives with complex anions

Derivatives of rare earth oxoselenates(IV) with other complex oxo-anions have not been studied systematically. The only examples known so far are the diselenite-nitrates $\text{R}(\text{Se}_2\text{O}_5)(\text{NO}_3) \cdot 3\text{H}_2\text{O}$ ($\text{R} = \text{Pr-Lu}, \text{Y}$) (Valkonen and Ylinen, 1979; Niinistö et al., 1980) and the complex perchlorate $(\text{H}_3\text{O})\text{Nd}(\text{SeO}_3)(\text{HSeO}_3)(\text{ClO}_4)$ (Wickleder, 2005b). Both compounds might be of certain interest as NLO materials because they crystallize with non-centrosymmetric space groups. The diselenite-nitrates were obtained from a solution of the rare earth oxides and SeO_2 in nitric acid. For the yttrium compound, a single crystal structure determination has been performed. The orthorhombic crystal structure (space group $P2_12_12_1$) shows the Y^{3+} ions in coordination of two monodentate and one chelating $\text{Se}_2\text{O}_5^{2-}$ groups, three H_2O molecules and one nitrate ion. The $\text{Se}_2\text{O}_5^{2-}$ groups connect the Y^{3+} ions to cationic layers according to $\infty^2[\text{Y}(\text{H}_2\text{O})_{3/1}(\text{Se}_2\text{O}_5)_{3/3}]^+$ that are oriented parallel to the (001) plane. The nitrate ions are situated between the layers with one oxygen atom being attached to Y^{3+} (fig. 19, left). The layers are connected by hydrogen bonds involving the nitrate ions and the water molecules.

Similarly, $(\text{H}_3\text{O})\text{Nd}(\text{SeO}_3)(\text{HSeO}_3)(\text{ClO}_4)$ crystallizes from a solution of Nd_2O_3 and SeO_2 in perchloric acid. The compound is non-centrosymmetric (space group $P2_1$) and shows a typical layered structure (fig. 19, right). In this case, the layers are electro-neutral and have the composition $\infty^2[\text{Nd}(\text{HSeO}_3)_{4/4}(\text{SeO}_3)_{3/3}]$. The coordination number of Nd^{3+} is nine due to the chelating attachment of two HSeO_3^- ions. The layers are separated by both, H_3O^+ and ClO_4^- ions. The latter are not coordinated to Nd^{3+} ions but fixed by hydrogen bonds involving HSeO_3^- and H_3O^+ ions between the layers.

3.3. Cationic derivatives of selenates(IV)

3.3.1. Alkali metal containing oxo-selenates(IV)

The number of ternary selenites containing alkali metals (A) is limited and a detailed investigation of the systems $\text{R}_2(\text{SeO}_3)_3 \cdot \text{A}_2\text{SeO}_3$ ($= \text{R}_2\text{O}_3 \cdot \text{A}_2\text{O} \cdot 4\text{SeO}_2$) is urgently needed. The two sodium selenites $\text{NaR}(\text{SeO}_3)_2$ ($\text{R} = \text{La}, \text{Y}$) have been obtained hydrothermally with Na_2CO_3 , R_2O_3 , and SeO_2 as initial compounds (Morris et al., 1990). The lanthanum compound shows the La^{3+} ions in tenfold coordination of oxygen atoms, which are part of three $\text{Se}(1)\text{O}_3^{2-}$ and four $\text{Se}(2)\text{O}_3^{2-}$ ions, respectively. Three of the selenite groups are chelating ligands. In accordance with the formulation $\infty^3[\text{La}(\text{Se}(1)\text{O}_3)_{3/3}(\text{Se}(2)\text{O}_3)_{4/4}]^-$, a three-dimensional anionic network incorporates the Na^+ ions for charge balance. With respect to the distances Na-O , the coordination number of Na^+ can be given as $5 + 2$. A three-dimensional anionic sublattice is also found for the yttrium compound but due to the smaller ionic radius of Y^{3+} when compared to La^{3+} , the coordination number decreases to seven. Five monodentate and

one chelating SeO_3^{2-} ions are attached to the Y^{3+} ions and the linkage of the polyhedra according to ${}_{\infty}^3[\text{Y}(\text{Se}(1)\text{O}_3)_{3/3}(\text{Se}(2)\text{O}_3)_{3/3}]^-$ provides channels that are occupied by the Na^+ ions exhibiting a coordination number of 5 + 3.

The lithium compound $\text{Li}_3\text{Lu}_5(\text{SeO}_3)_9$ has been obtained accidentally as a by-product in the reaction of Lu_2O_3 and SeO_2 to form $\text{Lu}_2(\text{SeO}_3)_3$ in a LiBr flux (Wontcheu, 2004; Wontcheu and Schleid, 2004b). It shows a monoclinic crystal structure with five crystallographically different Lu^{3+} ions. All of the latter are surrounded by six SeO_3^{2-} ligands but the coordination number is eight for two of the cations and seven for the remaining three due to the chelating coordination modes of two and one selenite groups, respectively. The distances Lu–O cover the typical range from 2.14 to 2.55 Å. Six of the nine crystallographically different SeO_3^{2-} groups are coordinated by three Lu^{3+} ions; three have four Lu^{3+} neighbours. The linkage of the $[\text{LuO}_8]$ and $[\text{LuO}_7]$ polyhedra by selenite groups leads to a complicated three-dimensional network in which the Li^+ ions occupy different holes providing the coordination numbers 4 + 1, 5, and 4 + 2 for the cations. The coordination polyhedra around the lithium ions are trigonal bipyramids in two cases and an elongated octahedron for the third Li^+ ion. The oxide atoms around the Li^+ ions belong to five and four selenite ions, respectively.

The solid state reaction of Tm_2O_3 , TmCl_3 , SeO_2 , and CsCl at 830 °C in silica tubes led to single crystals of two different compounds. One is the selenite $\text{Tm}_2(\text{SeO}_3)_3$ (see section 3.1), the second one is the complex chloride-selenite $\text{CsTmCl}_2(\text{SeO}_3)$ (Wontcheu and Schleid, 2003c; Wontcheu, 2004). It shows the Tm^{3+} ions in pentagonal bipyramidal coordination of five oxygen and two chlorine atoms that form the apices of the bipyramide. The oxygen atoms are donated by three monodentate and one chelating SeO_3^{2-} ligands. The selenite anions are surrounded by four Tm^{3+} ions so that infinite layers ${}_{\infty}^2[\text{TmCl}_{2/1}(\text{SeO}_3)_{4/4}]^-$ are formed. These layers are stacked along the c-axis of the monoclinic unit cell, and between the layers, the Cs^+ ions are situated. They are mainly coordinated by six Cl^- ions and by one oxygen atom at a distance of 3.19 Å. Two distant oxygen atoms at 3.83 and 4.08 Å contribute to a small extent to the coordination sphere of Cs^+ . It is astonishing that $\text{CsTmCl}_2(\text{SeO}_3)$ is the only representative of this family of compounds. Considering the frequent use of cesium halides as flux one would expect Cs-based compounds to be found more often as by-products. Further investigations seem to be necessary to optimize preparative conditions for these phases.

The bromide $\text{CsSm}_{21}\text{Br}_{16}(\text{SeO}_3)_{24}$ has been obtained in a reaction that aimed at the preparation of $\text{SmBr}(\text{SeO}_3)$. The complex selenite is *pseudo*-tetragonal (table 12) and is built from layers of the composition $[\text{Sm}_{14}(\text{SeO}_3)_{24}]$ that alternate with layers of the Br^- ions along the c-axis (Ruck and Schmidt, 2003). Within the $[\text{Sm}_{14}(\text{SeO}_3)_{24}]$ layers, the Sm^{3+} ions are exclusively coordinated by oxygen atoms. The layers are further connected by Sm^{3+} ions that are surrounded by both oxygen atoms and bromide ions. For electro-neutrality reasons, some of the Sm^{3+} ions between the layers are substituted by Cs^+ ions that originate from the used CsBr flux. Powder diffraction investigations show that other alkali metal ions can substitute for Sm^{3+} if the respective bromides are used as flux (Ruck and Schmidt, 2003).

Another complex cesium selenite, $\text{CsEu}_4\text{O}_3\text{Cl}_3(\text{SeO}_3)_2$, has been obtained as a side-product in a solid state reaction aiming at the synthesis of $\text{Eu}_4\text{O}_3\text{Cl}_2(\text{SeO}_3)_2$ (Wontcheu, 2004). As observed in the oxide-halide-selenites discussed in section 3.2.3, the O^{2-} -centered metal tetrahedra that are condensed to infinite layers are found again. However, in this case

Table 12
Crystallographic data of cationic oxo-selenate(IV) derivatives

Compound	Space group	Lattice parameters						Reference
		a (Å)	b (Å)	c (Å)	α (deg)	β (deg)	γ (deg)	
NaY(SeO ₃) ₂	<i>P2₁cn</i>	5.397(2)	8.525(2)	12.765(2)				Morris et al., 1990
NaLa(SeO ₃) ₂	<i>P2₁/n</i>	6.696(4)	6.761(4)	13.199(5)		101.51(3)		Morris et al., 1990
Li ₃ Lu ₅ (SeO ₃) ₉	<i>P2₁/n</i>	13.9385(5)	13.9451(2)	14.0948(2)		113.006(1)		Wontcheu and Schleid, 2004b
CsTmCl ₂ (SeO ₃)	<i>P2₁/n</i>	6.5892(5)	6.8926(6)	17.525(1)		99.093(7)		Wontcheu and Schleid, 2003c
CsSm ₂₁ Br ₁₆ (SeO ₃) ₂₄	<i>Bbab</i>	15.797(2)	15.797(2)	17.963(2)				Ruck and Schmidt, 2003
CsEu ₄ O ₃ Cl ₃ (SeO ₃) ₂	<i>P$\bar{1}$</i>	5.4509(2)	8.7999(3)	15.9744(7)	81.036(2)	89.992(2)	71.926(2)	Wontcheu, 2004
Cu ₃ ErO ₂ Cl(SeO ₃) ₂	<i>Pmnm</i>	6.299(1)	9.430(3)	6.967(2)				Berrigan and Gatehouse, 1996
CuLa ₂ (SeO ₃) ₄	<i>P2₁/c</i>	10.512(1)	7.136(1)	8.431(1)		110.61(1)		Harrison and Zhang, 1997a
CuNd ₂ (SeO ₃) ₄	<i>P2₁/c</i>	10.512(1)	7.044(1)	8.306(1)		110.59(1)		Ben Hamida, 2004
CuSm ₂ (SeO ₃) ₄	<i>P2₁/c</i>	10.504(3)	6.966(2)	8.225(2)		110.48(2)		Wickleder and Ben Hamida, 2003
CuEu ₂ (SeO ₃) ₄	<i>P2₁/c</i>	10.482(3)	6.931(1)	8.190(2)		110.46(3)		Ben Hamida, 2004
CuGd ₂ (SeO ₃) ₄	<i>P2₁/c</i>	10.510(2)	6.935(1)	8.185(2)		110.53		Wickleder and Ben Hamida, 2003
MnNdCl(SeO ₃) ₂	<i>P$\bar{1}$</i>	7.078(1)	7.301(2)	8.080(2)	86.88(2)	71.76(2)	64.37(2)	Ben Hamida, 2004
MnSmCl(SeO ₃) ₂	<i>P$\bar{1}$</i>	7.008(2)	7.241(2)	8.043(2)	86.90(3)	71.57(3)	64.33(3)	Wickleder and Ben Hamida, 2003
CoLaCl(SeO ₃) ₂	<i>P$\bar{1}$</i>	7.122(2)	8.899(2)	11.966(2)	97.31(3)	105.52(2)	107.98(2)	Ben Hamida, 2004
CoSmCl(SeO ₃) ₁	<i>P$\bar{1}$</i>	7.123(1)	8.895(2)	12.162(2)	72.25(1)	71.27(1)	72.08(1)	Wickleder and Ben Hamida, 2003
CoTbCl(SeO ₃) ₂	<i>P$\bar{1}$</i>	7.069(1)	8.796(2)	11.890(3)	97.63(3)	105.49(3)	107.80(3)	Ben Hamida, 2004
CuGdCl(SeO ₃) ₂	<i>P$\bar{1}$</i>	7.043(4)	9.096(4)	12.010(7)	70.84(4)	73.01(4)	70.69(4)	Wickleder and Ben Hamida, 2003
CoNd ₁₀ Cl ₁₂ (SeO ₃) ₈	<i>P2/c</i>	15.699(2)	15.699(2)	19.171(2)		114.00(1)		Ben Hamida and Wickleder, 2005

only three of the four metal ions are involved in $[\text{OR}_4]$ tetrahedra so that the condensation of the tetrahedra is even higher than observed for $\text{R}_4\text{O}_3\text{Cl}_2(\text{SeO}_3)_2$ ($\text{R} = \text{Er}, \text{Yb}$). The sheets are arranged parallel to the (001) plane of the monoclinic unit cell and are separated by the fourth Eu^{3+} ion that is in eightfold coordination of four oxygen and four Cl^- ligands and by the Cs^+ ions that are coordinated by eight Cl^- ions with *pseudo*-cubic coordination polyhedra. The different functionalities of the Eu^{3+} ions in the structure are reflected in the Eu–O distances; those Eu^{3+} ions that are involved in the sheets of condensed $[\text{OEu}_4]$ tetrahedra show very short bond length from 2.24 to 2.32 Å while the Eu^{3+} ion situated between the layers has nearest contacts between 2.44 and 2.74 Å.

3.3.2. Transition metal containing oxo-selenates(IV)

Recently, it turned out that the SeO_3^{2-} ion is a suitable ligand for linking rare earth and transition metal ions. On one hand, this may enrich the structural chemistry of rare earth selenites enormously via engaging the large number of transition metals. But what seems to be of much greater importance is, that a new family of compounds having the potential to show interesting magnetic phenomena due to the presence of both paramagnetic f- and d-element ions can be developed. For this purpose, it is desirable to realize different arrangements of the cations with respect to each other. This can be achieved by different stoichiometries of the cations in the compound, and furthermore, with respect to the knowledge from other polynary selenites, by the incorporation of halide anions into the lattice.

To date, examples for pure selenites are limited to the isotypic copper compounds $\text{CuR}_2(\text{SeO}_3)_4$ ($\text{R} = \text{La}, \text{Nd-Tb}$) (Harrison and Zhang, 1997a; Wickleder and Ben Hamida, 2003; Ben Hamida, 2004). They have been obtained from the reaction of CuO , R_2O_3 , and SeO_2 in the appropriate ratio by solid state or hydrothermal reactions. The hydrothermal reactions work also when metal nitrates are used instead of the oxides. All of the selenites show a deep blue color. In the crystal structure, the Cu^{2+} ions are in square-planar coordination of oxygen atoms that belong to four monodentate SeO_3^{2-} ions. The selenite groups are coordinated to two Cu^{2+} ions leading to layers of the composition ${}_{\infty}^2[\text{Cu}(\text{Se}(1)\text{O}_3)_{4/2}]^{2-}$. These are alternatively stacked in the direction of the a-axis with layers that are formed by the linkage of R^{3+} ions and selenite groups. The sheets contain the R^{3+} ions in tenfold coordination of oxygen atoms that belong to three chelating and four monodentate selenite ions, and according to the formulation ${}_{\infty}^2[\text{R}(\text{Se}(1)\text{O}_3)_{2/2}(\text{Se}(2)\text{O}_3)_{5/5}]^-$ two crystallographically different SeO_3^{2-} groups are involved. Only the $\text{Se}(1)\text{O}_3^{2-}$ ions connect the $[\text{Cu}(\text{Se}(1)\text{O}_3)_{4/2}]^{2-}$ layers as can be seen in fig. 20.

While to date the pure transition metal containing rare earth selenites are restricted to copper as the transition metal, the chloride-selenites $\text{MRCl}(\text{SeO}_3)_2$ allow greater variation of the transition metal M. They have been prepared with $\text{M} = \text{Mn}, \text{Co}, \text{Cu}$ and for most of the larger rare earth metals (Wickleder and Ben Hamida, 2003; Ben Hamida, 2004). The synthesis can be done by the reaction of the transition metal oxides, MO , with rare earth trichlorides and SeO_2 . Alternatively, the transition metal chlorides can serve as Cl^- source, and R is added in form of the oxides. In any case, the reactions are carried at 800 °C in evacuated silica ampoules, and excess of the chloride component is helpful if single crystals are desired.

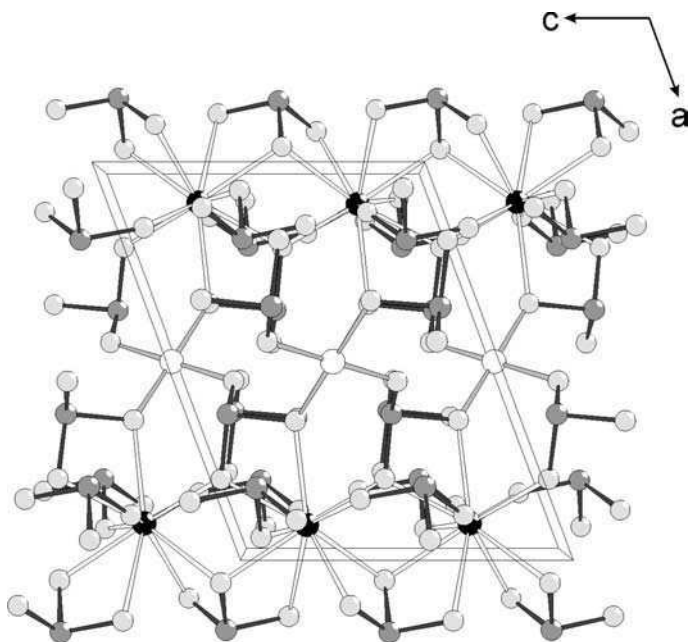


Fig. 20. Perspective view of the crystal structure of the copper selenites $\text{Cu}_2(\text{SeO}_3)_4$ ($R = \text{La, Nd-Tb}$) along [010].

In the isotypic manganese compounds $\text{MnRCl}(\text{SeO}_3)_2$ ($R = \text{Nd, Sm}$), the R^{3+} ion is coordinated by eight oxygen atoms and one Cl^- ligand. The oxygen atoms belong of three $\text{Se}(1)\text{O}_3^{2-}$ and two $\text{Se}(2)\text{O}_3^{2-}$ ions. Three selenite ions act as chelating ligands, the remaining are monodentate. Similarly to the copper compounds described above, the R^{3+} ions in $\text{MnRCl}(\text{SeO}_3)_2$ ($R = \text{Nd, Sm}$) are connected by selenite groups to layers according to $\infty^2[\text{R}(\text{Se}(1)\text{O}_3)_{3/3}(\text{Se}(2)\text{O}_3)_{2/2}\text{Cl}_{1/1}]^{2-}$. The Mn^{2+} ions are situated between these layers. They are octahedrally coordinated by four oxygen atoms and two chloride ions. The Cl^- ions are in *cis* orientation with respect to each other and the $[\text{MnCl}_2\text{O}_4]$ octahedra are connected via opposite edges (Cl-Cl and O-O , respectively) to infinite chains according to $\infty^1[\text{MnCl}_{2/2}\text{O}_{2/2}\text{O}_{2/1}]$ that are running between the $\infty^2[\text{R}(\text{Se}(1)\text{O}_3)_{3/3}(\text{Se}(2)\text{O}_3)_{2/2}\text{Cl}_{1/1}]^{2-}$ layers.

The structures of the respective chloride-selenites with $M = \text{Co, Cu}$ are very similar to the manganese compound just described. The connection of the R^{3+} ions by selenite groups to layers remains nearly the same and only the coordination number of one of the two crystallographically different R^{3+} ions decreases from 9 to 8 + 1. The coordination of the Co^{2+} ions in $\text{CoRCl}(\text{SeO}_3)_2$ is octahedral with four oxygen ligands and two Cl^- ions that are again in *cis*-position with respect to each other. The connection of the $[\text{CoO}_4\text{Cl}_2]$ octahedra is slightly different when compared to the observations for the manganese selenites. According to the formulation $\infty^1[\text{CoCl}_{2/2}\text{O}_{1/2}\text{O}_{3/1}]$, the linkage occurs via a common Cl-Cl edge but further

connection is achieved only via a common oxygen vertex, and not an O–O edge as found for $\text{MnRCl}(\text{SeO}_3)_2$ ($\text{R} = \text{Nd}, \text{Sm}$).

Owing to the electron configuration of Cu^{2+} (d^9), the coordination of this ion in $\text{CuGdCl}(\text{SeO}_3)_2$ is not ideally octahedral, but shows the typical tetragonal Jahn–Teller distortion; three oxygen atoms and one chloride ion are coordinated with short distances (Cu–O : 1.93–2.01 Å; Cu–Cl : 2.36 Å), and two further ligands ($1 \times \text{O}$ at 2.60 Å, $1 \times \text{Cl}$ at 2.80 Å) complete the distorted octahedron. Besides the difference in the M^{2+} coordination, $\text{CuGdCl}(\text{SeO}_3)_2$ has nearly the same structure as the manganese compounds. Thus, also in $\text{CuGdCl}(\text{SeO}_3)_2$ chains according to ${}_{\infty}^1[\text{CuCl}_{2/2}\text{O}_{2/2}\text{O}_{2/1}]$ are situated between the layers ${}_{\infty}^2[\text{Gd}(\text{Se}(1)\text{O}_3)_{3/3}(\text{Se}(2)\text{O}_3)_{2/2}\text{Cl}_{1/1}]^{2-}$. It is worthwhile to mention that the color of $\text{CuGdCl}(\text{SeO}_3)_2$ is light green in contrast to the deep blue color of the selenites $\text{CuR}_2(\text{SeO}_3)_4$ ($\text{R} = \text{La}, \text{Nd}, \text{Sm}, \text{Eu}, \text{Gd}$), what can be attributed to the different type of ligands and the different coordination geometry of Cu^{2+} .

A unique layer structure is found for the cobalt-based compound $\text{CoNd}_{10}\text{Cl}_8(\text{SeO}_3)_{12}$ (Ben Hamida and Wickleder, 2005). It has been obtained in form of blue single crystals in the reaction of CoCl_2 , Nd_2O_3 and SeO_2 . The majority of the Nd^{3+} ions and all of the selenite groups form one kind of a layer; the Cl^- ions build the second type. The layers are stacked in [102] direction of the monoclinic unit cell. The layers of the Nd^{3+} ions and the selenite groups have the composition $[\text{Nd}_7(\text{SeO}_3)_8]$ and seem to exhibit nearly tetragonal symmetry as can be seen in fig. 21 and also from the similar lengths of the a- and b-axis, respectively

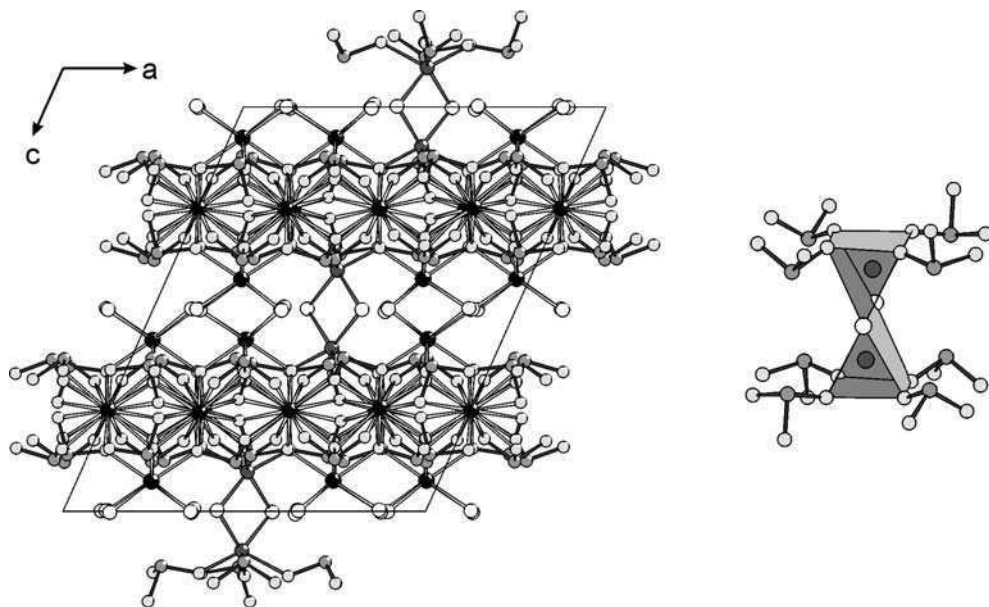


Fig. 21. Crystal structure of $\text{CoNd}_{10}\text{Cl}_8(\text{SeO}_3)_{12}$ viewed along [010]. The most characteristic feature of the structure are $[\text{Co}_2\text{Cl}_2(\text{SeO}_3)_8]$ dimers depicted on the right.

(table 12). Between the $[\text{Nd}_7(\text{SeO}_3)_8]$ and the Cl^- layers, the remaining three Nd^{3+} ions are located. They are coordinated by four oxygen atoms from selenite ions and four Cl^- ions in form of a square antiprism. Further connection of the sheets is achieved by the Co^{2+} ions. They have four oxygen and two chloride ligands. The coordination geometry of the $[\text{CoCl}_2\text{O}_4]$ polyhedron is a trigonal prism, and two of these prisms share a common edge to form dimers $[\text{Co}_2\text{Cl}_2\text{O}_8]$ (fig. 21). These dimers are the most characteristic feature of the crystal structure of $\text{CoNd}_{10}\text{Cl}_8(\text{SeO}_3)_{12}$. It should be mentioned that the crystal structure of $\text{CoNd}_{10}\text{Cl}_8(\text{SeO}_3)_{12}$ is closely related to that of $\text{CsSm}_{21}\text{Br}_{16}(\text{SeO}_3)_{24}$ (Ruck and Schmidt, 2003) that has been described above. This becomes more obvious if the formulae of the compounds are written as $\text{CoNd}_3\text{Cl}_8[\text{Nd}_7(\text{SeO}_3)_{12}]$ and $\text{Cs}_{0.5}\text{Sm}_{3.5}\text{Br}_8[\text{Sm}_7(\text{SeO}_3)_{12}]$, respectively, separating the cations that built the layers with the selenite groups in square brackets from those that are situated between the layers.

3.4. Properties of oxo-selenates(IV)

3.4.1. Thermal behaviour of oxo-selenates(IV)

The thermal decomposition of various selenites has been investigated. Table 13 summarizes the most important results that have been obtained to date. Unfortunately, not in every case the initial substances, intermediates, and products of the reactions are well characterized causing difficulties in the interpretation of the reactions.

The decomposition of selenite hydrates, $\text{R}_2(\text{SeO}_3)_3 \cdot x\text{H}_2\text{O}$, has been followed for nearly the complete rare earth series (Giesbrecht et al., 1962; Giolito and Giesbrecht, 1967; Perkovskaya, 1968; Savchenko et al., 1968; Petrov et al., 1973). According to the TG data, the water content x has been given as 4 in the most cases, except for La and Yb, where x is only 3. The first decomposition step is the dehydration that is observed in the range from 50 to 200 °C. The anhydrous selenites decompose in the same way as described in section 2.3.1. Thus, the oxides, R_2O_3 , are formed around 1000 °C, and the oxide-selenites $\text{R}_2\text{O}_2(\text{SeO}_3)$ are found as intermediates. In the case of $\text{R} = \text{Ce}, \text{Pr},$ and Tb , the residues are $\text{CeO}_2, \text{Pr}_6\text{O}_{11},$ and Tb_4O_7 , respectively.

More recently, the thermal behaviours of the acidic selenites $\text{Nd}(\text{HSeO}_3)(\text{SeO}_3) \cdot 2\text{H}_2\text{O}$ and $\text{Pr}(\text{HSeO}_3)(\text{SeO}_3)$ have been reported (de Pedro et al., 1994; Castro et al., 1994). According to these investigations, both compounds dehydrate in a first step to yield diselenite-selenites $\text{R}_2(\text{Se}_2\text{O}_5)(\text{SeO}_3)_2$ ($= \text{R}_2\text{Se}_4\text{O}_{11}$). For the neodymium compound, the dehydration process seems to occur in two steps. The authors mention that the diselenite-selenites are obtained in single crystalline form, however, structural data have not been given. Further decomposition leads to sesquiselenites $\text{R}_2(\text{SeO}_3)_3$, and SeO_3^{2-} rich diselenites $\text{R}_2(\text{Se}_2\text{O}_5)_{0.5}(\text{SeO}_3)_{2.5}$ ($= \text{R}_2\text{Se}_{3.5}\text{O}_{10}$) may occur as intermediates. Finally, the degradation of selenites $\text{R}_2(\text{SeO}_3)_3$ produces oxides, R_2O_3 as has been described in section 2.3.1.

Another group of acidic selenites that has been investigated, was said to have the composition $\text{RH}(\text{SeO}_3)_2 \cdot 2.5\text{H}_2\text{O}$ ($\text{R} = \text{Pr-Lu}, \text{Y}$) (Immonen et al., 1976). The structure of these phases is not known, but according to the lattice parameters that have been obtained from X-ray single crystal photographs it can be assumed that their structures are closely related to that of $\text{Nd}(\text{HSeO}_3)(\text{SeO}_3) \cdot 2\text{H}_2\text{O}$ (de Pedro et al., 1994). It is also possible that they have

Table 13
Thermal decomposition schemes of various oxo-selenites(IV)

Initial compound and reactions ¹⁾	Temperature range	Comments
$R_2(\text{SeO}_3)_3 \cdot x\text{H}_2\text{O}$; $x = 4$ or 3 (for La and Yb) $R_2(\text{SeO}_3)_3 \cdot x\text{H}_2\text{O} \rightarrow R_2(\text{SeO}_3)_3 + x\text{H}_2\text{O}\uparrow$	50–200 °C	Structures of the initial hydrates not known
$R(\text{HSeO}_3)(\text{SeO}_3) \cdot 2\text{H}_2\text{O}$ 1. $2R(\text{HSeO}_3)(\text{SeO}_3) \cdot 2\text{H}_2\text{O} \rightarrow R_2(\text{Se}_2\text{O}_5)(\text{SeO}_3)_2 + 5\text{H}_2\text{O}\uparrow$ 2. $2R_2(\text{Se}_2\text{O}_5)(\text{SeO}_3)_2 \rightarrow R_4(\text{Se}_2\text{O}_5)(\text{SeO}_3)_5 + \text{SeO}_2$ 3. $R_4(\text{Se}_2\text{O}_5)(\text{SeO}_3)_5 \rightarrow 2R_2(\text{SeO}_3)_3 + \text{SeO}_2$	70–270 °C 290–400 °C 520–590 °C	Structures of initial compounds known for R = Nd, Pr; dehydration may occur in two steps ($1 \times \text{H}_2\text{O} + 4 \times \text{H}_2\text{O}$); $R_4(\text{Se}_2\text{O}_5)(\text{SeO}_3)_5$ not necessarily seen
$R(\text{HSeO}_3)(\text{SeO}_3)$ 1. $2R(\text{HSeO}_3)(\text{SeO}_3) \rightarrow R_2(\text{Se}_2\text{O}_5)(\text{SeO}_3)_2 + \text{H}_2\text{O}\uparrow$ 2. $2R_2(\text{Se}_2\text{O}_5)(\text{SeO}_3)_2 \rightarrow R_4(\text{Se}_2\text{O}_5)(\text{SeO}_3)_5 + \text{SeO}_2$ 3. $R_4(\text{Se}_2\text{O}_5)(\text{SeO}_3)_5 \rightarrow 2R_2(\text{SeO}_3)_3 + \text{SeO}_2$	270–350 °C 290–400 °C 520–590 °C	Structures of initial compounds known for R = Nd, Pr; $R_4(\text{Se}_2\text{O}_5)(\text{SeO}_3)_5$ not necessarily seen
$R(\text{HSeO}_3)(\text{SeO}_3) \cdot 2.5\text{H}_2\text{O}$ 1. $2R(\text{HSeO}_3)(\text{SeO}_3) \cdot 2.5\text{H}_2\text{O} \rightarrow R_2(\text{Se}_2\text{O}_5)(\text{SeO}_3)_2 + 6\text{H}_2\text{O}\uparrow$ 2. $2R_2(\text{Se}_2\text{O}_5)(\text{SeO}_3)_2 + 8\text{H}_2 \rightarrow R_4\text{O}_4\text{Se}_3 + 5\text{SeO}_2 + 8\text{H}_2\text{O}$ 3. $2R_2(\text{Se}_2\text{O}_5)(\text{SeO}_3)_2 + 8\text{CO} \rightarrow R_4\text{O}_4\text{Se}_3 + 5\text{SeO}_2 + 8\text{CO}_2$	180–200 °C 490–530 °C 400–450 °C	Initial compounds possibly mistaken for $R(\text{HSeO}_3)(\text{SeO}_3) \cdot 2\text{H}_2\text{O}$; reaction carried out under reductive atmosphere (H_2 or CO); intermediates may occur during decomposition; further heating in H_2 leads to the formation of $R_2\text{O}_3$ due to H_2Se evolution; for R = Eu, the reduction leads to EuSe in both cases
$R_2(\text{SeO}_3)_3 \cdot x\text{H}_2\text{SeO}_3 \cdot n\text{H}_2\text{O}$; $x = 0.2\text{--}0.8$, $n = 4\text{--}5$ 1. $R_2(\text{SeO}_3)_3 \cdot x\text{H}_2\text{SeO}_3 \cdot n\text{H}_2\text{O} \rightarrow R_2(\text{SeO}_3)_3 \cdot x\text{H}_2\text{SeO}_3 + n\text{H}_2\text{O}\uparrow$ 2. $R_2(\text{SeO}_3)_3 \cdot x\text{H}_2\text{SeO}_3 \rightarrow R_2(\text{SeO}_3)_3 + x\text{H}_2\text{SeO}_3$	50–340 °C 380–550 °C	Structures of the initial compounds not known
$\text{NH}_4\text{R}(\text{SeO}_3)_2 \cdot x\text{H}_2\text{O}$; $x = 2$ for R = Sm and $x = 2.5$ for R = Gd 1. $\text{NH}_4\text{R}(\text{SeO}_3)_2 \cdot x\text{H}_2\text{O} \rightarrow \text{NH}_4\text{R}(\text{SeO}_3)_2 + x\text{H}_2\text{O}\uparrow$ 2. $\text{NH}_4\text{R}(\text{SeO}_3)_2 \rightarrow R_2(\text{SeO}_3)_3 + 2\text{NH}_3 + \text{SeO}_2 + \text{H}_2\text{O}$	80–200 °C 200–600 °C	Structures of the initial compounds not known
$\text{AGd}(\text{SeO}_3)_2 \cdot x\text{H}_2\text{O}$; $x = 2$ for A = K and $x = 2.5$ for A = Na 1. $\text{AGd}(\text{SeO}_3)_2 \cdot x\text{H}_2\text{O} \rightarrow \text{AGd}(\text{SeO}_3)_2 + x\text{H}_2\text{O}\uparrow$ 2. $\text{AGd}(\text{SeO}_3)_2 \rightarrow \text{AGdO}(\text{SeO}_3) + \text{SeO}_2$ 3. $2\text{AGdO}(\text{SeO}_3) \rightarrow \text{A}_2\text{Gd}_2\text{O}_3(\text{SeO}_3) + \text{SeO}_2$	80–240 °C 570–780 °C 830–1000 °C	Structures of the initial compounds not known; three dehydration steps for $\text{NaGdR}(\text{SeO}_3)_2 \cdot 2.5\text{H}_2\text{O}$; structures of decomposition products not known

¹⁾The selenites $R_2(\text{SeO}_3)_3$ that form in the reactions decompose according to the scheme mentioned in table 13.

been mistaken with the dihydrates. Besides these uncertainties, the investigation of the thermal behavior is interesting because the measurements have been carried out under reducing atmosphere using both H_2 and CO as reducing gases (Immonen et al., 1976). The first step of the decomposition is again the dehydration of the compounds, probably accompanied by the formation of $R_2(Se_2O_5)(SeO_3)_2$ ($= R_2Se_4O_{11}$) type phases. The next decomposition step results in the reduction of Se^{4+} to Se^{2-} and leads to oxide-selenides $R_4O_4Se_3$ (Khodadad et al., 1967), as has been confirmed by chemical analysis and X-ray powder diffraction. The formation of this product occurs independently from the type of reducing gas. However, the reaction starts at significantly lower temperatures when CO is involved. In both cases, inspection of the TG-curves gave evidence for intermediate compounds. The oxide-selenides, $R_4O_4Se_3$, are more stable in CO when compared to the H_2 atmosphere, owing to the formation of H_2Se at higher temperatures in the presence of hydrogen. The only exception of this reaction scheme is found for $R = Eu$, where $EuSe$ is observed as the final product.

A series of compounds with the general formula $R_2(SeO_3)_3 \cdot xH_2SeO_3 \cdot nH_2O$ has been obtained from rare earth hydroxides and selenious acid (D'Assunção et al., 1995). According to the chemical analyses, the content of H_2SeO_3 ranges from $x = 0.2$ to 0.8 and the number of H_2O molecules varies between 4 and 5. The constitution of these phases is not known. Upon heating, they are dehydrated in a first step, and at higher temperatures H_2SeO_3 is said to be expelled.

As pointed out previously, the number of structurally known rare earth selenites with alkali metal ions is very limited. Nevertheless, thermal investigations have been performed for a few compounds some thirty years ago. Based on chemical analyses they have the composition $AR(SeO_3)_2 \cdot xH_2O$ where A stands for Na , K , and NH_4 , $R = Nd$, Sm , Gd , Dy , and Er , and the water content x is 2 or 2.5. The ammonium compounds are of special interest because they decompose with formation of NH_3 and SeO_2 yielding the selenites $R_2(SeO_3)_3$. The process takes place in a wide temperature range from 200 to 600 °C (Erämetsä et al., 1973). The degradation of the sodium and potassium selenites is more complicated. It seems clear that the first decomposition step is dehydration. Considering the observed mass losses, further heating leads to oxide-selenites $A_2R_2O_2(SeO_3)_2$ and $A_2R_2O_3(SeO_3)$ ($A = Na, K$). The constitution of the latter has not been confirmed and the formation of product mixtures [$A_2R_2O_2(SeO_3)_2 = A_2(SeO_3) + R_2O_2(SeO_3)$ and $A_2R_2O_3(SeO_3) = A_2(SeO_3) + R_2O_3$] might also be possible.

3.4.2. Vibrational spectra of oxo-selenates(IV)

The undistorted SeO_3^{2-} ion has C_{3v} symmetry and four fundamental modes can be expected. They belong to the symmetry species A_1 ($2 \times$) and E ($2 \times$) so that all of them should occur in both IR and Raman spectra (Sathianandan et al., 1964). The frequencies for the stretching vibrations are usually found at 810 (ν_s) and 740 (ν_{as}) cm^{-1} while the bending modes occur at 425 (δ_s) and 372 (δ_{as}) cm^{-1} . However, in the crystal structures of the rare earth selenites the SeO_3^{2-} ions have mostly much lower symmetry so that a splitting of the bands is observed (Petrov et al., 1973; Bindu Gopinath et al., 1998). Furthermore, a factor group splitting may lead to more complex spectra. Table 14 surveys the typical frequency regions observed so far.

The energy of the $Se-O$ stretching modes is shifted to lower wavenumbers for the hydrogenselenites. The $Se-OH$ bond is usually significantly longer than the $Se-O$ bond which may

Table 14
Typical vibration energy ranges (cm^{-1}) of the SeO_3^{2-} ion in rare earth oxo-selenates(IV)

Vibration mode	ν_1 (A_1)	ν_2 (A_1)	ν_3 (E)	ν_4 (E)
Description	Symm. stretching	Symm. bending	Asymm. stretching	Asymm. bending
Range	790–890	420–510	660–760	330–410

decrease the vibration energies by about 100 cm^{-1} . Also, highly coordinated oxygen atoms of the selenite groups may lead to quite low vibration frequencies, but a differentiation is usually easy due to the presence of characteristic O–H vibrations in the case of HSeO_3^- . Thus vibrational spectroscopy is a good method to distinguish between selenites and hydrogen-selenites if structures are unknown. The same is true if diselenite ions, $\text{Se}_2\text{O}_5^{2-}$, are present in the compounds. The bridging oxygen atom shows distances Se–O around 1.8 \AA what is about $0.10\text{--}0.15 \text{ \AA}$ larger than the respective distances to the terminal oxygen atoms. The variation of this bond length is small so that the associated vibration band occurs in a narrow range between 550 and 650 cm^{-1} . Because of the absence of SeO_3^{2-} bands in this region, an observation of an absorption in that energy range can be taken as a solid proof for the presence of diselenite groups.

3.4.3. Thermochemical investigations of oxo-selenates(IV)

In recent years, a number of investigations have been performed to characterize the systems $\text{R}_2\text{O}_3/\text{SeO}_2$ and ROX/SeO_2 ($X = \text{Cl}, \text{Br}$) by thermochemical methods (Oppermann and Zhang-Preße, 2001; Oppermann et al., 2002a; Zhang-Preße and Oppermann, 2002; Oppermann et al., 2002b, 2003; Schmidt et al., 2004) (see also sections 3.1 and 3.2). Phase diagrams have been established by DTA measurements, and for a great number of compounds the enthalpies of formation were derived from their decomposition functions obtained from total pressure measurements and C_p values. Additionally, the enthalpies of formation were derived from the respective enthalpy of solution values. Selected data are summarized in tables 15 and 16.

It is worthwhile to mention that not all of the known compounds are necessarily observed in the thermochemical investigations, as can be seen from the existence of the phases $\text{R}_2\text{O}(\text{SeO}_3)_2$ ($= \text{R}_2\text{Se}_2\text{O}_7$) ($\text{R} = \text{Sm–Tm}$) and $\text{Sm}_2(\text{Se}_2\text{O}_5)_2(\text{SeO}_3)$ ($= \text{Sm}_2\text{Se}_3\text{O}_{13}$) (see section 3.1.3). Nevertheless, these investigations provide helpful data for the preparation of new compounds. This is especially true if single crystals are desired, because the thermochemical measurements show if one has to expect difficulties like incongruent melting or phase transitions. As an example, the phase diagram of the system $\text{Nd}_2\text{O}_3/\text{SeO}_2$ is shown in fig. 22 (Oppermann et al., 2002a). It shows the existence of five thermodynamically stable phases (also see section 3.1) and within the investigated temperature range three of them, $\text{Nd}_2\text{Se}_4\text{O}_{11}$, $\text{Nd}_2\text{Se}_{3.5}\text{O}_{10}$, and $\text{Nd}_2\text{Se}_3\text{O}_9$, melt peritectically with the melting points P_1 ($420 \pm 5 \text{ }^\circ\text{C}$), P_2 ($625 \pm 5 \text{ }^\circ\text{C}$), and P_3 ($1040 \pm 5 \text{ }^\circ\text{C}$). Furthermore, the compounds show various phase transitions (shown “ U_n ” in the diagram), which have to be considered for crystal growth experiments. The endothermic phase transition U_3 for $\text{Nd}_2\text{Se}_3\text{O}_9$ ($= \text{Nd}_2(\text{SeO}_3)_3$) was found to occur reversibly at $310 \pm 5 \text{ }^\circ\text{C}$, and the related enthalpy ΔH_{U_3} is $13.6 \pm 0.2 \text{ kJ/mol}$. As dis-

Table 15
Selected thermodynamical data of compounds in the systems R_2O_3/SeO_2

Compound	ΔH_f (298 K) (J/mol)	ΔS^0 (298 K) (J/mol·K)	C_p (298 K) (J/mol·K)
NdSeO ₅	-2190 ± 24	180 ± 17	168 ± 8
Nd ₂ Se _{1.5} O ₆	-2346 ± 33	202 ± 30	197 ± 8
Nd ₂ Se ₃ O ₉ ¹⁾	-2846 ± 39	302 ± 45	289 ± 13
Nd ₂ Se _{3.5} O ₁₀	-3030 ± 56	254 ± 66	316 ± 13
Nd ₂ Se ₄ O ₁₁	-3054 ± 63	423 ± 71	346 ± 8
SmSeO ₅	-2230 ± 17	155 ± 9	168 ± 4
Sm ₂ Se _{1.5} O ₆	-2418 ± 26	168 ± 25	196 ± 8
Sm ₂ Se ₃ O ₉ ²⁾	-2921 ± 40	269 ± 42	288 ± 2
Sm ₂ Se _{3.5} O ₁₀	-3077 ± 42	252 ± 50	316 ± 6
Sm ₂ Se ₄ O ₁₁	-3191 ± 42	304 ± 54	345 ± 13
YSeO ₅	-2248 ± 17	150 ± 18	146 ± 3
Y ₂ Se ₃ O ₉	-2893 ± 50	272 ± 59	250 ± 4
Y ₂ Se _{3.5} O ₁₀	-3002 ± 59	333 ± 84	300 ± 6
Y ₂ Se ₄ O ₁₁	-3105 ± 69	285 ± 84	330 ± 6

¹⁾Phase transition at 583 K; $\Delta H_T = 2.42 \pm 0.08$ J/mol · K.

²⁾Phase transition at 793 K; $\Delta H_T = 13.6 \pm 0.2$ J/mol · K.

Table 16
Selected thermodynamical data of compounds in the systems $R_2O_3/RX_3/SeO_2$ (X = Cl, Br)

Compound	ΔH_f (298 K, TP) ^{a)} (J/mol)	ΔH_f (298 K, SC) ^{b)} (J/mol)	ΔS^0 (298 K) (J/mol·K)
SmSeO ₃ Cl	-1317 ± 21	-1303 ± 8	157 ± 21
SmSe ₂ O ₅ Cl	-1561 ± 29	-1545 ± 9	253 ± 36
SmSe ₃ O ₇ Cl	-1780 ± 38	-1778 ± 10	339 ± 46
SmSeO ₃ Br	-1289 ± 23	-1250 ± 11	193 ± 21
SmSe ₂ O ₅ Br	-1564 ± 29	-1493 ± 11	223 ± 34
SmSe ₃ O ₇ Br	-1777 ± 42	-1737 ± 13	318 ± 46
Yb ₂ O(SeO ₃)Cl ₂	-2293 ± 20	-2303 ± 10	265 ± 15
YbSeO ₃ Cl	-1317 ± 30	-1281 ± 7	154 ± 30
YbSe ₂ O ₅ Cl	-1598 ± 40	-1508 ± 10	204 ± 40
YbSe ₃ O ₇ Cl	-1793 ± 40	-1739 ± 15	311 ± 50

^{a)}TP: data obtained from total pressure measurements.

^{b)}SC: data obtained from solution calorimetry.

cussed in section 3.1.2, this transition has been followed by X-ray diffraction methods and can be interpreted as a phase transition from structure type II to structure type I for the selenite Nd₂(SeO₃)₃. The findings for the system Sm₂O₃/SeO₂ are very similarly to those for the respective neodymium system. An endothermic phase transition has been also observed for

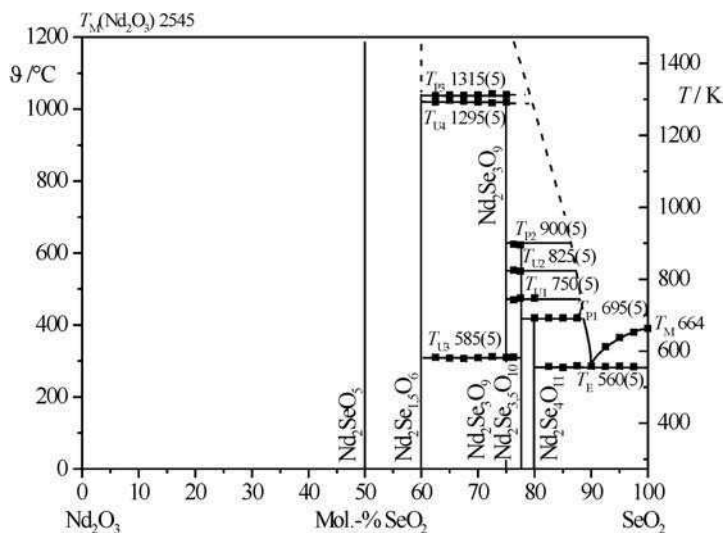


Fig. 22. Phase diagram of the system $\text{Nd}_2\text{O}_3/\text{SeO}_2$.

$\text{Sm}_2\text{Se}_3\text{O}_9$ ($= \text{Sm}_2(\text{SeO}_3)_3$) at $520 \pm 5^\circ\text{C}$ ($\Delta H = 2.42 \pm 0.08 \text{ kJ/mol}$), but this transformation has not been confirmed by diffraction experiments.

For the systems $\text{R}_2\text{O}_3\text{-SeO}_2\text{-H}_2\text{O}$ with $\text{R} = \text{Nd, Tm}$, solubility isotherms at 100°C have been determined recently (Gospodinov and Stancheva, 2001, 2003). According to these data in both cases the tetrahydrates $\text{R}_2(\text{SeO}_3)_3 \cdot 4\text{H}_2\text{O}$ form at low SeO_2 concentrations, and the acidic dihydrates $\text{R}(\text{HSeO}_3)(\text{SeO}_3) \cdot 2\text{H}_2\text{O}$ occur if the SeO_2 concentration increases. The latter are found over a wide SeO_2 concentration range and seem to be the unique phase on the SeO_2 -rich side of the thulium system. For neodymium, however, two additional compounds exist: $\text{Nd}(\text{HSeO}_3)_3$ and $\text{Nd}_2(\text{Se}_2\text{O}_5)_3 \cdot \text{H}_2\text{SeO}_3 \cdot \text{H}_2\text{O}$. Table 17 summarizes the data on the solubility isotherm for the neodymium system. For some of the phases structural data are available as it has been discussed in section 3.1.4.

4. Mixed-valent oxo-selenates(VI/IV)

A handful of compounds that contain selenate *and* selenite ions and thus are mixed valent with respect to the oxidation state of selenium are known. $\text{Er}_2(\text{SeO}_3)_2(\text{SeO}_4) \cdot 2\text{H}_2\text{O}$ was obtained via hydrothermal reaction of $\text{Er}(\text{NO}_3)_3 \cdot 5\text{H}_2\text{O}$ and SeO_2 (Morris et al., 1992b). Unfortunately, the crystal structure determination suffers from the disorder of the selenate group. Therefore, the presence of both oxidation states for Se has been proved by means of X-ray absorption near edge spectroscopy (XANES). The structure contains layers of eightfold coordinated Er^{3+} and SeO_3^{2-} ions, which are linked via the SeO_4^{2-} tetrahedra. The respective neodymium compound, $\text{Nd}_2(\text{SeO}_3)_2(\text{SeO}_4) \cdot 2\text{H}_2\text{O}$, has been prepared in the same way (Berdonosov et al.,

Table 17
Solubility isotherm of the system $\text{Nd}_2\text{O}_3/\text{SeO}_2/\text{H}_2\text{O}$ at 100 °C

Liquid phase (mass%)		Solid phase (mass%)		Compound
Nd_2O_3	SeO_2	Nd_2O_3	SeO_2	
5.3×10^{-3}	0.08	42.80	39.02	$\text{Nd}_2(\text{SeO}_3)_3 \cdot 4\text{H}_2\text{O}$
5.2×10^{-3}	0.87	38.89	37.25	$\text{Nd}_2(\text{SeO}_3)_3 \cdot 4\text{H}_2\text{O}$
7.5×10^{-3}	0.87	36.88	47.38	$\text{Nd}(\text{HSeO}_3)(\text{SeO}_3)_3 \cdot 2\text{H}_2\text{O}$
8.1×10^{-3}	5.22	29.50	40.41	$\text{Nd}(\text{HSeO}_3)(\text{SeO}_3)_3 \cdot 2\text{H}_2\text{O}$
8.4×10^{-3}	7.31	30.19	42.10	$\text{Nd}(\text{HSeO}_3)(\text{SeO}_3)_3 \cdot 2\text{H}_2\text{O}$
8.7×10^{-3}	15.20	32.90	45.38	$\text{Nd}(\text{HSeO}_3)(\text{SeO}_3)_3 \cdot 2\text{H}_2\text{O}$
8.6×10^{-3}	24.30	36.10	49.12	$\text{Nd}(\text{HSeO}_3)(\text{SeO}_3)_3 \cdot 2\text{H}_2\text{O}$
9.0×10^{-3}	29.51	36.52	49.76	$\text{Nd}(\text{HSeO}_3)(\text{SeO}_3)_3 \cdot 2\text{H}_2\text{O}$
1.0×10^{-2}	39.16	32.12	48.22	$\text{Nd}(\text{HSeO}_3)(\text{SeO}_3)_3 \cdot 2\text{H}_2\text{O}$
1.2×10^{-2}	42.27	26.03	47.57	$\text{Nd}(\text{HSeO}_3)(\text{SeO}_3)_3 \cdot 2\text{H}_2\text{O}$
2.2×10^{-2}	47.87	32.78	50.08	$\text{Nd}(\text{HSeO}_3)(\text{SeO}_3)_3 \cdot 2\text{H}_2\text{O}$
2.4×10^{-2}	49.08	27.50	50.63	$\text{Nd}(\text{HSeO}_3)(\text{SeO}_3)_3 \cdot 2\text{H}_2\text{O}$
2.5×10^{-2}	50.63	29.65	50.31	$\text{Nd}(\text{HSeO}_3)(\text{SeO}_3)_3 \cdot 2\text{H}_2\text{O}$
2.4×10^{-2}	50.63	26.09	61.60	$\text{Nd}(\text{HSeO}_3)_3$
2.6×10^{-2}	52.12	23.17	58.90	$\text{Nd}(\text{HSeO}_3)_3$
3.5×10^{-2}	56.65	26.09	62.79	$\text{Nd}(\text{HSeO}_3)_3$
3.0×10^{-2}	60.17	23.17	63.05	$\text{Nd}(\text{HSeO}_3)_3$
2.7×10^{-2}	60.17	26.62	65.90	$\text{Nd}_2(\text{Se}_2\text{O}_5)_3 \cdot \text{H}_2\text{SeO}_3 \cdot 2\text{H}_2\text{O}$
2.4×10^{-2}	63.55	20.62	65.51	$\text{Nd}_2(\text{Se}_2\text{O}_5)_3 \cdot \text{H}_2\text{SeO}_3 \cdot 2\text{H}_2\text{O}$
2.4×10^{-2}	69.15	24.48	67.00	$\text{Nd}_2(\text{Se}_2\text{O}_5)_3 \cdot \text{H}_2\text{SeO}_3 \cdot 2\text{H}_2\text{O}$
2.6×10^{-2}	73.20	23.02	68.10	$\text{Nd}_2(\text{Se}_2\text{O}_5)_3 \cdot \text{H}_2\text{SeO}_3 \cdot 2\text{H}_2\text{O}$
2.9×10^{-2}	76.86	25.04	68.54	$\text{Nd}_2(\text{Se}_2\text{O}_5)_3 \cdot \text{H}_2\text{SeO}_3 \cdot 2\text{H}_2\text{O}$

2004). It shows essentially the same structure than the erbium phase but one unit cell edge is doubled and the symmetry changes from Cc to $C2/c$. Nevertheless, a slight disorder of the selenate ion is still observable.

$\text{La}(\text{HSeO}_3)(\text{SeO}_4) \cdot 2\text{H}_2\text{O}$ was also obtained hydrothermally (Harrison and Zhang, 1997b). The structure shows the La^{3+} ions in ninefold coordination of oxygen atoms of three SeO_4^{2-} , three HSeO_3^- and two H_2O ligands. One of the hydrogenselenite ions is attached in a chelating manner. The HSeO_3^- groups connect the metal ions to double chains which are oriented in [100] direction and linked to more distant double chains by the SeO_4^{2-} tetrahedra. Although the hydrogen atoms were not located, hydrogen bonding can be assumed with the H_2O molecules and the HSeO_3^- ions as donors when judged from the donor acceptor distances which are around 3 Å.

One selenate-selenite is known containing additional halide ions, namely $\text{Pr}_4(\text{SeO}_3)_2(\text{SeO}_4)\text{F}_6$. It has been obtained in the form of light green single crystals during the decomposition of $\text{Pr}_2(\text{SeO}_4)_3$ in the presence of LiF in a gold ampoule (Göhausen and Wickleder, 2002). The monoclinic compound contains two crystallographically different Pr^{3+} ions. $\text{Pr}(1)^{3+}$ is surrounded by six fluoride ions and two chelating SeO_3^{2-} groups leading to a coordination number of ten. $\text{Pr}(2)^{3+}$ has four fluoride ions, three monodentate SeO_3^{2-} and two SeO_4^{2-}

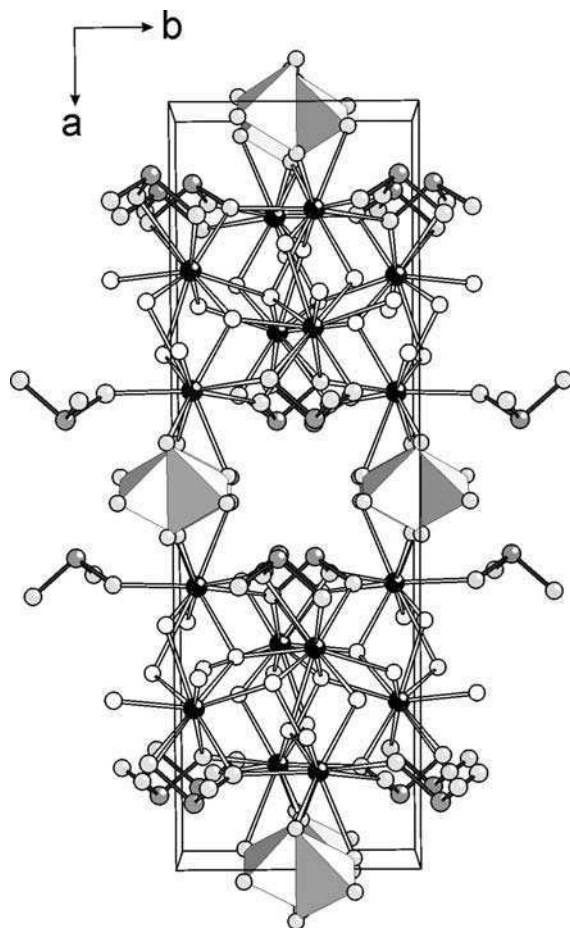


Fig. 23. Perspective view of the crystal structure of $\text{Pr}_4(\text{SeO}_3)_2(\text{SeO}_4)\text{F}_6$ along (001).

groups as neighbours. One of the latter acts as a chelating ligand, so the coordination number of $\text{Pr}(2)^{3+}$ is also 10. The selenite ions are themselves coordinated by five and the selenate ions by four Pr^{3+} ions. The coordination numbers of the F^- ions are three and four, respectively. The anions F^- and SeO_3^{2-} are arranged into layers parallel to the (100) plane along with the Pr^{3+} ions. The layers are connected along [100] via SeO_4^{2-} groups (fig. 23). The linkage of the coordination polyhedra leads to cavities in the crystal structure which incorporate the lone pairs of the selenite ions. The structure of $\text{Pr}_4(\text{SeO}_3)_2(\text{SeO}_4)\text{F}_6$ is very similar to those of $\text{La}_2(\text{SeO}_3)_3$ and LaFSeO_3 as may be seen by comparing the figs. 23, 17, and 8.

The only selenate-selenite containing an alkali metal ion is $\text{NaSm}(\text{SeO}_3)(\text{SeO}_4)$. It has also been obtained from a decomposition reaction. In this case $\text{Sm}_2(\text{SeO}_4)_3$ was decomposed in

the presence of NaCl (Göhausen and Wickleder, 2002). The reaction was carried out in a gold ampoule and led to light yellow single crystals. The crystal structure contains tenfold oxygen coordinated Sm^{3+} ions. The oxygen atoms belong to five SeO_3^{2-} and two SeO_4^{2-} ions. Two of the SeO_3^{2-} groups as well as one of the SeO_4^{2-} groups act as a chelating ligand. The sodium ions are surrounded by five SeO_4^{2-} ions and one SeO_3^{2-} group. One of the selenate ions is chelating leading to a coordination number of seven. Each selenite group is coordinated by six ($5 \times \text{Sm}^{3+}$ and $1 \times \text{Na}^+$), each selenate ion by seven cations ($5 \times \text{Na}^+$ and $2 \times \text{Sm}^{3+}$). Again, the structure provides empty voids for the incorporation of the lone pairs.

Acknowledgements

The own work that has been cited in this article has been supported by the Deutsche Forschungsgemeinschaft, Bonn, as part of the “Graduiertenkolleg 549” which is dealing with non-centrosymmetric crystals, and as part of the recent “Schwerpunktprogramm 1166” which covers the area of lanthanide-specific functionalities. I am grateful to my co-workers Dr. Ina Krügermann and Makram Ben Hamida for their diligent work in that field. Furthermore, I am deeply indebted to Prof. Dr. Gerd Meyer for his continued support during my time in Cologne. Finally I would like to thank Prof. Dr. Thomas Schleid for providing me structural data prior to publication.

References

- Aslanov, L.A., Farag, I.S.A., Ionov, V.M., Porai-Koshits, M., 1973. *Russ. J. Phys. Chem.* **47**, 1233.
- Barfiwala, U.A., Ajaonkar, V.R., 1995. *J. Therm. Anal.* **44**, 1463.
- Bard, A.J., Parsons, R., Jordan, J. (Eds.), 1985. *Standard Potentials in Aqueous Solution*. Dekker, New York.
- Ben Hamida, M., 2004. Diploma thesis, University of Cologne, Germany.
- Ben Hamida, M., Wickleder, M.S., 2005. Unpublished.
- Berdonosov, P.S., Shabalin, D.G., Olenev, A.V., Demianets, L.N., Dolgikh, V.A., Popovkin, B.A., 2003. *J. Solid State Chem.* **174**, 111.
- Berdonosov, P.S., Schmidt, P., Dityat'yev, O.A., Dolgikh, V.A., Lightfoot, P., Ruck, M., 2004. *Z. Anorg. Allg. Chem.* **630**, 1395.
- Berrigan, R., Gatehouse, B.M., 1996. *Acta Crystallogr.* **C52**, 496.
- Bindu Gopinath, A., Devanarayanan, S., Castro, A., 1998. *Spectrochim. Acta* **A54**, 785.
- Boatner, L.A., Beall, G.W., Abraham, M.M., Finch, C.B., Huray, P.G., Rappaz, M., 1980. In: Northrup, C.J. (Ed.), *Scientific Basis for Nuclear Waste Management*, vol. 2. Plenum, New York, p. 289.
- Bock, R., 1950. *Angew. Chem.* **62**, 375.
- Brauer, G. (Ed.), 1975. *Handbuch der Präparativen Anorganischen Chemie*, Bd. I. F. Enke Verlag, Stuttgart.
- Brezeanu, M., Patron, L., Carp, O., Mindru, I., Petre, N.L., 1999. Romanian Patent, application: RO 97-9701140 19970619.
- Castro, A., Enjalbert, R., de Pedro, M., Trombe, J.C., 1994. *J. Solid State Chem.* **112**, 418.
- Cruz, P.M., Spirandeli Crespi, M., Ribeiro, C.A., Ionashiro, M., Giolito, I., 1990. *Thermochim. Acta* **168**, 283.
- D'Assunção, L.M., da Costa, M.R., Ionashiro, M., 1995. *Ecl. Quim., São Paulo* **20**, 69.
- De Ávila Agostini, P.R., de Castilho Agostini, E., Giolito, I., Ionashiro, M., 1990a. *Thermochim. Acta* **168**, 273.
- De Ávila Agostini, P.R., de Castilho Agostini, E., Giolito, I., Ionashiro, M., 1990b. *Thermochim. Acta* **167**, 293.
- Delage, C., Carpy, A., H'Naifi, A., Goursolle, M., 1986. *Acta Crystallogr.* **C42**, 1475.

- de Pedro, M., Enjalbert, R., Castro, A., Trombe, J.C., Galy, J., 1994. *J. Solid State Chem.* **108**, 87.
- de Pedro, M., Trombe, J.C., Castro, A., 1995. *J. Mat. Sci. Lett.* **14**, 994.
- Erämetsä, O., Pakkanen, T., Niinistö, L., 1973. *Suom. Kemistil.* **B46**, 330.
- Felsche, J., 1973. *Struct. Bonding* [Berlin] **13**, 99.
- Gasnov, Y.M., Iskhakova, L.D., Trunov, V.K., 1985. *Zh. Neorg. Khim.* **30**, 3047.
- Giesbrecht, E., Perrier, M., Wendtlandt, W.W., 1962. *An. Acad. Brasil. Ciênc.* **34**, 37.
- Giolito, I., Giesbrecht, E., 1967. *An. Acad. Brasil. Ciênc.* **39**, 233.
- Giolito, I., Giesbrecht, E., 1969. *An. Acad. Brasil. Ciênc.* **41**, 517.
- Giolito, I., Ionashiro, M., 1981. *Thermochim. Acta* **46**, 77.
- Giolito, I., Ionashiro, M., 1988a. *Thermochim. Acta* **136**, 319.
- Giolito, I., Ionashiro, M., 1988b. *Thermochim. Acta* **136**, 335.
- Gmelin Handbook of Inorganic Chemistry, vol. **3**, D2, D3, 1980–1984, Springer Verlag, Berlin.
- Göhausen, I., Wickleder, M.S., 2000. *Z. Anorg. Allg. Chem.* **626**, 1725.
- Göhausen, I., Wickleder, M.S., 2001. *Z. Anorg. Allg. Chem.* **627**, 1115.
- Göhausen, I., Wickleder, M.S., 2002. *Z. Anorg. Allg. Chem.* **628**, 147.
- Gospodinov, G.G., Stancheva, M.G., 2001. *Monatsh. Chem.* **132**, 1031.
- Gospodinov, G.G., Stancheva, M.G., 2003. *J. Therm. Anal. Cal.* **73**, 835.
- Gupta, M.K., Surendra, L., Kaushik, S.M., Jere, G.V., 1982. *J. Solid State Chem.* **43**, 359.
- Harrison, W.T.A., 2000. *Acta Crystallogr.* **C56**, 627.
- Harrison, W.T.A., Zhang, Z., 1997a. *J. Solid State Chem.* **133**, 572.
- Harrison, W.T.A., Zhang, Z., 1997b. *Eur. J. Solid State Inorg. Chem.* **34**, 599.
- Hiltunen, L., Niinistö, L., 1976. *Cryst. Struct. Comm.* **5**, 567.
- Hájek, B., Novotna, N., Hradilová, J., 1979. *J. Less-Common Met.* **66**, 121.
- Held, P., Hellwig, H., Rühle, S., Bohatý, L., 2000. *J. Appl. Cryst.* **33**, 372.
- Iskhakova, L.D., 1995. *Kristallografiya* **40**, 631.
- Iskhakova, L.D., Tursina, A.I., 1989. *Kristallografiya* **34**, 1414.
- Iskhakova, L.D., Makarevich, L.G., 1996. *Zh. Neorg. Khim.* **41**, 1102.
- Iskhakova, L.D., Ovanisyan, S.M., Trunov, V.K., 1990a. *Kristallografiya* **35**, 1083.
- Iskhakova, L.D., Ovanisyan, S.M., Trunov, V.K., 1990b. *Kristallografiya* **35**, 1099.
- Iskhakova, L.D., Kozlova, N.P., Marugin, V.V., 1990c. *Kristallografiya* **35**, 1089.
- Iskhakova, L.D., Ovanisyan, S.M., Trunov, V.K., 1991. *Zh. Struk. Khim.* **32**, 30.
- Iskhakova, L.D., Ovanisyan, S.M., 1995. *Zh. Neorg. Khim.* **40**, 1768.
- Ionashiro, M., Giolito, I., 1980. *Thermochim. Acta* **38**, 285.
- Ionashiro, M., Giolito, I., 1982a. *Thermochim. Acta* **59**, 231.
- Ionashiro, M., Giolito, I., 1982b. *Thermochim. Acta* **56**, 375.
- Ionashiro, M., Giolito, I., 1988. *Thermochim. Acta* **136**, 327.
- Immonen, E., Koskenlinna, M., Niinistö, L., Pakkanen, T., 1976. *Finn. Chem. Lett.* **3**, 67.
- Karvinen, S., Niinistö, L., 1986. *Lanth. Actin. Res.* **1**, 169.
- Karvinen, S., Lumme, K., Niinistö, L., 1987. *J. Therm. Anal.* **32**, 919.
- Khodadad, P., Dugue, J., Adolphe, C., 1967. *Comptes Rend. Seanc. Acad. Scienc. Ser. C* **265**, 379.
- Koskenlinna, M., Valkonen, J., 1977. *Acta Chem. Scand.* **A31**, 457.
- Koskenlinna, M., Mutikainen, I., Leskelä, M., Niinistö, L., 1994. *Acta Crystallogr.* **C50**, 1384.
- Krügermann, I., 2002. PhD thesis, University of Cologne, Germany.
- Krügermann, I., Wickleder, M.S., 2002a. *Z. Anorg. Allg. Chem.* **628**, 2197.
- Krügermann, I., Wickleder, M.S., 2002b. *J. Solid State Chem.* **167**, 113.
- Krügermann, I., Wickleder, M.S., 2004. *Z. Naturforsch.* **59b**, 958.
- Leskelä, M., Hölsä, J., 1985. *Thermochim. Acta* **92**, 489.
- Leskelä, M., Niinistö, L., 1986. In: Gschneidner Jr., K.A., Eyring, L.R. (Eds.), *Handbook on the Physics and Chemistry of Rare Earths*, vol. **16**. Elsevier Science Publishers, New York, p. 203.
- McCarthy, G.J., White, W.B., Pfoertsch, D.E., 1978. *Mater. Res. Bull.* **13**, 1239.
- Meyer, S.F., Schleid, Th., 2002. *Z. Anorg. Allg. Chem.* **628**, 526.
- Morris, R.E., Hriljac, J.A., Cheetham, A.K., 1990. *Acta Crystallogr.* **C46**, 2013.
- Morris, R., Harrison, W.T.A., Stucky, G.D., Cheetham, A.K., 1992a. *Acta Crystallogr.* **C48**, 1182.
- Morris, R.E., Wilkinson, A.P., Cheetham, A.K., 1992b. *Inorg. Chem.* **31**, 4774.

- Nabar, M.A., Paralkar, S.V., 1976a. *Thermochim. Acta* **15**, 239.
- Nabar, M.A., Paralkar, S.V., 1976b. *Thermochim. Acta* **15**, 390.
- Nabar, M.A., Paralkar, S.V., 1980. *Thermochim. Acta* **35**, 287.
- Nabar, M.A., Ajgaonkar, V.R., 1981a. *Thermochim. Acta* **47**, 309.
- Nabar, M.A., Ajgaonkar, V.R., 1981b. *Thermochim. Acta* **51**, 381.
- Nabar, M.A., Ajgaonkar, V.R., 1982a. *Thermochim. Acta* **52**, 351.
- Nabar, M.A., Ajgaonkar, V.R., 1982b. *J. Appl. Cryst.* **15**, 573.
- Nabar, M.A., Ajgaonkar, V.R., 1985. *J. Less-Common. Met.* **106**, 211.
- Nabar, M.A., Khandekar, V.V., 1984. *J. Therm. Anal.* **29**, 1343.
- Nabar, M.A., Naik, V.R., 1998. *J. Alloys Compd.* **275–277**, 54.
- Nandi, J., Neogy, D., 1988. *Physica Status Solidi B* **149**, 275.
- Neogy, D., Nandy, J., 1982. *J. Chem. Phys.* **76**, 2591.
- Neogy, D., Nandy, J., 1983. *J. Phys. Chem. Solids* **44**, 943.
- Niinistö, L., Leskelä, M., 1987. In: Gschneidner Jr., K.A., Eyring, L.R. (Eds.), *Handbook on the Physics and Chemistry of Rare Earths*, vol. **18**. Elsevier Science Publishers, New York, p. 91.
- Niinistö, L., Valkonen, J., Ylinen, P., 1980. *Inorg. Nucl. Chem. Lett.* **16**, 13.
- Oppermann, H., Zhang-Preße, M., 2001. *Z. Naturforsch.* **56b**, 917.
- Oppermann, H., Zhang-Preße, M., Weck, S., Liebig, S., 2002a. *Z. Anorg. Allg. Chem.* **628**, 81.
- Oppermann, H., Dao Quoc, H., Zhang-Preße, M., Schmidt, P., Popovkin, B.A., Berdonosov, P.S., Dolgikh, V.A., 2002b. *Z. Anorg. Allg. Chem.* **628**, 891.
- Oppermann, H., Schmidt, P., Dao Quoc, H., Popovkin, B.A., Berdonosov, P.S., Dolgikh, V.A., 2003. *Z. Anorg. Allg. Chem.* **629**, 523.
- Ovanisyan, S.M., Iskhakova, L.D., 1988. *Kristallografiya* **33**, 1375.
- Ovanisyan, S.M., Iskhakova, L.D., 1989. *Kristallografiya* **34**, 57.
- Ovanisyan, S.M., Iskhakova, L.D., Trunov, V.K., 1986. *Kristallografiya* **31**, 1081.
- Ovanisyan, S.M., Iskhakova, L.D., Trunov, V.K., 1987a. *Zh. Neorg. Khim.* **32**, 896.
- Ovanisyan, S.M., Iskhakova, L.D., Trunov, V.K., 1987b. *Kristallografiya* **32**, 1148.
- Ovanisyan, S.M., Iskhakova, L.D., Trunov, V.K., 1988a. *Kristallografiya* **33**, 69.
- Ovanisyan, S.M., Iskhakova, L.D., Efremov, V.A., Trunov, V.K., 1988b. *Kristallografiya* **33**, 63.
- Perkovskaya, Yu.B., 1968. *Zh. Khim.* **8**, 24.
- Petrov, K.I., Ivanov, V.I., Voronskaya, G.N., 1969. *Struct. Chem. [USSR]* **10**, 310.
- Petrov, K.I., Voronskaya, G.N., Ivanov, V.I., 1970. *Russ. J. Inorg. Chem.* **15**, 317.
- Petrov, K.I., Golovin, Yu.M., Varfolomeev, M.B., Remennik, E.M., 1973. *Zh. Neorg. Khim.* **18**, 385.
- Petek, M., Abraham, M.M., Boatner, L.A., 1982. In: Topp, S.V. (Ed.), *Scientific Basis for Nuclear Waste Management*, vol. **4**. Elsevier-North-Holland, The Netherlands, p. 181.
- Prandtl, W., 1938. *Z. Anorg. Allg. Chem.* **238**, 321.
- Rosso, B., Perret, R., 1970. *Compt. Rend. C* **270**, 997.
- Ruck, M., Schmidt, P., 2003. *Z. Anorg. Allg. Chem.* **629**, 2133.
- Sathianandan, K., McCarty, L.D., Margrave, J.L., 1964. *Spectrochim. Acta* **20**, 957.
- Savchenko, G.S., Tananaev, I.V., Volodina, A.N., 1968. *Inorg. Mater.* **4**, 965.
- Schmidt, P., Dao Quoc, H., Oppermann, H., Ruck, M., Berdonosov, P.S., Dolgikh, V.A., Popovkin, B.A., 2004. *Z. Anorg. Allg. Chem.* **630**, 669.
- Shabalin, D.G., Berdonosov, P.S., Dolgikh, V.A., Oppermann, H., Schmidt, P., Popovkin, B.A., 2003. *Russ. Chem. Bull.* **52**, 98.
- Smolyakova, K.E., Efremov, A.A., Serebrennikov, V.V., 1973. *Russ. J. Phys. Chem.* **47**, 1389.
- Spirandeli Crespi, M., Ribeiro, C.A., Ionashiro, M., 1994. *Thermochim. Acta* **239**, 157.
- Stancheva, M., Petrova, R., Macicek, J., 1998. *Acta Crystallogr.* **C54**, 699.
- Suponitskii, Yu.L., Maier, A.I., Fedorov, V.V., Kravchenko, L.Kh., Doreshenko, N.A., Karapet'yants, M., 1969. *Russ. J. Phys. Chem.* **43**, 711.
- Thompson, L.C., 1979. In: Gschneidner Jr., K.A., Eyring, L.R. (Eds.), *Handbook on the Physics and Chemistry of Rare Earths*, vol. **3**. North-Holland, Amsterdam, p. 209.
- Valkonen, J., 1978a. *Acta Crystallogr.* **B34**, 1957.
- Valkonen, J., 1978b. *Acta Crystallogr.* **B34**, 3064.
- Valkonen, J., Niinistö, L., 1978. *Acta Crystallogr.* **B34**, 266.
- Valkonen, J., Leskelä, M., 1978. *Acta Crystallogr.* **B34**, 1323.
- Valkonen, J., Ylinen, P., 1979. *Acta Crystallogr.* **B35**, 2378.
- Valkonen, J., Niinistö, L., Eriksson, B., Larsson, L.O., Skoglund, U., 1975. *Acta Chem. Scand.* **A29**, 866.

- Vigdorchik, A.G., Malinovskii, Yu.A., 1990. *Sov. Phys. Crystallogr.* **35**, 223.
- Vigdorchik, A.G., Malinovskii, Yu.A., 1995. *Crystallogr. Rep.* **40**, 69.
- Wickleder, M.S., 2000a. *Z. Anorg. Allg. Chem.* **626**, 547.
- Wickleder, M.S., 2000b. *Z. Anorg. Allg. Chem.* **626**, 1468.
- Wickleder, M.S., 2001. *Z. Kristallogr. Suppl.* **18**, 139.
- Wickleder, M., 2002a. *Chem. Rev.* **102**, 2011.
- Wickleder, M.S., 2002b. *Z. Naturforsch.* **57b**, 1414.
- Wickleder, M.S., 2003. *Acta Crystallogr.* **E59**, i31–i32.
- Wickleder, M.S., Ben Hamida, M., 2003. *Z. Anorg. Allg. Chem.* **629**, 556.
- Wickleder, M.S., 2005a. *Z. Anorg. Allg. Chem.* **631**, submitted.
- Wickleder, M.S., 2005b. Unpublished.
- Wildner, M., 1994. *J. Solid State Chem.* **113**, 252.
- Wontcheu, J., 2004. PhD thesis, University of Stuttgart, Germany.
- Wontcheu, J., Schleid, Th., 2002a. *Z. Anorg. Allg. Chem.* **628**, 1941.
- Wontcheu, J., Schleid, Th., 2002b. *Z. Kristallogr. Suppl.* **19**, 138.
- Wontcheu, J., Schleid, Th., 2003a. *Z. Anorg. Allg. Chem.* **629**, 1463.
- Wontcheu, J., Schleid, Th., 2003b. *Z. Kristallogr. Suppl.* **20**, 158.
- Wontcheu, J., Schleid, Th., 2003c. *J. Solid State Chem.* **171**, 429.
- Wontcheu, J., Schleid, Th., 2004a. *Z. Kristallogr. Suppl.* **21**, 188.
- Wontcheu, J., Schleid, Th., 2004b. *Z. Anorg. Allg. Chem.* **630**, 1770.
- Wontcheu, J., Schleid, Th., 2005. *Z. Anorg. Allg. Chem.* **631**, 309.
- Zhang-Preße, M., Oppermann, H., 2002. *J. Therm. Anal. Cal.* **69**, 301.

This page intentionally left blank

Chapter 225

RARE-EARTH BETA-DIKETONATES

Koen BINNEMANS

*Katholieke Universiteit Leuven, Department of Chemistry, Celestijnenlaan 200F,
B-3001 Leuven Belgium*

E-mail: Koen.Binnemans@chem.kuleuven.be

Contents

1. Introduction	111	7.7. Nonlinear optical materials	203
2. Overview of β -diketone ligands and types of complexes	113	8. From materials to devices	205
3. Synthetic strategies	121	8.1. Chelates for lasers	205
4. Structural properties	128	8.2. Organic light-emitting diodes (OLEDs)	206
5. Physical and chemical properties	144	8.3. Liquid crystal displays (LCDs)	216
5.1. Aggregation state and melting point	144	8.4. Polymeric optical waveguides and amplifiers	217
5.2. Color	144	9. NMR shift reagents	218
5.3. Hydration states	153	9.1. Historical development and general principles	218
5.4. Kinetic stability	156	9.2. Achiral shift reagents	221
5.5. Solubility	157	9.3. Chiral shift reagents	226
5.6. Solution structure	157	10. Analytical applications	227
5.7. Electrochemical properties	158	10.1. Trace analysis of lanthanide ions	227
5.8. Thermodynamic properties	159	10.2. Trace analysis of organic and biomolecular compounds	229
5.9. Magnetic properties	159	10.3. Luminescent visualization of latent fingerprints	230
5.10. Crystal-field splittings	160	10.4. Chemical sensors	232
5.11. Infrared spectra	161	10.5. Stationary phases in gas chromatography	232
5.12. Chirality sensing	161	11. Applications of volatile complexes	233
5.13. Properties of hemicyanine dyes with β -diketonate counter ions	162	11.1. Volatile β -diketonate complexes	233
6. Luminescence of β -diketonate complexes	162	11.2. Gas chromatographic separation of the rare earths	237
6.1. Photoluminescence	162	11.3. Preparation of thin films by metal-organic chemical vapor deposition (MOCVD)	238
6.2. Electroluminescence	178	11.4. Preparation of thin films by atomic layer deposition (ALD)	241
6.3. Triboluminescence	179	11.5. Fuel additives	242
6.4. Sensitized chemiluminescence	183	12. Solvent extraction	243
7. From complexes to materials	185	13. Catalytic properties	247
7.1. Sol-gel glasses	185		
7.2. Ormosils	186		
7.3. β -Diketonates in polymer matrices	190		
7.4. β -Diketonates in zeolites	195		
7.5. Langmuir–Blodgett films (LB films)	197		
7.6. Liquid crystals	200		

14. Conclusions	250	References	251
Acknowledgements	251		

aa	acrylate
AAD	adamantylideneadamantane-1,2-dioxetane
AIBN	azobisisobutyronitrile
ALD	atomic layer deposition
ALE	atomic layer epitaxy
bath	4,7-diphenyl-1,10-phenanthroline (= bathophenanthroline)
bipy	2,2'-bipyridine
But	butyl
But ₄ N	tetrabutylammonium
CBP	4,4'- <i>N,N'</i> -dicarbazole-biphenyl
CN-PP	poly[2-(6'-cyano-6'-methyl-heptyloxy)-1,4-phenylene]
CPE	circularly polarized emission
CPL	circularly polarized luminescence
CTMAB	cetyltrimethylammonium bromide
CVD	chemical vapor deposition
dam	diantipirylmethane
dbso	di- <i>n</i> -butylsulfoxide
dbzso	dibenzylsulfoxide
D(fhd- <i>d</i>)	deuterated 1,1,1,2,2,6,6,7,7,7-decafluoro-3,5-heptanedione
dhsso	dihexylsulfoxide
diglyme	diethyleneglycol dimethyl ether
dipydike	1,3-(2-pyridyl)-propane-1,3-dione
distyphen	4,7-distyryl-1,10-phenanthroline
dmap	4-dimethylaminopyridine
dmbp	4,4'-dimethyl-2,2'-bipyridine
dme	dimethoxyethane; = monoglyme; = monoethyleneglycol dimethyl ether
dmop	2,9-dimethyl-1,10-phenanthroline (= 2,9-dimethyl- <i>o</i> -phenanthroline)
dmso	dimethylsulfoxide (used as ligand)
DMSO	dimethylsulfoxide (used as solvent)
dppz	dipyrido[3,2- <i>a</i> :2',3'- <i>c</i>]phenazine
ee	enantiomeric excess
epbm	1-ethyl-2-(2-pyridyl)benzimidazole
Et	ethyl
Et ₄ N	tetraethylammonium
GPTMS	3-glycidoxypropyltrimethoxysilane
Hacac	acetylacetone, 2,4-pentanedione
Hacac-F ₇	perfluoroacetylacetone, heptafluoroacetylacetone
Hbfa	benzoyl-2-furanolmethane
Hbpp	1,3-bis(3-pyridyl)-1,3-propanedione
Hbtfac	benzoyltrifluoroacetone

Hbzac	benzoylacetone, 1-phenyl-1,3-butanedione
Hctta	5-chlorosulfonyl-2-thenyltrifluoroacetone
Hdbbm	di(4-bromo)benzoylmethane
Hdbm	dibenzoylmethane, 1,3-diphenyl-1,3-propanedione
Hdcm	<i>d,d</i> -dicampholylmethane
Hdcnp	1,3-dicyano-1,3-propanedione
H ₂ dihed	<i>p</i> -di(4,4,5,5,6,6,6-heptafluoro-1,3-hexanedionyl)benzene
Hdmbm	4,4'-dimethoxydibenzoylmethane
Hdmh	2,6-dimethyl-3,5-heptanedione
Hdnm	dinaphthoylmethane
Hdpm	dipivaloylmethane, 2,2,6,6-tetramethyl-3,5-heptanedione; = Hthd and Htmhd
Hdppm	di(perfluoro-2-propoxypropionyl)methane
Hdtp	1,3-di(2-thienyl)-1,3-propanedione
Hfacam	3-(trifluoroacetyl)- <i>d</i> -camphor
Hfdh	6,6,6-trifluoro-2,2-dimethyl-3,5-hexanedione
Hfhhd	1,1,1,2,2,6,6,7,7,7-decafluoro-3,5-heptanedione
Hfod	6,6,7,7,8,8,8-heptafluoro-2,2-dimethyl-3,5-octanedione
Hftac	2-furyltrifluoroacetone; = 4,4,4-trifluoro-1-(2-furyl)-1,3-butanedione
Hhfac	hexafluoroacetylacetone, 1,1,1,5,5,5-hexafluoro-2,4-pentanedione
Hhfbc	3-(heptafluorobutyl)- <i>d</i> -camphor
Hhfth	4,4,5,5,6,6,6-heptafluoro-1-(2-thienyl)-1,3-hexanedione
Hmdbm	4-methoxydibenzoylmethane
Hmfa	4-methoxybenzoyl-2-furanoylmethane
Hmhd	6-methyl-2,4-heptanedione
Hntac	2-naphthoyltrifluoroacetone, 4,4,4-trifluoro-1-(2-naphthyl)-1,3-butanedione
Hpbm	2-(2-pyridyl)benzimidazole
H ₂ pdo	5,6-dihydroxy-1,10-phenanthroline
Hpmbp	1-phenyl-3-methyl-4-benzoyl-5-pyrazolone
Hpmbbp	1-phenyl-3-methyl-4(4-butylbenzoyl)-5-pyrazolone
Hpmip	1-phenyl-3-methyl-4-isobutyl-5-pyrazolone
Hpmtp	1-phenyl-3-methyl-4-trifluoroacetyl-5-pyrazolone
Hpop	3-(5-phenyl-1,3,4-oxadiazol-2-yl)-2,4-pentanedione
Hppa	3-phenyl-2,4-pentanedione
Hppd	3-[3',5'-bis(phenylmethoxy)phenyl]-1-(9-phenanthryl-1)propane-1,3-dione
Hpta	5,5-dimethyl-1,1,1-trifluoro-2,4-hexanedione; pivaloyltrifluoroacetone = Htpm
Hptp	1-phenyl-3-(2-thienyl)-1,3-propanedione
H(<i>t</i> -cam)	3-(<i>tert</i> -butylhydroxymethylene)- <i>d</i> -camphor
Htfac	1,1,1-trifluoro-2,4-pentanedione; trifluoroacetylacetone
Htfn	1,1,1,2,2,3,3,7,7,8,8,9,9,9-tetradecafluoro-4,6-nonanedione
Hthd	2,2,6,6-tetramethyl-3,5-heptanedione; = Hdpm and Htmhd
Htnb	4,4,4-trifluoro-1-(2-naphthyl)-1,3-butanedione (= Hntac)
Htpm	1,1,1-trifluoro-5,5-dimethyl-2,4-hexanedione; = Hpta
Htmhd	2,2,6,6-tetramethyl-3,5-heptanedione; = Hdpm and Hthd

Htmod	2,2,6,6-tetramethyl-3,5-octanedione
Htrimh	2,2,6-trimethyl-3,5-heptanedione
Htod	2,2,7-trimethyl-3,5-octanedione
Htta	2-thenoyltrifluoroacetone, 4,4,4-trifluoro-1-(2-thienyl)-1,3-butanedione
H ₂ bctot	1,10-bis(8'-chlorosulfo-dibenzothiophene-2'-yl)-4,4,5,5,6,6,7,7-octafluorodecane-1,3,8,10-tetraone
H ₂ bctot	1,10-bis(5'-chlorosulfo-thiophene-2'-yl)-4,4,5,5,6,6,7,7-octafluorodecane-1,3,8,10-tetraone
H ₂ bhhct	4,4'-bis(1'',1'',2'',2'',3'',3''-heptafluoro-4'',6''-hexanedione-6''-yl)-chlorosulfo- <i>o</i> -terphenyl
H ₂ btbct	4,4'-bis(1'',1'',1''-trifluoro-2'',4''-butanedione-6''-yl)-chlorosulfo- <i>o</i> -terphenyl
heptaglyme	heptaethyleneglycol dimethyl ether
Hex ₄ N	tetrahexylammonium
HMDS	hexamethyldisilazane
hmteta	hexamethyltriethylenetetramine
ITO	indium tin oxide
MCD	magnetic circular dichroism
MCM-41	Mobil Corporation Material 41
MCPL	magnetic circularly polarized luminescence
MOCVD	metalorganic chemical vapor deposition
monoglyme	monoethyleneglycol dimethyl ether; = dme
<i>n</i>	refractive index
OLED	organic light emitting diode
opb	1-octadecyl-2-(2-pyridyl)benzimidazole
ormosil	organically modified silicate
PBD	2- <i>tert</i> -butylphenyl-5-biphenyl-1,3,4-oxadiazole
Pc	phthalocyanine
pha	<i>N</i> -phenylacetamide
phen	1,10-phenanthroline
phenNO	1,10-phenanthroline- <i>N</i> -oxide
3-pic	3-picoline, 3-methylpyridine
4-pic	4-picoline, 4-methylpyridine
4-picO	4-picoline <i>N</i> -oxide
pip	piperidine
pipH ⁺	piperidinium
piphen	2-phenyl-imidazo[4,5- <i>f</i>]1,10-phenanthroline
pmdeta	pentamethyldiethylenetriamine
PMMA	poly(methylmethacrylate)
PMPS	poly(methylphenylsilane)
POF	polymer optical fiber
POFA	polymer optical fiber amplifier
PVC	poly(vinyl chloride)
PVK	poly(<i>N</i> -vinylcarbazole)
PVP	poly(vinylpyrrolidone)
PVV	poly(phenylene-vinylene)

py	pyridine
pyO	pyridine- <i>N</i> -oxide
pyr	pyrazine
salen	<i>N,N'</i> -ethylene bis(salicylideneimine)
salophen	<i>N,N'</i> -phenylene bis(salicylideneimine)
tbp	tri- <i>n</i> -butylphosphate
tbpo	tri- <i>n</i> -butylphosphine oxide
tetraglyme	tetraethyleneglycol dimethyl ether
terpy	2,2',6',2''-terpyridyl
TEOS	tetraethoxysilane
TFA	trifluoroacetic acid
thf	tetrahydrofuran (used as ligand)
THF	tetrahydrofuran (used as solvent)
tmeda	<i>N,N,N',N'</i> -tetramethylethylenediamine
TMOS	tetramethoxysilane
triglyme	triethyleneglycol dimethyl ether
TPD	4,4'-bis[<i>N</i> -(<i>p</i> -tolyl)- <i>N</i> -phenyl-amino]biphenyl; = <i>N,N'</i> -diphenyl- <i>N,N'</i> -(3-methyl phenyl)-1,1'-biphenyl-4,4'-diamine
tppo	triphenylphosphine oxide
Φ	luminescence quantum yield
η_{ext}	external quantum efficiency (of OLED)
η_{p}	power efficiency (of OLED)

1. Introduction

Rare-earth β -diketonates are complexes of β -diketones (1,3-diketones) with rare-earth ions. These complexes are the most popular and the most intensively investigated rare-earth coordination compounds. This popularity is partially due to the fact that many different β -diketones are commercially available and the fact that the synthesis of the corresponding rare-earth complexes is relatively easy. However, the main drive for the intense research activity on the rare-earth β -diketonates was and is still their potential of being used in several applications. The first rare-earth β -diketonates have been prepared by Urbain at the end of the 19th century (Urbain, 1897). He synthesized the tetrakis acetylacetonate complex of cerium(IV) and the hydrated tris acetylacetonate complexes of lanthanum(III), gadolinium(III) and yttrium(III). Over the years, four different periods of research interest in rare-earth β -diketonates can be distinguished. At the end of the 1950s and in the beginning of the 1960s, these compounds were explored as extractants in solvent–solvent extraction processes. In the middle of the 1960s, the rare-earth β -diketonates were recognized as potential active compounds for chelate lasers or liquid lasers. The Golden Years of the rare-earth β -diketonates was the period 1970–1985 when these compounds were frequently used as NMR shift reagents. In the 1990s, a new period of intense research activity on rare-earth β -diketonates started, now triggered by the ap-

plication of these compounds as electroluminescent materials in organic light emitting diodes (OLEDs), as volatile reagents for chemical vapor deposition or as catalysts in organic reactions.

Three main types of rare-earth β -diketonate complexes have to be considered: tris complexes, Lewis base adducts of the tris complexes (ternary rare-earth β -diketonates) and tetrakis complexes. The neutral tris complexes or tris(β -diketonates) have three β -diketonate ligands for each rare-earth ion and they can be represented by the general formula $[\text{R}(\beta\text{-diketonate})_3]$. Because the coordination sphere of the rare-earth ion is unsaturated in these six-coordinate complexes, the rare-earth ion can expand its coordination sphere by oligomer formation (with bridging β -diketonates ligands), but also by adduct formation with Lewis bases, such as water, 1,10-phenanthroline, 2,2'-bipyridine or tri-*n*-octylphosphine oxide. It is also possible to arrange four β -diketonate ligands around a single rare-earth ion and in this way tetrakis complexes or tetrakis(β -diketonates) with the general formula $[\text{R}(\beta\text{-diketonate})_4]^-$ are formed. These complexes are anionic and the electric neutrality is achieved by a counter cation. The cation can be an alkali-metal ion (Li^+ , Na^+ , K^+ , Cs^+ , Rb^+), but more often it is a protonated organic base (pyridinium, piperidinium, isoquinolinium, ...) or a quaternary ammonium ion (Et_4N , But_4N , Hex_4N , ...).

Although hundreds of different rare-earth β -diketonate complexes have been described in the literature, only few of them have been thoroughly investigated. The most popular luminescent rare-earth complex is $[\text{Eu}(\text{tta})_3(\text{phen})]$, where tta is the conjugated base of 2-thenoyltrifluoroacetone (Htta) and phen represents 1,10-phenanthroline. The most often used rare-earth β -diketonate complexes are however the $[\text{R}(\text{fod})_3]$ and the $[\text{R}(\text{thd})_3]$ complexes, where fod is the conjugate base of 6,6,7,7,8,8,8-heptafluoro-2,2-dimethyl-3,5-octanedione (Hfod) and thd is the conjugate base of 2,2,6,6-tetramethyl-3,5-heptanedione (Hthd). These compounds were originally developed as NMR shift reagents, but they have now found a wide use as volatile precursors for chemical vapor deposition, and the $[\text{R}(\text{fod})_3]$ complexes are also used as Lewis acid catalysts in organic reactions.

The popularity of the rare-earth β -diketonates is not reflected in an extensive review literature. Only two major reviews on rare-earth β -diketonates have been written in the past, namely the contribution of Forsberg in Gmelin Handbuch der anorganischen Chemie (Forsberg, 1981) and the book of Wenzel on NMR shift reagents (Wenzel, 1986). Other reviews had a wider scope, such as the book of Mehrotra on metal β -diketonates (Mehrotra et al., 1978), or were focused on one application such as NMR shift reagents or catalysis (see sections 9 and 13 of this Chapter). Properties of rare-earth β -diketonate complexes have been discussed in several of the previous chapters in this Handbook, but the information is fragmentary because these chapters were not focused on rare-earth β -diketonates as such. Thompson (1979) gives in Chapter 25 an overview of rare-earth coordination compounds with organic ligands and mentions shortly the rare-earth β -diketonates. Weber (1979) describes in Chapter 35 the rare-earth lasers, including the rare-earth chelate lasers. NMR shift reagents are discussed in Chapter 38 (Reuben and Elgavish, 1979). Long (1986) gives in Chapter 57 an overview of earlier work on β -diketonate complexes as catalysts in organic reactions. Shen and Ouyang (1987) review in Chapter 61 stereospecific polymerization by rare-earth coordination catalysts, and some of these catalysts are rare-earth β -diketonates.

Because research on rare-earth β -diketonates spans a period of more than one century, and because part of the older work has been published in lesser known journals or has not been described in detail in the review literature, much of the older work is overlooked by younger generations of researchers. It often happens in this field that nowadays results are presented as new research data, although these reported properties have been well-documented more than 40 years ago. This is especially true for luminescent rare-earth β -diketonates. This chapter gives an overview of the different types of rare-earth β -diketonate complexes, with emphasis on those properties that can be of interest for potential applications. This review does not describe only the new developments in the field, but also summarizes the most relevant data in the older literature.

First, I present the types of β -diketones that are being used for the preparation of rare-earth β -diketonate complexes. The different synthetic routes will be compared, and the most important physical properties of these complexes will be presented. An overview of the crystal structures of rare-earth β -diketonates is given. Because of the importance of the rare-earth β -diketonates as molecular luminescent materials, a large part of this chapter is devoted to fundamental aspects of these luminescent compounds. Following on the part on luminescence, other properties of the rare-earth β -diketonates are presented, in relation with the corresponding application (NMR shift reagents, precursors for chemical vapor deposition, catalyst, extracting agent, ...). Literature data have been collected up to the end of 2004.

Throughout this chapter, the β -diketones are denoted by their abbreviation, and a difference is made between the β -diketone and the corresponding β -diketonate ligand that is obtained by deprotonation of the β -diketone (i.e. the conjugate base of the β -diketone). For instance, Hacac stands for acetylacetonone, and acac is the acetylacetonate ligand. An overview of the different abbreviations can be found in the list at the beginning of this chapter, as well as in [table 1](#) and in [figs. 1 and 2](#). In the chapters of this Handbook, a difference is made between the terms “rare earths” and “lanthanides”, in the sense that the lanthanides are the elements with atomic number between 57 (lanthanum) and 71 (lutetium), whereas the rare earths represent the lanthanides together with the elements yttrium and scandium. This chapter describes the rare-earth β -diketonates and I will consistently use the term “rare-earth β -diketonates”, except in the parts that describe the luminescence behavior of these complexes, where I will use the term “lanthanide β -diketonates”. This is because scandium and yttrium are spectroscopically inactive.

2. Overview of β -diketone ligands and types of complexes

The β -diketones or 1,3-diketones bear two carbonyl groups that are separated by one carbon atom. This carbon atom is the α -carbon. In most β -diketones, the substituents on the α -carbon are hydrogen atoms. Only very few examples of rare-earth complexes of α -substituted β -diketonates are known. The substituent on the carbonyl function can be an alkyl group, a fluorinated alkyl group, an aromatic or an heteroaromatic group. The simplest β -diketone is acetylacetonone (Hacac), where the substituents on both carbonyl groups are methyl groups. All other β -diketones can be considered as derived from acetylacetonone by substitution of the

Table 1
Overview of β -diketones that can act in their deprotonated form as ligands for rare-earth ions

Abbreviation	Name	Synonym
Hacac	acetylaceton	2,4-pentanedione
Hacac-F ₇	perfluoroacetylaceton	heptafluoroacetylaceton 1,1,1,3,5,5,5-heptafluoro-2,4-pentanedione
Hbfa	benzoyl-2-furanoylmethane	
Hbpp	1,3-bis(3-pyridyl)-1,3-propanedione	
Hbtfac	benzoyltrifluoroacetone	
Hbzac	benzoylaceton	1-phenyl-1,3-butanedione
Hdbbm	di(4-bromo)benzoylmethane	
Hdcm	<i>d,d</i> -dicampholymethane	
Hdmbm	4,4'-dimethoxydibenzoylmethane	
Hdmh	2,6-dimethyl-3,5-heptanedione	
Hdnm	dinaphthoymethane	
Hdpm	dipivaloylmethane	2,2,6,6-tetramethyl-3,5-heptanedione
Hdppm	di(perfluoro-2-propoxypropionyl)methane	
Hdtp	1,3-di(2-thienyl)-1,3-propanedione	
Hfacam	3-(trifluoroacetyl)- <i>d</i> -camphor	
Hfdh	6,6,6-trifluoro-2,2-dimethyl-3,5-hexanedione	pivaloyltrifluoroacetone 5,5-dimethyl-1,1,1-trifluoro-2,4-hexanedione
Hfhf	1,1,1,2,2,6,6,7,7,7-decafluoro-3,5-heptanedione	
Hfod	6,6,7,7,8,8,8-heptafluoro-2,2-dimethyl-3,5-octanedione	
Hftac	2-furyltrifluoroacetone	4,4,4-trifluoro-1-(2-furyl)-1,3-butanedione
Hhfac	hexafluoroacetylaceton	1,1,1,5,5,5-hexafluoro-2,4-pentanedione
Hhfb	3-(heptafluorobutyl)- <i>d</i> -camphor	
Hhfh	4,4,5,5,6,6,6-heptafluoro-1-(2-thienyl)-1,3-hexanedione	

continued on next page

Table 1, *continued*

Abbreviation	Name	Synonym
Hmfa	4-methylbenzoyl-2-furanolmethane	
Hmhd	6-methyl-2,4-heptanedione	
Hntac	2-naphthoyltrifluoroacetone	4,4,4-trifluoro-1-(2-naphthyl)-1,3-butanedione
Hpop	3-(5-phenyl-1,3,4-oxadiazol-2-yl)-2,4-pentanedione	
Hppa	3-phenyl-2,4-pentanedione	
Hpta (= Htpm)	pivaloyltrifluoroacetone	5,5-dimethyl-1,1,1-trifluoro-2,4-hexanedione
Hptp	1-phenyl-3-(2-thienyl)-1,3-propanedione	
H(<i>t</i> -cam)	3-(<i>tert</i> -butylhydroxymethylene)- <i>d</i> -camphor	
Htfac	trifluoroacetylacetone	1,1,1-trifluoro-2,4-pentanedione
Htfn	1,1,1,2,2,3,3,7,7,8,8,9,9-tetradecafluoro-4,6-nonanedione	
Hthd (= Hdpm, Htmhd)	2,2,6,6-tetramethyl-3,5-heptanedione	dipivaloylmethane
Htmb	4,4,4,-trifluoro-1-(2-naphthyl)-1,3-butanedione	
Htmod	2,2,6,6-tetramethyl-3,5-octanedione	
Htrimh	2,2,6-trimethyl-3,5-heptanedione	
Htod	2,2,7-trimethyl-3,5-octanedione	
Htta	2-thenoyltrifluoroacetone	4,4,4-trifluoro-1-(2-thienyl)-1,3-butanedione

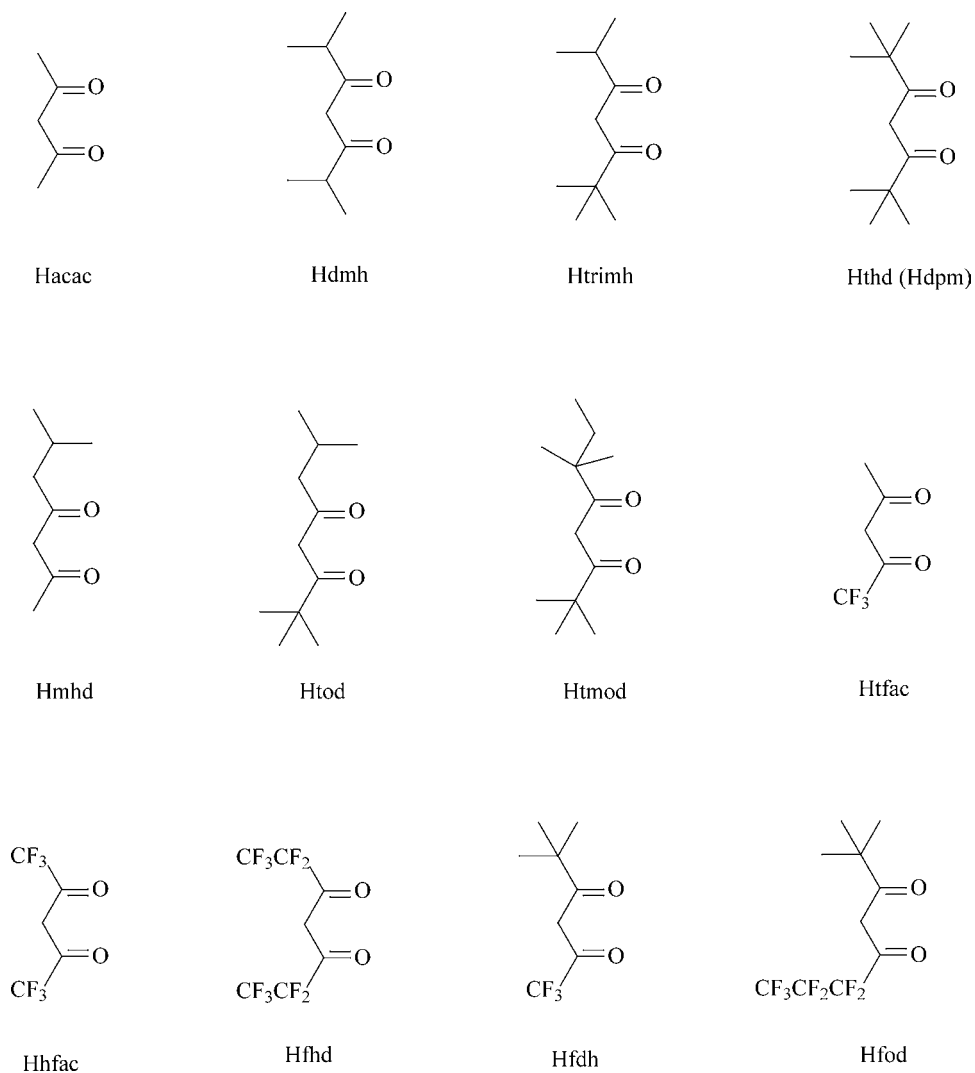


Fig. 1. Structures of β -diketones with aliphatic substituents. The molecules are in the keto form. The abbreviations are explained in [table 1](#).

CH_3 groups by other groups. Examples of other common β -diketones are benzoylacetone (Hbzac), benzoyltrifluoroacetone (Hbtfac), dibenzoylmethane (Hdbm), hexafluoroacetylacetone (Hhfac), 2-thenoyltrifluoroacetone (Htta), 2,2,6,6-tetramethyl-3,5-heptanedione (Hthd) and 6,6,7,7,8,8,8-heptafluoro-2,2-dimethyl-3,5-octanedione (Hfod). An overview of the β -diketones that are often used for complex formation with rare-earth ions are shown in [figs. 1 and 2](#), and in [table 1](#). The choice of the substituents influences the properties of the cor-

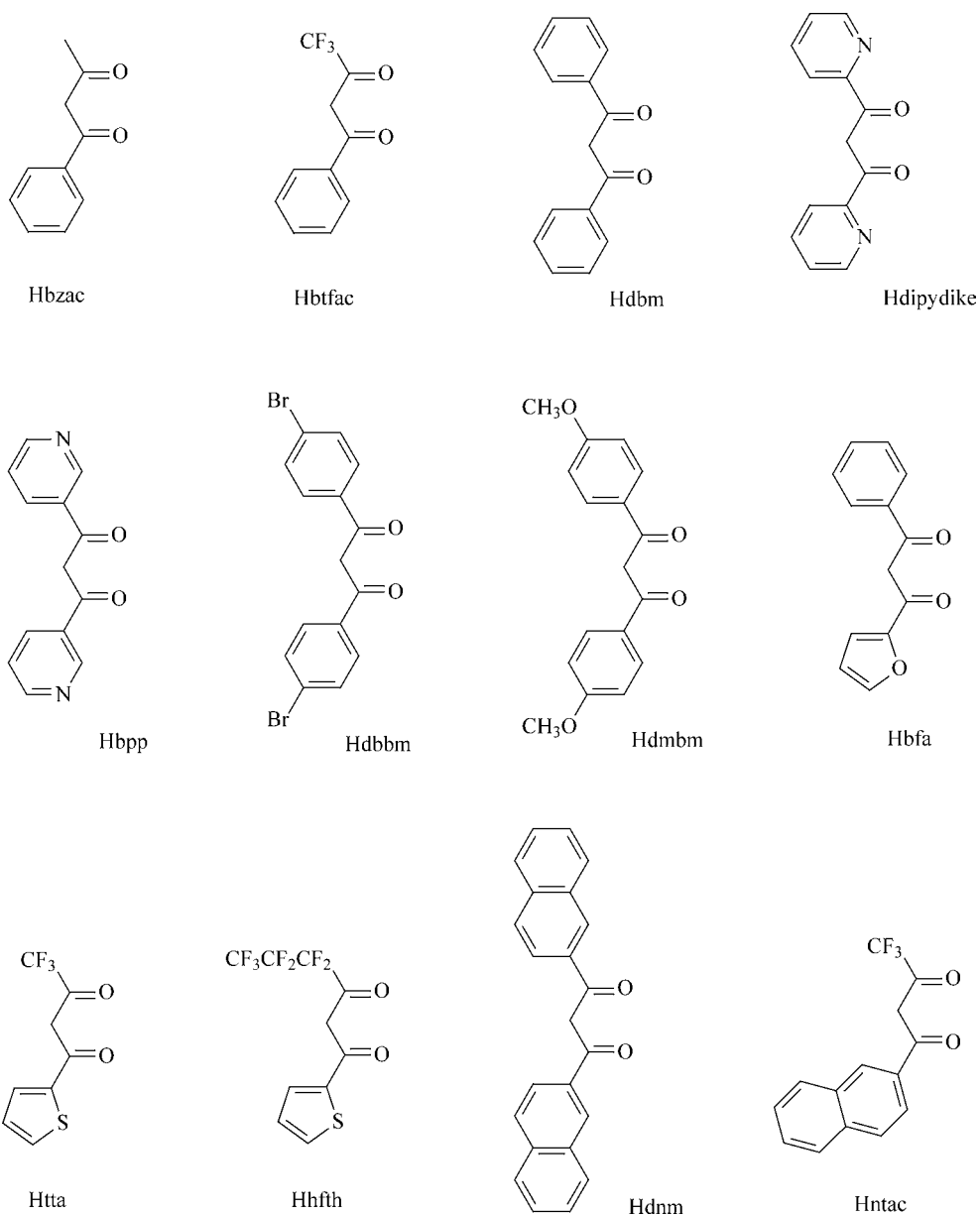


Fig. 2. Structures of β -diketones with aromatic and heterocyclic substituents. The molecules are in the keto form. The abbreviations are explained in table 1.

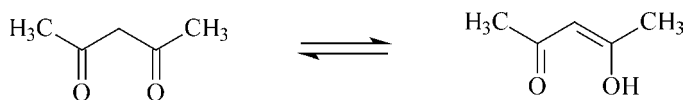


Fig. 3. Keto-enol equilibrium in acetylacetone.

responding rare-earth complexes. For instance, branched alkyl chains such as the *tert*-butyl group increase the solubility in organic solvents and the volatility. Perfluorinated alkyl groups increase the Lewis acidity. The β -diketones with aromatic substituents have a stronger light absorption than the β -diketones with only aliphatic substituents. The substituents have also an influence on the position of the energy levels of the ligand (singlet and triplet states). The position of the triplet is important, because this is one of the determining factors for the luminescence output. Many luminescent rare-earth β -diketonate complexes have ligands with one electron-donating group and one electron-withdrawing group in the same ligand. Examples are complexes of benzoyltrifluoroacetone or 2-thenoyltrifluoroacetone.

The β -diketones exhibit keto-enol tautomerism (fig. 3). In the enol form the H-atom of the alcohol function is hydrogen-bonded to the carbonyl O-atom. It is common practice to express the composition of a β -dicarbonyl system by the molar percentage of the enol tautomer at equilibrium, rather than by the equilibrium constant K ([enol form]/[keto form]). The amounts of keto- and enol form can be determined by integration of the keto and the enol resonance peaks in the ^1H NMR spectrum. The keto-enol tautomerism of β -diketones has been extensively reviewed by Emsley (1984). The position of the keto-enol equilibrium depends on a variety of factors such as the substituents on the β -dicarbonyl system, the solvent, the temperature and the presence of other species in solution that are capable of forming hydrogen bonds. The presence of an alkyl substituent on the α -carbon, decreases the amount of enol form. Whereas at room temperature 81% of the acetylacetone molecules are present in the enol form, this amount is reduced to 28% when a methyl group is placed in the α -position. Bulky alkyl groups such as the isopropyl group or the *sec*-butyl group depress the amount of enol form to almost 0%. The size of the α -substituent is not the only determining factor, since the presence of a chlorine group in the α -position increases the amount of enol form to 92%. On the other hand, a bromine group reduces the amount of enol form to 46%. The presence of a methyl group in the α -position depresses the amount of enol form in other β -diketones than acetylacetone. For instance, introduction of a methyl group in the α -position of benzoylacetone reduces the amount of enol form from 98% in pure benzoylacetone to 4% in the methyl-substituted benzoylacetone. Whereas in neat dibenzoylmethane, 100% of the molecules are in the enol form, 0% of the molecules of α -methyl dibenzoylmethane are present in the enol form. It is difficult to correlate the position of the keto-enol equilibrium to the bulkiness of substituents in the β -positions, although branching of the alkyl group increases the amount of the enol form (Koshimura et al., 1973). The presence of electron-withdrawing groups, such as CF_3 groups, favors the enol form (Burdett and Rogers, 1964). When four or more fluorine atoms are present in the molecule, the enolization is complete (Paskevich et al., 1981). For instance, 100% of the molecules of hexafluoroacetylacetone are in the enol form. Also phenyl groups favor the enol form (Burdett and Rogers, 1964). It was already

mentioned above that 100% of the molecules of dibenzoylmethane are in the enol form. The lower the polarity of the solvent, the higher is the percentage of the enol form. In CCl_4 , 94% of the acetylacetonone molecules are present in the enol form, whereas in acetonitrile this value is reduced to 36%. The amount of enol form decreases with increasing temperatures. As the degree of enolization increases, the acidity of the enol proton decreases (Hammond et al., 1959). In the case of unsymmetrically-substituted β -diketones, two different enol forms are possible. Lowe and Ferguson (1965) have shown that benzoylacetylacetones (with different substituents in the *para*-position of the phenyl group) are enolized towards the phenyl group.

When the β -diketone is deprotonated, the proton is removed from the α -carbon (if the β -diketone is in the keto form) or from the alcohol group (if the β -diketone is in the enol form). The acidity of the β -diketone depends on the substituents. Electron-withdrawing groups increase the acidity, whereas electron-donating groups decrease it. Because of the presence of the two carbonyl groups, the proton on the α -carbon is quite acidic and it can be removed by relatively weak bases. Examples of bases that are used for deprotonation of β -diketones are ammonia, sodium hydroxide, piperidine or pyridine. A much stronger base is needed to remove a second proton. The negative charge of the β -diketonate ligand is delocalized, as it is in the rare-earth β -diketonates, which form six-membered chelate rings.

Many β -diketones are commercially available at reasonable low prices, so that the synthesis of the rare-earth β -diketonates can often be restricted to the synthesis of the complexes, without the need to bother about the ligand synthesis. Only in the case that exotic β -diketones are needed or when new β -diketones are designed, the worker in the field of rare-earth β -diketonates has to synthesize the β -diketones himself/herself. The classic method for the synthesis of β -diketones is the Claisen condensation between a deprotonated methylketone and an ethyl or a methyl ester (Reid and Calvin, 1950; Barkley and Levine, 1951, 1953; Park et al., 1953; Springer et al., 1967; Wenzel et al., 1985c; Ohta et al., 1981; Ohta et al., 1994; Barbera et al., 1992; Fan and Lai, 1996). In general, the yields vary from 20 to 80%. For instance, benzoyltrifluoroacetone can be prepared by reaction between ethyl trifluoroacetate (1 eq.) and acetophenone (1 eq.) in dry diethyl ether, in the presence of sodium methoxide (1.05 eq.) as the base (Reid and Calvin, 1950). In the general procedure, the ester is added dropwise to the suspension of sodium methoxide in diethyl ether, followed by dropwise addition of the ketone. The ketone is added as the last component, in order to avoid self-condensation. The β -diketone is isolated by acidic workup. Solid β -diketones are purified by recrystallization. Liquid β -diketones can be purified by steam distillation or by vacuum distillation. Some authors purify the crude product by converting it first into the corresponding copper(II) complex. The copper(II) chelate is subsequently purified, for instance by recrystallization, and the pure β -diketone is obtained after decomposition of the copper(II) complex by a diluted aqueous sulfuric acid solution or by hydrogen sulfide. Instead of sodium methoxide, other bases can be used, for instance sodium ethoxide, sodium amide or sodium hydride (Paskevich et al., 1981). Dry diethyl ether can be replaced by benzene, toluene, dimethoxyethane or dimethyl sulfoxide (DMSO).

Ternary rare-earth β -diketonates contain one or two additional ligands besides the β -diketonate ligands. These ligands act as Lewis bases, and form adducts with tris β -diketonate complexes because of the tendency of the rare-earth ion to expand its coordination sphere

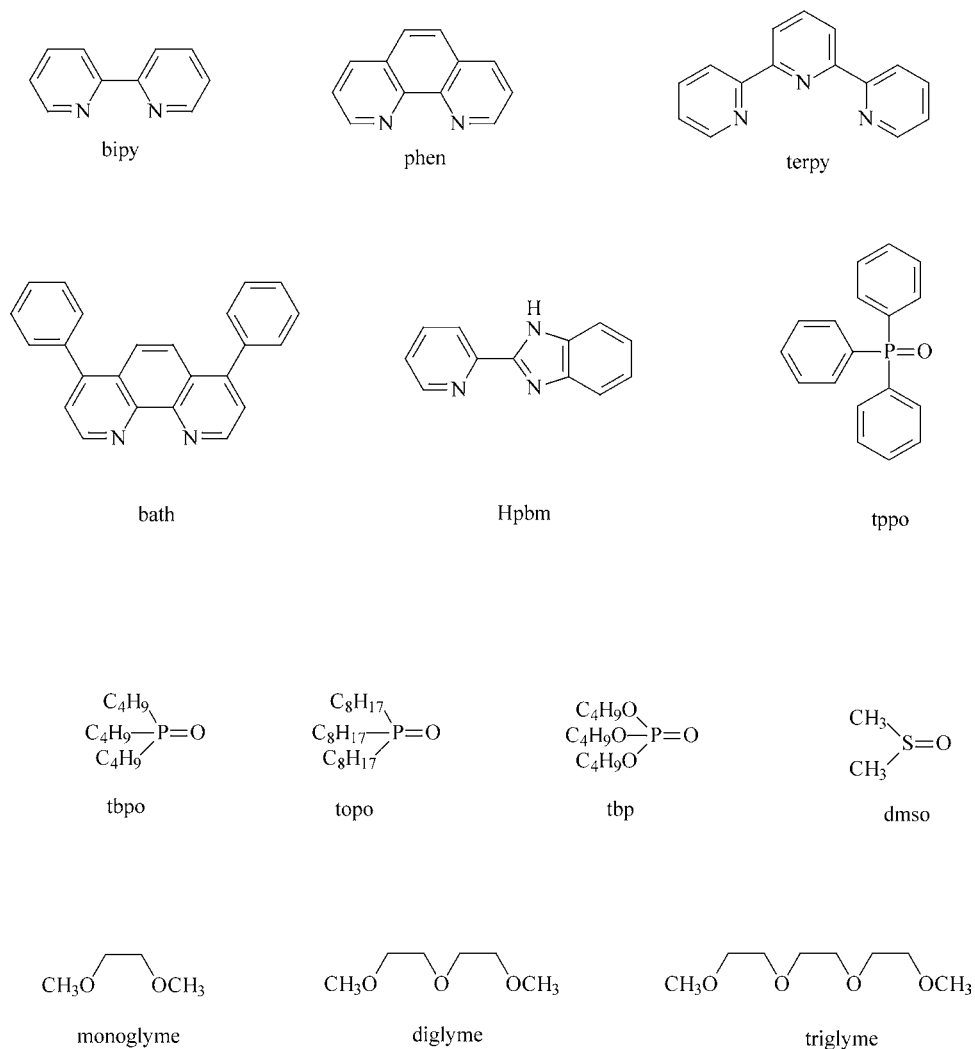


Fig. 4. Lewis bases that form adducts with rare-earth tris β -diketonates. Abbreviations: bipy = 2,2'-bipyridine; phen = 1,10-phenanthroline; terpy = 2,2',6',2''-terpyridyl; bath = bathophenanthroline or 4,7-diphenyl-1,10-phenanthroline; Hpbm = 2-(2-pyridyl)benzimidazole; tppo = triphenylphosphine oxide; tupo = tri-*n*-butylphosphine oxide; tupo = tri-*n*-octylphosphine oxide; tpo = tributylphosphate; dmsu = dimethylsulfoxide.

and to achieve a coordination number higher than six (typically eight or nine). Because the trivalent rare-earth ions are hard Lewis acids, the tris β -diketonate complexes form preferentially complexes with oxygen-donor or nitrogen-donor Lewis bases. An overview of Lewis bases that are often found in rare-earth β -diketonate complexes is given in [fig. 4](#). Two very

popular Lewis bases are the *N*-donor ligands 1,10-phenanthroline (phen) and 2,2'-bipyridine (bipy), because the resulting europium(III) complexes show often an intense luminescence. These *N*-donor ligands can be modified by substituents on the heterocycle ring. For instance 2,9-dimethyl-1,10-phenanthroline can be used instead of 1,10-phenanthroline (Holz and Thompson, 1993). New types of Lewis bases are the imidazo[4,5-*f*]1,10-phenanthroline, such as 3-ethyl-2-(4'-dimethylaminophenyl)-imidazo[4,5-*f*]1,10-phenanthroline or 2-(4'-dimethylaminophenyl) imidazo[4,5-*f*]1,10-phenanthroline (Bian et al., 2002). Another new type of Lewis bases are 1,4-diaza-1,3-butadiene derivatives (Fernandes et al., 2004).

3. Synthetic strategies

Although rare-earth β -diketonates have been known for more than one century, reliable synthetic procedures have been described only in 1964 (Bauer et al., 1964; Melby et al., 1964). Many of the earlier reported synthetic procedures gave impure compounds or compounds with an ill-defined composition. Moreover, much of these studies have been performed by physicists who neglected to fully characterize the materials they were measuring on. Several of the older papers on rare-earth β -diketonates describe tris complexes which are in reality either hydrates, hydroxy bis(β -diketonates), tetrakis complexes or polymeric materials. Without precautions, only tris chelates of β -diketonates with bulky substituents (e.g. [R(thd)₃] or [R(fod)₃]) can be obtained easily in anhydrous form. A number of earlier workers have used the so-called "piperidine method" described by Crosby et al. (1961). According to this method, the tris chelates were prepared by addition of piperidine to a solution of the corresponding rare-earth chloride and the β -diketone in water, ethanol or methanol. A modified procedure for the synthesis of dibenzoylmethanate complexes (Whan and Crosby, 1962) mentions that an alcoholic solution of the rare-earth chloride and an 25% excess of Hdbm was treated with piperidine and part of the solvent was evaporated to precipitate the rare-earth β -diketonate complex. The experimental procedure further mentions that it was necessary to heat the crude product for a prolonged time in vacuo at 125–150 °C to drive off an "extra mole of chelating agent". Experimental methods such as these were found very difficult to reproduce. It is not easy to get rid of all the excess of the β -diketone. Much of the confusion in the earlier works was caused by the fact that it was not realized that the rare-earth ions can have coordination numbers higher than six. In two often-cited papers that were published in the Journal of the American Chemical Society, Bauer et al. (1964) and Melby et al. (1964) give experimental procedures for the synthesis of the adducts of the tris and tetrakis complexes. The careful reader will not only notice that these papers not only follow each other in the same issue of JACS, but that moreover they have been received the same date (July 17, 1964) at the editorial office of the journal. Bauer et al. (1964) discusses three different methods to prepare rare-earth tetrakis β -diketonate complexes, and the authors also describe the synthesis of [Tb(tta)₃(phen)]. The different synthetic routes to the tetrakis complexes differ mainly in the type of base that has been used. The β -diketone and the rare-earth chloride are first dissolved in hot ethanol at a 4:1 molar ratio. In the case of the complexes with piperidinium as the counter ion, piperidine is a base strong enough to deprotonate the β -diketone, and no

other base has to be used. In the case of complexes with tetrapropylammonium counter ions, tetrapropylammonium hydroxide was used as the base and as provider for the counter ion. For the synthesis of complexes with *N*-hexadecylpyridinium counter ions, the counter ions was provided by *N*-hexadecylpyridinium chloride, and a 2.0 N NaOH solution was used as the base. In the case of [Tb(tta)₃(phen)], a 2.0 N NaOH solution was used as the base as well. 1,10-Phenanthroline was added, after the precipitated NaCl was filtered off. It should be noticed that in all cases, the rare-earth chloride salts was added to the β -diketone, before addition of the base. Melby et al. (1964) describe the synthesis of several hydrated tris complexes, Lewis base adducts of tris complexes and tetrakis complexes. The synthetic procedures vary from compound to compound. In contrast to the work of Bauer et al. (1964), Melby et al. (1964) add the rare-earth after deprotonation of the β -diketone by an appropriate base. The latter authors use not only hydrated rare-earth chloride salts as starting reagents, but hydrated rare-earth nitrate salts as well. Lewis base adducts of the tris complexes can be prepared by dissolving the anhydrous tris complex and the Lewis base in a suitable solvent (1:1 ratio for a bidentate Lewis base and a 1:2 ratio for a monodentate Lewis base). When adducts of bidentate Lewis bases are prepared, one can use hydrated tris complexes as the starting material, because the bidentate ligands will expel the water molecules out of the first coordination sphere (Melby et al., 1964). Charles and Ohlmann (1965a) prepared adducts of [R(dbm)₃] with monodentate Lewis bases (e.g. dmf, dmsO, pyridine, pyridine-*N*-oxide, piperidine) by dissolving anhydrous [R(dbm)₃] in an excess of the Lewis base, either as the pure liquid or as a solution in toluene. The adducts were isolated by evaporation of the excess of liquid or by precipitation with petroleum ether. Mattson et al. (1985) had difficulties in obtaining pure Lewis base adducts of [Eu(fod)₃], due to the high solubility of [Eu(fod)₃] in the usual organic solvents and the tendency of the corresponding Lewis base adducts to form an oil, and they had to carefully select the solvent system and the working conditions. For instance, [Eu(fod)₃(phen)] was obtained by mixing of equimolar quantities of [Eu(fod)₃] and 1,10-phenanthroline in a small volume of hexane. Crystals of the adduct were formed upon slow evaporation of the solvent at room temperature. The solid was recrystallized from heptane. [Eu(fod)₃(dmsO)] was made in ethyl acetate, [Eu(fod)₃(bipy)] in chloroform.

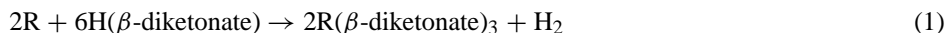
Most of the rare-earth β -diketonate complexes are prepared using the chloride as the rare-earth salt, although other studies mention the corresponding nitrate salt. Because of the greater coordinating power of nitrate ions in comparison with chloride ions, there is the possibility that if nitrate salts are used as a reagent for the synthesis of rare-earth β -diketonate complexes, the resulting complex contains a coordinating nitrate group. An example is the triboluminescent complex [Eu(NO₃)(tta)₂(tppo)₂] (Zhu et al., 1993). Melby et al. (1964) report that [Eu(tta)₃(tppo)₂] could only be prepared starting from europium(III) chloride, not from europium(III) nitrate. Attempts to synthesize this compound from europium(III) nitrate, gave [Eu(tta)₂(tppo)₂(NO₃)], even in the presence of an excess of triphenylphosphine oxide. [R(acac)(terpy)(NO₃)₂(H₂O)_{*n*}] complexes were prepared by Fukuda et al. (2002).

Lyle and Witts (1971) made a critical examination of different methods that have been used previously by other workers to prepare tris and tetrakis β -diketonate complexes of europium(III). They mention that the molar ratios in which the β -diketone, the base and the europium(III) salts are mixed, give only a rough guide to the stoichiometry of the reaction

product. Although it is generally recognized that a β -diketone:base:europium(III) ratio of 3:3:1 favors the formation of the tris complex, and a ratio 4:4:1 favors the formation of the tetrakis complex, unexpected results are possible. If water is not excluded from the reaction mixture, the tris complexes are invariably hydrated (monohydrate, dihydrate or even trihydrate), except when very bulky β -diketone ligands are used. In favorable cases, the hydrated tris complexes can be converted in the anhydrous forms (Belcher et al., 1969a). Dibenzoylmethanate complexes $[\text{R}(\text{dbm})_3] \cdot \text{H}_2\text{O}$ tend to decompose by hydrolysis on heating, and give a basic product, e.g. $[\text{R}(\text{dbm})_2(\text{OH})]$ (Ismail et al., 1969). Further studies have shown that the $[\text{R}(\text{dbm})_2(\text{OH})]$ compounds are polymeric. Differences from the predicted stoichiometries can be expected when a bidentate Lewis base is present in solution and when not enough base is used for the deprotonation of the β -diketone ligands. For instance, Wang et al. (1994c) obtained a compound with composition $[\text{Eu}(\text{dbm})_3(\text{bipy})](\text{Hdbm})$ when dibenzoylmethane and 2,2'-bipyridine were mixed with $\text{Eu}(\text{NO}_3)_3 \cdot 6\text{H}_2\text{O}$ in dry ethanol, in the absence of a base. The crystal structure of the compound shows that the neutral Hdbm molecule is non-coordinating.

Preparation of the anhydrous tris acetylacetonate complexes is very difficult (Liss and Bos, 1977). The general synthetic procedures will lead to hydrated complexes. Attempts to remove hydration water by vacuum drying often lead to partial hydrolysis, especially in the case of the heavy lanthanides. Koehler and Bos (1967) prepared the pure anhydrous tris acetylacetonate complexes of dysprosium(III), holmium(III) and erbium(III) by the reaction of the corresponding rare-earth hydride with purified acetylacetone. Later on, also pure anhydrous acetylacetonates of gadolinium(III), terbium(III) and yttrium(III) could be obtained by this method (Przystal et al., 1971), but not complexes of lanthanum(III), neodymium(III) and europium(III) (Liss and Bos, 1977). Liss and Bos (1977) were able to synthesize the anhydrous tris acetylacetonates by very careful vacuum drying. Dehydration was carried out in a vacuum of 10^{-5} – 10^{-6} Torr at 60–80 °C over periods of 5–8 days. This procedure lead to amorphous anhydrous tris acetylacetonates of lanthanum(III), neodymium(III), samarium(III), europium(III), gadolinium(III) and terbium(III). Crystalline $[\text{Nd}(\text{acac})_3]$, $[\text{Eu}(\text{acac})_3]$ and $[\text{Gd}(\text{acac})_3]$ were obtained by recrystallization from acetylacetone of the amorphous anhydrous acetylacetonates, under anhydrous conditions. Other methods to obtain anhydrous acetylacetonate complexes are discussed further in this section.

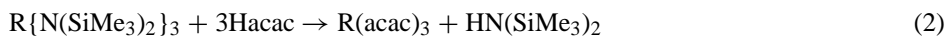
More than 95% of the rare-earth β -diketonate complexes described in the literature have been prepared by the metathesis reaction between the sodium or ammonium salt of a β -diketone and a rare-earth salt (chloride or nitrate) in water or ethanol as the solvent. In most cases, these methods work well, especially when the pH of the reaction mixture is controlled during the synthesis. Sometimes other synthetic routes have to be used, for instance when strictly anhydrous complexes are needed, or when complexes are wanted that are free of contaminating anions or cations. Complexes can be obtained by direct synthesis between a rare-earth metal and a β -diketone in an 1:3 molar ratio in an inert solvent (for instance toluene). Hydrogen gas is evolved and a tris β -diketonate complex is formed:



The tris β -diketonate complexes prepared in this way are free from contaminating ions such as sodium or chloride ions. It is evident that this method can be used only when the func-

tional groups of the β -diketone do not react with the rare-earth metal. Crisler (1975) prepared $[\text{Sm}(\text{acac})_3]$ by direct reaction between samarium metal and acetylacetone. When the β -diketone has a high acidity, such as in the case of hexafluoroacetylacetone (Hhfac), it is possible to make the rare-earth β -diketonate complexes by direct reaction rare-earth oxides. For instance, $[\text{R}(\text{hfac})_3(\text{diglyme})]$ complexes were prepared by reaction between the corresponding rare-earth oxide, hexafluoroacetylacetone and diglyme in a 1:3:1 molar ratio, and with toluene as solvent (Fragala et al., 1996, 1998; Malandrino et al., 2001; Evans et al., 2002). It is advisable to work with a slight excess of the rare-earth oxide, because the unreacted excess can easily be removed by filtration (Malandrino et al., 2001). For preparation of $[\text{Ce}(\text{hfac})_3(\text{diglyme})]$ and $[\text{Tb}(\text{hfac})_3(\text{diglyme})]$, the acetylacetonate complexes $[\text{Ce}(\text{acac})_3]$ and $[\text{Tb}(\text{acac})_3]$ were used instead of the oxides (Evans et al., 2002). The $[\text{R}(\text{hfac})_3(\text{diglyme})]$ complexes can be handled in air without decomposition.

Another synthetic route is the reaction between a β -diketone and a reactive rare-earth compound, such as a rare-earth bis(trimethylsilyl)amide $\text{R}\{\text{N}(\text{SiMe}_3)_2\}_3$ or a rare-earth isopropoxide $\text{R}(\text{O}^i\text{Pr})_3$. The $\text{R}\{\text{N}(\text{SiMe}_3)_2\}_3$ can be easily obtained by reaction between a suspension of RCl_3 in THF with $\text{K}[\text{N}(\text{SiMe}_3)_2]$ in toluene. The product is purified by sublimation. The reaction product that is formed between an acidic ligand such as a β -diketone and $\text{R}\{\text{N}(\text{SiMe}_3)_2\}_3$ is the volatile $\text{HN}(\text{SiMe}_3)_2$ that can be removed from the reaction mixture by evaporation. For example, the reaction between a rare-earth bis(trimethylsilyl)amide and acetylacetone is given by



Barash et al. (1993) obtained anhydrous $[\text{Y}(\text{acac})_3]_n$ by this method. The compound has a good solubility in hydrocarbon solvents. Because of its low volatility, it is assumed that the compound is not monomeric. Rare-earth isopropoxides can be prepared by reaction between a rare-earth metal and isopropanol. By reaction between the rare-earth isopropoxide and a β -diketone, isopropanol is formed:



The isopropanol can be removed by azeotropic distillation with benzene. The composition of several rare-earth isopropoxides do not correspond to the simple stoichiometric formula $\text{R}(\text{O}^i\text{Pr})_3$, but multinuclear aggregates such as $\text{R}_5\text{O}(\text{O}^i\text{Pr})_{13}$ are formed. Mehrotra et al. (1965) were the first to use this method for the preparation of anhydrous $[\text{Pr}(\text{acac})_3]$ and $[\text{Nd}(\text{acac})_3]$, and this method was extended to the synthesis of other rare-earth β -diketonate complexes (Misra et al., 1967; Sankhla and Kapoor, 1966; Hasan et al., 1968, 1969). Gleizes et al. (1993) prepared anhydrous $[\text{Y}(\text{thd})_3]$ by reaction between Hthd and $\text{Y}_5\text{O}(\text{O}^i\text{Pr})_{13}$ in toluene. Only few studies report on the use of organometallic rare-earth compounds as starting product for the synthesis of rare-earth β -diketonate complexes. Lim et al. (1996) obtained anhydrous tris(β -diketonato)lanthanum(III) complexes by reaction between tris(methyl)lanthanum and three equivalents of the β -diketone ligand in THF. The reagents were mixed at 0°C . Tris(methyl)lanthanum, $\text{La}(\text{CH}_3)_3$, was formed in-situ by reaction of anhydrous lanthanum(III)chloride with methyllithium in THF at -78°C , but the lanthanum compound is stable at room temperature. Anhydrous praseodymium acetylacetonates $[\text{Pr}(\text{acac})_3]$ and $\text{M}[\text{Pr}(\text{acac})_4]$ ($\text{M} = \text{Li}, \text{Na}$) were obtained via a solid state reaction

(steel ball milling) between anhydrous PrCl_3 and an alkali metal acetylacetonate (Zaitseva et al., 1998). The formation of a tris or a tetrakis complex depends on the molar ratios in which the reagents are mixed. Blackborow et al. (1976) prepared anhydrous tris acetylacetonate complexes of dysprosium(III) and erbium(III) by co-condensation at liquid nitrogen temperature (77 K) of acetylacetonone with metal atoms evaporated by a laser/thermal procedure.

The work of Van Staveren et al. (2000) shows that the choice of the solvent can have an influence on the type of complex that is formed. By reaction between erbium(III) triflate, hexafluoroacetylacetonone, cesium hydroxide and either 2,2'-bipyridine or 1,10-phenanthroline in methanol, the dinuclear complexes $[\text{Er}(\text{hfac})_2(\mu\text{-OCH}_3)(\text{bipy})]_2$ and $[\text{Er}(\text{hfac})_2(\mu\text{-OCH}_3)(\text{phen})]_2$ were formed, respectively. Methoxy groups are acting as bridging ligands. When the same reaction is performed in dry acetonitrile, the mononuclear complexes $[\text{Er}(\text{hfac})_3(\text{bipy})]$ and $[\text{Er}(\text{hfac})_3(\text{phen})]$ were formed.

The synthesis of complexes of perfluoroacetylacetonone (heptafluoroacetylacetonone, Hacac-F₇) turned out to be a difficult task (Petrov et al., 2002). Reaction of freshly precipitated $\text{Eu}(\text{OH})_3 \cdot n\text{H}_2\text{O}$ led to the formation of europium(III) trifluoroacetate, rather than to the formation of a β -diketonate complex. On the other hand, reaction between hydrated europium(III) acetate and perfluoroacetylacetonone in the presence of 1,10-phenanthroline gave the polynuclear complexes $[\text{Eu}_4(\text{phen})_4(\text{acac-F}_7)_4(\mu^3\text{-F})_4(\mu\text{-F})_2(\mu\text{-OCOCF}_3)_2]$ and $[\text{Eu}_2(\text{phen})_2(\text{acac-F}_7)_2(\mu\text{-OCOCF}_3)_4]$. Upon reaction between dry $\text{Eu}(\text{OAc})_3$ and Hacac-F₇ in dry dichloromethane at room temperature, the complex $[\text{Eu}(\text{acac-F}_7)_3(\text{HOAc})_3]$ was obtained. The reaction can formally be regarded as a proton transfer reaction from Hacac-F₇ to the coordinated acetate ligands. The complex contains three coordinated acetic acid molecules rather than acetate groups. It is possible to replace the weakly bound acetic acid molecules by Lewis bases such as tppo. In this way, $[\text{Eu}(\text{acac-F}_7)_3(\text{tppo})_2]$ was obtained. This complex was also prepared by reaction between europium(III) acetate and Hacac-F₇ in dry dichloromethane, in the presence of triphenylphosphine oxide. When triphenylphosphine oxide was replaced in the reaction by 2,2'-bipyridine, the dinuclear complex $[\text{Eu}_2(\text{acac-F}_7)_4(\text{OAc})_2]^{2-}[\text{bipyH}]_2^+$ was formed. Here, 2,2'-bipyridine acts as a base, rather than as a ligand. Although the synthesis of the acac-F₇ complexes requires strictly anhydrous conditions, the complexes are stable in moist air after synthesis.

Some tetrakis β -diketonate complexes can be transformed into the corresponding anhydrous tris complexes in good yield (Lyle and Witts, 1971). The choice of the base is a critical factor to make the procedure successful. The base should be strong enough to give adequate ionization of the β -diketonone for formation of the tetrakis complex. For instance, isoquinoline ($K_B = 2.5 \times 10^{-9}$) is too weak to deprotonate Hdbm, but deprotonation of this weak acid can be achieved by piperidine ($K_B = 1.6 \times 10^{-3}$). The adduct formed between the β -diketonone and the base should have an adequate thermal stability and volatility, so that it can be driven off of the tetrakis complex in the thermal decomposition reaction. Piperidine is often a good choice as the base when tris complexes are prepared starting from the tetrakis complex. However, the alkali metal hydroxides are a bad choice in this methodology. This synthetic procedure optimized by Lyle and Witts (1971) is an improved version of the "piperidine method" of Crosby et al. (1961), that has been described above. This is a good method to obtain anhy-

drous $[R(\text{dbm})_3]$ complexes. For instance, [Lyle and Witts \(1971\)](#) obtained $[\text{Eu}(\text{dbm})_3]$ in high yield by heating the piperidinium salt of the corresponding tetrakis complex at 135°C under vacuum for 24 hours.

Rare-earth β -diketonate complexes can be synthesized by extraction methods. [Halverson et al. \(1964a, 1964b\)](#) obtained Lewis base adducts of europium(III) β -diketonates by equilibration of an aqueous solution of europium(III) nitrate with a solution of the β -diketone (or its ammonium salt) and of the Lewis base in diethyl ether. As the Lewis base, trioctylphosphine oxide (topo), tributylphosphate (tbp) or dihexylsulfoxide (dhs) were used. The molar ratios Eu^{3+} :diketone:Lewis base were 1:3:2. The complexes are formed in the ether layer, and could be obtained as viscous oils from the ether solution. [Richardson and Sievers \(1971\)](#) prepared tris complexes of 1,1,1,5,5,6,6,7,7,7-decafluoro-2,4-heptanedione by extraction of an aqueous solution of the decafluoroheptanedione in diethyl ether. The rare-earth chlorides were used in 10 to 50% excess in order to prevent the formation of the corresponding tetrakis complexes. $[\text{Eu}(\text{tta})_3(\text{phen})]$ was prepared by extraction of an aqueous solution of europium(III) chloride, 2-thenoyltrifluoroacetone and 1,10-phenanthroline with benzene ([Melent'eva et al., 1966](#)). After separation of the benzene layer from the aqueous layer, the $[\text{Eu}(\text{tta})_3(\text{phen})]$ complex was precipitated by addition of petroleum ether to the benzene layer.

Evans was the first to prepare and characterize β -diketonate complexes of divalent lanthanide ions ([Evans et al., 1994](#)). $[\text{Eu}(\text{thd})_2(\text{dme})_2]$ and $[\text{Sm}(\text{thd})_2(\text{dme})_2]$ were obtained by reaction between 2 equivalents of Kthd and 1 equivalent of $[\text{EuI}_2(\text{thf})_2]$ or $[\text{SmI}_2(\text{thf})_2]$ in THF, followed by addition of 2 equivalents of dimethoxyethane (dme). In an attempt to prepare a complex with divalent europium from $[\text{Eu}(\text{hfac})_3(\text{diglyme})]$, [Evans et al. \(2002\)](#) investigated the reduction of this complex with potassium in toluene. Unexpectedly, crystals of $[\text{EuF}(\text{hfac})_3\text{K}(\text{diglyme})_2]$ were obtained. Reaction of $[\text{EuI}_2(\text{tf})_2]$ with Khfa gave the compound $[\text{Eu}(\text{hfac})_3(\text{diglyme})]$.

The standard procedure for purification of β -diketonates is by recrystallization. Often used recrystallization solvents are *n*-hexane (e.g. [Eisenbraut and Sievers, 1965](#)), *n*-heptane (e.g. [Mattson et al., 1985](#)), or toluene (e.g. [Ismail et al., 1969](#)). Other recrystallization solvents that have been used are ethyl acetate, ethanol and methanol. [Lyle and Witts \(1971\)](#) obtained crystalline $[\text{Eu}(\text{btfac})_3(\text{H}_2\text{O})_2]$ by addition of water to a solution of the complex in acetone. Complexes of β -diketonates that are dissolved in toluene or benzene can be precipitated by addition of petroleum ether or hexane to this solution. Volatile rare-earth β -diketonates such as $[\text{R}(\text{thd})_3]$ or $[\text{R}(\text{fod})_3]$ can be purified by vacuum sublimation. For instance, [Eisenbraut and Sievers \(1965\)](#) purified a series of $[\text{R}(\text{thd})_3]$ complexes by vacuum sublimation between 100 and 200°C . It is often observed that trials to purify β -diketonate complexes by recrystallization result in impurer compounds ([Lyle and Witts, 1971](#)). This is especially the case when dihydrates are recrystallized in hydrocarbon solvents and the water of hydration has to be recovered from the atmosphere. This is a slow process and the complex is more susceptible to decomposition. For instance, ligand rearrangement or ligand oxidation can take place. In order to avoid these problems with purification by recrystallization, it is advisable to use a synthetic method that eliminates the need for recrystallization. However, this is not always possible. Some rare-earth β -diketonate complexes are obtained in the form of a viscous oil, that crystallizes with difficulty or not at all. This is often a problem with complexes of highly

fluorinated ligands. These viscous oils can be contaminated by residues of ligands, but purification is not easy. One can try to isolate the rare-earth complex by differential solution in different solvents. Another possibility is to triturate the oil with water (Charles and Riedel, 1966). Liquid chromatography is not a good method for purification of rare-earth β -diketonate complexes, because of the labile nature of these compounds (Lyle and Witts, 1971). Desreux et al. (1972) mention that purification of $[\text{R}(\text{fod})_3]$ and $[\text{R}(\text{thd})_3]$ complexes on alumina of silica gel columns failed, because the complexes could not be eluted, even not with very polar solvents. Partial deactivation of the columns with dimethyldichlorosilane did not improve the elution.

Although the synthesis of rare-earth β -diketonate complexes is usually carried out in air, Eisentraut and Sievers (1965) found that the yields could be improved by evacuating the flask with the reaction mixture, after the rare-earth salt was added to a solution of the sodium salt of the β -diketone. The authors argue that lower yields of synthesis in air are caused by destructive air oxidation. Air oxidation during synthesis has been observed for transition metal β -diketonates as well, for instance for $[\text{Ni}(\text{thd})_2]$ (Johnson and Hammond, 1959).

Complexes of optically active β -diketones have been studied for their potential as chiral NMR shift reagents (see section 9.3). The most detailed study of these complexes (mainly europium(III) complexes) is the paper of McCreary et al. (1974). Attempts to purify these β -diketonate complexes by thin layer chromatography, molecular distillation or sublimation often resulted in decomposition of the complexes.

Cyclodextrins are cyclic oligosaccharides composed of six, seven and eight D-glucopyranose units linked by an $\alpha(1-4)$ glycoside linkage, which are termed α -, β -, and γ -cyclodextrin respectively (Szejtli, 1998). The cyclodextrins form inclusion compounds with different types of molecules. Brito et al. (1999) investigated the host guest interaction between β -cyclodextrin and $[\text{Eu}(\text{dbm})_3(\text{H}_2\text{O})_2]$ by spectroscopy. Braga et al. (2002) prepared β -cyclodextrin inclusion compounds that contain $[\text{Eu}(\text{ntac})_3(\text{H}_2\text{O})_x]$ and $[\text{Gd}(\text{ntac})_3(\text{H}_2\text{O})_x]$. The molar ratio of host to guest was either 3:1 or 1:1.

It is not only possible to synthesize rare-earth complexes with three or four β -diketonate ligands for each rare-earth ion; mono and bis β -diketonate complexes can be prepared as well when a suitable metal-to-ligand ratio is chosen for the synthetic procedure. In these complexes additional water molecules and/or hydroxy groups are present in the first coordination sphere of the rare-earth ion. Aquahydroxybis(β -diketonato)lanthanide(III) complexes, $[\text{R}(\beta\text{-diketonate})_2(\text{OH})(\text{H}_2\text{O})]$, were obtained by reaction of 2 eq. of the β -diketone ligand and 1 eq. of a rare-earth nitrate in methanol, upon dropwise addition of a 4% aqueous ammonia solution (Miyabayashi and Kinoshita, 1998). The reaction was complete after 1 hour stirring at room temperature. The melting point of the $[\text{Nd}(\text{bzac})_2(\text{OH})(\text{H}_2\text{O})]$ complex is 170 °C and that of $[\text{Nd}(\text{bzac})(\text{OH})_2(\text{H}_2\text{O})_2]$ is 183 °C, whereas that of $[\text{Nd}(\text{bzac})_3]$ is 180 °C. The authors claim in their patent application that the bis β -diketonate complexes have a better solubility and stability in polymerizable monomers such as styrene and methylmethacrylate than the corresponding tris β -diketonate complexes, so that these bis β -diketonate complexes are good starting materials for rare-earth-doped polymers.

Heteropolynuclear d-f complexes can be formed by adduct formation between a rare-earth tris β -diketonate and a transition metal complex. Sasaki et al. (1998, 2000) reported the

synthesis and structure of the dinuclear $[\text{Cu}(\text{salabza})\text{R}(\text{hfac})_3]$ complexes; where $\text{H}_2\text{salabza}$ is *N,N'*-bis(salicylidene)-2-aminobenzylamine, Hhfa is hexafluoroacetone and $\text{R} = \text{Gd}, \text{Lu}$. The complexes were formed by a reaction between a solution of $[\text{R}(\text{hfac})_3(\text{H}_2\text{O})_2]$ in methanol and a solution of $[\text{Cu}(\text{salabza})]$ in chloroform. Kuz'mina and coworkers (Aikhanyan et al., 1999; Kuz'mina et al., 2000a, 2000b) studied heterobimetallic complexes formed between $[\text{Cu}(\text{salen})]$ and $[\text{Ni}(\text{salen})]$ ($\text{H}_2\text{salen} = \text{N,N}'$ -bis(salicylidene)ethylenediamine) and different rare-earth β -diketonate complexes. Co-crystallization of an equimolar mixture of $[\text{Y}(\text{hfac})_3]$ and $[\text{Cu}(\text{acac})_2]$ in ethanol resulted in the formation of crystals of $[\text{Y}(\text{hfac})_3(\text{H}_2\text{O})_2\text{Cu}(\text{acac})_2]$. In these compounds, the $[\text{Y}(\text{hfac})_3(\text{H}_2\text{O})_2]$ and $[\text{Cu}(\text{acac})_2]$ molecules are linked by intermolecular hydrogen bonds to form zigzag chains (Kuz'mina et al., 2000b). This compound can thus not be considered as a genuine d-f complex. When the compound is heated in vacuum, a ligand exchange and evolution of $[\text{Cu}(\text{hfac})_2]$ into the gas phase is observed. This behavior with $[\text{Cu}(\text{acac})_2]$ is in contrast with that of $[\text{M}(\text{salen})]$ complexes ($\text{M} = \text{Cu}, \text{Ni}$) that form $[\text{M}(\text{salen})\text{R}(\text{hfac})_3]$ compounds (Ramade et al., 1997; Gleizes et al., 1998; Ryazanov et al., 2002). The rare-earth complexes of the type $[\text{R}(\text{hfac})_3]$, $[\text{R}(\text{fod})_3]$ and $[\text{R}(\text{pta})_3]$ were found to form complexes with $[\text{Cu}(\text{acacen})]$ or $[\text{Ni}(\text{acacen})]$, where H_2acacen is *N,N'*-ethylenebis(acetylacetonimine) (Kuz'mina et al., 2002). The resulting binuclear complexes sublimed without decomposition at temperatures of 200–240 °C at 0.01 mm Hg.

Acetylacetonate has been used as counter ion in rare-earth porphyrin complexes (Wang et al., 1974; Liu et al., 1994; Spyroulias et al., 1995; Jiang et al., 1995a, 1995b). In these complexes, the rare-earth ion can be bonded to one porphyrin ring and to one acac ligands so that a six-coordinate rare-earth complex is formed (Liu et al., 1994; Spyroulias et al., 1995), or two additional water molecules can be bonded so that the coordination sphere of the rare-earth ion is expanded to eight (Jiang et al., 1995a, 1995b). The spectroscopic properties of these complexes are determined by the porphyrin ligand and not by the β -diketonate ligand.

4. Structural properties

Detailed insight into the structure of the rare-earth β -diketonates was only possible after crystal structures could be determined by single crystal X-ray diffraction. At present, more than two hundred crystal structures of different types of rare-earth β -diketonate complexes can be found in the database of the Cambridge Crystallographic Data Centre. Crystal structures of tris complexes, tetrakis complexes, Lewis-base adducts of tris complexes and of dimers or oligomers are available. Whereas unsolvated tris complexes have a six-coordinate rare-earth ion, most of the rare-earth β -diketonate complexes are eight-coordinate. The coordination polyhedron of such eight-coordinate complexes can be described either by a dodecahedron (D_{2d} symmetry) or by an square antiprism (D_{4d} symmetry). These highly symmetric coordination polyhedra are never found in actual structures, but they are useful to classify or describe the coordination polyhedra of the complexes in a crystalline environment. Sometimes the coordination polyhedra are so heavily distorted that it is not possible to decide whether

the actual coordination polyhedron is closer to a dodecahedron or to a square antiprism. Typically, the symmetry at the rare-earth ion site is C_1 (no symmetry elements present). For this reason it is difficult to use the fine structure in the luminescence spectrum of europium(III) β -diketonate complexes to determine the site symmetry. Luminescence spectroscopy is only useful if the rare-earth ion is at a site of (relatively) high symmetry. An indication for the number of crystallographically non-equivalent sites in an europium(III) β -diketonate complex can be obtained from the number of lines observed for the ${}^5D_0 \rightarrow {}^7F_0$ transition. In $[\text{Ho}(\text{thd})_3(4\text{-pic})_2]$, the Ho^{3+} ion is at a site of C_2 symmetry (Horrocks et al., 1971). Besides the six- and eight-coordinate rare-earth β -diketonate complexes, complexes with coordination number seven, nine or even ten are also known. A selection of the rare-earth β -diketonate complexes for which crystallographic data are available, is given in tables 2 and 3. As can be seen, most of the crystals have a very low symmetry. An exception are the $[\text{R}(\text{dbm})_3(\text{H}_2\text{O})]$ complexes, that belong to the rhombohedral space group R3 (Kirby and Richardson, 1983). The crystal structure of $[\text{Ho}(\text{dbm})_3(\text{H}_2\text{O})]$ has been determined by Zalkin et al. (1969) (figs. 5 and 6). The rare-earth ion is seven-coordinate. The three dbm ligands form a trigonal prism around the rare-earth ion, and the (disordered) water molecule is lying on a threefold rotation axis. The nearly planar dbm ligands are arranged in a propeller-like fashion around the rare-earth ion. If the hydrogen atoms of the water molecule are neglected the coordination polyhedron of the $[\text{R}(\text{dbm})_3(\text{H}_2\text{O})]$ complexes has a C_3 symmetry. It is very uncommon to have such a high symmetry for a seven coordinate complex. So far, the number of crystal structures available for the tetrakis β -diketonate complexes is limited in comparison with the number of the tris complexes and adducts of tris complexes.

A structural feature of the rare-earth β -diketonates is that some of the compounds form crystals in which the rare-earth ion is inserted into one single type of coordination polyhedron, while in other compounds two different types of coordination polyhedra are present. Other rare-earth β -diketonates form two types of crystals in which the coordination polyhedron is different and which can be considered as isomers (Thompson and Berry, 2001). Two isomers are found for $[\text{Eu}(\text{tfac})_3(\text{H}_2\text{O})_2]$, where in one type of crystal the coordination polyhedron is a bicapped trigonal prism and in the other type a dodecahedron (Thompson and Berry, 2001). In $[\text{Eu}(\text{ntac})_3(\text{bipy})]$, one isomer is a bicapped trigonal prism and the other contains two slightly different square antiprisms (Thompson et al., 1998). Four different forms of $[\text{Eu}(\text{dbm})_3(\text{topo})]$ are known (Thompson and Berry, 2001). Two slightly different polyhedra are present in $[\text{Eu}(\text{thd})_3(\text{terpy})]$ (Holz and Thompson, 1988). In $[\text{Eu}(\text{thd})_3(\text{terpy})]$, the Eu^{3+} ion is nine-coordinate, with distorted tricapped trigonal prism as the coordination polyhedron. Thompson and Berry (2001) point to the fact that it is still unknown what factors influence the formation of compounds with multiple coordination sites for the central rare-earth ion and what factor leads to the formation of distinct geometrical isomers. The authors noticed that all the 1,10-phenanthroline adducts that have been characterized so far have a single coordination polyhedron, whereas several 2,2'-bipyridine adducts have two coordination polyhedra. This could lead to the conclusion that a flexible adduct molecule leads to the formation of different isomers, but in the adduct of 2,9-dimethyl-1,10-phenanthroline (which is a very rigid molecule) two different sites with a very different arrangement of the chelate rings

Table 2
Selection of rare-earth tris β -diketonate complexes for which crystal structures have been determined by single crystal X-ray diffraction

Compound	Crystal system	Space group	Refcode CDS*	Reference
[Sc(acac) ₃]	orthorhombic	Pbca (No. 61)	ACACSC	Andersen et al., 1973
[Sc(dbm) ₃]	triclinic	P $\bar{1}$ (No. 2)	JINPUR	Zaitseva et al., 1990
	monoclinic	P2 ₁ /c (No. 14)	JINPUR01	Zaitseva et al., 1990
[Y(acac) ₃ (H ₂ O) ₂](H ₂ O)	monoclinic	P2 ₁ /n (No. 14)	YACACT	Cunningham et al., 1967
[Y(acac) ₃ (phen)]	monoclinic	P2 ₁ /n (No. 14)	KUPSUJ	Liu et al., 1991
[Y(acac) ₃ (dmso)(H ₂ O)]·(dmso)	monoclinic	P2 ₁ /n (No. 14)	NUMFUW	Zharkova et al., 1998
[Y(bzac) ₃ (H ₂ O)]	triclinic	P $\bar{1}$ (No. 2)	PHBUAY	Cotton and Legzdins, 1968
[Y(hfac) ₃ (H ₂ O) ₂][Cu(acac) ₂]	monoclinic	P2 ₁ /n (No. 14)	COQDUH	Jung et al., 1998
[Y(thd) ₃]	orthorhombic	Pmn2 ₁ (No. 31)	HAHTOZ	Gleizes et al., 1993
[Y(thd) ₃ (H ₂ O)]	triclinic	P $\bar{1}$ (No. 2)	HAHTIT	Gleizes et al., 1993
[La(acac) ₃ (H ₂ O) ₂]	triclinic	P $\bar{1}$ (No. 2)	AQACAL	Philips et al., 1968
[La(acac) ₃ (phen)]	monoclinic	P2 ₁ /n (No. 14)	NAVYAK	Kuz'mina et al., 1997
[La(dbm) ₃ (dmop)]	monoclinic	P2 ₁ /n (No. 14)	HARYAA	Holz and Thompson, 1993
[La(dipydike) ₃] ₂	monoclinic	P2 ₁ /c (No. 14)	XEYYIJ	Brück et al., 2000
[La(hfac) ₃ (bipy) ₂]	monoclinic	C2/c (No. 15)	EBUXUU	Van Staveren et al., 2001
[La(hfac) ₃ (H ₂ O){Cu(salen)}]	monoclinic	P2 ₁ /n (No. 14)	RINQOU	Ramade et al., 1997
[La(hfac) ₃ (diglyme)]	monoclinic	P2 ₁ /c (No. 14)	ZIQXIG01	Malandrino et al., 1998a
[La(hfac) ₃ (monoglyme)]	monoclinic	P2 ₁ /c (No. 14)	KINDEQ	Malandrino et al., 1998a
[La(hfac) ₃ (triglyme)]	monoclinic	P2 ₁ /c (No. 14)	KINJOG	Malandrino et al., 1998a
[Ce(acac) ₃ (phen)]	monoclinic	P2 ₁ /n (No. 14)	PEKWEH	Christidis et al., 1998
[Ce(hfac) ₃ (diglyme)]	monoclinic	P2 ₁ /n (No. 14)	BAFXUC	Evans et al., 2002
[Pr(acac) ₃ (H ₂ O) ₂]	triclinic	P $\bar{1}$ (No. 2)	CAZGUF	Shen et al., 1983a
[Pr(acac) ₃ (phen)]	monoclinic	P2 ₁ /n (No. 14)	PELGOC	Christidis et al., 1998
[Sm(acac) ₃ (H ₂ O) ₂]	triclinic	P $\bar{1}$ (No. 2)	CAZHAM	Shen et al., 1983a
[Sm(acac) ₃ (phen)]	monoclinic	P2 ₁ /n (No. 14)	EDANUS	Urs et al., 2001
[Sm(hfac) ₃ (bipy)]·(bipy)	triclinic	P $\bar{1}$ (No. 2)	EBUYAB	Van Staveren et al., 2001
[Sm(hfac) ₃ (diglyme)]	monoclinic	P2 ₁ /n (No. 14)	BAFWIP	Evans et al., 2002
[Sm(thd) ₃ (dmap)]	monoclinic	P2 ₁ (No. 4)	XAXYAW	Clegg et al., 2000
[Sm(thd) ₃ (monoglyme)]	triclinic	P $\bar{1}$ (No. 2)	YEYLAP	Evans et al., 1994
[Nd(acac) ₃ (H ₂ O) ₂](acetone)	orthorhombic	Pbna (No. 60)	GAFDIA	Nakamura et al., 1986
[Nd(dbm) ₃ (H ₂ O)]	trigonal	R3 (No. 146)	ADBMDN	Kirby and Palmer, 1981a
[Nd(hfac) ₃ (diglyme)]	monoclinic	P2 ₁ /n (No. 14)	BAFYAJ	Evans et al., 2002

continued on next page

Table 2, *continued*

Compound	Crystal system	Space group	Refcode CDS*	Reference
[Nd(tta) ₃ (bipy)]	monoclinic	P2 ₁ /c (No. 14)	TTANDP	Leipoldt et al., 1976
[Nd(tta) ₃ (tppo) ₂]	triclinic	P $\bar{1}$ (No. 2)	TFPOND	Leipoldt et al., 1975
[Eu(acac) ₃ (phen)]	monoclinic	P2 ₁ /n (No. 14)	ACPNEU	Watson et al., 1972
[Eu(acac-F7) ₃ (tppo) ₂]	monoclinic	P2 ₁ /n (No. 14)	MIHNEW	Petrov et al., 2002
[Eu(btfac) ₃ (bipy)]	monoclinic	P2 ₁ /n (No. 14)	HILVED	Batista et al., 1998
[Eu(btfac) ₃ (H ₂ O) ₂]	orthorhombic	P2 ₁ 2 ₁ 2 ₁ (No. 19)	TOGHUS	Van Meervelt et al., 1996
[Eu(btfac) ₃ (tppo) ₂]	triclinic	P $\bar{1}$ (No. 2)	WIFWIR01	Van Meervelt et al., 1996
[Eu(dbm) ₃ (dmbp)](H ₂ O)	monoclinic	P2 ₁ /n (No. 14)	MAJZOM	Chen et al., 1999c
[Eu(dbm) ₃ (dmop)]	monoclinic	P2 ₁ /n (No. 14)	HARYEE	Holz and Thompson, 1993
[Eu(dbm) ₃ (phen)]	triclinic	P $\bar{1}$ (No. 2)	VADSEZ	Ahmed et al., 2003
[Eu(dbm) ₃ (terpy)]	monoclinic	P2 ₁ /n (No. 14)	KACTIR	Holz and Thompson, 1988
[Eu(dmh) ₃ (bipy)]	triclinic	P $\bar{1}$ (No. 2)	MUWYOS	Moser et al., 2000
[Eu(dmh) ₃ (phen)]	monoclinic	C2/c (No. 15)	MUWYIM	Moser et al., 2000
[Eu(fod) ₃ (H ₂ O) ₂]	triclinic	P $\bar{1}$ (No. 2)	DOMDEO	Vancoppemolle et al., 1983
[Eu(hfac) ₃ (bipy)(H ₂ O)]	triclinic	P $\bar{1}$ (No. 2)	–	Thompson et al., 2002
[Eu(hfac) ₃ (diglyme)]	monoclinic	P2 ₁ /n (No. 14)	KAFDOK01	Evans et al., 2002
		P2 ₁ /n (No. 14)	KAFDOK	Kang et al., 1997b
[Eu(hfac) ₃ (tppo) ₂]	monoclinic	P2 ₁ /c (No. 14)	MIHPEY	Petrov et al., 2002
[Eu(ntac) ₃ (bipy)]	monoclinic	P2 ₁ /c (No. 14)	UCICIS	Thompson et al., 1998
[Eu(ntac) ₃ (bipy)]-0.5(2-propanol)	orthorhombic	Pna2 ₁ (No. 33)	UCICEO	Thompson et al., 1998
[Eu(thd) ₃ (bipy)]	monoclinic	C2/c (No. 15)	–	Moser et al., 2000
[Eu(thd) ₃ (dmf) ₂]	triclinic	P $\bar{1}$ (No. 2)	EUTHDF10	Cunningham and Sievers, 1980
[Eu(thd) ₃ (monoglyme)]	monoclinic	P2 ₁ /c (No. 14)	YEYKUI	Evans et al., 1994
[Eu(thd) ₃ (phen)]	triclinic	P $\bar{1}$ (No. 2)	–	Malta et al., 1996
[Eu(thd) ₃ (py) ₂]	triclinic	P $\bar{1}$ (No. 2)	THMPEU10	Cramer and Seff, 1972
[Eu(tta) ₃ (H ₂ O) ₂]	monoclinic	P2 ₁ /c (No. 14)	AFTEU	White, 1976
[Eu(tta) ₃ (bipy)]	monoclinic	P2 ₁ /n (No. 14)	MAJZIG	Chen et al., 1999c
[Eu(tta) ₃ (bmbp)]	orthorhombic	Pca2 ₁ (No. 29)	YOJDIK	Zheng et al., 2002
[Eu(tta) ₃ (phen)]	triclinic	P $\bar{1}$ (No. 2)	MOYFEL	Hu et al., 1999
[Eu(tta) ₃ (tppo) ₂]	triclinic	P $\bar{1}$ (No. 2)	SABHIM	Li et al., 1988
[Gd(acac) ₃ (H ₂ O) ₂]	monoclinic	P2 ₁ /n (No. 14)	CEXPIE	Shen et al., 1983b
[Gd(hfac) ₃ (diglyme)]	monoclinic	P2 ₁ /n (No. 14)	TETZAT	Malandrino et al., 1996

continued on next page

Table 2, *continued*

Compound	Crystal system	Space group	Refcode CDS*	Reference
[Gd(hfac) ₃ (H ₂ O)(acetone)]	triclinic	P $\bar{1}$ (No. 2)	PORGIM	Plakatouras et al., 1994
[Gd(hfac) ₃ {Cu(salen)}]	monoclinic	P2 ₁ /n (No. 14)	RINQAG	Ramade et al., 1997
[Gd(thd) ₃ (monoglyme)]	triclinic	P $\bar{1}$ (No. 2)	YOMBIL	Baxter et al., 1995
[Gd(tta) ₃ (tppo) ₂]	triclinic	P $\bar{1}$ (No. 2)	SABHOS	Li et al., 1988
[Tb(acac-F7) ₃ (tppo) ₂]	monoclinic	P2 ₁ /n (No. 14)	MIHNUM	Petrov et al., 2002
[Tb(dbm) ₃ (dmop)]	monoclinic	P2 ₁ /n (No. 14)	HARYII	Holz and Thompson, 1993
[Tb(hfac) ₃ (diglyme)]	orthorhombic	Pna2 ₁ (No. 33)	BAFWUB	Evans et al., 2002
[Tb(hfac) ₃ (tppo) ₂]	monoclinic	P2 ₁ /n (No. 14)	MIHPIC	Petrov et al., 2002
[Tb(thd) ₃ (dmap)]	monoclinic	P2 ₁ (No. 4)	XAXXUP	Clegg et al., 2000
[Dy(thd) ₃ (H ₂ O)]	triclinic	P $\bar{1}$ (No. 2)	TMHPDY	Erasmus and Boeyens, 1971
[Ho(acac) ₃ (H ₂ O) ₂].H ₂ O	monoclinic	P2 ₁ /n (No. 14)	CUXQER	Kooijman et al., 2000
[Ho(acac) ₃ (H ₂ O) ₂].H ₂ O.(Hacac)	monoclinic	P2 ₁ /n (No. 14)	CUXQAN	Kooijman et al., 2000
[Ho(dbm) ₃ (H ₂ O)]	trigonal	R3 (No. 146)	PHPRHO10	Zalkin et al., 1969
[Ho(dbm) ₃ (dmop)]	monoclinic	P2 ₁ /n (No. 14)	HARYOO	Holz and Thompson, 1993
[Ho(hfac) ₃ (H ₂ O) ₂]	triclinic	P $\bar{1}$ (No. 2)	UCIMOI	Lee et al., 1998
[Ho(hfac) ₃ (H ₂ O) ₂](triglyme)	monoclinic	P2 ₁ /n (No. 14)	SIFZIQ01	Lee et al., 1998
[Ho(thd) ₃ (4-pic) ₂]	orthorhombic	Pbcn (No. 60)	HPHOPC	Horrocks et al., 1971
[Ho(thd) ₃ (pivalic acid)]	triclinic	P $\bar{1}$ (No. 2)	YEFWUB	Kuz'mina et al., 1994
[Er(acac) ₃ (H ₂ O) ₂]	monoclinic	P2 ₁ /n (No. 14)	CEXPQU	Shen et al., 1983b
[Er(hfac) ₃ (phen)]	monoclinic	C2/c (No. 15)	EBUXOO	Van Staveren et al., 2001
[Er(thd) ₃]	orthorhombic	Pmn2 ₁ (No. 31)	TMHDER	de Villiers and Boeyens, 1972
[Er(thd) ₃ (pivalic acid)]	triclinic	P $\bar{1}$ (No. 2)	YEWGAI	Kuz'mina et al., 1994
[Tm(acac) ₃ (H ₂ O) ₂].H ₂ O	monoclinic	P2 ₁ /n (No. 14)	CEXRAY	Shen et al., 1983b
[Tm(acac-F7) ₃ (tppo) ₂]	monoclinic	P2 ₁ /n (No. 14)	MIHPAU	Petrov et al., 2002
[Yb(acac) ₃]	triclinic	P $\bar{1}$ (No. 2)	FEBGAU	Batsanov et al., 1986
[Yb(acac) ₃ (H ₂ O)]	triclinic	P $\bar{1}$ (No. 2)	YBACAB	Cunningham et al., 1969
[Yb(acac) ₃ (H ₂ O) ₂]	triclinic	P $\bar{1}$ (No. 2)	ZASTIW	Martynenko et al., 1995
[Lu(fod) ₃ (H ₂ O)]	triclinic	P $\bar{1}$ (No. 2)	FMODLU	Boeyens and de Villiers, 1971
[Lu(thd) ₃]	orthorhombic	Pmn2 ₁ (No. 31)	LUTMHP	Onuma et al., 1976
[Lu(thd) ₃ (3-pic)]	monoclinic	P2 ₁ /c (No. 14)	MHPOLU10	Wasson et al., 1973

*Refcode CDS: reference code in the Cambridge Structural Database.

Table 3
Selection of rare-earth tetrakis β -diketonate complexes for which crystal structures have been determined by single crystal X-ray diffraction

Tetrakis unit	Counter ion	Crystal system	Space group	Refcode CDS*	Reference
[Y(hfac) ₄] ⁻	Cs ⁺	orthorhombic	Pbcn (No. 60)	CYSFAC10	Bennett et al., 1968
[La(tta) ₄] ⁻	quinolinium	triclinic	P $\bar{1}$ (No. 2)	DIBSUC	Wei et al., 1984
[Ce(tta) ₄] ⁻	isoquinolinium	monoclinic	P2 ₁ /c (No. 14)	QFTBCE	McPhail and Tschang, 1974
[Pr(tta) ₄] ⁻	tetrabutylammonium	monoclinic	P2/n (No. 13)	FODHUB	Criasia, 1987a
[Nd(tta) ₄] ⁻	pyridinium	monoclinic	P2 ₁ /c (No. 14)	THFAND	Leipoldt et al., 1977
[Sm(tta) ₄] ⁻	1,2-dimethylpyridinium	monoclinic	P2 ₁ /a (No. 14)	XOGYIB	Chen et al., 2000
[Sm(tta) ₄] ⁻	1,2,6-trimethylpyridinium	monoclinic	P2n (No. 7)	XOGYOH	Chen et al., 2000
[Sm(tta) ₄] ⁻	tetrabutylammonium	monoclinic	C2/c (No. 15)	FODJAJ	Criasia, 1987b
[Eu(bzac) ₄] ⁻	piperidinium	monoclinic	P2 ₁ /n (No. 14)	PIEUAC01	Rheingold and King, 1989
[Eu(dbm) ₄] ⁻	dimethylbenzylammonium	orthorhombic	Pca2 ₁ (No. 29)	XUXZAR	Xiong and You, 2002
[Eu(dbm) ₄] ⁻	imidazolium	orthorhombic	Pbcn (No. 60)	XIWTUS	Chen et al., 1999b
[Eu(dbm) ₄] ⁻	morpholinium	orthorhombic	Pca2 ₁ (No. 29)	XIRCAC	Zeng et al., 2000
[Eu(dbm) ₄] ⁻	triethylammonium	monoclinic	Ia (No. 9)	FIDNIP01	Cotton et al., 2001
[Eu(hfac) ₄] ⁻	Cs ⁺	orthorhombic	Pbcn (No. 60)	CEUHFA	Burns and Danford, 1969
[Eu(tta) ₄] ⁻	1,4-dimethylpyridinium	monoclinic	P2 ₁ /n (No. 14)	VAQDIA	Chen et al., 1998

*Refcode CDS: reference code in the Cambridge Structural Database.

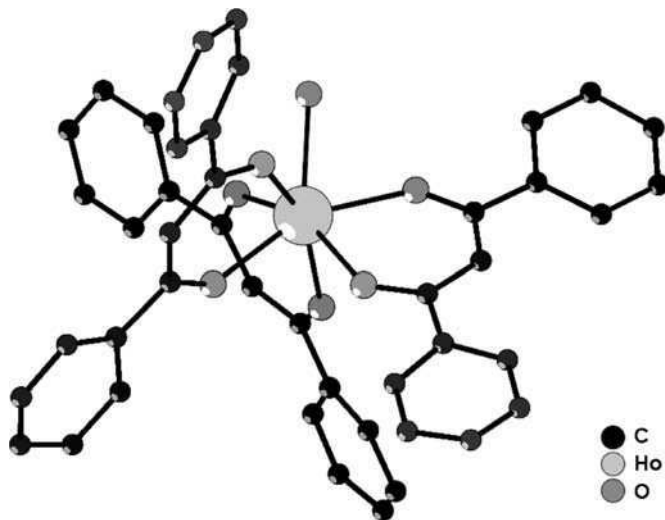


Fig. 5. Molecular structure of $[\text{Ho}(\text{dbm})_3(\text{H}_2\text{O})]$. The atomic coordinates are taken from Zalkin et al. (1969). No hydrogen atoms are shown.

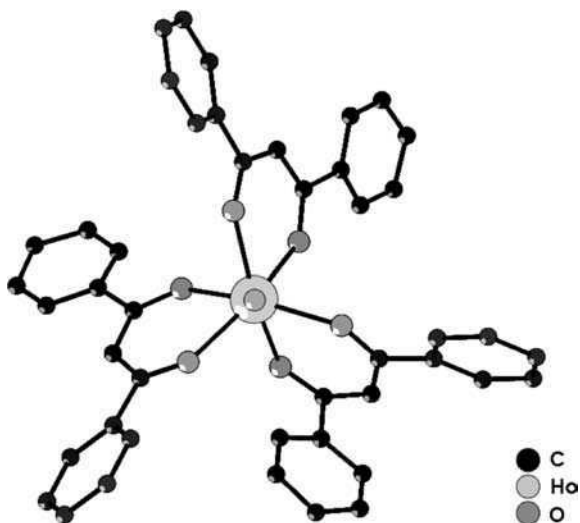


Fig. 6. Molecular structure of $[\text{Ho}(\text{dbm})_3(\text{H}_2\text{O})]$ with projection along the z -axis. The atomic coordinates were taken from Zalkin et al. (1969). No hydrogen atoms are shown.

exist (Holz and Thompson, 1993). $[\text{Eu}(\text{bzac})_3(\text{bipy})]$ has a single site with a distorted square antiprism as the coordination polyhedron (Moser et al., 2000). In $[\text{Nd}(\text{tfac})_3(\text{H}_2\text{O})_2]$, two geometric isomers coexist in the crystal lattice in a 74 to 26% ratio (Nakamura et al., 1986).

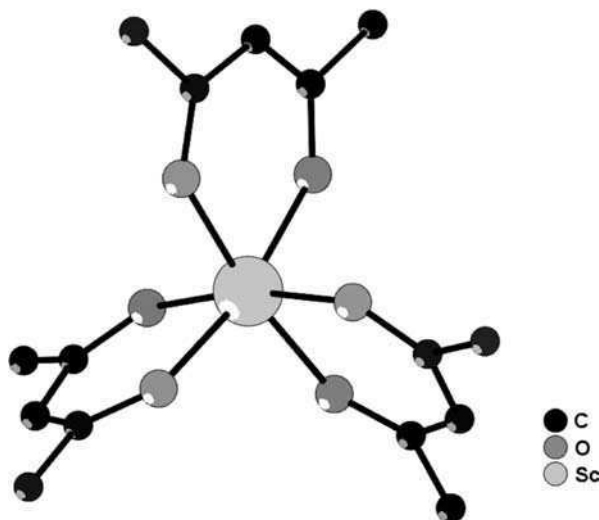


Fig. 7. Molecular structure of $[\text{Sc}(\text{acac})_3]$. The atomic coordinates are taken from Andersen et al. (1973). No hydrogen atoms are shown.

$[\text{Sc}(\text{acac})_3]$ crystallizes in the orthorhombic space group $Pbca$ (Andersen et al., 1973). The structure consists of discrete $\text{Sc}(\text{acac})_3$ molecules. The scandium(III) ion is six-coordinate, and the coordination polyhedron can be described as a slightly distorted octahedron (fig. 7). The site symmetry is close to D_3 . Another example of a six-coordinate scandium(III) β -diketonate complex is $[\text{Sc}(\text{dbm})_3]$ (Zaitseva et al., 1990). Two different crystal structures are described, one with a triclinic and one with a monoclinic cell. So far, no scandium(III) β -diketonates with coordination number higher than six have been described. Because of the small ion size of Sc^{3+} , coordination number six is the general rule for this rare-earth ion. Also in the trinuclear scandium(III) disiloxanediolate complex $[(\text{Ph}_2\text{SiO})_2\text{O}]_2\text{Sc}_3(\text{acac})_5$, the coordination number of Sc^{3+} is six as well (Lorenz et al., 2001) (fig. 8).

Coordination number seven is found in $[\text{Y}(\text{bzac})_3(\text{H}_2\text{O})]$ (Cotton and Legzdins, 1968). The coordination polyhedron is a distorted monocapped octahedron (with idealized C_{3v} symmetry). In the seven-coordinate complex $[\text{Lu}(\text{thd})_3(3\text{-pic})]$, the coordination polyhedron is a monocapped trigonal prism (Wasson et al., 1973). The idealized symmetry of such a coordination polyhedron is C_{2v} . The monocapped trigonal prism is also found in the crystal structures of, for instance, $[\text{Yb}(\text{acac})_3(\text{H}_2\text{O})]$ (Cunningham et al., 1969), $[\text{Lu}(\text{fod})_3(\text{H}_2\text{O})]$ (Boeyens and de Villiers, 1971), $[\text{Dy}(\text{thd})_3(\text{H}_2\text{O})]$ (Erasmus and Boeyens, 1971) and $[\text{Y}(\text{thd})_3(\text{H}_2\text{O})]$ (Gleizes et al., 1993). An example of a rare-earth β -diketonate complex with a non-coordinated polydentate ligand besides the above mentioned $[\text{Eu}(\text{thd})_3(\text{terpy})]$ complex, is $[\text{Eu}(\text{hfac})_3(\text{bipy})(\text{H}_2\text{O})]$ (Thompson et al., 2002). In the latter compound, a non-coordinated 2,2'-bipyridine molecule is located in the crystal lattice and disordered over two positions. Examples of crystal structures of eight-coordinate rare-earth β -diketonate complexes are

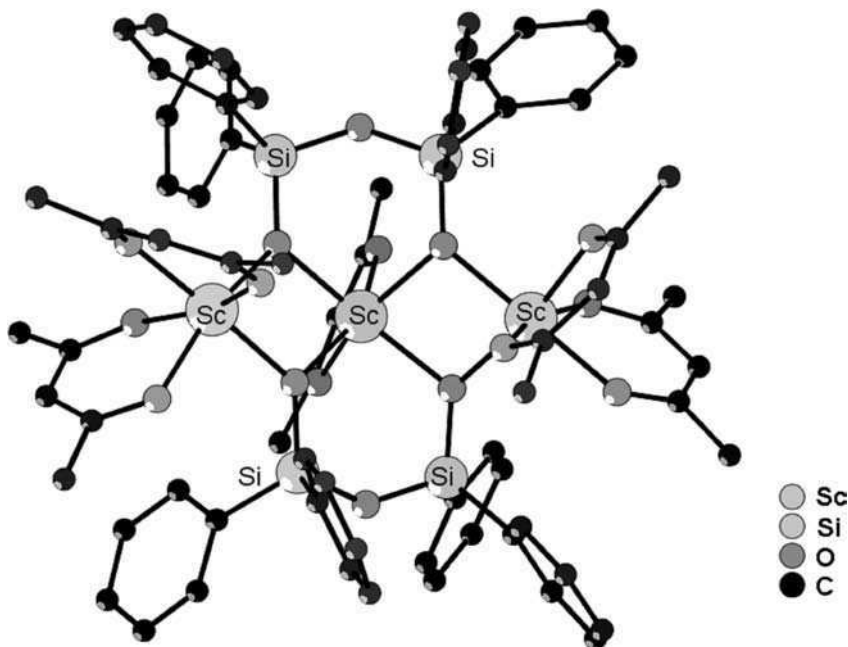


Fig. 8. Molecular structure of the trinuclear scandium(III) disiloxanediolate complex $[(\text{Ph}_2\text{SiO})_2\text{O}]_2\text{Sc}_3(\text{acac})_5$. The atomic coordinates are taken from Lorenz et al. (2001). No hydrogen atoms are shown.

the structures of $[\text{Eu}(\text{acac})_3(\text{phen})]$ (Watson et al., 1972) (fig. 9), $[\text{Eu}(\text{tta})_3(\text{H}_2\text{O})_2]$ (fig. 10) (White, 1976), and $\text{Cs}[\text{Eu}(\text{hfac})_4]$ (fig. 11) (Burns and Danford, 1969).

A special coordination mode is found in the lanthanum(III) complex of 1,3-(2-pyridyl)propane-1,3-dione (dipydike) (Brück et al., 2000). The molecular structure of $[\text{La}(\text{dipydike})_3]_2$ contains centrosymmetric dimers through bridging atoms of the β -diketonate ligands. The nitrogen atoms of the pyridyl group participates in the coordination. The lanthanum(III) ion is thus 10-coordinate. The coordination polyhedron formed by four terminal β -diketonate oxygens, four bridging β -diketonate oxygens and two terminal pyridyl nitrogens. The coordinating pyridyl groups are those of the bridging β -diketonate ligands.

A variation of the coordination number with the size of the lanthanide ion was found for a series of complexes of hexafluoroacetylacetonate (hfac) (Van Staveren et al., 2001). The trivalent ions at the beginning of the lanthanide series can accommodate two 2,2'-bipyridine or 1,10-phenanthroline ligands in the first coordination sphere besides three hexafluoroacetylacetonate ligands. This results in the formation of complexes with coordination number ten, for instance $[\text{La}(\text{hfac})_3(\text{phen})_2]$ or $[\text{La}(\text{hfac})_3(\text{bipy})_2]$ (figs. 12 and 13). The formation of 10-coordinate species is attributed to the presence of strong electron-withdrawing groups in the ligands. Due to the inductive effect of the CF_3 groups, the lanthanide ion becomes more positively charged. When the size of the lanthanide ions is large enough, a second bipy or phen ligand can be bound in order to compensate the higher positive charge. The ions

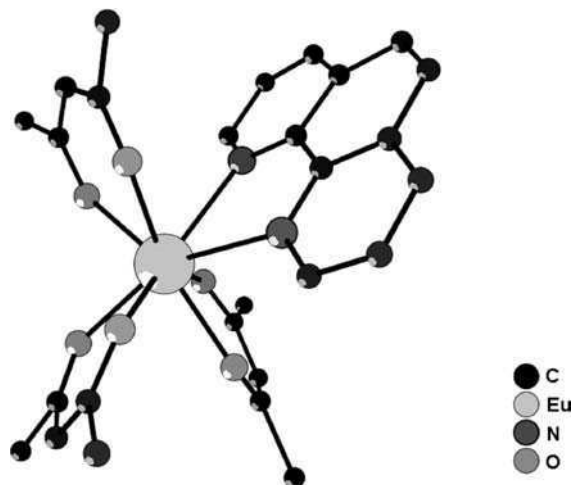


Fig. 9. Molecular structure of [Eu(acac)₃(phen)]. The atomic coordinates are taken from [Watson et al. \(1972\)](#). No hydrogen atoms are shown.

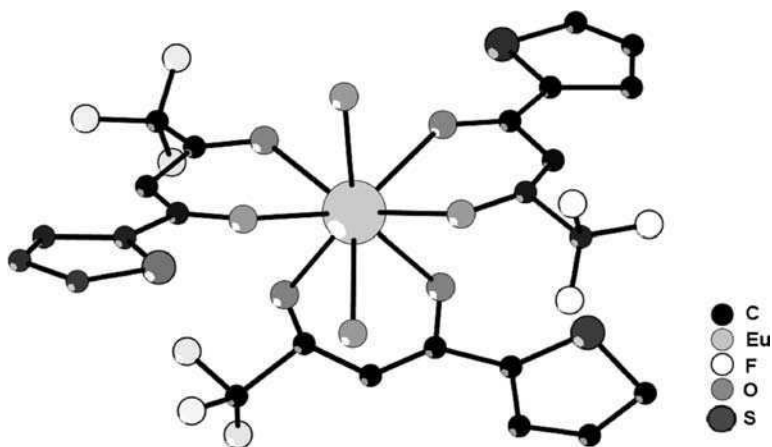


Fig. 10. Molecular structure of [Eu(tta)₃(H₂O)₂]. The atomic coordinates are taken from [White \(1976\)](#). No hydrogen atoms are shown.

in the second half of the lanthanide series have a smaller ionic radius and they form classical eight-coordinate complexes. Examples are [Ho(hfac)₃(phen)] or [Er(hfac)₃(bipy)]. Intermediate forms are possible for the ions in the middle of the lanthanide series. Although [Sm(hfac)₃(bipy)₂] could be obtained, the presence of a small amount of water resulted in the formation of [Sm(hfac)₃(bipy)(H₂O)]·(bipy), in which one coordinating and one non-

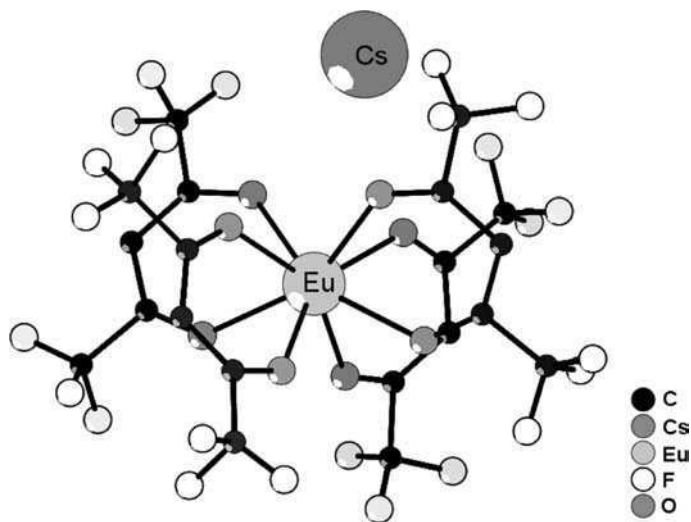


Fig. 11. Molecular structure of Cs[Eu(hfac)₄]. The atomic coordinates are taken from Burns and Danford (1969). No hydrogen atoms are shown.

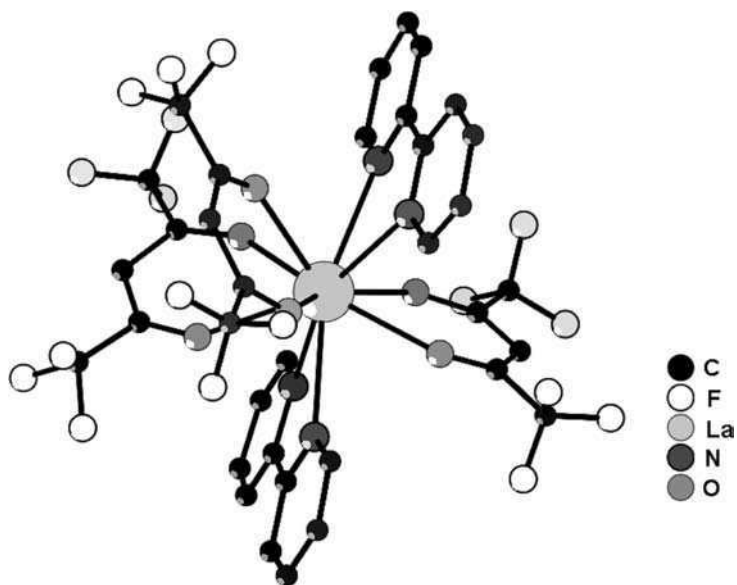


Fig. 12. Molecular structure of [La(hfac)₃(bipy)₂]. The atomic coordinates are taken from Van Staveren et al. (2001). No hydrogen atoms are shown.

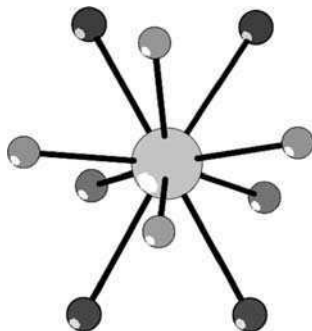


Fig. 13. Coordination polyhedron of the 10-coordinate La^{3+} ion in $[\text{La}(\text{hfac})_3(\text{bipy})_2]$. The atomic coordinates are taken from Van Staveren et al. (2001).

coordinating 2,2'-bipyridine molecule is present, in combination with a coordinating water molecule. The coordination number of the samarium(III) ion in this complex is nine.

The tendency of the trivalent rare-earth ions to adopt a high coordination number (typically 8 or 9) results in the formation of dimeric or polymeric species. Here β -diketonate ligands can act as bridging ligands between two or more metal centers. The tendency to form dimers is stronger for the lighter lanthanides than for the heavier lanthanides, due to the larger ionic radius of the lighter lanthanides. For instance, while the $[\text{R}(\text{thd})_3]$ complexes for $\text{R} = \text{La} - \text{Gd}$ crystallize as monoclinic dimers in the space group $\text{P}2_1/c$ (Erasmus and Boeyens, 1970; Baxter et al., 1995; Martynenko et al., 1998) (fig. 14), the heavier lanthanides form orthorhombic monomers with space group $\text{P}mn2_1$ (de Villiers and Boeyens, 1972; Onuma et al., 1976; Martynenko et al., 1998). An almost ideal trigonal prismatic structure has been observed for $[\text{Er}(\text{thd})_3]$ (de Villiers and Boeyens, 1972). Depending on the temperature, the terbium(III) complexes can occur in either monomeric or dimeric form. $[\text{Tb}_2(\text{thd})_6]$ undergoes an irreversible transition at 147°C from a monoclinic dimer to an orthorhombic monomer (Amano et al., 1980). The same behavior is found for the $[\text{Tb}_2(\text{tod})_6]$ complex, but at a lower temperature, namely 79°C (Andersen et al., 2002). $[\text{Y}_2(\text{tod})_6]$ is isostructural with $[\text{Tb}_2(\text{tod})_6]$ (Luten et al., 1996). In $[\{\text{Er}(\text{thd})_3\}_2(\text{tetraglyme})]$, two discrete $[\text{Er}(\text{thd})_3]$ moieties are linked by a bridging tetraglyme molecule (Darr et al., 1996) (fig. 15). The bridging occurs through the end pairs of oxygens of the polyether chain. The same structural motif is found in the crystal structures of $[\{\text{Y}(\text{thd})_3\}_2(\text{triglyme})]$ (Drake et al., 1993a), $[\{\text{Eu}(\text{thd})_3\}_2(\text{triglyme})]$ (Drake et al., 1993b), $[\{\text{Tb}(\text{thd})_3\}_2(\text{triglyme})]$ (Drake et al., 1993b) and $[\{\text{Gd}(\text{thd})_3\}_2(\text{heptaglyme})]$ (Baxter et al., 1995). In contrast, in $[\{\text{Gd}(\text{thd})_3\}_2(\text{tetraglyme})]$, the two $[\text{Gd}(\text{thd})_3]$ moieties are linked in an asymmetric manner, so that one of the oxygen atoms at the end of the polyether chain remains uncoordinated (Baxter et al., 1995). Poncelet and Hubert-Pfalzgraf (1989) reported the crystal structure of the cluster compound $[\text{Nd}_4(\text{acac})_{10}(\text{OH})_2]$, and Barash et al. (1993) that of $[\text{Y}_4(\text{acac})_{10}(\text{OH})_2]$. Xu and Raymond (2000) described an octameric lanthanum(III) cluster with pyrazolonate ligands. In the presence of $[\text{La}(\text{acac})_3]$, the rigid bis-tridentate pyrazolonate ligands self-assembled to a three dimensional ring structure with idealized D_{4d} symmetry. The lanthanum(III) ions are nine-coordinate and both distorted monocapped square antiprisms and

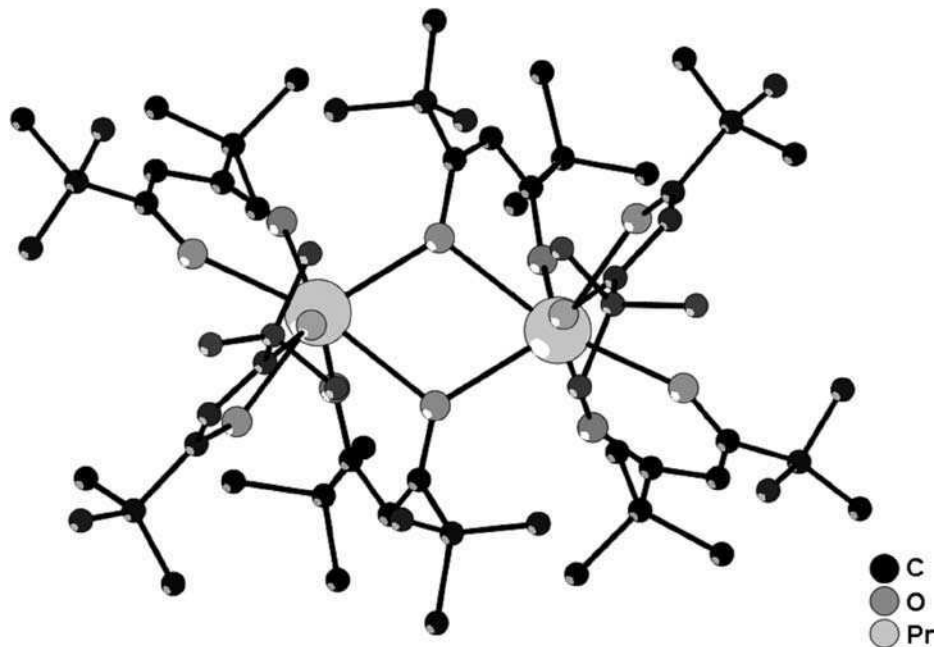


Fig. 14. Molecular structure of $[\text{Pr}_2(\text{thd})_6]$. The atomic coordinates are taken from [Erasmus and Boeyens \(1970\)](#). No hydrogen atoms are shown.

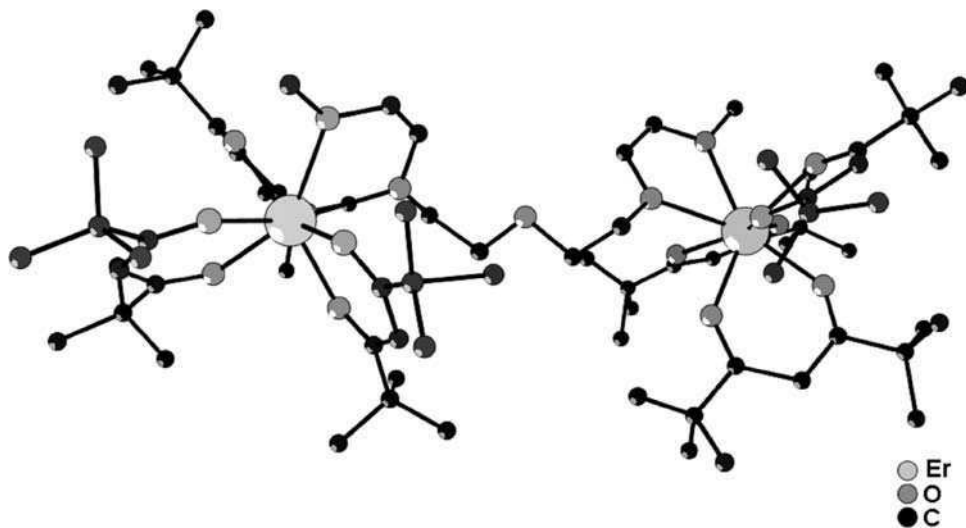


Fig. 15. Molecular structure of $[\text{Er}_2(\text{thd})_6(\text{tetraglyme})]$. The atomic coordinates are taken from [Darr et al. \(1996\)](#). No hydrogen atoms are shown.

distorted tricapped trigonal prisms can be recognized in the ring structure. Upon addition of triethylamine to a solution of hydrated rare-earth chlorides and benzoylacetone in methanol, nonanuclear rare-earth oxo-hydroxo clusters were formed (Xu et al., 2002). After crystallization from a methanol/chloroform mixture, the compounds had the composition $[R_9(\mu_4-O)_2(\mu_3-OH)_8(\mu-bzac)_8(bzac)_8]^- [HN(CH_2CH_3)_3]^+ \cdot (CH_3OH)_2(CHCl_3)$, where R = Sm, Eu, Gd, Dy and Er.

The complexes $[Ho(hfac)_3(H_2O)_2]$ and $[Ho(hfac)_3(H_2O)_2](triglyme)$ show polymeric chains by intermolecular hydrogen bonding (Lee et al., 1998). Whereas $[Ho(hfac)_3(H_2O)_2](triglyme)$ has a nearly linear polymeric chain, $[Ho(hfac)_3(H_2O)_2]$ has a zigzag chain. The molecules are linked by the hydrogen atoms of the coordinated water molecules and the oxygen atoms of the hfac ligands of $[Ho(hfac)_3(H_2O)_2]$. In contrast, in $[Ho(hfac)_3(H_2O)_2](triglyme)$, the molecules are linked by the hydrogen atoms of the coordinated water molecules and by the oxygen atoms of the triglyme. In the two complexes, the holmium(III) ion is eight-coordinate and the coordination polyhedron can be described as a distorted square antiprism. The closest Ho...Ho separation is 8.04 Å in $[Ho(hfac)_3(H_2O)_2]$ and 8.73 Å in $[Ho(hfac)_3(H_2O)_2](triglyme)$. Notice that the triglyme ligand in the $[Ho(hfac)_3(H_2O)_2](triglyme)$ is not coordinated to the holmium(III) ion, but it is in the second coordination sphere. The fact that coordinated water molecules can form intermolecular hydrogen bonds with the oxygen atoms of the β -diketonate, does not always result in formation of polymeric chains. For instance, in the seven-coordinate $[Y(thd)_3(H_2O)]$ complex, centrosymmetric dimeric associations are present due to hydrogen bonding (Gleizes et al., 1993). $[Y(hfac)_3(H_2O)_2][Cu(acac)_2]$ is composed of two metal components, $[Y(hfac)_3(H_2O)_2]$ and $[Cu(acac)_2]$ (Jung et al., 1998). The two components are connected through intermolecular hydrogen bonds and form infinite ribbons. The hydrogen bonds are formed between the water molecules coordinated to the yttrium(III) ion and the oxygen atoms of the acac ligand in $[Cu(acac)_2]$. The crystal structure of $[Y(hfac)_3(NITet)_2]$, where NITet is 2-ethyl-4,4,5,5-tetramethyl-4,5-dihydro-1*H*-imidazolyl-1-oxyl-3-oxide, consists of linear chains of $[Y(hfac)_3]$ units bridged by the nitronyl nitroxide radicals (Benelli et al., 1989b).

Cerium(IV) forms tetrakis complexes with β -diketonates. Two monoclinic polymorphs are known for $[Ce(acac)_4]$: α - $[Ce(acac)_4]$ and β - $[Ce(acac)_4]$. The α -form has been isolated after reaction between cerium(IV) hydroxide and an excess of acetylacetone (Matković and Grdenić, 1963; Titze, 1974). Addition of benzene to the same reaction mixture resulted in formation of the β -form (Titze, 1969) (fig. 16). The formation of the α - or β -form is solvent dependent. Behrsing et al. (2003) obtained α - $[Ce(acac)_4]$ by aerial oxidation of $[Ce(acac)_3(H_2O)_2]$ in dichloromethane, and β - $[Ce(acac)_4]$ by the same reaction in toluene. In both cases, one has to make sure that besides $[Ce(acac)_3(H_2O)_2]$ an excess of acetylacetone is present in the reaction mixture. Attempts to convert the β -form into the α -form by recrystallization in dichloromethane, resulted in significant reduction of cerium(IV) to cerium(III). The coordination polyhedron of cerium(IV) in α - $[Ce(acac)_4]$ has both been described as a distorted square antiprism (Titze, 1974), a dodecahedron (Allard, 1976) or a bicapped square antiprism (Steffen and Fay, 1978). The coordination polyhedron in β - $[Ce(acac)_4]$ is a square antiprism (Allard, 1976). The main difference between the α - and the β -form is the more pronounced folding of the acetylacetonate ligand in the β -form. Neutralization of a mixture of

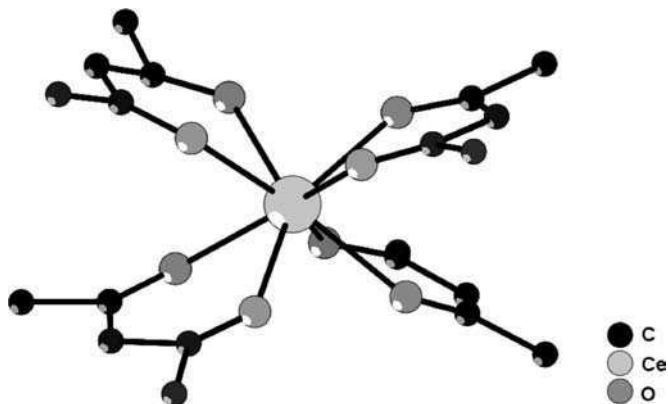


Fig. 16. Molecular structure of β -[Ce(acac)₄]. The atomic coordinates are taken from [Titze \(1969\)](#). No hydrogen atoms are shown.

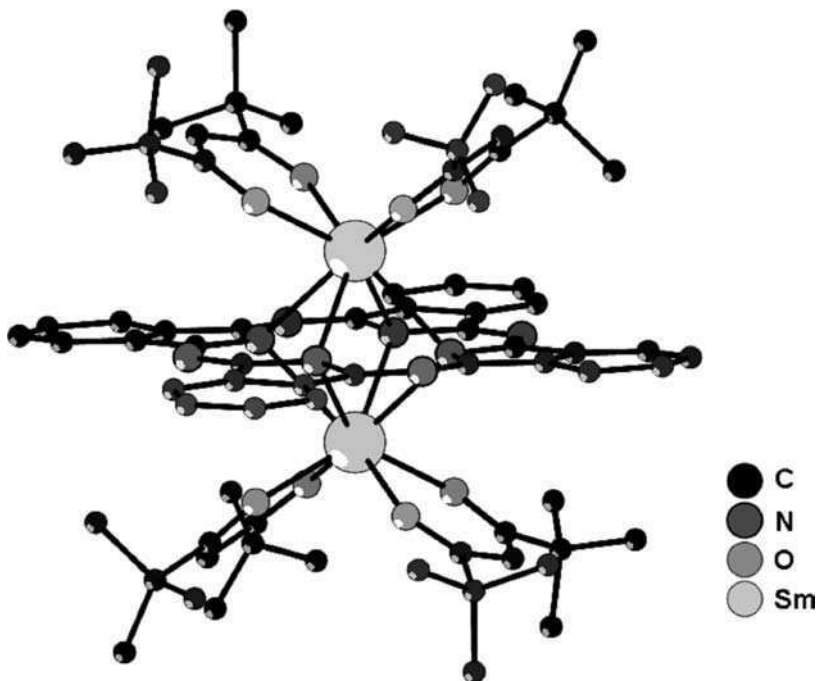


Fig. 17. Molecular structure of [Sm₂(thd)₄(Pc)]. The atomic coordinates are taken from [Sugimoto et al. \(1983\)](#). No hydrogen atoms are shown.

(NH₄)₄[Ce(NO₃)₆] and acetylacetonate with ammonia to pH 5 leads to the isolation of crystals of [Ce(acac)₄] \cdot 10H₂O ([Behrsing et al., 2003](#)). The crystals were unstable upon exposure to light and air. [Ce(acac)₄] \cdot 10H₂O forms a lamellar clathrate structure which crystallizes in the

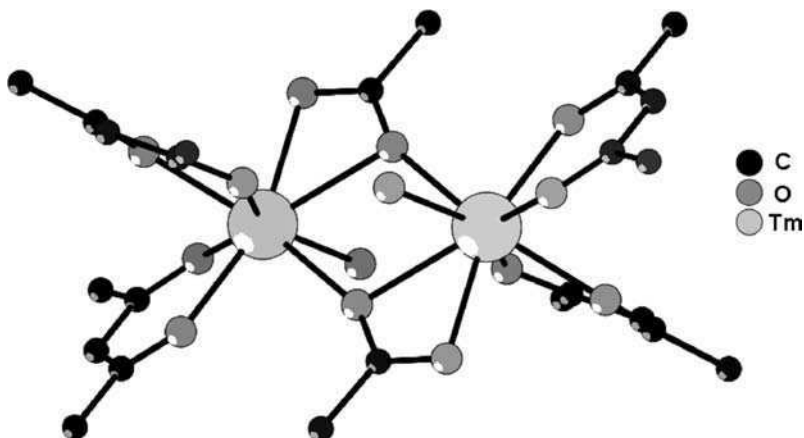


Fig. 18. Molecular structure of $[Tm_2(acac)_4(\mu_2-OAc)_2(H_2O)_2]$. The atomic coordinates are taken from Shen et al. (1983a, 1983b). No hydrogen atoms are shown.

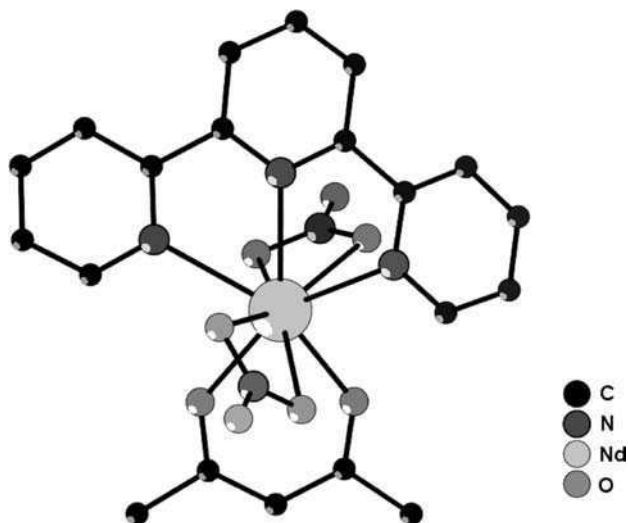


Fig. 19. Molecular structure of $[Nd(acac)(NO_3)_2(terpy)]$. The atomic coordinates are taken from Fukuda et al. (2002). No hydrogen atoms are shown.

monoclinic space group $P2_1/c$. Water molecules form undulating hydrogen-bonded sheets parallel to $[100]$. Sheets of discrete $[Ce(acac)_4]$ molecules are sandwiched between these layers. The cerium(IV) ions are eight-coordinate with a coordination polyhedron that is intermediate between a square antiprism and a dodecahedron.

Sugimoto et al. (1983) determined the crystal structure of the mixed β -diketonate–phthalocyanine complex $[\text{Sm}_2(\text{thd})_4(\text{Pc})]$ (fig. 17). The phthalocyanine ring is bridging the two samarium(III) centers. In some complexes, anions other than the β -diketonates are present. Examples are $[\text{Tm}_2(\text{acac})_4(\mu_2\text{-OAc})_2(\text{H}_2\text{O})_2]$ with bridging acetate groups (Shen et al., 1984) (fig. 18) and $[\text{Nd}(\text{acac})(\text{NO}_3)_2(\text{terpy})]$ (Fukuda et al., 2002) (fig. 19).

5. Physical and chemical properties

In this section, the properties of the rare-earth β -diketonates are discussed, as far as these properties are not described further in the text.

5.1. Aggregation state and melting point

The rare-earth β -diketonates are crystalline solids or viscous liquids. The compounds that are the easiest to obtain as crystalline solids are those of β -diketonates with aromatic substituents. On the other hand, complexes of β -diketonates with highly branched aliphatic groups have a strong tendency to form viscous oils. In general, the β -diketonate complexes are obtained as fine powders. Slow evaporation of a solution containing a complex can yield single crystals of a quality suitable for structure determination by X-ray diffraction. Reports on large crystals of rare-earth β -diketonate complexes are rare. Blanc and Ross (1965) obtained large crystals of $[\text{Eu}(\text{dbm})_4]^- (\text{Hex}_4\text{N})^+$ by slow evaporation of a solution of this complex in 2-butanone. According to these authors, the crystals were well-formed and completely clear. The crystals grew as approximately rectangular parallelepipeds of 1 cm in length and 0.3 cm on a side. X-ray studies showed that these crystals were monoclinic (space group $\text{P}2_1/c$). Kirby and Richardson (1983) obtained single crystals of $[\text{Eu}(\text{dbm})_3(\text{H}_2\text{O})]$ of a size large enough to measure polarized absorption spectra.

The melting point or decomposition points of rare-earth β -diketonate complexes are summarized in tables 4 and 5. For some complexes no melting point can be observed, because these complexes decompose before the melting point is reached. Typical examples of thermally unstable complexes are the acetylacetonate complexes and complexes of perfluorinated β -diketonates. Complexes of β -diketonates with long alkyl chains have lower melting points than complexes of β -diketonates with short alkyl chains. Springer et al. (1967) observed that hydration of anhydrous $[\text{R}(\text{fod})_3]$ complexes lower the melting point of the complexes.

5.2. Color

Most solid rare-earth β -diketonates are white, yellow or brown, and in general their color is determined by the color of the β -diketonate ligands. Only in the case of white β -diketonate ligands, the typical color of the lanthanide ion can be observed, for instance a greenish color for praseodymium(III) compounds and a blue-violet color for neodymium(III) compounds. Some europium(III) β -diketonates show a pink color in daylight, because of the intense photoluminescence of these compounds.

Table 4

Melting or decomposition temperatures of tris complexes of rare-earth β -diketonates and of their adducts with Lewis bases

Compound	Melting or decomposition point (°C)	Reference
[Sc(acac) ₃]	187–187.5	Morgan and Moss, 1914
[Sc(facam) ₃]	142.5–145	Feibush et al., 1972
[Sc(pta) ₃]	56.5–57.0	Shigematsu et al., 1969a
[Sc(thd) ₃]	152–155	Eisentraut and Sievers, 1965
[Sc(trimh) ₃]	88	Utsunomiya, 1972
[Sc(tta) ₃]	149	Purushottam and Raghava Rao, 1966
[Sc(tta) ₃ (bipy)]	179	Kononenko et al., 1965b
[Sc(tta) ₃ (phen)]	213	Kononenko et al., 1965b
[Y(acac) ₃ (phen)]	230–232	Kononenko et al., 1965a
[Y(facam) ₃]	207.5–209.5	Feibush et al., 1972
[Y(fod) ₃]	162–167	Springer et al., 1967
[Y(fod) ₃ (H ₂ O)]	108–112	Springer et al., 1967
[Y(fod) ₃ (bipy)]·2H ₂ O	83	Iftikhar et al., 1982
[Y(fod) ₃ (phen)]	105	Iftikhar et al., 1982
[Y(hfac) ₃ (triglyme)]	60–62	Leedham and Drake, 1996
[Y(hfac) ₃ (tetraglyme)]	74–76	Leedham and Drake, 1996
[Y(pta) ₃]	160.8–161.2	Shigematsu et al., 1969a
[Y(thd) ₃]	155–163	Song et al., 2003a
	173–175	Tasaki et al., 1997
	169–172.5	Eisentraut and Sievers, 1965
[Y(thd) ₃ (bipy)]	185–188	Timmer et al., 1998
[Y(thd) ₃ ((CH ₃) ₃ NO)]	199–202	Timmer et al., 1998
[Y(thd) ₃ (diglyme)]	86–89	Leedham and Drake, 1996
[Y(thd) ₃ (dmf)]	151–153	Timmer et al., 1998
[Y(thd) ₃ (dmsO)]	156–158	Timmer et al., 1998
[Y(thd) ₃ (Et ₃ PO)]	267–270	Timmer et al., 1998
[Y(thd) ₃ (4-Et-pyO)]	93–98	Timmer et al., 1998
[Y(thd) ₃ (hmteta)]	109–112	Leedham and Drake, 1996
[Y(thd) ₃ (phen)]	260–262	Timmer et al., 1998
[Y(thd) ₃ (Ph ₃ PO)]	263–265	Timmer et al., 1998
[Y(thd) ₃ (pyO)]	175–177	Timmer et al., 1998
[Y(thd) ₃ (pyr)]	185	Ansari and Ahmad, 1975
[Y(thd) ₃ (4- <i>tert</i> -But-pyO)]	97–100	Timmer et al., 1998
[Y(thd) ₃ (tmeda)]	145–150	Timmer et al., 1998
[Y(thd) ₃ (triglyme)]	77–81	Leedham and Drake, 1996
[Y(tmod) ₃]	94–96	Tasaki et al., 1997
[Y(trimh) ₃]	180–184	Utsunomiya, 1972
[Y(tta) ₃]	132	Purushottam and Raghava Rao, 1966
[Y(tta) ₃ (phen)]	246–248	Kononenko et al., 1965b
[La(acac) ₃]	274–275	Lim et al., 1996
[La(acac) ₃ (phen)]	219–220	Kononenko et al., 1965a
[La(acac) ₃ (tetraglyme)]	>250 (dec.)	Leedham and Drake, 1996
[La(bzac) ₃ (H ₂ O) ₂]	108–109	Sacconi and Ercoli, 1949

continued on next page

Table 4, *continued*

Compound	Melting or decomposition point (°C)	Reference
[La(dbm) ₃]	99–102	Lim et al., 1996
[La(facam) ₃]	205–207.5	Feibush et al., 1972
[La(fod) ₃]	215–230 (dec.)	Springer et al., 1967
[La(fod) ₃ (H ₂ O)]	215–230	Springer et al., 1967
[La(fod) ₃ (bipy)]·2H ₂ O	101	Iftikhar et al., 1982
[La(fod) ₃ (phen)]	95	Iftikhar et al., 1982
[La(hfac) ₃]	300 (dec.)	Lim et al., 1996
[La(hfac) ₃]·2H ₂ O	143–146	Lim et al., 1996
[La(hfac) ₃ (diglyme)]	74–76	Malandrino et al., 1995
[{La(hfac) ₃ } ₂ (heptaglyme)]	57–60	Leedham and Drake, 1996
[La(hfac) ₃ (triglyme)]	88–90	Malandrino et al., 1995
[La(tfac) ₃]	232–235 (dec.)	Lim et al., 1996
	243–246 (dec., in N ₂ atm.)	Lim et al., 1996
[La(tfac) ₃]·2H ₂ O	142–144	Lim et al., 1996
[La(thd) ₃]	238–248	Eisentraut and Sievers, 1965
	239–245	Berg and Acosta, 1968
	148–149	Belcher et al., 1969b
	229–230	Lim et al., 1996
	238–241 (in N ₂ atm.)	Lim et al., 1996
[La(thd) ₃ (phthalazine)]	132	Ansari and Ahmad, 1976
[La(thd) ₃ (pyr)]	218	Ansari and Ahmad, 1975
[La(thd) ₃ (triglyme)]	80–83	Leedham and Drake, 1996
[La(thd) ₃ (tetraglyme)]	41–44	Leedham and Drake, 1996
[La(tod) ₃]	172–176	Sievers and Wenzel, 1981
[La(tod) ₃]·2H ₂ O	95–97	Wenzel et al., 1985b
[La(tta) ₃]	135	Purushottam et al., 1965
[La(tta) ₃]·2H ₂ O	148–150	Charles and Ohlmann, 1965b
[La(tta) ₃ (phen)]	228–229	Kononenko et al., 1965b
[Ce(fdh) ₄]	123–127	Becht et al., 1993
[Ce(fdh) ₄ (phen)]	185–190	Becht et al., 1993
[Ce(fod) ₄]	149–150	McAleese et al., 1996a
[Ce(thd) ₄]	276	Selbin et al., 1971
	276–278	Hubert-Phalzgraf, 1992
[Ce(tod) ₄]	134–136	Wenzel et al., 1985b
	131.1	Andersen et al., 2002
[Ce(thd) ₃ (dme)]	>250 (dec.)	Leedham and Drake, 1996
[Ce(thd) ₃ (tmeda)]	190–193	Leedham and Drake, 1996
[Ce(thd) ₃ (triglyme)]	90–96 ^a	Leedham and Drake, 1996
[Ce(tmp) ₃]	138	Uhlemann and Dietze, 1971
[Ce(tta) ₃ (H ₂ O) ₂]	105	Uhlemann and Dietze, 1971
[Pr(acac) ₃ (phen)]	221–222	Kononenko et al., 1965a
[Pr(bzac) ₃ (H ₂ O) ₂]	106–108	Sacconi and Ercoli, 1949
[Pr(fod) ₃]	218–225 (dec.)	Springer et al., 1967
[Pr(fod) ₃ (H ₂ O)]	218–225 (dec.)	Springer et al., 1967

continued on next page

Table 4, *continued*

Compound	Melting or decomposition point (°C)	Reference
[Pr(fod) ₃ (bipy)]·2H ₂ O	83	Ifükhar et al., 1982
[Pr(hfac) ₃]	148–151	Berg and Acosta, 1968
[Pr(hfac) ₃ (diglyme) ₂]	85–88	Leedham and Drake, 1996
[Pr(hfac) ₃ (pmdeta)]	>250	Leedham and Drake, 1996
[Pr(facam) ₃]	211.5–213.5	Feibush et al., 1972
[Pr(thd) ₃]	222–224	Eisentraut and Sievers, 1965; Selbin et al., 1971; Berg and Acosta, 1968
[Pr(thd) ₃ (phthalazine)]	133	Ansari and Ahmad, 1976
[Pr(thd) ₃ (pyr)]	217–220	Ansari and Ahmad, 1975
[Pr(thd) ₃ (tetraglyme)]	83–86	Leedham and Drake, 1996
[Pr(tod) ₃]	219–223	Sievers and Wenzel, 1981
[Pr(trimh) ₃]	166–167	Utsunomiya, 1972
[Pr(tta) ₃]	164	Purushottam et al., 1965
[Nd(acac) ₃] (crystalline)	94	Liss and Bos, 1977
[Nd(acac) ₃ (phen)]	230–232	Kononenko et al., 1965a
[Nd(bzac) ₃ (H ₂ O) ₂]	106–108	Sacconi and Ercoli, 1949
[Nd(fod) ₃]	210–215 (dec.)	Springer et al., 1967
[Nd(fod) ₃ (H ₂ O)]	210–215 (dec.)	Springer et al., 1967
[Nd(fod) ₃ (bipy)]·2H ₂ O	80	Ifükhar et al., 1982
[Nd(hfac) ₃]·H ₂ O	115–121	Morris et al., 1963
[Nd(pmtfp) ₃ (dmsO) ₂]	152	Huang et al., 1988
[Nd(hfac) ₃ (diglyme)]	105	Evans et al., 2002
[Nd(pta) ₃]	126.5–128.0	Shigematsu et al., 1969a
[Nd(thd) ₃]	215–218	Eisentraut and Sievers, 1965
	191–192	Utsunomiya and Shigematsu, 1972
	218–220	Tasaki et al., 1997
	218–219	Berg and Acosta, 1968
	220	Fujinaga et al., 1981
[Nd(thd) ₃ (diglyme) ₂]	111–113	Leedham and Drake, 1996
[Nd(thd) ₃ (phthalazine)]	125–128	Ansari and Ahmad, 1976
[Nd(thd) ₃ (pyr)]	220	Ansari and Ahmad, 1975
[{Nd(thd) ₃ } ₂ (triglyme)]	74–77	Leedham and Drake, 1996
[Nd(tmod) ₃]	134–136	Tasaki et al., 1997
[Nd(tod) ₃]	228–230	Sievers and Wenzel, 1981
[Nd(trimh) ₃]	188–190	Utsunomiya, 1972
[Nd(tta) ₃]	181–182	Purushottam et al., 1965
[Nd(tta) ₃]·2H ₂ O	158	Charles and Ohlmann, 1965b
[Nd(tta) ₃ (phen)]	236–237	Kononenko et al., 1965b
[Sm(acac) ₃ (bipy)]	188–190	Kononenko et al., 1965a
[Sm(acac) ₃ (phen)]	223–225	Kononenko et al., 1965a
[{Sm(acac) ₃ } ₂ (heptaglyme)]	>250	Leedham and Drake, 1996
[Sm(bzac) ₃ (H ₂ O) ₂]	103–105	Sacconi and Ercoli, 1949
[Sm(hfac) ₃ (diglyme)]	116	Evans et al., 2002

continued on next page

Table 4, *continued*

Compound	Melting or decomposition point (°C)	Reference
[{Sm(hfac) ₃ } ₂ (tetraglyme)]	90–92	Leedham and Drake, 1996
[Sm(facam) ₃]	207.5–208.5	Feibush et al., 1972
[Sm(fod) ₃]	208–218 (dec.)	Springer et al., 1967
[Sm(fod) ₃ (H ₂ O)]	63–67	Springer et al., 1967
[Sm(fod) ₃ (bipy)]·2H ₂ O	76	Iftikhar et al., 1982
[Sm(pta) ₃]	113.1–118.0	Shigematsu et al., 1969a
[Sm(thd) ₃]	200–201	Selbin et al., 1971; Berg and Acosta, 1968
	195.5–198.5	Eisentraut and Sievers, 1965
	143–144	Hammond et al., 1963
[Sm(thd) ₃ (dme)]	96–98	Leedham and Drake, 1996
[Sm(thd) ₃ (dmf)]	146.5–147.5	Schimitschek et al., 1967
[Sm(thd) ₃ (phthalazine)]	125	Ansari and Ahmad, 1976
[Sm(thd) ₃ (py)]	133–135	Selbin et al., 1971
[Sm(thd) ₃ (pyr)]	217	Ansari and Ahmad, 1975
[Sm(trimh) ₃]	176–177	Utsunomiya, 1972
[Sm(tta) ₃]	148	Purushottam et al., 1965
[Sm(tta) ₃ (phen)]	241–243	Kononenko et al., 1965b
[Sm(tta) ₃ (tppo) ₂ (NO ₃)]	226	Fu et al., 2003
[Eu(acac) ₃] (amorphous)	160–170 (dec.)	Liss and Bos, 1977
[Eu(acac) ₃] (crystalline)	94	Liss and Bos, 1977
[Eu(acac) ₃ (bipy)]	200–202	Kononenko et al., 1965a
[Eu(acac) ₃ (H ₂ O) ₂]	147–148	Liang et al., 1970
[Eu(acac) ₃ (distyphen)]	255–260	Melby et al., 1964
[Eu(acac) ₃ (phen)]	250–255	Melby et al., 1964
	226–228	Kononenko et al., 1965a
[Eu(bzac) ₃ (phen)]	192–194	Bauer et al., 1964
	191–195	Anonymous, 2004
[Eu(btfac) ₃ (H ₂ O) ₂]	107–110	Charles and Riedel, 1966
	148–150	Liang et al., 1970
	93.6	Van Meervelt et al., 1996
[Eu(btfac) ₃ (bipy)]	193–194	Batista et al., 1998
[Eu(btfac) ₃ (phen)]	186–188 (dec.)	Anonymous, 2004
[Eu(btfac) ₃ (tppo) ₂]	136	Van Meervelt et al., 1996
[Eu(bzac) ₃ (H ₂ O) ₂]	100–104	Charles, 1967
[Eu(bzac) ₃ (bipy)]	173–174	Batista et al., 1998
[Eu(bzac) ₃ (phen)]	186–188	Butter and Kreher, 1965
[Eu(dbm) ₃ (phen)]	272–274	Anonymous, 2004
[Eu(dbm) ₃ (aniline)]	206–209	Charles and Ohlmann, 1965a
[Eu(dbm) ₃ (<i>n</i> -butylamine) ₂]	145–147	Charles and Ohlmann, 1965a
[Eu(dbm) ₃ (bipy)]	210–213	Melby et al., 1964
[Eu(dbm) ₃ (1,4-dioxane) ₂]	170–175	Charles and Ohlmann, 1965a
[Eu(dbm) ₃ (bath)]	191–192	Anonymous, 2004
[Eu(dbm) ₃ (dmf)]	133–138	Charles and Ohlmann, 1965a
[Eu(dbm) ₃ (dmsO) ₃]	112–115	Charles and Ohlmann, 1965a
[Eu(dbm) ₃ (4,7-dimethylphenanthroline)]	239–241	Anonymous, 2004

continued on next page

Table 4, *continued*

Compound	Melting or decomposition point (°C)	Reference
[Eu(dbm) ₃ (opb)]	119	Wang et al., 2002
[Eu(dbm) ₃ (phen)]	184–187	Bauer et al., 1964
	185–187	Melby et al., 1964
	172–173	Anonymous, 2004
[Eu(dbm) ₃ (piperidine) ₂]	183–185	Charles and Ohlmann, 1965a
[Eu(dbm) ₃ (py) ₂]	103–106	Charles and Ohlmann, 1965a
[Eu(dbm) ₃ (pyO)]	189–190	Charles and Ohlmann, 1965a
[Eu(dbm) ₃ (quinoline) ₂]	109–111	Charles and Ohlmann, 1965a
[Eu(dmh) ₃ (bipy)]	147–149	Moser et al., 2000
[Eu(dbm) ₃ (phen)]	181–183	Moser et al., 2000
[Eu(dnm) ₃ (phen)]	215–216	Anonymous, 2004, 2004
[Eu(fod) ₃]	205–212 (dec.)	Springer et al., 1967
[Eu(fod) ₃ (H ₂ O)]	59–67	Springer et al., 1967
[Eu(fod) ₃ (bipy)]	68–73	Mattson et al., 1985
[Eu(fod) ₃ (bipy)·2H ₂ O]	78	Iftikhar et al., 1982
[Eu(fod) ₃ (dmsO)]	165–168	Mattson et al., 1985
[Eu(fod) ₃ (phen)]	97–99.5	Mattson et al., 1985
[Eu(fod) ₃ (py) ₂]	70.5–72	Mattson et al., 1985
[Eu(fod) ₃ (4-picO)]	193.5–194.5	Mattson et al., 1985
[Eu(fod) ₃ (tppo) ₂]	220.5–223	Mattson et al., 1985
[Eu(hfac) ₃]	176–177	Berg and Acosta, 1968
	196	Halverson et al., 1964a, 1964b
[Eu(hfac) ₃ ·2H ₂ O]	181–182	Bhaumik, 1965a, 1965b
	110	Hellmuth and Mirzai, 1985
[Eu(hfac) ₃ (dhsO) ₂]	0	Halverson et al., 1964a, 1964b
[Eu(hfac) ₃ (diglyme)]	75–78	Kang et al., 1997a
	123–126 ^b	Malandrino et al., 2001
	114	Evans et al., 2002
[Eu(hfac) ₃ (dme)]	81.2	Malandrino et al., 2001
[Eu(hfac) ₃ (phen)]	257 (dec.)	Anonymous, 2004
[Eu(hfac) ₃ (terpy)]	235–240	Kang et al., 1997a
[Eu(hfac) ₃ (topo) ₂]	–10	Halverson et al., 1964a, 1964b
[Eu(mhd) ₃ (phen)]	186–189	Thompson and Berry, 2001
[Eu(pta) ₃]	113.8–114.0	Shigematsu et al., 1969a
[Eu(tpb) ₃ (phen)]	197–199	Bauer et al., 1964
[Eu(tfac) ₃ (dhsO) ₂]	15	Halverson et al., 1964a, 1964b
[Eu(tfac) ₃ (tbp) ₂]	10	Halverson et al., 1964a, 1964b
[Eu(tfac) ₃ (topo) ₂]	0	Halverson et al., 1964a, 1964b
[Eu(thd) ₃]	190–191	Selbin et al., 1971; Berg and Acosta, 1968
	187–189	Eisentraut and Sievers, 1965
	157	Halverson et al., 1964a, 1964b
[Eu(thd) ₃ (dme)]	176–178	Leedham and Drake, 1996
[Eu(thd) ₃ (phen)]	230–231	Malta et al., 1996
[Eu(thd) ₃ (py)]	135–138	Selbin et al., 1971
[Eu(thd) ₃ (pyr)]	211–214	Ansari and Ahmad, 1975
[{Eu(thd) ₃ } ₂ (tetraglyme)]	98–100	Leedham and Drake, 1996

continued on next page

Table 4, *continued*

Compound	Melting or decomposition point (°C)	Reference
[{Eu(thd) ₃ } ₂ (triglyme)]	111–114	Leedham and Drake, 1996
[Eu(thd) ₃ (topo) ₂]	5	Halverson et al., 1964a, 1964b
[Eu(trimh) ₃]	182–183	Utsunomiya, 1972
[Eu(tta) ₃]	180	Purushottam et al., 1965
	118–120	Ainitdinov et al., 1965
[Eu(tta) ₃ (bipy)]	221–223	Bauer et al., 1964
	221	Melent'eva et al., 1966
[Eu(tta) ₃ (opb)]	95–98	Wang et al., 2003
[Eu(tta) ₃ (4-picO) ₂]	234–236	Melby et al., 1964
[Eu(tta) ₃ (phen)]	242–244	Bauer et al., 1964
	247–249	Melby et al., 1964
	238–240	Kononenko et al., 1965b
	236–238	Melent'eva et al., 1966
[Eu(tta) ₃ (terpy)]	247–251	Melby et al., 1964
[Eu(tta) ₃ (tpo) ₂]	251–253	Melby et al., 1964
	169	Fu et al., 2003
[Gd(acac) ₃ (dme)]	126–135 ^c	Leedham and Drake, 1996
[Gd(acac) ₃ (phen)]	238–240	Kononenko et al., 1965a
[Gd(bzac) ₃ (H ₂ O) ₂]	100–101	Sacconi and Ercoli, 1949
[Gd(fod) ₃]	203–213 (dec.)	Springer et al., 1967
[Gd(fod) ₃ (H ₂ O)]	60–65	Springer et al., 1967
[Gd(fod) ₃ (bipy)]·2H ₂ O	84	Iftikhar et al., 1982
[Gd(pta) ₃]	162.1–164.0	Shigematsu et al., 1969a
[Gd(thd) ₃]	182–184	Eisentraut and Sievers, 1965
	183–184	Berg and Acosta, 1968
	176–177	Mitchell and Banks, 1971
	164–173	Song et al., 2003a
	174–175	Utsunomiya and Shigematsu, 1972
[Gd(thd) ₃ (diglyme) ₂]	77–79	Leedham and Drake, 1996
[{Gd(thd) ₃ } ₂ (triglyme)]	87–89	Leedham and Drake, 1996
[{Gd(thd) ₃ } ₂ (tetraglyme)]	88–91	Leedham and Drake, 1996
[{Gd(thd) ₃ } ₂ (heptaglyme)]	82–84	Leedham and Drake, 1996
[Gd(thd) ₃ (phthalazine)]	115–118	Ansari and Ahmad, 1976
[Gd(thd) ₃ (py)]	134–135	Selbin et al., 1971
[Gd(thd) ₃ (pyr)]	207–211	Ansari and Ahmad, 1975
[{Gd(thd) ₃ } ₂ (hmteta)]	91–93	Leedham and Drake, 1996
[Gd(trimh) ₃]	192–193	Utsunomiya, 1972
[Gd(tta) ₃]	122	Purushottam et al., 1965
[Gd(tta) ₃]·2H ₂ O	170 (dec.)	Charles and Ohlmann, 1965b
[Tb(acac) ₃ (bipy)]	208–210	Kononenko et al., 1965a
[Tb(acac) ₃ (phen)]	250–255	Melby et al., 1964
	225–227	Kononenko et al., 1965a
[Tb(hfac) ₃ (diglyme)]	85	Evans et al., 2002
[Tb(facam) ₃]	185–188	Feibush et al., 1972
[Tb(fod) ₃]	190–196	Springer et al., 1967

continued on next page

Table 4, *continued*

Compound	Melting or decomposition point (°C)	Reference
[Tb(fod) ₃ (H ₂ O)]	92–97	Springer et al., 1967
[Tb(fod) ₃ (bipy)]·2H ₂ O	74	Iftikhar et al., 1982
[Tb(pmip) ₃ (tppo) ₂]	195–196	Gao et al., 1999
[Tb(pta) ₃]	141.0–144.0	Shigematsu et al., 1969a
[Tb(thd) ₃]	177–180	Eisentraut and Sievers, 1965
	150–152	Selbin et al., 1971; Berg and Acosta, 1968
[Tb(thd) ₃ (tmeda)]	98–100	Leedham and Drake, 1996
[Tb(thd) ₃ (phthalazine)]	112–115	Ansari and Ahmad, 1976
[Tb(thd) ₃ (py)]	135–137	Selbin et al., 1971
[Tb(thd) ₃ (pyr)]	200–203	Ansari and Ahmad, 1975
[{Tb(thd) ₃ } ₂ (triglyme)]	86–89	Leedham and Drake, 1996
[{Tb(tfac) ₃ } ₂ (tetraglyme) ₂]	83–85	Leedham and Drake, 1996
[Tb ₂ (tod) ₆]	213.2	Andersen et al., 2002
[Tb(trimh) ₃]	195–198	Utsunomiya, 1972
[Tb(tta) ₃]	115	Purushottam et al., 1965
[Tb(tta) ₃ (phen)]	247–248	Bauer et al., 1964
[Dy(fod) ₃]	180–188	Springer et al., 1967
[Dy(fod) ₃ (H ₂ O)]	103–107	Springer et al., 1967
[Dy(fod) ₃ (bipy)]·2H ₂ O	85	Iftikhar et al., 1982
[Dy(pta) ₃]	150.0–151.4	Shigematsu et al., 1969a
[Dy(thd) ₃]	180–183.5	Eisentraut and Sievers, 1965
	182–183	Berg and Acosta, 1968
[{Dy(thd) ₃ } ₂ (heptaglyme)]	67–70	Leedham and Drake, 1996
[Dy(thd) ₃ (phthalazine)]	120	Ansari and Ahmad, 1976
[Dy(thd) ₃ (py)]	135–137	Selbin et al., 1971
[Dy(thd) ₃ (pyr)]	195–198	Ansari and Ahmad, 1975
[{Dy(thd) ₃ } ₂ (triglyme)]	85–87	Leedham and Drake, 1996
[Dy(trimh) ₃]	190–193	Utsunomiya, 1972
[Dy(tta) ₃]	193	Purushottam et al., 1965
[Dy(tta) ₃ (phen)]	243–244	Kononenko et al., 1965b
[Ho(fod) ₃]	172–178	Springer et al., 1967
[Ho(fod) ₃ (H ₂ O)]	103–111	Springer et al., 1967
[Ho(fod) ₃ (bipy)]·2H ₂ O	88	Iftikhar et al., 1982
[Ho(hfac) ₃ (H ₂ O) ₂]	124–130	Lee et al., 1998
[Ho(hfac) ₃ (H ₂ O) ₂]·triglyme	67–71	Kang et al., 1997b
[{Ho(hfac) ₃ } ₂ (tetraglyme)]	72–74	Leedham and Drake, 1996
[{Ho(tfac) ₃ } ₂ (hmteta)]	88–92	Leedham and Drake, 1996
[Ho(thd) ₃]	180–182.5	Eisentraut and Sievers, 1965
	178–180	Berg and Acosta, 1968
[Ho(thd) ₃ (dmf)]	151.5–154.5	Schimitschek et al., 1967
[Ho(thd) ₃ (phthalazine)]	125	Ansari and Ahmad, 1976
[Ho(thd) ₃ (py)]	134–135	Selbin et al., 1971
[Ho(thd) ₃ (pyr)]	183–187	Ansari and Ahmad, 1975
[{Ho(thd) ₃ } ₂ (triglyme)]	76–78	Leedham and Drake, 1996

continued on next page

Table 4, *continued*

Compound	Melting or decomposition point (°C)	Reference
[Ho(trimh) ₃]	190–192	Utsunomiya, 1972
[Ho(tta) ₃]	135	Purushottam et al., 1965
[Er(acac) ₃ (phen)]	228–230	Kononenko et al., 1965a
[Er(fod) ₃]	158–164	Springer et al., 1967
[Er(fod) ₃ (H ₂ O)]	104–112	Springer et al., 1967
[Er(fod) ₃ (bipy)]·2H ₂ O	95	Iftikhar et al., 1982
[Er(pta) ₃]	158.0–161.2	Shigematsu et al., 1969a
[Er(thd) ₃]	179–181	Eisentraut and Sievers, 1965; Berg and Acosta, 1968
	171–172	Utsunomiya and Shigematsu, 1972
[Er(thd) ₃ (H ₂ O)] _n	184	Darr et al., 1996
[Er(thd) ₃ (dme)]	94–96	Leedham and Drake, 1996
[Er(thd) ₃ (dmf)]	153–154	Schimitschek et al., 1967
[Er(thd) ₃ (diglyme) ₂]	72–74	Leedham and Drake, 1996
[{Er(thd) ₃ } ₂ (triglyme)]	80–82	Leedham and Drake, 1996
[{Er(thd) ₃ } ₂ (tetraglyme)]	77	Darr et al., 1996
[Er(thd) ₃ (phthalazine)]	116–120	Ansari and Ahmad, 1976
[Er(thd) ₃ (py)]	131–133	Selbin et al., 1971
[Er(thd) ₃ (pyr)]	168–171	Ansari and Ahmad, 1975
[Er(trimh) ₃]	142–144	Utsunomiya, 1972
[Er(tta) ₃]	125	Purushottam et al., 1965
[{Tm(acac) ₃ } ₂ (heptaglyme)]	83–85	Leedham and Drake, 1996
[Tm(fod) ₃]	140–146	Springer et al., 1967
[Tm(fod) ₃ (H ₂ O)]	110–115	Springer et al., 1967
[Tm(fod) ₃ (bipy)]·2H ₂ O	86	Iftikhar et al., 1982
[Tm(thd) ₃]	171.5–173.5	Eisentraut and Sievers, 1965
	170–173	Selbin et al., 1971; Berg and Acosta, 1968
[Tm(thd) ₃ (phthalazine)]	110–115	Ansari and Ahmad, 1976
[{Tm(thd) ₃ } ₂ (tetraglyme)]	71–73	Leedham and Drake, 1996
[{Tm(thd) ₃ } ₂ (triglyme)]	65–68	Leedham and Drake, 1996
[Tm(thd) ₃ (py)]	134–136	Selbin et al., 1971
[Tm(thd) ₃ (pyr)]	168–171	Ansari and Ahmad, 1975
[Tm(tta) ₃]	115	Purushottam et al., 1965
[Yb(fod) ₃]	125–132	Springer et al., 1967
[Yb(fod) ₃ (H ₂ O)]	112–115	Springer et al., 1967
[Yb(fod) ₃ (bipy)]·2H ₂ O	93	Iftikhar et al., 1982
[Yb(pta) ₃]	160.2–161.0	Shigematsu et al., 1969a
[Yb(thd) ₃]	166–169	Eisentraut and Sievers, 1965
	165–167	Selbin et al., 1971; Berg and Acosta, 1968
[Yb(thd) ₃ (diglyme)]	72–74	Leedham and Drake, 1996
[Yb(thd) ₃ (phthalazine)]	120–124	Ansari and Ahmad, 1976
[Yb(thd) ₃ (py)]	130–132	Selbin et al., 1971
[Yb(thd) ₃ (pyr)]	165	Ansari and Ahmad, 1975
[Yb(thd) ₃ (triglyme)]	68–70	Leedham and Drake, 1996

continued on next page

Table 4, *continued*

Compound	Melting or decomposition point (°C)	Reference
[Yb(trimh) ₃]	178–179	Utsunomiya, 1972
[Yb(tta) ₃]	145	Purushottam et al., 1965
[Y(fod) ₃ (bipy)]·2H ₂ O	90	Iftikhar et al., 1982
[Lu(fod) ₃]	118–125	Springer et al., 1967
[Lu(fod) ₃ (H ₂ O)]	111–115	Springer et al., 1967
[Lu(fod) ₃ (phen)]	115	Iftikhar et al., 1982
[Lu(pta) ₃]	160.0–163.2	Shigematsu et al., 1969a
[Lu(thd) ₃]	172–174	Eisentraut and Sievers, 1965
[Lu(thd) ₃ (py)]	125–127	Selbin et al., 1971
[Lu(trimh) ₃]	162–165	Utsunomiya, 1972
[Lu(tta) ₃]·2H ₂ O	170 (dec.)	Charles and Ohlmann, 1965b

^aPossibly dissolving in liberated triglyme.

^b[Eu(hfac)₃(diglyme)] undergoes a transition from the solid phase to a plastic phase at 71.4 °C. Complete melting occurs at 123–126 °C.

^cShows evidence of dissolving in dme.

5.3. Hydration states

The rare-earth β -diketonates are in general not hygroscopic, with the exception of the tris complexes. The tris complexes can form adducts with one, two or even three water molecules, resulting in seven-, eight- or nine-coordinate complexes. The most common of these hydrated complexes are the dihydrates. It is not possible to obtain anhydrous tris complexes by synthesis in an aqueous solution, except when afterwards a drying step in a (vacuum) oven is included. The problems encountered when one tries to dehydrate these complexes have been discussed in section 3. After dehydration, the anhydrous complexes start to take up water from the atmosphere and become hydrated again. The tendency to form hydrates is stronger when the complexes have fluorinated ligands, e.g. [R(fod)₃], because of the higher Lewis acidity of these ligands. Springer et al. (1967) noticed that anhydrous [Er(fod)₃] is transformed in contact with in air in a few seconds into the monohydrate complex. Complexes with very bulky ligands form a hydrophobic shell around the rare-earth ion, and this shell prevents that water molecules bind to the rare-earth ion. When crystalline forms of anhydrous [Nd(acac)₃] or [Eu(acac)₃] was exposed to the atmosphere, a loss of weight was observed (Liss and Boss, 1977). This weight loss was ascribed to a hydrolysis reaction:



The hydrolysis products melted around 130 °C, in contrast to the crystalline forms that melted at 94 °C. The hydrolysis products showed an IR peak in the OH stretch region. On the other hand when the amorphous forms of [Nd(acac)₃] and [Eu(acac)₃] were exposed to the atmosphere, a gain in weight was observed. The weight change corresponded to the formation of the monohydrate.

Table 5

Melting or decomposition temperatures of tetrakis β -diketonate complexes of rare earths, $Q^+[R(\beta\text{-diketonato})_4]^-$

Tetrakis unit	Counter ion Q^+	Melting or decomposition point ($^{\circ}C$)	Reference
[La(dbp) ₄] ⁻	triethylammonium	130	Melby et al., 1964
[La(hfac) ₄] ⁻	triethylammonium	130	Melby et al., 1964
[La(hfac) ₄] ⁻	2,6-lutidinium	130	Melby et al., 1964
[La(tta) ₄] ⁻	triethylammonium	135	Melby et al., 1964
[Pr(hfac) ₄] ⁻	triethylammonium	130	Melby et al., 1964
[Nd(dbp) ₄] ⁻	triethylammonium	130	Melby et al., 1964
[Nd(hfac) ₄] ⁻	triethylammonium	130	Melby et al., 1964
[Nd(hfac) ₄] ⁻	2,6-lutidinium	130	Melby et al., 1964
[Nd(hfac) ₄] ⁻	pyridinium	185	Melby et al., 1964
[Nd(tta) ₄] ⁻	triethylammonium	135	Melby et al., 1964
[Sm(hfac) ₄] ⁻	triethylammonium	130	Melby et al., 1964
[Eu(acac) ₄] ⁻	Na ⁺	345	Melby et al., 1964
[Eu(acac) ₄] ⁻	K ⁺	225	Melby et al., 1964
[Eu(btfac) ₄] ⁻	piperidinium	132	Melby et al., 1964
[Eu(btfac) ₄] ⁻	benzylammonium	68–70	Charles and Riedel, 1966
[Eu(btfac) ₄] ⁻	dibenzylammonium	152–153	Charles and Riedel, 1966
[Eu(btfac) ₄] ⁻	diethylammonium	135–136	Charles and Riedel, 1966
[Eu(btfac) ₄] ⁻	tetramethylammonium	217–218	Charles and Riedel, 1966
[Eu(btfac) ₄] ⁻	tetraethylammonium	152–153	Charles and Riedel, 1966
[Eu(btfac) ₄] ⁻	tetra- <i>n</i> -propylammonium	167–168	Charles and Riedel, 1966
[Eu(btfac) ₄] ⁻	tetra- <i>n</i> -butylammonium	136–137	Charles and Riedel, 1966
[Eu(btfac) ₄] ⁻	triethylammonium	87–88	Charles and Riedel, 1966
[Eu(btfac) ₄] ⁻	<i>n</i> -butylammonium	78–80	Charles and Riedel, 1966
[Eu(btfac) ₄] ⁻	2-hydroxyethylammonium	171–172	Charles and Riedel, 1966
[Eu(btfac) ₄] ⁻	piperidinium	170–172	Charles and Riedel, 1966
[Eu(btfac) ₄] ⁻	pyridinium	180–185	Charles and Riedel, 1966
[Eu(btfac) ₄] ⁻	quinolinium	155–157	Charles and Riedel, 1966
[Eu(btfac) ₄] ⁻	isoquinolinium	153–155	Charles and Riedel, 1966
[Eu(btfac) ₄] ⁻	tetramethylguanidium	154–155	Charles and Riedel, 1966
[Eu(bzac) ₄] ⁻	Na ⁺	220	Melby et al., 1964
[Eu(bzac) ₄] ⁻	piperidinium	141–142	Liang et al., 1970
[Eu(bzac) ₄] ⁻	tetrapropylammonium	158–166	Bauer et al., 1964
[Eu(dbm) ₄] ⁻	Na ⁺	167	Melby et al., 1964
[Eu(dbm) ₄] ⁻	K ⁺	300	Melby et al., 1964
[Eu(dbm) ₄] ⁻	Rb ⁺	286	Melby et al., 1964
[Eu(dbm) ₄] ⁻	Cs ⁺	280	Melby et al., 1964
[Eu(dbm) ₄] ⁻	hexadecyltrimethylammonium	163–164	Zhou et al., 1996
[Eu(dbm) ₄] ⁻	octadecyltriethylammonium	152–153	Zhou et al., 1996
[Eu(dbm) ₄] ⁻	tetramethylammonium	259	Melby et al., 1964
[Eu(dbm) ₄] ⁻	tetraethylammonium	230	Melby et al., 1964
[Eu(dbm) ₄] ⁻	triethylammonium	175	Melby et al., 1964
[Eu(dbm) ₄] ⁻	tetrapropylammonium	203–207	Bauer et al., 1964
[Eu(dbm) ₄] ⁻	diethylammonium	195–200	Bauer et al., 1964

continued on next page

Table 5, *continued*

Tetrakis unit	Counter ion Q ⁺	Melting or decomposition point (°C)	Reference
[Eu(dbm) ₄] ⁻	tetrahexylammonium	220–226	Bauer et al., 1964
[Eu(dbm) ₄] ⁻	azabicyclononane ion	164–168	Bauer et al., 1964
[Eu(dbm) ₄] ⁻	<i>N</i> -hexadecylpyridinium	193–197	Bauer et al., 1964
[Eu(dbm) ₄] ⁻	piperidinium	184–187 (α -form) 182–184 (β -form) 190	Bauer et al., 1964 Bauer et al., 1964 Melby et al., 1964
		188–193	Liang et al., 1970
[Eu(dtp) ₄] ⁻	piperidinium	180–186	Bauer et al., 1964
[Eu(dbp) ₄] ⁻	tetraethylammonium	152	Melby et al., 1964
[Eu(dbp) ₄] ⁻	triethylammonium	108	Melby et al., 1964
[Eu(hfac) ₄] ⁻	tetramethylammonium	190	Melby et al., 1964
[Eu(hfac) ₄] ⁻	triethylammonium	130	Melby et al., 1964
[Eu(hfac) ₄] ⁻	tetraethylammonium	153	Melby et al., 1964
[Eu(hfac) ₄] ⁻	2,4,6-collidinium	130	Melby et al., 1964
[Eu(hfac) ₄] ⁻	2,6-lutidinium	130	Melby et al., 1964
[Eu(hfac) ₄] ⁻	<i>N</i> -methylphenazinium	120	Melby et al., 1964
[Eu(hfac) ₄] ⁻	<i>N</i> -methylquinolinium	100	Melby et al., 1964
[Eu(hfac) ₄] ⁻	piperazinium	210	Melby et al., 1964
[Eu(hfac) ₄] ⁻	pyridinium	175	Melby et al., 1964
[Eu(nta) ₄] ⁻	<i>N</i> -hexadecylpyridinium	132–133	Zhou et al., 1995
[Eu(tbp) ₄] ⁻	isoquinolinium	150–151	Bauer et al., 1964
[Eu(tbp) ₄] ⁻	2,4,6-trimethylpyridinium	168–170	Bauer et al., 1964
[Eu(tfa) ₄] ⁻	isoquinolinium	111–114	Bauer et al., 1964
[Eu(tmb) ₄] ⁻	isoquinolinium	192–196	Bauer et al., 1964
[Eu(tta) ₄] ⁻	triethylammonium	133	Melby et al., 1964
[Eu(tta) ₄] ⁻	tetrapropylammonium	188–189	Bauer et al., 1964
[Eu(tta) ₄] ⁻	tetrahexylammonium	170–172	Bauer et al., 1964
[Eu(tta) ₄] ⁻	4-aminopyridinium	205–207	Chen et al., 2001
[Eu(tta) ₄] ⁻	2,4,6-collidinium	158	Melby et al., 1964
[Eu(tta) ₄] ⁻	isoquinolinium	170–171	Bauer et al., 1964
[Eu(tta) ₄] ⁻	<i>N</i> -methylisoquinolinium	168–170	Chen et al., 2001
[Eu(tta) ₄] ⁻	1,2-dimethylpyridinium	148–150	Chen et al., 2001
[Eu(tta) ₄] ⁻	2,4,6-trimethylpyridinium	159–160	Bauer et al., 1964
		125–126	Chen et al., 2001
[Eu(ptp) ₄] ⁻	tetrapropylammonium	189–193	Bauer et al., 1964
[Gd(dbm) ₄] ⁻	piperidinium	185–189 (α -form) 183–185 (β -form)	Bauer et al., 1964 Bauer et al., 1964
[Gd(hfac) ₄] ⁻	triethylammonium	130	Melby et al., 1964
[Tb(dbp) ₄] ⁻	triethylammonium	130	Melby et al., 1964
[Tb(dtp) ₄] ⁻	piperidinium	182–188	Bauer et al., 1964
[Tb(hfac) ₄] ⁻	triethylammonium	130	Melby et al., 1964
[Tb(hfac) ₄] ⁻	2,4,6-collidinium	135	Melby et al., 1964
[Tb(hfac) ₄] ⁻	2,6-lutidinium	130	Melby et al., 1964
[Tb(hfac) ₄] ⁻	pyridinium	185	Melby et al., 1964
[Tb(tta) ₄] ⁻	triethylammonium	158	Melby et al., 1964
[Tb(tta) ₄] ⁻	pyridinium	193	Melby et al., 1964

continued on next page

Table 5, *continued*

Tetrakis unit	Counter ion Q ⁺	Melting or decomposition point (°C)	Reference
[Tb(tta) ₄] [−]	2,4,6-trimethylpyridinium	155–157	Bauer et al., 1964
[Dy(hfac) ₄] [−]	triethylammonium	130	Melby et al., 1964
[Ho(hfac) ₄] [−]	triethylammonium	130	Melby et al., 1964
[Er(hfac) ₄] [−]	triethylammonium	130	Melby et al., 1964
[Yb(hfac) ₄] [−]	triethylammonium	130	Melby et al., 1964

5.4. Kinetic stability

The rare-earth β -diketonate complexes are kinetically labile, which means that in solution there is a fast exchange of ligands. Bhaumik (1965a, 1965b) was able to illustrate this behavior by an elegant experiment. Upon addition of a solution of Tb(NO₃)₃ in ethanol to a solution of [Eu(hfac)₃] in ethanol, the strong red luminescence of the europium(III) complex was readily replaced by the green luminescence of the [Tb(hfac)₃] complex. This effect was even more dramatic in the case of the acetylacetonate complexes. When a solution of Tb(NO₃)₃ was added to a weakly luminescent solution of [Eu(acac)₃], the intense green luminescence of [Tb(acac)₃] was observed. The fact that the β -diketonate complexes are kinetically labile, makes that after dissolution of a complex in a solvent, different species are formed in solution. For instance, when a tetrakis complex is dissolved, not only the tetrakis complex is present in solution, but also the corresponding tris and bis β -diketonate complexes. Cotton et al. (1966) investigated the ligand exchange in yttrium β -diketonate complexes. After mixing a solution of [(C₆H₅)₄As][Y(tfac)₄] and [(C₆H₅)₄As][Y(hfac)₄], five different species could be characterized: [Y(hfac)₄][−], [Y(hfac)₃(tfac)][−], [Y(hfac)₂(tfac)₂][−], [Y(hfac)(tfac)₃][−], and [Y(tfac)₄][−]. The ligand exchange equilibria for these yttrium(III) complexes with piperidinium counter ions have been studied by ¹H-NMR (Serpone and Ishayek, 1971). The ligand exchange of [Sc(acac)₃] in acetonitrile was studied by Hatakeyama et al. (1988). Luminescence spectroscopy has often been used to determine the distribution of β -diketonate species in solution. The equilibria not only depend on the type of β -diketonate ligand, but also on the solvent and on the concentration of the complex (Samelson et al., 1966). Halverson et al. (1964a, 1964b) mention that use of ethylene glycol as the solvent, results in a virtually complete decomposition of the complex [Eu(hfac)₃(topo)₂]. Mihara et al. (1994) studied the kinetics and the mechanism of ligand exchange between [Ce(acac)₄] and the free ligand Hacac in C₆D₆ and CD₃CN, by ¹H-NMR line broadening. The observed first-order rate constant depends on the concentration of Hacac in the enol form. The exchange rate was not influenced upon addition of H₂O to deuterated benzene, but addition of DMSO retarded the exchange rate. It is proposed that the exchange reaction proceeds through the formation of a nine-coordinate adduct, [Ce(acac)₄(Hacac)], followed by two parallel rate-determining steps, being the proton transfer from protonated Hacac to leaving acac, and the ring opening of acac in the adduct complex.

Not many data on the shelf-life of rare-earth β -diketonates are available. Charles and Ohlmann (1965a) mention that Lewis base adducts of [R(dbm)₃] could be stored at room temperature for periods longer than one year without decomposition.

5.5. Solubility

Eisentraut and Sievers (1968) determined the solubility of $[\text{Yb}(\text{thd})_3]$ in different solvents. The compound was found to be soluble in methylcyclohexane, benzene, chloroform, methanol, ethylacetate, ethanol, carbon tetrachloride and hexane. The compound is insoluble in water. The complex has the highest solubility in ethyl acetate: 0.70 g $[\text{Yb}(\text{thd})_3]$ is soluble in 1 ml of ethylacetate at 24 °C. The authors also observed that the solubility of the $[\text{R}(\text{thd})_3]$ complexes in organic solvents increases as the ionic radius of the rare-earth ion decreases.

Because the β -diketonate ligands form a lipophilic shell around the rare-earth ion, rare-earth β -diketonate complexes are well soluble in supercritical carbon dioxide, which is a non-polar solvent. Andersen et al. (2001) investigated the solubility of $[\text{Ce}(\text{acac})_4]$, $[\text{Ce}(\text{tod})_4]$, $[\text{Ce}(\text{thd})_4]$, $[\text{Tb}(\text{acac})_3]$, $[\text{Tb}(\text{tod})_3]$ and $[\text{Tb}(\text{thd})_3]$ in supercritical carbon dioxide. The solubilities were found to depend on the β -diketonate ligand and increase in the order $\text{acac} < \text{thd} < \text{tod}$. The rare-earth tod complexes are more than order of magnitude more soluble than the corresponding thd complexes. This behavior was explained by the fact that the tod ligands form a more compact ligand shell around the rare-earth ion than does thd (Andersen et al., 2002). Lin et al. (1998) studied the adduct formation of lanthanide β -diketonates with organophosphorus Lewis bases (tbp, tbpo, topo) in supercritical CO_2 . The β -diketonates in this study were Hfod and Hhfac.

5.6. Solution structure

The tetrakis β -diketonate complexes are assumed to be eight-coordinate. Their solution structure is intermediate between two ideal structures: the dodecahedron and the square antiprism (Samelson et al., 1966). Because of the labile nature of the complexes, it is evident that it is impossible to have one single species with an ideal coordination polyhedron in solution. In the past, there has been a debate on the question whether an eight-coordinate tetrakis complex can form an adduct with a solvent molecule, for instance acetonitrile, to form a nine-coordinate complex. Whereas Samelson et al. (1966) have suggested the existence of such nine-coordinate species, Shepherd (1966) could not obtain experimental evidence for such an hypothesis. Karraker (1967) compared the fine structure and the intensity of the absorption bands of rare-earth β -diketonate complexes in solution and in the solid state. He found that the absorption spectra of the six-coordinate tris complexes in polar solvents resembled those of the eight-coordinate complexes due to adduct formation with solvent molecules. The absorption spectra of the hydrated β -diketonate complexes in benzene resemble those of the six- and seven-coordinate complexes due to dehydration. Addition of water or of another solvent with oxygen donor ligands to a solution containing $[\text{Nd}(\text{fod})_3]$ or $[\text{Er}(\text{fod})_3]$ complexes resulted in marked changes in the shape and intensity of the so-called *hypersensitive transitions* (Karraker, 1971). This effect was attributed to adduct formation. Yatmirskii and Davidenko (1979) discussed the absorption spectra of rare-earth β -diketonate complexes in organic solvents. These authors also point to the existence of mono and bis β -diketonate complexes in solution. In non-polar solvents, the tetrakis complexes dissociate into tris complexes and a β -diketonate salt.

The rare-earth β -diketonates easily dimerize in non-polar solvents (Ismail et al., 1969; Bruder et al., 1974; Neilson and Shepherd, 1976; Kemlo et al., 1977). For instance, $[\text{Tb}(\text{acac})_3] \cdot 3\text{H}_2\text{O}$ exists in benzene as dimers at concentrations higher than 0.005 M (Neilson and Shepherd, 1976). Bruder et al. (1974) investigated the self-association of $[\text{Pr}(\text{fod})_3]$ and $[\text{Eu}(\text{fod})_3]$ in detail. The tendency of these complexes to self-associate can be related to the tendency of the rare-earth complexes to acquire a high coordination number. In the $[\text{R}(\text{fod})_3]$ complexes, the coordination number of the rare-earth ion is six, whereas the rare-earth ion has coordination number seven in the $[\text{R}_2(\text{fod})_6]$ dimers and coordination number eight in the $[\text{R}_3(\text{fod})_9]$ trimers. Coordination number seven can also be reached by a bridging water molecule: $[(\text{fod})_3\text{R}(\text{OH}_2)\text{R}(\text{fod})_3]$. The extent of self-association has the following solvent dependence: *n*-hexane > carbon tetrachloride > benzene > chloroform. The self-association is reduced in more polar solvents. Whereas self-association could be detected in carbon tetrachloride, this was not the case for these complexes dissolved in chloroform. Thus, in chloroform $[\text{Pr}(\text{fod})_3]$ and $[\text{Eu}(\text{fod})_3]$ are essentially present in monomeric form. The complexes of the larger lanthanides (the elements at the beginning of the lanthanide series) are more associated than the complexes of the smaller lanthanides, although the smaller lanthanide(III) ions have the highest Lewis acidity and can easier form adducts with Lewis bases. The reason for this opposite behavior is steric hindrance. In contrast to the $[\text{R}(\text{fod})_3]$ complexes, the $[\text{R}(\text{thd})_3]$ complexes are monomeric in solvents and in all concentrations (Bruder et al., 1974). It should be noticed that $[\text{R}(\text{thd})_3]$ ($\text{R} = \text{La} - \text{Sm}$) form anhydrous dimers in the solid state (Erasmus and Boeyens, 1970, 1971). The aggregation behavior of $[\text{Pr}(\text{fod})_3]$ and $[\text{Eu}(\text{fod})_3]$ has been studied by Desreux et al. (1972) as well.

Because of the preference of trivalent rare-earth ions for oxygen donor ligands, the interaction between 1,10-phenanthroline and rare-earth ions is very weak in aqueous solution. 1,10-Phenanthroline does not form stable complexes with rare-earth ions in water. However, when 3 equivalents of a β -diketone with an aromatic substituent (e.g. Hdbm, Hbtfa or Htta) are mixed with 1 equivalent of 1,10-phenanthroline and 1 equivalent of Eu^{3+} in aqueous solution, a highly luminescent ternary europium(III) complex is formed (Frey et al., 1994). No ternary complexes were formed in the case of Hacac, Hhfa or Hbzac. These experimental facts point to the existence of a synergistic coordination in ternary complexes of rare-earth ions with β -diketonate ligands that contain aromatic groups and 1,10-phenanthroline.

Recently, Pikramenou and coworkers (Bassett et al., 2004) studied rare-earth complexes of the bis(β -diketone) ligands 1,3-bis(3-phenyl-3-oxopropanoyl)benzene and 1,3-bis(3-phenyl-3-oxopropanoyl)-5-ethoxy-benzene. These complexes have a helical structure. Both triple-stranded neutral complexes of the type $[\text{R}_2\text{L}_3]$, and quadruple-stranded anionic complexes of the type $[\text{R}_2\text{L}_4]^{2-}$ are formed, where L is the deprotonated form of the bis(β -diketone) ligands. The solution structure of these complexes was studied in detail by NMR spectroscopy.

5.7. Electrochemical properties

Richter and Bard (1996) have investigated the electrochemical properties of several tetrakis(β -diketonato)europate(III) complexes with tetrabutylammonium or piperidinium counter ions by cyclic voltammetry. The cyclic voltammograms were similar to those of the free β -

diketone ligands. No waves were observed at potentials ≤ 500 mV where the thermodynamic reduction of free Eu^{3+} to Eu^{2+} occurs. This suggests that the f-orbitals of Eu^{3+} are screened by the ligand orbitals, which results in a redox behavior characteristic of ligand-based processes. The β -diketonate ligands can thus be reduced electrochemically without reduction of Eu^{3+} . Comparable results were obtained by Hemingway et al. (1975) for the complexes $[\text{Eu}(\text{dbm})_3(\text{pip})]$ and $[\text{Eu}(\text{dnm})_3(\text{pip})]$. Behrsing et al. (2003) studied the electrochemical behavior of $[\text{Ce}(\text{acac})_4]$ by cyclic voltammetry. Reduction of $[\text{Ce}(\text{acac})_4]$ gave well-defined cyclic voltammograms in acetonitrile and acetone, which indicates that the electrochemical process is quasi reversible. Matsumoto et al. (2000) have studied the redox behaviour of the same complex in acetonitrile.

5.8. Thermodynamic properties

Geira (2000) determined the standard molar enthalpies of the formation of $[\text{R}(\text{thd})_3]$ complexes ($\text{R} = \text{La}, \text{Pr}, \text{Nd}, \text{Sm}, \text{Gd}, \text{Dy}, \text{Ho}, \text{Er}$) in the crystalline state by calorimetry. Also the standard molar enthalpies of sublimation and the enthalpy changes of the complexes in the gaseous state were calculated. Other thermochemical studies include the determination of the standard molar enthalpies of formation of $[\text{La}(\text{acac})_3]$ and $[\text{La}(\text{bzac})_3]$ (Geira and Kakolowicz, 1988), the standard molar enthalpy of formation of $[\text{Pr}(\text{thd})_3]$ and $[\text{Ho}(\text{thd})_3]$ (Airoldi and Santos, 1993) and of $[\text{Sc}(\text{thd})_3]$, $[\text{Y}(\text{thd})_3]$ and $[\text{La}(\text{thd})_3]$ (Santos et al., 1997).

5.9. Magnetic properties

Shepherd (1967) measured the molar magnetic susceptibility of $[\text{Eu}(\text{btfac})_4]^-$ complexes with different counter ions (piperidinium, piperazinium, morpholinium, ammonium and benzyltrimethylammonium) between -150°C and 100°C . The magnetic susceptibility and magnetization of crystals of phosphoro-azo derivatives of europium(III) and terbium(III) β -diketonates have been measured (Borzechowska et al., 2002). A ferromagnetic spin-spin coupling was observed for the $[\text{Cu}(\text{salbza})\text{Gd}(\text{hfac})_3]$ complex, where H_2salbza is *N,N'*-bis(salicylidene)-2-aminobenzylamine (Sasaki et al., 2000). These authors also determined the crystal structure of the complex (fig. 20). For magnetic studies of d-f complexes, most often Gd^{3+} is selected as the rare-earth ion, because of the simplifying spin-only character of the $^8\text{S}_{7/2}$ ground state of this ion. The trivalent Gd^{3+} ion does not show magnetic anisotropy, so that the magnetic exchange interactions can be considered as being isotropic. Benelli et al. (1989a) prepared bis adducts between $[\text{R}(\text{hfac})_3]$ ($\text{R} = \text{Eu}, \text{Gd}$) and the nitronyl nitroxides 2-ethyl-4,4,5,5-tetramethyl-4,5-dihydro-1*H*-imidazolyl-1-oxyl-3-oxide and 2-phenyl-4,4,5,5-tetramethyl-4,5-dihydro-1*H*-imidazolyl-1-oxyl-3-oxide. Binding to the rare-earth ion occurs through the oxygen atom. The nitronyl nitroxides are organic radicals. A weak ferromagnetic coupling was observed between the gadolinium(III) ions and the nitronyl nitroxides, whereas the nitronyl nitroxides couple in an antiferromagnetic way to each other in the bis adducts. The ferromagnetic coupling was attributed to the fact that the magnetic orbital of the ligand has a non-zero overlap with the 6s-orbital of the gadolinium(III) ion. The fraction of the unpaired electrons transferred into the empty 6s-orbitals polarizes the 4f electron spins and forces them to be parallel to the unpaired spins of the radicals. The fact that two radical ligands are present for each gadolinium(III)

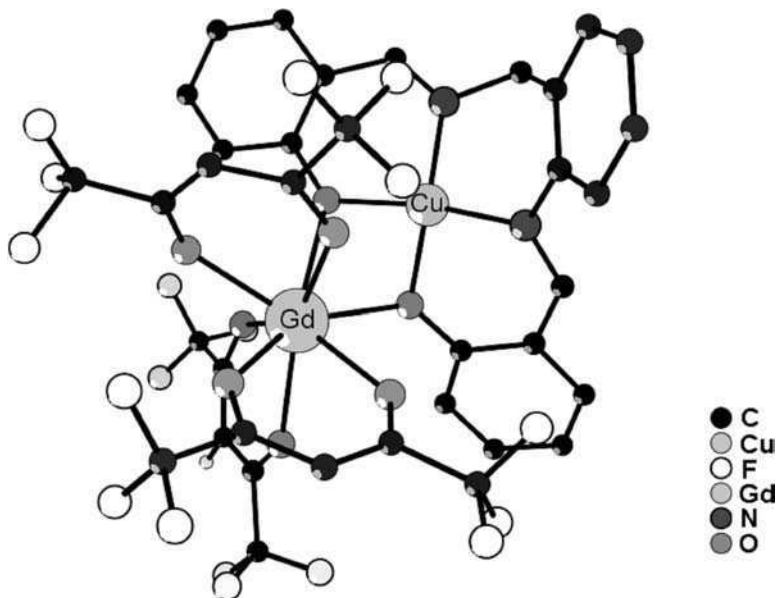


Fig. 20. Molecular structure of the $[\text{Cu}(\text{salbza})\text{Gd}(\text{hfac})_3]$ complex, where H_2salbza is N,N' -bis(salicylidene)-2-aminobenzylamine (Sasaki et al., 2000). No hydrogen atoms are shown.

ion makes the theoretical interpretation more difficult. Therefore, the authors made adducts with one nitronyl nitroxide per gadolinium(III) ion: $[\text{Gd}(\text{hfac})_3(\text{NITiPr})(\text{H}_2\text{O})]$, where NITiPr is 2-isopropyl-4,4,5,5-tetramethyl-4,5-dihydro-1*H*-imidazolyl-1-oxyl-3-oxide (Benelli et al., 1990). The crystal structure of the corresponding europium(III) compound could be obtained. The coordination polyhedron is a highly distorted dodecahedron. Magnetic measurements on the gadolinium(III) compound show that the ferromagnetic coupling between the gadolinium(III) ion and the nitronyl nitroxide occurs essentially in an isotropic way, and not in a dipolar way. The same type of coupling has found in adducts of $[\text{Gd}(\text{hfac})_3]$ with pyridine-substituted nitronyl nitroxide radicals (Benelli et al., 1992). When the gadolinium(III) ion in these adducts with organic radicals is replaced by other paramagnetic rare-earth ions, the theoretical interpretation of the magnetic data becomes much more difficult, because of the magnetic anisotropy of the ground state. Magnetic anisotropy measurements were performed on the $[\text{Ho}(\text{hfac})_3(\text{NITet})]$ complex, where NITet is 2-ethyl-4,4,5,5-tetramethyl-4,5-dihydro-1*H*-imidazolyl-1-oxyl-3-oxide (Benelli et al., 1993). Magnetic measurements were also performed on $[\text{R}(\text{hfac})_3(\text{NITet})]$ ($\text{R} = \text{Tb}, \text{Dy}, \text{Ho}$). The compounds show magnetic phase transitions between 1.2 K and 3.2 K.

5.10. Crystal-field splittings

The fine-splitting in the absorption, excitation and luminescence spectra of rare-earth β -diketonate complexes is due to the crystal-field perturbation. The splitting patterns is determined by the symmetry of the coordination polyhedron around the rare-earth ion and by

the crystal field strength. A detailed description of the crystal-field perturbation in rare-earth complexes can be found in the review paper of [Görlner-Walrand and Binnemans \(1996\)](#). Few studies describe the crystal-field perturbation in lanthanide β -diketonate complexes theoretically. [Bjorklund et al. \(1968\)](#) studied the crystal-field splitting of $(\text{Et}_4\text{N})[\text{Eu}(\text{dbm})_4]$. [Kirby and Richardson \(1983\)](#) performed a crystal-field study of $[\text{Eu}(\text{dbm})_3(\text{H}_2\text{O})]$, on the basis of spectroscopic data obtained from polarized absorption measurements, and (unpolarized) luminescence measurements. [Tsaryuk et al. \(2000\)](#) determined the phenomenological B_q^k crystal field parameters for a series of adducts of $[\text{Eu}(\text{thd})_3]$ with substituted 1,10-phenanthrolines. [Kirby and Palmer \(1981a, 1981b\)](#) had chosen $[\text{R}(\text{dbm})_3(\text{H}_2\text{O})]$ ($\text{R} = \text{Nd}, \text{Eu}, \text{Ho}, \text{Er}$) as model compounds to test the dynamic-coupling model that is used to describe the intensities of f–f transitions between crystal-field levels. A detailed analysis of the f–f intensities of $[\text{Eu}(\text{dbm})_3(\text{H}_2\text{O})]$ was made by [Kirby and Richardson \(1983\)](#), and by [Dallara et al. \(1984\)](#). [Szczewski et al. \(1995\)](#) compared the EPR spectra of the gadolinium(III) β -diketonate complexes $[\text{Gd}(\text{acac})_3(\text{H}_2\text{O})_3]$, $[\text{Gd}(\text{tta})_3(\text{H}_2\text{O})_2]$ and $[\text{Gd}(\text{bzac})_3(\text{H}_2\text{O})_2]$ with those of polycarboxylate complexes.

5.11. Infrared spectra

Over the years, there has been a lot of dispute about the assignment of some absorption bands in the infrared (IR) spectra of metal complexes of β -diketonates, including the rare-earth β -diketonates. More particularly, the polemic was about the positions of the C=O and C=C stretching vibrations in the infrared spectra. [Bellamy and Branch \(1954\)](#) assigned the bands at 1580 cm^{-1} and 1520 cm^{-1} to the C=O and C=C stretching modes respectively. These assignments were reversed by [Nakamoto and Martell \(1960\)](#). [Mikami et al. \(1967\)](#) supported the assignments made by Nakamoto and Martell, although the two modes were shown to be slightly coupled. [Pinchas et al. \(1967\)](#) concluded on the basis of the infrared spectra of ^{13}C and ^{18}O labeled $[\text{Cr}(\text{acac})_3]$ and $[\text{Mn}(\text{acac})_3]$ complexes, that the assignment made by Bellamy and Branch is the correct one. [Liang et al. \(1970\)](#) assigned the absorption bands observed in the infrared spectrum of $[\text{Eu}(\text{acac})_3(\text{H}_2\text{O})_2]$ at 1600 cm^{-1} and 1515 cm^{-1} to the C=O and C=C stretching vibrations respectively. Replacement of a methyl group by a trifluoromethyl group strengthens the C=O and C=C bonds, but weakens the Eu–O bond. The former two bands are therefore shifted to higher wavenumbers, while the latter is shifted to lower wavenumbers. [Misumi and Iwasaki \(1967\)](#) studied the infrared spectra of the tris acetylacetonate complexes of praseodymium(III), neodymium(III), europium(III), gadolinium(III), dysprosium(III) and erbium(III). Their assignments of the C=O and C=C stretching vibrations should be corrected, according to the findings of [Pinchas et al. \(1967\)](#). The R–O vibrations were found in the regions $420\text{--}432\text{ cm}^{-1}$ and $304\text{--}322\text{ cm}^{-1}$. The R–O stretching vibrations shift to higher wavenumbers from praseodymium(III) to erbium(III).

5.12. Chirality sensing

[Tsukube et al. \(2001\)](#) found that upon addition of chiral amino alcohols to rare-earth complexes of non-chiral β -diketonates, such as $[\text{R}(\text{thd})_3]$ or $[\text{R}(\text{fod})_3]$, a circular dichroism (CD) signal could be observed. It was suggested that tris β -diketonate complexes can be used for

chirality sensing, because the sign of the CD signal depends on the configuration of the amino alcohol. This method could be applied to determine the enantiomeric excess in mixtures of enantiomers of amino alcohols.

5.13. *Properties of hemicyanine dyes with β -diketonate counter ions*

Tetrakis rare-earth β -diketonate complexes can act as counter ions for hemicyanine dyes (also called stilbazolium dyes). Typically stilbazolium dyes have halide counter ions, but these halide counter ions can be replaced by anionic tetrakis β -diketonate complexes $[\text{R}(\text{pmbp})_4]^-$, where Hpmbp is 1-phenyl-3-methyl-4-benzoyl-5-pyrazolone (Wang et al., 1994c, 1995a; Li et al., 1996). The rare-earth ions studied were restricted to La, Nd, Dy and Yb. Structural changes of the hemicyanine chromophore include changing the two methyl groups of the amino-nitrogen by ethyl groups, or changing the $\text{C}_{16}\text{H}_{33}$ chain by a $\text{C}_{18}\text{H}_{37}$ chain. The intense red color of these compounds is not due to the rare-earth complex but to the hemicyanine counter ion. The strong absorption bands of the hemicyanine chromophore overwhelm those of the f–f transitions, but Binnemans (2000) could observe f–f transitions of Nd^{3+} in this type of compounds. The intensity and the positions of the absorption bands of the hemicyanine chromophore depend on the solvent (Binnemans et al., 1999c). This strong solvatochromism is an indication for the good non-linear optical properties of these complexes. Another interesting property of these compounds is the observation of a photoelectrical signal. A double lipid membrane doped with an ytterbium(III) complex containing a hemicyanine chromophore showed a small electric current through the membrane when illuminated with a continuous light source (Xiao et al., 1994). The group of Huang prepared similar complexes in which the $\text{C}=\text{C}$ linking group was replaced by an azo group ($\text{N}=\text{N}$) (Gao et al., 1996a, 1996b).

6. Luminescence of β -diketonate complexes

6.1. *Photoluminescence*

One of the most interesting features of trivalent lanthanide ions is their photoluminescence. Several lanthanide ions show luminescence in the visible or near-infrared spectral regions upon irradiation with ultraviolet light. The color of the emitted light depends on the lanthanide ion. For instance, Eu^{3+} emits red light, Tb^{3+} emits green light and Tm^{3+} emits blue light. Yb^{3+} , Nd^{3+} and Er^{3+} are well-known for their near-infrared luminescence. When the light emission by lanthanide ions is discussed, one uses the term “luminescence”, rather than the terms “fluorescence” or “phosphorescence”. The reason is that the terms fluorescence and phosphorescence are used to describe light emission by organic molecules, and that these terms incorporate information on the emission mechanism: *fluorescence* is singlet-to-singlet emission and *phosphorescence* is triplet-to-triplet emission. In the case of the lanthanides, the emission is due to transitions inside the 4f-shell, i.e. these transitions are intraconfigurational f–f transitions. Because the partially filled 4f-shell is well shielded from its environment by the closed $5s^25p^6$ shell, the ligands in the first and second coordination sphere perturb the electronic configurations of the trivalent lanthanide ions only to a very limited extent. This

shielding is responsible for the specific properties of lanthanide luminescence, more particularly for the narrow-band emission and for the long lifetimes of the excited states. Depending on the method of excitation, different types of luminescence are considered, e.g. *photoluminescence* (emission after excitation by irradiation with electromagnetic radiation), *electroluminescence* (emission by recombination of electrons and holes under the influence of an electric field), *chemiluminescence* (non-thermal production of light by a chemical reaction) or *triboluminescence* (emission observed by applying mechanical stress to crystals or by fracture of crystals).

Although the photoluminescence by lanthanide ions is an efficient process, the lanthanide ions suffer from weak light absorption. Because the molar absorptivities ε of most of the transitions in the absorption spectra of the trivalent lanthanide ions are less than $10 \text{ l mol}^{-1} \text{ cm}^{-1}$, only a small amount of radiation can be absorbed by direct excitation in the 4f levels. Since the luminescence intensity is not only proportional to the luminescence quantum yield, but also to the amount of light absorbed, weak light absorption results in weak luminescence. However the problems of weak light absorption can be overcome by the so-called "antenna effect". Weissman (1942) discovered that intense metal-centered luminescence can be observed for lanthanide complexes with organic ligands upon excitation in an absorption band of the organic ligand. Because of the intense absorption bands of organic chromophores, much more light can be absorbed by the organic ligand than by the lanthanide ion itself. Subsequently, the excitation energy is transferred from the organic ligand to the lanthanide ion by intramolecular energy transfer. Weissman (1942) first observed this phenomenon for the europium(III) complex of salicylaldehyde, but in his seminal paper he also studied the europium(III) complexes of benzoylacetone, dibenzoylmethane and *meta*-nitrobenzoylacetone. It took about 20 years before the importance of Weissman's work was appreciated, although Sevchenko and Trofimov (1951) showed that his experiments could be reproduced. But after the mechanisms of the energy transfer from the organic ligand to the lanthanide ion has been investigated in the early 1960s and after one realized that the lanthanide β -diketonate complexes could have potential as the active component in chelate lasers, an intense research activity has been going on in the field of luminescent materials based on lanthanide β -diketonates.

The commonly accepted mechanism of energy transfer from the organic ligands to the lanthanide ion is that of Crosby and Whan (Crosby et al., 1961, 1962; Whan and Crosby, 1962) (fig. 21). Upon irradiation with ultraviolet light, the organic ligands of the lanthanide complex are excited to a vibrational level of the first excited singlet state ($S_1 \leftarrow S_0$). The molecule undergoes fast *internal conversion* to lower vibrational levels of the S_1 state, for instance through interaction with solvent molecules. The excited singlet state can be deactivated radiatively to the ground state (molecular fluorescence, $S_1 \rightarrow S_0$), or can undergo non-radiative *intersystem crossing* from the singlet state S_1 to the triplet state T_1 . The triplet state T_1 can be deactivated radiatively to the ground state S_0 , by the spin-forbidden transition $T_1 \rightarrow S_0$. This results in molecular phosphorescence. Alternatively, the complex may undergo a non-radiative transition from the triplet state to an excited state of the lanthanide ion. After this indirect excitation by energy transfer, the lanthanide ion may undergo a radiative transition to a lower 4f-state by characteristic line-like photoluminescence, or it may be deactivated by radiationless processes. According to Whan and Crosby (1962) the main cause of radiationless

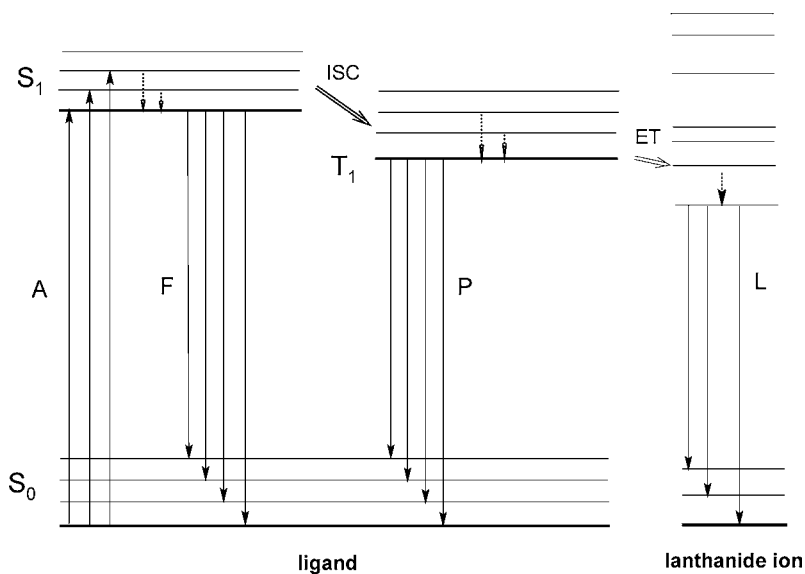


Fig. 21. Photophysical processes in lanthanide β -diketonate complexes (antenna effect). Abbreviations: A = absorption, F = fluorescence, P = phosphorescence, L = lanthanide-centered luminescence, ISC = intersystem crossing, ET = energy transfer.

deactivation of the lanthanide ion is the vibronic coupling with the ligand and solvent molecules. Although [Kleinerman \(1964\)](#) proposed a mechanism of direct transfer of energy from the excited triplet state S_1 to the energy levels of the lanthanide ion, this mechanism is now considered to be not important. Luminescence by the lanthanide ion is only possible from certain levels, that are termed *resonance levels*. The main resonance levels are $^4G_{5/2}$, 5D_0 , 5D_4 and $^4F_{9/2}$ for respectively Sm^{3+} , Eu^{3+} , Tb^{3+} and Dy^{3+} . If the lanthanide ion is excited to a non-emitting level, either directly by excitation in the 4f-levels or indirectly by energy transfer, the excitation energy is dissipated via radiationless processes until a resonance level is reached. Radiative transitions become then competitive with the non-radiative processes and metal-centered emission can be observed. Line-emission by a lanthanide ion is only possible if the radiationless deactivation, the molecular fluorescence and phosphorescence can be minimized. In order to populate a resonance level of the lanthanide ion, it is necessary that the lowest triplet state of the complex is located at an energy nearly equal or above the resonance level of the lanthanide ion, not below. When the energy levels of the organic ligands are below that of the resonance level of the lanthanide ion, the molecular fluorescence or phosphorescence of the ligand is observed, or no light emission at all. The luminescence observed for a specific lanthanide complex is therefore a sensitive function of the energy of the lowest triplet level of the complex relative to a resonance level of the lanthanide ion. Because the position of the triplet level depends on the type of ligand, is it therefore possible to control the luminescence intensity observed for a given lanthanide ion by variation of the ligand ([Filipescu et al., 1964](#)). The position of the triplet level is also temperature dependent, so that

the luminescence caused by indirect excitation through the organic ligands is much more temperature sensitive than luminescence caused by direct excitation of the 4f-levels (Weissman, 1942). Sato and Wada (1970) investigated the relationship between the efficiency of the intermolecular energy transfer from the triplet state to the lanthanide ion and the energy difference between the triplet state and resonance levels of the lanthanide ions. The authors determined the energy of the triplet states by measuring the phosphorescence spectra of gadolinium(III) β -diketonate complexes at 77 K in an EPA solution (5 parts of diethyl ether, 5 parts of 3-methylpentane and 5 parts of ethanol by volume). Because the 4f-levels of Gd^{3+} are located above the triplet levels, no metal-centered emission can be observed for Gd^{3+} . Moreover, the presence of a heavy paramagnetic ion enhances the intersystem crossing from the singlet to the triplet state, because of mixing of triplet and singlet states ("paramagnetic effect") (Tobita et al., 1984, 1985). By the spin-orbit coupling the triplet state acquires partially a singlet character and the selection rules can be relaxed. By the presence of the gadolinium(III) ion, the decay time of the triplet state is reduced (Bhaumik and El-Sayed, 1965). Often cryogenic temperatures are necessary to observe phosphorescence, because otherwise the triplet state is deactivated by radiationless processes. Also the fluorescence competes with the phosphorescence. At 77 K, the solvent quenching of the triplet state is negligible. The triplet levels are always located at a lower energy than the singlet levels. Although energy transfer to the lanthanide ion takes place from the lowest triplet level T_1 , it is sometimes possible to observe in the phosphorescence spectrum higher lying triplet states such as T_2 as well. The efficiency of the energy transfer is proportional to the overlap between the phosphorescence spectrum and the absorption spectrum of the lanthanide ion. The overlap decreases as the triplet state energy increases. A close match between the energy of the triplet state and the energy of the receiving 4f-level of the lanthanide ion is not desirable neither, because back transfer of the lanthanide ion to the triplet state can occur. Many of the europium(III) β -diketonate complexes show an intense luminescence, but most β -diketonate complexes are not good ligands to sensitize the luminescence of terbium(III) ions. The reason is that the triplet level of many β -diketonate ligands with aromatic substituents is below that of the resonance level 5D_4 of Tb^{3+} . Often, terbium β -diketonate complexes show weak or no luminescence at room temperature, although sometimes stronger luminescence it observed at liquid nitrogen temperatures. Besides, europium(III) and terbium(III) complexes, visible photoluminescence can be expected for the β -diketonate complexes of samarium(III) and dysprosium(III) (Freeman and Crosby, 1963). Weak visible or near-infrared emission is possible for the complexes of praseodymium(III), neodymium(III), holmium(III), erbium(III), thulium(III) and ytterbium(III). It has already been mentioned that no metal-centered photoluminescence can be observed for gadolinium(III) complexes, because of the high energy of the 4f-levels. Because lanthanum(III) has an empty 4f-shell and lutetium(III) a filled 4f-shell, no metal-centered luminescence can be observed for the complexes of these ions. Serafin and coworkers (Sager et al., 1965; Filipescu et al., 1964) investigated the influence of different substituents on the β -diketonate ligands on the intramolecular energy transfer. They determined the position of the first excited singlet S_1 by measuring the absorption spectra of the complexes. The absorption intensities don't change much on changing the substituents of the β -diketonate. The authors found that the position of S_1 does not affect directly the energy transfer from the β -diketonate ligand to

the lanthanide ion. On the other hand, the intersystem crossing (singlet-to-triplet transition), depends on the substituents. When the energy transfer from the ligand to the lanthanide ion is inefficient, the metal-centered luminescence is weak and at the same time an emission band due to the molecular phosphorescence is observed. One can say that in these cases, the triplet state is only partially quenched by the lanthanide ion. When the lanthanide luminescence is absent, the intensity of the phosphorescence band can approach that of the corresponding gadolinium(III) complex. The efficiency of the energy transfer from the organic ligand to the lanthanide ion, is proportional to the overlap between the ligand phosphorescence spectrum and the absorption spectrum of the lanthanide(III) ion (Iwamuro et al., 2000).

Wu and Su (2001) investigated the intramolecular energy relaxation processes of $[\text{R}(\text{tta})_3(\text{H}_2\text{O})_2]$ complexes ($\text{R} = \text{Nd}, \text{Eu}, \text{Gd}$) by photoacoustic spectroscopy. Yang et al. (1999) performed a similar study on $[\text{Eu}(\text{dbm})_3(\text{phen})]$ and $[\text{Eu}_{0.8}\text{R}_{0.2}(\text{dbm})_3(\text{phen})]$ complexes ($\text{R} = \text{Nd}^{3+}, \text{Gd}^{3+}, \text{Tb}^{3+}$), and Yu et al. (2003) on $[\text{Nd}(\text{dbm})_3(\text{H}_2\text{O})]$ and $[\text{Nd}(\text{dbm})_3(\text{phen})]$. Photoacoustic spectroscopy is a complementary technique to luminescence spectroscopy, because it can monitor non-radiative relaxation.

As mentioned above, europium(III) β -diketonate complexes show often an intense luminescence. However, the luminescence intensities are strongly dependent on the type of β -diketone, and on the type of complex. Moreover, it is very often difficult, not to say impossible to compare the luminescence output of different samples. The luminescence intensity is not only related to the quantum yield of luminescence, but also to the amount of absorbed radiation. For this reason, the luminescence of solid samples will also depend on the position of the sample in the light beam that is used for excitation. The luminescence intensity of lanthanide chelates that are excited in the ligand bands is much more dependent on the temperature than the luminescence that is observed upon direct excitation in the f-f levels. It is possible to find some regularities in the luminescence output of europium(III) β -diketonates. The weakest luminescence is observed for the tris complexes. Lewis base adducts give higher intensities, and the tetrakis β -diketonate complexes gives the highest luminescence intensity. Aliphatic β -diketones (acetylacetonone, trifluoroacetylacetonone or hexafluoroacetylacetonone) give weakly luminescent europium complexes, because of the large energy gap between the resonance levels of the europium ion and the triplet state of the ligand, which makes energy transfer to the europium ion inefficient (Filipescu et al., 1964). Combinations of aromatic and aliphatic substituents on the β -diketones (benzoylacetonone, benzoyltrifluoroacetonone, thenoyltrifluoroacetonone) give europium complexes with a more intense luminescence. In these systems, the energy transfer from the ligand to the lanthanide ion is more efficient. The increase in luminescence intensity in such systems is also attributed to the increased anisotropy around the europium ion (Filipescu et al., 1964). Among the Lewis base adducts, a complex that is well-known for its good luminescence properties is $[\text{Eu}(\text{tta})_3(\text{phen})]$ (figs. 22 and 23). Among the terbium complexes, strong luminescence is observed for the tris complexes of acetylacetonone, di-*p*-fluorodibenzoylmethane and trifluoroacetylacetonone (Filipescu et al., 1964). The highest luminescence intensity is observed for terbium(III) complexes of acetylacetonone (Yang et al., 1994a, 1994b). In order to obtain luminescent terbium(III) β -diketonate complexes with aromatic substituents, complexes of 1-indoleacetylacetonone and 3-indoleacetylacetonone were prepared (Wu et al., 1992a, 1992b; Wu and Yang, 1992). The reason for this choice was that

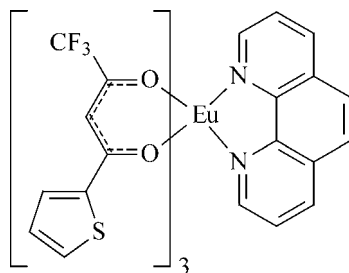


Fig. 22. Structure of the luminescent europium(III) β -diketonate complex $[\text{Eu}(\text{tta})_3(\text{phen})]$.

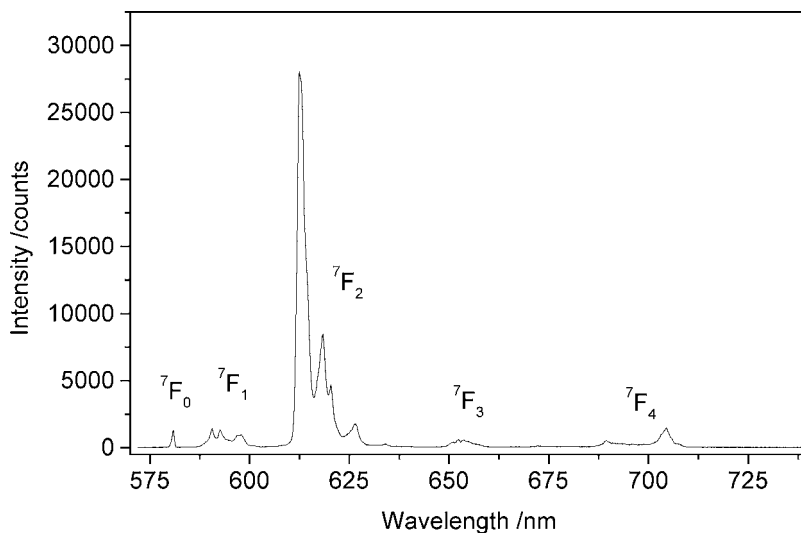


Fig. 23. Luminescence spectrum at 77 K of $[\text{Eu}(\text{tta})_3(\text{phen})]$ in a KBr pellet. The excitation wavelength is 396 nm. All the transitions start from the $^5\text{D}_0$ state.

the triplet level of the indole group is at a higher energy than the energy of the triplet level of a phenyl group. Yang et al. (1994a, 1994b) stated that the presence of a rigid planar structure in the complex causes a higher intensity of the sensitized luminescence, because such structure allows a better energy transfer. The fact that a stronger luminescence is observed for $[\text{Eu}(\text{tta})_3(\text{phen})]$ than for $[\text{Eu}(\text{tta})_3(\text{bipy})]$ is in agreement with this rule.

Typically, the luminescent lanthanide complexes are excited by ultraviolet radiation. By adduct formation of $[\text{Eu}(\text{fod})_3]$ with bis(*N,N*-dimethylamino)benzophenone (Michler's ketone) in benzene, Werts et al. (1999) obtained an europium(III) complex that could be excited by blue light at ca. 450 nm (fig. 24). It was shown by UV-VIS titration that a 1:1 adduct is formed between Michler's ketone and the β -diketonate complex. However, the adduct formation could only be observed in non-coordinating solvents, and also water molecules were found to compete with Michler's ketone for binding to the $[\text{Eu}(\text{fod})_3]$ complex. The adduct

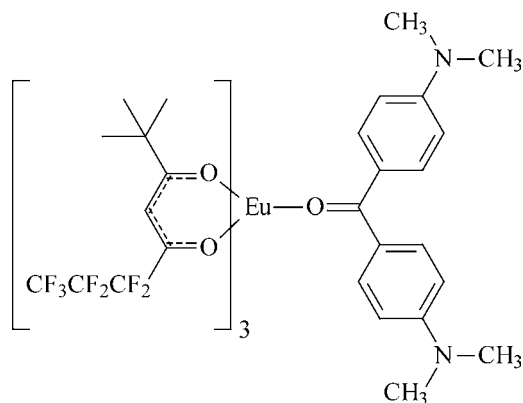


Fig. 24. Adduct formed between $[\text{Eu}(\text{fod})_3]$ and Michler's ketone (Werts et al., 1999).

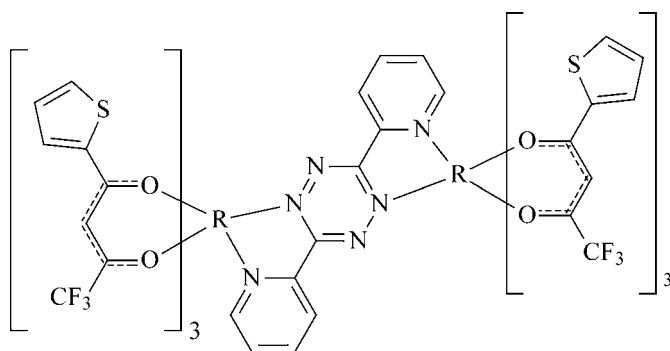


Fig. 25. Rare-earth complexes of 3,6-bis(2-pyridyl)tetrazine (Shavaleev et al., 2003b). R = Gd, Er, Yb.

could not be isolated in the solid state, although it could be trapped in a methylcyclohexane glass at 77 K. Upon variation of the β -diketonate ligand, it was found that the adduct with $[\text{Eu}(\text{thd})_3]$ was strongly luminescent as well, but only a weak luminescence could be observed for the adduct of $[\text{Eu}(\text{hfac})_3]$. Mononuclear and dinuclear adducts of $[\text{R}(\text{tta})_3]$ (R = Nd, Er, Yb) with 3,6-bis(2-pyridyl)tetrazine showed near-infrared luminescence upon excitation with visible light (520 nm) in a low-energetic transition centered on the 3,6-bis(2-pyridyl)tetrazine ligand (Shavaleev et al., 2003b) (fig. 25). Sabbatini et al. (1996) and Lis et al. (2002) gave an overview of applications of lanthanide luminescence that are based on the sensitization of the luminescence by the presence of organic chromophores.

The luminescence of europium(III) complexes can be quenched by a low-lying ligand-to-metal charge-transfer state (LMCT state) (Blasse, 1976; Napier et al., 1975; Sabbatini et al., 1993). Such a LMCT state can deactivate the excited singlet and/or triplet states of the ligand. An et al. (2002) studied the quenching of the $^5\text{D}_1$ state in Eu^{3+} doped $[\text{Gd}(\text{thd})_3]$ by a low-lying ligand-to-metal charge transfer state. Villata et al. (1999) discussed the photoinduced

electron transfer as the main deactivation mechanism of $[\text{Eu}(\text{fod})_3]$ in organic solutions. Upon steady state irradiations of the complex at 300 nm, Eu^{3+} is photochemically reduced to Eu^{2+} .

The *luminescence quantum yield* Φ is an important quantity for evaluation of the efficiency of the emission process in luminescence materials. The quantum yield is defined as the ratio of the number of emitted photons to the number of absorbed photons per time unit (Fery-Forgues and Lavabre, 1999):

$$\Phi = \frac{\text{number of emitted photons}}{\text{number of absorbed photons}}. \quad (5)$$

The luminescence quantum yield is directly related to the rate constants for radiative deactivation (k_r) and non-radiative deactivation (k_{nr}), by the relationship:

$$\Phi = \frac{k_r}{k_r + k_{nr}}. \quad (6)$$

The factor k_r is temperature-independent. The non-radiative rate constant contains contributions from a temperature-independent term, which accounts for the deactivation to the ground state, and a temperature-dependent term which can play a role when upper-lying short-lived excited states are thermally accessible (Thompson et al., 2002). Determination of quantum yields is not an easy task. The measurement of *absolute quantum yields* is critical and requires special equipment, because it is necessary to know the amount of excited light received by the sample. These measurements are done by the use of scattering agents and integrating spheres to calibrate the system. For routine work, one is often satisfied with the determination of *relative quantum yields*. In this case the quantum yield of the unknown is compared with that of a reference sample:

$$\Phi_X = \left(\frac{A_R}{A_X}\right) \left(\frac{E_X}{E_R}\right) \left(\frac{n_X}{n_R}\right)^2 \Phi_R, \quad (7)$$

where Φ is the luminescence quantum yield, A is the absorbance at the excitation wavenumber, E is the area under the corrected emission curve (expressed in number of photons), and n is the refractive index of the solvents used. The subscripts R and X refer to the reference and to the unknown, respectively. The ideal absorbance for luminescence measurements lies between 0.04 and 0.05. When the absorbance is above 0.05, the emission intensity can no longer be assumed proportional to the concentration of the analyte (no linear relationship between the emission intensity and the concentration). Only when the sample and the reference have the same absorbance at the excitation wavelength, and absorbance up to 0.5 can be tolerated. When the absorbance is too low, the impurities from the medium may become important with respect to the amount of analyte. Moreover, at low concentrations the dissociation of the complex in solution can be a problem, especially when the formation constants are not very high (as is often the case for rare-earth β -diketonate complexes). It is advisable to use the same excitation wavelength for measuring the luminescence of the standard and of the unknown. One should not choose the excitation wavelength on the edge of an excitation band, because upon excitation on the edge, a slight change in wavelength will induce a large change in the amount of light absorbed. When the same solvent is used for both the reference and the unknown, the

factor $(n_X/n_R)^2$ will be equal to unity. For lanthanide complexes, the quantum yield depends upon the ligand (or metal) transition that is excited, because sensitization of the lanthanide ion can go through several energy migration paths, the efficiency of which depends on the peculiar levels involved. For integration of the emission spectra, the spectra have to be expressed as a function of the wavenumber (cm^{-1}) and not as a function of the wavelength. Of course, the luminescence quantum yield have to be determined by the use of corrected emission spectra. Finding a suitable reference (standard) is often a big problem, especially when one wants to perform measurements on luminescent materials that emit in the near-infrared region. The reference has to emit in the same region as the lanthanide ion of interest does. Most of the fluorescence standards are organic compounds that show broad band emission, whereas the lanthanide ions exhibit line-like emission. For determination of luminescence quantum yield on europium(III), cresyl violet ($\Phi = 54\%$ in methanol) or rhodamine 101 ($\Phi = 100\%$ in ethanol) can be used as standards (Eaton, 1998). For terbium(III) complexes, quinine sulfate ($\Phi = 54.6\%$ in 0.5 M aqueous H_2SO_4) and 9,10-diphenylanthracene ($\Phi = 90\%$ in cyclohexane) can be used (Eaton, 1998). Another standard for lanthanide complexes emitting in the visible region is $[\text{Ru}(\text{bipy})_3]\text{Cl}_2$ ($\lambda_{\text{ex}} = 400 \text{ nm}$, $\Phi = 2.8\%$ in water) (Nakamura, 1982). Bünzli and coworkers (Chauvin et al., 2004) proposed the use of europium(III) and terbium(III) tris(dipicolinates) as secondary standards for luminescence quantum yield determination.

For solid samples, standard phosphors can be used (de Sá et al., 2000; Bril and De Jager-Veenis, 1976a, 1976b; de Mello Donegá et al., 1996a, 1996b). The relevant expression is:

$$\Phi_X = \left(\frac{1 - R_R}{1 - R_X} \right) \left(\frac{\phi_X}{\phi_R} \right) \Phi_R, \quad (8)$$

where R is the amount of reflected excitation radiation and ϕ is the integrated photon flux (photons s^{-1}). Commercial phosphors that can be used as standard for luminescence quantum yields are $\text{Y}_2\text{O}_3:3\% \text{Eu}^{3+}$ (YOX-U719 Philips, $\Phi = 99\%$) for europium(III) emission and $\text{GdMgB}_5\text{O}_{10}:\text{Tb}^{3+}, \text{Ce}^{3+}$ (CBT-U734 Philips, $\Phi = 95\%$) for terbium(III) (Malta et al., 1998). A solid standard that is easily obtainable is sodium salicylate, which has a broad band emission with a maximum at 450 nm, and a luminescence quantum yield of 60% at room temperature (Bril and De Jager-Veenis, 1976b; Gonçalves e Silva et al., 2000). One of the few examples of direct determination of absolute quantum yield of β -diketonates is the work of Gudmundson et al. (1963). These authors determined the absolute quantum efficiency of $[\text{Eu}(\text{tta})_3]$ in acetone by a calorimetric method. By this technique the temperature rise of the samples due to non-radiative deactivation is measured. The quantum efficiency in acetone at 25 °C was determined as 0.56 ± 0.08 . Only the ${}^5\text{D}_0 \rightarrow {}^7\text{F}_2$ transition was considered, because the authors argue that this transition accounts for more than 95% of the total emission of the complex. For the determination of the luminescence quantum yields, it is not necessary to record emission spectra at high resolution (Haas and Stein, 1971). The errors on the experimentally determined luminescence quantum yields can be quite high (up to 30%), so one has to be careful with drawing conclusions when quantum yields of different systems are compared. The luminescence quantum efficiency of $[\text{Eu}(\text{nta})_3(\text{dmsO})_2]$ (0.75) is one of the highest observed for solid europium(III) complexes (Carlos et al., 2003).

Whereas the luminescence quantum yield gives an idea of the luminescence quenching in the whole system, the luminescence decay time indicates the extent of quenching at the emitting ion site only. [Bhaumik \(1964\)](#) studied the temperature variation of the luminescence quantum yield and the decay times of various europium(III) β -diketonate complexes in various solvents. Although the luminescence decay times of the complexes are quite different from one another at room temperature, the values for the different complexes are very much the same at 77 K (ca. 450 μ s). This indicates that the rate of quenching at the Eu^{3+} site approaches a constant value at this temperature. Fluorine substitution in the ligand results in a decrease of the quenching and thus in an increase of the decay time at room temperature (up to a factor 2). Although the decay times of the europium(III) complexes are similar at 77 K, this is not the case for the corresponding luminescence quantum yields. This gives an indication of the fact that quenching not only occurs at the rare-earth ion site, but in the ligand as well. The luminescence quantum yields of the fluorinated complexes was found to be higher than those of the non-fluorinated complexes. During a time-resolved study of the spectroscopic properties of tris and tetrakis complexes of europium(III) with dibenzoylmethane ligands in glass-forming solvents, [Watson et al. \(1975\)](#) observed that the $^5\text{D}_0$ emission intensity rised exponentially from an apparent initial intensity to a maximum within several microseconds, and decayed exponentially on a much longer (millisecond) timescale. The emission of the $^5\text{D}_1$ level was found to decay on a microsecond time scale, and the rise time of the $^5\text{D}_0$ emission is virtually identical with the decay time of the $^5\text{D}_1$ emission. It is an interesting phenomenon that the lifetime of the tris complexes is shorter than that of the tetrakis complexes at 77 K, but the reverse is true at room temperature. The glass-forming solvents used by the authors were: (a) diethyl ether–2-methylbutane (EP); (b) diethyl ether–2-methylbutane–ethanol (EPA); (c) methanol–ethanol (ME); (d) methylcyclohexane–2-methylbutane (MCHIP). In all cases, equal volume parts of the different components have been taken.

[Charles and Riedel \(1966\)](#) compared the relative intensities and the fine structure of the $^5\text{D}_0 \rightarrow ^7\text{F}_1$ and $^5\text{D}_0 \rightarrow ^7\text{F}_2$ transitions of many tetrakis europium(III) complexes of benzoyltrifluoroacetone. The luminescence intensity of the tetrakis complexes is much higher than that of the corresponding hydrated tris complex. [Shepherd \(1966\)](#) found that the counter ion of tetrakis europium(III) complexes influences the fine structure of the luminescence spectrum in non-polar solvents, whereas the spectra in polar solvents are cation independent. This effect was ascribed to ion-pairing in non-polar solvents, which disturbs the first coordination sphere of the europium(III) ion. [Bjorklund et al. \(1968\)](#) analyzed theoretically the crystal-field splitting observed in the emission spectrum of the tetraethylammonium tetrakis(dibenzoylmethanato)europate(III) at 77 K. The effect of different alkali-metal counter ions on the luminescence spectra of $\text{M}^+[\text{Eu}(\text{bzac})_4]^-$ ($\text{M}^+ = \text{Na}^+, \text{K}^+, \text{Rb}^+, \text{Cs}^+$) have been investigated by high-resolution spectroscopy ([Murray et al., 1989](#)). The authors found a descent in symmetry when the size of the cation increased. The following symmetries were assigned for the different compounds: sodium, D_4 ; potassium, C_4 or C_{4v} ; rubidium, D_{2d} ; cesium, D_2 . Thompson and coworkers ([Moser et al., 2000](#); [Thompson and Berry, 2001](#)) point to the fact that it is very difficult to assign the geometry of the coordination polyhedron in europium(III) β -diketonate complexes based on the fine

Table 6

Luminescence lifetimes of europium(III) β -diketonate complexes in the solid state at room temperature. The emitting state is 5D_0

Compound	Lifetime (ms)	Reference
[Eu(btfac) ₃ (H ₂ O) ₂]	0.17	de Mello Donegá et al., 1997
[Eu(tta) ₃ (H ₂ O) ₂]	0.260	Malta et al., 1997
[Eu(btfac) ₃ (H ₂ O) ₂]	0.329	Qian et al., 2001
[Eu(dmbm) ₃ (phen)]	0.34	Bünzli et al., 1994
[Eu(mdbm) ₃ (phen)]	0.37	Bünzli et al., 1994
[Eu(btfac) ₃ (phenNO)]	0.37	de Mello Donegá et al., 1997
[Eu(bzac) ₃ (H ₂ O) ₂]	0.41	Alves et al., 1997
[Eu(bzac) ₃ (phen)]	0.43	Alves et al., 1997
[Eu(dbm) ₃ (phen)]	0.43	Bünzli et al., 1994
[Eu(bzac) ₃ (phenNO)]	0.46	Alves et al., 1997
[Eu(mfa) ₃ (phen)]	0.47	Bünzli et al., 1994
[Eu(tta) ₃ (ptso) ₂]	0.598	Gonçalves e Silva et al., 2000
[Eu(bzac) ₃ (phen)]	0.61	Bünzli et al., 1994
[Eu(tta) ₃ (dbzso) ₂]	0.714	Malta et al., 1997
[Eu(tta) ₃ (dmsO) ₂]	0.72	Brito et al., 2000
[Eu(hfac) ₃ (monoglyme)]	0.93	Malandrino et al., 2001
[Eu(hfac) ₃ (diglyme)]	0.96	Malandrino et al., 2001
[Eu(tta) ₃ (phen)]	0.976	Gonçalves e Silva et al., 2000
[Eu(dbm) ₃ (phen)]	1.993	Yan et al., 1997

structure of the luminescence spectrum, because of the low symmetry of the coordination site (often as low as C₁).

Malta and coworkers (Malta et al., 1997, 2002; Malta and Gonçalves e Silva, 1998; Faustino et al., 2000; de Sá et al., 2000) made a theoretical study of the intramolecular energy transfer and the luminescence quantum yields of europium(III) β -diketonate complexes. These theoretical insights can lead to a more rational design of luminescent lanthanide complexes. To describe the electronic structure of the organic part of the compounds and the coordination geometries, the so-called *sparkle model* was used (de Andrade et al., 1994, 1995, 1996; Rocha et al., 2004). This model provides the energies of the ligand singlet and triplet states, as well as the matrix elements that are required for the energy transfer rates between the ligand and the lanthanide ion. Lifetime measurements of [Eu(fod)₃] dissolved in the homologous series of *n*-alcohols give lifetimes between 425 and 475 μ s for the OH-alcohols, and between 800 and 900 μ s for the OD-alcohols (Schuurmans and Lagendijk, 2000). Table 6 presents an overview of the measured radiative lifetime for different europium(III) complexes.

Springer et al. (1967) observed that water enhances the luminescence of solid [Eu(fod)₃] and [Tb(fod)₃] complexes. Voloshin and coworkers (Kazakov et al., 1998d; Ostakhov et al., 1998; Voloshin et al., 2000a, 2000b, 2000c, 2000d, 2001a) studied this phenomenon in detail and found that addition of water to toluene solutions of lanthanide β -diketonates enhance both the luminescence intensity and luminescence lifetime. A condition is that the concentration of the β -diketonate complex in toluene is at least 10⁻⁴ M. The effect was observed for complexes of samarium(III) (Voloshin et al., 2000a, 2000b, 2000c, 2000d), europium(III)

(Kazakov et al., 1998d; Ostakhov et al., 1998; Voloshin et al., 2001a), terbium(III) (Voloshin et al., 2000a, 2000b, 2000c, 2000d). However at the same time, addition of water to toluene solutions of neodymium(III), dysprosium(III) and ytterbium(III) β -diketonates quenches the luminescence (Voloshin et al., 2000a, 2000b, 2000c, 2000d). The observation of the visible luminescence by addition of water is surprising, because it is well-known that water molecules can efficiently quench the luminescence of lanthanide ions through non-radiative exchange of the electronic energy of the lanthanide ion to the high-energy vibrational modes of the OH-groups ($\nu = 3300\text{--}3500\text{ cm}^{-1}$) (Beeby et al., 1999). The luminescence quenching by water molecules is inversely proportional to the energy gap between the emitting state and the ground state manifold. The energy gap between the luminescent state and the ground state manifold is approximately 10200 cm^{-1} for Yb^{3+} , 12000 cm^{-1} for Eu^{3+} , and 15000 cm^{-1} for Tb^{3+} . The excited states of Eu^{3+} and Yb^{3+} can be quenched by the third harmonic of the OH oscillator, and the excited state of Tb^{3+} by the fourth harmonic. However, in toluene at concentrations higher than 10^{-4} M , the lanthanide β -diketonates show significant concentration quenching due to formation of dimers. These dimers have lower luminescence quantum yields compared to the monomers due to energy losses both in the ligand and in the lanthanide ion. The presence of water in toluene causes dissociation of the poorly luminescent dimers to give monomers which are more strongly luminescent. Because of the strong quenching effect of water molecules on the near-infrared luminescence of lanthanide ions, the monomers of these complexes do not show luminescence.

Praseodymium(III) β -diketonate complexes can emit both visible and near-infrared luminescence (Voloshin et al., 2001b), from two excited states ($^3\text{P}_0$ and $^1\text{D}_2$). The near-infrared emission is more efficient than the visible luminescence. By choosing a ligand with an appropriate position of the triplet level relative to the $^3\text{P}_0$ and the $^1\text{D}_2$ levels, the emission from these two excited states can be tuned. For instance $[\text{Pr}(\text{tta})_3(\text{H}_2\text{O})_2]$ emits from the $^1\text{D}_2$ level only, because the triplet level is located below the $^3\text{P}_0$ level. On the other hand, $[\text{Pr}(\text{acac})_3(\text{H}_2\text{O})_2]$ and $[\text{Pr}(\text{dbm})_3(\text{H}_2\text{O})_2]$ emit from the two levels, because of the high-lying triplet state. By replacing the hydrogen atom in the α -position of neodymium(III) hexafluoroacetate by a deuterium and by replacement of the two coordinated H_2O molecules by D_2O molecules, it is possible to observe a strong near-infrared luminescence for this complex dissolved in CD_3OD (Hasegawa et al., 1996) or in DMSO-d_6 (Yanagida et al., 2000). The latter authors also incorporated the $[\text{Nd}(\text{hfa-D})_3(\text{D}_2\text{O})_2]$ in polymethylmethacrylate and in polyhexafluoroisopropylmethacrylate. By replacement of the C–H bond in the hexafluoroacetylacetate by a C–D bond, and by replacement of the O–H vibrations by O–D vibrations, the radiationless deactivation could be reduced to a large extent. This work has been extended to neodymium(III) complexes with other perfluorinated β -diketonates having a deuterium atom in the α -position (Iwamuro et al., 2000). The solvents used for the optical studies were methanol- d_4 and THF- d_8 . The most efficient near-infrared photoluminescence was observed for the tris[bis(pentafluorobenzoyl)methanato]neodymium(III) complex. The luminescence lifetime of the complexes dissolved in THF- d_8 was between 2.1 and 4.5 μs . Meshkova and coworkers (Meshkova et al., 1997, 1998, 2000; Meshkova and Topilova, 1998; Bol'shoi et al., 1997; Topilova et al., 1991, 1997; Rusakova et al., 1992) investigated the luminescence of lanthanide complexes of β -diketonates with perfluoroalkyl chains. In a series of

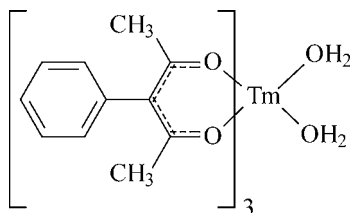


Fig. 26. Blue-emitting thulium(III) complex of 3-phenyl-2,4-pentanedione, $[\text{Tm}(\text{ppa})_3(\text{H}_2\text{O})_2]$ (Serra et al., 1998a, 1998b).

perfluorinated analogues of benzoylacetone is was found that both the luminescence intensity, the quantum yield, the lifetime and the absorptivity increased as a function of the number of carbon atoms in the perfluoroalkyl chain. This means that complexes formed by benzoyltrifluoroacetone ($R_F = \text{CF}_3$) show a less intense luminescence than complexes of comparable β -diketonates $R_F\text{COCH}_2\text{COC}_6\text{H}_5$ where the CF_3 group of benzoyltrifluoroacetone has been replaced by longer perfluorinated alkyl chains ($R_F = \text{C}_3\text{F}_7\text{--C}_8\text{F}_{17}$). The good luminescence performance is attributed to the formation of a hydrophobic shell around the lanthanide ion by the long perfluoroalkyl chains, so that water molecules cannot coordinate to the central lanthanide ion and cannot quench the luminescence. Because the improvement in luminescence output is small when the C_6F_{13} chain is replaced by an C_8F_{17} chain, it was concluded that it makes not much sense to use β -diketonates with even longer perfluoroalkyl chains. The luminescence was not only investigated for lanthanide ions that emit in the visible region (Eu^{3+} , Sm^{3+}), but also for the lanthanide ions that emit in the near infrared (Nd^{3+} , Yb^{3+}). The luminescence behavior of the tris complexes of lanthanides with fluorinated β -diketonates are comparable to that of the ternary complexes with 1,10-phenanthroline or 2,2'-bipyridine, and much better than the luminescence behavior of the tris complexes of non-fluorinated β -diketonates. Another type of ligand are those that are derived from 2-thenoyltrifluoroacetone where the CF_3 group is replaced by longer perfluoroalkyl chains. Yuan and Matsumoto (1996) also found that perfluoroalkyl chains have an enhancing effect on the luminescence of top-adducts of europium(III) β -diketonate complexes.

The thulium(III) complex of 3-phenyl-2,4-pentanedione, $[\text{Tm}(\text{ppa})_3(\text{H}_2\text{O})_2]$ is special in the sense that it is a rare example of a blue-emitting rare-earth β -diketonate (Serra et al., 1998a, 1998b) (fig. 26). Moreover, it is one of the few examples of rare-earth complexes of an α -substituted β -diketone. Upon excitation at 335 nm, characteristic emission bands of Tm^{3+} are observed at 478 nm ($^1\text{G}_4 \rightarrow ^3\text{H}_6$), 650 nm ($^1\text{G}_4 \rightarrow ^3\text{F}_4$) and 770 nm ($^1\text{G}_4 \rightarrow ^3\text{H}_6$). Thulium(III) centered photoluminescence was unexpected for this complex, because the triplet level is below the resonance level of thulium(III). It is assumed that the $^1\text{G}_4$ resonance level of thulium(III) is populated directly via transfer of the excitation energy from a charge transfer energy level.

Ward and coworkers (Shavaleev et al., 2003a) showed that the near-infrared emission of lanthanide complexes can be sensitized by visible light excitation of the electronic transitions localized on the d-metal metal chromophore of heterodinuclear d-f complexes,

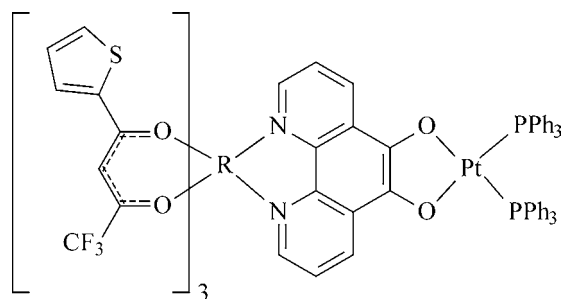


Fig. 27. Heteronuclear rare-earth complexes with a $\text{Pt}(\text{PPh}_3)_2(\text{catechol})_2$ chromophore (Shavaleev et al., 2002).
 $\text{R} = \text{La, Nd, Gd, Er, Yb}$.

Table 7
 Intensity ratios $I(^5\text{D}_0 \rightarrow ^7\text{F}_2)/I(^5\text{D}_0 \rightarrow ^7\text{F}_1)$ of europium(III) β -diketonate complexes

Complex	Intensity ratio	Reference
[Eu(hfac) ₃ (diglyme)]	6.6	Malandrino et al., 2001
[Eu(tta) ₃ (H ₂ O) ₂]	8.90	Brito et al., 2002
[Eu(tta) ₃ (opb)]	11.0	Wang et al., 2003
[Eu(hfac) ₃ (monoglyme)]	11.0	Malandrino et al., 2001
[Eu(tta) ₃ (tppo) ₂]	12.99	Brito et al., 2002
[Eu(tta) ₃ (pha) ₂]	15.50	Brito et al., 2002
[Eu(dmbm) ₃ (phen)]	16.9	Bünzli et al., 1994
[Eu(mfa) ₃ (phen)]	17.7	Bünzli et al., 1994
[Eu(bzac) ₃ (phen)]	17.8	Bünzli et al., 1994
[Eu(dbm) ₃ (phen)]	18.1	Bünzli et al., 1994
[Eu(tta) ₃ (dbzso) ₂]	20.25	Brito et al., 2002
[Eu(tta) ₃ (ptsso) ₂]	20.85	Brito et al., 2002
[Eu(mdbm) ₃ (phen)]	27.6	Bünzli et al., 1994

followed by metal-to-metal ($d \rightarrow f$) energy transfer. This principle was illustrated for platinum(II)–lanthanide(III) complexes $[\text{P}(\text{Ph}_3)_2\text{Pt}(\mu\text{-pdo})\text{R}(\text{tta})_3]$, where 5,6-dihydroxy-1,10-phenanthroline (H_2pdo) was chosen as a bisbidentate bridging ligand between a $[\text{R}(\text{tta})_3]$ complex and a platinum(II) moiety with PPh_3 ligands, and where $\text{R} = \text{Nd, Er}$ or Yb (fig. 27). These authors also made heterodinuclear rhenium(I)–lanthanide(III) complexes, that contain both a $\{\text{Re}(\text{CO})_3\text{Cl}(\text{diimine})\}$ and a $[\text{R}(\text{tta})_3]$ luminophor (Shavaleev et al., 2002, 2003c). The near-infrared emitting lanthanide ions quench the visible luminescence of the rhenium(I)-containing luminophor, which indicates that energy transfer to the lanthanide ion takes place.

In order to compare the luminescence intensities of europium(III) complexes, the ratio between the area under the emission curve of the hypersensitive $^5\text{D}_0 \rightarrow ^7\text{F}_2$ and of the magnetic-dipole allowed $^5\text{D}_0 \rightarrow ^7\text{F}_1$ can be reported. This corresponds to the intensity ratio $I(^5\text{D}_0 \rightarrow ^7\text{F}_2)/I(^5\text{D}_0 \rightarrow ^7\text{F}_1)$. These values for different europium(III) β -diketonates are listed in table 7. The higher this ratio is, the more intense is the red emission of the hypersensi-

tive ${}^5D_0 \rightarrow {}^7F_2$ transition. In general, the ratio is (much) larger than one for the β -diketonate complexes. When the ${}^5D_0 \rightarrow {}^7F_2$ transition is less intense than the ${}^5D_0 \rightarrow {}^7F_1$ transition, the emission light is orange (Thompson and Kuo, 1988). Many authors try to interpret this intensity ratio in terms of the symmetry of the Eu^{3+} site. They state that the higher the intensity ratio is, the lower is the symmetry. Of course, it is true that the ${}^5D_0 \rightarrow {}^7F_2$ transition is forbidden in a centrosymmetric system and that in this case the magnetic dipole transition ${}^5D_0 \rightarrow {}^7F_1$ is the most intense transition in the luminescence spectrum, but it is very difficult to quantify deviations from a centrosymmetric system. Moreover, the intensity of the hypersensitive transition ${}^5D_0 \rightarrow {}^7F_2$ is not only determined by the site symmetry, but by other factor such as the ligand polarizability as well. For samarium(III) complexes an analogous intensity ratio can be considered (Brito et al., 2002), namely $({}^4G_{5/2} \rightarrow {}^6H_{9/2})/({}^4G_{5/2} \rightarrow {}^6H_{5/2})$. The magnetic dipole transition ${}^4G_{5/2} \rightarrow {}^6H_{5/2}$ is found around 560 nm, and the electric-dipole transition ${}^4G_{5/2} \rightarrow {}^6H_{9/2}$ is found around 650 nm. The latter transition is the most intense in the spectrum.

It is possible to enhance the luminescence of europium(III), terbium(III), samarium(III) or dysprosium(III) β -diketonates in a micellar environment by addition of an excess of β -diketonate complexes of Y^{3+} , La^{3+} , Lu^{3+} or Gd^{3+} . This phenomenon is called “*co-luminescence*” and is due to an intermolecular energy transfer from the complexes of the enhancing ion (e.g. Y^{3+}) to the complexes of the emitting ion (e.g. Eu^{3+}). Because the concentration of the donor complexes is in general much higher than the concentration of the acceptor complexes, each acceptor complex is surrounded by many donor complexes and the emission of the acceptor is enhanced (Xu et al., 1992; Lis et al., 2002). In section 10.1, we described how co-luminescence can be used to improve the detection limit in the case of determination of trace amounts of lanthanide ions by luminescence. Terbium(III) ions can enhance the luminescence of europium(III) by intermolecular energy transfer from terbium(III) to europium(III) ions (Li et al., 1993).

The adduct formation between europium(III) β -diketonate complexes and Lewis bases can be studied by luminescence titrations (Brittain, 1979a, 1979b, 1980; Brittain and Richardson, 1976b). The principle is that the tris β -diketonate complexes are only very weakly luminescent in a non-coordinating solvent such as CCl_4 , in contrast to the adducts that are formed upon addition of the Lewis base. It is found that the formation constant depends on the Lewis acidity of the β -diketonate complex and the highest values are found for the complexes of highly fluorinated β -diketonates. Of course, the formation constant also depends on the Lewis basicity of the substrate.

Most luminescence studies on rare-earth β -diketonate complexes focus on the intensities of the electronic $f-f$ transitions. Only few studies deal with the luminescence vibronic spectra of β -diketonates. Tsaryuk et al. (1997, 1998) studied the intensity distribution in the vibronic sidebands of the electronic transitions of europium(III) β -diketonate complexes with different 1,10-phenanthroline derivatives (1,10-phenanthroline, 3,4,7,8-tetramethyl-1,10-phenanthroline, 4,7-diphenyl-1,10-phenanthroline and 5-nitrophenanthroline), and with 2,2'-bipyridine. Introduction of a nitro group in the 5-position of 1,10-phenanthroline leads to luminescence quenching in adducts of europium(III) β -diketonates with 1,10-phenanthroline (Tsaryuk et al., 2003).

Serra et al. (1998a, 1998b) trapped luminescent europium(III) and terbium(III) β -diketonates in K_2SO_4 crystals, and obtained in such a way *luminescent hourglass inclusions*. This work was inspired by the well-known hourglass crystals consisting of organic dyes trapped into K_2SO_4 crystals (Kahr et al., 1994, 1996).

Linearly polarized absorption and luminescence spectra of the tetrahexylammonium salt of tetrakis(dibenzoylmethanato)europate(III) single crystal were obtained by Blanc and Ross (1965). The crystal had a monoclinic symmetry. On the basis of the selection rules, the authors conclude that the site-symmetry must be close to S_4 . The site symmetry cannot be as high as S_4 , because of the overall monoclinic symmetry of the crystal. The research groups of Bazan and Heeger (Yang et al., 2002; Srdanov et al., 2002) observed polarized luminescence from $[Eu(dnm)_3(\text{phen})]$ in stretched polyethylene films. This work is discussed in section 7.3.

A chiral lanthanide complex emits elliptically polarized light, or to say it in other words, emits unequal amounts of left and right circularly polarized light. The emitted light can be analyzed in terms of the so-called *circular intensity differential*, $\Delta I = I_L - I_R$, or in terms of the total luminescence intensity, $I = I_L + I_R$ (Brittain, 1983, 1989). Here, I_L and I_R are the intensities of the emitted left and right circularly polarized light respectively. The quantity $g_{em} = 2\Delta I/I$ is the *emission anisotropy factor* (Riehl and Richardson, 1976; Richardson and Riehl, 1977). In *circularly polarized luminescence* (CPL) spectroscopy, ΔI is measured as a function of the wavelength. This technique is also called *circularly polarized emission* (CPE) spectroscopy. CPL spectra of chiral europium(III) β -diketonate spectra have been studied in detail (Brittain and Richardson, 1976a; Brittain, 1982a, 1982b; Chan and Brittain, 1981, 1985). For instance, the CPL spectra of the chiral shift reagent $[Eu(\text{facam})_3]$ in different neat and mixed achiral solvent systems have been measured by Brittain and Richardson (1976a). These studies showed that the CPL signals are very sensitive to the nature of the complex-solvent interactions and to the structure of the complex-solvent adducts. In simple $[Eu(\text{facam})_3]$ complexes dissolved in non-coordinating solvents, no CPL is observed. However, the binding of a substrate (Lewis base) leads to the formation of a ternary complex and this ternary complex exhibits strong CPL signals. Interestingly, optical activity can be induced in achiral β -diketonate complexes by adduct formation with chiral Lewis bases, or by dissolving the achiral complex in a chiral solvent ((Brittain and Richardson, 1977; Yang and Brittain, 1981; Brittain and Johnson, 1985). Brittain and Richardson (1977) observed CPL signals for the achiral complexes $[Eu(\text{fod})_3]$, $[Eu(\text{bzac})_3]$ and $[Eu(\text{dbm})_3]$ dissolved in the chiral solvent α -phenylethylamine. Here α -phenylethylamine acts both as the solvent and the adduct forming Lewis base. Brittain and Johnson (1985) investigated by CPL the ternary complexes formed by different the europium(III) β -diketonato complexes and the chiral (*R*)-(+)-methyl *p*-tolyl sulfoxide (MTS). The sulfoxide is able to form 1:1 or 1:2 adducts with the tris β -diketonate complexes.

Richardson and Brittain (1981) measured magnetic circularly polarized luminescence (MCPL) spectra of the complexes $[Eu(\text{thd})_3]$, $[Eu(\text{fod})_3]$, $[Eu(\text{dbm})_3]$ and $[Eu(\text{bzac})_3]$ dissolved in DMSO and DMF. MCPL is the emission analogy of magnetic circular dichroism (MCD) (Riehl and Richardson, 1977; Richardson and Riehl, 1977). In an MCPL experiment, a static magnetic field is applied to the sample, with the magnetic field lines parallel to the direction in which the emission light is detected. The Zeeman perturbation caused by the mag-

netic field will force the molecules to emit elliptically polarized light (i.e. unequal amount of left and right circularly polarized light). The aim of the study was to determine the symmetry of the europium complexes in these solvent systems, on the basis of the crystal field fine structure of the ${}^5D_0 \rightarrow {}^7F_J$ ($J = 0-4$) transitions. MCPL is a better technique to resolve crystal-field fine structure of complexes in solution than simple photoluminescence, because ΔI is a signed quantity. Moreover, MCPL is not restricted to chiral complexes. Whereas no changes in the total luminescence spectra were observed when the applied magnetic field strength was varied from 0 T to 4.2 T, the intensities of the MCPL bands (ΔI) were found to vary linearly with the magnetic field strength. The MCPL spectra could be interpreted in terms of Faraday B terms, which means that no degenerate energy levels are present in the complexes when no magnetic field is applied. The main conclusion of the study was thus that all the europium complexes have a non-axial symmetry. The absence of splitting of the ${}^5D_0 \rightarrow {}^7F_0$ transition indicated that only one monomeric species exist in solution. Later on Richardson and coworkers (Foster et al., 1983) extended these studies to the complexes [Eu(hfac)₃], [Eu(tfac)₃], [Eu(bpp)₃], [Eu(ftac)₃] and [Eu(ftac)₃(phen)]. MCPL spectra were measured in DMF and in methanol. The spectra of the tris complexes were found to show small solvent effects, what can be explained by the fact that these coordinating solvents act as Lewis bases and can form adducts with the tris β -diketonate complexes. For [Eu(ftac)₃(phen)], no solvent effects were observed in the MCPL spectra. All the complexes have a non-axial symmetry with a strong orthorhombic component. The authors found that the $I({}^5D_0 \rightarrow {}^7F_2)/I({}^5D_0 \rightarrow {}^7F_1)$ ratio in the total luminescence spectra can be correlated with the ligand polarizability (higher ratios for highly polarizable ligands). The $I({}^5D_0 \rightarrow {}^7F_2)/I({}^5D_0 \rightarrow {}^7F_1)$ ratio was also found to be sensitive to the ligand environment.

Rikken and Raupach (1997) were the first to observe magneto-chiral anisotropy (magneto-chiral dichroism), by studying the magneto-chiral luminescence anisotropy of solutions of the two enantiomers of the optically active europium(III) complex [Eu(tfc)₃] in alternating magnetic fields. The magneto-chiral anisotropy implies that the optical properties of chiral systems are different for light propagating parallel or antiparallel to the direction of the magnetic field lines. It can be considered as arising either from a magnetically induced change of natural optical activity, or from the difference in magnetic optical activity of the two enantiomers in a chiral medium. However, this effect is very weak and difficult to observe.

The luminescence observed for [Ce(thd)₄] is broad band emission and is due to a transition between the higher-energy ligand-to-metal charge transfer (LMCT) state and the lowest-energy LMCT state (Kunkely and Vogler, 2001). The LMCT excitation of [Ce(thd)₄] induces a reduction of cerium(IV) to cerium(III), and an oxidation of the ligand. The emission can be viewed as emission of cerium(III) from a metal-centered fd excited state which is generated by electron transfer from the thd ligand to cerium(IV). This behavior corresponds to that it observed for [Ru(bipy)₃]³⁺.

6.2. Electroluminescence

Electroluminescence is luminescence generated in materials under the influence of an external electric field. The light emission is caused by the recombination of electron and holes in the

material. The electroluminescence of lanthanide complexes and its application in organic light emitting diodes (OLEDs) is discussed in section 8.2.

6.3. Triboluminescence

Triboluminescence is the emission of light caused by the application of mechanical stress to crystals or by fracture of crystals (Walton, 1977; Zink, 1978; Sweeting, 2001). This phenomenon is also known as *mechanoluminescence*, *piezoluminescence* or *fractoluminescence*. The term triboluminescence comes from the Greek 'tribein', which means 'to rub'. Although triboluminescent materials have been known for 400 years (Francis Bacon observed triboluminescence when crushing sugar crystals in 1605), there is still no satisfying theory to give a general explanation for triboluminescence. Because the mechanism of triboluminescence is not completely understood yet, no predictions can be made whether or not a compound will exhibit an intense triboluminescence. This hampers the rational design of efficient triboluminescent materials. Over the years, evidence has been accumulated that separation of electric charges during fracture is a necessary condition for triboluminescence and that triboluminescence is caused by the recombination of charges separated during fracture (Dickinson et al., 1984; Das, 1973). It has been assumed that only piezoelectric (non-centrosymmetric) crystals can exhibit triboluminescence, because only such crystals can develop opposite electric charges on the opposing faces of a fracture. Zink and coworkers estimated that the correlation between triboluminescence activity and a non-centrosymmetric space group is more than 95% (Zink et al., 1976; Hocking et al., 1992). However, there are several examples of centrosymmetric crystals that are triboluminescent, and many non-centrosymmetric crystals do not show triboluminescence. Sweeting points out that impurities or disorder may play an important role in the triboluminescence activity of centrosymmetric materials (Sweeting and Rheingold, 1987; Sweeting et al., 1992; Sweeting, 2001). Rheingold and King proposed that in ionic solids that can cleave along intrinsically charged planes a non-piezoelectric surface-charging can occur, which can lead to triboluminescence, without the need of non-centrosymmetric crystal structure (Rheingold and King, 1989).

In 1966, Hurt et al. (1966) reported on the very intense triboluminescence of triethylammonium tetrakis(dibenzoylmethanato)europate(III), $(\text{Et}_3\text{NH})^+[\text{Eu}(\text{dbm})_4]^-$ (fig. 28). The triboluminescence of this compound can be observed by the naked eye. Evidence was offered for an europium-centered triboluminescence (observation of the $^5\text{D}_0 \rightarrow ^7\text{F}_2$ transition) and for the fact that the fracture process excited the ligand, which subsequently transferred the excitation energy to the europium ion. Sweeting and Rheingold (1987) found that $(\text{Et}_3\text{NH})^+[\text{Eu}(\text{dbm})_4]^-$ exists in two crystal modifications, one of which is triboluminescent and the other not. Both forms crystallize in the centrosymmetric monoclinic space group $I2/a$. The non-triboluminescent form contained co-crystallized dichloromethane solvent molecules. The triboluminescent form did not contain solvent molecules in its crystal, but was disordered. Because the two crystal forms had the same photoluminescence spectrum in the solid state, the authors concluded that the dichloromethane molecules do not quench the triboluminescence by quenching the photoluminescence. The authors claim that the disorder in the aromatic rings of the triboluminescent form is a sufficient condition to permit charge separation upon

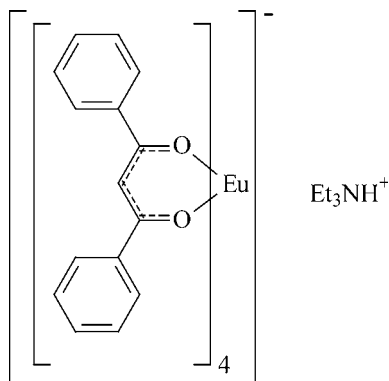


Fig. 28. Structure of the triboluminescent complex triethylammonium tetrakis dibenzoylmethanato europate(III), $(\text{Et}_3\text{NH}^+)[\text{Eu}(\text{dbm})_4]^-$.

cleavage, by creating randomly distributed sites of slightly different ionization potential and electron affinities at the faces of developing cracks. The voltage developed across the growing crack is adequate to cause an electric discharge through the surrounding gas. This discharge excited the phenyl rings of the ligands which in turn excite the f-levels of Eu^{3+} . This explanation is supported by the fact that in the non-triboluminescent form of $(\text{Et}_3\text{NH}^+)[\text{Eu}(\text{dbm})_4]^-$ no disorder is present. The triboluminescence of $(\text{Et}_3\text{NH}^+)[\text{Eu}(\text{dbm})_4]^-$ disappears when its crystals are crushed under several liquids such as dichloromethane, hexane, ethanol and water. The subsequent recovery of the triboluminescence upon removal of the liquids suggests that air is necessary for the triboluminescence and that the triboluminescence is caused by a gas discharge. Sweeting and Rheingold believe that their finding of the importance of disorder for triboluminescence of $(\text{Et}_3\text{NH}^+)[\text{Eu}(\text{dbm})_4]^-$ can be generalized to a theory which states that disorder is a sufficient condition for the triboluminescence of other centrosymmetric crystals. A non-centrosymmetric space group is neither necessary nor sufficient for triboluminescence. The $(\text{Et}_3\text{NH}^+)[\text{Eu}(\text{dbm})_4]^-$ compound of Sweeting and Rheingold has been often cited as the classical example of a disordered but non-centrosymmetric triboluminescent crystal. However, Cotton et al. (2001) reinvestigated the crystal structure of $(\text{Et}_3\text{NH}^+)[\text{Eu}(\text{dbm})_4]^-$ and found that Sweeting and Rheingold (1987) made an error in their crystal structure determination and that the crystals do not belong to the centric space group $I2/a$ but to the non-centric (and apolar) space group Ia . The possibility of second-harmonic generation (SHG) in $(\text{Et}_3\text{NH}^+)[\text{Eu}(\text{dbm})_4]^-$ also shows that this compound is non-centric (Sage et al., 1999a). Cotton and Huang (2003) confirmed that the space group $P2_1/n$ assigned by Rheingold and King (1989) to the triboluminescent and centrosymmetric crystals of piperidinium tetrakis(benzoylacetonato)europate(III) is correct. Thus centrosymmetric lanthanide compounds can exhibit triboluminescence.

The intense triboluminescence of $(\text{Et}_3\text{NH}^+)[\text{Eu}(\text{dbm})_4]^-$ stimulated further research towards analogous compounds. An obvious substitution is to replace the triethylammonium group by other protonated nitrogen bases: 2-hydroxyethylammonium (Xiong and You, 2002), pyrrolidinium (Xiong and You, 2002), dimethylbenzylammonium (Hurt et al., 1966; Xiong

and You, 2002), 2-methylpyridinium (Chen et al., 1999a), imidazolium (Chen et al., 1999b), morpholinium (Zeng et al., 2000). Different tetrakis(2-thenoyltrifluoroacetato)europate(III) complexes have been investigated as well, with the counter ion being 1,4-dimethylpyridinium (Chen et al., 1998), 1,2-dimethylpyridinium, 1,2,6-trimethylpyridinium, *N*-methylisoquinolinium and 4-aminopyridinium (Chen et al., 2001). Crystals of 1,4-dimethylpyridinium tetrakis(2-thenoyltrifluoroacetato)europate(III) are centrosymmetric (Chen et al., 1998). The observed triboluminescence is correlated with the disorders of the S atoms and the F atoms. No triboluminescence could be observed for the analogous 4-methylpyridinium (Huang et al., 1992), *N*-ethylpyridinium (Wei et al., 1983), and 3,6-bis(dimethylamine)-diphenyliodonium (Chen et al., 1997) compounds. All these compounds crystallize in centrosymmetric space groups, but in contrast to the 1,4-dimethylpyridinium compound, their S and F atoms do not exhibit disorder. Besides the tetrakis(β -diketonato)europate(III) complexes, triboluminescence has been reported for the Lewis base adducts of tris(β -diketonato)europium(III) complexes for instance [Eu(tta)₃(phen)] (Takada et al., 1997, 2000; Chen et al., 1999c; Zheng et al., 2002; Sage and Bourhill, 2001; Bourhill et al., 2001). Triboluminescence has also been described for the complex [Eu(NO₃)(tta)₂(tppo)₂], that contains a nitrate group in the first coordination sphere (Zhu et al., 1993). Although most triboluminescent complexes are monomeric species, one paper described a dinuclear β -diketonato europium(III) complex, being [Eu₂(tta)₆(pyO)₂] with pyridine-*N*-oxide as the μ^2 -bridging group (Chen et al., 1997, 2002).

Takada et al. (1997) investigated the triboluminescence of [Eu(tta)₃(phen)] and analogous compounds with substituted 1,10-phenanthrolines dispersed in polycarbonate polymer films. These polymer films were obtained by casting a dichloromethane solution containing the europium complex (10 wt%) and the polycarbonate (90 wt%) on a glass substrate. [Eu(tta)₃(phen)] and [Eu(tta)₃(5-methyl-phen)] showed triboluminescence in powder form which was strong enough to be visible in daylight, [Eu(tta)₃(5-phenyl-phen)] and [Eu(tta)₃(bath)] did not. On the other hand, in the polymer-dispersed films, all the four complexes exhibited triboluminescence and the emission intensity was almost identical for the four complexes. The fact that non-triboluminescent complexes in powder form became triboluminescent when dispersed in a polymer film suggests that the excitation mechanism are different in powder and in the polymer film. Electron impact is proposed as the mechanism of triboluminescence in the polymer-dispersed films. This effect can be caused by discharge due to the strong electric field arising from frictional electrification between the film and substrate.

The triboluminescence spectra of the europium(III) complexes are very similar to the corresponding solid-state photoluminescence spectra. The triboluminescence is in general weaker than the photoluminescence and only the most intense transitions of the photoluminescence spectrum can be observed in the triboluminescence spectrum. The other transitions are too weak to be observed. Thus europium(III) complexes exhibit a red triboluminescence due to the $^5D_0 \rightarrow ^7F_2$ transition. The difference in luminescence intensity between triboluminescence and photoluminescence may result from the different excitation mechanisms: triboluminescence results from excitation by mechanical stress and photoluminescence from excitation by ultraviolet radiation (Chen et al., 2001). Triboluminescence most likely occurs inside the crystal as cracks are formed and the triboluminescence

light must pass through the crystal to reach the detector, but photoluminescence is also emitted from the whole surface. Takada et al. (2000) investigated the triboluminescence of [Eu(tta)₃(phen)] by microphotography and their study shows that triboluminescence is only generated on crack surfaces. The metal-centered triboluminescence of the europium complexes is in contrast to the triboluminescence of classical triboluminescent materials, such as sucrose. In sucrose the triboluminescence is due to a gas discharge upon fracture. In air, its triboluminescence spectrum is identical to that of the $^3\Pi_u \rightarrow ^3\Pi_g$ transition in a nitrogen discharge, with several emission peaks between 300 and 420 nm (Zink et al., 1976; Sweeting, 2001). At present, it is not fully clear yet whether in europium(III)-containing triboluminescent materials first a nitrogen discharge takes place and that subsequently this emission of light is used to excite the organic ligand of the β -diketonate complex before finally the excitation energy is transferred to the europium(III) ion. The only known europium complex that shows at the same time a gas discharge spectrum and an europium-centered spectrum is [Eu(tta)₃(phen)] (Takada et al., 1997). (Et₃NH)⁺[Eu(dbm)₄]⁻ not only shows triboluminescence in air, but also under helium, carbon dioxide, argon and sulfur hexafluoride with negligible differences in luminescence intensity (Sweeting, 2001). On the other hand, the piperidinium analogue of (Et₃NH)⁺[Eu(dbm)₄]⁻ gave no emission under helium. The pyridinium compound is triboluminescent when placed under helium, but not when recrystallized under helium.

Although very few quantitative data are available for the triboluminescence intensities and thus the performance of different triboluminescent materials are difficult to compare, there is evidence that the strongest triboluminescence intensity is exhibited by the morpholinium tetrakis(dibenzoylmethanato)europate(III) complex (Zeng et al., 2000). At ambient temperatures its triboluminescence is circa eight times more intense than that of triethylammonium tetrakis(dibenzoylmethanato)-europate(III) complex, which occupies the second place among the most efficient triboluminescent materials. This very strong triboluminescence is attributed to the co-existence of disorder in the chelating ring and the non-centrosymmetric crystal structure. The strong dependence of small structural changes on the crystal structure and hence on the triboluminescence activity, is illustrated that in contrast to morpholinium tetrakis(dibenzoylmethanato)europate(III), *N*-methylmorpholinium tetrakis(dibenzoylmethanato)europate(III) shows no triboluminescence at ambient temperature (Zeng et al., 2000). The failure to observe a SHG-signal for the latter compound, may indicate that it crystallizes in a centrosymmetric space group and that disorder is not important (Xiong et al., 1999).

Most of the studies on triboluminescent lanthanide β -diketonate complexes focus on europium(III) as the emitting ion, but triboluminescent complexes of terbium(III), samarium(III) and dysprosium(III) have also been described (Chen et al., 1999d, 2000; Clegg et al., 2000; Sage and Bourhill, 2001). For instance, an intense green triboluminescence was observed for *p*-dimethylaminopyridine tris(1,3-*tert*-butyl-2,4-propanedionato)terbium(III).

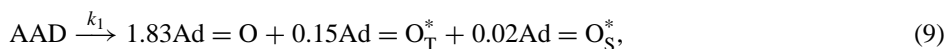
For a long time, triboluminescent materials were of academic interest only. Recently, the use of triboluminescent materials as smart sensors for structural damage monitoring has been suggested (Sage et al., 1999a, 1999b; Sage and Bourhill, 2001). Such sensors have great promise for real-time monitoring of both the magnitude and location of damages, caused by

dynamic impact events, in composite structures. Composites are modern engineering materials, which typically consist of epoxy resins reinforced with carbon fibers. These composites combine high strength and stiffness with light weight. Although composites are expensive, they are widely used in airplanes, high performance cars, sports equipment, . . . Composite panels have the disadvantage that under heavy impact they will often deform and fracture on the opposite side to that where the impact occurred. Once the impact is over and the panel has sprung back in its original shape, the damage can hardly be seen, although the composite material will now have a much lower strength. A triboluminescent compound embedded in a composite material can indicate the occurrence of structural damage by emitting light upon fracture. Besides indicating the onset of damage, the intensity of the triboluminescent light gives information on the severity of the damage. The sensor has to be designed in such a way that there is a linear relationship between the total light output from the sensor and the impact energy. However, below a certain threshold value for the impact energy, no light should be given out. The threshold value has to correspond to the impact energy that damages the material. In this way, the sensor detects damage, but will not produce false signals at lower energies. The light emitted by the triboluminescent sensor embedded into a composite material can be collected by an optical fiber and guided to a detector.

6.4. Sensitized chemiluminescence

Chemiluminescence is the non-thermal production of light by a chemical reaction (Gundermann, 1965; Haas, 1967; Cormier et al., 1973; Schreiner et al., 1983). This phenomenon occurs when an energy-releasing reaction produces a molecule in an electronically excited state and this molecule returns to the ground state by emission of light. The rare-earth β -diketonate complexes act as sensitizer of chemiluminescence. They receive the excitation energy from the excited-state species produced by the chemical reaction, and release the excitation energy by metal-centered luminescence. The direct chemiluminescence of the emissive excited-state molecules is quenched by this energy transfer. The chemiluminescence of rare-earth-containing compounds, including rare-earth β -diketonates has been reviewed by Elbanowski et al. (2000).

Rare-earth β -diketonates have been often used to enhance the emission intensity of the chemiluminescence originating from the thermal decomposition of 1,2-dioxetanes. A well-known example is adamantylideneadamantane-1,2-dioxetane, which is often abbreviated AAD (Kazakov et al., 1998c; Voloshin et al., 2000a, 2000b, 2000c). The thermolysis of the four-membered cyclic peroxide AAD results in the formation of singlet ($\text{Ad} = \text{O}_\text{S}^*$) and triplet ($\text{Ad} = \text{O}_\text{T}^*$) excited adamantanone states. The yield are given by eq. (9) (Schuster et al., 1975):



where k_1 is the rate constant of the AAD thermolysis reaction. The excited singlet state releases its energy by direct chemiluminescence ($\lambda_{\text{max}} = 420 \text{ nm}$). The chemiluminescence spectrum observed for the AAD decomposition is identical with the fluorescence spectrum of adamantanone ($\text{Ad} = \text{O}$). The structures of AAD and adamantone are shown in fig. 29. The chemiluminescence of the excited singlet state of adamantanone, $\text{Ad} = \text{O}_\text{S}^*$, is quenched

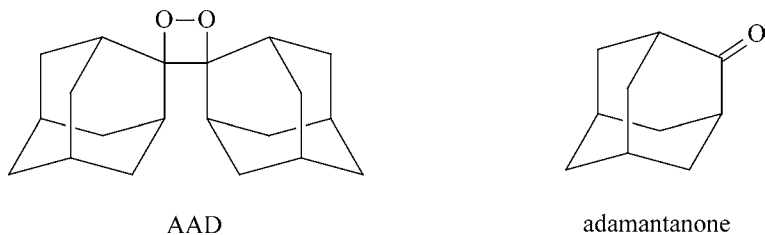


Fig. 29. Structures of adamantlylideneadamantane-1,2-dioetane (AAD) and adamantone.

upon addition of lanthanide β -diketonates and emission bands typical of the corresponding lanthanide ion appear. For all the lanthanide β -diketonates investigated, but for europium compounds, the photoluminescence and the chemiluminescence spectra coincide. For the europium β -diketonates, for instance $[\text{Eu}(\text{fod})_3]$, the chemiluminescence is not only observed from the $^5\text{D}_0$ and $^5\text{D}_1$ levels and the $^5\text{D}_1$ -chemiluminescence at 540 nm is much more efficient than the $^5\text{D}_1$ photoluminescence (Sharipov et al., 1990; Voloshin et al., 2000b). Although only very few studies report on visible photoluminescence of praseodymium(III) in solution, it is possible to observe visible chemiluminescence for $[\text{Pr}(\text{fod})_3]$ and $[\text{Pr}(\text{thd})_3]$ (Kazakov et al., 1998a). Not only visible chemiluminescence has been studied, but also the sensitized near infrared chemiluminescence of ytterbium(III) and neodymium(III) complexes (Voloshin et al., 2000a, 2000c), and of praseodymium(III) complexes (Kazakov et al., 1998b, 1998c). The chemi-excitation of the lanthanide ions occur via several mechanisms. First, the energy from the excited singlet state $\text{Ad} = \text{O}_\text{S}^*$ can be transferred to the singlet state L_S^* of the β -diketonate ligand. This process is followed by intersystem crossing to the β -diketonate triplet state L_T^* and energy transfer to the lanthanide ion (eq. (10)):



This process only occurs when the singlet excited state of the β -diketonate is at a lower energy than the singlet state of the adamantane. This is the case for $[\text{Ln}(\text{tta})_3] \cdot n\text{H}_2\text{O}$ and $[\text{Ln}(\text{btfac})_3] \cdot n\text{H}_2\text{O}$ complexes, but not for $[\text{Ln}(\text{fod})_3] \cdot n\text{H}_2\text{O}$, $[\text{Ln}(\text{acac})_3] \cdot n\text{H}_2\text{O}$ or $[\text{Ln}(\text{thd})_3] \cdot n\text{H}_2\text{O}$ complexes (Voloshin et al., 2000b). Secondly, the lanthanide complexes can be excited by energy transfer from the triplet state of the adamantane to the triplet state of the β -diketonate, followed by energy transfer to the lanthanide ion (eq. (11)):



This mechanism is possible for the lanthanide complexes of Htta, Hbtfa, Hfod, Hacac and Hthd. A third mechanism for chemi-excitation of the lanthanide ion is the intracomplex energy transfer to the excited levels of R^{3+} . This mechanism is of importance for lanthanide β -diketonates that have an unsaturated coordination sphere, such as $[\text{R}(\text{fod})_3]$ or $[\text{R}(\text{thd})_3]$. AAD can coordinate through the peroxide oxygens to the lanthanide ion and the latter catalyzes the AAD decomposition. The highest chemiluminescence intensity is observed for complexes that catalyze the AAD decomposition, e.g. $[\text{Eu}(\text{fod})_3]$ and $[\text{Dy}(\text{thd})_3]$. For instance

the chemiluminescence intensity of $[\text{Eu}(\text{fod})_3]$ is 100 times higher than that of the corresponding tta and btfa complexes. Because of the intracomplex energy transfer chemiluminescence starting from the $^5\text{D}_1$ level of Eu^{3+} is so intense. The complex formation in benzene of adamantanone with $[\text{Eu}(\text{fod})_3]$ in the ground and excited states was investigated by Ostakhov et al. (1997). Kazakov et al. (1996a, 1996b) investigated the thermolysis of AAD adsorbed on Silipore in the presence of $[\text{Eu}(\text{fod})_3]$ by chemiluminescence methods. The chemiluminescence spectra and the mechanisms were found to be the same as those in toluene solution. However, in solution the chemiluminescence intensity increases linearly with the $[\text{Eu}(\text{fod})_3]$ concentration, whereas for $[\text{Eu}(\text{fod})_3]$ on Silipore the chemiluminescence intensity varies exponentially as a function of the $[\text{Eu}(\text{fod})_3]$ concentration. Upon mechanical impact on solid particles of the complex $[\text{Eu}(\text{fod})_3(\text{AAD})]$, light emission was observed (Kazakov et al., 1995; Antipin et al., 1996). It was shown that this luminescence is chemiluminescence and not triboluminescence. Wildes and White (1971) have studied the thermal decomposition of trimethyldioxetane in the presence of $[\text{Eu}(\text{tta})_3(\text{phen})]$. The authors consider the system as a chemical source of monochromatic light, because 80% of the emitted light appears in a single band at 613 nm having a total width at half-height of about 5 nm (this is the $^5\text{D}_0 \rightarrow ^7\text{F}_2$ transition).

Studies of lanthanide-sensitized chemiluminescence on systems other than the thermolysis of 1,2-dioxetanes, include the thermolysis of diphenyldiazomethane in the presence of oxygen (Nazarov, 2000), the system $\text{H}_2\text{O}_2\text{-NaOH}$ (Kaczmarek et al., 2003) and the oxidation of hydrazine by hypochlorite (Tsaplev, 1997). Given the fact that up to date the sensitized chemiluminescence of rare-earth β -diketonate complexes has been explored for only a limited number of chemiluminescent reactions, it can be anticipated that a wealth of original research will be conducted in the near future.

7. From complexes to materials

7.1. Sol-gel glasses

Inorganic glasses are excellent transparent host matrices for trivalent lanthanide ions, and lanthanide-doped glasses have been intensively studied in the past. However, it is not easy to sensitize lanthanide luminescence in inorganic glasses, especially not when no co-doping with transition metal ions is made. Because inorganic glasses (for instance silicate, phosphate, fluoride or fluorophosphate glasses) are typically processed at very high temperatures, up to temperatures above 1000 °C, these host matrices cannot be used to trap highly luminescent lanthanide complexes such as lanthanide β -diketonates. Molecular lanthanide complexes are thermally not stable enough to withstand the high processing temperatures and the organic ligands will be decomposed. It is possible to prepare silicate and other glasses by a low-temperature route, namely by the *sol-gel route*. *Sol-gel glasses* are obtained by controlled hydrolysis of metal alkoxides. For instance, silicon alkoxides react with water and undergo hydrolysis and polycondensation, which leads to the formation of a silicate network. Besides the type of alkoxide used for the hydrolysis, important reaction parameters are r ($= \text{H}_2\text{O}(\text{mol})/\text{Si}(\text{mol})$), solvent, catalyst, pH, temperature and pressure. Water is used as a reagent in the hydrolysis reaction, but is also a by-product of the condensation reaction. A mo-

lar ratio $r = 2$ is sufficient for a complete reaction. Under most conditions however, the hydrolysis of the alkoxide is incomplete and the condensation reactions proceed simultaneously. In this case, complete hydrolysis is achieved only when $r > 10$. Alkoxysilanes and water are immiscible. Therefore a solvent in which both components are soluble, such as an alcohol, is used. The hydrolysis can be catalyzed by an acid or a base. The most often used precursors for the preparation of silica glasses via a sol-gel route are tetraethoxysilane ($\text{Si}(\text{OC}_2\text{H}_5)_4$, TEOS, also named tetraethyl orthosilicate) and tetramethoxysilane ($\text{Si}(\text{OCH}_3)_4$, TMOS, also named tetramethoxy orthosilicate). Hydrolysis of TEOS is slower than that of TMOS, because of the retarding effect of the bulkier ethoxy groups. A *sol* is a colloidal suspension of solid particles in a liquid. A *gel* is a two-component system that consists of a continuous solid and fluid phase of colloidal dimensions. The *sol-gel process* thus involves the formation of a colloidal suspension (*sol*) and further polymerization of the sol to form an inorganic network in a continuous liquid phase (*gel*). A gel from which all volatile liquids have been removed, is called a *xerogel*. Drying of the gel to obtain a (monolithic) xerogel is not the only possible processing route. A film can be made by spinning, spraying the sol or by dipping the substrate in the sol. The reader is referred to the excellent book of [Brinker and Scherer \(1990\)](#) for more information on the synthesis, structure and application of sol-gel glasses.

[Matthews and Knobbe \(1993\)](#) were the first to dope rare-earth β -diketonate complexes in a silica sol-gel glass prepared by hydrolysis of TEOS. They studied the luminescence behavior of the complexes $[\text{Eu}(\text{tta})_3(\text{H}_2\text{O})_2]$ and $(\text{pipH})[\text{Eu}(\text{tta})_4]$. The authors selected these complexes because they display an intense photoluminescence and because they are highly soluble in *N,N*-dimethylformamide (DMF). DMF is often added to starting mixture for the preparation of sol-gel glasses, since this additive prevents that the glass cracks during the drying process ([Adachi and Sakka, 1987, 1988](#)). Sol-gel glasses doped with europium(III) β -diketonate complexes showed a much higher luminescence intensity than sol-gel glasses doped with EuCl_3 . [Yan et al. \(1997\)](#) incorporated the ternary rare-earth complexes $[\text{Eu}(\text{dbm})_3(\text{phen})]$ and $[\text{Tb}(\text{acac})_3(\text{phen})]$ into a silica sol-gel glass. The luminescence lifetime of the complexes in the sol-gel matrix was found to be longer than for the pure complexes in the solid state. [Strek et al. \(1999\)](#) investigated the luminescence properties of the europium(III) complexes $[\text{Eu}(\text{acac})_3(\text{H}_2\text{O})_2]$, $[\text{Eu}(\text{bzac})_3(\text{H}_2\text{O})_2]$, $[\text{Eu}(\text{acac})_3(\text{phen})]$ and $[\text{Eu}(\text{bzac})_3(\text{phen})]$ in silica sol-gel glasses. Crystal-field fine structure could be observed in the emission spectra. A $[\text{Eu}(\text{tta})_3]$ -doped sol-gel film was made by dip-coating of a sol co-doped with europium(III) chloride and Htta ([Hao et al., 1999](#)). Upon heat treatment the europium(III) β -diketonate complex is gradually formed, which is evident from an increase in luminescence intensity. However, at temperatures above 130°C the luminescence intensity decreases rapidly due to thermal decomposition of the complex. The in-situ synthesis of europium(III) β -diketonate complexes was also used by [Fan et al. \(2004\)](#).

Not all sol-gel glasses are silica glasses. For instance, [Reisfeld et al. \(2001\)](#) investigated the luminescence of $[\text{Eu}(\text{dbm})_3]$ in a zirconia (ZrO_2) film.

7.2. Ormosils

The purely inorganic glasses that are prepared by controlled hydrolysis of metal alkoxides have some disadvantages in the sense that the solubility of the molecular luminescent lan-

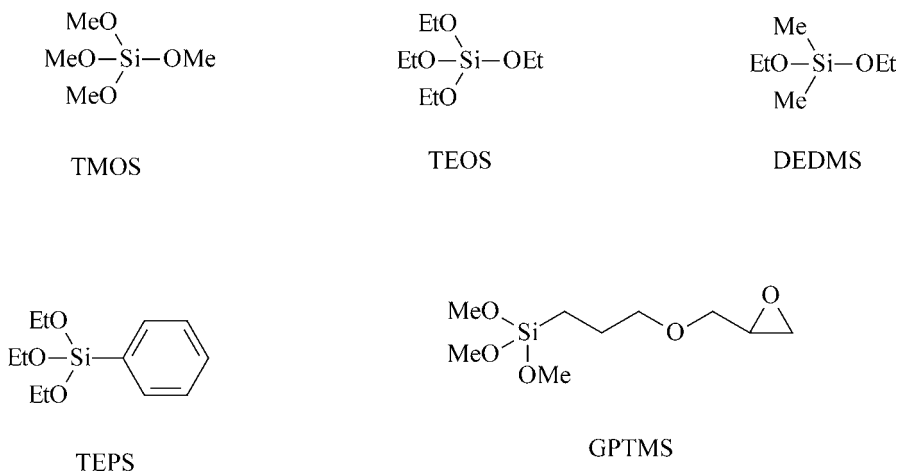


Fig. 30. Tetraalkoxysilane and organoalkoxysilane precursors for sol-gel glasses and ormosils. TMOS = tetramethoxysilane; TEOS = tetraethoxysilane; DEDMS = diethoxydimethylsilane; TEPS = triethoxyphenylsilane; GPTMS = 3-(glycidyloxypropyl)trimethoxysilane.

thanide complexes in this host is low (a few wt% at maximum). Moreover, these glasses easily crack. The water present in the pores make long drying methods necessary. These disadvantages can be overcome by designing organic/inorganic hybrid materials. Silicon-containing hybrid materials are known under the specific name *organically modified silicates (ormosils)*. The hybrid materials can be classified according to the bonding between the organic and inorganic part of the network (Sanchez and Ribot, 1994). In Class I materials, organic molecules are blended into the inorganic network. In Class II materials, the inorganic and organic constituents are linked via covalent bonds. Most of the ormosils are made by co-condensation of TEOS or TMOS with an organosilicon compounds that contains two or three alkoxide groups. An overview of important tetraalkoxysilane and organoalkoxysilane precursors used for sol-gel synthesis of ormosils is given in fig. 30.

Li et al. (1999) prepared luminescent ormosils that contained [Eu(tta)₃(phen)]. The ormosils were obtained by hydrolysis of tetraethoxysilane (TEOS) and triethoxyphenylsilane (TEPS) in a THF–EtOH–H₂O mixed solvent that contained DMF. The emission intensity of the composite material increased after immersing in a dilute ammonia solution. It is argued that part of the europium(III) β -diketonate complex is decomposed in the ormosil, because of protonation of the β -diketonate ligands by the protons provided by the solvents and the acidic silanol groups. Treatment of the ormosil with ammonia deprotonates the β -diketone, which again binds the Eu³⁺ ion. When the europium(III)-doped ormosil samples were treated with hexamethyldisilazane (HMDS), the luminescence intensity increased markedly due to the replacement of the hydroxyl groups in the matrix by trimethylsilyl groups (–OSi(CH₃)₃). This modification reduces the radiationless deactivation (multiphonon relaxation) of the excited states of Eu³⁺ by the matrix. Additionally, the ammonia released by the trimethylsilylation by hexamethyldisilazane has the same effect as a treatment with a dilute ammonia solution.

[Eu(btfac)₃(H₂O)₂] was incorporated in a sol-gel matrix that was formed by hydrolysis of vinyltriethoxysilane (Qian et al., 2001). On the basis of the splitting of the ⁷F_J levels, the authors concluded that the site symmetry of Eu³⁺ in the matrix is C₁, C₂ or C_s. Later on, the [Eu(tta)₃(bipy)]-containing hybrids were also investigated (Qian et al., 2002a). The latter authors doped [Eu(tta)₃(tpo)₂] in the same type of glass matrix, and investigated the temperature dependence of the lifetime of the ⁵D₀ level (Qian et al., 2002b). The lifetime remained almost constant in the temperature range between 13 and 100 K, but above 100 K the lifetime decreased with increasing temperature. Li et al. (2000) made a composite material by hydrolysis of tetraethoxysilane and vinyltrimethoxysilane, and they polymerized methyl methacrylate in the sol to PMMA with a radicalar reaction, with benzoyl peroxide as the initiator. The composite silicate-PMMA matrix was doped with [Eu(tta)₃(phen)]. The authors chose this matrix because the refractive index of PMMA (*n* = 1.4920) is close to that of SiO₂ glass (*n* = 1.4589), so that light scattering can be reduced. Yan (2003) doped [Tb(acac)₃(phen)] in a SiO₂/PMMA hybrid matrix. Yan and You (2002) incorporated [Tb(acac)₃(dam)] into a hybrid SiO₂/PEMA matrix (PEMA = polyethylmethacrylate). The emission intensity increased with increasing Tb³⁺ concentration and no evidence for concentration quenching was observed. This is in contrast with the terbium(III) complex in the pure PEMA polymer matrix, where the luminescence intensity reached a maximum for a Tb³⁺ content of 1%. This difference is attributed to the fact that the terbium complex can be better dispersed in the hybrid matrix than in the PEMA polymer. Guo et al. (2003) incorporated the ternary terbium(III) complex [Tb(tfac)₃(phen)] into an ormosil matrix derived from TEOS and 3-glycidoxypropyltrimethoxysilane (GPTMS). The luminescence lifetime of the terbium(III) complex in the hybrid matrix was longer than that of the same complex in a silica matrix or that of the pure [Tb(tfac)₃(phen)] complex. [Eu(fod)₃(H₂O)₂] was doped into an inorganic-organic hybrid material, that was formed by hydrolysis of TEOS and *N*-[3-(trimethoxysilyl)propyl]-ethylenediamine (de Farias et al., 2002a). The europium(III) complex was introduced in the hybrid matrix after synthesis of the matrix, and stirring an ethanolic solution of the europium(III) complex with the insoluble matrix. Qian and Wang (2001) prepared in situ an [Eu(tta)₃(tpo)₂] complex in an ormosil matrix made of a starting mixture of TEOS, 3-glycidoxypropyltrimethoxysilane and methyl methacrylate (+0.4 wt% of benzoyl peroxide). A solution of Htta, tppo and EuCl₃ in ethanol (3:2:1 molar ratio) was added to the starting solution for sol-gel synthesis. The precursor solution became a wet gel after a few days of gelation at 40 °C. A transparent monolithic sample was obtained after a prolonged drying period. The [Eu(tta)₃(tpo)₂] complex was formed in the sol-gel matrix by heat treatment at 100 °C for 24 hours. The intensity of the ⁵D₀ → ⁷F₂ transition in the heat-treated sample was a factor of about 1400 higher than in the sample before heat treatment. The β-diketonate complex had to be prepared in situ because it is not stable under the conditions at which the sol-gel matrix is synthesized (pH = 2). Upon co-doping of an ormosil made of TEOS and 3-glycidoxypropyltrimethoxysilane with [Eu(tta)₃] and [Tb(ssa)] (where H₃ssa is sulphosalicylic acid), europium(III)- and terbium(III)-centered emission could be observed simultaneously (Fan et al., 2002). By adjusting the ratio of the concentration of the metal complexes, the luminescence color could be tuned. Di-ureasils are made of a polyethylene chains of varying length that are grafted via both ends to a

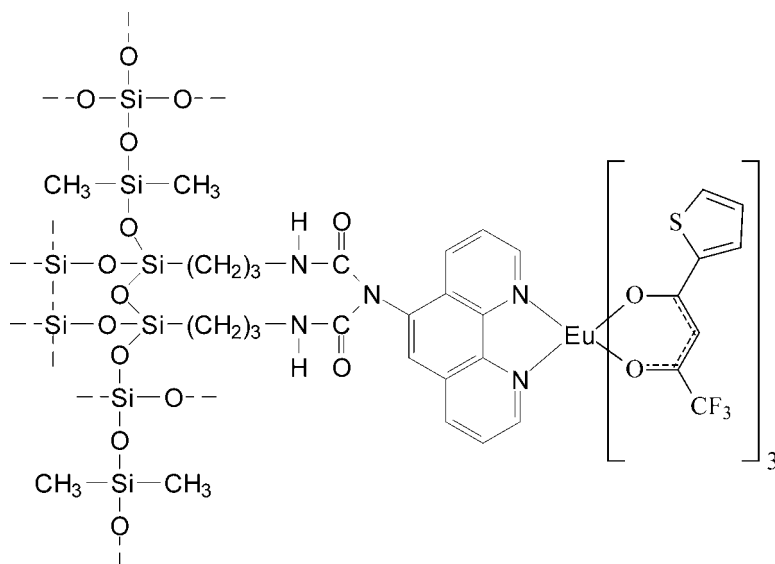


Fig. 31. $[\text{Eu}(\text{tta})_3(\text{phen})]$ complex covalently links to an ormosil matrix (after Binnemans et al., 2004).

silica network. These hybrid materials form transparent, elastomeric monoliths, and are able to dissolve luminescent guest molecules in high concentration (Bekiari et al., 1999; Carlos et al., 1999, 2000a, 2000b, 2002; Sá Ferreira et al., 2001). Carlos et al. (2002) doped complexes of Eu^{3+} , Tb^{3+} and Tm^{3+} with benzoyltrifluoroacetate ligands into these di-ureasils. Moleski et al. (2002) introduced $[\text{Eu}(\text{tta})_3(\text{bipy})]$ into thin films of di-ureasil gels.

Nassar et al. (2001) covalently bound β -diketones (Hacac, Hbtfa, Hdbm and Hhfa) to a functionalized silica that was obtained by a sol-gel reaction between TEOS and 3-chloropropyltrimethoxysilane. The β -diketones in their sodium form reacted with the functionalized silica, so that the β -diketones became linked to the silica matrix via the α -carbon. Afterwards complexes of the β -diketones with Eu^{3+} were formed, in the presence of 1,10-phenanthroline or 2,2'-bipyridine as co-ligands. Sigoli et al. (2001) prepared a macroporous silica matrix by hydrothermal treatment of Pyrex glass. The silanol groups on the surface of this matrix were modified by reaction with 3-chloropropyltrimethoxysilane, and the modified matrix was subsequently reacted with $[\text{Eu}(\text{tta})_3(\text{H}_2\text{O})_2]$. The luminescence of this material was compared with the one of the $[\text{Eu}(\text{tta})_3(\text{H}_2\text{O})_2]$ complex adsorbed on the surface of the macroporous silica (that was not treated with 3-chloropropyltrimethoxysilane). The matrix with adsorbed europium complex has a slightly smaller $({}^5\text{D}_0 \rightarrow {}^7\text{F}_2)/({}^5\text{D}_0 \rightarrow {}^7\text{F}_1)$ intensity ratio than the matrix with the anchored europium complex. Binnemans et al. (2004) used 5-amino-1,10-phenanthroline to covalently link the luminescent $[\text{Eu}(\text{tta})_3(\text{phen})]$ complex to an ormosil matrix (fig. 31). The glass matrix was prepared by first reacting 5-amino-1,10-phenanthroline with 3-(triethoxysilyl)propyl isocyanate, and the resulting compound was condensed with tetramethoxysilane (TEOS) and diethoxydimethylsilane (DEDMS) at a neutral

pH to a sol-gel glass. Reaction of the sol-gel glass with $[\text{Eu}(\text{tta})_3(\text{H}_2\text{O})_2]$ resulted in the final luminescent ormosil material.

7.3. β -Diketonates in polymer matrices

Polymers are interesting host matrices for lanthanide complexes, including β -diketonate complexes. These materials have several advantages. First of all, by incorporation of luminescent lanthanide complexes, useful optical materials can be obtained. Powdered samples of lanthanide complexes, either in the neat form or dispersed into potassium bromide pellets, can be used for fundamental spectroscopic and photophysical properties, but the processability of such powder samples is low. In order to make them suitable for applications, the lanthanide complexes can be incorporated into polymers. Polymers are much easier to process. For instance, polymer films can be obtained by spin coating or by melt casting. It is not only possible to obtain polymer films, but objects of virtually any desired shape (sheets, rods, fibers, ...) or size can be made from polymeric materials. Polymers have several advantages over glasses besides the better processability, such as lighter weight and flexibility. In general the production of polymers is cheaper than that of glasses, and much less energy is required. The lanthanide β -diketonate complexes can be incorporated in many types of optical transparent polymers. Examples are polymethylmethacrylate (PMMA), polyvinylalcohol (PVA), polyethylene (PE), polystyrene (PS), polyurethanes, polyesters, polycarbonates, polyimides and epoxy resins. Of interest as a host matrix for infrared luminescent lanthanide complexes are fluorinated or deuterated polymers (fig. 32). Examples of perfluorinated polymers are CYTOP (Cyclic Transparent Optical Polymer; developed by Asahi Glass Company) and poly(hexafluoro isopropyl methacrylate) (P-FiPMA). An example of a deuterated polymer is deuterated poly(methylmethacrylate) (PMMA- d_8).

There are different methods for incorporating rare-earth β -diketonate complexes into polymers. First of all, one has to make the difference between host-guest systems and systems in which the rare-earth complexes are an integral part of the polymer. In a host-guest system, the rare-earth complex is dissolved into the polymer matrix. To make host-guest systems, two techniques can be used (Gao et al., 1998). The first technique involves dissolution of the rare-earth complexes directly into the monomer. After addition of an appropriate initiator,

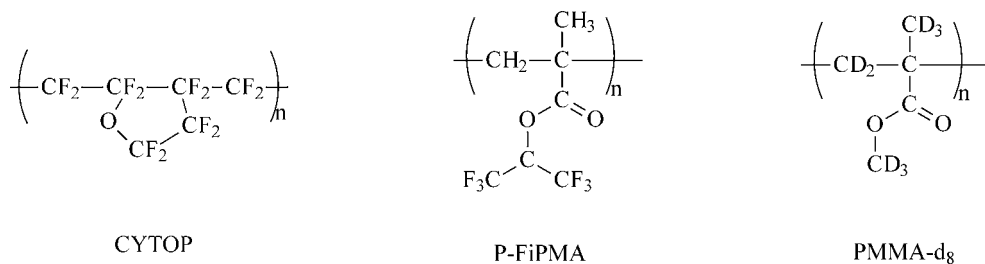


Fig. 32. Examples of fluorinated and deuterated polymers that can be used as a host matrix for near-infrared emitting rare-earth β -diketonate complexes.

the monomer solution is polymerized by either thermal polymerization or photopolymerization to form a uniformly doped polymer. According to the second technique, the rare-earth complex and the pure polymer are both dissolved in a co-solvent. The solvent is then evaporated, and a uniformly doped polymer is obtained. Rare-earth complexes that contain polymerizable groups can be copolymerized together with another monomer. This results in a copolymer in which the rare-earth complex is part of the polymer backbone or of the side chain. Alternatively, a polymer with pendant ligand such as 1,10-phenanthroline can form adducts with tris β -diketonate complexes. By incorporation of β -diketonate complexes into polymers the dissociation of the complexes that is often observed in solution can be suppressed, although it is sometimes difficult to exclude dissociation. One has to be aware of the fact that during the processing of the polymer, the complexes can dissociate in coordinating solvents. Gao et al. (1998) investigated the effect of dissociation of the samarium(III) and europium(III) β -diketonate complexes on the optical properties of the doped PMMA polymers. In contrast to the benzoyltrifluoroacetato complexes, the hexafluoroacetylacetonato complexes $[\text{Sm}(\text{hfac})_4]^- (\text{Et}_4\text{N})^+$ and $[\text{Eu}(\text{hfac})_4]^- (\text{Et}_4\text{N})^+$ were found to be quite stable and do not show evidence for dissociation. By dispersion β -diketonate complexes into polymers, it is possible to reduce the concentration quenching of the luminescence.

The first experiments on optical materials based on polymers doped with β -diketonate complexes go back to the 1960's when rare-earth β -diketonates have been tested as active components in chelate lasers (see section 8.1). For instance, Wolff and Pressley (1963) doped $[\text{Eu}(\text{tta})_3]$ into a polymethylmethacrylate (PMMA) matrix and observed laser action in this material. Huffmann (1963a) described laser action of $[\text{Tb}(\text{tta})_3]$ in these same type of polymer matrix. After this initial interest in lanthanide-doped polymers, during the next three decades not much further research has been done on these materials. Recently, luminescent lanthanide-containing polymers regained interest, because of their possible application in light-emitting diodes (LEDs) and in optical amplifiers and waveguides. The application of rare-earth doped polymers in LEDs is reviewed in section 8.2, and the application in optical amplifiers and waveguides in section 8.3. Here we also mention the reviews of Kuriki et al. (2002) and of Kido and Okamoto (2002) in the thematic *Chemical Reviews* issue "*Frontiers in Lanthanide Chemistry*".

The luminescence behavior of $[\text{Eu}(\text{dbm})_3]$ and $[\text{Eu}(\text{dbm})_3(\text{phen})]$ in PMMA was investigated (Liu et al., 2003, 2004b). Europium(III) doped polymer films were made by dissolution of PMMA and the europium(III) complex in chloroform, followed by casting of the solution on a clean glass or quartz slide, and evaporation of the solvent. The lifetimes of the $^5\text{D}_0$ level of the two complexes in PMMA were found to be different. The decay curve of $[\text{Eu}(\text{dbm})_3(\text{phen})]$ in PMMA could be fitted by a single exponential function, whereas the decay of $[\text{Eu}(\text{dbm})_3]$ in PMMA is bi-exponential. These results indicate that all Eu^{3+} ions experience the same environment in $[\text{Eu}(\text{dbm})_3(\text{phen})]$, but different environments in $[\text{Eu}(\text{dbm})_3]$. Liu et al. (2004a) doped $[\text{Eu}(\text{dbm})_3(\text{H}_2\text{O})_2]$ and $[\text{Eu}(\text{tta})_3(\text{H}_2\text{O})_2]$ complexes into a poly(vinylpyrrolidone) (PVP) matrix. It was shown by XRD that the complexes can be dispersed well in the polymer matrix. There is evidence that the water molecules in the complexes are partially replaced by C=O groups of the PVP polymer. The absorption and

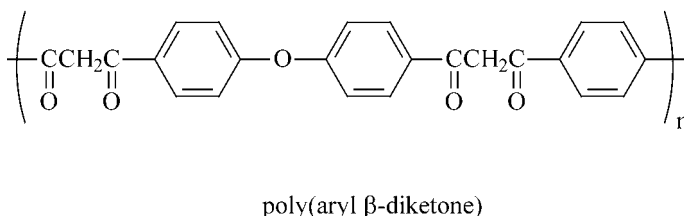
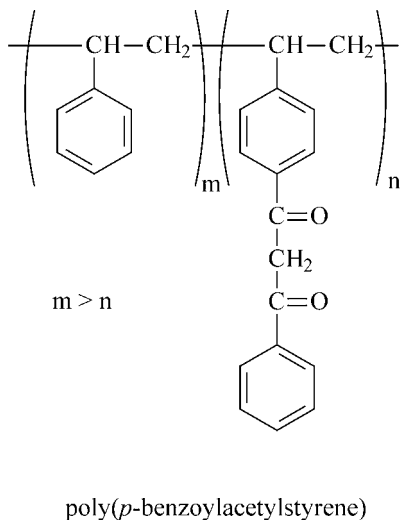


Fig. 33. Polymeric β -diketones (adapted after Ueba et al., 1980).

luminescence spectra of $[\text{Sm}(\text{dbm})_3]$ in PMMA were measured by Dong et al. (2004). These authors also determined the Judd–Ofelt intensity parameters for this system.

Ueba et al. (1980) made europium(III) complexes of β -diketone-containing polymers (fig. 33). In this way, it was possible to attach the Eu^{3+} ion directly to the polymer, either through the backbone or through the side chain. The europium-containing polymers were prepared by adding an EuCl_3 solution in tetrahydrofuran and methanol (1:1 v/v) to a tetrahydrofuran solution of the polymers (1–2% solution). The pH of the solution was adjusted to pH 8 by adding piperidine. The polymer precipitated and could be recovered by filtration. The luminescence intensity reached a maximum at an Eu^{3+} content of 1% wt and remained constant with further increasing Eu^{3+} content.

Upon addition of dibenzoylmethanate ligand to a styrene-co-acrylic acid oligomer complex, Tang and coworkers (Tang et al., 1999a) found an increase of the photoluminescence intensity of Eu^{3+} . These authors (Tang et al., 1999b) also observed an intense luminescence

for a ternary complex formed between europium(III) ion, dbm ligands and oligoacrylic acid. Pagnot et al. (2000) investigated by scanning near-field optical microscopy (SNOM) the photostability of $[\text{Eu}(\text{dbm})_4](\text{piperidinium})$ complexes in polystyrene thin films. As could be expected, the photostability of this β -diketonate complex was found to be quite low. de Farias et al. (2002b) doped $[\text{Eu}(\text{fod})_3(\text{H}_2\text{O})_2]$ and $[\text{Eu}(\text{fod})_3(\text{terpy})]$ into films of 3-trimethylsilylpropyl)ethylene diamine and of an acrylic resin, and these authors studied the luminescence properties of these films. The luminescence properties of $[\text{Eu}(\text{tta})_3(\text{H}_2\text{O})_2]$ into an epoxy resin were investigated by Parra et al. (2002). The epoxy resin was a diglycidyl ether of bisphenol-A (Araldite GT 7004). The epoxy matrix acts as an antenna which absorbs light and channels it to the europium(III) ion. The same authors also doped $[\text{Tb}(\text{acac})_3(\text{H}_2\text{O})_4]$ in the epoxy resin (Parra et al., 2004). Allan et al. (1992) tested europium(III) tetrakis β -diketonate complexes as pigments for polystyrene. Oxygen sensors made of fluoropolymers doped with europium(III) complexes are described in section 10.4.

Kuriki et al. (2001, 2002) doped the complexes of deuterated 1,1,1,2,2,6,6,7,7,7-decafluoro-3,5-heptanedione, $[\text{R}(\text{fhd-}d)_3]$ ($\text{R} = \text{Pr, Nd, Er, Tm}$) into a perfluorocarbon liquid (3M PF-5080) and into the perfluorinated polymer CYTOP. A comparison of the peak positions in the emission spectrum of $[\text{Nd}(\text{fhd-}d)_3]$ in PMMA- d_8 with that of the same complex in a perfluorocarbon liquid shows that the ${}^4\text{F}_{3/2} \leftarrow {}^4\text{I}_{9/2}$ transition in PMMA- d_8 is shifted to shorter wavelengths (Kuriki et al., 2002).

Wang et al. (2000b) made europium(III) containing copolymers by co polymerization of methyl methacrylate and $[\text{Eu}(\beta\text{-diketonato})_2(\text{aa})]$ complexes that contain two β -diketonate ligands (tta, acac, bzac and dbm) and one acrylate ligand. The europium(III) complexes were synthesized by the reaction of 1 equivalent of europium(III) isopropoxide with 2 equivalents of a β -diketonate and 1 equivalent of acrylic acid in a 1:1 mixture of anhydrous 2-propanol and anhydrous benzene. The copolymers were prepared by radical copolymerization of the europium(III) complexes with methyl methacrylate in DMF, using AIBN as the initiator. The copolymers were found to be soluble in chloroform, 1,2-dichloroethane, THF, benzene and toluene, and could be easily cast into uniform thin films with good mechanical flexibility and high thermal stability. The number average molecular weight (M_n) of the copolymers was in the range between 53700 and 72600, whereas the polydispersity index (PDI) was between 4.79 and 5.96. These M_n values are lower than of the homopolymer PMMA that was obtained by the same polymerization technique, whereas at the same time the polydispersity was higher. The luminescence intensities, the luminescence lifetimes and the intensity ratio (${}^5\text{D}_0 \rightarrow {}^7\text{F}_2$)/(${}^5\text{D}_0 \rightarrow {}^7\text{F}_1$) of the europium(III)-containing copolymers are higher than those of the corresponding europium(III)-containing monomers and of blends of the europium(III) complexes with PMMA. The emission intensities increased linearly with increasing europium(III) content, and no significant concentration quenching of the luminescence could be observed in the concentration range between 0 and 6.39 mol% Eu^{3+} . This latter effect is due to the fact that the europium(III) complexes are uniformly distributed along the polymer backbone, so that $\text{Eu}(\text{III})\text{-Eu}(\text{III})$ interactions are avoided. The luminescence intensity of the copolymers depend on the β -diketonate ligand and increased in the order $\text{acac} < \text{bzac} < \text{dbm} < \text{tta}$. A luminescent europium(III)-containing copolymer suitable for OLED applications was prepared by radical copolymerization of 9-vinylcarbazole, methyl methacry-

late and [Eu(bzac)₂(phen)(aa)] complex. The carbazole group was incorporated for its hole-transporting properties. The function of the europium(III) compound is electron transport and light emission (see also section 8.2). Not only acrylate groups have been used to graft rare-earth β -diketonate complexes to a polymer matrix, but also neutral N-donor polydentate ligands such as 2,2'-bipyridine. Pei and coworkers (Pei et al., 2002) grafted [Eu(dbm)₃], [Eu(tta)₃] and [Eu(ntac)₃] to a fluorene type of conjugated polymer by complex formation via 2,2'-bipyridine groups in the side chains. The complexes were prepared by heating at reflux for 2 days a solution of the polymer and an europium(III) complex in a 1:1 mixture of THF and ethanol. The authors made special efforts to purify the europium(III)-containing polymer. After synthesis, the polymer was placed in a Soxhlet-extractor and extracted with hot acetone for 2 days, in order to remove all the excess of the europium(III) β -diketonate complex. In these electroluminescent polymers, the blue light emitted by the fluorene groups is transformed into red light by energy transfer to the europium(III) ion. The best efficiency for energy transfer from the blue-emitting conjugated polymer to the europium(III) ion was observed for the [Eu(dbm)₃] complex. No concentration nor self-quenching was observed. Feng and coworkers (Feng et al., 1998) formed lanthanide(III) grafted polymers by reaction between [Eu(tta)₃] and polymer-bound triphenylphosphine, triphenylarsine, triphenylstibine, or triphenylbismutine. It was assumed that the P, As, Sb or Bi group of the polymer interacts with the lanthanide(III) ion (R = Sm³⁺, Eu³⁺, Tb³⁺). Among the europium(III)-containing polymers, the best luminescence performance was observed for the polymer-bound triphenylarsine system. By coupling a functionalized dibenzoylmethane ligand to poly(lactic acid) through an ester bond, site-isolated luminescent europium(III) complexes were obtained (Bender et al., 2002).

Linearly polarized photoluminescence arises from lanthanide ions doped into uniaxial single crystal hosts, such as LaCl₃, LaF₃ or LiYF₄. Lanthanide ions doped in polycrystalline materials or lanthanide complexes in solution give unpolarized photoluminescence. Because the lanthanide β -diketonate complexes are obtained as polycrystalline or as single crystals too small for optical spectroscopy, the luminescence of lanthanide β -diketonates is unpolarized. Polarized luminescence could be useful for several applications (for instance for obtaining polarized light sources) and it is therefore a challenge to obtain linearly polarized emission from lanthanide chelates. Two mechanisms can lead to polarized emission from lanthanide ions (Feofilov, 1961): (a) polarized absorption by oriented ligands; (b) polarized emission depending on the site-symmetry of the lanthanide ion. The research groups of Bazan and Heeger (Yang et al., 2002; Srdanov et al., 2002) were able to observe polarized emission from [Eu(dnm)₃(phen)] in stretched polyethylene films. The presence of the rigid naphthyl groups allows the three β -diketonate ligands to align parallel to the direction in which the polymer film has been stretched. This results in a quasi-uniaxial alignment of the chelate complex. The emission of Eu³⁺ was found to be highly polarized. When the luminescence was detected with the polarization parallel to the orientation direction of the film, intensity of the strongest emission line of the ⁵D₀ → ⁷F₂ manifold (ca. 612 nm) increased by a factor of 10 when the polarization of the incident beam was changed from perpendicular to parallel to the orientation direction of the film. The reason of these intensity differences is that the aligned chromophores of the β -diketonate ligands absorb light more strongly when the incident light beam is parallel

to the orientation direction of the polymer film. More light absorption by the ligands means that more energy can be transferred to the Eu^{3+} ion. When the experimental setup is changed, so that the incident light beam is always parallel to the orientation direction of the film and that now the luminescence is detected either parallel or perpendicular to the orientation direction, the crystal-field transitions of the ${}^5\text{D}_0 \rightarrow {}^7\text{F}_J$ transitions are found to be polarized. However, in this case the differences in total luminescence intensity are less pronounced. The fact that the crystal-field fine structure of the ${}^5\text{D}_0 \rightarrow {}^7\text{F}_2$ transitions in solid $[\text{Eu}(\text{dnm})_3(\text{phen})]$ differs from the fine structure observed for $[\text{Eu}(\text{dnm})_3(\text{phen})]$ in the stretched polymer film, indicates that the β -diketonate ligands re-arrange upon stretching.

7.4. β -Diketonates in zeolites

Zeolites are microporous crystalline aluminosilicates, whose general formula can be represented as $\text{M}_{x/n}^{n+}[(\text{AlO}_2)_x(\text{SiO}_2)_y] \cdot m\text{H}_2\text{O}$ (Breck, 1974; Barrer, 1978; van Bekkum et al., 1991). Their structure consists of $[\text{AlO}_4]^{5-}$ and $[\text{SiO}_4]^{4-}$ tetrahedra linked by bridging oxygen atoms to a three-dimensional network. The negative electric charge generated in the framework when a silicon atom is isomorphically replaced by an aluminum atom, must be compensated by counter-ions M^{n+} present in the micropores of the zeolite. In this way, zeolites act as ion exchangers. The pores of the zeolites have a very regular shape and size and are defined by the crystal structure of the zeolites. A typical feature of zeolites is also the presence of large central cavities, the so-called *super cages*.

Zeolites in which the sodium counter ions have been replaced by lanthanide ions, are starting materials for efficient luminescent materials. The luminescence efficiency of purely Eu^{3+} -doped zeolites is very low (quantum yield lower than 1% for Eu-X) (Sendor and Kynast, 2002). Although this is partly due to the presence of water molecules in the zeolite cage, dehydration experiments show that this is not the only cause: even after dehydration the quantum yield remained as low as 5%. The main cause seems to be a low-lying $\text{O} \rightarrow \text{Eu}^{3+}$ charge transfer band, which efficiently deactivates the excited state of Eu^{3+} . Because of the weak absorption by the $f-f$ transitions of Eu^{3+} , the total luminescence output remains low, and one has to rely on the antenna effect to increase the luminescence efficiency. A tremendous gain in luminescence intensity is observed when the europium ions in the cage are complexed with β -diketonate ligands. Sendor and Kynast (2002) found an increase by a factor of 350 after treatment of a $\{\text{Eu}_8\text{-X}\}$ sample (i.e. a zeolite-X with 8 Eu^{3+} ions per unit cell) with an excess of Htta, followed by washing and rehydration. The rehydration step is necessary for complex formation. Otherwise the Htta ligands cannot be deprotonated in the zeolite cage and the Eu^{3+} ions cannot be released from the walls of the super cage. The luminescence efficiency depends on the $\text{Eu}:\text{tta}$ ratio. A strongly emissive species was found to be $\{[\text{Eu}(\text{tta})_3]\text{-X}\}$, where the complexes remain attached to the zeolite cage. Increasing of the number of Eu^{3+} ions per unit cell results in an exaltation of the luminescence intensity up to 8 Eu^{3+} per unit cell. Further addition of Eu^{3+} leads to a decrease in the luminescence intensity. The corresponding complex can be represented as $\{[\text{Eu}_8(\text{tta})_{13,5}]\text{-X}\}$. Bright luminescent materials could also be obtained by encapsulating $[\text{Eu}(\text{tta})_3(\text{phen})]$ in to the zeolite cage. In this case, the β -diketonate complex is no longer linked to the walls of the zeolite cage. The increase in luminescence intensity of

Eu³⁺-doped zeolites by complex formation with β -diketonate ligands can be illustrated by a spectacular experiment (Sendor and Kynast, 2002). {Eu₈-X} does hardly show visible luminescence upon irradiation by a 366 nm UV source. However when solid Htta is added to a vial containing {Eu₈-X} powder and the mixture shaken, a bright red luminescence is visible within a few seconds.

Alvaro et al. (1998) investigated the encapsulation of europium benzoyltrifluoroacetate complexes in zeolite-Y and mordenite. The Eu:ligand ratio was in all cases lower than the ratio expected for a 1:3 complex. For instance, for zeolite-Y no Eu:ligand ratios higher than 1:1.35 could be obtained. Because of steric hindrance, the pores of the zeolite-Y and mordenite are too small to host a [Eu(bfa)₃] or even a [Eu(bfa)₂]⁺ complex. The most abundant species seems to be [Eu(bfa)]²⁺. Encapsulation of the europium complexes in the zeolite matrix resulted in an increase of the luminescence lifetime in comparison with the complexes in solution. An increase in lifetime by a factor 2 was found when the zeolite-Y containing [Eu(bfa)]²⁺ complex was dehydrated and rehydrated by D₂O. Surprisingly no difference in lifetime was found when a zeolite-Y containing Eu³⁺ without organic ligands was treated by the same procedure.

The mesoporous silicate MCM-41 (Mobil Corporation Material 41) is closely related to the zeolites. MCM-41 contains a hexagonal array of mesoporous with a pore diameter ranging between 20 and 100 Å (Kresge et al., 1992; Beck et al., 1992). These pores are large enough to encapsulate rare-earth β -diketonate complexes, without the need of the “ship-in-the-bottle” approach which is necessary for introduction of these complexes in classic zeolites. Xu et al. (2000) were the first to use MCM-41 as a host for a luminescent europium β -diketonate complex. Before encapsulation of [Eu(tta)₄]⁻(C₅H₅NC₁₆H₃₃)⁺, the authors modified MCM-41 with *N*-(3-trimethoxysilyl)ethylethylenediamine in order to reduce the number of silanol groups in the host matrix. The high energy vibrations of the Si-OH groups would otherwise quench the luminescence of the europium ion, at least to some extent. The most remarkable property of the europium complex in the modified MCM-41 is the very strong intensity of the hypersensitive transition ⁵D₀ → ⁷F₂ at 612 nm. The author even report that the intensity ratio (⁵D₀ → ⁷F₂)/(⁵D₀ → ⁷F₁) is +∞, because the ⁵D₀ → ⁷F₁ could not be observed. Of all the luminescent europium complexes presently known, this material has the highest color purity. The intensity ratio for the same europium complex in unmodified MCM-41 is only 5.5. The intensity increase has been attributed to the reduced size of the pores in the modified MCM-41 (14.26 Å) in comparison with the unmodified MCM-41 (29.31 Å). The europium complex with a diameter of about 12 Å can enter the pores of the modified MCM-41 matrix, but NH-groups of the modifying agent form strong H-bonds with the F-atoms of the thenoyltrifluoroacetate ligands. Due to this H-bonding the symmetry of the complex is decreased, and this renders the electric dipole transition ⁵D₀ → ⁷F₂ dominant. The luminescence lifetime of the complex [Eu(tta)₄]⁻(C₅H₅NC₁₆H₃₃)⁺ in the modified MCM-41 matrix (2.18 ms) is much longer than that of neat [Eu(tta)₄]⁻(C₅H₅NC₁₆H₃₃)⁺ powder (0.84 ms). Encapsulation of the europium complex in the MCM-41 host improved the photostability of the complex as well. Fu et al. (2002) modified MCM-41 by 3-aminopropyltriethoxysilane (APTES) or *N*-[(3-triethoxysilyl)propyl]ethylenediamine (TEPED), and encapsulated the europium complex [Eu(dbm)₃(phen)] in the modified hosts. In this case, the (⁵D₀ → ⁷F₂)/(⁵D₀ → ⁷F₁) ratio was

much lower (2.7 for the host modified by APTES and 1.7 for the host modified by TEPED) than for the tetrakis(thenoyltrifluoroacetato)europate(III) complex discussed above. Yao et al. (2000) encapsulated the $[\text{Eu}(\text{tta})_3]$ complex in the mesoporous molecular sieve MCM-41. The $[\text{Eu}(\text{tta})_3]$ molecules were found to be present within the cetyltrimethylammonium micelles that were used as template to prepare MCM-41. Acid treatment of the molecular sieve to remove the surfactant template also removed the europium(III) complex. Europium luminescence was not observed in the precursor solution that was used to make the molecular sieve. A luminescent complex is formed upon heat treatment, because the tta molecules can then diffuse to the Eu^{3+} sites to form $[\text{Eu}(\text{tta})_3]$ complexes. The luminescence lifetime of $[\text{Eu}(\text{tta})_3]/\text{MCM-41}$ (228 μs) was found to be similar to that measured for $[\text{Eu}(\text{tta})_3]$ in ethanolic solution (226 μs). Fernandes et al. (2002) incorporated $[\text{Eu}(\text{thd})_3]$ and $[\text{Eu}(\text{dbm})_3]$ complexes in MCM-41, either by wet impregnation of the MCM-41 with a solution of the europium(III) complex or by reaction between the matrix and the europium(III) complex in the gas phase. The europium(III) complexes were immobilized on the silica matrix by grafting them on the free silanol groups at the surface. The luminescence spectra of the europium(III) complexes were modified after incorporation in the MCM-41, but ligand-to-metal energy transfer could still be observed.

7.5. Langmuir–Blodgett films (LB films)

The Langmuir–Blodgett technique allows the deposition of ordered monolayers or ordered multilayers on a substrate. The method is applicable to amphiphilic molecules, i.e. molecules with a polar head group and an apolar chain. It is also possible to incorporate smaller molecules into a Langmuir–Blodgett film, but then amphiphilic co-reagents have to be used. In order to make a Langmuir–Blodgett film (LB-film), the compound is first dissolved in chloroform and the chloroform solution is poured on to a water surface in a so-called Langmuir trough, which is a water basin coated with Teflon[®]. The amphiphilic molecules are present at the water/air interface, so that their polar head groups are pointing toward the water, and their apolar chains toward the air. The molecules float freely on the water surface, and no order exists. The molecules can be considered as forming a “2D gas phase”. When two parallel barriers are moved over the water surface toward each other, the amphiphilic molecules are forced to come closer to one another. At a certain point when the area between the barriers is small enough, the molecules start to feel one another, and they no longer move independently of one another. They can now be considered as forming a liquid phase. When the barriers are further brought together, the molecules are forced to line up with the alkyl chains perpendicular to the water surface, and now an ordered monolayer is formed on the water surface: the Langmuir monolayer. In the latter, the molecules are ordered as in of a crystalline solid. The monolayers can be transferred to a substrate by dipping the substrate into the ordered monolayer. Repetition of the procedure results in the formation of a multilayer. Depending on the fact that the substrate is hydrophobic or hydrophilic, or depending on the way of dipping, different types of multilayers (X, Y or Z-type) can be obtained.

Tetrakis complexes of rare-earth β -diketonates with amphiphilic quaternary ammonium ions or *N*-alkylpyridinium ions as counter ions were often the material of choice to

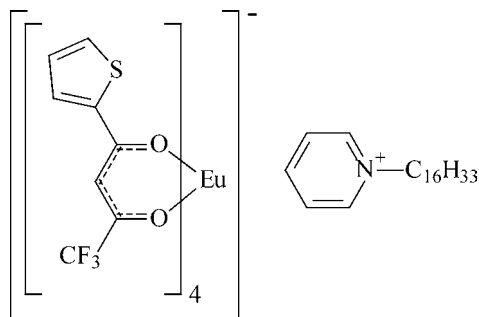


Fig. 34. Structure of $[\text{Eu}(\text{tta})_4]^- (\text{N-hexadecylpyridinium})^+$ (Wang et al., 1991).

produce luminescent Langmuir–Blodgett films. Examples of quaternary ammonium salts are cetyltrimethylammonium (hexadecyltrimethylammonium) or octadecyltriethylammonium. Wang et al. (1991) prepared a strongly luminescent amphiphilic europium(III) complex, $[\text{Eu}(\text{tta})_4]^- (\text{N-hexadecylpyridinium})^+$ (fig. 34). The complex was too hydrophilic to form stable LB-films, and addition of stearic acid was needed for LB-film formation. $[\text{Eu}(\text{pmbp})_4]^- (\text{N-hexadecylpyridinium})^+$ has better film forming properties, but the complex is only weakly luminescent (Huang et al., 1991). Zhou et al. (1996) investigated the luminescence of $[\text{Eu}(\text{dbm})_4]^- (\text{Et}_3\text{NC}_{18}\text{H}_{37})^+$ and $[\text{Eu}(\text{dbm})_4]^- (\text{Me}_3\text{NC}_{16}\text{H}_{33})^+$ in LB-films. $[\text{Eu}(\text{tta})_4]^- (\text{Me}_3\text{NC}_{16}\text{H}_{33})^+$ cannot form a stable monolayer on a pure water surface, because of dissolution (Liu et al., 1998). However, a stable monolayer could be obtained by saturation of the aqueous phase by complex $[\text{Eu}(\text{tta})_4]^-$ ions, and by making mixed monolayers with octadecylamine. Qian et al. (1995) studied monolayers and multilayers of $[\text{Eu}(\text{tta})_4]^- [(\text{C}_{18}\text{H}_{37})_2\text{N}(\text{CH}_3)_2]^+$. LB-films of terbium(III) pyrazolone complexes show an intense green photoluminescence (Zhao et al., 1997). Langmuir–Blodgett films incorporating tetrakis β -diketonate complexes with ferrocene-containing counter ions are also known (Gao et al., 1995b; Xia et al., 1996). An increase in luminescence intensity was observed after Langmuir–Blodgett films of europium(III) bis(hexadecyl)phosphate were dipped in an aqueous solution of benzoyltrifluoroacetone (Serra et al., 1994).

Jiang et al. (1995a, 1995b) found that tris(2-thenoyltrifluoroacetato)mono(9-octadecyl-4,5-diazafluorene)europium could be used to form stable Langmuir–Blodgett films that are strongly luminescent (fig. 35). The luminescence intensity of this complex in an LB-film was 11-fold larger than that of $[\text{Eu}(\text{tta})_4]^- (\text{N-hexadecylpyridinium})^+$ in a mixed LB-film with stearic acid. Wang et al. (2003) made an amphiphilic Lewis base adduct of a tris complex by reaction between $[\text{Eu}(\text{tta})_3(\text{H}_2\text{O})_2]$ and 1-octadecyl-2-(2-pyridyl)benzimidazole (fig. 36). The complex $[\text{Eu}(\text{tta})_3(\text{opb})]$ formed a stable monolayer on a pure water subphase and Langmuir–Blodgett films could be deposited on a hydrophilic quartz substrate. Although the $[\text{Eu}(\text{tta})_3(\text{opb})]$ complex showed an intense luminescence in powder form, the complex incorporated in an LB-films was only weakly luminescent. The quenching of the luminescence was attributed to aggregate formation.

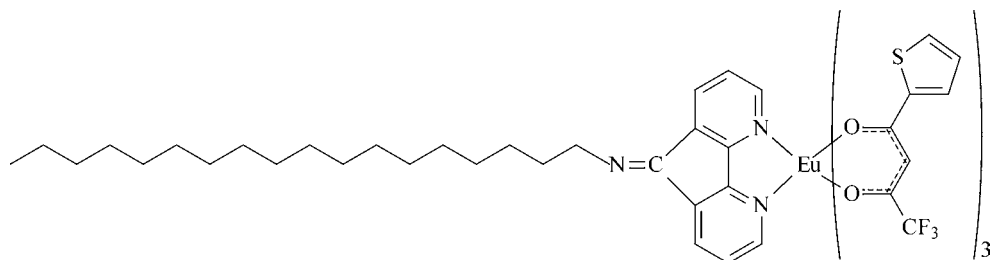


Fig. 35. Structure of tris(2-thenoyltrifluoroacetato)mono(9-octadecylimino-4,5-diazafluorene)europium(III) (Jiang et al., 1995a, 1995b).

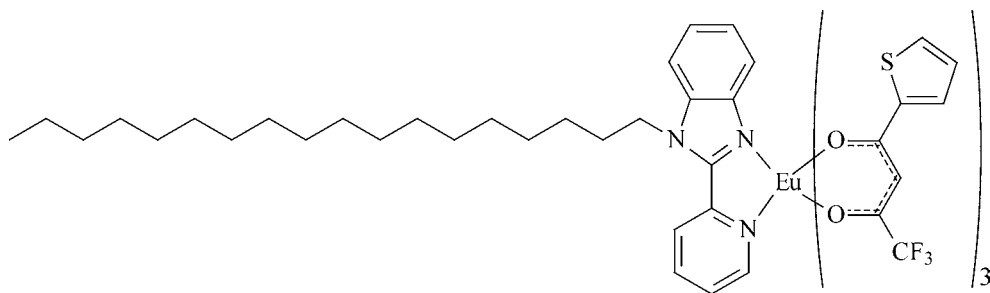


Fig. 36. The amphiphilic europium(III) complex $[\text{Eu}(\text{tta})_3(\text{opb})]$ (Wang et al., 2002, 2003).

Considerable efforts were made to incorporate the highly luminescent complexes $[\text{Eu}(\text{tta})_3(\text{phen})]$ and $[\text{Sm}(\text{tta})_3(\text{phen})]$ into Langmuir–Blodgett films. This is not an easy task, because these complexes are lacking the long alkyl chains that are typical of amphiphilic rare-earth β -diketonate complexes. In order to obtain Langmuir–Blodgett films of a good quality, it is necessary to understand the monolayer behavior of these complexes. The selection of an appropriate subphase is a critical factor in the fabrication of monolayers at the air/water interface with a stable surface behavior. When an aqueous solution saturated with 2-thenoyltrifluoroacetone, 1,10-phenanthroline and $[\text{Eu}(\text{tta})_3(\text{phen})]$ was used as a composite subphase, both dissolution and dissociation of the $[\text{Eu}(\text{tta})_3(\text{phen})]$ complexes were inhibited, so that reproducible π -A isotherms and uniformly distributed crystalline monolayers were obtained (Gao et al., 1996a). Arachidic acid was used for the dispersion of the monolayer. By addition of an appropriate amount of arachidic acid to a solution of $[\text{Eu}(\text{tta})_3(\text{phen})]$ in chloroform, stable monolayers consisting of $[\text{Eu}(\text{tta})_3(\text{phen})]$ and arachidic acid were obtained, and the $[\text{Eu}(\text{tta})_3(\text{phen})]$ were found to be dispersed homogeneously in the monolayer. Further work showed that with the aid of arachidic acid, the monolayer of $[\text{Eu}(\text{tta})_3(\text{phen})]$ and arachidic acid (in 1:1 molar ratio) and the monolayers of $[\text{Sm}(\text{tta})_3(\text{phen})]$ and arachidic acid (in 1:1 molar ratio) could be successfully transferred onto hydrophobic glass substrates, so that Langmuir–Blodgett films could be obtained (Zhang et al., 1997b). The arachidic acid molecules are nearly perpendicular to the substrate surface. The arachidic acid does not influence the luminescence of the

lanthanide complexes (Zhang et al., 1997c). When an amount of tri-*n*-octylphosphine oxide (topo) was mixed with the arachidic acid, the luminescence performance of the LB-films was improved (Zhang et al., 1997c). It was also found that the luminescence of the europium(III) complex is enhanced in mixed Langmuir–Blodgett films containing both [Eu(tta)₃(phen)] and [Y(tta)₃(phen)] besides arachidic acid (Zhong and Yang, 1998). This effect is due to co-luminescence, a phenomenon mentioned in section 6.1: energy can be transferred from the triplet state of [Y(tta)₃(phen)] to the triplet state of [Eu(tta)₃(phen)] by an intermolecular energy transfer mechanism. The distance for the energy transfer from [Y(tta)₃(phen)] to [Eu(tta)₃(phen)] is less than 30 Å. Zhang and Yang (2000) incorporated [Tb(tta)₃(phen)], [Tb(acac)₃(phen)], [Tb(tfac)₃(phen)] and [Tb(hfac)₃(phen)] into Langmuir–Blodgett films with the aid of arachidic acid. [Tb(tta)₃(phen)] orients between the arachidic acid molecules within the layers, whereas the other terbium complexes packed up to multilayers between the head groups of arachidic acid molecules in the same layer. The luminescence intensity of the green-emitting LB-films could be modulated by changing the wavelength of the excitation light. The differences observed in the monolayer behavior of terbium(III) β -diketonates were also found for the corresponding samarium(III) and europium(III) complexes (Zhang and Yang, 2001). An enhanced europium(III) luminescence was observed in LB-films that contain both [Eu(tta)₃(phen)] and [Tb(tta)₃(phen)], together with arachidic acid (Zhong et al., 2001). The excitation energy is transferred from the terbium(III) to the europium(III) complex by intermolecular energy transfer. A self-organized ring pattern was observed for a [Sm(tta)₃(phen)] complex in a Langmuir–Blodgett film formed from a [Sm(tta)₃(phen)]–stearic acid mixture (Zhang et al., 2001). Mixed monolayers of [Eu(tta)₃(topo)₂] and stearic acid could be deposited on a solid substrate (Huang et al., 1999).

Many examples of hemicyanine dyes with rare-earth tetrakis β -diketonate complexes incorporated into Langmuir–Blodgett films have been described in the literature. These materials are discussed in section 7.7. The rare-earth complex does not only improve the quality of the LB-films, but better nonlinear optical properties were found as well. Pavier et al. (1997) investigated the photoluminescence of LB-films in which ytterbium(III) complexes of pyrazolone ligands were used as counter ions. The fluorescence of the hemicyanine ligand was observed in the visible region, and metal-centered luminescence of Yb³⁺ in the near-infrared region.

7.6. Liquid crystals

Liquid crystals (or mesogens) form a state of matter with a molecular order between that of a highly ordered crystalline solid and a disordered liquid (Demus et al., 1998; Collings and Hird, 1997; Collings, 1990). Liquid crystals are fluid (they flow like a liquid), but their physical properties (electric permittivity, heat conductivity, viscosity, . . .) are anisotropic. This means that different values can be measured for a given physical property, depending on the direction in which this property is measured. Typical liquid crystals have a rod-like or a disk-like shape, so that the molecules used to produce these compounds must have a pronounced shape-anisotropy. A mesogenic compound is transformed into a liquid-crystalline state, either upon heating a solid compound (thermotropic liquid crystals) or by addition of a solvent (lyotropic liquid crystals). The liquid-crystalline state is also called a *mesophase*.

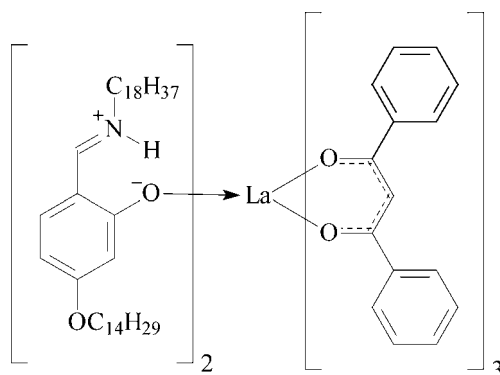


Fig. 37. Lewis base adduct of $[\text{La}(\text{dbm})_3]$ and a non-mesomorphic salicylaldehyde Schiff's base. The compound melts at 95°C and exhibits a monotropic smectic A phase upon cooling below 81°C .

Liquid crystals are of technological importance. They are for instance the active components in a liquid-crystal displays (LCDs). It is possible to combine the properties of liquid crystals, i.e. anisotropy, switchable by an external electric field, with those of transition metal ions (redox behavior, color) by incorporating metal ions into a liquid crystal. Liquid-crystalline metal complexes are named “*metallomesogens*” (Giroud-Godquin and Maitlis, 1991; Espinet et al., 1992; Hudson and Maitlis, 1993; Serrano, 1996; Bruce, 1996; Donnio and Bruce, 1999; Donnio et al., 2003). Rare-earth-containing liquid crystals have been reviewed extensively by Binnemans and Görlner-Walrand (2002). Most of the liquid-crystalline rare-earth complexes that have been reported in the literature hitherto are Schiff base complexes. Although Swager and coworkers (Trzaska et al., 1999) showed that β -diketones could be used to obtain eight-coordinate metallomesogens with zirconium(IV) as the central metal ion, attempts to synthesize liquid-crystalline rare-earth complexes with these mesogenic ligands were unsuccessful for a long time. The main reason is that the commonly used synthetic routes to rare-earth β -diketonate complexes do not work for the mesogenic β -diketones, mainly due to solubility problems: the solvents in which the ligands are soluble do not dissolve the rare-earth precursor salts.

Binnemans and coworkers showed that it is possible to obtain mesomorphic rare-earth complexes by forming Lewis-base adducts of simple rare-earth tris β -diketonate complexes with mesogenic ligands. More particularly, they studied bisadducts of $[\text{R}(\text{dbm})_3]$ complexes (Hdbm = 1,3-diphenyl-1,3-propanedione or dibenzoylmethane) with a salicylaldehyde Schiff base ligand (fig. 37) (Binnemans and Lodewyckx, 2001; Binnemans et al., 2003). The adducts are monotropic liquid crystals, exhibiting a smectic A phase upon cooling of the isotropic liquid. The crystal structure of $[\text{La}(\text{dbm})_3\text{L}_2]$, where L is *N*-butyl-2-hydroxy-4-methoxybenzaldehyde was described (fig. 38). The temperature difference between the melting point and the clearing point of the monotropic mesophase increases over the lanthanide series. The complexes of the heavier lanthanides were not liquid-crystalline. Galyametdinov and coworkers prepared tris complexes of the lanthanides with 1,3-bis(*p*-tetradecyloxyphenyl)-

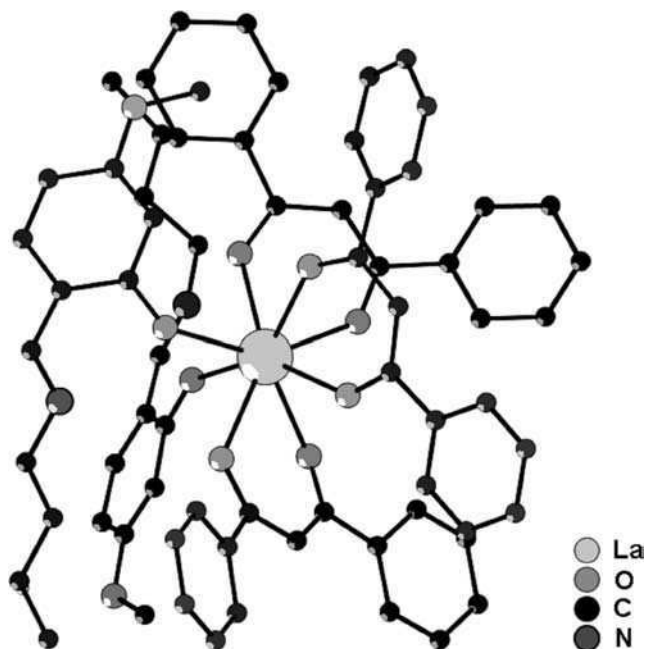


Fig. 38. Molecular structure of $[\text{La}(\text{dbm})_3\text{L}_2]$, where L is *N*-butyl-2-hydroxy-4-methoxybenzaldehyde. The atomic coordinates are taken from Binnemans et al. (2003). No hydrogen atoms are shown.

1,3-propanedione, where the coordination sphere was saturated by 1,10-phenanthroline, 2,2'-bipyridine or substituted 2,2'-bipyridines (Galyametdinov et al., 2002a, 2002b). This was the first example of a lanthanide complex where the mesomorphism was induced by the β -diketonate ligand. The complexes form monotropic smectic A phases or monotropic highly ordered smectic phases (that were not studied in detail).

Other attempts to obtain liquid-crystalline rare-earth complexes via Lewis-adduct formation with rare-earth tris β -diketonate complexes were less successful.

Hapiot and Boyaval studied adducts of $[\text{R}(\text{tta})_3]$ and cholesteryl nonanoate and cholesteryl tetradecanoate (Boyaval et al., 1999; Hapiot and Boyaval, 2001). By means of IR, ^1H -, ^{13}C - and ^{19}F -NMR spectroscopy, including 2D NMR and relaxation techniques, they were able to show that a 1:1 adduct was formed between $[\text{R}(\text{tta})_3]$ ($\text{Ln} = \text{Nd}, \text{Sm}, \text{Eu}$) and the cholesteryl ester, and that bonding of the cholesteryl ester and the metal ion occurs through both oxygen atoms of the ester. This type of bonding can be considered as a pseudo-chelate type. The authors argue that the absence of a mesophase in the adducts is not only due to the large size of the $[\text{R}(\text{tta})_3]$ moiety, but also to a twisted conformation of the ligands, so that the overall structure of the adduct is not rod-like.

Wang et al. (1995b) reported thermotropic mesomorphism for tetrakis 1-phenyl-3-methyl-4-benzoyl-5-pyrazolanato lanthanate complexes with amphiphilic hemicyanines as counter ions. However, further study revealed that these complexes are not liquid-crystalline

(Binnemans et al., 1999a), whereas the corresponding hemicyanine bromides are (Binnemans et al., 1999b).

An alternative approach to obtain luminescent liquid crystals is to use the host–guest concept: a luminescent lanthanide complex is dissolved in a liquid-crystalline matrix. This approach allows one to optimize the luminescence and mesomorphic properties of the liquid-crystal mixture independently. Boyaval et al. investigated the luminescence of lanthanide complexes in a cholesteric liquid crystal mixture (Boyaval et al., 1999, 2001). Binnemans and Moors (2002) showed that a nematic liquid crystal can be an interesting host matrix to study the spectroscopic properties of luminescent lanthanide complexes. These authors doped the β -diketonate complex [Eu(tta)₃(phen)] into the nematic liquid crystals *N*-(4-methoxybenzylidene)-4-butylaniline (MBBA) and 4-*n*-pentyl-4'-cyanobiphenyl (5CB) and observed narrow-band red photoluminescence with a well-resolved crystal field splitting. Later on, these authors extended their studies to lanthanide β -diketonate complexes emitting in the near-infrared (Ln = Nd, Er, Yb) (Van Deun et al., 2003).

7.7. Nonlinear optical materials

Rare-earth β -diketonate complexes with hemicyanine or related chromophores have been studied for their potential as nonlinear optical materials (NLO materials). Such nonlinear optical materials could have applications in the domains of opto-electronics and photonics (Verbiest et al., 1997). Nonlinearity of the optical properties means that when a molecule is placed in an intense light beam, there is no linear relationship between the induced electric dipole moment and the applied electric field. When a molecule is subjected to an intense light field, the induced dipole moment is given by eq. (12).

$$\mu_i = \sum_{j,k,l} (\alpha_{ij} E_j + \beta_{ijk} E_j E_k + \gamma_{ijkl} E_j E_k E_l + \dots). \quad (12)$$

The summation runs over repeated indices. μ_i is the *i*-th component of the induced electric dipole moment and E_i are components of the applied electro-magnetic field. The coefficients α_{ij} , β_{ijk} and γ_{ijkl} are components of the *linear polarizability*, the *first hyperpolarizability*, and the *second hyperpolarizability tensor*, respectively. The first term on the right hand side of eq. (12) describes the linear response of the incident electric field, whereas the other terms describe the nonlinear response. The β tensor is responsible for second order nonlinear optical effects such as *second harmonic generation* (SHG, frequency doubling), *frequency mixing*, *optical rectification* and the *electro-optic effect*. The β tensor vanishes in a centrosymmetric environment, so that most second-order nonlinear optical materials that have been studied so far consists of non-centrosymmetric, one-dimensional charge-transfer molecules. At the macroscopic level, observation of the nonlinear optical susceptibility requires that the molecular non-symmetry is preserved over the physical dimensions of the bulk structure.

Because compounds with a hemicyanine (aminostyrylpyridinium) chromophore exhibit a large charge separation between the ground state and the excited state, they are good candidates for nonlinear optical materials. Nonlinear optical effects can be observed both in solution and in organized systems (Langmuir–Blodgett films or in single crystals). The nonlin-

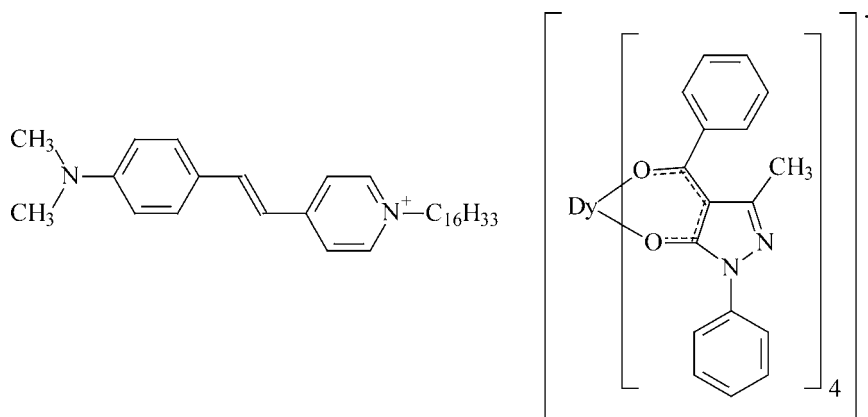


Fig. 39. Stilbazolium dye with a tetrakis(pyrazolonato)dysprosate(III) complex as the counter ion (Wang et al., 1994a, 1994b).

ear optical properties of hemicyanine compounds with halogenide counter ions were investigated by for instance Bruce et al. (1994), Lupo et al. (1988) and by Grummt et al. (1996). Wang et al. (1994a, 1994b) synthesized hemicyanine compounds with an anionic rare-earth tetrakis β -diketonate compounds as counter ions, instead of halogenide counter ions (fig. 39). The use of a tetrakis complex as the anion not only improved the film forming properties (important for the preparation of LB-films), but also improved the nonlinear optical properties due to a better charge separation in the hemicyanine chromophore. The nonlinear optical properties of these types of complexes have been studied in detail (Zhou et al., 1994; Huang et al., 1995). The first hyperpolarizability was determined from second harmonic generation experiments after incorporation into an LB-film. A crystal structure of a hemicyanine dye with a $[\text{La}(\text{tta})_4]^-$ counter ion is available (Wang et al., 1995c). Zhao et al. (1995) investigated the influence of a gas atmosphere (vapors of chloroform, acetic acid and isopropanol) on the generation of the second harmonic in an LB-film. The gas atmosphere has a pronounced effect on the SHG-signal. Wostyn et al. (2001a) used this type of compounds to test an improved technique for the suppression of the multiphonon fluorescence contribution in hyper-Rayleigh scattering. Hyper-Rayleigh scattering allows the determination of the first polarizability of molecules in solution (Clays and Persoons, 1991). The hyperpolarizability in the hemicyanines with tetrakis β -diketonate counter ions was found to be independent of the nature of the rare-earth ions (Wostyn et al., 2001b). These authors come to the conclusion that the strategy to enhance the film-forming properties by using rare-earth-containing counter ions in hemicyanine complexes is not effective in improving the molecular nonlinear optical properties.

Not only hemicyanine dyes, but also azo dyes have been studied for their nonlinear optical properties. In these compounds the C=C group of the hemicyanine group is replaced by a N=N group (Li et al., 1995, 1996; Gao et al., 1995a, 1996b). Another type of complex is the one in which the pyridinium ion is covalently linked to a ferrocene group (Gao et al., 1995b).

8. From materials to devices

8.1. *Chelates for lasers*

The possibility to use rare-earth β -diketonate complexes for the design of lasers gave a strong impulse to the spectroscopic study of these complexes in the early 1960's. In a 1962 Nature paper, Schimitschek and Schwarz (1962) pointed to the fact that europium complexes have optical properties that make them very attractive as potential laser materials. The authors suggested that laser action should be experimentally verified for these complexes dissolved in both organic solvents or in a polymer matrix. Around the same time, the potential application of rare-earth chelates in lasers has been suggested by other authors as well (Whan and Crosby, 1962; Filipescu et al., 1962). In 1963, Lempicki and Samelson (1963) were the first to obtain stimulated emission at 613.1 nm ($^5D_0 \rightarrow ^7F_2$ transition) from an alcohol solution (3:1 ethanol:methanol) of europium benzoylacetate at -150°C , by pumping with a xenon flash lamp. The threshold energy was between 1790 and 1920 J. This threshold is the amount of energy that must be delivered to the laser device to bring it to point at which the onset of laser action is observed. Samelson et al. (1964c) observed room temperature operation of a europium(III) chelate laser. From then on, a considerable number of studies on laser action of europium(III) and terbium(III) β -diketonate complexes in frozen organic solutions and in polymers were reported within a few years (for instance: Samelson et al., 1964a, 1964b, 1964c; Lempicki et al., 1964; Lempicki and Weise, 1967; Schimitschek, 1963; Schimitschek et al., 1965a, 1965b, 1966, 1967, 1969; Schimitschek and Nehring, 1964; Nehring et al., 1964; Brecher et al., 1968; Lempicki and Weise, 1967; Wolff and Pressley, 1963; Huffmann, 1963a; 1963b, 1964; Bhaumik et al., 1964; Bazhulin et al., 1965; Bjorklund et al., 1967; Meyer et al., 1964a, 1964b; Meyer, 1965; Seitz, 1969; Verron and Meyer, 1966; de Witte and Meyer, 1967; Crozet and Meyer, 1967; Aristov and Maslyukov, 1968; Altman and Geller, 1969; Ross and Blanc, 1967; Batyaev, 1971). The ligands include benzoylacetone, dibenzoylmethane, trifluoroacetylacetone, thenoyltrifluoroacetone and benzoyltrifluoroacetone. A great deal of this work has been done by physicists on poorly characterized or on impure compounds. During these studies it was realized that, in contrast to earlier belief, rare-earth tris β -diketonate complexes are much less common than Lewis base adducts of these tris complexes and than the tetrakis β -diketonate complexes. It was shown that the active components in most successful laser systems were the tetrakis complexes (Brecher et al., 1965). Although in most of the studies on laser chelates, europium(III) has been chosen as the emitting ion, some studies report on laser action of terbium(III) complexes (Huffmann, 1963a, 1963b; Bjorklund et al., 1967; Samelson et al., 1964c, 1967), whereas Whittaker (1970) observed laser action by neodymium(III) in a tetrakis thenoyltrifluoroacetate complex prepared from a didymium salt (mixture of praseodymium and neodymium salts).

Strong light absorption by the β -diketonate ligands is an advantage for sensitizing the luminescence of lanthanide ions by the antenna effect, but this property limits the usefulness of the rare-earth β -diketonate complexes as laser materials. In order to achieve uniform excitation of the solutions containing the rare-earth chelate at the concentration required for laser

action (ca. 0.01 M), only thin samples (ca. 1–6 mm) could be used (Samelson et al., 1964b; Ross and Blanc, 1967). Therefore, most of the studies of liquid lasers have been performed on laser solutions in a capillary tube or on rare-earth doped polymers drawn to fibers. Another problem with the chelate lasers is the low photostability of the rare-earth β -diketonate complexes under ultraviolet irradiation. This severely limits the lifetime of these laser systems. Thirdly, the lasing thresholds are high for these chelate lasers at room temperature (1000–3000 J). Because of the high input energy needed, excessive warming of the laser solutions can be a problem. To circumvent the latter, circulation of the liquid through the cell and cooling with an external heat exchanger have been proposed (Schimitschek et al., 1966). Finally, the energy output of the rare-earth chelate lasers is low, because of the existence of efficient pathways for the radiationless deactivation of the excited states.

The most commonly used solvents for the study of the laser action are a 2:1:1 mixture of β -ethoxypropionitrile, β -ethoxyethanol and acetonitrile (EAA), a 1:1:1 mixture of propionitrile, butyronitrile and isobutyronitrile (“nitrile solvent”), a 3:1 ethanol–methanol mixture, a 3:1 ethanol–DMF mixture, and acetonitrile. Some of the mixed solvent systems remain liquid to temperatures as low as -150°C . However, the β -diketonate complexes are not always stable for a long time in such solutions. For instance, Schimitschek et al. (1965b) mention that europium(III) β -diketonate complexes degrade in the 3:1 ethanol:methanol mixture. Fry and Pirie (1965) found that in this alcohol mixture, $[\text{Eu}(\text{bzac})_3(\text{H}_2\text{O})]$ decomposed upon heating the solution to 70°C or upon irradiation with ultraviolet radiation. The main decomposition products were ethyl acetate and acetophenone, which indicates that benzoylacetate underwent a reverse Claisen condensation. Brecher et al. (1965) discussed the dissociation in solution of the tetrakis complexes into mixtures of non-lasing tris complexes and free β -diketonate anions.

For a long time after 1970, no research has been done on rare-earth chelate lasers. In 1995, Taniguchi et al. (1995a) demonstrated ultra-low threshold lasing due to morphology-dependent resonances from the europium complex $[\text{Eu}(\text{dbm})_3(\text{phen})]$ dissolved in liquid microdroplets with ca. $90\ \mu\text{m}$ diameters. These microdroplets consisted of a viscous ethanol–glycerol mixture. The same year, authors from the same research consortium (Taniguchi et al., 1995b), described a solid chelate laser based on $[\text{Eu}(\text{dbm})_3(\text{phen})]$ dispersed into polystyrene spheres. The advantage of this type of chelate laser in comparison with the liquid chelate laser, is that the former is free of solvent effects.

8.2. Organic light-emitting diodes (OLEDs)

Light emitting diodes (LEDs) will probably become the most important type of light source for artificial lighting in the 21st century, and will probably drive out the incandescent lamps and even the mercury-containing discharge lamps. Typically, a LED consists of inorganic p - and n -type semiconductors. The holes and electrons are driven to the p – n junction by the applied electric field. The electrons and holes recombine at this p – n junction, and the excess of energy is given off as visible or infrared radiation. In a LED, electrical energy is transformed into light (electroluminescence). In *organic light emitting diodes* (OLEDs), the active components are organic molecules instead of inorganic semiconductors. OLEDs are mainly developed for

display applications. One hopes to use OLEDs for the design of large flat panel displays with a very wide viewing angle. The advantages of OLEDs are that they are easier and cheaper to fabricate than their inorganic counter parts, that they can be made very large (luminescent sheets) and that they can be deposited on almost every substrate including flexible ones, like plastics (flexible displays). Although the phenomenon of organic electroluminescence was discovered by Pope in 1963, the development of the first OLEDs began in the Chemistry Division of Kodak Research Laboratories at the end of the 1970s (Hung and Chen, 2002). One has to mention here the pioneering work of Tang and Van Slyke (1987), who introduced an injection type of electroluminescent device that operated at driving voltages as low as a few volts. They used a hole transport layer for hole injection from the electrode into the emitting organic layer and they used tris(8-hydroxyquinolino)aluminum(III) (AlQ) as the emissive material. Tris(8-hydroxyquinolino)aluminum(III) emits bright green light. This multilayer device had a luminance of more than 1000 cd/m² below 10 V with an external quantum efficiency of 1% (i.e. one photon is emitted for 100 injected electrons). Another milestone was the work of Burroughes et al. (1990). Their OLED consisted of a single layer of the π -conjugated polymer poly(phenylene-vinylene) (PVV) between metallic electrodes. Since that time, a lot of research efforts have been invested in optimizing the performance of OLEDs and now OLEDs with a broad variety of emitting colors are available (Hung and Chen, 2002).

An OLED consists of very thin layers sandwiched by two electrodes. These layers can be deposited by various techniques such as chemical vapor deposition, plasma deposition, or spin coating from a solution. Electrons are injected into the emitting layer from the cathode, and holes are injected from the anode. The cathode is typically a layer of a metal with a low work function such as aluminum, magnesium, calcium or a magnesium:aluminum alloy. The anode is typically a transparent layer of indium tin oxide (ITO). The recombination of the injected holes with the injected electrons allows the formation of singlet and triplet excitons. Because of spin statistics, 75% of the recombinations give rise to triplet excitons and 25% to singlet excitons. Only singlet excitons can produce electroluminescence. The triplet excitons decay non-radiatively and do not generate electroluminescence. For this reason, the maximum internal quantum efficiency of an OLEDs is limited to 25%. Different types of OLEDs have been described (fig. 40). A *single-layer OLED* is made of a single organic layer sandwiched between the cathode and the anode. This layer must not only possess a high quantum efficiency for photoluminescence, but the layer must also have good hole and electron transport properties. In a *two-layer OLED*, one organic layer is specifically chosen to transport holes and the other layer is chosen to transport electrons. Recombination of the hole–electron pair takes place at the interface between the two layers, which generates electroluminescence. In a *three-layer OLED* an additional layer is placed between the hole transporting layer and the electron transporting layer. The emitting layer is primarily the site of hole–electron recombination and thus of electroluminescence. This cell structure is useful for emissive materials that do not possess high carrier (either electron or hole) transport properties. In an OLED, electrons are transported via the lowest unoccupied molecular orbital (LUMO). The LUMO is analogous to the conduction band of semiconductors. Holes are transported via the highest occupied molecular orbital (HOMO). The HOMO can be compared with the valence band of a semiconductor.

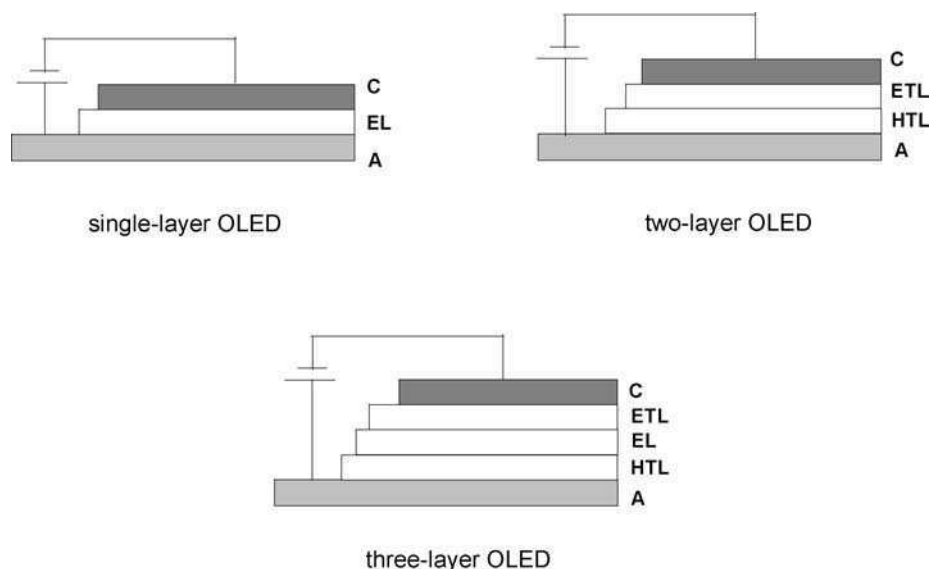


Fig. 40. Different types of OLED cells. C = cathode (typically aluminum); EL = emitter layer; ETL = electron transport layer; HTL = hole transport layer; A = anode (typically ITO glass).

The performance of OLEDs are tested by measuring the current density–voltage and the luminance–voltage characteristics. The *turn-on-voltage* is defined as the voltage necessary to have a luminance of 1 cd/m^2 . Ideally, this value should be as low as possible, but in many lanthanide-based OLEDs the values are between 5 and 10 V. The luminance will increase with increasing voltage up to a maximum value. Increasing the voltage further will then cause a decrease of luminance. In OLEDs one can distinguish the *external quantum efficiency* (η_{ex}) and the *power efficiency* (η_{p}). The external quantum efficiency is defined as the ratio of the number of emitted quanta to the number of charge carriers. The power efficiency is the ratio of the luminous flux emitted by the OLED and the consumed electric power. Molecules often used as active components in OLEDs are depicted in fig. 41.

Kido and Okamoto (2002) published a review article on lanthanide-containing OLEDs. In theory, incorporation of lanthanide complexes in the emitting layer of OLEDs offers two main advantages: (i) improved color saturation and (ii) higher efficiency of the OLED. Because of the sharp emission bands of the trivalent lanthanide ions (with a full-width at half maximum of less than 10 nm), lanthanide luminescence is highly monochromatic. This results in a much better color saturation than when organic molecules are used as the emissive material. In this case the band widths of the emission bands are typically around 80 to 100 nm. A saturated monochromatic emission is necessary for the development of full-color displays based on OLEDs. Broad emission bands will give dull colors. As mentioned above, the efficiency of OLEDs is limited to 25% by spin statistics. However, when lanthanide complexes are used,

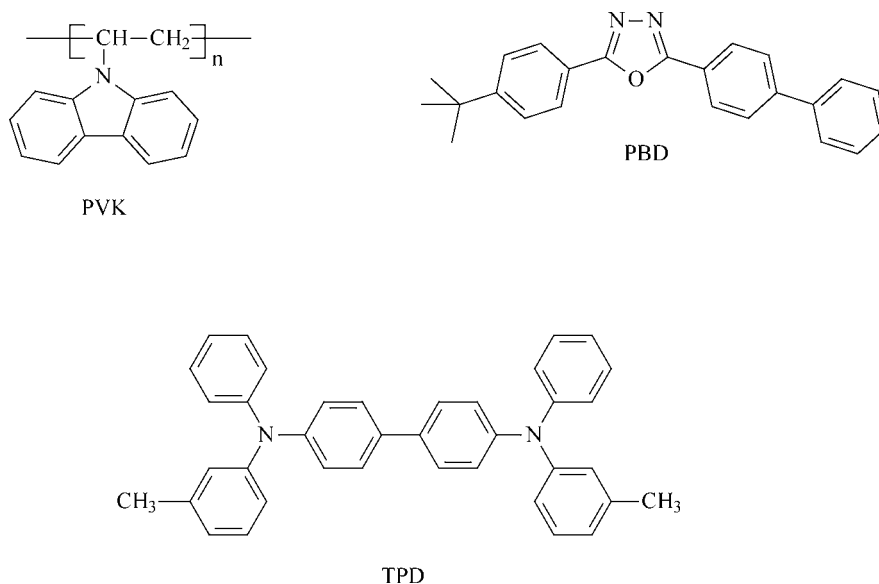


Fig. 41. Active components in OLEDs; the hole-transporting materials poly(*N*-vinylcarbazole) (PVK) and *N,N'*-diphenyl-*N,N'*-bis-(3-methylphenyl)-1,1'-biphenyl-4,4'-diamine (TPD), and the electron-transporting material 2-*tert*-butylphenyl-5-biphenyl-1,3,4-oxadiazole (PBD).

the efficiency is in theory not limited because the excitation energy can be transferred both from an excited singlet or triplet to the lanthanide ion.

Although one often predicts a bright future for lanthanide-doped OLEDs, it has been learned from practice that the use of lanthanide complexes in OLEDs generates several problems. One difficulty is the poor film-forming properties of low-molecular weight lanthanide coordination compounds. Other problems are the low electroluminescence efficiency (due to poor charge-carrier transporting properties), and the bad long-term stability of the rare-earth complexes.

Kido and coworkers were the first to propose a lanthanide complex as the emissive material in an OLED (Kido et al., 1990). These authors built an electroluminescent device consisting of *N,N'*-diphenyl-*N,N'*-(3-methylphenyl)-1,1'-biphenyl-4,4'-diamine (TPD) as the hole injecting layer and [Tb(acac)₃] as the emitting and electron transporting layer. The cathode was an aluminum layer and the anode an ITO-coated glass plate. The OLED was made by vacuum deposition. The green emitting OLED had a luminance of 7 cd/m². This value is very low, but the importance of this paper is the proof-of-principle. The electroluminescence spectrum was found to be identical with the corresponding photoluminescence spectrum. The relative intensities of the emission bands were independent of the current density. It should be noticed that the [Tb(acac)₃] compound described in this paper was not characterized, so it is not clear whether the compound under investigation was an hydrate or a partially hydrolyzed compound. Later on, these authors made a red-emitting OLED based on

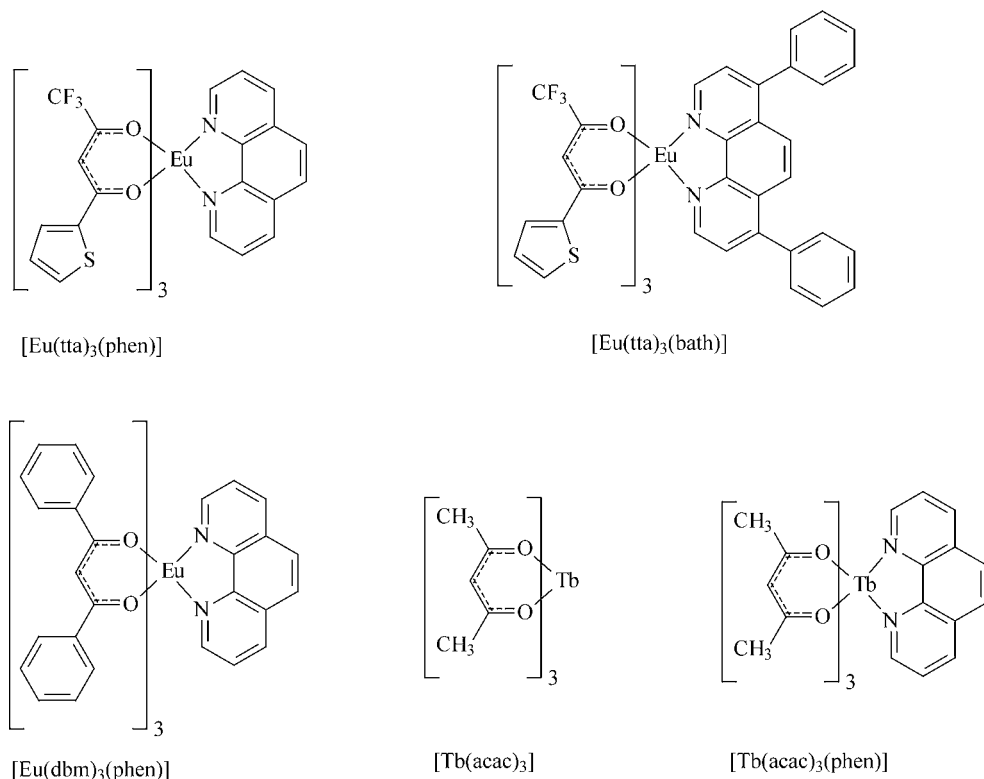


Fig. 42. Low-molecular weight red emitting europium(III) β -diketonate complexes and green emitting terbium(III) β -diketonate complexes that are used as active component in the emitter layer of lanthanide-doped OLEDs.

an europium(III) compound (Kido et al., 1991). Their electroluminescence cell consisted of 2-*tert*-butylphenyl-5-biphenyl-1,3,4-oxadiazole (PDB) as the electron transporting layer and poly(methylphenylsilane) (PMPS) as the hole transporting layer doped with [Eu(tta)₃]. Luminescence started at 12 V, and a maximum luminescence intensity of 0.3 cd/m² was obtained at 18 V. By replacing the [Eu(tta)₃] complex by [Eu(dbm)₃(phen)], a luminance of 460 cd/m² could be achieved (Kido et al., 1994). In the same way, the efficiency of the green-emitting OLED could be improved to 90 cd/m² by use of [Tb(acac)₃(phen)] instead of [Tb(acac)₃] (Kido et al., 1996). The structure of low-molecular weight europium(III) and terbium(III) β -diketonate complexes often used in lanthanide-based OLEDs are shown in fig. 42.

The first types of lanthanide-based OLEDs were prepared by vacuum deposition of the different layers (hole injection layer, emitting layer, electron transport layer, cathode) on the ITO substrate. This technique is applicable only for volatile and thermally stable lanthanide complexes. Unfortunately, most volatile lanthanide β -diketonate complexes are not the ones with the best luminescence properties. Many β -diketonate complexes cannot be sublimed without

considerable thermal decomposition, or give deposited layers of an inferior quality. The films of lanthanide β -diketonates produced by vacuum deposition have poor charge-carrier properties. Especially the transport of electrons is problematic. Because of the unbalanced injection and transport of charge carriers, recombination often takes place at sites other than the emitting layer. This not only leads to low electroluminescence efficiency, but also to a reduced lifetime of the OLED.

One approach to improve the OLEDs based on lanthanide compounds, is to replace the tris β -diketonate complexes by Lewis base adducts (i.e. by ternary complexes). In this way, not only the volatility and the thermal stability can be improved, but also the film forming properties and the carrier-transport ability. This approach was already illustrated above for the work of Kido and coworkers (Kido et al., 1994, 1996), who used 1,10-phenanthroline as the Lewis base. Although 1,10-phenanthroline is often used as Lewis base to form ternary complexes (Kido et al., 1994, 1996; Takada et al., 1994; Sano et al., 1995; Campos et al., 1996; Dirr et al., 1997; Li et al., 1997; Liu et al., 1997; Jabbour et al., 1999; Miyamoto et al., 1999; Zhu et al., 2000a; Zhao et al., 2000; Pyo et al., 1999; Lee et al., 1999; McGehee et al., 1999; Takada et al., 2001; Zhong et al., 2002; Jiang et al., 2002b; Zheng et al., 2002c; Ohmori et al., 1998, 2001), better results are often obtained when 4,7-diphenyl-1,10-phenanthroline (bathophenanthroline, bath) is used instead (Sano et al., 1995; Wang et al., 1997; Okada et al., 1999; Liang et al., 2000a, 2000b; Zheng et al., 2002b). Other phenanthroline derivatives that have been applied to make electroluminescent ternary europium complexes are 5-amino-1,10-phenanthroline, 4,7-dimethyl-1,10-phenanthroline, 1,10-phenanthroline disulfonic acid, and 5-chloro-1,10-phenanthroline (Kim et al., 2000). Tsaryuk et al. (2002) discussed the problem of optimizing the performance of ternary complexes of europium(III) β -diketonates with 1,10-phenanthroline for OLED applications. 2,2'-Bipyridine is much less popular than 1,10-phenanthroline to form ternary complexes (Zheng et al., 2002a). Huang et al. (2002a) made ternary complexes with 2-(2-pyridyl)benzimidazole (Hpbm) and 1-ethyl-2-(2-pyridyl)benzimidazole (epbm). The ligands derived from 2-(2-pyridyl)benzimidazole have the advantage that they can be easily substituted by alkyl chains on the benzimidazole group. The europium complex made of 1-octadecyl-2-(2-pyridyl)benzimidazole (opb), [Eu(dbm)₃(opb)] has a melting point of 119 °C, and starts to decompose at 337 °C (Wang et al., 2002). The large temperature interval between the melting point and the onset of thermal decomposition facilitates processing of this complex by vacuum vapor deposition. Moreover, the long alkyl chain stabilizes the amorphous phase. It is known that crystallization of the emissive layer has an unfavorable effect on the electroluminescence. Gao et al. (2003) studied the performance of the [Eu(dbm)₃(piphen)] complex, where piphen is 2-phenyl-imidazo[4,5-f]1,10-phenanthroline. Another type of 1,10-phenanthroline derivative is dipyrido[3,2-a:2',3'-c]phenazine (dppz). This ligand was used to make [Eu(tta)₃(dppz)] complexes (Sun et al., 2002). Hu et al. (2000a, 2000b) chose triphenyl phosphine oxide (tppo) as the reagent to make ternary [Eu(dbm)₂(tppo)] complexes, and the corresponding OLEDs had a high luminance (up to 380 cd/m²). In order to improve the charge-transport properties, an oxadiazole-functionalized β -diketone ligand has been designed and the electroluminescence of the corresponding tris β -diketonate dihydrate was studied (Wang et al., 2001) (fig. 43). The turn-on-voltage of the device was 8 V. At 15 V the luminance was 100 cd/m² ($\eta_{\text{ex}} = 1.1\%$), and

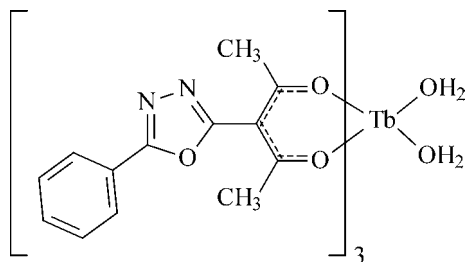


Fig. 43. Structure of an oxadiazole-functionalized terbium(III) β -diketonate (Wang et al., 2001).

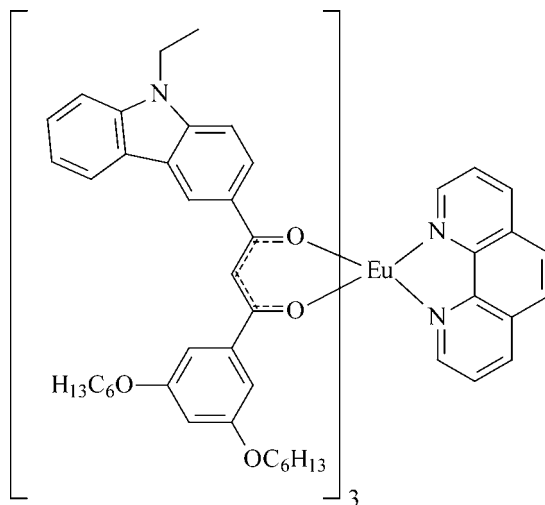


Fig. 44. Structure of tris[1-(*N*-ethylcarbazoyl)(3',5'-hexyloxybenzoyl)methane](1,10-phenanthroline)europium(III) (Robinson et al., 2000).

at 20 V the luminance increased to 550 cd/m^2 ($\eta_{\text{ex}} = 0.6\%$). The improved charge transport was evident from the high current densities (25 mA/cm^2 at 15 V, and 275 mA/cm^2 at 20 V). The same type of device with $[\text{Tb}(\text{acac})_3]$ as the emitter has current densities of only 0.6 and 1.3 mA/cm^2 under the same conditions. The terbium compound described by Wang et al. (2001) has two water molecules in the first coordination sphere. The luminescence efficiency could be enhanced by replacing these water molecules by a bidentate Lewis base. Liang et al. (2003) used 2-(2-pyridyl)benzimidazole functionalized with an oxadiazole group to form a ternary complex with $[\text{Eu}(\text{dbm})_3]$. The complex tris[1-(*N*-ethylcarbazoyl)(3',5'-hexyloxybenzoyl)methane](1,10-phenanthroline)europium(III) was designed to incorporate the same complex groups that improve both the electron transport (1,10-phenanthroline) and hole transport (the carbazole fragment) (Robinson et al., 2000) (fig. 44). Moreover, crystallization was prevented by the presence of six hexyloxy groups and a stable amorphous phase

was obtained. Noto et al. (2001) studied the electroluminescence of an OLED that contained the complex $[\text{Eu}(\text{dbm})_2(\text{dcnp})(\text{phen})]$, where $\text{H}(\text{dcnp})$ is 1,3-dicyano-1,3-propanedione.

Instead of depositing the emissive layer by vacuum vapor deposition, it is also possible to dope the lanthanide complex into a polymer matrix. In this case the lanthanide complex and the polymer are dissolved in a suitable solvent and the emissive layer is cast directly from solution by spin coating (Kido et al., 1991; McGehee et al., 1999; Yu et al., 2000; Liang et al., 2001; Jiang et al., 2002b). The doped polymers have several advantages. First of all, the thermal decomposition of the electroluminescent complexes by vacuum sublimation is avoided. Secondly, the processing of the films is simplified. Thirdly, the polymer have better film forming properties than the low-molecular weight lanthanide complexes. Fourthly, the polymer matrix can have good hole- and electron-transporting properties, so that the electroluminescence is improved. Finally, the energy of blue-emitting polymers can be transferred to the lanthanide complex. Heeger and coworkers (McGehee et al., 1999) reported red-emitting OLEDs with a high color saturation, in which the energy from the blue-emitting conjugated polymer poly[2-(6'-cyano-6'-methyl-heptyloxy)-1,4-phenylene] (CN-PPP) is transferred to europium β -diketonate complexes. The complexes that were studied are: $[\text{Eu}(\text{acac})_3(\text{phen})]$, $[\text{Eu}(\text{bzac})_3(\text{phen})]$, $[\text{Eu}(\text{dbm})_3(\text{phen})]$ and $[\text{Eu}(\text{dnm})_3(\text{phen})]$. The external quantum efficiency of the OLEDs incorporating these complexes were respectively 0.03%, 0.1%, 0.7% and 1.1%. The best performance was thus observed for the OLED based on $[\text{Eu}(\text{dnm})_3(\text{phen})]$. In order to have a good energy transfer from the polymer to the europium(III) complex, the position of the triplet level of the β -diketonate ligand has to lie above the $^5\text{D}_0$ level of Eu^{3+} , and there must be an overlap between the emission spectrum of the polymer and the absorption spectrum of the β -diketonate. Diaz-Garcia et al. (2002) investigated the energy transfer from the OLED-components PVK, PBD and TPD to the rare-earth complexes $[\text{Eu}(\text{tmhd})_3]$, $[\text{Eu}(\text{tfc})_3]$ and $[\text{Sm}(\text{tmhd})_3]$. To have a better intramolecular energy transfer, Jiang et al. (2002b) prepared β -diketones bearing two phenanthryl groups. However, energy transfer from the β -diketonates to the Eu^{3+} ion proved to be efficient. These authors also synthesized dendron-substituted β -diketones to provide site isolation of the europium ion in the corresponding complexes; this results in less self-quenching of the luminescence (Jiang et al., 2002a). It is possible to bind the lanthanide complexes directly onto the polymer backbone. Zhao et al. (1999a) linked a europium complex consisting of two dibenzoylmethanate (dbm) ligands and one 1,10-phenanthroline group to a copolymer of methacrylate and acrylic acid. The efficiency of the OLED made of this material was low; the luminance was only 0.32 cd/m^2 at 18 V. Ling et al. (2002) made a copolymer containing both a europium(III) complex and carbazole groups. However, a LED based on this polymer had a very high turn-on voltage (24 V) and a very low luminance (0.228 cd/m^2 at 29 V). Pei et al. (2002) designed conjugated polymers with europium(III) β -diketonate complexes grafted to fluorene-type conjugated polymers through pendant 2,2'-bipyridine groups in the side chains. An OLED based on this conjugated polymer has a turn-on voltage of 15 V, an external electroluminescence efficiency of 0.07% and a luminance of about 11 cd/m^2 at 25 V. Although most of the lanthanide complexes applied in OLEDs are ternary complexes (Lewis base adducts of tris β -diketonate complexes), there is evidence that the tetrakis β -diketonate complexes give a good performance as well. This was illustrated for $\text{Li}[\text{Eu}(\text{tta})_4]$, $\text{Na}[\text{Eu}(\text{tta})_4]$ and $\text{K}[\text{Eu}(\text{tta})_4]$ (Yu et al.,

2000). An advantage of these complexes is their good solubility in organic solvents such as chloroform, ethanol, acetonitrile and acetone. This facilitates their processing by spin coating. Water-soluble β -diketonate complexes were obtained by functionalizing dibenzoylmethane in the 4-position by an oligo-ethylene oxide chain, or by formation of ternary complexes with a sulfonic acid substituted-phenanthroline (Anonymous, 2004). The performance of the tetrakis complex $(\text{pyH})^+[\text{Eu}(\text{tta})_4]^-$ in OLEDs was studied by Liang et al. (1997).

The most popular lanthanide ion for incorporation in OLEDs is without doubt the europium(III) ion. An overview of the development in the field of red-emitting OLEDs is summarized in table 8. Most of the electroluminescent europium(III) complexes have dibenzoylmethanate (dbm) or thenoyltrifluoroacetate (tta) as the β -diketonate ligand. Also the electroluminescence of the green-emitting terbium(III) β -diketonate complexes has been well-investigated (Kido et al., 1990; Liang et al., 1997; Li et al., 1997; Gao et al., 1999; Wang et al., 2000a; Moon et al., 2001; Christou et al., 2000; Zheng et al., 2002b, 2002d; Pyo et al., 1999; Zhao et al., 2000). Hong et al. (2000) designed a white light emitting OLED, consisting of $[\text{Dy}(\text{acac})_3(\text{phen})]$ as the emitting layer and poly(*N*-vinylcarbazole) (PVK) as the hole transporting layer. The white emission was obtained by a superposition of a yellow emission band (${}^4\text{F}_{9/2} \rightarrow {}^6\text{H}_{13/2}$ transition at 580 nm) and of a blue emission band (${}^4\text{F}_{9/2} \rightarrow {}^6\text{H}_{15/2}$ transition at 480 nm). The white emission was found to be independent of the drive voltage. These authors were also able to make a OLEDs emitting narrow-band blue light (482 nm) by incorporation of the $[\text{Tm}(\text{acac})_3(\text{phen})]$ complex (Hong et al., 1999). Zhang et al. (1997a) observed a change in emission color from green-white to red when the temperature of the compound $[(\text{Eu}_{0.1}\text{Gd}_{0.9})(\text{tta})_3(\text{tppo})_2]$ was increased from 77 K to 300 K. At cryogenic temperatures, triplet emission (phosphorescence) of the organic ligand is observed, while at higher temperatures the phosphorescence is quenched by the europium(III) ion and the typically red luminescence of Eu^{3+} is seen. An OLED based on this compound could be used for temperature-monitoring. Samarium(III) complexes give orange electroluminescence. This was illustrated by an OLED incorporating the $[\text{Sm}(\text{tta})_3(\text{tppo})_2]$ complex (Reyes et al., 2002). Infrared luminescence was obtained by use of $[\text{Yb}(\text{dbm})_3(\text{bath})]$ (Kawamura et al., 2000; Hong et al., 2001a, 2001b), $[\text{Nd}(\text{dbm})_3(\text{bath})]$ (Kawamura et al., 1999), $[\text{Er}(\text{acac})_3(\text{phen})]$ (Sun et al., 2000). However, in each case the efficiency was very low. $[\text{Pr}(\text{dbm})_3(\text{bath})]$ generates both visible and infrared light (Hong et al., 2001a, 2001b). The infrared emission of this complex consists of three bands, at 1015 nm, 1065 nm and 1550 nm. The bands were assigned to the ${}^1\text{D}_2 \rightarrow {}^3\text{F}_3$, ${}^1\text{D}_2 \rightarrow {}^3\text{F}_4$ and ${}^1\text{D}_2 \rightarrow {}^1\text{G}_4$ transition respectively. The emitting level is thus ${}^1\text{D}_2$ and not ${}^1\text{G}_4$. The typical ${}^1\text{G}_4 \rightarrow {}^3\text{H}_3$ band at 1320 nm was absent. Huang et al. (2002b) used the terbium complex tris-(1-phenyl-3-methyl-4-isobutyryl-5-pyrazolone)-bis(triphenyl phosphine oxide), $[\text{Tb}(\text{pmip})_3(\text{tppo})_2]$, not as the emissive layer, but as the electron-transporting layer in a blue-emitting OLED. Chu et al. (2002) made a bifunctional organic diode containing $[\text{Y}(\text{acac})_3(\text{phen})]$ for both light-to-electricity conversion (photovoltaic cell) or electricity-to-light conversion (OLED).

Kido et al. (1996) made a white-emitting OLED by combining in the emissive layer $[\text{Eu}(\text{dbm})_3(\text{phen})]$ for red emission, $[\text{Tb}(\text{dbm})_3(\text{phen})]$ for green emission and TPD for blue emission. TPD has also hole-transporting properties. Tris(8-hydroxyquinolino)aluminum(III) was used as the electron-transporting layer. Zhao et al. (1999b) obtained white emis-

Table 8
Europium(III) β -diketonate complexes in OLEDs^a

Emitter layer	L (cd/m ²)	V (V)	J (mA/cm ²)	η_{ext} (%)	η_{p} (lm/W)	Reference
[Eu(tta) ₃]/PMPS	0.3	18	–	–	–	Kido et al., 1991
[Eu(tta) ₂ (pmbbp)(phen)]	16	12.5	125	–	–	Zhu et al., 2000b
[Eu(tta) ₃ (phen)]	30	15	182	–	–	Lee et al., 1999
Na[Eu(tta) ₄]/PVK	36.7	26	–	–	–	Yu et al., 2000
[Eu(dbm) ₃ (phen)]	50	15	–	–	–	Heil et al., 2001
[Eu(tfac) ₃ (bpy)]	68	20	–	–	–	Zheng et al., 2002a
[EuY(tta) ₆ (phen) ₂]	99	11	246.5	–	–	Zhu et al., 2000a
[Eu(dbm) ₃ (tppo)]	320	14.5	–	–	–	Hu et al., 2000b
[Eu(dbm) ₃ (OXD-PyBM)]	322	21	–	1.7	–	Liang et al., 2003
[Eu(dbm) ₃ (bath)]	400	15	–	–	–	Liang et al., 2000b
[Eu(tta) ₃ (phen)]/PBD,PVK	417	25	175	–	–	Male et al., 2002
[Eu(dtp) ₃ (bath)]	450	15	200	–	–	Okada et al., 1999
[Eu(dbm) ₃ (phen)]/PBD (1/3)	460	16	–	–	–	Kido et al., 1994
[Eu(tta) ₃ (phen)]/CBP (1%)	505	12	0.4	1.4	–	Adachi et al., 2000
[Eu(dbm) ₃ (bath)]/TPD (3/1)	820	18	0.6	1.0	1.0	Liang et al., 2000a
[Eu(DCNP)(dbm) ₂ (phen)]/PBD (10%)	924	–	0.17	3.5	2.0	Liu et al., 1997
[Eu(tta) ₃ (dppz)]/CBP (4.5%)	1670	13.6	1.23	2.1	2.1	Sun et al., 2002

^aParameters: operating voltage (V), current density (J), external quantum efficiency (η_{ext}), luminance (L), power efficiency (η_{p}).

sion from an OLED containing $[\text{Eu}_x\text{Tb}_{1-x}(\text{acac})_3(\text{phen})]$ in the emissive layer. Pyo et al. (2000) designed a white-emitting OLED based on $[\text{Eu}(\text{tta})_3(\text{phen})]$, $[\text{Tb}(\text{acac})_3(\text{Cl-phen})]$ and TPD. Here, Cl-phen is a chlorine-substituted phenanthroline group. A voltage tunable OLED was obtained by using a mixed samarium(III) and europium(III) complex, $[\text{Sm}_{0.7}\text{Eu}_{0.3}(\text{tta})_3(\text{tppo})_2]$ (Reyes et al., 2004). Raising the voltage of the device results in a gradual change of the red emission colour to a yellowish one, due to a higher contribution of triplet emission by the tta ligands.

8.3. Liquid crystal displays (LCDs)

Liquid crystal displays are being widely used for several technological applications, such as the displays of calculators or the screens of laptop computers. LCDs have the advantage of a low power consumption and they are flat (in contrast to the cathode ray tube monitors), but they have some disadvantages as well: a restricted viewing angle and a low brightness. These are mainly due to the use of dichroic sheet polarizers and absorbing color filters in the LC cell. Those optical components are inefficient in the sense that they lose a large part of the incident light. Major improvements in LCD performance can be expected when an LC cell without polarizers and color filters would be designed. A very promising concept is the *luminescent LCD*, which is an emissive type of display, just as the cathode ray tube is. Luminescent lanthanide complexes, including β -diketonate complexes, can play an important role in the development of this type of display. The idea of a luminescent LCD is not new. The first one to explore this concept was Larrabee, who added luminescent molecules to a nematic liquid crystal (Larrabee, 1973, 1976). These luminescent molecules were excited with an UV source and emission was controlled electrically by the alignment of the liquid crystal (the *nematic 'guest-host effect'*). Yu and Labes suggested to use an electric field induced cholesteric to nematic phase transition as the basis of a luminescent LCD (Yu and Labes, 1977; Labes, 1979). The cholesteric "off" state absorbs the excitation light stronger than the nematic "on" state, so that the emission of the luminescent additive is intense in the "off" state and is reduced in the "on" state. The authors used the red-emitting europium(III) complex $[\text{Eu}(\text{tta})_3(\text{H}_2\text{O})_2]$ as the luminescent additive and could reach a contrast ratio of 9:1 (differences in intensities between the "off" and the "on" state). A third approach to luminescent LCDs is replacement of the absorbing color filter by a luminescent layer. However, the development of luminescent LCDs slowed down. At that time the quality of the LCD was high enough to meet all the needs. Secondly, there were no convenient UV-sources available (except the mercury discharge lamp). Presently, the situation is different. The growing market for flat computer monitors makes luminescent LCDs attractive again. The newly developed UV-LEDs have advantages as LCD backlights: light, thin, mercury-free and noiseless. The application of UV-LED as backlights for luminescent LCDs was explored by Sato et al. (1998) and by Yamaguchi et al. (1999). Work done in the Philips Research Laboratories describes the use of lanthanide β -diketonate complexes incorporated in a polymer sheet, and excited by UV-LEDs (Boerner et al., 2000a, 2000b).

8.4. Polymeric optical waveguides and amplifiers

Telecommunication is an important aspect of our present society. Due to the intensive use of Internet there is a need for fast data transfer. Presently, the most often used information carriers are still electric pulses that are transmitted through copper wires. However, if light is used instead of electricity, the speed of data transfer can be increased up to a factor 10^6 . For long-distance transfer of light signals, special optical glass cables have been developed. An *optical cable* consists of a very transparent core and a transparent covering layer (the cladding), which must have a lower refractive index than that of the core material. If a cable is fabricated in such a configuration, light will stay inside the core by total reflection and can be transmitted over a certain distance. Glass is superior to polymers in transparency, but not in mechanical properties. Glass is brittle and as a consequence the core of the glass optical cables needs to be very thin (ca. 0.1 mm) in order to have some flexibility without the problem of fracture. For this reason, one uses in general the term 'glass optical fibers' instead of 'glass optical cables'. The small diameter makes coupling of fibers difficult and time-consuming. For local-area fiber networks in particular, huge numbers of couplings are necessary. Therefore, the use of optical glass fibers is a very expensive option for those applications. As polymers are far more ductile than glass, larger core diameters up to 1 mm or more are feasible without losing flexibility. However, polymers do suffer from a lower transparency. This means that their application is limited to local-area networks. Transmission loss (expressed in dB/km or in dB/m) is an important parameter to determine the performance of an optical fiber. Transparent polymers applied as *polymer optical fibers* (POFs) are poly(methyl methacrylate) (PMMA), polystyrene and polycarbonate. PMMA is the most transparent bulk material known at this moment and is most widely used. A drawback of PMMA is its low glass transition temperature. Above 80 °C, softening and a consequential loss of properties sets in, so that PMMA cannot be used above this temperature. This limits its applicability tremendously. Materials with a higher glass transition temperature, such as polycarbonates are applicable, but they suffer from high intrinsic optical losses, resulting in low transmission distances. Two different types of optical fibers are the *step-index optical fibers* and the *graded-index optical fibers*. In the step-index optical fiber, the refractive index is constant along the fiber core cross-section and immediately changes (step-wise) to the refractive index of the cladding. The refractive index of a graded-index optical fiber has a maximum along the fiber axis and decreases gradually in the radial direction until it merges into the constant index of the cladding. Light rays propagate via discrete paths through a fiber. Each distinct path is called a *mode* and corresponds to a certain angle of incidence. Consequently, different modes take different times to travel along the fiber. The total number of light modes which can be coupled in an optical fiber is defined by the *numerical aperture* (NA), which is limited by the refractive index difference between cladding and core.

In order to extend the distance onto which an optical signal can be transmitted by a polymer optical fiber, loss of energy has to be compensated by coupling the polymer optical fiber to an *optical amplifier*. Such an optical amplifier contains a luminescent material emitting at the same wavelength as the signal beam. The luminescent material needs to be pumped by a laser beam, which excites the molecules to a higher energy level and generates population inversion of the electronic states. A beam traveling through the amplifying medium stimulates

the emission of light with the same wavelength and phase. In a *polymer optical fiber amplifier (POFA)*, emission is stimulated by the attenuated signal, and the intensity of the signal is amplified. Laser pumping is necessary to achieve and retain the population inversion. *Planar optical waveguides* are related to the optical fiber amplifiers. A planar optical waveguide has a sandwich structure in which a layer of a transparent polymeric material is covered on either side with a layer of a transparent optical material having a lower refractive index. Planar optical waveguides can also be used for amplification of optical signals. They are easier to manufacture and optical pumping can be achieved more conveniently because they can be irradiated by the pump laser over the entire area of the layer.

Lanthanide complexes, including lanthanide β -diketonate complexes, have been often tested as a luminescent materials in polymer optical fiber amplifiers and in planar optical waveguides. This research has been reviewed by Kuriki et al. (2002).

Kobayashi et al. (1997) made graded index polymer optical fibers of PMMA doped with the europium(III) complexes $[\text{Eu}(\text{tta})_3]$ and $[\text{Eu}(\text{hfac})_3]$. An increase in luminescence intensity was observed when 20 wt% of triphenyl phosphate was added to the polymer, whereas the luminescence intensity decreased upon addition of benzyl *n*-butyl phthalate. The attenuation loss of the graded index PMMA fiber doped with $[\text{Eu}(\text{hfac})_3]$ was found to be 0.4 dB/m around 650 nm. Lin et al. (1996) doped the fluorinated neodymium(III) complex $[\text{Nd}(\text{hfac})_3]$ into a fluorinated polyimide (UI-trade 9000 series of the Amoco Chemical Company) and used this material to prepare waveguides. Although they observed photoluminescence at 880, 1060 and 1330 nm, the luminescence intensity was weak. Kuriki et al. (2000) prepared a graded index optical fiber of deuterated PMMA- d_8 doped with the neodymium(III) complex of deuterated hexafluoroacetone, $[\text{Nd}(\text{hfa-}d)_3]$ or with the neodymium(III) complex of deuterated 1,1,1,2,2,6,6,7,7,7-decafluoro-3,5-heptanedione, $[\text{Nd}(\text{fhd-}d)_3]$.

9. NMR shift reagents

9.1. Historical development and general principles

Nuclear magnetic resonance (NMR) spectroscopy is nowadays one of the most powerful techniques available to the chemist to elucidate the structure of organic compounds. However, in order to measure chemical shifts, coupling constants and peak integrations, the NMR signals should be clearly separated. Overlap is not a serious problem in ^{13}C NMR spectra, but is more likely to occur in ^1H NMR spectra. At the time when the only NMR spectrometers available at a reasonable price were operating at a low frequency (60 or 90 MHz), not only complex molecules such as steroids gave spectra with overlapping peaks, but it was even impossible to obtain well-resolved proton NMR spectra of simple molecules such as 1-hexanol. The interpretation of proton NMR spectra can be made easier by application of NMR shifts reagents. These are paramagnetic metal complexes which induce changes in the chemical shifts of protons close to an electronegative substituent with a lone electron pair (e.g. amino, hydroxyl or carbonyl groups). The ability of certain lanthanide complexes to induce large changes in chemical shifts with relatively small line broadening effects made them popular as *NMR shift*

reagents. One uses also the term '*lanthanide shift reagents*' (abbreviated to LSR) for them. Most of these shift reagents are lanthanide β -diketonate complexes. These complexes are stable, soluble in organic solvents (when a proper choice of β -diketone ligand is made) and are known to expand their coordination sphere by adduct formation with ligands having lone electron pairs.

The ability of paramagnetic substances to shift NMR resonances has been attributed to two processes: the contact and the dipolar interactions. The contact interaction operates through bonds. The contribution from the contact interaction arises from the delocalization of the unpaired electron from the shift reagent to the atoms of the substrate. The ease with which this happens varies for different nuclei. For a saturated molecule the effect is usually restricted to atoms which are a few bonds away from the shift reagent. The dipolar (or pseudo-contact) interaction is due to the direct effect of the magnetic moment of the unpaired electron on the nuclei of the substrate. The effect is transmitted through space and is inversely proportional to the cube of the distance between the two nuclei. The use of lanthanide shift reagents in simplifying NMR spectra is not only based on resolution of overlapping multiplets, but also on the ability to reduce second-order spectra (i.e. spectra in which the value of the coupling constant J is comparable to the value of the chemical shift δ) to first-order spectra ($\delta \gg J$).

In September 1969, Hinckley published a seminal paper on lanthanide-induced shifts in the proton NMR spectrum of cholesterol by addition of the paramagnetic dipyridine-adducts of tris(dipivalomethanato)europium(III), $[\text{Eu}(\text{thd})_3(\text{py})_2]$ (Hinckley, 1969). His measurements showed downfield shifts of specific proton resonances of cholesterol by 0.02 to 3.5 ppm and the addition of the europium(III) complex did not cause an appreciable line broadening of the signals. Hinckley realized the potential of lanthanide complexes as NMR shift reagents in inducing changes in the chemical shifts in proton NMR spectra. He found that the magnitudes of the induced shifts vary linearly as the reciprocal of the cube of the distance of the ^1H nucleus from the site of coordination (the hydroxyl group in the case of cholesterol). Shortly after this discovery, Sanders and Williams (1970) described the use of the pyridine-free europium(III) compound $[\text{Eu}(\text{thd})_3]$. Addition of $[\text{Eu}(\text{thd})_3]$ to benzylalcohol or 1-hexanol gave shifts up to 15 ppm. The anhydrous tris complex is a much more efficient NMR shift reagent than the pyridine bis-adduct, because of the competition between pyridine and the organic substrate for the free coordination sites in the europium(III) complex. Sanders and Williams (1971) have estimated the relative order of complexation of various functional groups with $[\text{Eu}(\text{thd})_3]$ as judged from relative shifts in comparable molecules: amines > alcohols > ketones > aldehydes > ethers > esters > nitriles. Briggs et al. (1970) found that tris(dipivalomethanato)praseodymium(III), $[\text{Pr}(\text{thd})_3]$, shifts proton resonances upfield and that these upfield shifts are larger than the downfield displacements by $[\text{Eu}(\text{thd})_3]$. The analogous complexes of neodymium, samarium, terbium, dysprosium and holmium induce shifts to higher field, whereas the erbium, thulium and ytterbium complexes induce shifts to lower fields (Crump et al., 1970; Ahmad et al., 1971; Armitage and Hall, 1971). Whidesides and Lewis (1970) described the use of a chiral lanthanide shift reagent, tris-[(3-*tert*-butylhydroxymethylene) *d*-camphorato]europium(III), for determination of enantiomeric purity. In Rondeau and Sievers (1971) first described the lan-

thanide complexes of 6,6,7,7,8,8,8-heptafluoro-2,2-dimethyl-3,5-octanedione, Hfod, as shift reagent. The $[R(\text{fod})_3]$ compounds are considerable more soluble in NMR solvents such as CCl_4 and CDCl_3 , and have found to induce larger shifts than $[R(\text{thd})_3]$ complexes in many substrates. They are suitable shift reagents for weak Lewis bases such as ethers, esters and nitriles. The $[\text{Eu}(\text{fod})_3]$, $[\text{Pr}(\text{fod})_3]$ and $[\text{Yb}(\text{fod})_3]$ complexes became the most widely used of the various commercially available NMR shift reagents. Suitable shift reagents for soft Lewis bases such as alkenes, aromatics and halogenated compounds are the binuclear silver-lanthanide β -diketonate complexes introduced by [Wenzel et al. \(1980\)](#).

In the 1970's and 1980's several review papers devoted to lanthanide NMR shift reagents have been published ([Campbell, 1971](#); [von Ammon and Fischer, 1972](#); [Becker, 1972](#); [Peterson and Wahl, 1972](#); [Horrocks, 1973](#); [Sievers, 1973](#); [Slonim and Bulai, 1973](#); [Cockerill et al., 1973](#); [Williams, 1974](#); [Voronov, 1974](#); [Reuben, 1975a, 1975b](#); [Flockhart, 1976](#); [Sullivan, 1978](#); [Reuben and Elgavish, 1979](#); [Inagaki and Miyazawa, 1981](#); [Forsberg, 1981](#)). A very comprehensive overview of the use of tris(β -diketonato)lanthanide complexes as NMR shift reagents can be found in the book of [Wenzel \(1987\)](#). Recent developments have been reviewed by [Forsberg \(1996\)](#) and by [Peters et al. \(1996\)](#).

The main use of NMR shift reagents was in the separation of overlapping multiplets in proton NMR spectra of organic compounds which are able to coordinate to a lanthanide ion. It is also possible to obtain information on the molecular structure in solution by fitting the dipolar contribution to the bound shift of the complex between the shift reagent and the substrate to the so-called *McConnell–Robertson equation* ([McConnell and Robertson, 1958](#)).

With the advent of modern high-frequency Fourier-Transform NMR spectrometers at the end of the 1980's, the importance of NMR shift reagents faded. The proton NMR spectra recorded on a high-frequency NMR spectrometer (>250 MHz) are much easier analyzable than the ones recorded at a lower frequency. The corresponding signals are narrower and thus better resolved. The spectra are more likely to be of first order. In cases where the proton resonances are difficult to assign, one can rely on spin decoupling experiments, or on two-dimensional NMR techniques (COSY, NOESY, ...). It should be noticed that one can be faced with problems of excessive signal broadening when using lanthanide shift reagents on high-frequency NMR spectrometers, due to the slower tumbling rate of the shift reagent donor complex compared to the free donor ([Bulsing et al., 1981](#)). Such broadening is more important when NMR spectra are recorded at high frequency. The multidimensional NMR techniques have also facilitated the determination of the conformation of organic molecules in solution, and limited the importance of lanthanide shift reagents in this application. The chiral NMR shift reagents are still more often used than the achiral analogues, since the former can be used for the determination of the optical purity (enantiomeric excess) of chiral organic molecules. Fast recording FT-NMR spectra of compounds with long relaxation times is a problem due to saturation effects. By adding a shift reagent, the relaxation time can be reduced and the accumulation time for recording an NMR spectrum can be shortened significantly. Lanthanide shift reagents are re-gaining importance in field such as protein structure determination ([Geraldés and Luchinat, 2003](#)).

9.2. Achiral shift reagents

The achiral shifts reagents are lanthanide complexes of achiral β -diketones, such as Hthd (Hdpm) and Hfod. Not all trivalent lanthanide ions can be employed in NMR shift reagents (Wenzel, 1987). Lanthanum(III) and lutetium(III) are useless, because they are diamagnetic. Cerium(III) is unstable and tends to be oxidized to diamagnetic cerium(IV) in β -diketonate complexes. Promethium(III) is radioactive and has only short-living isotopes. Although gadolinium(III) is paramagnetic and is the most often used ion in magnetic resonance imaging (MRI) contrast agents, it cannot be used as NMR shift reagent. The reason is that the ground state of the $4f^7$ electronic configuration of gadolinium(III) is isotropic and will not produce pseudo-contact shifts in the NMR spectrum of a substrate. Addition of a gadolinium(III) complex to the substrate will cause only severe line broadening.

Complexes of Pr, Nd, Sm, Tb, Dy, and Ho are upfield shift reagents with relative ordering of the shifts $Dy > Tb > Ho > Pr > Nd > Sm$. Complexes with Eu, Er, Yb, and Tm are downfield shift reagents with a relative ordering $Tm > Er > Yb > Eu$. This ordering has been determined from the isotropic shifts for the most shifted resonances in 1-hexanol, 4-picoline, 4-picoline *N*-oxide and 4-vinylpyridine, with $[R(dpm)_3]$ as the metal of the shift reagent was varied (Horrocks and Sipe, 1971, 1972). The magnitude and direction of the shift can be related to the magnetic anisotropy of the lanthanide complex (Bleaney, 1972; Horrocks and Sipe, 1971).

One might conclude from these results that dysprosium and thulium are the best metals to use in NMR shift reagents. However, these metal are seldom applied in shift reagents, because of too severe line broadening which blurs the fine structure in the proton NMR spectrum. The line broadening with a shift reagent is proportional to the square of the chemical shift (Reuben and Leigh, 1972). Secondly, dysprosium and thulium cause such large shifts that can make finding and assigning all the resonances difficult. The shifts induced by the less powerful lanthanide ions are still large enough to produce first-order proton NMR spectra, and in this case line broadening is less a problem. Therefore, europium is the preferred metal in downfield shift reagents, whereas praseodymium is used in upfield shift reagents. In some studies, ytterbium complexes are used as downfield shift reagent.

In general, downfield reagents are preferred over the upfield analogs (Wenzel, 1987). The resonances furthest downfield in the unshifted spectrum are usually closest to the electron withdrawing groups that bond to the shift reagent. These resonances often exhibit the largest shift and remain the furthest downfield in the shifted spectrum. A first-order spectrum with an upfield shift reagent requires a complete inversion of the spectrum. The resonances of nuclei closest to the electron-withdrawing group are now furthest upfield. Larger shifts are necessary to achieve a first-order spectrum with an upfield shift reagent than with a downfield reagent. The inversion of NMR spectra with upfield shift reagents can contradict our sense of NMR spectra. In some cases, praseodymium(III) complexes have been applied to move the resonances of methyl groups to still higher fields (Belanger et al., 1971a, 1971b).

The tris(β -diketonato)europium(III) complexes are the most popular shift reagents for the study of achiral substrates. The europium(III) complexes induce shifts large enough for most applications and the line broadening is so slight that the fine structure due to coupling remains

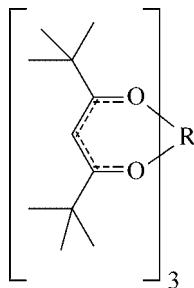


Fig. 45. Structure of the NMR shift reagents $[R(\text{thd})_3]$, where $R = \text{Pr, Eu, Yb}$. The complexes are also known under the abbreviation $[R(\text{dpm})_3]$. Hthd stands for 2,2,6,6-tetramethyl-3,5-heptanedione and Hdpm stands for dipivaloylmethane.

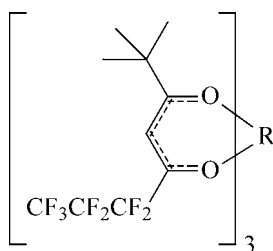


Fig. 46. Structure of the NMR shift reagents $[R(\text{fod})_3]$, where $R = \text{Pr, Eu, Yb}$. Hfod stands for 6,6,7,7,8,8,8-heptafluoro-2,2-dimethyl-3,5-octanedione.

intact. One can wonder why europium(III) can be used in shift reagents, although the non-degenerate 7F_0 ground state of the Eu^{3+} ion cannot cause contact or pseudo-contact shifts. The reason is that the first excited state, 7F_1 , is only about 300 cm^{-1} above the ground state and is significantly populated at room temperature. The 7F_1 state accounts for the shift properties of the europium(III) ion.

Lanthanide complexes with a wide variety of achiral β -diketonate ligands have been tested for use as NMR shift reagents. However, only two types of complexes have found a widespread application: those with the ligands 2,2,6,6-tetramethyl-3,5-heptanedione (Hdpm or Hthd), and 6,6,7,7,8,8,8-heptafluoro-2,2-dimethyl-3,5-octanedione (Hfod) (figs. 45 and 46). Please notice that the abbreviations Hdpm and Hthd are used for one and the same β -diketonate. It is evident that the abbreviation Hthd is derived from the systematic name of 2,2,6,6-tetramethyl-3,5-heptanedione, whereas dpm notation comes from the trivial name dipivaloylmethane. Still another abbreviation for 2,2,6,6-tetramethyl-3,5-heptanedione is Htmhd. Although the abbreviation dpm is more often used than thd in the case of NMR contrast agents, we will use thd, because this abbreviation is currently more popular, and this abbreviation is also used by workers in the field of volatile rare-earth β -diketonate complexes (see section 11). The $[R(\text{thd})_3]$ and the $[R(\text{fod})_3]$ complexes are available from several commercial

sources (especially those with Ln = Pr, Eu or Yb). The [R(fod)₃] complexes have several advantages over the [R(thd)₃] complexes. First of all, they are much more soluble in common NMR solvents than the [R(thd)₃] complexes. The low solubility of the latter compounds restricts their application in some cases. Secondly, the [R(fod)₃] complexes are more effective shift reagents than the [R(thd)₃] complexes, in the sense that they induce a larger chemical shift for the same concentration of shift reagent. They are suitable shift reagents for weak donor compounds such as ethers, ketones and esters. The explanation given for this superior behavior is that the -C₃F₇ group of the fod ligands withdraws electron density from the lanthanide ion, so that the [R(fod)₃] complexes are stronger Lewis acids than the corresponding [R(thd)₃] complexes (Rondeau and Sievers, 1971; Sievers, 1980). Stronger Lewis acids are able to build more stable complexes with weak Lewis bases than weaker Lewis acids do. Or to say it in other words: the lanthanide ion in the [R(fod)₃] complexes is harder than in the [R(thd)₃] complexes. A disadvantage of the [R(fod)₃] complexes is that they are very hygroscopic and difficult to keep in an anhydrous form. The well-known complexes [R(acac)₃] and [R(dbm)₃] are of little value because of the hygroscopic nature of the acetylacetonate complexes and the low solubility of the dibenzoylmethanate complexes in NMR solvents (Sanders and Williams, 1971). It was also argued that lanthanide β-diketonate complexes with less bulky substituents than [R(thd)₃] or [R(fod)₃] are inefficient as shift reagents, because of the lack of a preferred orientation of the substrate molecules when the stereochemical rigidity and the bulky substituents of the chelate rings are absent (Sanders and Williams, 1971; Horrocks and Sipe, 1971).

The NMR solvents should not contain polar groups, in order to avoid a strong interaction between the solvent and the shift reagent. Therefore, one is restricted to solvents such as CCl₄, CDCl₃, CS₂ or C₆D₆. As mentioned above, the solubility of the [R(thd)₃] complexes is rather low. For instance, the solubility of Eu(thd)₃ in CCl₄ or CDCl₃ is ca. 0.2 mol/l or ca. 150 mg/ml, and ca. 0.1 mol/l or 70 mg/ml in deuterated benzene (Pohl, 1971). The solubility of the [R(thd)₃] complexes increases by a factor of more than three in the presence of substrates with polar groups, so that solutions containing a shift reagent concentration larger than 300 mg/ml can be obtained. The solubility of the [R(fod)₃] complexes is more than 400 mg/ml. The magnitude of the lanthanide induced shift is a function of the solvent (Wenzel, 1987). The largest shifts are observed in non-polar solvents such as *n*-heptane or cyclohexane, intermediate shifts are observed in CCl₄ and CS₂, and smaller shifts occur in benzene and chloroform. The shift in CDCl₃ is about 80% of the value observed for the shift in CCl₄, and the shift in C₆D₆ is about 90% of the value in CCl₄. It is recommended that CCl₄ is used for quantitative studies and that solvents such as CDCl₃ and C₆D₆ should only be employed for qualitative studies (separation of overlapping signals) (Arduini et al., 1973). There is still no satisfying explanation for explanation of the solvent effect on the lanthanide induced shifts (Wenzel, 1987). It is not known whether a solvent such as CDCl₃ lowers the association constant by competition with the substrate for the lanthanide ion. Some arguments are against this competing mechanism. For instance, no significant shift of the proton resonance of CHCl₃ is observed in the presence of a shift reagent (Raber et al., 1980). The solvent used in studies of NMR shift reagents should be carefully dried prior to use. It is presumed that the reference compound tetramethylsilane (TMS) exhibits no shift in the presence of a lanthanide

shift reagent. The TMS resonance often interferes with the resonances shifted by upfield shift reagents, and in such cases benzene is recommended as an internal standard (Shapiro and Johnston, 1972).

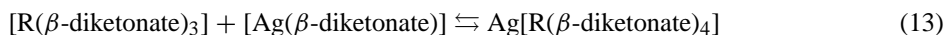
To avoid a strong dilution of the solution containing the substrate, it is recommended to add the shift reagent in solid form, rather than in the form of a concentrated solution. One has to be cautious not to measure the NMR spectrum before all the shift reagents has dissolved, because even the smallest amount of undissolved shift reagent has a deteriorating effect on the resolution. In case of doubt, the solution should be filtered through a plug of glass wool. A strong line broadening is also observed in cases when the tris(β -diketonato)lanthanide(III) is contaminated by lanthanide oxide or hydroxide impurities. The shift reagent can be purified by vacuum sublimation. The shift reagents should also be carefully dried, preferentially in vacuum (1 Torr) at 100–115 °C over P₂O₅ for 24 hours (Wenzel, 1987). Peters et al. (1981) showed that in commercial [R(fod)₃] shift reagents, adducts of the type [R(fod)₃]-Mfod (M = Na, K) are often present as impurities. A shift reagent contaminated with [R(fod)₃]-Mfod can be purified by shaking a CHCl₃ solution of the shift reagent with an aqueous solution of LnCl₃. Alternatively, a CHCl₃ solution of the impure shift reagent can be shaken a 0.1 N aqueous HCl solution to yield a mixture of [R(fod)₃] and Hfod. Hfod can be removed by recrystallization or by selective adsorption into zeolite NaX.

The *tert*-butyl group of pure [Eu(thd)₃] exhibits a relatively broad resonance signal at $\delta = +0.5$ ppm. In the presence of complex forming molecules this resonance is shifted upfield to the range from $\delta = -0.5$ ppm to $\delta = -2$ ppm (Pohl, 1971). The corresponding signal in [Pr(thd)₃] can be found at $\delta = +1.4$ ppm and is shifted after addition of complex forming molecules to the range from $\delta = +3$ ppm to $\delta = +5$ ppm. In both cases, the spectral range of interest of the organic substrate is free from the disturbing *tert*-butyl signal of the lanthanide complex. Fully deuterated lanthanide shift reagents are available for difficult cases in which interference with the resonances of the lanthanide complex occurs. Another approach to eliminate the *tert*-butyl resonances it is to use highly fluorinated ligands (Wenzel, 1987). Examples of such ligands are 1,1,1,5,5,6,6,7,7,7-decafluoro-2,4-heptanedione (Sievers et al., 1976; Dyer et al., 1973), 1,1,1,2,2,6,6,7,7,7-decafluoro-3,5-heptanedione (Burgett and Warner, 1972; Burgett, 1975; Morrill et al., 1975) and 1,1,1,2,2,3,3,7,7,8,8,9,9,9-tetradecafluoro-4,6-nonanedione (Morrill et al., 1975). Although the lanthanide complexes prepared from these ligands induce larger shifts in organic substrates than the classic reagents [R(thd)₃] and [R(fod)₃], they only found a limited use, because they are more difficult to prepare and to store in an anhydrous crystalline form.

When there is a strong interaction between the substrate molecules and the lanthanide shift reagents, the optimum shift is observed at less than stoichiometric ratios between the substrate and the shift reagent, namely at molar ratio of 0.5 to 0.7 mole of shift reagent to 1.0 mole of substrate (Pohl, 1971). Higher concentration of shift reagents do not result in a larger shift, but only in a line broadening (which fastly increases with increasing concentration of the shift reagent). The fact that only one NMR spectrum is observed and not the superposition of the NMR spectra of the non-coordinated and the coordinated substrate molecules, despite that an excess of the substrate is present, indicates that a fast exchange of the substrate molecules coordinated to the lanthanide ions takes place. Horrocks and Sipe (1971) observed a

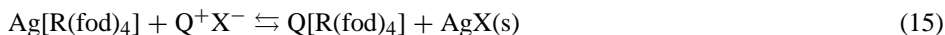
linear dependence of the shift on the $[R(\text{thd})_3]/[\text{substrate}]$ ratio for values of the quantity less than 0.2.

The $[R(\text{thd})_3]$ and $[R(\text{fod})_3]$ shift reagents are effective on compounds containing the basic heteroatoms oxygen and nitrogen, but do not bind to and do not shift the NMR signals of soft Lewis bases such as alkenes, aromatics, halogenated compounds and phosphines. Evans et al. (1975) reported shifts in the spectra of alkenes by using silver heptafluorobutyrate in combination with lanthanide tris(β -diketonates). In these systems the alkene is bound to silver heptafluorobutyrate which acts as a bridge between the alkene and the lanthanide shift reagent. Damska and Janowski (1980a, 1980b) used $[\text{Pr}(\text{fod})_3]$ with silver trifluoroacetate to resolve the proton resonances of the xylene isomers. Wenzel et al. (1980) reported the use of binuclear lanthanide(III)–silver(I) shift reagents for aromatic compounds. They made silver complexes of Hfod and of 1,1,1-trifluoro-2,4-pentanedione, Htfa, and found that these complexes $[\text{Ag}(\text{fod})]$ and $[\text{Ag}(\text{tfac})]$ are better bridging compounds between aromatics and lanthanide shift reagents than silver heptafluorobutyrate and silver trifluoroacetate are. The original work on shift reagents for aromatics has been extended to alkenes, halogenated compounds and phosphines (Wenzel and Sievers, 1981, 1982a, 1982b; Offermann and Mannschreck, 1981; Smith, 1981; Krasutsky et al., 1982; Wenzel and Lalonde, 1983). The equilibria involved with the binuclear shift reagents and a substrate are (Wenzel and Russett, 1987; Wenzel, 1987):



It is thus assumed that the active species is an ion pair between silver(I) and a lanthanide(III) tetrakis(β -diketonate) complex. It is still not known what the driving force for the formation of the $\text{Ag}[R(\beta\text{-diketonate})_4]$ from $[R(\beta\text{-diketonate})_3] + [\text{Ag}(\beta\text{-diketonate})]$ is. The formation constant of $\text{Ag}[R(\text{fod})_3]$ is about 500 M^{-1} (Raber and Hajek, 1986). For substrates which bind only weakly to silver (aromatic and chlorinated compounds), it is advantageous when pentane is substituted for CDCl_3 as NMR solvent (Wenzel, 1984). Because of pentane resonances in the region between $\delta = 1$ and $\delta = 4$ ppm, pentane cannot be used as a solvent to study compounds which have proton resonances in this spectral range. Wenzel and Lalonde (1983) reported that the silver complexes $[\text{Ag}(\text{tta})]$ and $[\text{Ag}(\text{hfth})]$ are more stable than the $[\text{Ag}(\text{fod})]$ and $[\text{Ag}(\text{tfac})]$ complexes which were used in the earlier studies on binuclear shift reagents. They are less light-sensitive and have a longer shelf life. The applications of binuclear lanthanide(III)–silver(I) NMR shift reagents have been reviewed by Wenzel (1986, 1987). Whereas in the case the simple achiral lanthanide shift reagents, europium(III) complexes are recommended for obtaining upfield shifts, the ytterbium(III) complexes are the best choice in the case of binuclear lanthanide(III)–silver(I) shift reagents. With the binuclear reagents containing Eu^{3+} the shifts are often too small to be of practical value. The silver(I) bridge between the substrate and the lanthanide(III) ion increases the distance between the lanthanide(III) ion and the resonating nucleus, so that not only the shift is reduced but at the same time the line broadening as well. Binuclear praseodymium(III)–silver(I) complexes can be used for obtaining downfield shifts. The recommended pair is $[\text{Pr}(\text{fod})_3]$ – $[\text{Ag}(\text{tfac})]$. For halogenated substrates, reasonable shifts can be obtained by using dysprosium(III) complexes (Wenzel and Sievers, 1981).

The lanthanide tetrakis(β -diketonate) complexes are effective NMR shift reagents for organic salts (Wenzel and Zaia, 1985, 1987). The active $[\text{R}(\beta\text{-diketonate})_4]$ species are formed in situ by reaction between an organic salt and $\text{Ag}[\text{R}(\beta\text{-diketonate})_4]$. For instance when organic ammonium halide Q^+X^- is added to a solution of $\text{Ag}[\text{R}(\text{fod})_4]$ in chloroform, the silver halide AgX precipitates from the solution and $\text{Q}[\text{R}(\text{fod})_4]$ is formed:



The proton resonances of the alkyl group are shifted by the lanthanide tetrakis(β -diketonate). The shift is considerably larger with $[\text{R}(\text{fod})_4]^-$ than with $[\text{R}(\text{fod})_3]$. Besides ammonium salts, sulfonium and isothiuronium salts have been tested. In the case of organic salts there is no need to use $\text{Ag}[\text{Yb}(\text{fod})_4]$ for obtaining upfield shifts, the shift obtained by using $\text{Ag}[\text{Eu}(\text{fod})_4]$ are large enough.

The organic substrate can be recovered after completion of the shift reagent experiment (Juneau, 1977). The solution containing a mixture of the substrate and the shift reagent is poured on top of a chromatography column (1 × 10 cm) filled with active silica gel and swelled with chloroform. The column is first eluted with 25 ml of chloroform, followed by 15 ml of a chloroform/methanol mixture (80:20 v/v). The shift reagent is collected in the first fractions. When an europium(III) complex is used, it can be detected in the fractions by its bright red photoluminescence under UV-radiation. Alumina can also be used as the stationary phase (Stolzenberg et al., 1971; Desreux et al., 1972). The lanthanide shift reagent should not be re-used after recovery of the substrate, because it can be partially hydrolyzed or contaminated.

9.3. Chiral shift reagents

The development of chiral shift reagents permits a direct determination of the optical purity (enantiomeric excess, ee) of chiral substances with no need for sample derivatization and no need for actual enantiomer resolution. When a mixture of substrate enantiomers is treated with an optically pure lanthanide shift reagent, one can often see separate NMR signals corresponding to the two enantiomers. Peak integration allows direct measurement of the relative amount of substrate enantiomers (Wenzel, 1987; Rothchild, 1989). The enantiomeric shift difference is symbolized by $\Delta\Delta\delta$. The chiral lanthanide shift reagents give rather unpredictable enantiomeric shift differences: the substrate proton resonances that are shifted by the smallest amount on adduct formation with the shift reagent may give the largest values of $\Delta\Delta\delta$ (McGoran et al., 1979; Goering et al., 1974). The first example of a chiral shift reagent was the tris-[(3-*tert*-butylhydroxymethylene) *d*-camphorato]europium(III) complex described by Whidesides and Lewis (1970). Later on many different chiral shift reagents have been developed, but most of these compounds are based on camphor derivatives. The most effective of these ligands are the CF_3 derivative 3-(trifluoroacetyl)-*d*-camphor (Hfacam) (fig. 47), and the C_3F_7 derivative 3-(heptafluorobutyryl)-*d*-camphor (Hhfb). The lanthanide induced shifts are in general larger for the $[\text{R}(\text{hfb})_3]$ complexes than for the $[\text{R}(\text{facam})_3]$ complexes, but the enantiomeric resolution shows no consistent pattern (Goering et al., 1974).

Another ligand of interest is di(perfluoro-2-propoxypropionyl)methane, because its europium(III) complex gives a superior enantiomeric resolution in comparison with $[\text{Eu}(\text{hfb})_3]$

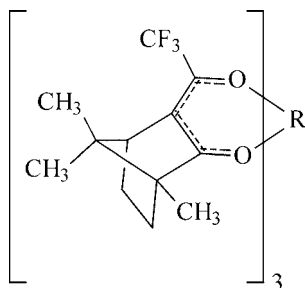


Fig. 47. Structure of the chiral NMR shift reagents $[R(\text{facam})_3]$, where $R = \text{Pr, Eu or Yb}$. Hfacam stands for 3-(trifluoroacetyl)-*d*-camphor or 3-trifluoromethylhydroxymethylene-*d*-camphor.

and because only the hydrogen resonance of the methine groups overlaps with the proton resonances of the substrate (Kawa et al., 1982). Although the most widely used chiral shift reagents are $[R(\text{hfb})_3]$ and $[R(\text{facam})_3]$, the complexes of *d,d*-dicampholylmethane (Hdcm) give the best optical resolution (McCreary et al., 1974; Whitesides et al., 1976). McCreary et al. (1974) discovered the effectiveness of the $[\text{Eu}(\text{dcm})_3]$ during a study of various campholyl and fencholyl derivatives of methane. Europium(III) complexes are first choices for chiral shift reagents (Wenzel, 1987). Line broadening has to be kept to a minimum, in order to achieve good enantiomeric resolution. Moreover a downfield shift reagent is preferred.

The optical purity of chiral alkenes or aromatics can be determined by using chiral binuclear lanthanide(III)–silver(I) shift reagents (Wenzel, 1987). These shift reagents are the chiral analogues of the binuclear shift reagents described in section 9.2, and can be formed from a chiral lanthanide tris(β -diketonate) and a chiral or an achiral silver β -diketonate. The best enantiomeric resolution with ytterbium(III) agents was achieved with $[\text{Yb}(\text{hfb})_3]$ - $[\text{Ag}(\text{fod})]$, $[\text{Yb}(\text{facam})_3]$ - $[\text{Ag}(\text{tta})]$ and $[\text{Yb}(\text{facam})_3]$ - $[\text{Ag}(\text{facam})]$ (Wenzel et al., 1985a). The most efficient couple is $[\text{Yb}(\text{facam})_3]$ - $[\text{Ag}(\text{facam})]$, but suffers from a limited solubility in CDCl_3 (Wenzel and Sievers, 1982a, 1982b) and from the low photostability of $[\text{Ag}(\text{facam})]$. Binuclear complexes formed using Hdcm as the ligand are not effective for enantiomeric resolution, probably because the ligand is too sterically demanding to allow formation of $[\text{R}(\text{dcm})_4]^-$ complexes (Wenzel, 2000).

10. Analytical applications

10.1. Trace analysis of lanthanide ions

Neutral lanthanide complexes can be dissolved in micelles formed by non-ionic surfactants such as polyoxyethylene isooctylphenol (*Triton X-100*) or nonaoxyethylene dodecyl ether (*BL-9EX*). This approach is useful to obtain highly luminescent aqueous lanthanide solutions. The free aqueous lanthanide ions are only very weakly luminescent, because of the low molar absorptivities ϵ of the lanthanide *f*–*f* transitions ($\epsilon \leq 10 \text{ mol}^{-1} \text{ l cm}^{-1}$) and because the water molecules in the first coordination sphere quench the excited states very ef-

ficiently. By forming coordination complexes with strongly absorbing organic ligands such as β -diketonates, the luminescence efficiency can be increased. By complex formation with organic ligands, water molecules can be expelled from the first coordination sphere too. Three bidentate monocharged ligands result in a neutral six coordinate complex. Coordination number six is low for lanthanide ions (CN 8 or 9 is more common), so it is very likely that the coordination sphere is expanded by taking up two or three water molecules. The water molecules can be removed from the first coordination sphere by forming Lewis-base adducts with neutral molecules, such as 1,10-phenanthroline (*phen*) or tri-*n*-octylphosphine oxide (*topo*). However, these neutral Lewis base adducts have a very low solubility in water. They can be solubilized by addition of a surfactant. As mentioned above, a non-ionic surfactant is often used.

Highly luminescent lanthanide complexes dissolved inside micelles have found application in the spectrofluorimetric determination of lanthanide ions (Sm^{3+} , Eu^{3+} , Tb^{3+} and Dy^{3+}). Micellar systems provide a means of much faster and easier analysis than when the highly luminescent, but hydrophobic lanthanide complexes have to be separated from the aqueous solution in a separate solvent extraction step. Arnaud and Georges (1997) showed that by using the ternary complex $[\text{Eu}(\text{tta})_3(\text{topo})_2]$ in a micellar solution of *Triton X-100* detection limits as low as $6 \times 10^{-12} \text{ mol l}^{-1}$ can be achieved. The luminescence intensity was a linear function of the europium(III) concentration over six order of magnitude from 10^{-11} to $10^{-5} \text{ mol l}^{-1}$. It is interesting to note that most of the *Htta* exists outside the micelle, in the bulk aqueous phase, whereas the $[\text{Eu}(\text{tta})_3]$ and $[\text{Eu}(\text{tta})_3(\text{topo})_2]$ complexes were found to exist inside the micelle (Taketatsu, 1981). In these analysis procedures, solutions of the β -diketonate ligand and the coligand are added to the solution containing europium(III) ions. It is possible to determine by spectrofluorimetry simultaneously traces of samarium and europium (Taketatsu and Sato, 1979; Zhu et al., 1991a, 1991b), or even of a ternary mixture of samarium, europium and terbium (Gao et al., 1987; Zhu et al., 1990). The method can also be adapted for analysis by flow injection spectrofluorimetry (Aihara et al., 1986a, 1986b). The most often used β -diketone in analytical determination of europium or samarium is 2-thenoyltrifluoroacetone (*Htta*) (Arnaud and Georges, 1997; Arnaud et al., 1998; Si et al., 1991; Erostyak et al., 1995; Yang et al., 1989, 1998; Brennetot and Georges, 2000; Arnaud and Georges, 2003; Sita et al., 1997; Biju et al., 2000; Ci and Lan, 1989; Xu et al., 1991), because this ligand is known to form strongly luminescent complexes with europium(III). Other β -diketones that are used for determination of lanthanides are benzoylacetone (Yang et al., 1990a; Xu et al., 1991), dibenzoylmethane (Yang et al., 1990b; Zhu et al., 1991a, 1991b; Hu et al., 1997; Hornyak et al., 1997), hexafluoroacetylacetone (Williams and Guyon, 1971) or pivaloyltrifluoroacetone (Xu and Hemmilä, 1992a, 1992b). The co-luminescence of lanthanide complexes was mentioned in section 6.1. The luminescence of europium(III), terbium(III), samarium(III) or dysprosium(III) complexes in micellar environment can be enhanced by addition of an excess of yttrium(III), lanthanum(III), lutetium(III) or gadolinium(III) complexes. The luminescence enhancement is due to energy transfer from the latter complexes to the complexes with emitting lanthanide ions. The $\text{Sm(III)-tta-phen-Gd(III)-Triton X-100}$ system was applied to the determination of trace amounts of samarium rare-earth oxides. A detection limit of $8 \times 10^{-12} \text{ mol/l}$ could be

reached (Ci and Lan, 1989). By the use of the same system, europium and samarium could be determined simultaneously, although the detection limit was higher than when samarium was determined separately: 5×10^{-10} mol/l (Yang et al., 1989). The detection limit of europium in this method was as low as 7.5×10^{-12} mol/l. The europium(III) luminescence in the Eu(III)-tta-CTMAB-Triton X-100 system can be enhanced by addition of terbium(III) ions (Zhu et al., 1992) or by gadolinium(III) ions (Zhu et al., 1991a, 1991b). A detection limit as low as 10^{-13} mol/l was obtained for the Eu(III)-dibenzo-18-crown-6-Triton X-100 system by addition of Tb(III) (Sita et al., 1997). The method was applied to the determination of europium in oxides of lanthanum, praseodymium and gadolinium. Trace amounts of europium in yttrium and gadolinium oxides were determined by the Eu(III)-tta-topo-Triton X-100 system in the presence of an excess of Tb(III) (Biju et al., 2000).

Beltyukova and Balamantsarashvili (1995) determined the europium content in samples by luminescence intensity measurements of the $[\text{Eu}(\text{tta})_3(\text{phen})]$ after preconcentration by adsorption of the complex on solid polyurethane foam. The method has been tested for the determination of the europium content of scandium(III) oxide. Concentration as low as $10^{-6}\%$ could be detected. Addition of surfactants to the solution resulted in a decrease of the luminescence intensity, because less complex is adsorbed in the presence of the surfactant.

10.2. Trace analysis of organic and biomolecular compounds

Europium β -diketonate complexes are being used as fluorescent labels in *time-resolved luminescent immunoassay* (Soini and Lovgren, 1987; Hemmilä et al., 1984; Sabbatini et al., 1996; Hemmilä, 1995; Hemmilä et al., 1995; Hemmilä and Mikkala, 2001). Immunoassays are based on the immunoreaction between an antibody that is used as the immunoreagent and the antigen that has to be analyzed. In the *dissociation-enhanced lanthanide fluoroimmunoassay* (DELFLIA, from LKB Wallac and Pharmacia), the immunoreagent is labeled for immunoreactions with an isothiocyanatophenyl-EDTA-Eu(III) or N^1 -(*p*-isothiocyanatobenzyl)diethylenetriamine- N^1, N^2, N^3, N^4 -tetraacetate-Eu(III) by binding to an amino group of the antibody. After the immunoreaction and separation of the labeled immunocomplex, the europium(III) ions are released from the complex by lowering the pH (to pH 2–3). By treatment of the europium(III)-containing solution with a mixture of 2-naphthoyltrifluoroacetate (ntac)-trioctylphosphine oxide (topo) and Triton X-100, the strongly luminescent ternary europium(III) complex $[\text{Eu}(\text{ntac})_3(\text{topo})_2]$ is formed. The function of the non-ionic surfactant Triton X-100 is to dissolve the europium complex in a micellar phase (the β -diketonate complex has a low solubility in water). The function of trioctylphosphine oxide (topo) is to shield the Eu^{3+} from water molecules by occupying the vacant coordination sites in the β -diketonate complex. The luminescence is measured in a time-resolved mode, in order to get rid of the background fluorescence of the organic compounds present in solution. Because the DELFLIA system has some drawbacks such as the need for the time-consuming conversion of a non-fluorescent europium(III) label into the luminescent $[\text{Eu}(\text{ntac})_3(\text{topo})_2]$ complex, or the fact that the system is vulnerable to contamination by europium(III) in the environment due to the excess of the reagents nta and topo (Diamandis, 1988; Mathis, 1993), research is going on to improve this fluoro-immunoassay system. An alternative is

the use of a β -diketone that can be covalently bound to proteins, such as 5-chlorosulfonyl-2-thenoyltrifluoroacetone (Hctta) (Ci and Yang, 1992; Ci et al., 1995; Yang et al., 1994a, 1994b). Because the stability of the europium(III) complexes formed by this ligand is quite low, a large excess of Eu(III) has to be used to shift the equilibrium to the europium(III) complex. More stable europium(III) complexes can be obtained by the use of tetradentate β -diketonates (Yuan and Matsumoto, 1997, 1998; Matsumoto and Yuan, 2003). Examples are 4,4'-bis(1'',1'',1'',2'',2'',3'',3''-heptafluoro-4'',6''-hexanedione-6''-yl)-chlorosulfo-*o*-terphenyl, H₂(bhhct), (Yuan et al., 1998), 4,4'-bis(1'',1'',1''-trifluoro-2'',4''-butanedione-6''-yl)-chlorosulfo-*o*-terphenyl, H₂(btbct) (Wu and Zhang, 2002), 1,10-bis(5'-chlorosulfo-dibenzothiophene-2'-yl)-4,4,5,5,6,6,7,7-octafluorodecane-1,3,8,10-tetraone, H₂(bcot) (Yuan and Matsumoto, 1997), and 1,10-bis(5'-chlorosulfo-thiophene-2'-yl)-4,4,5,5,6,6,7,7-octafluorodecane-1,3,8,10-tetraone, H₂(bctot) (Wu et al., 2002) (fig. 48).

Addition of tta anions to an europium(III)-containing Schiff's base macrocycle increased the luminescence intensity markedly (Vallarino, 1997). The tta anion coordinates to the europium-macrocycle without disrupting the macrocycle structure. The author developed a protocol for the use of these systems as luminescent markers for cytological imaging.

Luminescent europium(III) β -diketonate complexes have been used in the time-resolved luminescence determination of organic compounds in trace amount after separation of a mixture by high-performance liquid chromatography (HPLC) (Matsumoto et al., 2002). Matsumoto et al. (2002) developed a new β -diketone that is able to bind to analytes with amino and phenolic hydroxyl groups and whose europium complexes can be used as a luminescent label for HPLC: 5-(4'-chlorosulfo-1',1''-diphenyl-4'-yl)-1,1,1,2,2-pentafluoro-3,5-pentanedione (Hcdpp). This ligand was applied to the determination of estrogens. The phenolic hydroxyl group of the estrogens could be covalently bound to the chlorosulfonyl group of Hcdpp. The labeled analytes were separated by HPLC, and after separation europium(III) chloride, *topo* and Triton X-100 were added by post-column introduction to the eluent. Estrone, 17 β -estradiol, ethynylestradiol and estriol were measured by a time-resolved fluorescence detector with detection limits between 0.60 and 0.65 ng/ml.

10.3. Luminescent visualization of latent fingerprints

Lanthanide β -diketonate complexes find application for the visualization of latent fingerprints. When someone touches an object a latent fingerprint is left behind on the surface. The latent fingerprints consists in water-soluble components (amino acids, amines, monosaccharides, urea and lactic acid) and lipid components (triglycerides and fatty acids); they are hardly visible and can easily be damaged or wiped away. Because fingerprints can be used for identification of suspects of a crime, development and visualization of these latent fingerprints is of prime importance in forensic research. One of the most often used method for developing latent fingerprints is to expose an object suspected of containing finger prints to the vapors of a monomeric cyanoacrylate ester. The vapors are preferentially deposited into the fingerprint residues and the various components in the fingerprint residue catalyze the polymerization of the cyanoacrylate ester. The cyanoacrylate developed fingerprints can be visualized by illumination with an ultraviolet lamp after staining or dusting them by fluo-

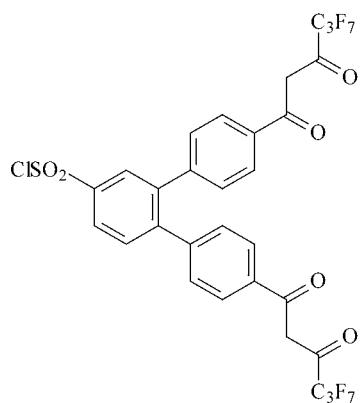
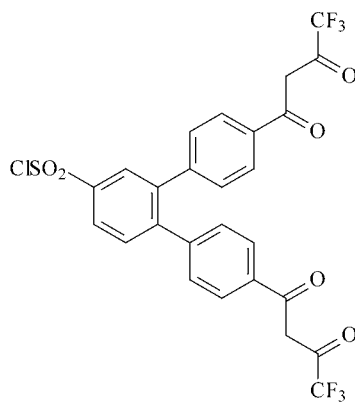
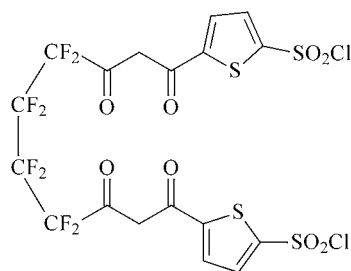
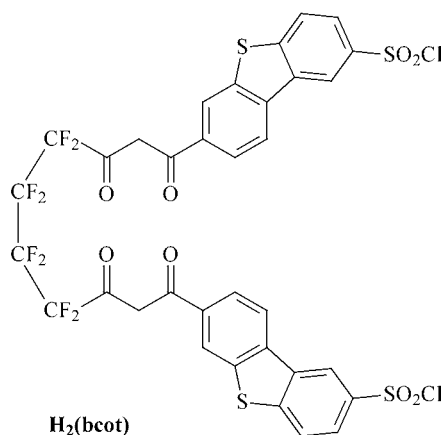
**H₂(bhhct)****H₂(btbtct)****H₂(bctot)****H₂(bcot)**

Fig. 48. Tetradentate β -diketonates that are used to form highly luminescent europium(III) complexes for time-resolved luminescence immunoassay.

rescent dyes or pigments, or exposing the developed prints to fluorescent dye vapors. Typical fluorescent dyes are Rhodamine 6G, Ardox or Brilliant Yellow. Alternatively, one can use an europium chelate. Misner et al. (1993) penetrated the cyanoacrylate developed latent prints with a solution of europium(III) thenoyltrifluoroacetate in a water/2-butanone mixture. When the solvent evaporated, the luminescent dye was trapped in the print. The luminescent dye was called TEC, after "Thenoyl Europium Chelate". Advantages of TEC are the narrow emission bands and the large Stokes shift. A large Stokes shift is desir-

able, because it allows easy blocking of the excitation light by a filter. TEC was found to give much brighter prints than the classic fluorescent dyes (Wilkinson and Misner, 1994; Wilkinson and Watkin, 1993). Even better results were obtained by Lock et al. (1995) with [Eu(tta)₃(phen)] as the luminescent dye and petroleum ether as the solvent. The NMR contrast agent [Eu(fod)₃] allows direct visualization of latent fingerprints without the need of preceding treatment with cyanoacrylate ester (Caldwell et al., 2001), because [Eu(fod)₃] is able of direct reaction with the fingerprint components.

10.4. Chemical sensors

Amao et al. (2000a) developed an oxygen sensitive optical sensor based on luminescence intensity changes of [Eu(tta)₃(phen)] immobilized in a polystyrene-2,2,2-trifluoromethylmethacrylate polymer film. Later on, these authors extended the work to other europium complexes, but [Eu(tta)₃(phen)] was found to be the superior luminescent compounds for this application (Amao et al., 2000b). The reason for the choice of a fluorinated polymer for the film is the high oxygen permeability of these materials. The luminescence intensity decreases with increasing oxygen concentration, because the luminescence is quenched by oxygen. The sensor can be calibrated by exposing the film to atmospheres of 100% argon (I_0) and 100% oxygen (I_{100}). The ratio I_0/I_{100} was found to be 2.40 in the case of [Eu(tta)₃(phen)]. Based on the same principle, Amao et al. (2000c, 2001) designed an oxygen sensor based on [Tb(acac)₃(phen)] absorbed on an alumina film.

Tsukube and coworkers (Mahajan et al., 2003) used rare-earth tris β -diketonate complexes for sensing of chloride ions by luminescence spectroscopy. When 3 equivalent of chloride ions were added to a solution of [Eu(fod)₃] in acetonitrile, the intensity of the $^5D_0 \rightarrow ^7F_2$ transition increases by a factor of 2. The Cl⁻ anion-responsive luminescence could be detected by the naked eye. The response upon addition of Br⁻, I⁻ or ClO₄⁻ to [Eu(fod)₃] was much smaller than the response upon addition of Cl⁻, and the luminescence formed by the former anions could not be detected visually. The [R(fod)₃] complexes were also used for the construction of an ion-selective electrode, where the rare-earth complexes were incorporated in a PVC membrane.

10.5. Stationary phases in gas chromatography

The ability of the coordinatively unsaturated tris(β -diketonato)lanthanide complexes to expand their coordination sphere by adduct formation with Lewis bases is not only of importance for their application as NMR shift reagents (see section 9). This ability can also be used to prepare liquid stationary phases for gas chromatography, which are able to separate organic compounds on the basis of their nucleophilicity. Feibush et al. (1972) studied the retention of different alkanes, alkenes, alcohols, ketones and ethers by GC columns with solutions of [R(β -diketonato)₃] complexes in squalane as the stationary phase. Brooks and Sievers (1973) investigated by GC the interaction of ketones and alcohols with a stationary phase consisting of the NMR shift reagent [Eu(fod)₃] in squalane. The alcohols were found to form more stable complexes with [Eu(fod)₃] than ketones. Picker and Sievers (1981) considered the use

of pre-columns containing rare-earth β -diketonates to retain selectively and separate nucleophilic species from non-nucleophilic species. As the rare-earth component the europium(III) complex of the ligand *p*-di(4,4,5,5,6,6,6-heptafluoro-1,3-hexanedionyl)benzene, H₂(dihed), has been used. The complex had the empirical formula [Eu₂(dihed)₂(OH)₂(H₂O)_x]. At high temperature this complex loses water and polymerizes. The [Eu(dihed)]_x column could selectively retain oxygen donor molecules such as esters. Kowalski (1985, 1991) investigated a stationary phase consisting of [Pr(fod)₃] or [Eu(fod)₃] in poly(dimethylsiloxane) to separate mixtures of nucleophilic compounds. The separation ability of the stationary phases based on lanthanide β -diketonates has been interpreted in terms of the HSAB-principle (hard and soft acids and bases): the lanthanide chelates are 'hard acids' and interact primarily with 'hard bases' e.g. aliphatic alcohols, and to a lesser extent with 'softer bases', such as carbonyl compounds and aliphatic ethers, and very weakly with cyano compounds, with aromatic compounds and alkenes (Kowalski, 1998b). Stationary phases containing tris[3-(trifluoromethylhydroxymethylene)-(+)-camphorato]lanthanide complexes (R = Pr, Eu, Er, Dy, Yb) dissolved in polydimethylsiloxane have been used for the enantioselective separation of racemic mixtures of chiral alcohols and ketones (Kowalski, 1998a). The thermal stability of these kinds of stationary phases containing lanthanide β -diketonates could be improved by free radical crosslinking by 2,2'-azobis(2-methylpropionitrile) (Kowalski, 1992). The gas-chromatographic separation of volatile rare-earth β -diketonate complexes is described in section 11.2.

11. Applications of volatile complexes

11.1. Volatile β -diketonate complexes

Most rare-earth complexes have a very low vapor pressure and it is difficult to transform them from the solid or liquid state into the vapor phase. The reason is that many of these complexes are oligomers and/or exhibit strong intramolecular forces. With the advent of gas chromatography in the beginning of the 1960s, attempts were made to obtain volatile rare-earth complexes in order to separate a mixture of rare earths by this method. In view of the popularity of rare-earth β -diketonates at that time as luminescent materials, several researchers have tried to design volatile rare-earth β -diketonates. Firstly fluorinated ligands such as hexafluoroacetylacetone, Hhfa, have been used, since it was known that fluorine reduces the intramolecular forces (Bhaumik, 1965a, 1965b). Although the [R(hfac)₃] complexes sublime, they show considerable thermal decomposition at the sublimation temperature (Richardson and Sievers, 1971). Typical organic molecules that can be purified by (vacuum) sublimation, such as camphor, have an isometric shape. It has tried to obtain volatile rare-earth complexes by using β -diketonates with bulky substituents. High volatility was observed for complexes of 2,2,6,6-tetramethyl-3,5-heptanedione, Hthd (Eisentraut and Sievers, 1965) and of 6,6,7,7,8,8,8-heptafluoro-2,2-dimethyl-3,5-octanedione, Hfod. The volatility of the β -diketonate complexes depends on the extent of fluorination. Thus the complexes containing highly fluorinated ligands are more volatile than complexes with fewer fluorines substituted

for hydrogens, in the order $[R(\text{hfac})_3] \gg [R(\text{tfac})_3] > [R(\text{fod})_3] \gg [R(\text{acac})_3]$ (Sievers and Sadlowski, 1978). It is thought that the fluorine atoms in the outer periphery of the rare-earth complex reduces the van der Waals interactions and the intermolecular hydrogen bonding.

The volatility of these complexes increases when the radius of the trivalent lanthanide ion decreases (Eisentraut and Sievers, 1967). For instance, the vapor pressure at 200 °C increases from 0.2 mm for the $[\text{La}(\text{thd})_3]$ complex to ca. 5 mm for the $[\text{Yb}(\text{thd})_3]$ complex (Sicre et al., 1969). Possible explanations for the size-related trend in volatility have been discussed (Sicre et al., 1969). The smaller the ionic radius of the rare-earth ion is, the smaller is the size of the corresponding β -diketonate complex. In smaller complexes, the local dipoles of the polar groups decrease or are better shielded from the attractive forces of neighboring molecules, so that the intermolecular forces decrease. The smaller complexes have less tendency to form oligomers. Mass effects can be ruled out because the volatility of the $[\text{Y}(\text{thd})_3]$ complexes is comparable to the volatility of the complexes $[\text{Ho}(\text{thd})_3]$ and $[\text{Er}(\text{thd})_3]$. Although Y^{3+} , Ho^{3+} and Er^{3+} have a similar ionic radius, Ho^{3+} and Er^{3+} ions have a much greater mass than the Y^{3+} ion (Eisentraut and Sievers, 1965). A mixture of $[\text{R}(\text{thd})_3]$ complexes can be separated on a thermal-gradient fractional sublimation apparatus (Eisentraut and Sievers, 1965). $[\text{Ce}(\text{thd})_4]$ is more volatile than the $[\text{R}(\text{thd})_3]$ complexes (Song et al., 2003a). Chou and Wang (1996) developed a mathematical model to predict the evaporation rates of $[\text{Ce}(\text{thd})_4]$ from the surface of the solid precursor. Hydrated β -diketonate complexes do not sublime, but partial thermal decomposition occurs (Leskelä et al., 1991a; Cunningham et al., 1967). The $[\text{R}(\text{acac})_3]$ complexes are practically non-volatile because they have the tendency to polymerize in order to achieve a coordination number higher than six. For instance the non-volatile compound $[\text{Y}_4(\text{acac})_{10}(\text{OH})_2]$ is formed from $[\text{Y}(\text{acac})_3(\text{H}_2\text{O})_3]$ upon heating (Barash et al., 1993). The volatility of such complexes can be improved by replacing the water molecules in the first coordination sphere by dimethylformamide (DMF) or tri-*n*-butylphosphin oxide (Richardson and Sievers, 1971). Timmer et al. (1998) report a very high volatility for the adduct of $[\text{Y}(\text{thd})_3]$ with the triamine $(\text{CH}_3)_2\text{NCH}_2\text{CH}_2\text{N}(\text{CH}_3)\text{CH}_2\text{CH}_2\text{N}(\text{CH}_3)_2$, despite the much higher molecular mass of this adduct in comparison with $[\text{Y}(\text{thd})_3]$. Also $[\text{Y}(\text{thd})_3(\text{pyO})]$ and $[\text{Y}(\text{thd})_3(4\text{-tert-But-pyO})]$ were found to be more volatile than the parent compound $[\text{Y}(\text{thd})_3]$. Hydrated lanthanide tris acetylacetonates can be volatilized by mixing the solid compound with 1,10-phenanthroline, because the mixing results in the formation of volatile, mononuclear $[\text{R}(\text{acac})_3(\text{phen})]$ complexes (Kuzmina et al., 2000c). Studies with Lewis bases other than 1,10-phenanthroline (for instance with hexamethylphosphorotriamide or acetylacetonimine) showed that a volatile complex is formed only in the cases when the mononuclear complexes are stable towards thermal dissociation. Addition of acetic acid to binary mixtures $[\text{Nd}(\text{thd})_3]$ - $[\text{Er}(\text{thd})_3]$ and $[\text{Ho}(\text{thd})_3]$ - $[\text{Er}(\text{thd})_3]$ enhances the separation of these mixtures by vacuum sublimation (Fenkhuu et al., 1996).

The volatility of the β -diketonate complexes can also be increased by formation of the tetrakis complexes, because the latter are mononuclear. The first volatile heterobimetallic compound was the ionic $\text{Cs}[\text{Y}(\text{hfac})_4]$, which Lippard (1966) sublimed without decomposition both in air and in vacuum. Addition of alkali metal acetylacetonate to $[\text{R}(\text{acac})_3]$ complexes results in the formation of volatile $\text{M}[\text{R}(\text{acac})_4]$ complexes ($\text{M} = \text{Li}, \text{Na}, \text{Cs}$) (Zaitseva

et al., 1995, 1999). A synergistic effect on the volatility of the $[\text{R}(\text{acac})_3]$ was observed upon addition of a highly volatile complex such as $[\text{Zr}(\text{acac})_4]$ (Kuzmina et al., 2000c).

Sicre et al. (1969) measured the vapor pressure of the $[\text{R}(\text{thd})_3]$ complexes as a function of the temperature. With the exception of the lanthanum complex, a sharp break was observed in the Clapeyron–Clausius plots (vapor pressure versus temperature) at a temperature matching the melting point of the corresponding complex. The $[\text{R}(\text{thd})_3]$ complexes exhibit a vapor pressure of 1 mm at temperatures from 170 °C for $[\text{Lu}(\text{thd})_3]$ to 225 °C for $[\text{La}(\text{thd})_3]$. More than half of the $[\text{R}(\text{thd})_3]$ complexes exhibit a higher vapor pressure than the saturated hydrocarbon *n*-tetracosane (vapor pressure: 1 mm at 184 °C). This was unexpected, given the higher molecular mass of the $[\text{R}(\text{thd})_3]$ complexes (empirical formula: $\text{C}_{33}\text{H}_{57}\text{O}_6\text{R}$) than that of *n*-tetracosane ($\text{C}_{24}\text{H}_{50}$). Moreover it was always thought that the more ionic bonding with the larger resulting dipoles in the β -diketonate complex would render them more volatile. It was argued that the bulky ligands form a hydrocarbon shell around the complex, which shields the polar groups from interactions with the neighboring molecules. The sublimation enthalpies of the $[\text{R}(\text{thd})_3]$ complexes are in the range 174–185 kJ mol^{-1} for the lighter lanthanides (La–Tb) and in the range 150–160 kJ mol^{-1} for the heavier lanthanides (Tb–Yb) (Amano et al., 1980, 1981). The difference in sublimation enthalpies between the heavier and lighter lanthanides has been discussed by Amano et al. (1979) and was attributed to a difference in crystal structure (monoclinic dimers for the lighter lanthanides and orthorhombic dimers for the heavier lanthanides). The sublimation behavior of volatile rare-earth β -diketonates is summarized in table 9.

The volatility of the $[\text{R}(\text{thd})_3]$ complexes makes them suitable for mass spectrometry studies. Mass spectra have been reported for $[\text{Y}(\text{thd})_3]$ (Girichev et al., 1993), $[\text{Gd}(\text{thd})_3]$ (Hirayama et al., 1985), $[\text{Tb}(\text{thd})_3]$ (Leskelä et al., 1991a), $\text{Y}(\text{hfac})_3$ (Gleizes et al., 1998) and $[\text{Ce}(\text{thd})_4]$ (Leskelä et al., 1996; Leskelä et al., 1991b). Mészáros-Szecsényi et al. (2002) carried out evolved gas analysis (EGA) on $[\text{Sc}(\text{thd})_3]$ and found $[\text{Sc}(\text{thd})_2]^+$ as the major scandium-containing species in the gas phase at 200–300 °C. Peters et al. (1982) were able to demonstrate by means of electron impact mass spectrometry that dimeric (or higher) associates of $[\text{Eu}(\text{fod})_3]$ and $[\text{Yb}(\text{fod})_3]$ occur in the gas phase, even under the conditions of high vacuum at which the mass spectrometry was performed. It was also shown that in the gas phase 1:1 and 1:2 adducts of $[\text{R}(\text{fod})_3]$ with *n*-propylamine exist. Compounds of the type $[\text{R}(\text{fod})_3]\cdot\text{Mfod}$ ($\text{M} = \text{Na}, \text{K}, \text{Rb}, \text{Cs}$), which are frequently present in commercial NMR shift reagents (Peters et al., 1981), could also be detected by mass spectrometry. Lippard (1966, 1967) studied the mass spectra of $\text{Cs}[\text{Y}(\text{hfac})_4]$. An intense peak at $m/z = 843$ was assigned to the $\text{Cs}[\text{hfac})_3]^+$ ion. This result indicates that the cesium ion is strongly bound to the complex, and that loss of a hfac ligand precedes loss of Cs^+ . A possible explanation is strong ion-pairing between the cesium ion and the fluorine atoms of the hfac ligands.

Shibata and coworkers (Shibata et al., 1985, 1986a, 1986b, 1986c) studied the molecular structure of $[\text{R}(\text{thd})_3]$ complexes ($\text{R} = \text{Pr}, \text{Sm}, \text{Eu}, \text{Gd}, \text{Tb}, \text{Dy}, \text{Ho}, \text{Er}, \text{Y}$) by gas-phase electron-diffraction. The experimental data were consistent with a monomeric trigonal prismatic structure and it was stated that the rare-earth site has a C_3 symmetry. The observed R–O distances reflect the lanthanide contraction. The *tert*-butyl groups rotate freely. The chelate rings are folded around the O··O axes (twisted chelate rings). However, Giricheva et al.

Table 9
Sublimation behavior of volatile rare-earth β -diketonates

Compound	Sublimation range (°C)*	Reference	Sublimation enthalpy (kJ mol ⁻¹)	Reference
[Y(thd) ₃]	215–251	Harima et al., 1990	–	–
[La(thd) ₃]	–	–	180	Amano et al., 1981
			144	Sicre et al., 1969
[Pr(thd) ₃]	249–290	Leskelä et al., 1991a	179	Amano et al., 1981
			166	Sicre et al., 1969
[Nd(thd) ₃]	–	–	159	Sicre et al., 1969
[Sm(thd) ₃]	232–274	Leskelä et al., 1991a	181	Amano et al., 1981
			151	Sicre et al., 1969
[Eu(thd) ₃]	229–266	Leskelä et al., 1991a	180	Amano et al., 1981
			201	Amano et al., 1979
			166	Sicre et al., 1969
[Gd(thd) ₃]	225–254	Leskelä et al., 1991a	162	Amano et al., 1979
[Tb(thd) ₃]	222–257	Leskelä et al., 1991a	174 (dimer)	Amano et al., 1981
			151 (monomer)	Amano et al., 1981
			142	Amano et al., 1979
[Dy(thd) ₃]	–	–	134	Amano et al., 1979
[Ho(thd) ₃]	–	–	153	Amano et al., 1981
			132	Sicre et al., 1969
[Er(thd) ₃]	–	–	154	Amano et al., 1981
			133	Sicre et al., 1969
[Tm(thd) ₃]	217–245	Leskelä et al., 1991a	156	Amano et al., 1981
			132	Sicre et al., 1969
[Yb(thd) ₃]	216–250	Leskelä et al., 1991a	156	Amano et al., 1981
			133	Sicre et al., 1969
[Ce(thd) ₄]	246–254	Leskelä et al., 1991a	–	–
	140–200/150 Pa	Richardson et al., 1968		
[Ce(thd) ₃ (phen)]	130–250/150 Pa	Leskelä et al., 1996	–	–
[Ce(tmp) ₃]	160–210/50 Pa	Becht et al., 1993	–	–
[Ce(fdh) ₄]	140/13.3 Pa	Becht et al., 1993	–	–
[Ce(fdh) ₄ (phen)]	170/13.3 Pa	Becht et al., 1993	–	–

*Determined by thermogravimetry.

(2003) point to the fact that the electron diffraction data may be described by two alternative models, one assuming a C₃ symmetry and another assuming a D₃ symmetry. Ab initio and DFT calculations on [Lu(thd)₃] gave structures which are comparable with those derived from the experimental data (Belova et al., 2004). The gas-phase configuration of [La(thd)₃] was found to be different from that of the other [R(thd)₃] complexes (Giricheva et al., 2002), in the sense that the former complex has planar chelate rings. An antiprismatic trigonal structure was proposed for [Sc(acac)₃], with a C₃ symmetry (Ezhov et al., 1998) or a D₃ symmetry (Belova et al., 2002).

A few spectroscopic studies have been performed on lanthanide β -diketonates in the vapor phase. UV-spectroscopy has been used to determine the concentration of the rare-earth

complexes in the vapor phase (Bhaumik, 1965a, 1965b; Rappoli and DeSisto, 1996). Jacobs et al. (1975) studied the photophysical properties of $[\text{Tb}(\text{thd})_3]$ in the vapor phase. The luminescence lifetime was found to decrease from $1.2 \mu\text{s}$ at 230°C to $0.2 \mu\text{s}$ at 300°C . Dao and Twarowski (1986) measured the luminescence lifetimes of $[\text{Eu}(\text{thd})_3]$ and $[\text{Eu}(\text{fod})_3]$ in the gas phase as a function of the temperature. $[\text{Eu}(\text{fod})_3]$ has a much longer lifetime than $[\text{Eu}(\text{thd})_3]$ at comparable temperatures: $6.8 \mu\text{s}$ for $[\text{Eu}(\text{fod})_3]$ at 190°C and $0.93 \mu\text{s}$ for $[\text{Eu}(\text{thd})_3]$ at 200°C . The luminescence lifetimes are independent of the presence of argon as a buffer gas and of the vapor pressure of the europium(III) chelate.

11.2. Gas chromatographic separation of the rare earths

In the 1960s attempts were made to separate mixtures of rare earths by gas chromatography (Moshier and Sievers, 1965; Eisentraut and Sievers, 1965; Shigematsu et al., 1969a, 1969b; Robards et al., 1987, 1988; Sokolov, 1988). Earlier experiments failed because of the low volatility and the thermal instability of the rare-earth complexes known at that time (Moshier and Sievers, 1965). For instance, the $[\text{R}(\text{acac})_3]$ complexes are unsuitable for gas chromatographic separation. The metal complexes must have a vapor pressure on the order of 0.1 to 1 mm to move through the column at a reasonable rate. Eisentraut and Sievers (1965) found that the $[\text{R}(\text{thd})_3]$ complexes were volatile and stable enough to separate them. A benzene solution of the complexes was injected in the gas chromatograph and separated on a column filled with the apolar stationary phase Apiezon N. The authors were surprised to find out that the retention times could not be correlated with the molecular mass of the complexes, but rather with the ionic radius of the rare-earth ion. Thus, the yttrium complex $[\text{Y}(\text{thd})_3]$ has about the same retention time as the erbium complex $[\text{Er}(\text{thd})_3]$, although the atomic mass of yttrium is about one-half of that of erbium (see also the discussion in section 10.1). The retention does not vary linearly, but exponentially with the ionic radius. For instance, when $[\text{Sc}(\text{thd})_3]$ is eluted from the column under given conditions after 2 minutes, the retention time of $[\text{Ho}(\text{thd})_3]$ is 4 minutes and that of $[\text{Nd}(\text{thd})_3]$ is 15 minutes. Under these conditions, it takes several hours to elute $[\text{La}(\text{thd})_3]$. Because the complexes of fluorinated β -diketones have a higher volatility than the complexes of the non-fluorinated β -diketones, the fluorinated rare-earth complexes have a sufficient high vapor pressure at relatively low column temperatures. It is even possible to elute them at a temperature close to room temperature. The lower column temperatures needed for elution, reduces the problem of thermal decomposition. One reason why the rare-earth β -diketonates are more suitable for application in gas chromatography than other volatile rare-earth complexes (e.g. alkoxides) is that they do not exhibit high reactivity towards atmospheric moisture or oxygen. This greatly facilitates sample preparation or handling. Fujinaga and coworkers (1971, 1974) found that gas chromatographic separation of volatile metal chelates could be improved by mixing ligand vapor with the carrier gas. The addition of a constant small amount of ligand vapor to the carrier gas suppresses the dissociation of the metal chelates in the column and releases the metal chelates adsorbed on the solid support. These authors used this method to separate mixtures of $[\text{R}(\text{tfac})_3]$ complexes by gas chromatography (Fujinaga et al., 1976). Although earlier work in the 1960s (Moshier and Sievers, 1965) has shown that the $[\text{R}(\text{acac})_3]$ are unsuitable for separation of

the rare earths, some authors continued to work with these compounds (Spitsyn et al., 1982; Magazeeva et al., 1986). Butts and Banks (1970) were the first to report on mixed ligand systems for gas chromatography. They separated the elements of the rare-earth series in the form of the $[R(\text{hfac})_3(\text{tbp})_2]$ complexes. These complexes were found to have a much higher thermal stability than the $[R(\text{hfac})_3]$ complexes. Sieck and Banks (1972) extended this work to other ternary complexes of fluorinated β -diketonates and neutral Lewis bases.

Gas chromatography of rare-earth β -diketonates is not only of interest for the separation of mixtures of rare earths. The method can also be used for trace metal analysis. First, formation of the volatile chelates is achieved by extraction of the rare-earth ions with the β -diketonate ligands from an aqueous solution into an immiscible organic solvent. Alternatively, direct reaction between the ligand and the metal ions in the aqueous solution can be used (in the absence of a solvent). After elution, the volatile rare-earth β -diketonate complexes can be detected by conventional detectors such as the flame ionization detector (FID) or the thermal conductivity detector (TCD). Because the $[R(\text{tfac})_3]$ and the $[R(\text{fod})_3]$ complexes contain electronegative fluorine atoms, they can be selectively detected at low concentrations by an electron capture detector (ECD) (Sievers and Sadlowski, 1978). Burgett and Fritz (1972, 1973) studied the separation and quantitative determination of rare earths by gas chromatography of $[R(\text{thd})_3(\text{dbso})_3]$ complexes.

11.3. Preparation of thin films by metal-organic chemical vapor deposition (MOCVD)

Chemical vapor deposition (CVD) is a process that involves deposition of a solid material from a gaseous phase. The precursor gases (often diluted in carrier gases) are delivered into the reaction chamber at temperatures close to room temperature. As the precursor gases pass over or come into contact with a heated substrate, they react or decompose forming a solid phase, which is deposited on the substrate. The substrate temperature is critical and can influence the reactions that will take place. CVD coatings are usually only a few microns thick and are generally deposited at relatively slow rates, on the order of a few hundred microns per hour. Because materials are deposited from the gaseous state during CVD, the precursors must be volatile, but must have at the same time a thermal stability high enough to allow the precursors to be delivered to the reactor. Liquid precursors are preferred over solid precursors, because liquids can be flash-vaporized with excellent reproducibility and negligible decomposition. In contrast, the sublimation of solids is often slow and non-reproducible and leaves troublesome residues. Sintering of solid precursors also affects volatility. For the ease of handling, the compounds should be air and moisture stable. When the precursors are volatile coordination compounds or organometallics, the term *metal-organic chemical vapor deposition* (MOCVD) is coined.

The most intensively used precursors for MOCVD of lanthanide complexes are the 2,2,6,6-tetramethyl-3,5-heptanedionate (thd) chelates (Tiitta and Niinistö, 1997). Because of the tendency of trivalent cerium to be oxidized to tetravalent cerium, $[\text{Ce}(\text{thd})_3]$ is very unstable and cannot be used as a precursor for MOCVD. However, the oxidation state +III of $[\text{Ce}(\text{thd})_3]$ can be stabilized by adding 1,10-phenanthroline to saturate the coordination sphere of the cerium(III) ion (Uhlemann and Dietze, 1971). The salt used to prepare the $[\text{Ce}(\text{thd})_3(\text{phen})]$

complex has an influence on its properties (Leskelä et al., 1996). $[\text{Ce}(\text{thd})_4]$ is often used as a precursor to obtain CeO_2 thin films, but the chemical and physical properties of $[\text{Ce}(\text{thd})_4]$ are strongly dependent on the methods of synthesis (Song et al., 2002). Because of thermal decomposition during evaporation, solid $[\text{Ce}(\text{thd})_4]$ should be volatilized at temperatures lower than 200°C (Song et al., 2002). The thd complexes have relatively high melting points, and they have to be used as solid precursors. In order to obtain precursors that can be used in the liquid state, Tasaki et al. (1997) designed lanthanide complexes with much lower melting points, by replacing the Hthd β -diketone ligand by 2,2,6,6-tetramethyl-3,5-octanedione (Htmod). The complexes with fluorinated ligands, such as $[\text{R}(\text{hfac})_3]$ or $[\text{R}(\text{fod})_3]$, have a high volatility and are thermally stable, but have the disadvantage that fluorine-containing species frequently contaminate the oxide film deposits (Chadwick et al., 1996; McAleese and Steele, 1998) and that toxic decomposition products are formed. Contamination by fluorides can be reduced by using moist oxygen to assist decomposition and to remove the fluorine-containing species from the deposit (McAleese et al., 1996a; McAleese and Steele, 1998). This can be considered as an in-situ defluorination technique. But, it has been advised to avoid the use of fluorinated precursors for the production of epitaxial or high quality films (Leedham and Drake, 1996). A new class of anhydrous, volatile and thermally stable MOCVD precursors are the adducts of tris(β -diketonato) complexes with polyethers such as monoglyme or diglyme. These Lewis bases saturate the coordination sphere of the lanthanide ion, so that the complexes maintain their monomeric character and the vapor pressure and stability is increased. The complex $[\text{Eu}(\text{hfac})_3(\text{diglyme})]$ was investigated by Kang et al. (1997a) and was found to sublime intact. The synthetic procedure for the compound was improved by Malandrino et al. (2001) and these authors also studied the analogous compound $[\text{Eu}(\text{hfac})_3(\text{monoglyme})]$. The glyme adducts of the $[\text{R}(\text{thd})_3]$ proved to be good candidates as MOCVD precursors too (Leedham and Drake, 1996).

The β -diketonate precursors can be used for the deposition of rare-earth oxide layer, either alone or in combination with other metal oxides. Examples of binary rare-earth oxides prepared by MOCVD include La_2O_3 (Bonnet et al., 1995), CeO_2 (McAleese et al., 1996a; Pan et al., 1998a; Lo Nigro et al., 2003), Pr_2O_3 (Bonnet et al., 1995), Nd_2O_3 (Langlet and Shannon, 1990; Bonnet et al., 1995), Sm_2O_3 (Bonnet et al., 1995), Eu_2O_3 (Bonnet et al., 1995), Gd_2O_3 (Bonnet et al., 1995; McAleese et al., 1996b), Dy_2O_3 (Bonnet et al., 1995), Er_2O_3 (Bonnet et al., 1995; Hubbard and Espinoza, 2000) and Sc_2O_3 (Xu et al., 2001). Not only oxides have been prepared by MOCVD, but also rare-earth fluoride thin films, for example LaF_3 (Malandrino et al., 1998a; Condorelli et al., 2000), CeF_3 (Lo Nigro et al., 2002), and GdF_3 (Malandrino et al., 1996). Other rare-earth compounds prepared by MOCVD include SrCeO_3 (Pan et al., 1998b), LaNiO_3 (Gorbenko and Bosak, 1998), PrGaO_3 (Han et al., 1993b), NdGaO_3 (Han et al., 1992), LaAlO_3 (Malandrino et al., 1997, 1998b), YAlO_3 (Han et al., 1993a), $\text{Ce}_{1-x}\text{Gd}_x\text{O}_{2-x/2}$ (McAleese and Steele, 1998), Gd_2O_3 -doped CeO_2 (Song et al., 2003a, 2003b), Eu_2O_3 -doped Y_2O_3 (Hirata et al., 1997), $(\text{La},\text{Pr})_{0.7}(\text{Ca},\text{Sr})_{0.3}\text{MnO}_3$ (Gorbenko et al., 1997), yttria-stabilized zirconia (Chour et al., 1997; Itoh and Matsumoto, 1999; Akiyama et al., 2002; Chevalier et al., 2003), RuO_2 -doped yttria-stabilized zirconia (Kimura and Goto, 2003) and ytterbium-doped InP (Whitney et al., 1988; Williams and Wessels, 1990). A lot of research activities have been devoted to obtain

thin films of the high-temperature superconductor $\text{YBa}_2\text{Cu}_3\text{O}_{7-x}$ and related compounds by MOCVD (Panson et al., 1989; Yamane et al., 1988; Dickinson et al., 1989; Ozawa, 1991; Busch et al., 1991; Matsuno et al., 1992; Leskelä et al., 1993; Thomas et al., 1993; Yamaguchi et al., 1989, 1994; Richards et al., 1995; Otway and Obi, 1997; Weiss et al., 1997; Galindo et al., 2000; Polyakov et al., 2000; Zama et al., 2000; Meng et al., 2002). In most of these studies, $[\text{Y}(\text{thd})_3]$ has been used as the precursor for the yttrium component. Panson et al. (1989) chose $[\text{Y}(\text{fod})_3]$ as the precursor. Developments in this field have been plagued by the difficulties in finding a suitable precursor for the barium component (Wahl et al., 2000; Tiitta and Niinistö, 1997). For instance, $[\text{Ba}(\text{thd})_2]$ has a strong tendency to self-associate. This results in a strong dependence of both the composition and the volatility on the method of synthesis.

Many of the materials can be prepared as thin films by MOCVD contain at least two different metal elements (e.g. LaNiO_3 or $\text{Y}_2\text{BaCu}_3\text{O}_7$). Their preparation requires as many precursors as metal elements that have to be deposited. A new approach is the use a single-source precursor, i.e. a volatile heterometallic compound, which contain all the metallic elements to be deposited (Gleizes, 2000). This approach allows a simplification of the MOCVD process and the reactor design. A good control of the gas phase composition up to the deposition zone is possible. The use of a single-source precursor is of great importance for the growth of thin films of the high-temperature superconductor $\text{Y}_2\text{BaCu}_3\text{O}_7$, because not only three different metals have to be deposited, but also because of difficulties inherent to the barium precursors for CVD (see above). High-molecular weight heterometallic precursors have the disadvantage of low volatility, but this can be overcome by performing the MOCVD process under ultra-high vacuum. Gleizes and coworkers (Gleizes et al., 1998, 1999; Kuzmina et al., 2001) developed a strategy to synthesize volatile f-d complexes, i.e. complexes that contain both a lanthanide ion and a d-transition metal ion. They used d-metal complexes with *O-O'-N-N'* donor Schiff base ligands $[\text{M}(\text{Q})]$ as neutral ligands to coordinatively saturate tris(β -diketonato)lanthanide(III) complexes $[\text{R}(\text{dik})_3]$, so that heterobimetallic complexes with general formula $[\text{M}(\text{Q})\text{Ln}(\text{dik})_3]$ are obtained. The first examples of these complexes were $[\text{Ni}(\text{salen})\text{Y}(\text{hfac})_3]$ and $[\text{Ni}(\text{salen})\text{Gd}(\text{hfac})_3]$ (Gleizes et al., 1998). Later on, the studies were extended by variation of the Schiff base ligand (i.e. salophen instead of salen) and of the β -diketone (i.e. Hpta or Hthd instead of Hhfa) (Gleizes et al., 1999; Kuzmina et al., 2001). It was shown by thermogravimetry and sublimation experiments that the volatility of the complexes mainly depends on the nature of the d-metal Schiff base complex. For instance, $[\text{Cu}(\text{salophen})\text{Ln}(\text{hfac})_3]$ complexes are less volatile than $[\text{Cu}(\text{salen})\text{Ln}(\text{hfac})_3]$ complexes, due to the stronger $\pi-\pi$ interactions between overlapping $[\text{Cu}(\text{salophen})]$ entities than between $[\text{Cu}(\text{salen})]$. On the other hand, the complexes $[\text{M}(\text{salen})\text{Ln}(\text{hfac})_3]$ and $[\text{M}(\text{salen})\text{Ln}(\text{pta})_3]$ have very comparable volatilities, although $[\text{R}(\text{hfac})_3]$ and $[\text{R}(\text{pta})_3]$ complexes have a similar volatility. Mass spectrometric studies of $[\text{Ni}(\text{salen})\text{Y}(\text{hfac})_3]$ have shown that both the heterobimetallic complex and the monometallic parent complexes $[\text{Ni}(\text{salen})]$ and $[\text{Y}(\text{hfac})_3]$ exist in the vapor phase (Gleizes et al., 1999). Due to the relatively low thermal stability of $[\text{M}(\text{salen})\text{R}(\beta\text{-diketonate})_3]$ complexes, the partial vapor pressure of the homometallic dissociation products rapidly increases with increasing temperature. Replacement of $[\text{M}(\text{salen})]$ by the more volatile $[\text{M}(\text{acacen})]$ (H_2acacen is the condensation product

of acetylacetonone with 1,2-diaminoethane) resulted in heterobimetallic complexes, much less sensitive to dissociation upon sublimation (Kuzmina et al., 2001). Jardin et al. (1995) tested [La(thd)₃] as a volatile lanthanum(III) compound for the preparation of a ZBLAN fluoride glass (ZrF₄-BaF₂-LaF₃-AlF₃-NaF glass), but the authors could not obtain a homogeneous phase due to the low volatility or stability of the zirconium(IV)-containing or the barium(II)-containing precursors.

11.4. Preparation of thin films by atomic layer deposition (ALD)

Atomic layer epitaxy (ALE) is a variant of MOCVD and was developed by T. Suntola in Finland in the 1970s (Suntola and Antson, 1977; Suntola, 1989). He used the acronym ALE to describe the layer-by-layer growth mechanism and the resulting epitaxial film. However, such and epitaxial growth can only be achieved on matching single crystal substrates. Growth on amorphous substrates such as glass, leads to amorphous films and the name *atomic layer deposition (ALD)* should be preferred.

An ALD growth process proceeds by exposing the substrate alternatively to vaporized anion and cation precursors (Niinistö, 1998; Jones and Chalker, 2003). The substrate area is purged with inert gas between the precursor pulses to eliminate gas-phase reactions and to remove reaction products. In an ideal case, one monolayer of the first reactant is chemisorbed on the substrate and this layer reacts with the second precursor pulsed onto the substrate, resulting in the formation of a solid film (Nieminen et al., 2001a). In practice, a full monolayer growth per cycle is not achieved due to the bulkiness of the precursors, but only a distinct fraction of a monolayer is deposited during one cycle (Gourba et al., 2003). The deposition process is based on alternating chemisorption of the precursors, surface reaction and desorption. ALD can be used to deposit conformal and uniform thin films in a reproducible way. Thickness control of the film by the number of deposition cycles is accurate and easy when the deposition is carried out within certain temperature limit, i.e. the 'ALD window'. ALD is a self-limiting deposition process where the growth rate is independent of growth parameters such as temperature, vapor pressure, precursor fluxes and pulse and purge times (Suntola, 1989; Niinistö et al., 1996). In comparison with classic MOCVD, ALD has some advantages (Gourba et al., 2003). First of all, gas phase reactions between the precursors are avoided. Secondly, the film thickness is easily controllable by the number of reaction cycles. Thirdly, the ALD process can be carried out at relatively low temperatures. The ALD process is especially suitable for applications where exact control of the film thickness is needed or where deposition have to be performed on uneven or porous substrates (Putkonen et al., 2002). In the past, the applications of ALD have been mainly focused on binary systems, such as oxides or sulphides, but recently ternary and quaternary systems are being investigated as well.

Atomic layer deposition has been used to obtain a variety of thin rare-earth binary oxide films: Sc₂O₃ (Putkonen et al., 2001a), Y₂O₃ (Mölsä et al., 1994; Putkonen et al., 2001b), La₂O₃ (Nieminen et al., 2001b) and CeO₂ (Mölsä and Niinistö, 1994; Päiväsaari et al., 2002). Typically, the [R(thd)₃] complexes have been used as the precursor, except for CeO₂, that is prepared starting from [Ce(thd)₄]. Rare-earth oxide thin films have several potential applications. The large dielectric constant makes CeO₂ advantageous for stable capacitor devices for large scale integration (Becht et al., 1993). CeO₂ has a high refractive index and

good transmittance in the visible part and near-infrared of the electromagnetic spectrum, and it is therefore an interesting material for optical devices (McDevitt and Braun, 1964; Wahid et al., 1992). It can also be used for a resistive type of oxygen sensor for combustion gases (Fang et al., 2000). Potential applications of lanthanum oxide thin films include dielectric layers in devices (Mahalingam et al., 1981) and protective coatings (Bonnet et al., 1994).

Lanthanum sulfide, La_2S_3 , thin films were grown by ALD, with $[\text{La}(\text{thd})_3]$ and H_2S as the precursors (Kukli et al., 1998). The films grown below 400°C were amorphous. At 500°C films of well-defined cubic $\gamma\text{-La}_2\text{S}_3$ could be deposited. However, the films contained a significant amount of oxygen and carbon, probably originating from the $[\text{La}(\text{thd})_3]$ precursor. Upon annealing at $510\text{--}730^\circ\text{C}$, the material reacted with residual oxygen in the bulk of the film in lanthanum oxysulfide, $\text{La}_2\text{O}_2\text{S}$, and other oxysulfides were formed. Films of lanthanum sulfide are of interest because of the wide transmission range in the infrared. Cerium-doped strontium sulfide thin films are promising high-brightness blue phosphors for thin film electroluminescent flat panel displays. The luminescence properties of this material depend on the concentration, distribution and oxidation state of cerium in the SrS host lattice and on the crystallinity of the thin films (Heikkinen et al., 1998). Only cerium(III) is luminescent, not cerium(IV). In ALD deposition of SrS:Ce thin films, $[\text{Ce}(\text{thd})_4]$ and $[\text{Sr}(\text{thd})_2]$ have been used as the precursors (Leskelä et al., 1991b; Heikkinen et al., 1998; Niinistö, 1997). During the deposition process, cerium(IV) is reduced to cerium(III) by hydrogen sulfide. $[\text{Ce}(\text{thd})_3(\text{phen})]$ and $[\text{Ce}(\text{tpm})_3]$ have also been used as the cerium precursor (Leskelä et al., 1996). The electroluminescence properties were found to be dependent on the cerium precursor used. Enhanced electroluminescence in comparison with $[\text{Ce}(\text{thd})_4]$ was obtained with $[\text{Ce}(\text{thd})_3(\text{phen})]$. The luminescence color shifted towards the blue with the fluorinated precursor $[\text{Ce}(\text{tpm})_3]$, but the luminance was poor and the growth rate of strontium sulfide decreased. $[\text{Ce}(\text{thd})_3(\text{phen})]$ sublimed in two stages, which indicates a partial release of the 1,10-phenanthroline adduct molecules during the sublimation process. Terbium-doped calcium sulfide thin films were grown by ALD (Karpinska et al., 1995). The films showed a bright green photoluminescence at room temperature.

Among the films of ternary compounds prepared by ALD are the ABO_3 perovskite types of LaCoO_3 (Seim et al., 1997) and LaGaO_3 (Nieminen et al., 2001a). These materials have potential applications as electrodes, sensors, catalysts, superconductors and ferroelectrics. The electric and magnetic properties of these perovskites can be controlled by changing the combination of the metals A and B and by variation of the oxygen stoichiometry. In these studies, $[\text{La}(\text{thd})_3]$ is used as the lanthanum precursor and this compound is decomposed during the ALD process by ozone. Haukka et al. (1997) studied the growth of mixed LaCeCuO oxides on porous high surface area alumina by ALD. Films of $\text{YBa}_2\text{Cu}_3\text{O}_7$ could be deposited by ALD at 450°C , which exhibited superconductivity after oxygen annealing (Mölsä, 1991; Niinistö et al., 1996; Leskelä et al., 1993).

11.5. Fuel additives

Their high volatility and solubility in non-polar organic solvents make rare-earth complexes suitable as fuel additive for combustion engines (Sievers and Sadlowski, 1978;

Sievers and Wenzel, 1981; Hartle, 1977). The rare-earth β -diketonates exhibit antiknock activity and may promote combustion. Of the different rare-earth β -diketonates studied, the $[\text{R}(\text{thd})_3]$ complexes exhibited the greatest antiknock activity (Sievers and Sadlowski, 1978). Although the $[\text{Ce}(\text{thd})_3]$ complex was found to be superior to every single pure $[\text{R}(\text{thd})_3]$ complex, a mixture of $[\text{R}(\text{thd})_3]$ complexes performed equally well. This finding is important because such a mixture can be prepared from mixed rare-earth oxides or even from a cheap raw rare-earth ore. However, it was discovered that the $[\text{R}(\text{thd})_3]$ complexes promote the degradation of hydrocarbon fuel to such an extent that they are virtually useless as fuel additives (Sievers and Wenzel, 1981). In order to overcome these problems, the new β -diketone 2,2,7-trimethyl-3,5-octanedione, Htod, was designed and the corresponding $[\text{R}(\text{tod})_3]$ complexes were prepared (Sievers and Wenzel, 1981; Wenzel et al., 1985b). Besides the absence of the undesirable side-effect of degradation of the hydrocarbon fuel, the $[\text{R}(\text{tod})_3]$ complexes have two additional advantages over $[\text{R}(\text{thd})_3]$ complexes: their higher solubility in hydrocarbon solvents and the fact that the Htod ligand can be prepared from cheaper starting materials (neopentanoic acid and methylisobutyl ketone). A typical additive concentrate contains 5 wt% solutions of $[\text{R}(\text{tod})_3]$ in xylene.

The fuel additives eliminate carbonaceous deposits from the walls of the combustion chambers. These unwanted deposits reduce the volume of the combustion chamber, so that the engine compression ratio increases, which in turn causes a proportional increase in the octane number requirement of the engine. The deposits catalyze the combustion process with a resulting tendency to cause pre-ignition. Because of reduction of the heat transfer rate through the cylinder walls by the deposits, the combustion temperature increases. Under these conditions the engine exhibits a larger tendency to knock (Sievers and Wenzel, 1981). The rare-earth oxides which are formed during the combustion of the rare-earth containing fuel additives may act as high-surface catalysts dispersed in the combustion and exhaust system (Sievers and Sadlowski, 1978). These rare-earth oxides catalyze the low-temperature oxidation of organic compounds and the decomposition of nitrogen oxides, so that they reduce the emission of harmful combustion products.

12. Solvent extraction

Solvent extraction is an important chemical separation process. A metal ion is extracted from an aqueous phase to an immiscible organic phase by an extraction agents, which is often an acidic organic compound such a β -diketone. In the aqueous phase the extracting agent is deprotonated and the deprotonated ligand forms a complex with the metal ions present in the aqueous solution. When the complex is neutral, it is better soluble in the apolar organic phase than in the aqueous solution, which causes the metal complex to be transferred from the aqueous to the organic phase. The organic phase is typically chloroform, dichloromethane, diethyl ether, benzene toluene, cyclohexane or petroleum ether, but it can also consist in the pure extracting agent. The *synergistic effect* in solvent extraction is the enhancement of the extraction of a metal ion with an acidic extracting agent by the addition of a neutral ligand (Mathur,

1983). Examples of synergistic agents are tri-*n*-butylphosphate (tbp), tri-*n*-octylphosphine oxide (topo), 1,10-phenanthroline (phen) or 2,2'-bipyridine. The synergistic effect is important for the extraction of rare-earth ions. The mechanism of this effect is a better solubility of the ternary rare-earth complexes of the extracting agent and the synergistic agents in comparison with the hydrated complex formed when the extracting agent is present alone. The extraction of rare-earth ions with β -diketones has been intensively investigated in the 1950s, when this process was of importance for the separation of fission products in the uranium fuel rods of nuclear power plants.

Acetylacetone and benzoylacetone are not good reagents to extract trivalent rare-earth ions from an aqueous to an organic phase in the absence of synergistic reagents (Brown et al., 1960; Moeller et al., 1965). This is probably due to the fact that these β -diketones form hydrated complexes with rare-earth ions, which are too hydrophilic to allow extraction into an apolar organic phase. Because of the possibility to form water-free complexes with the rare-earth ions, dipivaloylmethane (Hthd) is a much better extracting reagent (Sweet and Parlett, 1968). The synergism in the extraction of trivalent rare-earth ions has been studied by many workers (Healy, 1961a, 1961b; Yoshida, 1966; Scribner and Kotecki, 1965; Shigematsu et al., 1966, 1967, 1969b, 1970).

Fluorinated substituents have often been introduced into extractants. The acidity of the extracting agent is increased by the electron-withdrawing effect of the fluorinated group, and the extracting agent can be used to extract metal ions from more acidic aqueous solutions. For instance, the acid dissociation constant of acetylacetone (Hacac) is $pK_a = 8.82$, whereas the pK_a value of 2-thenoyltrifluoroacetone (Htta) is 6.23. A popular ligand for the solvent extraction of rare earths is 2-thenoyltrifluoroacetone (Htta). Therefore, metal ions are extractable from aqueous solution at a lower pH with Htta than with Hacac. The fact that the fluorinated β -diketonates can be used for extraction from acidic solution is of importance for the extraction of metal ions that are easily hydrolyzed. 2-Thenoyltrifluoroacetone is a very popular extracting agent, and was developed for the extraction of rare-earths from nuclear fuel wastes (Reid and Calvin, 1950). It is either used alone (Poskanzer and Foreman, 1961; Alstad et al., 1974), or in combination with various synergistic agents (Newman and Klotz, 1972; Bhatti et al., 1980; Bhatti and Duyckaerts, 1983; Nakamura and Suzuki, 1986, 1988; Dukov, 1993; Dukov and Jordanov, 1998, 1999). In the presence of quaternary ammonium ions Q^+ , the rare-earth ions are extracted as $Q^+[R(tta)_4]^-$ species (Khopkar and Mathur, 1977; Genov et al., 1977; Dukov and Genov, 1980, 1981; Noro and Sekine, 1993a, 1993b; Atanassova et al., 2002). The hydration number of rare-earth complexes of 2-thenoyltrifluoroacetone obtained by extraction into chloroform is about 3 from lanthanum(III) to holmium(III), and decreases than steadily to 2.4 for lutetium(III) (Hasegawa et al., 1999). Desreux et al. (1978) investigated the synergistic extraction of Eu^{3+} by Htta with 1H -NMR. Other β -diketonates than 2-thenoyltrifluoroacetone used for the extraction of rare-earth ions are hexafluoroacetylacetone, benzoylacetone and pivaloyltrifluoroacetone (Nakamura and Suzuki, 1986; Le et al., 1997; Matsubayashi and Hasegawa, 2001). Le et al. (1997) compared the extraction of the rare-earth ions by benzoyltrifluoroacetone and the α -substituted β -diketone 4,4,4-trifluoro-3-methyl-1-phenylbutane-1,3-dione. The authors found that rare earths were extracted at a lower pH with benzoyltrifluoroacetone than with 4,4,4-trifluoro-3-methyl-1-phenylbutane-1,3-dione, due to

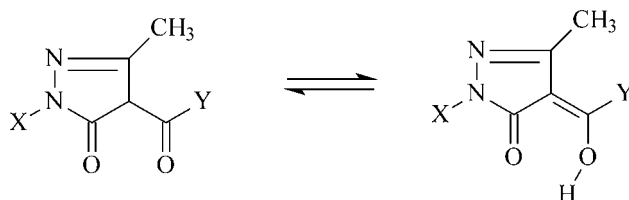


Fig. 49. General formula of 1-aryl-3-methyl-4-acyl-5-pyrazolones in the keto form (left) and in the enol form (right). X is an aromatic group and Y can be an aromatic or an aliphatic group.

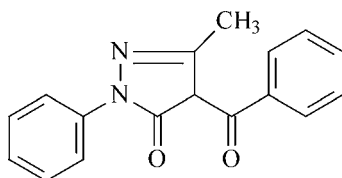


Fig. 50. Structure of 1-phenyl-3-methyl-5-benzoyl-5-pyrazolone (Hpmbp) in the keto form.

the higher acidity of the former. However, the separation of the rare earths was better with 4,4,4-trifluoro-3-methyl-1-phenylbutane-1,3-dione, because of the smaller bite angle of this ligand. Further research showed that the separability of the rare-earth ions is improved by shorter O...O distances in the metal complexes (i.e. a smaller bite angle) (Umetani et al., 2000). If the β -diketone is modified by the introduction of bulky substituents at suitable positions to create a steric effect, the O...O distances can be controlled and the separation can be improved. Nakamura et al. (2002) investigated the synergistic extraction of rare earths by 1-phenyl-3-isoheptyl-1,3-propanedione with 2,2'-bipyridine, 1,10-phenanthroline and 2,9-dimethyl-1,10-phenanthroline.

The acylpyrazoles can be considered as α -substituted β -diketones. 1-Phenyl-3-methyl-4-benzoyl-5-pyrazolone (Hpmbp) and other 1-aryl-3-methyl-4-acyl-5-pyrazolone are versatile extraction reagents for rare-earth ions (Roy and Nag, 1978; Umetani et al., 1980; Sasayama et al., 1983; Umetani and Freiser, 1987; Mukai et al., 1990, 1997, 2003) (figs. 49 and 50). The pK_a values of the 4-acyl-5-pyrazolones are between 2.5 and 4.0, so that these extractants are more acidic than 2-thenoyltrifluoroacetone. Several authors have investigated the solvent extraction of rare-earth ions with mixtures of acylpyrazolones and quaternary ammonium salts (Sasaki and Freiser, 1983; Dukov and Genov, 1986). Umetani et al. (2000) investigated the extraction of rare-earth ions with several 4-acyl-3-methyl-1-phenyl-5-pyrazolones, and discussed the separability in terms of the O...O distances. Bis(4-acylpyrazol-5-one) derivatives are formed by linking two 4-acylpyrazol-5-one units by a polymethylene spacer of varying length (Miyazaki et al., 1992) (fig. 51). The solvent extraction of scandium(III) and yttrium(III) with these extracting agents has been investigated. 3-Phenyl-4-benzoyl-5-isoxazolone is a highly acidic extracting agent ($pK_a = 1.23$) (Jyothi and Rao, 1987, 1988, 1989, 1990) that can be used for the extraction of rare-earth ions (Le et al., 1993) (fig. 52).

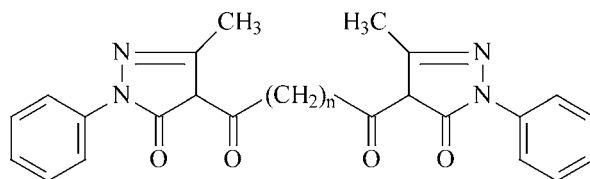


Fig. 51. Structure of bis(4-acylpyrazol-5-one) derivatives, with a polymethylene chain of varying length (Miyazaki et al., 1992).

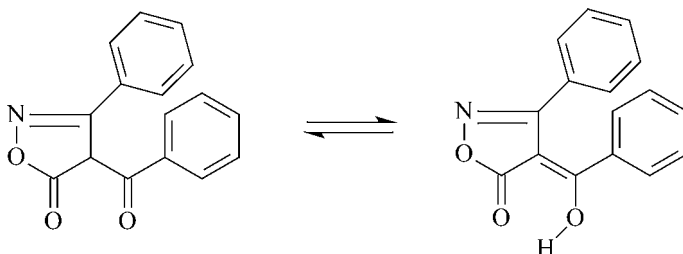


Fig. 52. Structure of 3-phenyl-4-benzoyl-5-isoxazolone in the keto form (left) and in the enol form (right).

Noro and Sekine (1992) noticed that the solvent extraction of Eu^{3+} with benzoyltrifluoroacetone into carbon tetrachloride was enhanced by the addition of bulky cations such as the tetrabutylammonium ion. This was attributed to the fact that the tetrakis complex $[\text{Eu}(\text{btfac})_4]^-$ is extracted as an ion pair with tetrabutylammonium, $[\text{Eu}(\text{btfac})_4]^- (\text{C}_4\text{H}_9)_4\text{N}^+$, and that this ion pair is more easily extracted than the tris complex $[\text{Eu}(\text{btfac})_3]$. Similar results were obtained for the extraction of Pr^{3+} and Nd^{3+} with 2-thenoyltrifluoroacetone (Noro and Sekine, 1993a, 1993b).

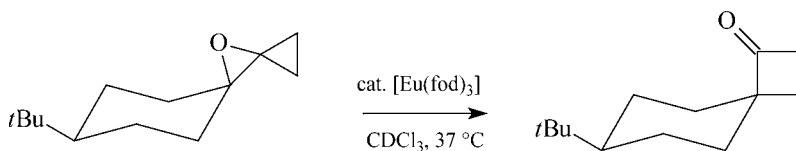
Because of their lipophilic character and because they form adducts with anions, $[\text{R}(\text{fod})_3]$ complexes are used as carriers of anions in liquid membrane transport (Tsukube et al., 1996b). The most efficient transport properties were found for the chloride ions. Ramkumar et al. (1998) studied the transport of chloride and bromide ions through a Nafion 117 cation exchange membrane by $[\text{R}(\text{tta})_3]$ complexes ($\text{R} = \text{Pr}, \text{Eu}$). The β -diketonate complexes were immobilized by precipitation on the polymer membrane. Tsukube and coworkers (Tsukube et al., 1996c, 1998, 2002; Tsukube and Shinoda, 2002) used tris complexes of fod for the extraction of zwitterionic amino acids from an aqueous phase to a dichloromethane phase. Good extractability was found for the hydrophobic amino acids phenylalanine, tryptophan, leucine, valine and phenylglycine, whereas the hydrophilic amino acids glycine and alanine were hardly extracted. The rare-earth ion is important in the extraction process, because of its ability to expand its coordination sphere by adduct formation. $[\text{Cu}(\text{fod})_2]$ is unable to transfer the amino acids from the aqueous to the organic phase. The adducts of amino acids with the rare-earth tris β -diketonate complexes can be used to transport amino acids through a liquid membrane consisting of dichloromethane. When a rare-earth complex of a chiral β -diketone

is used as the extracting agent, enantioselective extraction of amino acids is possible. Examples are the tris complexes of 3-(heptafluoropropylhydroxymethylene)-camphorate (Tsukube et al., 1998). Whereas the extractability decreases with decreasing size of the rare-earth ion, the enantioselectivity had the reversed order. The highest enantiomeric excess (49% ee) was observed for L-glycine with ytterbium(III) tris[(3-heptafluoropropylhydroxymethylene)-(+)-camphorate]. The type of β -diketonate has a pronounced effect on the enantioselective extraction. Rare-earth complexes of 3-(trifluoromethylhydroxymethylene)-camphorates showed only a modest enantiomer selectivity (<10% ee). The naturally occurring ionophore lasalocid enhances the extraction of $[R(acac)_3]$ complexes from an aqueous solution into a carbon tetrachloride solution (Tsukube et al., 1996a). This effect was described as supramolecular extraction based on a 1:1 complexation between lasalocid and the rare-earth complex.

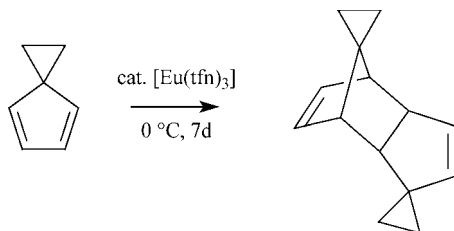
13. Catalytic properties

Many organic reactions are catalyzed by Lewis acids. Typical examples are Friedel–Crafts reactions (alkylations, acetylations), Fries rearrangement, Diels–Alder reactions, aldol reactions, Michael reactions and epoxide ring openings (Yamamoto, 2000). The classic strong Lewis acids such as $AlCl_3$, $FeCl_3$, $SnCl_4$, $TiCl_4$, or BF_3 are very efficient catalysts, but are often so reactive that they are not compatible with sensitive functional groups and their chemoselectivity is very low. Rare-earth salts have been used as mild Lewis acids in applications for which the above mentioned strong Lewis acids are unsuitable. Very often the rare-earth triflates, $R(CF_3SO_3)_3$ have been applied as mild water-compatible Lewis acid catalysts. Several excellent reviews have been published on this topic (Molander, 1989, 1992; Imamoto, 1994; Kobayashi, 1994, 1999; Kobayashi et al., 2002). Because the tris(β -diketonato)lanthanide(III) complexes that are being used as NMR shift reagents, and especially the compounds with highly fluorinated ligands, are Lewis acids, it is not unrealistic to assume that these NMR shift reagents can act as catalysts. Probably the first report of a reaction catalyzed by an NMR shift reagent was the rearrangement of oxaspiropentane to cyclobutanone under the action of $[Eu(fod)_3]$ (scheme 1) (Trost and Bogdanowicz, 1973a, 1973b).

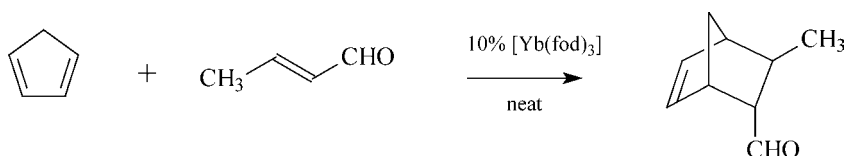
Lanthanide β -diketonates have been used as catalysts in Diels–Alder reactions. The first example of a lanthanide-catalyzed cycloaddition was the dimerization of spiro[2.4]hepta-4,6-diene by $[Eu(tfn)_3]$ (Morrill et al., 1975) (scheme 2). In the absence of the europium(III) complex no dimerization took place. Because of the mild experimental conditions, this catalyst has potential in Diels–Alder reactions where acid labile components are combined. An example is the cycloaddition of cyclopentadiene with acrolein (Danishefsky and Bednarski, 1985).



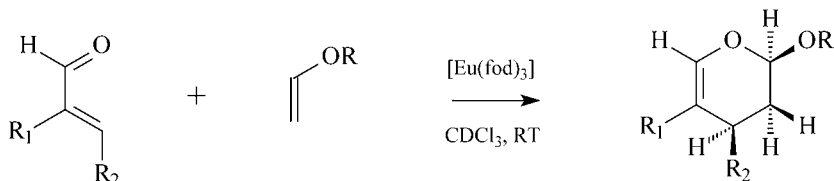
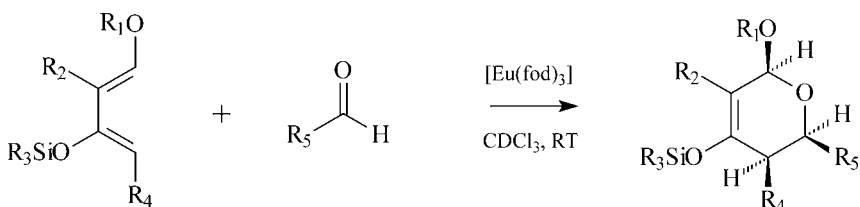
Scheme 1.



Scheme 2.



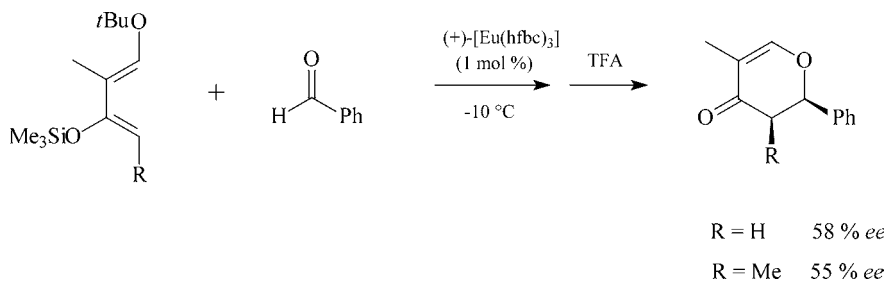
Scheme 3.



Scheme 4.

Most dienes react with acrolein at room temperature in 1–2 days. In most of the examples studied, the *endo*-adduct was formed in excess. For instance, in the case of crotonaldehyde as dienophile, the *endo:exo* ratio was 10:1 (scheme 3).

Intense research on the use of NMR shift reagents as mild Lewis catalysts started after Danishefsky reported that $[\text{Eu}(\text{fod})_3]$ could catalyze hetero Diels–Alder reactions of the type shown in scheme 4 (Bednarski and Danishefsky, 1983). Because of the high turnover rate, small amounts of the catalyst (0.5 mol%) were sufficient to perform the reactions smoothly at room temperature within 1–2 days. Heating has to be avoided because of the fragile character



Scheme 5.

of both the reagents and the reaction products. Shortly afterwards, it has been shown that $[\text{Yb}(\text{fod})_3]$ could be used in this type of reactions as well (Danishefsky and Bednarski, 1984). Probably because of the higher Lewis acidity of Yb^{3+} , $[\text{Yb}(\text{fod})_3]$ is a more active catalyst than $[\text{Eu}(\text{fod})_3]$.

In general, the $[\text{R}(\text{fod})_3]$ complexes are efficient catalysts for promoting the cycloaddition of electron-rich dienes with aldehydes. Many examples of Diels–Alder and hetero Diels–Alder reactions where $[\text{R}(\text{fod})_3]$ is used as the catalyst, have been reported in the literature (Ruano et al., 2002; Wada et al., 1996; Dujardin et al., 1997, 1998, 2001; Bauer, 1996; Bauer et al., 1996; Jarczuk and Jezewski, 1996; Helliwell et al., 1999). Other reactions catalyzed by $[\text{R}(\text{fod})_3]$ complexes include ene reactions (Deaton and Ciufoloni, 1997; Ciufolini et al., 1997), 1,3-dipolar cycloadditions (Tamura et al., 1999), radical-mediated allylations (Nagano and Kuno, 1994; Nagano et al., 1996), aldol reactions (Gu et al., 1992a, 1992b; Terada et al., 1992; Mikami et al., 1991a), ring closure of vinylic epoxy alcohols (Oka et al., 1997), rearrangement of allylic esters (Shull et al., 1996; Dai and Lee, 1999; Dai et al., 2000, 2001a, 2001b). Seven-, eight- and nine-membered cyclic ethers could be made by $[\text{Eu}(\text{fod})_3]$ -mediated reactions (Oka et al., 1997, 1998; Saitoh et al., 2003a, 2003b). $[\text{Eu}(\text{fod})_3]$ can be a valuable reagent for the synthesis of natural product, as shown by Saitoh et al. (2003b) for the total synthesis of (+)-laurallene.

$[\text{Eu}(\text{dppm})_3]$ is an efficient catalyst for the reaction of aldehydes or α,β -unsaturated aldehydes with ketene silyl acetals (Mikami et al., 1991b, 1993, 2002; Terada et al., 1994). Hdppm is di(perfluoro-2-propoxypropionyl)methane. The $[\text{Eu}(\text{dppm})_3]$ complex has a strong Lewis acidity due to the highly fluorinated ligand. It was originally developed by Ishikawa and coworkers (Kawa et al., 1982) as a chiral shift reagent (fig. 53).

Bednarski et al. (1983) were the first to report an example of asymmetric catalysis with the chiral NMR shift reagent (+)- $[\text{Eu}(\text{hfbc})_3]$ (scheme 5). The cyclocondensation reaction exhibits a modest enantioselectivity for the *l*-isomer.

Anwander and coworkers (Gerstberger et al., 1999) immobilized rare-earth complexes on the mesoporous silicate MCM-41 by first grafting $[\text{R}\{\text{N}(\text{SiHMe}_2)_2\}_3(\text{thf})_x]$ onto MCM-41, followed by surface-confined ligand exchange with Hfod. This procedure yielded $[\text{MCM-41}]\text{R}(\text{fod})_x(\text{thf})_y$ ($\text{R} = \text{Sc}, \text{Y}, \text{La}$). The performance of this catalyst was tested in the hetero Diels–Alder reaction between *trans*-1-methoxy-3-trimethylsilyloxy-1,3-butadiene and benzaldehyde. A comparable activity was found for the yttrium(III) and scandium(III) com-

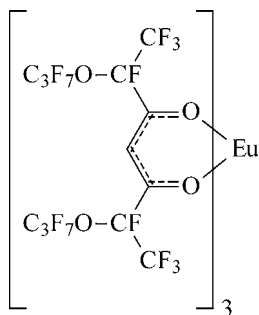


Fig. 53. Structure of tris[di(perfluoro-2-propoxypropionyl)methanato]europium(III), [Eu(dppm)₃].

plexes, whereas the activity of the lanthanum(III) complex was slightly lower. [MCM-41]R(fod)_x(thf)_y was found to be a superior catalyst both to the homogeneous system ([R(fod)₃] dissolved in a solvent) and to the material that was obtained by reaction between [Y(fod)₃] and dehydrated MCM-41. The immobilized catalyst had a long term stability, although it was less reactive in the beginning of the reaction. Keller et al. (1997) used polysiloxane-tethered β -diketonate complexes of praseodymium(III) and europium(III) as catalysts for the Danishefsky-type Diels–Alder reactions.

14. Conclusions

During the last 50 years, hundreds, not to say thousands of research papers on rare-earth β -diketonates have been published, and there is a strong evidence that these rare-earth coordination compounds will remain popular in the near future. The rare-earth β -diketonates are excellent compounds to test theoretical models in the field of spectroscopy or photophysics. Although the luminescent properties of these complexes have been explored to test their applicability in chelate lasers, organic light emitting diodes and planar optical waveguides, it is very unlikely that the rare-earth β -diketonate complexes will ever be used in real commercial devices, because of their low photochemical stability. The rare-earth β -diketonates are decomposed under the conditions required for materials processing (e.g. UV curing of polymers) or under the operating conditions (e.g. UV pumping of chelate lasers). For stability reasons, it is unlikely that OLEDs based on rare-earth β -diketonates will find a commercial application, in spite of the intense research efforts in this area. The rare-earth β -diketonates were widely used in the 1970s and 1980s as NMR shift reagents, but this application is now of minor importance, because of the availability of high-field NMR spectrometers. The use of NMR shift reagents is now largely restricted to specialty applications, such as determination of the enantiomeric purity of chiral compounds. The rare-earth β -diketonates are more likely to find use in applications that are based on their volatility, such as reagents for chemical vapor deposition. Here the low photochemical stability of the compounds is not a major issue, because the β -diketonates are decomposed after deposition to oxides or other inorganic rare-earth

compounds anyway. In luminescence application that don't require a long term photochemical stability of the compounds, the rare-earth β -diketonates are useful. Examples of such applications are fingerprint analysis or fluorimetric analysis (trace analysis of rare earths or fluoroimmunoassay). Rare-earth β -diketonates can be of further interest as mild Lewis acids in for instance Diels–Alder reactions. It can be assumed that in this case $[\text{Pr}(\text{fod})_3]$, $[\text{Eu}(\text{fod})_3]$ and especially $[\text{Yb}(\text{fod})_3]$ will be used, because of the commercial availability of these compounds as NMR shift reagents and because of their higher Lewis acidity in comparison with other β -diketonate complexes.

Acknowledgements

The author thanks the F.W.O.-Flanders (Belgium) for a postdoctoral fellowship. He also wishes to acknowledge all those scientists who were so kind to send him reprints of their work upon request. The crystal structures were drawn by Dr. Peter Nockemann.

References

- Adachi, T., Sakka, S., 1987. *J. Mater. Sci.* **22**, 4407.
- Adachi, T., Sakka, S., 1988. *J. Non-Cryst. Solids* **99**, 118.
- Adachi, C., Baldo, M.A., Forrest, S.R., 2000. *J. Appl. Phys.* **87**, 8049.
- Ahmad, N., Bhacca, N.S., Selbin, J., Wander, J.D., 1971. *J. Am. Chem. Soc.* **93**, 2564.
- Ahmed, M.O., Liao, J.L., Chen, X.W., Shen, S.A., Kaldis, J.H., 2003. *Acta Cryst.* **E59**, m29.
- Aihara, M., Arai, M., Taketatsu, T., 1986a. *Analyst* **111**, 641.
- Aihara, M., Arai, M., Tomitsugu, T., 1986b. *Anal. Lett.* **19**, 1907.
- Aikihanyan, A.S., Malkerova, I.P., Kuz'mina, N.P., Gleizes, A., Julve-Olsina, M., Sanz, J.L., Eremenko, I.L., 1999. *Russian J. Inorg. Chem.* **44**, 907 [*Zh. Neorg. Khim.* **44**, 969].
- Ainitdinov, Kh.A., Lebedev, O.L., Michurina, A.V., 1965. *Opt. Spectr. USSR* **18**, 303.
- Airoldi, C., Santos, L.S., 1993. *Struct. Chem.* **4**, 323.
- Akiyama, Y., Imaishi, N., Shin, Y.K., Jung, S.C., 2002. *J. Crystal Growth* **241**, 352.
- Allan, J.R., Carson, B.R., Gerrard, D.L., Birmie, J., 1992. *Eur. Polym. J.* **28**, 609.
- Allard, B., 1976. *J. Inorg. Nucl. Chem.* **38**, 2109.
- Alstad, J., Augustson, L.H., Farbu, L., 1974. *J. Inorg. Nucl. Chem.* **36**, 899.
- Altman, D.E., Geller, M., 1969. US Patent 3,470,493.
- Alvaro, M., Fornes, V., Garcia, S., Garcia, H., Scaiano, J.C., 1998. *J. Phys. Chem. B* **102**, 8744.
- Alves Jr., S., Almeida, F.V., de Sá, G.F., de Mello Donegá, C., 1997. *J. Lumin.* **72–74**, 478.
- Amano, A., Sato, A., Suzuki, S., 1979. *Radiochem. Radioanal. Lett.* **39**, 441.
- Amano, A., Sato, A., Suzuki, S., 1980. *Chem. Lett.*, 537.
- Amano, A., Sato, A., Suzuki, S., 1981. *Bull. Chem. Soc. Jpn.* **54**, 1368.
- Amao, Y., Okura, I., Miyashita, T., 2000a. *Chem. Lett.*, 934.
- Amao, Y., Okura, I., Miyashita, T., 2000b. *Bull. Chem. Soc. Jpn.* **73**, 2663.
- Amao, Y., Okura, I., Miyashita, T., 2000c. *Chem. Lett.*, 1286.
- Amao, Y., Ishikawa, Y., Okura, I., Miyashita, T., 2001. *Bull. Chem. Soc. Jpn.* **74**, 2445.
- An, Y.Z., Schramm, G.A.E., Berry, M.T., 2002. *J. Lumin.* **97**, 7.
- Andersen, T.J., Neuman, M.A., Melson, G.A., 1973. *Inorg. Chem.* **12**, 927.
- Andersen, W.C., Sievers, R.E., Lagalante, A.F., Bruno, T.J., 2001. *J. Chem. Eng. Data* **46**, 1045.
- Andersen, W.C., Noll, B.C., Sellers, S.P., Whildin, L.L., Sievers, R.E., 2002. *Inorg. Chim. Acta* **336**, 105.
- Anonymous, 2004. H.W. Sands Corp., <http://www.hwsands.com/index.html>.
- Ansari, M.S., Ahmad, N., 1975. *J. Inorg. Nucl. Chem.* **37**, 2099.
- Ansari, M.S., Ahmad, N., 1976. *Acta Chim. (Budapest)* **91**, 429.

- Antipin, V.A., Voloshin, A.I., Ostakhov, S.S., Kazakov, V.P., 1996. *Russian Chem. Bull.* **45**, 1099.
- Arduini, A., Armitage, I.M., Hall, L.D., Marshall, A.G., 1973. *Carbohydr. Res.* **31**, 255.
- Aristov, A.V., Maslyukov, Yu.S., 1968. *Zh. Prikl. Spektrosk.* **8**, 717.
- Armitage, I., Hall, L.D., 1971. *Can. J. Chem.* **49**, 2770.
- Arnaud, N., Georges, J., 1997. *Analyst* **122**, 143.
- Arnaud, N., Georges, J., 2003. *Spectrochimica Acta A* **59**, 1829.
- Arnaud, N., Vaquer, E., Georges, J., 1998. *Analyst* **123**, 261.
- Atanassova, M., Jordanov, V.M., Dukov, I.L., 2002. *Hydrometallurgy* **63**, 41.
- Barash, E.U., Coan, P.S., Lobkovskii, E.B., Streib, W.E., Caulton, K.G., 1993. *Inorg. Chem.* **32**, 497.
- Barbera, J., Cativiela, C., Serrano, J.L., Zurbano, M., 1992. *Liq. Cryst.* **11**, 887.
- Barkley, L.B., Levine, R., 1951. *J. Am. Chem. Soc.* **73**, 4625.
- Barkley, L.B., Levine, R., 1953. *J. Am. Chem. Soc.* **75**, 2059.
- Barrer, R.M., 1978. *Zeolites and Clays as Sorbents and Molecular Sieves*. Academic Press, London.
- Bassett, A.P., Magennis, S.W., Glover, P.B., Lewis, D.J., Spencer, N., Parsons, S., Williams, R.M., De Cola, L., Pikramenou, Z., 2004. *J. Am. Chem. Soc.* **126**, 9413.
- Batista, H.J., de Andrade, A.V.M., Longo, R.L., Simas, A.M., de Sá, G.F., Ito, N.K., Thompson, L.C., 1998. *Inorg. Chem.* **37**, 3542.
- Batsanov, A.S., Struchkov, Yu.T., Trembovetskii, G.V., Murav'eva, I.A., Martynenko, L.I., Spitsin, V.I., 1986. *Dokl. Akad. Nauk* **289**, 903.
- Batyaev, I.M., 1971. *Russian Chem. Rev.* **40**, 622.
- Bauer, H., Blanc, J., Ross, D.L., 1964. *J. Am. Chem. Soc.* **86**, 5125.
- Bauer, T., 1996. *Tetrahedron: Asymm.* **7**, 981.
- Bauer, T., Chapuis, C., Jezewski, A., Kozak, J., Jurczak, J., 1996. *Tetrahedron Asymm.* **5**, 1391.
- Baxter, I., Drake, S.R., Hursthouse, M.B., Malik, K.M.A., McAleese, J., Otway, D.J., Plakatouras, J.C., 1995. *Inorg. Chem.* **34**, 1384.
- Bazhulin, P.A., Derkacheva, L.D., Distanov, B.G., Peregudov, G.V., Prokhorov, A.P.M., Sololovskaya, A.I., Shigorin, D.N., 1965. *Opt. Spectrosc.* **18**, 298.
- Becht, M., Gerfin, T., Dahmen, K.-H., 1993. *Chem. Mater.* **5**, 137.
- Beck, J.S., Vartuli, J.C., Roth, W.J., Leonowicz, M.E., Cresge, C.T., Smith, K.D., Chu, C.T.W., Olson, D.H., Sheppard, E.W., Mccullen, S.B., Higgins, J.B., Schlenker, J.L., 1992. *J. Am. Chem. Soc.* **114**, 10834.
- Becker, E.D., 1972. *Appl. Spectrosc.* **26**, 421.
- Bednarski, M., Danishefsky, S., 1983. *J. Am. Chem. Soc.* **105**, 3716.
- Bednarski, M., Maring, C., Danishefsky, S., 1983. *Tetrahedron Lett.* **24**, 3451.
- Beeby, A., Clarkson, I.M., Dickins, R.S., Faulkner, S., Parker, D., Royle, L., de Sousa, A.S., Williams, G., Woods, M., 1999. *J. Chem. Soc. Perkin Trans.* **2**, 493.
- Behrsing, T., Bond, A.M., Deacon, G.B., Forsyth, C.M., Forsyth, M., Kamble, K.J., Skelton, B.W., White, A.H., 2003. *Inorg. Chim. Acta* **352**, 229.
- Bekiari, V., Lianos, P., Judenstein, P., 1999. *Chem. Phys. Lett.* **307**, 310.
- Belanger, P., Freppel, C., Tizane, D., Richter, J.C., 1971a. *Chem. Comm.*, 266.
- Belanger, P., Freppel, C., Tizane, D., Richter, J.C., 1971b. *Can. J. Chem.* **49**, 1985.
- Belcher, R., Majer, J., Perry, R., Stephen, W.I., 1969a. *J. Inorg. Nucl. Chem.* **31**, 471.
- Belcher, R., Dudeney, A.W.L., Stephen, W.I., 1969b. *J. Inorg. Nucl. Chem.* **31**, 625.
- Bellamy, L.J., Branch, R.F., 1954. *J. Chem. Soc.*, 4491.
- Belova, N.V., Giricheva, N.I., Girichev, G.V., Shlykov, S.A., Tverdova, N.V., Kuz'mina, N.P., Zaitseva, I.G., 2002. *J. Struct. Chem.* **43**, 56.
- Belova, N.V., Girichev, G.V., Hinchley, S.L., Kuzmina, N.P., Rankin, D.W.H., Zaitzeva, I.G., 2004. *Dalton Trans.*, 1715.
- Beltyukova, S., Balamantsarashvili, G., 1995. *Talanta* **42**, 1833.
- Bender, J.L., Corbin, P.S., Fraser, C.L., Metcalf, D.H., Richarson, F.S., Thomas, E.L., Urbas, A.M., 2002. *J. Am. Chem. Soc.* **124**, 8526.
- Benelli, C., Caneschi, A., Gatteschi, D., Pardi, L., Rey, P., Shum, D.P., Carlin, R.L., 1989a. *Inorg. Chem.* **28**, 272.
- Benelli, C., Caneschi, A., Gatteschi, D., Pardi, L., Rey, D., 1989b. *Inorg. Chem.* **28**, 3230.
- Benelli, C., Caneschi, A., Fabretti, A.C., Gatteschi, D., Pardi, L., 1990. *Inorg. Chem.* **29**, 4153.
- Benelli, C., Caneschi, A., Gattaschi, D., Pardi, L., 1992. *Inorg. Chem.* **31**, 741.
- Benelli, C., Caneschi, A., Gattaschi, D., Sessoll, R., 1993. *Inorg. Chem.* **32**, 4797.
- Bennett, M.J., Cotton, F.A., Legzdins, P., Lippard, S.J., 1968. *Inorg. Chem.* **7**, 1770.
- Berg, E.W., Acosta, J.J.C., 1968. *Anal. Chim. Acta* **40**, 101.
- Bhatti, M.S., Duyckaerts, G., 1983. *Anal. Chim. Acta* **149**, 369.

- Bhatti, M.S., Desreux, J.F., Duyckaerts, G., 1980. *J. Inorg. Nucl. Chem.* **42**, 767.
- Bhaumik, M.L., 1964. *J. Chem. Phys.* **40**, 3711.
- Bhaumik, M.L., 1965a. *J. Inorg. Nucl. Chem.* **27**, 243.
- Bhaumik, M.L., 1965b. *J. Inorg. Nucl. Chem.* **27**, 261.
- Bhaumik, M.L., El-Sayed, M.A., 1965. *J. Phys. Chem.* **69**, 275.
- Bhaumik, M.L., Fletcher, P.C., Nugent, L.J., Lee, S.M., Higa, S., Telk, C.L., Weinberg, M., 1964. *J. Phys. Chem.* **68**, 1490.
- Bian, Z.Q., Wang, K.Z., Jin, L.P., 2002. *Polyhedron* **21**, 313.
- Biju, V.M., Reddy, M.L.P., Rao, T.P., Kannan, G., Mishra, A.K., Balasubramanian, N., 2000. *Anal. Lett.* **33**, 2271.
- Binnemans, K., 2000. *J. Alloys Compds* **303/304**, 125.
- Binnemans, K., Görrler-Walrand, C., 2002. *Chem. Rev.* **102**, 2303.
- Binnemans, K., Lodewyckx, K., 2001. *Angew. Chem.* **113**, 248 [*Angew. Chem. Int. Ed.* **40**, 242].
- Binnemans, K., Moors, D., 2002. *J. Mater. Chem.* **12**, 3374.
- Binnemans, K., Bex, C., Bruce, D.W., 1999a. *Liq. Cryst.* **26**, 771.
- Binnemans, K., Bex, C., Van Deun, R., 1999b. *J. Incl. Phenom. Macrocycl. Chem.* **35**, 63.
- Binnemans, K., Bex, C., Venard, A., De Leebeeck, H., Görrler-Walrand, C., 1999c. *J. Mol. Liq.* **83**, 283.
- Binnemans, K., Lodewyckx, K., Parac-Vogt, T.N., Van Deun, R., Tinant, B., Van Hecke, K., Van Meervelt, L., 2003. *Eur. J. Inorg. Chem.*, 3028.
- Binnemans, K., Lenaerts, P., Driesen, K., Görrler-Walrand, C., 2004. *J. Mater. Chem.* **14**, 191.
- Bjorklund, S., Kellmeyer, G., Hurt, C.R., McAvoy, N., Filipescu, N., 1967. *Appl. Phys. Lett.* **10**, 160.
- Bjorklund, S., Filipescu, N., McAvoy, N., Degnan, J., 1968. *J. Phys. Chem.* **72**, 970.
- Blackborow, J.R., Edy, C.R., von Gustorf, E.A.K., Scrivanti, A., Wolfbeis, O., 1976. *J. Organomet. Chem.* **108**, C32.
- Blanc, J., Ross, D.L., 1965. *J. Chem. Phys.* **43**, 1286.
- Blasse, G., 1976. *Struct. Bond.* **26**, 43.
- Bleaney, B., 1972. *J. Magn. Reson.* **8**, 91.
- Boerner, H., Justel, T., Nikol, H., 2000a. US Patent 6,165,631.
- Boerner, H., Justel, T., Nikol, H., Ronda, C., 2000b. US Patent 6,051,925.
- Boeyens, J.C.A., de Villiers, J.P.R., 1971. *J. Cryst. Mol. Struct.* **1**, 297.
- Bol'shoi, D.B., Meshkova, S.B., Topilova, Z.M., Lozinskii, M.O., Shapiro, Yu.E., 1997. *Opt. Spekt.* **83**, 678.
- Bonnet, G., Lachkar, M., Laprin, J.P., Colson, J.C., 1994. *Solid State Ionics* **72**, 344.
- Bonnet, G., Lachkar, M., Colson, J.C., Larpin, J.P., 1995. *Thin Solid Films* **261**, 31.
- Borzechowska, M., Trush, V., Turowska-Tyrk, I., Amirkhaniv, W., Legendziewicz, J., 2002. *J. Alloys Compds* **341**, 98.
- Bourhill, G., Palsson, L.O., Samuel, I.D.W., Sage, I.C., Oswald, I.D.H., Duignan, J.P., 2001. *Chem. Phys. Lett.* **336**, 234.
- Boyaval, J., Hapiot, F., Li, C., Isaert, N., Warengem, M., Cayette, P., 1999. *Mol. Cryst. Liq. Cryst. A* **330**, 1387.
- Boyaval, J., Li, C., Hapiot, F., Warengem, M., Isaert, N., Guyot, Y., Boulon, G., Cayette, P., 2001. *Mol. Cryst. Liq. Cryst.* **359**, 337.
- Braga, S.S., Sá Ferreira, R.A., Gonçalves, I.S., Pillinger, M., Rocha, J., Teixeira-Dias, J.J.C., Carlos, L.D., 2002. *J. Phys. Chem. B* **106**, 11430.
- Brecher, C., Samelson, H., Lempicki, A., 1965. *J. Chem. Phys.* **42**, 1081.
- Brecher, C., Lempicki, A., Samelson, H., 1968. US Patent 3,405,372.
- Breck, D.W., 1974. *Zeolite Molecular Sieves: Structure Chemistry and Use*. Wiley, New York.
- Brennetot, R., Georges, J., 2000. *Spectrochim. Acta* **A56**, 703.
- Briggs, J., Frost, G.H., Hart, F.A., Moss, G.P., Staniforth, M.L., 1970. *Chem. Comm.*, 749.
- Bril, A., De Jager-Veenis, W., 1976a. *J. Res. Nat. Bureau Stand.* **80A**, 401.
- Bril, A., De Jager-Veenis, W., 1976b. *J. Electrochem. Soc.* **123**, 396.
- Brinker, C.J., Scherer, G.W., 1990. *Sol-Gel Science*. Academic Press, San Diego.
- Brito, H.F., Carvalho, C.A.A., Malta, O.L., Passos, J.J., Menezes, J.F.S., Sinisterra, R.D., 1999. *Spectrochim. Acta A* **55**, 2403.
- Brito, H.F., Malta, O.L., Menezes, J.F.S., 2000. *J. Alloys Compds* **303-304**, 336.
- Brito, H.F., Malta, O.L., Felinto, M.C.F.C., Teotonio, E.E.S., Menezes, J.F.S., Silva, C.F.B., Tomiyama, C.S., Carvalho, C.A.A., 2002. *J. Alloys Compds* **344**, 293.
- Brittain, H.G., 1979a. *J. Am. Chem. Soc.* **101**, 1733.
- Brittain, H.G., 1979b. *J. Chem. Soc., Dalton Trans.*, 1187.
- Brittain, H.G., 1980. *Inorg. Chem.* **19**, 640.
- Brittain, H.G., 1982a. *Polyhedron* **2**, 261.
- Brittain, H.G., 1982b. *J. Chem. Soc. Dalton Trans.*, 2059.

- Brittain, H.G., 1983. *Coord. Chem. Rev.* **48**, 243.
- Brittain, H.G., 1989. In: Bünzli, J.-C.G., Choppin, G.R. (Eds.), *Lanthanide Probes in Life, Chemical and Earth Sciences; Theory and Practice*. Elsevier, Amsterdam, pp. 295–319.
- Brittain, H.G., Johnson, C.R., 1985. *Inorg. Chem.* **24**, 4465.
- Brittain, H.G., Richardson, F.S., 1976a. *J. Am. Chem. Soc.* **98**, 5858.
- Brittain, H.G., Richardson, F.S., 1976b. *J. Chem. Soc., Dalton Trans.*, 2253.
- Brittain, H.G., Richardson, F.S., 1977. *J. Am. Chem. Soc.* **99**, 65.
- Brooks, J.J., Sievers, R.E., 1973. *J. Chromatographic Sci.* **11**, 303.
- Brown, W.B., Steinbach, J.F., Wagner, W.F., 1960. *J. Inorg. Nucl. Chem.* **13**, 119.
- Bruce, D.W., 1996. In: Bruce, D.W., O'Hare, D. (Eds.), *Inorganic Materials*. 2nd edition. Wiley, Chichester, p. 429.
- Bruce, D.W., Denning, R.G., Grayson, M., Le Lagadec, R., Lai, K.K., Pickup, B.T., Thornton, A., 1994. *Adv. Mater.: Optics Electron.* **4**, 293.
- Brück, S., Hilder, M., Junk, P.C., Kynast, U.H., 2000. *Inorg. Chem. Comm.* **3**, 666.
- Bruder, A.H., Tanny, S.R., Rockefeller, H.A., Springer Jr., C.S., 1974. *Inorg. Chem.* **13**, 880.
- Bulsing, J.M., Sanders, J.K.M., Hall, L.D., 1981. *J. Chem. Soc., Chem. Comm.*, 1201.
- Bünzli, J.-C.G., Moret, E., Foiret, V., Schenk, K.J., Wang, M.Z., Jin, L.P., 1994. *J. Alloys Compds* **207/208**, 107.
- Burdett, J.L., Rogers, M.T., 1964. *J. Am. Chem. Soc.* **86**, 2105.
- Burgett, C.A., 1975. US Patent 3,867,418.
- Burgett, C.A., Fritz, J.S., 1972. *Anal. Chem.* **44**, 1738.
- Burgett, C.A., Fritz, J.S., 1973. *Talanta* **20**, 363.
- Burgett, C.A., Warner, P., 1972. *J. Magn. Reson.* **8**, 87.
- Burns, J.H., Danford, M.D., 1969. *Inorg. Chem.* **8**, 1780.
- Burroughes, J.H., Bradley, D.D.C., Brown, A.R., Marks, R.N., Mackay, K., Friend, R.H., Burns, P.L., Holmes, A.B., 1990. *Nature* **347**, 539.
- Busch, H., Fink, A., Müller, A., 1991. *J. Appl. Phys.* **70**, 2450.
- Butter, E., Kreher, K., 1965. *Z. Naturforsch. A* **20**, 408.
- Butts, W.C., Banks, C.V., 1970. *Anal. Chem.* **42**, 133.
- Caldwell, J.P., Henderson, W., Kim, N.D., 2001. *J. Forensic Sci.* **46**, 1332.
- Campbell, J.R., 1971. *Aldrichimica Acta* **4**, 55.
- Campos, R.A., Kovalev, I.P., Guo, Y., Wakili, N., Skotheim, T., 1996. *J. Appl. Phys.* **80**, 7144.
- Carlos, L.D., Sá Ferreira, R.A., de Zea Bermudez, V., Molina, C., Bueno, L.A., Ribeiro, S.J.L., 1999. *Phys. Rev. B* **60**, 10042.
- Carlos, L.D., Sá Ferreira, R.A., de Zea Bermudez, V., 2000a. *Electrochim. Acta* **45**, 1555.
- Carlos, L.D., Messaddeq, Y., Brito, H.F., Sá Ferreira, R.A., de Zea Bermudez, V., Ribeiro, S.J.L., 2000b. *Adv. Mater.* **12**, 594.
- Carlos, L.D., Sá Ferreira, R.A., Rainho, J.P., de Zea Bermudez, V., 2002. *Adv. Funct. Mater.* **12**, 1.
- Carlos, L.D., de Mello Donegá, C., Albuquerque, R.Q., Alves Jr., S., Menezes, J.F.S., Malta, O.L., 2003. *Mol. Phys.* **101**, 1037.
- Chadwick, D., McAleese, J., Senkiw, K., Steele, B.C.H., 1996. *Applied Surface Sci.* **99**, 417.
- Chan, H.K., Brittain, H.G., 1981. *J. Inorg. Nucl. Chem.* **43**, 2399.
- Chan, H.K., Brittain, H.G., 1985. *Polyhedron* **4**, 39.
- Charles, R.G., 1967. *Inorg. Synth.* **9**, 37.
- Charles, R.G., Ohlmann, R.C., 1965a. *J. Inorg. Nucl. Chem.* **27**, 119.
- Charles, R.G., Ohlmann, R.C., 1965b. *J. Inorg. Nucl. Chem.* **27**, 255.
- Charles, R.G., Riedel, E.P., 1966. *J. Inorg. Nucl. Chem.* **28**, 3005.
- Chauvin, A.S., Gumy, F., Imbert, D., Bünzli, J.-C.G., 2004. *Spectrosc. Lett.* **37**, 517.
- Chen, B.T., Zhang, Y.G., Gao, L., Wang, M.Z., 1997. *Acta Chimica Sinica* **55**, 553.
- Chen, X.F., Liu, S.H., Duan, C.Y., Xu, Y.H., You, X.Z., Ma, J., Min, N.B., 1998. *Polyhedron* **17**, 1883.
- Chen, X.F., Liu, S.H., Ma, J., 1999a. *Chinese J. Inorg. Chem.* **15**, 252.
- Chen, X.F., Liu, S.H., Yu, Z., Cheung, K.K., Ma, J., Min, N.B., You, X.Z., 1999b. *J. Coord. Chem.* **47**, 349.
- Chen, X.F., Zhu, X.H., Xu, Y.H., Raj, S.S.S., Öztürk, S., Fun, H.K., Ma, J., You, X.Z., 1999c. *J. Mater. Chem.* **9**, 2919.
- Chen, X.F., Zhu, X.H., Chen, W., Vittal, J.J., Tan, G.K., Wu, J., You, Y.Z., 1999d. *J. Coord. Chem.* **52**, 97.
- Chen, X.F., Zhu, X.H., Chen, W., Vittal, J.J., Tan, G.K., Wu, J., You, X.Z., 2000. *J. Coord. Chem.* **52**, 97.
- Chen, X.F., Duan, C.Y., Zhu, X.H., You, X.Z., Raj, S.S.S., Fun, H.K., Wu, J., 2001. *Mater. Chem. Phys.* **72**, 11.
- Chen, X.F., Zhu, X.H., Xu, Y.H., Raj, S.S.S., Fun, H.K., Wu, J., You, X.Z., 2002. *J. Coord. Chem.* **55**, 421.
- Chevalier, S., Kilo, M., Borchardt, G., Larpin, J.P., 2003. *Appl. Surface Sci.* **205**, 188.
- Chou, K.S., Wang, W.M., 1996. *Thermochimica Acta* **286**, 75.
- Chour, K.W., Chen, J., Xu, R., 1997. *Thin Solid Films* **304**, 106.

- Christidis, P.C., Tossidis, I.A., Pachalidis, D.G., Tzavelas, L.C., 1998. *Acta Cryst.* **C54**, 1233.
- Christou, V., Salata, O.V., Ly, T.Q., Cappechi, S., Bailey, N.J., Cowley, A., Chippindale, A.M., 2000. *Synth. Met.* **111**, 7.
- Chu, B., Fan, D., Li, W.L., Hong, Z.R., Li, R.G., 2002. *Appl. Phys. Lett.* **81**, 10.
- Ci, Y.X., Lan, Z.H., 1989. *Anal. Chem.* **61**, 1063.
- Ci, Y.X., Yang, X.D., 1992. *Chin. Chem. Lett.* **3**, 1007.
- Ci, Y.Y., Yang, X.A., Chang, W.B., 1995. *J. Immunol. Methods* **179**, 233.
- Ciufolini, M.A., Deaton, M.V., Zhu, S.R., Chen, M.Y., 1997. *Tetrahedron* **53**, 16299.
- Clays, K., Persoons, A., 1991. *Phys. Rev. Lett.* **66**, 2980.
- Clegg, W., Sage, I., Oswald, I., Brough, P., Bourhill, G., 2000. *Acta Cryst.* **C56**, 1323.
- Cockerill, A.F., Davies, G.L.O., Harden, R.C., Rackham, D.M., 1973. *Chem. Rev.* **73**, 553.
- Collings, P.J., 1990. *Liquid Crystals: Nature's Delicate Phase of Matter*. Princeton University Press, Princeton.
- Collings, P.J., Hird, M., 1997. *Introduction to Liquid Crystals: Chemistry and Physics*. Taylor and Francis, London.
- Condorelli, G.G., Gennaro, S., Fragala, I.L., 2000. *Chem. Vap. Depos.* **6**, 185.
- Cormier, J.M., Hercules, D.M., Lee, J. (Eds.), 1973. *Chemiluminescence and Bioluminescence*. Plenum, New York.
- Cotton, F.A., Huang, P.L., 2003. *Inorg. Chim. Acta* **346**, 223.
- Cotton, F.A., Legzdins, P., 1968. *Inorg. Chem.* **7**, 1777.
- Cotton, F.A., Legzdins, P., Lippard, S.J., 1966. *J. Chem. Phys.* **45**, 3461.
- Cotton, F.A., Daniels, L.M., Huang, P.L., 2001. *Inorg. Chem. Comm.* **4**, 319.
- Cramer, R.E., Seff, K., 1972. *Acta Cryst.* **B28**, 3281.
- Criasia, R.T., 1987a. *Inorg. Chim. Acta* **133**, 189.
- Criasia, R.T., 1987b. *Inorg. Chim. Acta* **133**, 195.
- Crisler, L.R., 1975. US Patent 3,919,274.
- Crosby, G.A., Whan, R.E., Alire, R.M., 1961. *J. Chem. Phys.* **34**, 743.
- Crosby, G.A., Whan, R.E., Freeman, J.J., 1962. *J. Am. Chem. Soc.* **66**, 2493.
- Crozet, P., Meyer, Y., 1967. *Nature* **213**, 1115.
- Crump, D.R., Sanders, J.K.M., Williams, D.H., 1970. *Tetrahedron Lett.*, 4419.
- Cunningham, J.A., Sievers, R.E., 1980. *Inorg. Chem.* **19**, 595.
- Cunningham, J.A., Sands, D.E., Wanger, W.F., 1967. *Inorg. Chem.* **6**, 499.
- Cunningham, J.A., Sands, D.E., Wagner, W.F., Richardson, M.R., 1969. *Inorg. Chem.* **8**, 22.
- Dai, W.M., Lee, M.Y.H., 1999. *Tetrahedron Lett.* **40**, 2397.
- Dai, W.M., Mak, W.L., Wu, A.X., 2000. *Tetrahedron Lett.* **41**, 7101.
- Dai, W.M., Wu, A., Hamaguchi, W., 2001a. *Tetrahedron Lett.* **42**, 4211.
- Dai, W.M., Wu, A.X., Lee, M.Y.H., Lai, K.W., 2001b. *Tetrahedron Lett.* **42**, 4215.
- Dallara, J.J., Reid, M.F., Richardson, F.S., 1984. *J. Phys. Chem.* **88**, 3587.
- Damska, A., Janowski, A., 1980a. *Chemia Analityczna* **25**, 77.
- Damska, A., Janowski, A., 1980b. *Org. Magn. Reson.* **13**, 122.
- Danishefsky, S., Bednarski, M., 1984. *Tetrahedron Lett.* **25**, 721.
- Danishefsky, S., Bednarski, M., 1985. *Tetrahedron Lett.* **26**, 2507.
- Dao, P., Twarowski, A.J., 1986. *J. Chem. Phys.* **85**, 6823.
- Darr, J.A., Mingos, D.M.P., Hibbs, D.E., Hursthouse, M.B., Malik, K.M.A., 1996. *Polyhedron* **15**, 3225.
- Das, J.N., 1973. *J. Phys.* **B23**, 962.
- de Andrade, A.V.M., da Costa Jr., N.B., Simas, A.M., de Sá, G.F., 1994. *Chem. Phys. Lett.* **227**, 349.
- de Andrade, A.V.M., da Costa Jr., N.B., Simas, A.M., de Sá, G.F., 1995. *J. Alloys Compds* **225**, 55.
- de Andrade, A.V.M., Longo, R.L., Simas, A.M., de Sá, G.F., 1996. *J. Chem. Soc., Faraday Trans.* **92**, 1835.
- de Farias, R.F., Alves Jr., S., Belian, M.F., de Sá, G.F., 2002a. *Opt. Mater.* **18**, 431.
- de Farias, R.F., Alves Jr., S., Belian, M.F., Vieira, M.P.R.S., de Souza, J.M., Pedrosa, G.G., de Sa, G.F., 2002b. *Solid State Sci.* **4**, 1343.
- de Mello Donegá, C., Alves Jr., S., de Sá, G.F., 1996a. *Chem. Comm.*, 1199.
- de Mello Donegá, C., Ribeiro, S.J.L., Gonçalves, R.R., Blasse, G., 1996b. *J. Phys. Chem. Solids* **57**, 1727.
- de Mello Donegá, C., Alves Jr., S., de Sá, G.F., 1997. *J. Alloys Compds* **250**, 422.
- de Sá, G.F., Malta, O.L., de Mello Donegá, C., Simas, A.M., Longo, R.L., Santa-Cruz, P.A., da Silva Jr., E.F., 2000. *Coord. Chem. Rev.* **196**, 165.
- de Villiers, J.P.R., Boeyens, J.C.A., 1972. *Acta Cryst.* **B28**, 2335.
- de Witte, O., Meyer, Y., 1967. *J. Chim. Phys.* **64**, 186.
- Deaton, M.V., Ciufolini, M.A., 1997. *Tetrahedron Lett.* **34**, 2409.
- Demus, D., Goodby, J., Gray, G.W., Spiess, H., Vill, V. (Eds.), 1998. *Handbook of Liquid Crystals*, vol. **1-3**. Wiley-VCH, Weinheim.

- Desreux, J.F., Fox, L.E., Reilley, C.R., 1972. *Anal. Chem.* **44**, 2217.
- Desreux, J.F., Massaux, J., Duyckaerts, G., 1978. *J. Inorg. Nucl. Chem.* **40**, 1159.
- Diamandis, E.P., 1988. *Clin. Biochem.* **21**, 139.
- Diaz-Garcia, M.A., Fernandez De Avila, S., Kyzuk, M.G., 2002. *Appl. Phys. Lett.* **81**, 3924.
- Dickinson, J.T., Brix, L.B., Jensen, L.C., 1984. *J. Phys. Chem.* **88**, 1698.
- Dickinson, P.H., Geballe, T.H., Sanjurjo, A., Hildenbrand, D., Craig, G., Zisk, M., Collman, J., Banning, S.A., Sievers, R.E., 1989. *J. Appl. Phys.* **66**, 444.
- Dirr, S., Wiese, S., Johannes, H.-H., Ammermann, D., Böehler, A., Grahm, W., Kowalsky, W., 1997. *Synth. Met.* **91**, 53.
- Dong, N., Chen, B., Yin, M., Ning, L.X., Zhang, Q.J., Xia, S.D., 2004. *J. Rare Earths* **22**, 31.
- Donnio, B., Bruce, D.W., 1999. *Struct. Bond.* **95**, 193.
- Donnio, B., Guillon, D., Deschenaux, R., Bruce, D.W., 2003. In: Fujita, A., Powell, C., Creutz, M., McCleverty, J.A., Meyer, T.J. (Eds.), *Comprehensive Coordination Chemistry II*, vol. 7. Elsevier, Oxford, pp. 357–627.
- Drake, S.R., Hursthouse, M.B., Malik, K.M.A., Miller, S.A.S., Otway, D.J., 1993a. *Inorg. Chem.* **32**, 4464.
- Drake, S.R., Lyons, A., Otway, D.J., Slawin, A.M.Z., Willimas, D.J., 1993b. *J. Chem. Soc., Dalton Trans.*, 2379.
- Dujardin, G., Maudet, M., Brown, E., 1997. *Tetrahedron Lett.* **38**, 1555.
- Dujardin, G., Martel, A., Brown, E., 1998. *Tetrahedron Lett.* **39**, 8647.
- Dujardin, G., Leconte, S., Coutable, L., Brown, E., 2001. *Tetrahedron Lett.* **42**, 8849.
- Dukov, I.L., 1993. *Monatsh. Chem.* **124**, 689.
- Dukov, I.L., Genov, L., 1980. *Acta Chim. Acad. Sci. Hung.* **104**, 329.
- Dukov, I.L., Genov, L., 1981. *J. Inorg. Nucl. Chem.* **43**, 412.
- Dukov, I.L., Genov, L., 1986. *Solv. Extr. Ion Exch.* **4**, 999.
- Dukov, I.L., Jordanov, V.M., 1998. *Solv. Extr. Ion Exch.* **16**, 1151.
- Dukov, I.L., Jordanov, V.M., 1999. *Monatsh. Chem.* **130**, 865.
- Dyer, D.S., Cunningham, J.A., Brooks, J.J., Sievers, R.E., Rondeau, R.E., 1973. In: Sievers, R.E. (Ed.), *Nuclear Magnetic Shift Reagents*. Academic Press, New York, p. 21.
- Eaton, D.F., 1998. *Pure Appl. Chem.* **60**, 1107.
- Eisenbraut, K.J., Sievers, R.E., 1965. *J. Am. Chem. Soc.* **87**, 5254.
- Eisenbraut, K.J., Sievers, R.E., 1967. *J. Inorg. Nucl. Chem.* **29**, 1931.
- Eisenbraut, K.J., Sievers, R.E., 1968. *Inorg. Synth.* **11**, 94.
- Elbanowski, M., Makowska, B., Staninski, K., Kaczmarek, M., 2000. *J. Photochem. Photobiol. A* **130**, 75.
- Emsley, J., 1984. *Struct. Bonding* **57**, 147.
- Erasmus, C.S., Boeyens, J.C.A., 1970. *Acta Cryst.* **B26**, 1843.
- Erasmus, C.S., Boeyens, J.C.A., 1971. *J. Cryst. Mol. Struct.* **1**, 83.
- Erostyak, J., Buzady, A., Kozma, L., Hornyak, I., 1995. *Spectrosc. Lett.* **28**, 473.
- Espinat, P., Esteruelas, M.A., Oro, L.A., Serrano, J.L., Sola, E., 1992. *Coord. Chem. Rev.* **117**, 215.
- Evans, F.D., Tucker, J.N., de Villardi, G.C., 1975. *J. Chem. Soc., Chem. Comm.*, 205.
- Evans, W.J., Schreeve, W.L., Ziller, W.J., 1994. *Inorg. Chem.* **33**, 6435.
- Evans, W.J., Giarikos, D.G., Johnston, M.A., Greci, M.A., Ziller, J.W., 2002. *J. Chem. Soc. Dalton Trans.*, 520.
- Ezhov, Y.S., Komarov, S.A., Sevast'yanov, V.G., 1998. *J. Struct. Chem.* **39**, 514.
- Fan, P.C., Lai, C.K., 1996. *J. Chin. Chem. Soc.* **43**, 337.
- Fan, X.P., Wang, Z.Y., Wang, M.Q., 2002. *J. Lumin.* **99**, 247.
- Fan, X.P., Wu, X.P., Wang, M.Q., Qiu, J.B., Kawamoto, Y., 2004. *Mater. Lett.* **58**, 2217.
- Fang, G., Liu, Z., Liu, C., Yao, K.L., 2000. *Sens. Actuators* **B66**, 46.
- Faustino, W.M., Rocha, G.B., Gonçalves e Silva, F.R., Malta, O.L., de Sá, G.F., Simas, A.M., 2000. *J. Molec. Struct. (Theochem)* **527**, 245.
- Feibush, B., Richardson, M.F., Sievers, R.E., Springer Jr., C.S., 1972. *J. Am. Chem. Soc.* **94**, 6717.
- Feng, H.Y., Jian, S.H., Jian, Y.P., Lei, Z.Q., Wang, R.M., 1998. *J. Appl. Polymer Sci.* **68**, 1605.
- Fenkhuva, L., Kuz'mina, N.P., Martynenko, L.I., 1996. *Russian J. Coord. Chem.* **22**, 540.
- Feofilov, P.P., 1961. *The Physical Basis of Polarized Emission*. Consultants Bureau, New York.
- Fernandes, A., Dexpert-Ghys, J., Brouca-Cabarrecq, C., Philippot, E., Gleizes, A., Galarneau, A., Brunel, D., 2002. *Studies Surf. Sci. Catal.* **142**, 1371.
- Fernandes, J.A., Sá Ferreira, R.A., Pillinger, M., Carlos, L.D., Gonçalves, I.S., Ribeiro-Claro, P.J.A., 2004. *Eur. J. Inorg. Chem.*, 3913.
- Fery-Forgues, S., Lavabre, D., 1999. *J. Chem. Educ.* **76**, 1260.

- Filipescu, N., Kagan, M.R., McAvoy, N., Serafin, F.A., 1962. *Nature* **196**, 467.
- Filipescu, N., Sager, W.F., Serafin, F.A., 1964. *J. Phys. Chem.* **68**, 3324.
- Flockhart, B.D., 1976. *CRC Crit. Rev. Anal. Chem.* **6**, 69.
- Forsberg, J.H., 1981. Complexes with diketones and polyketones. In: *Gmelin Handbuch der Anorganischen Chemie*. Springer, Berlin, p. 65. Sc, Y, La-Lu (Syst. No. 39) Rare-Earth Elements, Part D3, Ch. 5.
- Forsberg, J.H., 1996. In: Gscheidner Jr., K.A., Eyring, L. (Eds.), *Handbook on the Physics and Chemistry of Rare Earths*, vol. **23**. North-Holland, Amsterdam, Ch. 153.
- Foster, D.R., Richardson, F.S., Vallarino, L.M., Shillady, D., 1983. *Inorg. Chem.* **22**, 4002.
- Freeman, J.J., Crosby, G.A., 1963. *J. Am. Chem. Soc.* **67**, 2717.
- Frey, S.T., Gong, M.L., De Horrocks Jr., W., 1994. *Inorg. Chem.* **33**, 3229.
- Fry, F.H., Pirie, W.R., 1965. *J. Chem. Phys.* **43**, 3761.
- Fu, L.S., Xu, Q.H., Zhang, H.J., Li, L.S., Meng, Q.G., Xu, R.R., 2002. *Mater. Sci. Eng. B* **88**, 68.
- Fu, Y.J., Wong, T.K.S., Yan, Y.K., Hu, X., 2003. *J. Alloys Comps* **358**, 235.
- Fujinaga, T., Kuwamoto, T., Kimoto, T., 1976. *Talanta* **23**, 753.
- Fujinaga, T., Kuwamoto, T., Murai, S., 1971. *Talanta* **18**, 429.
- Fujinaga, T., Kuwamoto, T., Murai, S., 1974. *Anal. Chim. Acta* **71**, 141.
- Fujinaga, T., Kuwamoto, T., Sugiura, K., Ichiki, S., 1981. *Talanta* **28**, 295.
- Fukuda, Y., Nakao, A., Hayashi, K., 2002. *J. Chem. Soc., Dalton Trans.*, 527.
- Galindo, V., Sénateur, J.P., Abrutis, A., Teiserskis, A., Weiss, F., 2000. *J. Crystal Growth* **208**, 357.
- Galyametdinov, Yu.G., Turanova, O.A., Van, V., Knyazev, A.A., Haase, W., 2002a. *Dokl. Chem.* **384**, 144 [Dokl. Akad. Nauk **384**, 206].
- Galyametdinov, Yu.G., Malykhina, L.V., Haase, W., Driesen, K., Binnemans, K., 2002b. *Liq. Cryst.* **29**, 1581.
- Gao, D.Q., Bian, Z.Q., Wang, K.Z., Jin, L.P., Huang, C.H., 2003. *J. Alloys Comps* **358**, 188.
- Gao, J.Z., Wang, X.W., He, J., Bai, G.B., 1987. *Inorg. Chim. Acta* **140**, 273.
- Gao, L.H., Wang, K.Z., Huang, C.H., Zhao, X.S., Xia, X.H., Li, T.K., Xu, J.M., 1995a. *Chem. Mater.* **7**, 1047.
- Gao, L.H., Wang, K.Z., Zhao, X.S., Xia, X.H., Xu, J.M., Li, T.K., 1995b. *Chem. Lett.*, 1049.
- Gao, X., Liu, H.G., Zhang, R.J., Yang, K.Z., 1996a. *Thin Solid Films* **284-285**, 39.
- Gao, L.H., Wang, K.Z., Huang, C.H., Zhou, Y.F., Li, T.K., Xu, J.M., Zhao, X.S., Xia, X.H., 1996b. *Thin Solid Films* **286**, 237.
- Gao, R.Y., Koeppen, C., Zheng, G.Q., Garito, A.F., 1998. *Appl. Opt.* **37**, 7100.
- Gao, X.C., Cao, H., Huang, C.H., Umitami, S., Chen, G.Q., Jiang, P., 1999. *Synth. Met.* **99**, 127.
- Geira, E., 2000. *J. Chem. Thermodynamics* **32**, 821.
- Geira, E., Kakolowicz, W., 1988. *J. Thermal Anal.* **33**, 977.
- Genov, L., Dukov, I.L., Kassabov, G.I., 1977. *Acta Chim. Acad. Sci. Hung.* **95**, 361.
- Geraldes, C.F.G.C., Luchinat, C., 2003. In: Sigel, A., Sigel, H. (Eds.), *The Lanthanides and Their Interrelations with Biosystems*. In: *Metal Ions in Biosystems*, vol. **40**. Marcel Dekker, New York, Ch. 14.
- Gerstberger, G., Palm, C., Anwander, R., 1999. *Chem. Eur. J.* **5**, 997.
- Girichev, G.V., Giricheva, N.I., Belova, N.V., Kaul', A.R., Kuz'mina, N.P., Gorbenco, Yu., 1993. *Russ. J. Inorg. Chem.* **38**, 320.
- Giricheva, N.I., Belova, N.V., Shlykov, S.A., Girichev, G.V., Vogt, N., Tverdova, N.V., Vogt, J., 2002. *J. Mol. Struct.* **605**, 171.
- Giricheva, N.I., Belova, N.V., Girichev, G.V., Tverdova, N.V., Shlykov, S.A., Kuzmina, N.P., Zaitseva, I.G., 2003. *J. Struct. Chem.* **44**, 771.
- Giroud-Godquin, A.M., Maitlis, P.M., 1991. *Angew. Chem. Int. Ed. Engl.* **30**, 375.
- Gleizes, A.N., 2000. *Chem. Vap. Deposition* **6**, 155.
- Gleizes, A., Sans-Lenain, S., Medus, D., Hovnanian, N., Miele, P., Foulon, J.-D., 1993. *Inorg. Chim. Acta* **209**, 47.
- Gleizes, A., Julve, M., Kuzmina, N., Alikhanyan, A., Lloret, F., Malkerova, I., Sanz, J.L., Senocq, F., 1998. *Eur. J. Inorg. Chem.*, 1169.
- Gleizes, A.N., Senocq, F., Julve, M., Sanz, J.L., Kuzmina, N., Troyanov, S., Malkerova, I., Alikhanyan, A., Ryazanov, M., Rogachev, A., Dedlovskaya, E., 1999. *J. Phys. IV France* **9**, 943.
- Goering, H.L., Eikenberry, J.N., Koerner, G.S., Latimer, C.J., 1974. *J. Am. Chem. Soc.* **96**, 1493.
- Gonçalves e Silva, F.R., Menezes, J.F.S., Rocha, G.B., Alves, S., Brito, H.F., Longo, R.L., Malta, O.L., 2000. *J. Alloys Comps* **303-304**, 364.
- Gorbenco, O.Yu., Bosak, A.A., 1998. *J. Crystal Growth* **186**, 181.
- Gorbenco, O.Yu., Kaul, A.R., Babushkina, N.A., Belova, L.M., 1997. *J. Mater. Chem.* **7**, 747.

- Görrler-Walrand, C., Binnemans, K., 1996. Rationalization of crystal-field parametrization. In: Gschneidner Jr., K.A., Eyring, L. (Eds.), *Handbook on the Physics and Chemistry of Rare Earths*, vol. **23**. North-Holland, Amsterdam, p. 121, Chapter 155.
- Gourba, E., Ringuedé, A., Cassir, M., Billard, A., Päiväsaari, J., Niinistö, J., Putkonen, M., Niinistö, L., 2003. *Ionics* **9**, 15.
- Grummt, U.W., Feller, K.H., Lehmann, F., Colditz, R., Gadonas, R., Pugzlys, A., 1996. *Thin Solid Films* **284–285**, 904.
- Gu, J.H., Terada, M., Mikami, K., Nakai, T., 1992a. *Tetrahedron Lett.* **33**, 1465.
- Gu, J.H., Okamoto, M., Terada, M., Mikami, K., Nakai, T., 1992b. *Chem. Lett.*, 1169.
- Gudmundson, R.A., Marsh, O.J., Matovich, E., 1963. *J. Chem. Phys.* **39**, 272.
- Gundermann, K.D., 1965. *Angew. Chem. Int. Ed. Engl.* **4**, 566.
- Guo, J.F., Fu, L.S., Li, H.R., Zheng, Y.X., Meng, Q.G., Wang, S.B., Liu, F.G., Zhang, H.J., 2003. *Mater. Lett.* **57**, 3899.
- Haas Jr., J.W., 1967. *J. Chem. Educ.* **44**, 396.
- Haas, Y., Stein, G., 1971. *J. Phys. Chem.* **75**, 3668.
- Halverson, F., Brinen, J.S., Leto, J.R., 1964a. *J. Chem. Phys.* **40**, 2790.
- Halverson, F., Brinen, J.S., Leto, J.R., 1964b. *J. Chem. Phys.* **41**, 157.
- Hammond, G.S., Borduin, W.G., Guter, G.A., 1959. *J. Am. Chem. Soc.* **81**, 4682.
- Hammond, G.S., Nonhebel, D.C., Wu, C.H.S., 1963. *Inorg. Chem.* **2**, 73.
- Han, B., Neumayer, D., Schultz, D.L., Marks, T.J., Zhang, H., David, V.P., 1992. *Appl. Phys. Lett.* **61**, 3047.
- Han, B., Neumayer, D.A., Schultz, D.L., Hinds, B.J., Marks, T.J., Zhang, H., Dravid, V.P., 1993a. *Chem. Mater.* **5**, 14.
- Han, B., Neumayer, D.A., Marks, T.J., Rudman, D.A., Zhang, H., David, V.K., 1993b. *Appl. Phys. Lett.* **63**, 3639.
- Hao, X.P., Fan, X.P., Wang, M.Q., 1999. *Thin Solid Films* **353**, 223.
- Hapiot, F., Boyaval, J., 2001. *Magn. Reson. Chem.* **39**, 15.
- Harima, H., Ohnishi, H., Hanaoka, K., Tachibana, K., Kobayashi, M., Hoshinouchi, S., 1990. *Jpn. J. Appl. Phys.* **29**, 1932.
- Hartle, R.J., 1977. US Patent 4,036,605.
- Hasan, M., Kumar, K., Dubey, S., Misra, S.N., 1968. *Bull. Chem. Soc. Jpn.* **41**, 2619.
- Hasan, M., Misra, S.N., Kapoor, R.N., 1969. *Indian J. Chem.* **7**, 519.
- Hasegawa, Y., Murakoshi, K., Wada, Y., Yanagida, S., Kim, J.H., Nakashima, N., Yamanaka, T., 1996. *Chem. Phys. Lett.* **248**, 8.
- Hasegawa, Y., Ishiwata, E., Ohnishi, T., Choppin, G.R., 1999. *Anal. Chem.* **71**, 5060.
- Hatakeyama, Y., Kido, H., Harada, M., Timoyasu, H., Fukutomi, H., 1988. *Inorg. Chem.* **27**, 992.
- Haukka, S., Lindblad, M., Suntola, T., 1997. *Appl. Surface Sci.* **112**, 23.
- Healy, T.V., 1961a. *J. Inorg. Nucl. Chem.* **19**, 314.
- Healy, T.V., 1961b. *J. Inorg. Nucl. Chem.* **19**, 328.
- Heikkinen, H., Johansson, L.-S., Nykänen, E., Niinistö, L., 1998. *Appl. Surface Sci.* **133**, 205.
- Heil, H., Steiger, J., Schmechel, R., van Seggern, H., 2001. *J. Appl. Phys.* **90**, 5357.
- Helliwell, M., Philips, I.M., Pritchard, R.G., Stoodley, R.J., 1999. *Tetrahedron Lett.* **40**, 8651.
- Hellmuth, K.-H., Mirzai, H., 1985. *Fresenius Z. Anal. Chem.* **321**, 124.
- Hemingway, R.E., Park, S.M., Bard, A.J., 1975. *J. Am. Chem. Soc.* **97**, 200.
- Hemmilä, I., 1995. *J. Alloys Comps* **225**, 480.
- Hemmilä, I., Mukkala, V., 2001. *Crit. Rev. Lab. Clin. Sciences* **38**, 441.
- Hemmilä, I., Dakubu, S., Mukkala, V., Siitari, H., Lövgren, T., 1984. *Anal. Biochem.* **137**, 335.
- Hemmilä, I., Ståhlberg, T., Mottram, P., 1995. *Bioanalytical Applications of Labelling Technologies*, 2nd edition. Wallac Oy, Turku.
- Hinckley, C.C., 1969. *J. Am. Chem. Soc.* **91**, 5160.
- Hirata, G.A., McKittrick, J., Avalos-Borja, M., Siqueiros, J.M., Devlin, D., 1997. *Appl. Surface Sci.* **113–114**, 509.
- Hirayama, C., Charles, R.G., Straw, R.D., Sullivan, P.G., 1985. *Thermochim. Acta* **88**, 407.
- Hocking, M.B., Vandervoort-Maarschalk, F.W., McKiernan, J., Zink, J.I., 1992. *J. Lumin.* **51**, 323.
- Holz, R.C., Thompson, L.C., 1988. *Inorg. Chem.* **27**, 4640.
- Holz, R.C., Thompson, L.C., 1993. *Inorg. Chem.* **32**, 5251.
- Hong, Z.R., Li, W.L., Zhao, D.X., Liang, C.J., Liu, X.Y., Peng, J.B., Zhao, D., 1999. *Synth. Met.* **104**, 165.
- Hong, Z.R., Li, W.L., Zhao, D.X., Liang, C.J., Liu, X.Y., Peng, J.B., Zhao, D., 2000. *Synth. Met.* **111–112**, 43.
- Hong, Z.R., Liang, C.J., Li, R.G., Zhao, D., Fan, D., Li, W.L., 2001a. *Thin Solid Films* **391**, 122.
- Hong, Z.R., Liang, C.J., Li, R.G., Zang, F.X., Fan, D., Li, W.L., Hung, L.S., Lee, S.T., 2001b. *Appl. Phys. Lett.* **79**, 1942.

- Hornyak, I., Erostyak, J., Buzady, A., Kaszas, A., Kozma, L., 1997. *Spectrosc. Lett.* **30**, 1475.
- Horrocks, W.DeW., 1973. *NMR of Paramagnetic Molecules: Principles and Applications*. Academic Press, New York, Ch. 12.
- Horrocks Jr., W.DeW., Sipe III, J.P., 1971. *J. Am. Chem. Soc.* **93**, 6800.
- Horrocks Jr., W.DeW., Sipe III, J.P., 1972. *Science* **177**, 994.
- Horrocks Jr., W.DeW., Sipe III, J.P., Lubner, J.R., 1971. *J. Am. Chem. Soc.* **93**, 5258.
- Hu, L., Li, J., Song, G., 1997. *Anal. Lett.* **30**, 945.
- Hu, M.L., Huang, Z.Y., Chen, Y.Q., Wang, S., Lin, J.J., Hu, Y., Xu, D.J., Xu, Y.Z., 1999. *Chin. J. Chem.* **17**, 637.
- Hu, W.P., Matsamura, M., Wang, M.Z., Jin, L.P., 2000a. *Appl. Phys. Lett.* **77**, 4271.
- Hu, W.P., Matsumura, M., Wang, M.Z., Jin, L.P., 2000b. *Jpn. J. Appl. Phys.* **39**, 6445.
- Huang, C.H., Deng, A.P., Han, Y.Z., Xu, G.X., Lin, X.Y., Zheng, Q.T., Shen, F.L., Zhang, S.D., 1988. *Acta Chim. Sin.* **4**, 315.
- Huang, C.H., Zhu, X.Y., Wang, K.Z., Xu, G.X., Xu, Y., Liu, Y.Q., Zhang, P., Wang, X.P., 1991. *Chin. Chem. Lett.* **2**, 741.
- Huang, C.H., Zhu, X.Y., Guo, F.W., Song, J.Q., Xu, Z.H., Liao, C.S., 1992. *Acta Scientiarum Naturalium Universitatis Pekinensis* **28**, 428.
- Huang, C.H., Wang, K.Z., Xu, G.X., Zhao, X.S., Xie, X.M., Xu, Y., Liu, Y.Q., Xu, L.G., Li, T.K., 1995. *J. Phys. Chem.* **99**, 14397.
- Huang, H.X., Liu, H.G., Xue, Q.B., Qian, D.J., 1999. *Colloids Surf. A* **154**, 327.
- Huang, L., Wang, K.Z., Huang, C.H., Gao, D.Q., Jin, L.P., 2002a. *Synth. Met.* **128**, 241.
- Huang, L., Tian, H., Li, F.Y., Gao, D.Q., Huang, Y.Y., Huang, C.H., 2002b. *J. Lumin.* **97**, 55.
- Hubbard, K.M., Espinoza, B.F., 2000. *Thin Solid Films* **366**, 175.
- Hubert-Phalzgraf, L.G., 1992. *Appl. Organomet. Chem.* **6**, 627.
- Hudson, S.A., Maitlis, P.M., 1993. *Chem. Rev.* **93**, 861.
- Huffmann, E.H., 1963a. *Phys. Lett.* **7**, 237.
- Huffmann, E.H., 1963b. *Nature* **200**, 158.
- Huffman, E.H., 1964. *Nature* **203**, 1373.
- Hung, L.S., Chen, C.H., 2002. *Mater. Sci. Eng. R* **39**, 143.
- Hurt, C.R., McAvoy, N., Bjorklund, S., Filipescu, N., 1966. *Nature* **212**, 179.
- Ifitkhar, K., Sayeed, M., Ahmad, N., 1982. *Inorg. Chem.* **21**, 80.
- Imamoto, T., 1994. *Lanthanides in Organic Synthesis*. Academic Press, London.
- Inagaki, F., Miyazawa, T., 1981. *Prog. Nucl. Magn. Reson. Spectrosc.* **14**, 67.
- Ismail, M., Lyle, S.J., Newbery, J.E., 1969. *J. Inorg. Nucl. Chem.* **31**, 1715.
- Itoh, K.I., Matsumoto, O., 1999. *Thin Solid Films* **345**, 29.
- Iwamuro, M., Wada, Y., Kitamura, T., Nakashima, N., Yanagida, S., 2000. *Phys. Chem. Chem. Phys.* **2**, 2291.
- Jabbour, G.E., Wang, J.F., Kippelen, B., Peyghambarian, N., 1999. *Jpn. J. Appl. Phys.* **38**, L1553.
- Jacobs, R.R., Weber, M.J., Pearson, R.K., 1975. *Chem. Phys. Lett.* **34**, 80.
- Jarczuk, J., Jezewski, A., 1996. *Tetrahedron: Asymm.* **7**, 1413.
- Jardin, M., Guery, J., Jacoboni, C., 1995. *J. Non-Cryst. Solids* **184**, 204.
- Jiang, J.Z., Wei, L.L., Gao, P.L., Gu, Z.N., Machia, K.I., Adachi, G.Y., 1995a. *J. Alloys Compds* **225**, 363.
- Jiang, W., Wang, K.Z., Huang, C.H., Xu, G.X., 1995b. *J. Rare Earths* **13**, 241.
- Jiang, X.Z., Jen, A.K.Y., Phelan, G.D., Huang, D.Y., Londergan, T.M., Dalton, L.R., Register, R.A., 2002a. *Thin Solid Films* **416**, 212.
- Jiang, X.Z., Jen, A.K.Y., Huang, D.Y., Phelan, G.D., Londergan, T.M., Dalton, L.R., 2002b. *Synth. Met.* **125**, 331.
- Johnston, K.E., Hammon, G.S., 1959. *U.S. Atomic Energy Commission Report IS-215*, 64 p.
- Jones, A.C., Chalker, P.R., 2003. *J. Phys. D.: Appl. Phys.* **R36**, 80.
- Juneau, G.P., 1977. *Anal. Chem.* **49**, 2375.
- Jung, Y.S., Lee, J.H., Park, K., Cho, S.I., Kang, S.J., 1998. *Bull. Korean Chem. Soc.* **19**, 699.
- Jyothi, A., Rao, G.N., 1987. *Chem. Scr.* **27**, 367.
- Jyothi, A., Rao, G.N., 1988. *Bull. Chem. Soc. Jpn.* **61**, 4497.
- Jyothi, A., Rao, G.N., 1989. *Polyhedron* **8**, 1111.
- Jyothi, A., Rao, G.N., 1990. *Talanta* **37**, 431.
- Kaczmarek, M., Staninski, K., Elbanowski, M., 2003. *J. Photochem. Photobiol. A* **154**, 273.
- Kahr, B., Clow, J.K., Paeterson, M.L., 1994. *J. Chem. Educ.* **71**, 584.
- Kahr, B., Jang, S.H., Subramony, J.A., Kelly, M.P., Bastin, L., 1996. *Adv. Mater.* **11**, 941.
- Kang, S.J., Jung, Y.K., Sohn, Y.S., 1997a. *Bull. Korean Chem. Soc.* **18**, 75.
- Kang, S.J., Jung, Y.S., Sohn, Y.S., 1997b. *Bull. Korean Chem. Soc.* **18**, 266.
- Karpinska, L., Godlewski, M., Leskelä, M., Niimistö, L., 1995. *J. Alloys Compds* **225**, 544.

- Karraker, D.E., 1967. *Inorg. Chem.* **6**, 1863.
- Karraker, D.E., 1971. *J. Inorg. Nucl. Chem.* **33**, 3713.
- Kawa, H., Yamaguchi, F., Ishikawa, N., 1982. *Chem. Lett.*, 153.
- Kawamura, Y., Wada, Y., Hasegawa, Y., Iwamuro, M., Kitamura, T., Yanagida, S., 1999. *Appl. Phys. Lett.* **74**, 3245.
- Kawamura, Y., Wada, Y., Iwamuro, M., Kitamura, T., Yanagida, S., 2000. *Chem. Lett.*, 280.
- Kazakov, V.P., Voloshin, A.I., Ostakhov, S.S., Ableeva, N.S., 1996a. *High Energy Chem.* **30**, 267.
- Kazakov, V.P., Voloshin, A.I., Ostakhov, S.S., Ableeva, N.S., 1996b. *High Energy Chem.* **30**, 413.
- Kazakov, V.P., Voloshin, A.I., Shavaleev, N.M., 1998a. *Mendeleev Comm.*, 110.
- Kazakov, V.P., Voloshin, A.I., Ostakhov, S.S., Zharinova, E.V., 1998b. *Russian Chem. Bull.* **47**, 386.
- Kazakov, V.P., Voloshin, A.I., Shavaleev, N.M., 1998c. *J. Photochem. Photobiol. A* **119**, 177.
- Kazakov, V.P., Voloshin, A.I., Ostakhov, S.S., Shavaleev, N.M., 1998d. *Mendeleev Comm.*, 47.
- Kazakov, V.P., Antipin, V.A., Voloshin, A.I., Khusainova, I.A., 1995. *Russian Chem. Bull.* **44**, 1774.
- Keller, F., Weinmann, H., Schurig, V., 1997. *Chem. Ber./Recueil* **130**, 879.
- Kemlo, J.A., Neilson, J.D., Shepherd, T.M., 1977. *Inorg. Chem.* **16**, 1111.
- Khopkar, P.K., Mathur, J.N., 1977. *J. Inorg. Nucl. Chem.* **39**, 2063.
- Kido, J., Okamoto, Y., 2002. *Chem. Rev.* **102**, 2357.
- Kido, J., Nagai, K., Ohashi, Y., 1990. *Chem. Lett.*, 657.
- Kido, J., Nagai, K., Okamoto, Y., Skotheim, T., 1991. *Chem. Lett.*, 1267.
- Kido, J., Hayase, H., Hongawa, K., Nagai, K., 1994. *Appl. Phys. Lett.* **65**, 2124.
- Kido, J., Ikeda, W., Kimura, M., Nagai, K., 1996. *Jpn. J. Appl. Phys.* **35**, L394.
- Kim, Y.K., Pyo, S.W., Choi, D.S., Hue, H.S., Lee, S.H., Ha, Y.K., Lee, H.S., Kim, J.S., Kim, W.Y., 2000. *Synth. Met.* **111–112**, 113.
- Kimura, T., Goto, T., 2003. *Thin Solid Films* **167**, 240.
- Kirby, A.F., Palmer, R.A., 1981a. *Inorg. Chem.* **20**, 1030.
- Kirby, A.F., Palmer, R.A., 1981b. *Inorg. Chem.* **20**, 2544.
- Kirby, A.F., Richardson, F.S., 1983. *J. Phys. Chem.* **87**, 2544.
- Kleinerman, M., 1964. *Bull. Am. Phys. Soc.* **9**, 265.
- Kobayashi, S., 1994. *Synlett.*, 889.
- Kobayashi, S. (Ed.), 1999. *Lanthanides: Chemistry and Uses in Organic Synthesis*. Springer Verlag, Berlin.
- Kobayashi, S., Sugiura, M., Kitagawa, H., Lam, W.W.L., 2002. *Chem. Rev.* **102**, 2227.
- Kobayashi, T., Nakatsuka, S., Iwafuji, T., Kuriki, K., Imai, N., Nakamoto, T., Claude, C.D., Sasaki, K., Koike, Y., 1997. *Appl. Phys. Lett.* **71**, 2421.
- Koehler, J.M., Bos, W.G., 1967. *Inorg. Nucl. Chem. Lett.* **3**, 545.
- Kononenko, L.I., Melent'eva, E.V., Vitkun, R.A., Poluektov, N.S., 1965a. *Ukr. Khim. Zh.* **31**, 1031.
- Kononenko, L.I., Tischenko, M.A., Viktkun, R.A., Poluektov, N.S., 1965b. *Russian J. Inorg. Chem.* **10**, 1341 [*Zh. Neorg. Khim.* **10**, 2465].
- Kooijman, H., Nijssen, F., Spek, A.L., Schip, F., 2000. *Acta Cryst.* **C56**, 156.
- Koshimura, H., Saito, J., Okuno, T., 1973. *Bull. Chem. Soc. Jpn.* **46**, 632.
- Kowalski, W.J., 1985. *J. Chromatogr.* **349**, 457.
- Kowalski, W.J., 1991. *Chromatographia* **31**, 168.
- Kowalski, W.J., 1992. *Chromatographia* **34**, 266.
- Kowalski, W.J., 1998a. *Chem. Anal. (Warsaw)* **43**, 69.
- Kowalski, W.J., 1998b. *J. Chromatogr. A* **793**, 390.
- Krasutsky, P.A., Yurchenko, A.G., Radionov, V.N., 1982. *Tetrahedron Lett.* **23**, 3719.
- Kresge, C.T., Leonowitz, M.E., Roth, W.J., Vartuli, J.C., Beck, J.S., 1992. *Nature* **359**, 710.
- Kukli, K., Heikkinen, H., Nykänen, E., Niinistö, L., 1998. *J. Alloys Compds* **275–277**, 10.
- Kunkely, H., Vogler, A., 2001. *J. Photochem. Photobiol. A* **146**, 63.
- Kuriki, K., Kobayashi, T., Imai, N., Tamura, T., Tagaya, A., Koike, Y., Okamoto, Y., 2000. *Proc. SPIE* **3939**, 28.
- Kuriki, K., Nishihara, S., Nishizawa, Y., Tagaya, A., Okamoto, Y., Koike, Y., 2001. *Electron. Lett.* **37**, 415.
- Kuriki, K., Koike, Y., Okamoto, Y., 2002. *Chem. Rev.* **102**, 2347.
- Kuz'mina, N.P., Pisarevskii, A.P., Martynenko, L.I., Struchkov, Yu.T., 1994. *Koord. Khim.* **20**, 707.
- Kuz'mina, N.P., Chugarov, N.V., Pisarevsky, A.P., Martynenko, L.I., 1997. *Koord. Khim.* **23**, 450.
- Kuz'mina, N.P., Rogachev, A.Y., Spiridonov, F.M., Dedlovskaya, E.M., Ketsko, V.A., Gleizes, A., Battiston, J., 2000a. *Russian J. Inorg. Chem.* **45**, 1340 [*Zh. Neorg. Khim.* **45**, 1468].
- Kuz'mina, N.P., Kupriyanova, G.N., Troyanov, S.I., 2000b. *Russian J. Coord. Chem.* **26**, 367 [*Koord. Khim.* **26**, 390].
- Kuzmina, N.P., Martynenko, L.I., Chugarov, N.V., Zaitseva, I.G., Grigoriev, A.N., Yakushevich, A.N., 2000c. *J. Alloys Compds* **308**, 158.
- Kuzmina, N., Malkerova, I., Ryazanov, M., Alikhanyan, A., Rogachev, A., Gleizes, A.N., 2001. *J. Phys. IV France* **11**, 661.

- Kuz'mina, N.P., Ryazanov, M.V., Ketsko, V.Z., Gleizes, A.N., 2002. *Russian J. Inorg. Chem.* **47**, 26 [*Zh. Neorg. Khim.* **47**, 30].
- Labes, M.M., 1979. US Patent 4,176,918.
- Langlet, M., Shannon, R.D., 1990. *Thin Solid Films* **186**, L1.
- Larrabee, R.D., 1973. *RCA Rev.* **34**, 329.
- Larrabee, R.D., 1976. US Patent 3,960,753.
- Le, Q.T.H., Umetani, S., Takahara, H., Matsui, M., 1993. *Anal. Chim. Acta* **272**, 293.
- Le, Q.T.H., Umetani, S., Suzuki, M., Matsui, M., 1997. *J. Chem. Soc., Dalton Trans.*, 643.
- Lee, J.H., Jung, Y.S., Sohn, Y.S., Kang, S.J., 1998. *Bull. Korean Chem. Soc.* **19**, 231.
- Lee, M.H., Pyo, S.W., Lee, H.S., Choi, J.S., Kim, J.S., Kim, Y.K., Lee, S.H., Kim, W.Y., Ju, S.H., Lee, C.H., 1999. *J. Korean Phys. Soc.* **35**, S436.
- Leedham, T.J., Drake, S.R., 1996. US Patent 5,504,195.
- Leipoldt, J.G., Bok, L.D.C., Laubscher, A.E., Basson, S.S., 1975. *J. Inorg. Nucl. Chem.* **37**, 2477.
- Leipoldt, J.G., Bok, L.D.C., Basson, S.S., Laubscher, A.E., 1976. *J. Inorg. Nucl. Chem.* **38**, 1477.
- Leipoldt, J.G., Bok, L.D.C., Basson, S.S., Laubscher, A.E., Van Vollenhoven, J.S., 1977. *J. Inorg. Nucl. Chem.* **39**, 301.
- Lempicki, A., Samelson, H., 1963. *Phys. Lett.* **4**, 133.
- Lempicki, A., Weise, K.H., 1967. US Patent 3,319,183.
- Lempicki, A., Samelson, H., Brecher, C., 1964. *J. Chem. Phys.* **41**, 1214.
- Leskelä, M., Niinistö, L., Nykänen, E., Soininen, P., Tiitta, M., 1991a. *Thermochim. Acta* **175**, 91.
- Leskelä, M., Niinistö, L., Sillanpää, R., Tiitta, M., 1991b. *Acta Chem. Scand.* **45**, 1086.
- Leskelä, M., Mölsä, H., Niinistö, L., 1993. *Supercond. Sci. Technol.* **6**, 627.
- Leskelä, T., Vasama, K., Härkönen, G., Sarkio, P., Lounasmaa, M., 1996. *Adv. Mater. Optics Electron.* **6**, 169.
- Li, Y.G., Yang, Y.S., Li, Y.Y., Mak, T.W.C., 1988. *Jiegou Huaxue (Chin.) (Chinese J. Struct. Chem.)* **7**, 165.
- Li, H., Huang, C.H., Zhao, Y.L., Li, T.K., Bai, J., Zhao, X.S., Xia, X.H., 1995. *Solid State Comm.* **94**, 731.
- Li, H., Huang, C.H., Zhou, D., Xu, L., Li, T.K., Zhao, X.S., Xie, X., 1996. *Progr. Nat. Sci.* **6**, 96.
- Li, W.L., Yu, J.Q., Sun, G., Hong, Z., Yu, Y., Zhao, Y., Peng, J.B., Tsutsui, T., 1997. *Synth. Met.* **91**, 263.
- Li, H.H., Inoue, S., Machida, K.I., Adachi, G.Y., 1999. *Chem. Mater.* **11**, 3171.
- Li, H.R., Zhang, H.J., Lin, J., Wang, S.B., Yang, K.Y., 2000. *J. Non-Cryst. Solids* **278**, 218.
- Li, W., Li, W., Yu, G., Wang, Q., Gin, Y., 1993. *J. Alloys Comps* **191**, 107.
- Liang, C.Y., Schimitschek, E.J., Trias, J.A., 1970. *J. Inorg. Nucl. Chem.* **32**, 811.
- Liang, C.J., Li, W.L., Hong, Z.R., Liu, X.Y., Peng, J.B., Liu, L., Lu, Z.Y., Xie, M.Q., Liu, Z.B., Yu, J.Q., Zhao, D.Q., 1997. *Synth. Met.* **91**, 151.
- Liang, C.J., Zhao, D., Hong, Z.R., Zhao, D.X., Li, X.Y., Li, W.L., Peng, J.B., Yu, J.Q., Lee, C.S., Lee, S.T., 2000a. *Appl. Phys. Lett.* **76**, 67.
- Liang, C.J., Hong, Z.R., Liu, X.Y., Zhao, D.X., Zhao, D., Li, W.L., Peng, J.B., Yu, J.Q., Lee, C.S., Lee, S.T., 2000b. *Thin Solid Films* **359**, 14.
- Liang, Y.J., Lin, Q., Zhang, H.J., Zhang, Y.X., 2001. *Synth. Met.* **123**, 377.
- Liang, F.S., Zhou, Q.G., Cheng, Y.X., Wang, L.X., Ma, D.G., Jing, X.B., Wang, F.S., 2003. *Chem. Mater.* **15**, 1935.
- Lim, J.T., Hong, S.T., Lee, J.C., Lee, I.K., 1996. *Bull. Korean Chem. Soc.* **17**, 1023.
- Lin, S., Feuerstein, R.J., Mickelson, A., 1996. *J. Appl. Phys.* **79**, 2868.
- Lin, Y.H., Wu, H., Smart, N., Wai, C.M., 1998. *J. Chromatogr. A* **793**, 107.
- Ling, Q.D., Yang, M.J., Zhang, W.G., Lin, H.Z., Yu, G., Bai, F.L., 2002. *Thin Solid Films* **417**, 127.
- Lippard, S.J., 1966. *J. Am. Chem. Soc.* **88**, 4300.
- Lippard, S.J., 1967. *Prog. Inorg. Chem.* **8**, 124.
- Lis, S., Elbanowski, M., Makowska, M., Hnatejko, Z., 2002. *J. Photochem. Photobiol. A* **150**, 233.
- Liss, I.B., Bos, W.G., 1977. *J. Inorg. Nucl. Chem.* **39**, 443.
- Liu, W.S., Zhu, Y., Tan, M.Y., 1991. *J. Coord. Chem.* **24**, 107.
- Liu, G.F., Shi, T.S., Liu, X.X., 1994. *Polyhedron* **13**, 2255.
- Liu, L., Li, W.L., Hong, Z.R., Peng, J.B., Liu, X.Y., Liang, C.J., Liu, Z.B., Yu, J.Q., Zhao, D.X., 1997. *Synth. Met.* **91**, 267.
- Liu, H.G., Lan, W.Z., Yang, K.Z., Zhu, G.Y., Zhang, H.W., 1998. *Thin Solid Films* **323**, 235.
- Liu, H.G., Park, S.T., Jang, K.W., Zhang, W.S., Seo, H.J., Lee, Y.I., 2003. *Mater. Chem. Phys.* **82**, 84.
- Liu, H.G., Lee, Y.I., Qin, W.P., Jang, K.W., Feng, X.S., 2004a. *Mater. Lett.* **58**, 1677.
- Liu, H.G., Park, S.T., Jang, K.W., Feng, X.S., Kim, C.D., Seo, H.J., Lee, Y.I., 2004b. *J. Lumin.* **106**, 47.
- Lo Nigro, R., Malandrino, G., Fragala, I.L., Bettinelli, M., Speghini, A., 2002. *J. Mater. Chem.* **12**, 2816.
- Lo Nigro, R., Toro, R., Malandrino, G., Fragala, I.L., 2003. *Chem. Mater.* **15**, 1434.
- Lock, E.R.A., Mazzella, W.D., Margot, P., 1995. *J. Forensic Sci.* **40**, 654.

- Long, J.R., 1986. Implications in Organic Synthesis. In: Gschneidner Jr., K.A., Eyring, L. (Eds.), Handbook on the Physics and Chemistry of Rare Earths, vol. 8. North-Holland, Amsterdam, p. 335.
- Lorenz, V., Fischer, A., Jacob, K., Brüser, W., Edelmann, F.T., 2001. Chem. Eur. J. **7**, 848.
- Lowe Jr., J.U., Ferguson, L.N., 1965. J. Org. Chem. **30**, 3000.
- Lupo, D., Prass, W., Scheunemann, U., Laschewsky, A., Ringsdorf, H., Ledoux, I., 1988. J. Opt. Soc. Am. B **5**, 300.
- Luten, H.A., Rees Jr., W.S., Goedken, V.L., 1996. Chem. Vap. Depos. **2**, 149.
- Lyle, S.J., Witts, A.D., 1971. Inorg. Chem. Acta **5**, 481.
- Magazeeva, N.V., Martynenko, L.I., Muraveva, I.A., Sokolov, D.N., Spitsyn, V.I., 1986. Bull. Acad. Sci. USSR, Div. Chem. Sci. **35**, 1645.
- Mahajan, R.K., Kaur, I., Kaur, R., Uchida, S., Onimaru, A., Shinoda, S., Tsukube, H., 2003. Chem. Comm., 2238.
- Mahalingam, T., Radhakrishnan, M., Balasubramanian, C., 1981. Thin Solid Films **78**, 229.
- Malandrino, G., Licata, R., Castelli, F., Fragala, I.L., Benelli, C., 1995. Inorg. Chem. **34**, 6233.
- Malandrino, G., Incontro, O., Castelli, F., Fragala, I.L., 1996. Chem. Mater. **8**, 1292.
- Malandrino, G., Frassica, A., Fragala, I.L., 1997. Chem. Vap. Depos. **3**, 306.
- Malandrino, G., Benelli, C., Castelli, F., Fragala, I.L., 1998a. Chem. Mater. **10**, 3434.
- Malandrino, G., Fragala, I.L., Scardi, P., 1998b. Chem. Mater. **10**, 3765.
- Malandrino, G., Bettinelli, M., Speghini, A., Fragala, I.L., 2001. Eur. J. Inorg. Chem., 1039.
- Male, N.A.H., Salata, O.V., Christou, V., 2002. Synth. Met. **126**, 7.
- Malta, O.L., Gonçalves e Silva, F.R., 1998. Spectrochim. Acta **A54**, 1593.
- Malta, O.L., Couto dos Santos, M.A., Thompson, L.C., Ito, N.K., 1996. J. Lumin. **69**, 77.
- Malta, O.L., Brito, H.F., Menezes, J.F.S., Gonçalves e Silva, F.R., Alves Jr., S., Farias Jr., F.S., de Andrade, A.V.M., 1997. J. Lumin. **75**, 255.
- Malta, O.L., Brito, H.F., Menezes, J.F.S., Gonçalves e Silva, F.R., de Mello Donegá, C., 1998. Chem. Phys. Lett. **282**, 233.
- Malta, O.L., Batista, H.J., Carlos, L.D., 2002. Chem. Phys. **282**, 21.
- Martynenko, L.I., Burova, S.A., Pisarevskii, A.P., 1995. Koord. Khim. **21**, 424.
- Martynenko, L.I., Kuz'mina, N.P., Grigor'ev, A.N., 1998. Russian J. Inorg. Chem. **43**, 1038 [Zh. Neorg. Khim. **43**, 1131].
- Mathis, G., 1993. Clin. Chem. **39**, 1953.
- Mathur, J.N., 1983. Solvent Extr. Ion Exch. **1**, 349.
- Matković, B., Grdenić, D., 1963. Acta Cryst. **16**, 456.
- Matsubayashi, I., Hasegawa, Y., 2001. Anal. Sci. **17**, 221.
- Matsumoto, K., Tsukahara, Y., Uemara, T., Tsunoda, K., Kume, H., Kawasaki, S., Tadano, J., Matsuya, T., 2002. J. Chromatogr. B **773**, 135.
- Matsumoto, K., Yuan, J.C., 2003. In: Sigel, A., Sigel, H. (Eds.), The Lanthanides and Their Interrelations with Biosystems. In: Metal Ions in Biosystems, vol. 40. Marcel Dekker, New York, Chapter 6.
- Matsumoto, M., Kodama, H., Funahashi, S., Takagi, H.D., 2000. Inorg. React. Mech. **2**, 19.
- Matsuno, S., Uchikawa, F., Utsinomiya, S., Nakabayashi, S., 1992. Appl. Phys. Lett. **60**, 2427.
- Matthews, L.R., Knobbe, E.T., 1993. Chem. Mater. **5**, 1697.
- Mattson, S.M., Abramson, E.J., Thompson, L.C., 1985. J. Less-Common Met. **112**, 373.
- McAleese, J., Steele, B.C.H., 1998. Corrosion Sci. **40**, 113.
- McAleese, J., Plakatouras, J.C., Steele, B.C.H., 1996a. Thin Solid Films **280**, 152.
- McAleese, J., Plakatouras, J.C., Steele, B.C.H., 1996b. Thin Solid Films **286**, 64.
- McConnell, H.M., Robertson, R.E., 1958. J. Chem. Phys. **29**, 1361.
- McCreary, M.D., Lewis, D.W., Wernick, D.L., Whitesides, G.M., 1974. J. Am. Chem. Soc. **96**, 1038.
- McDevitt, N.T., Braun, W.L., 1964. Spectrochim. Acta **20**, 799.
- McGehee, M.D., Bergstedt, T., Zhang, C., Saab, A.P., O'Regan, M.B., Bazan, G.C., Srdanov, V.I., Heeger, A.J., 1999. Adv. Mater. **11**, 1349.
- McGoran, E.C., Cutter, B., Morse, K., 1979. J. Chem. Educ. **56**, 122.
- McPhail, A.T., Tschang, P.S.W., 1974. J. Chem. Soc., Dalton Trans., 1165.
- Mehrotra, R.C., Misra, T.N., Misra, S.N., 1965. Indian J. Chem. **3**, 525.
- Mehrotra, R.C., Bohra, R., Gaur, D.P., 1978. Metal β -Diketonates and Allied Derivatives. Academic Press, London.
- Melby, L.R., Rose, N.J., Abramson, E., Caris, J.C., 1964. J. Am. Chem. Soc. **86**, 5117.
- Melent'eva, E.V., Kononenko, L.I., Poluektov, N.S., 1966. Ukr. Khim. Zh. **32**, 1147.
- Meng, G.Y., Song, H.Z., Wang, H.B., Xia, C.R., Peng, D.K., 2002. Thin Solid Films **409**, 105.

- Meshkova, S.B., Topilova, Z.M., 1998. *Ukr. Khim. Zh.* **64**, 89.
- Meshkova, S.B., Topilova, Z.M., Lozinskii, M.O., Rusakova, N.V., Bol'shoi, D.V., 1997. *J. Anal. Chem.* **52**, 852 [*Zh. Anal. Khim.* **52**, 939].
- Meshkova, S.B., Shapiro, Yu.E., Kuz'min, V.E., Artemenko, A.G., Rusakova, N.V., Pykhteeva, E.G., Bol'shoi, D.V., 1998. *Russian J. Coord. Chem.* **24**, 669.
- Meshkova, S.B., Kuz'min, V.E., Shapiro, Yu.E., Topilova, Z.M., Yudanov, I.V., Bol'shoi, D.V., Antonovich, V.P., 2000. *J. Anal. Chem.* **55**, 102.
- Mészáros-Szecsényi, K., Päiväsääri, J., Putkonen, M., Niinistö, L., Pokol, G., 2002. *J. Thermal Anal. Calorimetry* **69**, 65.
- Meyer, Y., 1965. *J. Phys. (Paris)* **26**, 558.
- Meyer, Y., Poncet, H., Verron, M., 1964a. *Compt. Rend.* **259**, 103.
- Meyer, Y., Astier, R., Simon, J., 1964b. *Compt. Rend.* **259**, 4604.
- Mihara, T., Tomiyasu, H., Jung, W.K., 1994. *Polyhedron* **13**, 1747.
- Mikami, K., Terada, M., Matsuzawa, H., 2002. *Angew. Chem. Int. Ed.* **41**, 3554.
- Mikami, K., Terada, M., Nakai, T., 1991a. *Tetrahedron: Asymm.* **2**, 993.
- Mikami, K., Terada, M., Nakai, T., 1991b. *J. Org. Chem.* **56**, 5456.
- Mikami, K., Terada, M., Nakai, T., 1993. *J. Chem. Soc., Chem. Comm.*, 343.
- Mikami, M., Nakagawa, I., Shimanouchi, T., 1967. *Spectrochim. Acta* **A23**, 1037.
- Misner, A., Wilkinson, D., Watkin, J., 1993. *J. Forensic Ident.* **43**, 154.
- Misra, S.N., Misra, T.N., Mehrotra, R.C., 1967. *Indian J. Chem.* **5**, 372.
- Misumi, S., Iwasaki, N., 1967. *Bull. Chem. Soc. Jpn.* **40**, 550.
- Mitchell, J.W., Banks, C., 1971. *Anal. Chim. Acta* **57**, 415.
- Miyabayashi, T., Kinoshita, J., 1998. *US Patent* 5,792,822.
- Miyamoto, Y., Uekawa, M., Ikeda, H., Kaifu, K., 1999. *J. Lumin.* **81**, 159.
- Miyazaki, S., Mukai, H., Umetani, S., Kihara, S., Matsui, M., 1992. *Anal. Chim. Acta* **259**, 25.
- Moeller, T., Martin, D.F., Thompson, L.C., Ferrus, R., Feistel, G., Randall, W.J., 1965. *Chem. Rev.* **65**, 1.
- Molander, G.A., 1989. Lanthanide reagents in organic synthesis. In: Hartley, F.R. (Ed.), *Organometallic Compounds in Organic and Biological Syntheses*. In: *The Chemistry of the Metal-Carbon Bond*, vol. **5**. Wiley, New York, p. 319.
- Molander, G., 1992. *Chem. Rev.* **92**, 29.
- Moleski, R., Stathatos, E., Bekiari, V., Lianos, P., 2002. *Thin Solid Films* **416**, 279.
- Mölsä, H., 1991. M.Sc. Thesis, Helsinki University of Technology, Espoo.
- Mölsä, H., Niinistö, L., 1994. *Mat. Res. Symp. Proc.* **335**, 341.
- Mölsä, H., Niinistö, L., Utriainen, M., 1994. *Adv. Mater. Opt. Electron.* **4**, 389.
- Moon, D.G., Salata, O.V., Etechells, M., Dobson, P.J., Christou, V., 2001. *Synth. Met.* **123**, 355.
- Morgan, G.T., Moss, H.W., 1914. *J. Chem. Soc.*, 189.
- Morrill, T.C., Clark, R.A., Bilobran, D., Youngs, D.S., 1975. *Tetrahedron Lett.* **397**, 1207.
- Morris, M.L., Moshier, R.W., Sievers, R.E., 1963. *Inorg. Chem.* **2**, 411.
- Moser, D.F., Thompson, L.C., Young Jr., V.G., 2000. *J. Alloys Compds* **303/304**, 121.
- Moshier, R.W., Sievers, R.E., 1965. *Gas Chromatography of Metal Chelates*. Pergamon Press, Oxford.
- Mukai, H., Umetani, S., Matsui, M., 1997. *Anal. Sci.* **13**, 145.
- Mukai, H., Umetani, S., Matsui, M., 2003. *Solvent Extr. Ion Exch.* **21**, 73.
- Mukai, H., Miyazaki, S., Umetani, S., Kihara, S., Matsui, M., 1990. *Anal. Chim. Acta* **239**, 277.
- Murray, G.M., Pesterfield, L.L., Stump, N.A., Schweitzer, G.K., 1989. *Inorg. Chem.* **28**, 1994.
- Nagano, H., Kuno, Y., 1994. *J. Chem. Soc., Chem. Comm.*, 987.
- Nagano, H., Kuno, Y., Omori, Y., Iguchi, M., 1996. *J. Chem. Soc., Perkin Trans.* **1**, 389.
- Nakamoto, K., Martell, A.E., 1960. *J. Phys. Chem.* **32**, 588.
- Nakamura, K., 1982. *Bull. Chem. Soc. Jpn.* **55**, 2697.
- Nakamura, S., Suzuki, N., 1986. *Polyhedron* **5**, 1805.
- Nakamura, S., Suzuki, N., 1988. *Polyhedron* **7**, 155.
- Nakamura, M., Nakamura, R., Nagai, K., Shimoi, M., Tomada, S., Takeuchi, Y., Ouchi, A., 1986. *Bull. Chem. Soc. Jpn.* **59**, 332.
- Nakamura, S., Takei, S., Akiba, K., 2002. *Anal. Sci.* **18**, 319.
- Napier, G.D.R., Neilson, J.D., Shepherd, T.M., 1975. *Chem. Phys. Lett.* **31**, 328.
- Nassar, E.J., Serra, O.A., Calefi, P.S., Manso, C.M.C.P., Neri, C.R., 2001. *Mater. Res.* **4**, 18.
- Nazarov, A.M., 2000. *High Energy Chem.* **34**, 301.
- Nehring, R.B., Schimitschek, E.J., Trias, J.A., 1964. *Phys. Lett.* **12**, 198.
- Neilson, J.D., Shepherd, T.M., 1976. *J. Chem. Soc., Faraday Trans.* **72**, 557.

- Newman, L., Klotz, P., 1972. *Inorg. Chem.* **11**, 2150.
- Nieminen, M., Lehto, S., Niinistö, L., 2001a. *J. Mater. Chem.* **11**, 3148.
- Nieminen, M., Putkonen, M., Niinistö, L., 2001b. *Appl. Surface Sci.* **174**, 155.
- Niinistö, L., 1997. *Annali di Chimica* **87**, 221.
- Niinistö, L., 1998. *Curr. Opin. Solid State Mater. Sci.* **3**, 147.
- Niinistö, L., Ritala, M., Leskelä, M., 1996. *Mater. Sci. Eng. B* **41**, 23.
- Noro, J., Sekine, T., 1993a. *Bull. Chem. Soc. Jpn.* **66**, 804.
- Noro, J., Sekine, T., 1993b. *J. Alloys Compds* **192**, 132.
- Noro, J., Sekine, T., 1992. *Bull. Chem. Soc. Jpn.* **65**, 1910.
- Noto, M., Irie, K., Era, M., 2001. *Chem. Lett.*, 320.
- Offermann, W., Mannschreck, A., 1981. *Tetrahedron Lett.* **22**, 3227.
- Ohmori, Y., Ueta, H., Kurosaka, Y., Hamada, Y., Yoshino, K., 1998. *Jpn. J. Appl. Phys.* **37**, L798.
- Ohmori, T., Kajii, H., Sawatani, T., Ueta, H., Yoshino, K., 2001. *Thin Solid Films* **393**, 407.
- Ohta, K., Akimoto, H., Fujimoto, T., Yamamoto, I., 1994. *J. Mater. Chem.* **4**, 61.
- Ohta, K., Yokoyama, M., Kusabayashi, S., Mikawa, H., 1981. *Mol. Cryst. Liq. Cryst.* **69**, 131.
- Oka, T., Fujiwara, K., Murai, A., 1997. *Tetrahedron Lett.* **38**, 8053.
- Oka, T., Fujiwara, K., Murai, A., 1998. *Tetrahedron* **54**, 21.
- Okada, K., Wang, Y.F., Chen, T.M., Kitamura, M., Nakaya, T., Inoue, H., 1999. *J. Mater. Chem.* **9**, 3023.
- Onuma, S., Onoue, H., Shibata, S., 1976. *Bull. Chem. Soc. Jpn.* **49**, 644.
- Ostakhov, S.S., Voloshin, A.I., Kazakov, V.P., Khusainiova, I.A., 1997. *Chem. Phys. Rep.* **16**, 101.
- Ostakhov, S.S., Voloshin, A.I., Kazakov, V.P., Shavaleev, N.M., 1998. *Russian Chem. Bull.* **47**, 1466.
- Otway, D.J., Obi, B., Rees Jr., W.S., 1997. *J. Alloys Compds* **251**, 254.
- Ozawa, T., 1991. *Thermochimica Acta* **174**, 185.
- Pagnot, T., Audebert, P., Tribillon, G., 2000. *Chem. Phys. Lett.* **322**, 572.
- Päiväsääri, A., Putkonen, M., Niinistö, L., 2002. *J. Mater. Chem.* **12**, 1828.
- Pan, M., Meng, G.Y., Xin, H.W., Chen, C.S., Peng, D.K., Lin, Y.S., 1998a. *Thin Solid Films* **324**, 89.
- Pan, M., Meng, G.Y., Chen, C.S., Peng, D.K., Lin, Y.S., 1998b. *Mater. Lett.* **36**, 44.
- Panson, A.J., Charles, R.G., Schmidt, D.N., Szedon, J.R., Machiko, G.J., Braginski, A.I., 1989. *Appl. Phys. Lett.* **53**, 1756.
- Park, J.D., Brown, H.A., Lacher, J.R., 1953. *J. Am. Chem. Soc.* **75**, 4753.
- Parra, D.F., Brito, H.F., Do Rosario Matos, J., Dias, L.C., 2002. *J. Appl. Polym. Sci.* **83**, 2716.
- Parra, D.F., Mucciolo, A., Brito, H.F., 2004. *J. Appl. Polymer Sci.* **94**, 865.
- Paskevich, K.I., Saloutin, V.I., Postovskii, I.Ya., 1981. *Russian Chem. Rev.* **50**, 180 [*Usp. Khim.* **50**, 325].
- Pavier, M.A., Richardson, T., Searle, T.M., Huang, C.H., Li, H., Zhou, D., 1997. *Supramol. Sci.* **4**, 437.
- Pei, J., Liu, X.L., Yu, W.L., Lai, Y.H., Niu, Y.H., Cao, Y., 2002. *Macromolecules* **35**, 7274.
- Peters, J.A., Schuyl, P.J.W., Bovée, W.M.M.J., Alberts, J.H., Van Bekkum, H., 1981. *J. Org. Chem.* **46**, 2784.
- Peters, J.A., Schuyl, P.J.W., Knol-Kalkman, A.H., 1982. *Tetrahedron Lett.* **23**, 4497.
- Peters, J.A., Huskens, J., Raber, D.J., 1996. *Prog. Nucl. Magn. Reson. Spectrosc.* **28**, 283.
- Peterson Jr., M.R., Wahl Jr., H.W., 1972. *J. Chem. Educ.* **49**, 790.
- Petrov, V.A., Marshall, W.J., Grushin, V.V., 2002. *Chem. Comm.*, 520.
- Philips, T., Sands, D.E., Wagner, W.F., 1968. *Inorg. Chem.* **7**, 2295.
- Picker, J.E., Sievers, R.E., 1981. *J. Chromatography* **203**, 29.
- Pinchas, S., Silver, B.L., Laulich, I., 1967. *J. Chem. Phys.* **46**, 1506.
- Plakatouras, J.C., Baxter, I., Hursthouse, M.B., Malik, K.M.A., McAleese, J., Drake, S.R., 1994. *Chem. Comm.*, 2455.
- Pohl, L., 1971. *Merck Kontakte* **1**, 17.
- Polyakov, O.V., Badalyan, A.M., Belyi, V.I., 2000. *Chemistry for Sustainable Development* **8**, 255.
- Poncellet, O., Hubert-Pfalzgraf, L.G., 1989. *Polyhedron* **8**, 2183.
- Poskanzer, A.M., Foreman, B.M., 1961. *J. Inorg. Nucl. Chem.* **16**, 323.
- Przystal, J.K., Bos, W.G., Liss, I.B., 1971. *J. Inorg. Nucl. Chem.* **33**, 679.
- Purushottam, D., Ramachandra Rao, V., Raghava Rao, Bh.S.V., 1965. *Indian J. Chem.* **33**, 182.
- Purushottam, D., Raghava Rao, Bh.S.V., 1966. *Indian J. Chem.* **4**, 109.
- Putkonen, M., Nieminen, M., Niinistö, J., Niinistö, L., 2001a. *Chem. Mater.* **13**, 4701.
- Putkonen, M., Sajavaara, T., Johansson, L.-S., Niinistö, L., 2001b. *Chem. Vap. Deposition* **7**, 44.
- Putkonen, M., Sajavaara, T., Niinistö, J., Johansson, L.-S., Niinistö, L., 2002. *J. Mater. Chem.* **12**, 442.

- Pyo, S.W., Lee, M.H., Lee, H.S., Kim, J.S., Kim, Y.K., Hoe, H.S., Lee, S.H., 1999. *J. Korean Phys. Soc.* **35**, S173.
- Pyo, S.W., Lee, S.P., Lee, H.S., Kwon, O.K., Hoe, H.S., Lee, S.H., Ha, Y.K., Kim, Y.K., Kim, J.S., 2000. *Thin Solid Films* **363**, 232.
- Qian, G.D., Wang, M.Q., 2001. *Mater. Res. Bull.* **36**, 2289.
- Qian, D.J., Nakahara, H., Fukuda, K., Yang, K.Z., 1995. *Chem. Lett.*, 175.
- Qian, G.D., Wang, M.Q., Yang, Z., 2001. *J. Non-Cryst. Solids* **286**, 235.
- Qian, G.D., Wang, M.Q., Yang, Z., 2002a. *J. Phys. Chem. Solids* **63**, 1829.
- Qian, G.D., Yang, Z., Wang, M.Q., 2002b. *J. Non-Cryst. Solids* **96**, 211.
- Raber, D.J., Hajek, M., 1986. *Magn. Reson. Chem.* **24**, 297.
- Raber, D.J., Johnston Jr., M.D., Janks, C.M., Perry, J.W., Jackson III, G.F., 1980. *Org. Magn. Reson.* **14**, 32.
- Ramade, I., Kahn, O., Jeannin, Y., Robert, F., 1997. *Inorg. Chem.* **36**, 930.
- Ramkumar, J., Unnikrishnan, E.K., Maiti, B., Mathur, P.K., 1998. *J. Membrane Sci.* **141**, 283.
- Rappoli, B.J., DeSisto, W.J., 1996. *Appl. Phys. Lett.* **68**, 2726.
- Reid, J.C., Calvin, M., 1950. *J. Am. Chem. Soc.* **72**, 2948.
- Reisfeld, R., Saraidarov, T., Pietraszkiewicz, M., Lis, S., 2001. *Chem. Phys. Lett.* **349**, 266.
- Reuben, J., Elgavish, G.A., 1979. Shift reagents and NMR of paramagnetic lanthanide complexes. In: Gschneidner Jr., K.A., Eyring, L. (Eds.), *Handbook on the Physics and Chemistry of Rare Earths*, vol. 4. North-Holland, Amsterdam, p. 483.
- Reuben, J., 1975a. *Prog. Nucl. Magn. Reson. Spectrosc.* **9**, 1.
- Reuben, J., 1975b. *Naturwiss.* **62**, 172.
- Reuben, J., Leigh Jr., J.S., 1972. *J. Am. Chem. Soc.* **94**, 2789.
- Reyes, R., Hering, E.N., Cremona, M., da Silva, C.F.B., Brito, H.F., Achete, C.A., 2002. *Thin Solid Films* **420–421**, 23.
- Reyes, R., Cremona, M., Teotonio, E.E.S., Brito, H.F., Malta, O.L., 2004. *Chem. Phys. Lett.* **396**, 54.
- Rheingold, A.M., King, W., 1989. *Inorg. Chem.* **28**, 1715.
- Richards, B.C., Cook, S.L., Pinch, D.L., Andrews, G.W., Lengeling, G., Schulte, B., Jürgensen, H., Shen, Y.Q., Vase, P., Freltoft, T., Spee, C.I.M.A., Linden, J.L., Hitchman, M.L., Shamlan, S.H., Brown, A., 1995. *Physica C* **252**, 229.
- Richardson, F.S., Brittain, H.G., 1981. *J. Am. Chem. Soc.* **103**, 18.
- Richardson, M.F., Sievers, R.E., 1971. *Inorg. Chem.* **10**, 498.
- Richardson, F.S., Riehl, J.P., 1977. *Chem. Rev.* **77**, 773.
- Richardson, M.M., Wagner, W.F., Sands, D.E., 1968. *J. Inorg. Nucl. Chem.* **30**, 1275.
- Richter, M.M., Bard, A.J., 1996. *Anal. Chem.* **68**, 2641.
- Riehl, J.P., Richardson, F.S., 1976. *J. Chem. Phys.* **65**, 1011.
- Riehl, J.P., Richardson, F.S., 1977. *J. Chem. Phys.* **66**, 1988.
- Rikken, G.L.J.A., Raupach, E., 1997. *Nature* **390**, 493.
- Robards, K., Patsalides, E., Dilli, S., 1987. *J. Chromatography* **411**, 1.
- Robards, K., Clarke, S., Patsalides, E., 1988. *Analyst* **113**, 1757.
- Robinson, M.R., O'Regan, M.B., Bazan, G.C., 2000. *Chem. Comm.*, 1645.
- Rocha, G.B., Freire, R.O., da Costa, N.B., de Sá, G.F., Simas, A.M., 2004. *Inorg. Chem.* **43**, 2346.
- Rondeau, R.E., Sievers, R.E., 1971. *J. Am. Chem. Soc.* **93**, 1522.
- Ross, D.L., Blanc, J., 1967. *Adv. Chem. Ser.* **71**, 155.
- Rothchild, R., 1989. *J. Chem. Educ.* **66**, 814.
- Roy, A., Nag, K., 1978. *J. Inorg. Nucl. Chem.* **40**, 331.
- Ruano, J.L.G., Gutiérrez, L.G., Castro, A.M.M., Yuste, F., 2002. *Tetrahedron: Asymm.* **13**, 2003.
- Rusakova, N.V., Topilova, Z.M., Meshkova, S.B., Lozinskii, M.O., Gevaza, Yu.I., 1992. *Zh. Neorg. Khim.* **37**, 116.
- Ryazanov, M., Nikiforov, V., Lloret, F., Julve, M., Kuzmina, N., Gleizes, A., 2002. *Inorg. Chem.* **41**, 1816.
- Sá Ferreira, R.A., Carlos, L.D., Gonçalves, R.R., Ribeiro, S.J.L., de Zea Bermudez, V., 2001. *Chem. Mater.* **13**, 2991.
- Sabbatini, N., Guardigli, M., Lehn, J.M., 1993. *Coord. Chem. Rev.* **123**, 201.
- Sabbatini, N., Guardigli, M., Manet, I., 1996. Antenna effect in encapsulation complexes of lanthanide ions. In: Gschneidner Jr., K.A., Eyring, L. (Eds.), *Handbook on the Physics and Chemistry of Rare Earths*, vol. 23. North-Holland, Amsterdam, p. 69.
- Sacconi, L., Ercoli, R., 1949. *Gazz. Chim. Ital.* **79**, 731.
- Sage, I., Bourhill, G., 2001. *J. Mater. Chem.* **11**, 231.
- Sage, I., Badcock, R., Humberstone, L., Geddes, N., Kemp, M., Bourhill, G., 1999a. *Smart. Mater. Struct.* **8**, 504.
- Sage, I., Badcock, R., Humberstone, L., Geddes, N., Kemp, M., Bishop, S., Bourhill, G., 1999b. *SPIE* **3675**, 169.

- Sager, W.F., Filipescu, N., Serafin, F.A., 1965. *J. Phys. Chem.* **69**, 1092.
- Saitoh, T., Suzuki, T., Onodera, N., Sekiguchi, H., Hagiwara, H., Hoshi, T., 2003a. *Tetrahedron Lett.* **44**, 2709.
- Saitoh, T., Suzuki, T., Sugimoto, M., Hagiwara, H., Hoshi, T., 2003b. *Tetrahedron Lett.* **44**, 3175.
- Samelson, H., Brecher, C., Lempicki, A., 1967. *J. Chim. Phys.* **64**, 165.
- Samelson, H., Lempicki, A., Brophy, V.A., Brecher, C., 1964a. *J. Chem. Phys.* **40**, 2547.
- Samelson, H., Lempicki, A., Brecher, C., 1964b. *J. Chem. Phys.* **40**, 2553.
- Samelson, H., Lempicki, A., Brecher, C., Brophy, V.A., 1964c. *Appl. Phys. Lett.* **5**, 173.
- Samelson, H., Brecher, C., Lempicki, A., 1966. *J. Molec. Spectrosc.* **19**, 349.
- Sanchez, C., Ribot, F., 1994. *New J. Chem.* **18**, 1007.
- Sanders, J.K.M., Williams, D.H., 1970. *Chem. Comm.*, 422.
- Sanders, J.K.M., Williams, D.H., 1971. *J. Am. Chem. Soc.* **93**, 641.
- Sankhla, B.S., Kapoor, R.N., 1966. *Can. J. Chem.* **44**, 1369.
- Sano, T., Fujita, M., Fuji, T., Hamada, Y., Shibata, K., Kuroki, K., 1995. *Jpn. J. Appl. Phys.* **34**, 1883.
- Santos Jr., L.S., Roca, S., Airoldi, C., 1997. *J. Chem. Thermodynamics* **29**, 661.
- Sasaki, M., Horiuchi, H., Kumagai, M., Sakamoto, M., Sakiyama, H., Nishida, Y., Sadaoka, Y., Ohba, M., Okawa, H., 1998. *Chem. Lett.*, 911.
- Sasaki, M., Manseki, K., Horiuchi, H., Kumagai, M., Sakamoto, M., Sakiyama, H., Nishida, Y., Saki, M., Sadaoka, Y., Ohba, M., Okawa, H., 2000. *J. Chem. Soc., Dalton Trans.*, 259.
- Sasaki, Y., Freiser, H., 1983. *Inorg. Chem.* **22**, 2289.
- Sasayama, K., Umetani, S., Matsui, M., 1983. *Anal. Chim. Acta* **149**, 253.
- Sato, S., Wada, M., 1970. *Bull. Chem. Soc. Jpn.* **43**, 1955.
- Sato, Y., Takahashi, N., Sato, S., 1998. *Jpn. J. Appl. Phys.* **37**, L129.
- Schimitschek, E.J., 1963. *Appl. Phys. Lett.* **3**, 117.
- Schimitschek, E.J., Nehring, R.B., 1964. *J. Appl. Phys.* **35**, 2786.
- Schimitschek, E.J., Schwarz, E.G.K., 1962. *Nature* **196**, 832.
- Schimitschek, E.J., Trias, J.A., Nehring, R.B., 1965a. *J. Appl. Phys.* **36**, 867.
- Schimitschek, E.J., Nehring, R.B., Trias, J.A., 1965b. *J. Chem. Phys.* **42**, 788.
- Schimitschek, E.J., Nehring, R.B., Trias, J.A., 1966. *Appl. Phys. Lett.* **9**, 103.
- Schimitschek, E.J., Nehring, R.N., Trias, J.A., 1967. *J. Chim. Phys.* **64**, 173.
- Schimitschek, E.J., Nehring, R.B., Trias, J.A., 1969. US Patent 3,450,641.
- Schreiner, R., Testen, M.E., Skhashiri, B.Z., Dirreen, G.E., Williams, L.G., 1983. In: Shkhashiri, B.Z. (Ed.), *Chemical Demonstrations: A Handbook for Teachers of Chemistry*, vol. 1. The University of Wisconsin Press, Madison, pp. 125–204.
- Schuster, G.B., Turro, N.J., Steinmetzer, H.-C., Schaap, A.P., Faler, G., Adam, W., Liu, J.C., 1975. *J. Am. Chem. Soc.* **97**, 7110.
- Schuurmans, F.J.P., Lagendijk, A., 2000. *J. Chem. Phys.* **113**, 3310.
- Scribner, W.G., Kotecki, A.M., 1965. *Anal. Chem.* **37**, 1304.
- Seim, H., Nieminen, M., Niinistö, L., Fjellvåg, H., Johansson, L.-S., 1997. *Appl. Surface Sci.* **112**, 243.
- Seitz, R., 1969. US Patent 3,477,037.
- Selbin, J., Ahmad, N., Bhacca, N., 1971. *Inorg. Chem.* **10**, 1383.
- Sendor, D., Kynast, U., 2002. *Adv. Mater.* **14**, 1570.
- Serpone, N., Ishayek, R., 1971. *Inorg. Chem.* **10**, 2650.
- Serra, O.A., Nasser, E.J., Kodaira, C.A., Neri, C.R., Cazlefi, P.S., Rosa, I.L.V., 1998a. *Spectrochim. Acta* **A54**, 2077.
- Serra, O.A., Nasser, E.J., Calefi, P.S., Rosa, I.L.V., 1998b. *J. Alloys Comps* **275–277**, 838.
- Serra, O.A., Rosa, I.L.V., Medeiros, C.L., Zaniquelli, M.E.D., 1994. *J. Lumin.* **60–61**, 112.
- Serrano, J.L. (Ed.), 1996. *Metallomesogens, Synthesis, Properties and Applications*. VHC, Weinheim.
- Sevchenko, A.N., Trifimov, A.K., 1951. *J. Exp. Theor. Phys.* **21**, 220.
- Shapiro, B.L., Johnston Jr., M.D., 1972. *J. Am. Chem. Soc.* **94**, 8185.
- Sharipov, G.L., Voloshin, A.I., Kazakov, V.P., Tolstikov, G.A., 1990. *Dokl. Akad. Nauk SSSR* **315**, 425.
- Shavaleev, N.M., Moorcraft, L.P., Pope, S.J.A., Bell, Z.R., Faulkner, S., Ward, M.D., 2003a. *Chem. Comm.*, 1134.
- Shavaleev, N.M.M., Bell, Z.R., Accorsi, G., Ward, M.D., 2003b. *Inorg. Chim. Acta* **351**, 159.
- Shavaleev, N.M., Pope, S.J.A., Bell, Z.R., Faulkner, S., Ward, M.D., 2003c. *Dalton Trans.*, 808.
- Shavaleev, N.M., Bell, Z.R., Ward, M.D., 2002. *Dalton Trans.*, 3925.
- Shen, C., Fan, Y.G., Wang, Y.T., Liu, G.F., Lu, P.Z., 1983a. *Jilin Daxue Ziran Kex. Xue. (Chin.) (Acta Sci. Nat. Univ. Jil.)*, 103.

- Shen, C., Fan, Y.G., Wang, Y.T., Liu, G.F., Lu, P.Z., 1983b. *Gaodeng Xuexiao Huaxue Xuebao* (Chin.) (Chem. J. Chin. Univ.) **4**, 769.
- Shen, C., Fan, Y.G., Wang, Y.T., Liu, G.F., Weng, G.F., 1984. *Jilin Daxue Ziran Kex. Xue.* (Chin.) (Acta Sci. Nat. Univ. Jil.), 99.
- Shen, Z.Q., Ouyang, J., 1987. Rare earth coordination catalysts in stereospecific polymerization. In: Gschneidner Jr., K.A., Eyring, L. (Eds.), *Handbook on the Physics and Chemistry of Rare Earths*, vol. **9**. North-Holland, Amsterdam, p. 395.
- Shepherd, T.M., 1966. *Nature* **5063**, 745.
- Shepherd, T.M., 1967. *J. Phys. Chem.* **71**, 4137.
- Shibata, S., Iijima, K., Kimura, S., 1985. *J. Mol. Struct.* **131**, 113.
- Shibata, S., Iijima, K., Inuzuka, T., 1986a. *J. Mol. Struct.* **140**, 65.
- Shibata, S., Iijima, K., Inuzuka, T., 1986b. *J. Mol. Struct.* **144**, 181.
- Shibata, S., Iijima, K., Inuzuka, T., Kimura, S., Sato, T., 1986c. *J. Mol. Struct.* **144**, 351.
- Shigematsu, T., Tabushi, M., Matsui, M., Honjyo, T., 1966. *Bull. Chem. Soc. Jpn.* **39**, 165.
- Shigematsu, T., Tabushi, M., Matsui, M., Honjyo, T., 1967. *Bull. Chem. Soc. Jpn.* **40**, 2807.
- Shigematsu, T., Matsui, M., Utsunomiya, K., 1969a. *Bull. Chem. Soc. Jpn.* **42**, 1278.
- Shigematsu, T., Tabushi, M., Matsui, M., Honjyo, T., 1969b. *Bull. Chem. Soc. Jpn.* **42**, 976.
- Shigematsu, T., Honjyo, T., Tabushi, M., Matsui, M., 1970. *Bull. Chem. Soc. Jpn.* **43**, 793.
- Shull, B.K., Sakai, T., Koreeda, M., 1996. *J. Am. Chem. Soc.* **118**, 11690.
- Si, Z.K., Zhu, G.Y., Li, J., 1991. *Analyst* **116**, 309.
- Sicre, J.E., Dubois, J.T., Eisentraut, K.J., Sievers, R.E., 1969. *J. Am. Chem. Soc.* **91**, 3476.
- Sieck, R.F., Banks, C.V., 1972. *Anal. Chem.* **44**, 2307.
- Sievers, R.E., 1980. US Patent 4,206,132.
- Sievers, R.E., Sadlowski, J.E., 1978. *Science* **201**, 217.
- Sievers, R.E., Wenzel, T.J., 1981. US Patent 4,251,233.
- Sievers, R.E. (Ed.), 1973. *Nuclear Magnetic Shift Reagents*. Academic Press, New York.
- Sievers, R.E., Brooks, J.J., Cunningham, J.A., Rhine, W.E., 1976. *Adv. Chem. Ser.* **150**, 222.
- Sigoli, F.A., Brito, H.F., Jafelicci Jr., M., Davalos, M.R., 2001. *Int. J. Inorg. Mater.* **3**, 755.
- Sita, M., Rao, T.P., Lyer, C.S.P., Damodaran, A.D., 1997. *Talanta* **44**, 423.
- Slonim, I.Y., Bulai, A.K., 1973. *Russ. Chem. Rev.* **42**, 904.
- Smith, W.B., 1981. *Org. Magn. Reson.* **17**, 124.
- Soini, E., Lovgren, T., 1987. *CRC Crit. Rev. Anal. Chem.* **18**, 105.
- Sokolov, D.N., 1988. *Usp. Khim.* **57**, 1670.
- Song, H.Z., Wang, H.B., Zhang, J., Peng, D.K., Meng, G.Y., 2002. *Mater. Res. Bull.* **37**, 1487.
- Song, H.Z., Jiang, Y.Z., Xia, C.G., Meng, G.Y., Peng, D.K., 2003a. *J. Cryst. Growth* **250**, 423.
- Song, H.Z., Wang, H.B., Zha, S.W., Peng, D.K., Meng, G.Y., 2003b. *Solid State Ionics* **156**, 249.
- Spitsyn, V.I., Muraveva, I.A., Martynenko, L.L., Sokolov, D.N., Golubtsova, V.I., 1982. *Zh. Neorg. Khim.* **27**, 853.
- Springer Jr., C.S., Meek, D.W., Sievers, R.E., 1967. *Inorg. Chem.* **6**, 1105.
- Spyroulias, G.A., Sioubara, M.P., Coutsolelos, A.G., 1995. *Polyhedron* **14**, 3563.
- Srdanov, V.I., Robinson, M.R., Bu, X., Bazan, G.C., 2002. *Appl. Phys. Lett.* **80**, 3042.
- Steffen, W.L., Fay, R.C., 1978. *Inorg. Chem.* **17**, 779.
- Stolzenberg, G.E., Zayskie, R.G., Olson, P.A., 1971. *Anal. Chem.* **43**, 908.
- Strek, W., Sokolnicki, J., Legendziewicz, J., Maruszewski, K., Reisfeld, R., Pavich, T., 1999. *Opt. Mater.* **13**, 41.
- Sugimoto, H., Higashi, T., Maeda, A., Mori, M., Masuda, H., Taga, T., 1983. *Chem. Comm.*, 1234.
- Sullivan, G.R., 1978. *Top. Stereochem.* **10**, 287.
- Sun, P.P., Duan, J.P., Shih, H.T., Cheng, C.H., 2002. *Appl. Phys. Lett.* **81**, 792.
- Sun, R.G., Wang, Y.Z., Zheng, Q.B., Zhang, H.J., Epstein, A.J., 2000. *J. Appl. Phys.* **87**, 7589.
- Suntola, T., 1989. *Mater. Sci. Rep.* **4**, 261.
- Suntola, T., Antson, J., 1977. US Patent 4,058,430.
- Sweet, T.R., Parlett, H.W., 1968. *Anal. Chem.* **40**, 1885.
- Sweeting, L.M., 2001. *Chem. Mater.* **13**, 854.
- Sweeting, L.M., Rheingold, A.L., 1987. *J. Am. Chem. Soc.* **109**, 2652.
- Sweeting, L.M., Cashel, M.L., Rosenblatt, M.M., 1992. *J. Lumin.* **52**, 281.
- Szejtli, J., 1998. *Chem. Rev.* **98**, 1743.
- Szyczewski, A., Krzyminiwski, R., Lis, S., Pietrzak, J., Elbanowski, M., 1995. *Radiat. Phys. Chem.* **45**, 935.
- Takada, N., Tsutsui, T., Saito, S., 1994. *Jpn. J. Appl. Phys.* **33**, 863.
- Takada, N., Sugiyama, J., Katoh, R., Minami, N., Hieda, S., 1997. *Synth. Met.* **91**, 351.
- Takada, N., Hieda, S., Sugiyama, J., Katoh, R., Minami, N., 2000. *Synth. Met.* **111–112**, 587.
- Takada, N., Peng, J., Minami, N., 2001. *Synth. Met.* **121**, 1745.
- Taketatsu, T., 1981. *Chem. Lett.*, 1057.
- Taketatsu, T., Sato, A., 1979. *Anal. Chim. Acta* **108**, 429.

- Tamura, O., Mita, N., Gotanda, K., Yamada, K., Nakano, T., Katagiri, R., Sakamoto, M., 1999. *Heterocycles* **46**, 95.
- Tang, B., Jin, L.P., Zheng, X.J., Zhu, L.Y., 1999a. *Spectrochim. Acta A* **55**, 1731.
- Tang, B., Jin, L.P., Zheng, X.J., Yang, M.S., 1999b. *J. Appl. Polymer Sci.* **74**, 2588.
- Tang, C.W., Van Slyke, S.A., 1987. *Appl. Phys. Lett.* **51**, 913.
- Taniguchi, H., Tomisawa, H., Kido, J., 1995a. *Appl. Phys. Lett.* **66**, 1578.
- Taniguchi, H., Kido, J., Nishiyama, M., Sasaki, S., 1995b. *Appl. Phys. Lett.* **67**, 1060.
- Tasaki, Y., Satoh, M., Yoshizawa, S., Kataoka, H., Hikada, H., 1997. *Jpn. J. Appl. Phys.* **36**, 6871.
- Terada, M., Gu, J.H., Deka, D.C., Mikami, K., Nakai, T., 1992. *Chem. Lett.*, 29.
- Terada, M., Naki, T., Mikami, K., 1994. *Inorg. Chim. Acta* **222**, 377.
- Thomas, O., Hudner, J., Östling, M., Mossang, E., Chenevier, B., Weiss, F., Boursier, D., Senateur, J.P., 1993. *J. Alloys Compds* **195**, 287.
- Thompson, L.C., 1979. Complexes. In: Gschneidner Jr., K.A., Eyring, L. (Eds.), *Handbook on the Physics and Chemistry of Rare Earths*, vol. **3**. North-Holland, Amsterdam, p. 209.
- Thompson, L.C., Berry, S., 2001. *J. Alloys Compds* **323–324**, 177.
- Thompson, L.C., Kuo, S.C., 1988. *Inorg. Chim. Acta* **149**, 305.
- Thompson, L.C., Atchison, F.W., Young Jr., V.G., 1998. *J. Alloys Compds* **265/268**, 765.
- Thompson, L., Legendziewicz, J., Cybinska, J., Pan, L., Brennessel, W., 2002. *J. Alloys Compds* **341**, 312.
- Tiitta, M., Niinistö, L., 1997. *Chem. Vap. Deposition* **3**, 167.
- Timmer, K., Cook, S.L., Spee, C., 1998. US Patent 5,837,321.
- Titze, H., 1969. *Acta Chem. Scand.* **23**, 399.
- Titze, H., 1974. *Acta Chem. Scand.* **A28**, 1079.
- Tobita, S., Arakawa, M., Tanaka, I., 1984. *J. Phys. Chem.* **88**, 2697.
- Tobita, S., Arakawa, M., Tanaka, I., 1985. *J. Phys. Chem.* **89**, 5649.
- Topilova, Z.M., Rusakova, N.V., Meshkova, S.B., Lozinskii, M.O., Kudryavtseva, L.S., Kononenko, L.I., 1991. *Zh. Anal. Khim.* **46**, 863.
- Topilova, Z.M., Meshkova, S.B., Bol'shoi, D.V., Lozinskii, M.O., Shapiro, Yu.E., 1997. *Zh. Neorg. Khim.* **42**, 99.
- Trost, B.M., Bodanowicz, M., 1973a. *J. Am. Chem. Soc.* **95**, 2038.
- Trost, B.M., Bodanowicz, M., 1973b. *J. Am. Chem. Soc.* **95**, 5321.
- Trzaska, S.T., Zheng, H.X., Swager, T.M., 1999. *Chem. Mater.* **11**, 130.
- Tsaplev, Yu.B., 1997. *Zh. Fiz. Khim.* **71**, 730.
- Tsaryuk, V.I., Zolin, V.F., Kudryashova, A.A., 1997. *Synth. Met.* **91**, 357.
- Tsaryuk, V., Zolin, V., Legendziewicz, J., 1998. *Spectrochim. Acta* **A54**, 2247.
- Tsaryuk, V., Legendziewicz, J., Puntus, L., Zolin, V., Sokolnicki, J., 2000. *J. Alloys Compds* **300/301**, 464.
- Tsaryuk, V., Zolin, V., Legendziewicz, J., Sokolnicki, J., Kudryashova, V., 2002. In: Neyts, K., De Visschere, D., Poelman, P. (Eds.), *Proceedings of the 11th International Workshop on Inorganic Electroluminescence and the 2002 International Conference on the Science and Technology of Emissive Displays and Lighting (Ghent, Belgium, 23–26 September 2002)*. Ghent University, Belgium, p. 165.
- Tsaryuk, V., Zolin, V., Legendziewicz, J., 2003. *J. Lumin.* **102/103**, 744.
- Tsukube, H., Shinoda, S., 2002. *Chem. Rev.* **102**, 2389.
- Tsukube, H., Takeishi, H., Yoshida, Z., 1996a. *Inorg. Chim. Acta* **251**, 1.
- Tsukube, H., Uenishi, J., Shiba, H., Yonemitsu, O., 1996b. *J. Membrane Sci.* **114**, 187.
- Tsukube, H., Shinoda, S., Uenishi, J., Shiode, M., Yonemitsu, O., 1996c. *Chem. Lett.*, 969.
- Tsukube, H., Shinoda, S., Uenishi, J., Kanatani, T., Itoh, H., Shiode, M., Iwachido, T., Yonemitsu, O., 1998. *Inorg. Chem.* **37**, 1585.
- Tsukube, H., Hosokubo, M., Wada, M., Shinoda, S., Tamiaki, H., 2001. *Inorg. Chem.* **40**, 740.
- Tsukube, H., Shinoda, S., Tamiaki, H., 2002. *Coord. Chem. Rev.* **226**, 227.
- Ueba, Y., Banks, E., Okamoto, Y., 1980. *J. Appl. Polym. Sci.* **25**, 2007.
- Uhlemann, E., Dietze, F., 1971. *Z. Anorg. Allgem. Chem.* **386**, 329.
- Umetani, S., Freiser, H., 1987. *Inorg. Chem.* **26**, 3179.
- Umetani, S., Kawase, Y., Le, Q.T.H., Matsui, M., 2000. *J. Chem. Soc., Dalton Trans.*, 2787.
- Umitani, S., Matsui, M., Toei, J., Tsunenobu, T., 1980. *Anal. Chim. Acta* **113**, 315.
- Urbain, G., 1897. *Comp. Rend.* **124**, 618.
- Urs, U.K., Shalini, K., Cameron, T.S., Shivashankar, S.A., Guru Row, T.N., 2001. *Acta Cryst.* **E57**, m457.
- Utsunomiya, K., 1972. *Anal. Chim. Acta* **59**, 147.
- Utsunomiya, K., Shigematsu, T., 1972. *Anal. Chim. Acta* **58**, 411.
- Vallarino, L.M., 1997. *J. Alloys Compds* **249**, 69.

- van Bekkum, H., Flanigen, E.M., Jansen, J.C. (Eds.), 1991. Introduction to Zeolite Science and Practice. Elsevier, Amsterdam.
- Vancoppemolle, A., Declercq, J.P., Van Meerssche, M., 1983. *Eur. Cryst. Meeting* **8**, 193.
- Van Deun, R., Moors, D., De Fré, B., Binnemans, K., 2003. *J. Mater. Chem.* **123**, 1520.
- Van Meervelt, L., Froyen, A., D'Olieslager, W., Walrand-Görller, C., Drisque, I., King, G.S.D., Maes, S., Lenstra, A.T.H., 1996. *Bull. Soc. Chim. Belg.* **105**, 377.
- Van Staveren, D.R., Haasnoot, J.G., Manotti Lanfredi, A.M., Menzer, S., Nieuwenhuizen, P.J., Spek, A.L., Ugozzoli, F., Weyhermüller, T., Reedijk, J., 2000. *Inorg. Chim. Acta* **307**, 81.
- Van Staveren, D.R., van Albada, G.A., Haasnoot, J.G., Kooijman, H., Manotti Lanfredi, A.M., Nieuwenhuizen, P.J., Spek, A.L., Ugozzoli, F., Weyhermüller, T., Reedijk, J., 2001. *Inorg. Chim. Acta* **315**, 163.
- Verbiest, T., Houbrechts, S., Kauranen, M., Clays, K., Persoons, A., 1997. *J. Mater. Chem.* **7**, 2175.
- Veron, M., Meyer, Y., 1966. *Fr. Patent* 1453474 (C.A. 67 (1967) 16686).
- Villata, L.S., Wolcan, E., Féliz, M.R., Capparelli, A.L., 1999. *J. Phys. Chem. A* **103**, 5661.
- Voloshin, A.I., Shavaleev, N.M., Kazakov, V.P., 2000a. *J. Photochem. Photobiol. A* **131**, 61.
- Voloshin, A.I., Shavaleev, N.M., Kazakov, V.P., 2000b. *J. Photochem. Photobiol. A* **136**, 203.
- Voloshin, A.I., Shavaleev, N.M., Kazakov, V.P., 2000c. *J. Lumin.* **91**, 49.
- Voloshin, A.I., Shavaleev, N.M., Kazakov, V.P., 2000d. *J. Photochem. Photobiol. A* **134**, 111.
- Voloshin, A.I., Shavaleev, N.M., Kazakov, V.P., 2001a. *J. Lumin.* **93**, 191.
- Voloshin, A.I., Shavaleev, N.M., Kazakov, V.P., 2001b. *J. Lumin.* **93**, 199.
- von Ammon, R., Fischer, R.D., 1972. *Angew. Chem. Int. Ed.* **11**, 675 [*Angew. Chem.* **84**, 737].
- Voronov, V.K., 1974. *Russ. Chem. Rev.* **43**, 432.
- Wada, E., Pei, W., Yasuoka, H., Chin, U., Kanemasa, S., 1996. *Tetrahedron* **52**, 1205.
- Wahid, P.F., Sundaram, K.B., Sisk, P.J., 1992. *Opt. Laser Technol.* **24**, 263.
- Wahl, G., Stadel, O., Gorbenco, O., Kaul, A., 2000. *Pure Appl. Chem.* **72**, 2167.
- Walton, A.J., 1977. *Adv. Phys.* **26**, 887.
- Wang, C.P., Venteicher, R.F., Horrocks Jr., W.DeW., 1974. *J. Am. Chem. Soc.* **96**, 7149.
- Wang, J.F., Wang, R.Y., Yang, J., Zheng, Z.P., Carducci, M.D., Cayou, T., Peyghambarian, N., Jabbour, G.E., 2001. *J. Am. Chem. Soc.* **123**, 6179.
- Wang, K.Z., Huang, C.H., Gao, G.Q., Xu, G.X., Cui, D.F., Fan, Y., 1991. *Chem. J. Chin. Univ.* **14**, 150.
- Wang, K.Z., Jiang, W., Huang, C.H., Xu, G.X., Xu, L.G., Li, T.K., Zhao, X.S., Xie, X.M., 1994a. *Chem. Lett.* 1761.
- Wang, K.Z., Huang, C.H., Xu, G.X., Xu, Y., Liu, Y.Q., Zhu, D.B., Zhao, X.S., Xie, X.M., Wu, N.Z., 1994b. *Chem. Mater.* **6**, 1986.
- Wang, M.Z., Jin, L.P., Cai, G.L., Liu, S.X., Huang, J.L., Qin, P.W., Huang, S.H., 1994c. *J. Rare Earths* **12**, 166.
- Wang, K.Z., Wu, N.Z., Huang, C.H., Xu, G.X., Xu, Y., Liu, Y.Q., Zhu, D.B., Liu, L.Y., Wang, W.C., 1995a. *Chem. J. Chinese Univ.* **16**, 1.
- Wang, K.Z., Huang, C.H., Xu, G.X., Zhou, Q.F., 1995b. *Solid State Chem.* **95**, 223.
- Wang, K.Z., Huang, C.H., Xu, G.X., Wang, R.J., 1995c. *Polyhedron* **14**, 23.
- Wang, K.Z., Li, L.J., Liu, W.M., Xue, Z.Q., Huang, C.H., Lin, J.H., 1997. *Mater. Res. Bull.* **31**, 993.
- Wang, H.B., Song, H.Z., Xia, C.R., Peng, D.K., Meng, G.Y., 2000a. *Mater. Res. Bull.* **35**, 2363.
- Wang, L.H., Wang, W., Zhang, W.G., Kang, E.T., Huang, W., 2000b. *Chem. Mater.* **12**, 2212.
- Wang, K.Z., Huang, L., Gao, L.H., Huang, C.H., Jin, L.P., 2002. *Solid State Comm.* **122**, 233.
- Wang, K.Z., Gao, L.H., Huang, C.H., 2003. *J. Photochem. Photobiol. A* **156**, 39.
- Wasson, S.J.C., Sands, D.E., Wagner, W.F., 1973. *Inorg. Chem.* **12**, 187.
- Watson, W.H., Williams, R.J., Stemple, N.R., 1972. *J. Inorg. Nucl. Chem.* **34**, 501.
- Watson, M.M., Zenger, R.P., Yardley, J.T., Stucky, G.D., 1975. *Inorg. Chem.* **14**, 2675.
- Weber, M.J., 1979. Rare earth lasers. In: Gschneidner Jr, K.A., Eyring, L. (Eds.), *Handbook on the Physics and Chemistry of Rare Earths*, vol. **4**. North-Holland, Amsterdam, p. 275.
- Wei, A.Z., Teng, M.K., Dai, J.B., Liang, D.C., 1983. *J. Struct. Chem. (Chinese)* **2**, 237.
- Wei, A.Z., Teng, M.K., Dai, J.B., Liang, D.C., Sun, J.B., 1984. *Zhongguo Kexue Jishu Daxue Xuebao* **14**, 140.
- Weiss, F., Schmatz, U., Pisch, A., Felten, F., Pignard, S., Sénateur, J.P., Abrutis, A., Fröhlich, K., Selbmann, D., Klippe, L., 1997. *J. Alloys Comps* **251**, 264.
- Weissman, S.I., 1942. *J. Chem. Phys.* **10**, 214.
- Wenzel, T.J., 1984. *J. Org. Chem.* **49**, 1834.
- Wenzel, T.J., 1986. In: Morill, A. (Ed.), *Lanthanide Shift Reagents in Stereochemical Analysis*. VCH Publishers, Weinheim, pp. 151–173.

- Wenzel, T.J., 1987. *NMR Shift Reagents*. CRC Press, Boca Raton, Florida.
- Wenzel, T.J., 2000. In: *Encyclopedia of Spectroscopy and Spectrometry*, vol. 1. Academic Press, London, pp. 411–421.
- Wenzel, T.J., Lalonde Jr., D.R., 1983. *J. Org. Chem.* **48**, 1951.
- Wenzel, T.J., Zaia, J., 1985. *J. Org. Chem.* **50**, 1322.
- Wenzel, T.J., Zaia, J., 1987. *Anal. Chem.* **59**, 562.
- Wenzel, T.J., Russett, M.D., 1987. *J. Chem. Educ.* **64**, 979.
- Wenzel, T.J., Sievers, R.E., 1981. *Anal. Chem.* **53**, 393.
- Wenzel, T.J., Sievers, R.E., 1982a. *J. Am. Chem. Soc.* **104**, 382.
- Wenzel, T.J., Sievers, R.E., 1982b. *Anal. Chem.* **54**, 1602.
- Wenzel, T.J., Bettes, T.C., Sadlowski, J.E., Sievers, R.E., 1980. *J. Am. Chem. Soc.* **102**, 5903.
- Wenzel, T.J., Ruggles, A.C., Lalonde Jr., D.R., 1985a. *Magn. Reson. Chem.* **23**, 778.
- Wenzel, T.J., Williams, E.J., Haltiwanger, R.C., Sievers, R.E., 1985b. *Polyhedron* **4**, 369.
- Wenzel, T.J., Williams, E.J., Sievers, R.E., 1985c. *Inorg. Synth.* **23**, 144.
- Werts, M.H.V., Duin, M.A., Hofstraat, H., Verhoeven, J.W., 1999. *Chem. Comm.*, 799.
- Whan, R.E., Crosby, G.A., 1962. *J. Mol. Spectrosc.* **8**, 315.
- White, J.G., 1976. *Inorg. Chim. Acta* **16**, 159.
- Whidesides, G.M., Lewis, D.W., 1970. *J. Am. Chem. Soc.* **92**, 6979.
- Whitesides, G.M., McCreary, M., Lewis, D., 1976. US Patent 3,950,135.
- Whitney, P.S., Uwai, K., Nakagome, H., Takahei, K., 1988. *Appl. Phys. Lett.* **53**, 2074.
- Whittaker, B., 1970. *Nature* **228**, 157.
- Wildes, P.D., White, E.H., 1971. *J. Am. Chem. Soc.* **93**, 6286.
- Wilkinson, D.A., Watkin, J.E., 1993. *Forensic Sci. Int.* **60**, 67.
- Wilkinson, D.A., Misner, A.H., 1994. *J. Forensic Ident.* **44**, 387.
- Williams, D.E., Guyon, J.C., 1971. *Anal. Chem.* **43**, 139.
- Williams, D.H., 1974. *Pure Appl. Chem.* **40**, 25.
- Williams, D.M., Wessels, B.W., 1990. *Appl. Phys. Lett.* **56**, 566.
- Wolff, N.E., Pressley, R.J., 1963. *Appl. Phys. Lett.* **2**, 152.
- Wostyn, K., Binnemans, K., Clays, K., Persoons, A., 2001a. *Rev. Sci. Instr.* **72**, 3215.
- Wostyn, K., Binnemans, K., Clays, K., Persoons, A., 2001b. *J. Phys. Chem. B* **105**, 5169.
- Wu, F.B., Zhang, C., 2002. *Anal. Biochem.* **311**, 57.
- Wu, F.B., Han, S.Q., Zhang, C., He, Y.F., 2002. *Anal. Chem.* **74**, 5882.
- Wu, R.H., Su, Q.D., 2001. *J. Mol. Struct.* **559**, 195.
- Wu, S.L., Yang, Y.S., 1992. *J. Alloys Compds* **180**, 403.
- Wu, S.L., Wu, W.L., Yang, Y.S., 1992a. *J. Alloys Compds* **180**, 391.
- Wu, S.L., Wu, Y.L., Yang, Y.S., 1992b. *J. Alloys Compds* **180**, 399.
- Xia, W.S., Ye, X.Z., Huang, C.H., Gan, L.B., Wang, K.Z., Luo, C.P., 1996. *J. Rare Earths* **14**, 167.
- Xiao, Y.J., Gao, X.X., Huang, C.H., Wang, K.Z., 1994. *Chem. Mater.* **6**, 1910.
- Xiong, R.G., You, X.Z., 2002. *Inorg. Chem. Comm.* **5**, 677.
- Xiong, R.G., Zuo, J.L., Yu, Z., You, X.Z., Chen, W., 1999. *Inorg. Chem. Comm.* **2**, 490.
- Xu, G., Wang, Z.M., He, Z., Lu, Z., Liao, C.S., Yan, C.H., 2002. *Inorg. Chem.* **41**, 6802.
- Xu, J.D., Raymond, K.N., 2000. *Angew. Chem. Int. Ed.* **39**, 2745.
- Xu, Q.H., Li, L.S., Li, B., Yu, J.H., Xu, R.R., 2000. *Microporous Mater.* **38**, 351.
- Xu, Y.Y., Hemmilä, I.A., 1992a. *Anal. Chim. Acta* **256**, 9.
- Xu, Y.Y., Hemmilä, I.A., 1992b. *Talanta* **39**, 759.
- Xu, Y.Y., Hemmilä, I.A., Lövgren, T.N., 1992. *Analyst* **117**, 1061.
- Xu, Z., Daga, A., Chen, H., 2001. *Appl. Phys. Lett.* **79**, 2782.
- Xu, Y.Y., Hemmilä, I., Mukkala, V., Holttinen, S., Lövgren, T., 1991. *Analyst* **116**, 1155.
- Yamaguchi, R., Ito, Y., Sato, Y., Sato, S., 1999. *Mol. Cryst. Liq. Cryst. A* **331**, 2417.
- Yamaguchi, T., Aoki, S., Sadakata, N., Kohno, O., Osanai, H., 1989. *Appl. Phys. Lett.* **55**, 1582.
- Yamaguchi, T., Iijima, Y., Hirano, N., Nagaya, S., Kohno, O., 1994. *Jpn. J. Appl. Phys.* **33**, 6150.
- Yamamoto, H. (Ed.), 2000. *Lewis Acids in Organic Synthesis*. Wiley-VCH, Weinheim.
- Yamane, H., Matsumoto, H., Hirai, T., Iwasaki, H., Watanabe, K., Kobayashi, N., Muto, Y., Kurosawa, H., 1988. *Appl. Phys. Lett.* **53**, 1548.
- Yan, B., 2003. *Mater. Lett.* **57**, 2535.
- Yan, B., You, J.Y., 2002. *J. Rare Earths* **20**, 404.
- Yan, B., Zhang, H.J., Wang, S.B., Ni, J.Z., 1997. *Mater. Chem. Phys.* **51**, 92.
- Yanagida, S., Hasegawa, Y., Wada, Y., 2000. *J. Lumin.* **87–89**, 995.
- Yang, C.Y., Srdanov, V., Robinson, M.R., Bazan, G.C., Heeger, A.J., 2002. *Adv. Mater.* **14**, 980.
- Yang, J., Zhu, G., Wang, H., 1989. *Analyst* **114**, 1417.

- Yang, J., Zhou, H., Ren, X., Li, C., 1990a. *Anal. Chim. Acta* **238**, 307.
- Yang, J., Ren, X., Zou, H., Shi, R., 1990b. *Analyst* **115**, 1505.
- Yang, W., Mo, Z.L., Teng, X.L., Chen, M., Gao, J.Z., Yuan, L., Kang, J.W., Ou, Q.Y., 1998. *Analyst* **123**, 1745.
- Yang, X.C., Brittain, H.G., 1981. *Inorg. Chem.* **20**, 4273.
- Yang, X.D., Ci, Y.Y., Chang, W.B., 1994a. *Anal. Chem.* **66**, 2590.
- Yang, Y.S., Gong, M.L., Li, Y.Y., Lei, H.Y., Wu, S.L., 1994b. *J. Alloys Compds* **207/208**, 112.
- Yang, Y.T., Su, Q.D., Zhao, G.W., 1999. *Spectrochim. Acta* **55**, 1527.
- Yao, Y.F., Zhang, M.S., Shi, J.X., Gong, M.L., Zhang, H.J., Yang, Y.S., 2000. *J. Rare Earths* **18**, 186.
- Yatmirskii, K.B., Davidenko, N.K., 1979. *Coord. Chem. Rev.* **27**, 223.
- Yoshida, H., 1966. *Bull. Chem. Soc. Jpn.* **39**, 1810.
- Yu, G., Liu, Y.Q., Wu, X., Zhu, D.B., Li, H.Y., Jin, L.P., Wang, M.Z., 2000. *Chem. Mater.* **12**, 2537.
- Yu, L.J., Labes, M.M., 1977. *Appl. Phys. Lett.* **31**, 719.
- Yu, X.J., Song, H.Y., Su, Q.D., 2003. *J. Molec. Struct.* **644**, 119.
- Yuan, J., Matsumoto, K., 1997. *J. Pharm. Biomed. Anal.* **15**, 1397.
- Yuan, J., Matsumoto, K., 1998. *Anal. Chem.* **70**, 596.
- Yuan, J., Matsumoto, K., Kimura, H., 1998. *Anal. Chem.* **70**, 596.
- Yuan, J.L., Matsumoto, K., 1996. *Anal. Sci.* **12**, 31.
- Zaitseva, E.G., Baidina, I.A., Stabnikov, P.A., Borisov, S.V., Igumenov, I.K., 1990. *Zh. Strukt. Khim.* **31**, 184.
- Zaitseva, I.G., Kuzmina, N.P., Martynenko, L.I., 1995. *J. Alloys Compds* **225**, 393.
- Zaitseva, I.G., Kuz'mina, N.P., Martynenko, L.I., Makhaev, V.D., Borisov, A.P., 1998. *Russian J. Coord. Chem.* **43**, 728.
- Zaitseva, I.G., Kuz'mina, N.P., Martynenko, L.I., 1999. *Russian J. Coord. Chem.* **25**, 811.
- Zalkin, A., Templeton, D.H., Karraker, D.G., 1969. *Inorg. Chem.* **8**, 2680.
- Zama, H., Tanaka, N., Morishita, T., 2000. *J. Crystal Growth* **221**, 440.
- Zeng, X.R., Xiong, R.G., You, X.Z., Cheung, K.K., 2000. *Inorg. Chem. Comm.* **3**, 341.
- Zhang, R.J., Zheng, S.P., Wang, M.Q., Yang, K.Z., Li, J.B., Hu, J.F., 2001. *Thin Solid Films* **396**, 229.
- Zhang, R.J., Yang, K.Z., 2000. *Thin Solid Films* **371**, 235.
- Zhang, R.J., Yang, K.Z., 2001. *Colloids Surf. A* **178**, 177.
- Zhang, X.M., Sun, R.G., Zheng, Q.B., Kobayashi, T., Li, W.L., 1997a. *Appl. Phys. Lett.* **71**, 2596.
- Zhang, R.J., Liu, H.G., Yang, K.Z., Si, Z.K., Zhu, G.Y., Zhang, H.W., 1997b. *Thin Solid Films* **295**, 228.
- Zhang, R.J., Liu, H.G., Zhang, C.R., Yang, K.Z., Zhu, G.Y., Zhang, H.W., 1997c. *Thin Solid Films* **302**, 223.
- Zhao, D.X., Li, W.L., Hong, Z., Liang, C.J., Zhao, D., Peng, J.B., Liu, X.Y., 1999a. *Jpn. J. Appl. Phys.* **38**, L46.
- Zhao, D., Li, W., Hong, Z., Liu, X., Liang, C., Zhao, D., 1999b. *J. Lumin.* **82**, 105.
- Zhao, D., Hong, X.Z.R., Liang, C.J., Zhao, D., Liu, X.Y., Li, W.L., Lee, C.S., Lee, S.T., 2000. *Thin Solid Films* **363**, 208.
- Zhao, X.S., Xie, X.M., Xia, X.H., Li, H., Wang, K.Z., Huang, C.H., Li, T.K., Xu, L.G., 1995. *Thin Solid Films* **263**, 13.
- Zhao, Y.L., Zhou, D.J., Yao, G.Q., Huang, C.H., 1997. *Langmuir* **13**, 4060.
- Zharkova, Ya.N., Troyanov, S.I., Martynenko, L.I., Dzyubenko, N.G., Chugarov, N.V., 1998. *Koord. Khim.* **24**, 60.
- Zheng, Y.X., Lin, J., Liang, Y.J., Zhou, Y.H., Guo, C., Wang, S.B., Zhang, H.J., 2002a. *J. Alloys Compds* **336**, 114.
- Zheng, Y.X., Lin, J., Liang, Y.J., Lin, Q., Yu, Y.N., Wang, S.B., Guo, C., Zhang, H.J., 2002b. *Opt. Mater.* **20**, 273.
- Zheng, Y.X., Liang, J.Y., Zhang, H.J., Lin, Q., Chuan, G., Wang, S.B., 2002c. *Mater. Lett.* **53**, 52.
- Zheng, Y.X., Lin, J., Liang, Y.J., Lin, Q., Yu, Y.N., Guo, C., Wang, S.B., Zhang, H.J., 2002d. *Mater. Lett.* **54**, 424.
- Zheng, Z.P., Wang, J.F., Liu, H., Carducci, M.D., Peyghambarian, N., Jabbour, G.E., 2002. *Acta Cryst.* **C58**, m50.
- Zhong, G.L., Yang, K.Z., 1998. *Langmuir* **14**, 5502.
- Zhong, G.L., Wang, Y.H., Wang, C.K., Yang, K.Z., 2001. *Thin Solid Films* **385**, 234.
- Zhong, G.L., Kim, K.K., Jin, J.I., 2002. *Synth. Met.* **129**, 193.
- Zhou, D.J., Huiang, C.H., Wang, K.Z., Xu, G.X., Zhao, X.S., Mie, X.M., Xu, L.G., Li, T.K., 1994. *Langmuir* **10**, 1910.
- Zhou, D.J., Huang, C.H., Yao, G.Q., Bai, J., Li, T.K., 1996. *J. Alloys Compds* **235**, 156.
- Zhou, D.J., Wang, K.Z., Huang, C.H., Xu, G.X., Xu, L.G., Li, T.K., 1995. *Solid State Comm.* **93**, 167.
- Zhu, G.Y., Si, Z.K., Yang, J.G., Ding, J., 1990. *Anal. Chim. Acta* **231**, 157.

- Zhu, G.Y., Si, Z.K., Liu, P., 1991a. *Anal. Chim. Acta* **245**, 109.
- Zhu, G.Y., Si, Z.K., Ping, L., Wei, J., 1991b. *Anal. Chim. Acta* **247**, 37.
- Zhu, G., Si, Z., Jiang, W., Li, W., Li, J., 1992. *Spectrochim. Acta* **A7**, 1009.
- Zhu, W.G., Jiang, Q., Lu, Z.Y., Wei, X.Q., Xie, M.G., Zou, D.C., Tsutsui, T., 2000a. *Thin Solid Films* **363**, 167.
- Zhu, W.G., Jiang, Q., Lu, Z.Y., Wei, X.Q., Xie, M.G., Zou, D.C., Tsutsui, T., 2000b. *Synth. Met.* **111–112**, 445.
- Zhu, W.X., Zhou, J.G., Zhu, N.J., 1993. *J. Rare Earths* **11**, 161.
- Zink, J.I., 1978. *Acc. Chem. Res.* **11**, 289.
- Zink, J.I., Hardy, G.E., Sutton, J.E., 1976. *J. Phys. Chem.* **80**, 248.

Chapter 226

MOLECULAR RECOGNITION AND SENSING VIA RARE EARTH COMPLEXES

Satoshi SHINODA, Hiroyuki MIYAKE and Hiroshi TSUKUBE*

Department of Chemistry, Graduate School of Science, Osaka City University,
Sugimoto, Sumiyoshi-ku, Osaka 558-8585, Japan

E-mail: tsukube@sci.osaka-cu.ac.jp

Contents

List of symbols and acronyms	274	3.2.4. Chirality sensing with metal-based CPL	306
1. Introduction	274	4. Magnetic sensing via rare earth probes	308
2. Coordination chemistry and molecular recognition	278	4.1. Rare earth complexes for NMR sensing	308
2.1. Coordination and recognition of neutral substrates	278	4.1.1. Introduction	308
2.2. Coordination and recognition of charged substrates	280	4.1.2. Chirality sensing in aqueous solutions	312
2.3. Coordination and recognition of chiral substrates	283	4.1.3. Chirality sensing with hybrid probes	314
3. Optical sensing via rare earth probes	284	4.1.4. Chirality sensing with dynamic probes	315
3.1. Rare earth complexes for luminescence sensing	284	4.1.5. Chirality sensing with high resolution NMR spectrometers	315
3.1.1. Introduction	284	4.2. Rare earth complexes for MRI sensing	317
3.1.2. Luminescence sensing of neutral and anionic substrates	288	4.2.1. Introduction	317
3.1.3. Luminescence sensing of cationic substrates	296	4.2.2. pH-sensing	319
3.1.4. Luminescence sensing of biological substrates	298	4.2.3. O ₂ -sensing	323
3.2. Rare earth complexes for CD sensing	301	4.2.4. Sensing of metal cations	324
3.2.1. Introduction	301	4.2.5. Temperature sensing	325
3.2.2. Chirality sensing with ligand-based CD	301	4.2.6. MRI sensing with supramolecular probes	326
3.2.3. Chirality sensing with metal-based CD	305	4.2.7. Sensing of natural supramolecules	328
		5. Conclusion	330
		Acknowledgements	330
		References	331

* Corresponding author.

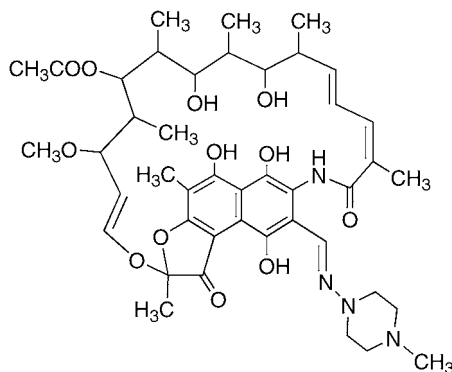
List of symbols and acronyms

acac	acetylacetonato (= 2,4-pentanedionato)	ESI	electrospray ionization
Ala	alanine	LIS	lanthanide induced shift
ATP	adenosine triphosphate	MRI	magnetic resonance imaging
BINOL	1,1'-bi-2-naphthol	MS	mass spectrometry
CD	circular dichroism	MTPA	α -methoxy- α - (trifluoromethyl)phenylacetic acid
CPL	circularly polarized luminescence	NIR	near-infrared
CSR	chiral shift reagent	NMR	nuclear magnetic resonance
cyclen	1,4,7,10-tetraazacyclododecane	terpy	2,2':6'2''-terpyridine
EDTA	ethylenediaminetetraacetic acid		
ee	enantiomeric excess		

1. Introduction

Rare earth metals possess characteristic 4f open-shell configurations and exhibit interesting variability across the periodic series (Richardson, 1982; Alexander, 1995; Piguet and Bünzli, 1999; Kaltsoyannis, 1999). For example, the effective ionic radii of their trivalent states range between 0.98 Å and 1.16 Å in the octa-coordinated complexes, and decrease in order of atomic numbers (Shannon, 1976). Since the electron transfer ability, Lewis acidity, light-emitting efficiency, and magnetic function of the rare earth cation systematically vary, we can select the most suitable one and use it in the tailor-made synthesis of functional rare earth materials. The trivalent rare earth cations are used as spectroscopic probes, because they have similar coordination geometry and ionic radii to those of biologically active Ca²⁺ cation. When they replace Ca²⁺ cations in biological systems, structural and environmental information around the metal center can be spectroscopically read out. Salvadori et al. (1984) typically employed Yb³⁺ ion to characterize the complex behaviors between rifamycin **1** (scheme 1) and Ca²⁺ ion. Several –OH groups in its chiral cyclic skeleton were demonstrated to coordinate with the Ca²⁺ ion in a multidentate fashion. Messori et al. (1986) revealed that Yb³⁺ ion bound transferrin, iron carrier protein, up to a metal-to-protein ratio of 2:1, and concluded that the two binding sites of the transferrin were indistinguishable or had comparable affinities. Furthermore, luminescent materials, light converters (Sabbatini and Guardigli, 1993; Parker, 2000; Kuriki et al., 2002), nuclear magnetic resonance (NMR) and magnetic resonance imaging (MRI) reagents (Aime et al., 1998; Caravan et al., 1999), and organic and biological catalysts (Imamoto, 1994; Komiyama et al., 1999; Molander and Romero, 2002; Kobayashi et al., 2002) were developed from rare earth complexes, and successfully employed in the fields of chemistry, biology, medicine and materials science.

This chapter describes unique molecular recognition properties of the rare earth complexes as well as their applications in specific probing and sensing of the targeted substrates. “Molecular recognition” is one of main subjects in all areas of molecular-based

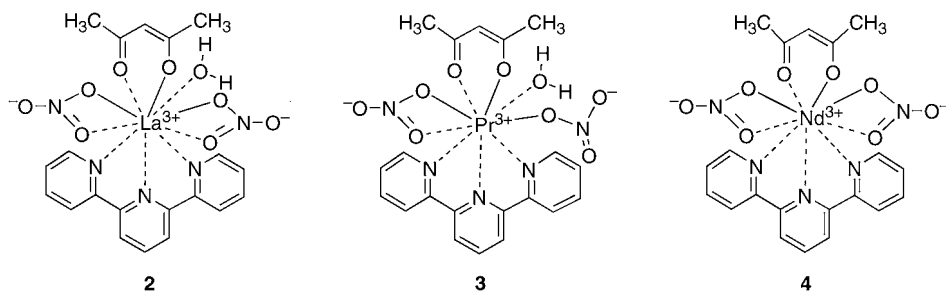


1

Scheme 1.

biology, physics, and chemistry. This has primarily been emphasized by natural products such as proteins, nucleic acids, sugars, amino acids, hormones, and antibiotics, and also by drugs, foods, and synthetic chemicals. When the rare-earth-containing receptor binds with a particular substrate, specific interactions may occur in the inner and/or outer coordination sphere. Since the resulting interactions often modify the complex characteristics, the precise information of the substrate can be read out by monitoring them (Miyake et al., 2001; Tsukube and Shinoda, 2002).

Rare earth complexes have high coordination numbers and characteristic geometry which are principally dependent on the natures of coordinating ligands, rare earth center, competitive solvents, and outer sphere interactions. Most trivalent rare earth cations typically form octa- or nona-coordinated complexes, in which mechanical distortions are usually required to accommodate steric interactions. Since their coordination bonds have little or no directionality, such steric constraints directly influence the complex structure and stability. Fukuda et al. (2002) compared crystal structures of highly coordinated complexes including 13 kinds of rare earth centers, with acetylacetonate and terpyridine ligands as well as additional nitrate anion and water molecule (fig. 1). The nature of the metal ions significantly reflects the structures of the highly coordinated complexes: (a) the largest La^{3+} cation gives a deca-coordinated complex, $[\text{La}(\text{terpy})(\text{acac})(\text{NO}_3)_2\text{H}_2\text{O}]$ **2**, which has four chelating ligands (tridentate terpy, bidentate acac, and two NO_3^-) and one water molecule; (b) the smaller Pr^{3+} cation forms a nona-coordinated complex, $[\text{Pr}(\text{terpy})(\text{acac})(\text{NO}_3)_2\text{H}_2\text{O}]$ **3**, in which one NO_3^- anion is monodentate while the other one is bidentate; and (c) the Nd^{3+} and other smaller cations also yield nona-coordinated complexes such as $[\text{Nd}(\text{terpy})(\text{acac})(\text{NO}_3)_2]$ **4**, but no water molecule is bound to the metal ion. The coordination bonds involved in these rare earth complexes have principally an ionic nature, and the spherical trivalent metal ions form kinetically labile and stereochemically versatile complexes. Therefore, the designed rare earth metal complexes meet the requirements for acting as selective receptors of external guest ligands.



	2	3	4
Size of metal center	Large	Medium	Small
Coordination number	10	9	9
Ligand components	5	5	4

Fig. 1. Effect of the size of the rare earth ion on complexation behavior.

	La	Ce	Pr	Nd	Pm	Sm	Eu	Gd	Tb	Dy	Ho	Er	Tm	Yb	Lu	
	57	58	59	60	61	62	63	64	65	66	67	68	69	70	71	
<i>Luminescence</i>				●		○	●		●	○		●		●		
<i>CD</i>	○	○	○	○	○	○	○	●	○	●	○	○	○	○	●	○
<i>NMR</i>	○			●			●	●			●				●	○
<i>MRI</i>								○	●							

Fig. 2. Optical and magnetic sensing with rare earth complexes. Solid circle—very important, open circle—important.

The rare earth complexes have potential not only in molecular recognition but also in sensing and probing of the targeted substrates (Tsukube et al., 2002a). Fig. 2 outlines applicability of rare earth complexes in optical and magnetic sensing. They exhibit fascinating spectroscopic properties based on internal $4f \rightarrow 4f$ electronic transitions. Although their low transition probabilities require sensitization by the ligand to achieve intense luminescence, these luminescent sensing materials have the crucial advantage of micro- to milli-second lifetimes. Actually, several types of Nd^{3+} , Eu^{3+} , Tb^{3+} , Er^{3+} and Yb^{3+} complexes have already been used as luminescent tags for labeling biological substrates, in which efficient energy transfer from chromophoric ligands to the metal ion occurs. Guest-responsive luminescent rare earth complexes have recently been developed (Bruce et al., 2000; Gunnlaugsson et al., 2002; Montalti et al., 2001). Both the intensity and splitting patterns of the observed emission signals give detailed information on microenvironments around the excited rare earth ion. Fig. 3 typically illustrates the chirality-responsive luminescence of Tb^{3+} tripodal complexes. Two diastereomeric tris(2-pyridylmethyl)amine derivatives **5** include a remarkable difference

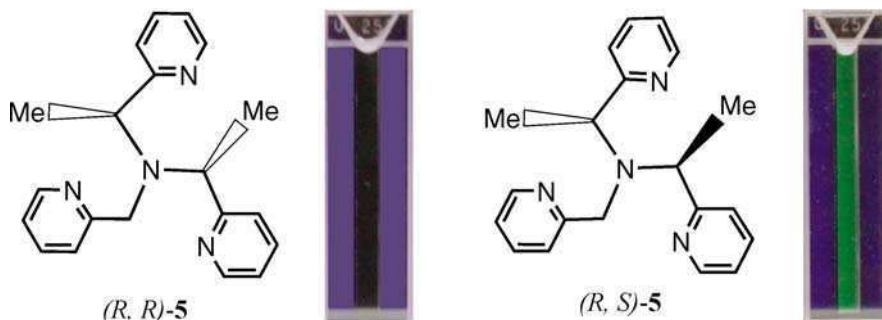


Fig. 3. Visual sensing of ligand chirality: non-luminescent Tb^{3+} -(*R,R*)-5 complex; and luminescent Tb^{3+} -(*R,S*)-5 complex. Reproduced, with permission, after Yamada et al. (2003).

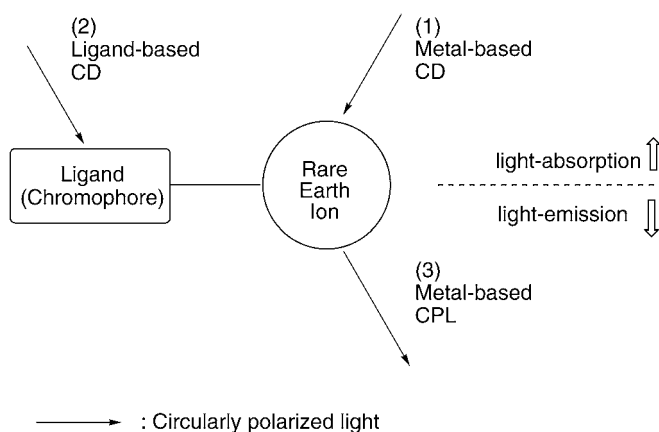


Fig. 4. CD and CPL phenomena with rare earth complexes.

in Tb^{3+} luminescence intensity, which is large enough to be recognized by the naked eye (Yamada et al., 2003). Although several organic fluorescent receptors have been developed as optical sensing materials, these rare earth complexes can visually sense the precise molecular information of the specific substrate via highly coordinated ternary complexes.

Chiroptical information from the rare earth complexes also gives deep insights into the ligand coordination geometry, stereochemistry, electronic state, and other environment-dependent parameters. Since chiral rare earth complexes exhibit circular dichroism (CD) and/or circularly polarized luminescence (CPL) spectra (fig. 4), stereochemistry of the specific guest can be read out using three types of CD methods (Kuroda and Saito, 2000): (1) the rare earth centers themselves exhibit CD spectra based on $f-f$ transitions under chiral coordination environments (metal-based CD); (2) achiral, chromophoric ligands coordinating with rare earth ions give intense CD signals upon complexation with polydentate chiral substrates

(ligand-based CD); and (3) rare earth metal-based circularly polarized luminescence behaviors are observed with some emissive rare earth complexes (metal-based CPL). In these processes, the initial ligands should be carefully chosen and combined with suitable rare earth ions to control the competitive coordinations of substrates, solvents, and other molecules. When a racemic rare earth complex with highly chromophoric ligands is employed as a probe, direct coordination of a chiral external substrate often induces intense ligand-based CD signals (Nakanishi and Dillon, 1971; Tsukube and Shinoda, 2002). Several rare earth complexes further present metal-based CD signals upon ternary complexation with chiral substrates, though they are often too weak to be useful as sensors. The instruments for CPL measurements are now commercially available, and a number of emissive Eu^{3+} , Tb^{3+} , and Dy^{3+} complexes have been characterized as CPL probes.

Several rare earth complexes with a large number of unpaired 4f electrons and considerable associated electronic magnetic moments are known to be effective NMR and MRI probes. Although their theory and practical applications have been reviewed elsewhere (Aime et al., 1998; Caravan et al., 1999), recent advances in this field are summarized below from the stand-point of molecular recognition chemistry and sensing technology. A number of Pr^{3+} , Sm^{3+} , Eu^{3+} , Dy^{3+} , and Yb^{3+} complexes are commercially available NMR shift reagents, which provide spectral simplification and resolution enhancement. Since these shift reagents give angular and distance information around the metal centers, they have further potential as paramagnetic biological probes to gain structural information on amino acids, nucleotides, and proteins. A series of Gd^{3+} complexes have received particular attention as MRI contrast agents for medical imaging. Additional smart MRI contrast agents are currently required to exhibit high sensitivity toward external stimuli such as pH and P_{O_2} , and intracellular concentrations of specific analytes.

In this chapter, we first overview basic coordination and molecular recognition chemistry of rare earth complexes, and then detail their recent applications in sensing and probing processes. There are many possibilities for their uses in optical and magnetic sensings of the targeted substrates, but many difficulties nonetheless remain in the practical design of such rare earth complexes. As described below, several multidentate macrocyclic and acyclic chelators were successfully developed to generate structurally defined rare earth complexes. Some of them exhibit characteristic molecular recognition profiles based on the formation of highly coordinated ternary complexes, and also act as luminescence, CD, NMR, and MRI sensors for specific guests.

2. Coordination chemistry and molecular recognition

2.1. Coordination and recognition of neutral substrates

When the rare earth cation is coordinatively unsaturated by the primary ligands, additional neutral or anionic substrates coordinate onto the metal ion to form a highly coordinated ternary complex. Fig. 5 schematically illustrates a complexation process in which europium tris(2,2,6,6-tetramethyl-3,5-heptanedionate) $\mathbf{6}(\text{Eu}^{3+})$ binds two pyridine molecules to yield

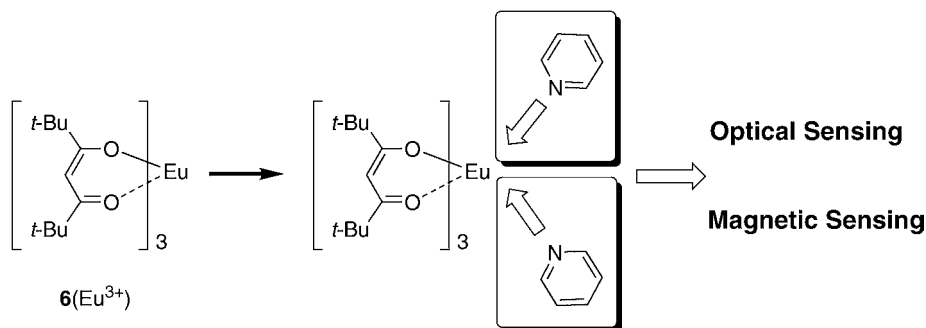


Fig. 5. Highly coordinated ternary complex between europium tris(β -diketonate) **6** and two pyridine molecules.

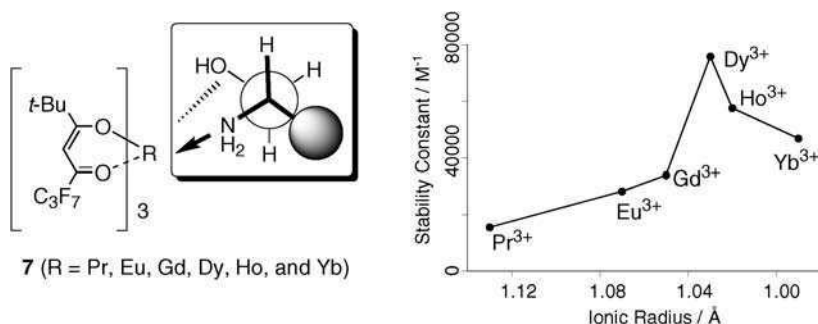


Fig. 6. Stability constants of highly coordinated ternary complexes between rare earth tris(β -diketonates) **7** and (*S*)-2-amino-3-methyl-1-butanol. Redrawn, with permission, after Tsukube et al. (2001).

a highly coordinated species (Cramer and Seff, 1972; LaPlanche and Vanderkooi, 1983). In this highly coordinated complex, the Eu^{3+} cation was electrically neutralized by three β -diketonate anions and further bound two pyridine substrates to achieve octa-coordination. Similar highly coordinated complexes were isolated, in which various nitrogen- and oxygen-containing substrates were included. Since additional coordination of these external substrates induces a geometrical rearrangement of the primary β -diketonate ligands in the inner coordination sphere, the optical and magnetic properties of the rare earth tris(β -diketonates) vary with the nature of the additional substrates. Therefore, this type of rare earth complexes have a potential as effective receptors and sensing devices.

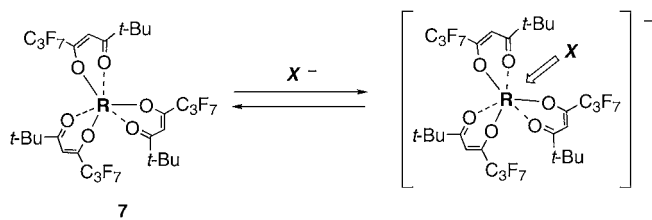
Tsukube et al. (2001) systematically determined $\log K$ values of the highly coordinated ternary complexes between rare earth tris(6,6,7,7,8,8,8-heptafluoro-2,2-dimethyl-3,5-octanedionates) **7** and 2-amino-3-methyl-1-butanol in $\text{CH}_3\text{OH}/\text{CH}_2\text{Cl}_2$ (1/99) (fig. 6). The $\log K$ values increase in the order $\text{Pr}^{3+} < \text{Eu}^{3+} < \text{Gd}^{3+} < \text{Dy}^{3+} > \text{Ho}^{3+} > \text{Yb}^{3+}$, though the ionic radii of the rare earth centers decrease in the order $\text{Pr}^{3+} > \text{Eu}^{3+} > \text{Gd}^{3+} > \text{Dy}^{3+} > \text{Ho}^{3+} > \text{Yb}^{3+}$. The smaller rare earth ions were confirmed to induce shorter and stronger

coordination bonds with amino alcohols, but the resulting complexes have larger steric repulsion between the amino alcohol and the β -diketonate ligands. Yang and Brittain (1982) reported similar stability constants between amino alcohols and europium tris(β -diketonates) in CHCl_3 . Since this type of rare earth complexes exhibit much larger $\log K$ values for amino alcohols than for the corresponding monoalcohol, monoamine, and diol substrates, they work well as chemo-selective receptors for bidentate amino alcohols.

2.2. Coordination and recognition of charged substrates

Although there has been extensive development of various organic receptors to monitor the targeted anions of biological, environmental, clinical, and industrial interests (Schmidtchen and Berger, 1997; Beer and Gale, 2001; Wiskur et al., 2001), rare earth complexes were only recently recognized as effective candidates for this purpose (Parker et al., 2002; Tsukube and Shinoda, 2002). The rare earth tris(β -diketonates) typically have suitable features as selective anion receptors: (1) several vacant coordination sites on the rare earth center are available for external anionic species; (2) coordination and recognition of the external anion are modified by an adequate combination of rare earth ion and primary ligand; and (3) stability, solubility, and Lewis acidity are enhanced by use of fluorinated ligands. Table 1 summarizes the stability constants of highly coordinated ternary complexes between rare earth tris(β -diketonates) **7** and four kinds of inorganic anions (Mahajan et al., 2003). Each rare earth complex forms 1:1 ternary complexes with several inorganic anions, and prefers the smaller (harder) Cl^- anion to the larger (softer) Br^- , I^- or ClO_4^- anions. The K values for Cl^- greatly depend on the nature of the rare earth cation but exhibit a different trend from that of ionic radii: K value, $\text{Pr}^{3+} < \text{Eu}^{3+} \approx \text{Dy}^{3+} > \text{Yb}^{3+}$; ionic radius of octa-coordinated rare earth ion $\text{Pr}^{3+} > \text{Eu}^{3+} > \text{Dy}^{3+} > \text{Yb}^{3+}$ (Shannon, 1976). As described in the case of bidentate amino

Table 1
Stability constants of highly coordinated ternary complexes between rare earth tris(β -diketonates) **7** and inorganic anions



Complex	Stability constant (K (M^{-1})) in CDCl_3			
	Cl^-	Br^-	I^-	ClO_4^-
7 (Pr^{3+})	[450]	79	*	93
7 (Eu^{3+})	600	84	*	52
7 (Dy^{3+})	[610]	28	20	15
7 (Yb^{3+})	[94]	[11]	16	5

*Too small to be determined. []: partially insoluble.

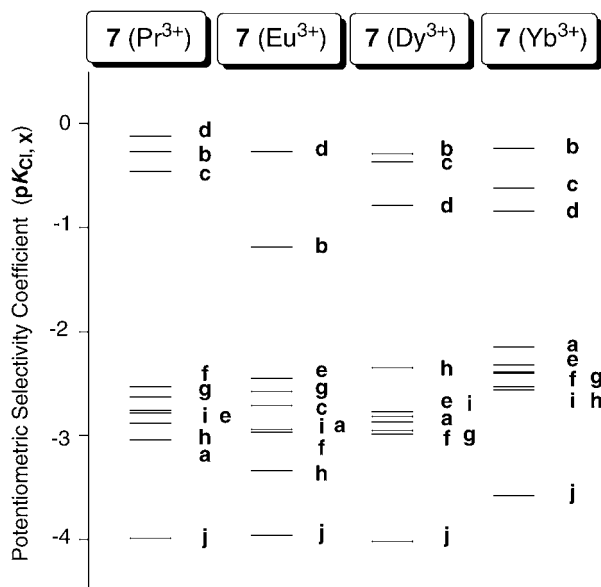


Fig. 7. Potentiometric selectivity coefficients toward Cl^- for ion-selective electrodes based on rare earth tris(β -diketonates) **7**. (a = F^- , b = Br^- , c = I^- , d = SCN^- , e = OH^- , f = HCO_3^- , g = CH_3CO_2^- , h = NO_3^- , i = ClO_4^- , j = SO_4^{2-}). Reproduced, with permission, after Mahajan et al. (2003).

alcohols, the smallest Yb^{3+} cation provides the largest steric repulsion between β -diketonates and the guest Cl^- anion.

The rare earth tris(β -diketonates) **7** also act as anion-selective electrode devices based on characteristic anion coordination. When they are incorporated in poly(vinyl chloride) membrane electrodes, near Nernstian responses are found for Cl^- anion (Mahajan et al., 2003). Fig. 7 indicates that the rare earth complex-based electrodes are highly selective towards Cl^- in comparison with F^- , Br^- , I^- , SCN^- , OH^- , HCO_3^- , CH_3CO_2^- , NO_3^- , ClO_4^- , and SO_4^{2-} . Although Br^- , I^- , and SCN^- anions compete with Cl^- in the Pr^{3+} , Dy^{3+} , and Yb^{3+} complexes, the Eu^{3+} complex gives satisfactorily high selectivity coefficients for Cl^- : $\text{p}K_{\text{Cl,Br}} = -1.19 \gg \text{p}K_{\text{Cl,I}} = -2.71 > \text{p}K_{\text{Cl,ClO}_4} = -2.94$. The corresponding copper bis(β -diketonate) exhibits extremely low electrode response and anion selectivity, indicating that the rare earth complex offers unique anion-selective sensing at the water/polymer membrane interface.

Trivalent rare earth cations form complexes with a series of hydroxycarboxylic acids and amino acids in aqueous solutions, some of which are listed in fig. 8. Earlier studies of Katzin (1968, 1969) revealed that these biological substrates effectively act as bidentate ligands toward the rare earth cations. Rare earth complexes with multidentate chelators were recently applied as receptors for zwitterionic amino acids of biological and artificial interests. Aime et al. (2001a) characterized the complexation behaviors of zwitterionic amino acids with oc-

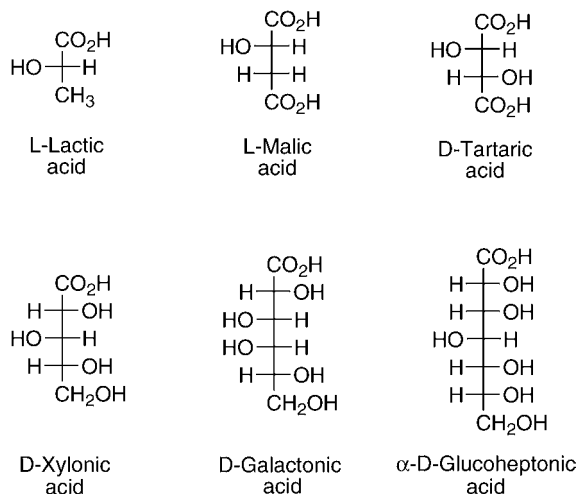
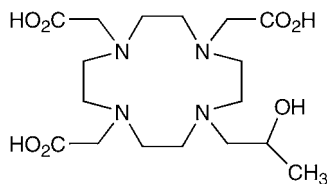


Fig. 8. A series of water-soluble substrates for rare earth complexation.



8

Scheme 2.

tadtentate cyclen **8**-Gd³⁺ complex (scheme 2) in aqueous media, and proposed that the -NH₃⁺ part of the amino acid guest interacts with the bound water molecule on the rare earth center. The rare earth tris(β -diketonates) **7** efficiently extract phenylalanine, tryptophan, leucine, and phenylglycine from neutral aqueous solutions into organic media, though more hydrophilic alanine and glycine are rarely extracted (Tsukube et al., 1996a, 1998). When the -CO₂⁻ part of the amino acid is directly coordinated to the neutral rare earth complex, the resulting anionic species was thought to interact intramolecularly with the -NH₃⁺ function of the amino acid. These rare earth tris(β -diketonates) further mediate transport of amino acids across bulk liquid membranes (Tsukube et al., 1996b). The rare earth complex is an effective carrier under neutral pH conditions, forming a highly coordinated ternary complex with amino acid on one side of the membrane. The ternary complex moves across the membrane and releases the guest amino acid into a receiving aqueous phase. In addition to oligopyridine derivatives and β -diketonate ligands, polyaminocarboxylic acid ligands such as EDTA analogs were reported

to form highly coordinated ternary complexes with rare earth ions and amino acids in aqueous solutions (Kido et al., 1991). Therefore, rare earth complexes including multidentate ligands act as effective receptors of charged substrates.

2.3. Coordination and recognition of chiral substrates

Chirality is an important information involved in many biological and artificial processes. Its recognition requires that the receptor forms diastereomeric complexes with a pair of substrate enantiomers, which have different structures and/or stability constants (Tsukube and Shinoda, 2000). Since the observed differences between the diastereomers are usually small, chiral recognition is one of the most difficult tasks in molecular recognition chemistry and sensing technology. The rare earth tris(β -diketonates) with chiral ligands **9** achieve enantioselective extraction of amino acids from neutral aqueous solution (Tsukube et al., 1996a, 1998). As illustrated in fig. 9, the extractability of tryptophan is dependent on the ionic radius, and decreases from Pr^{3+} or Eu^{3+} to Er^{3+} and then to Yb^{3+} . The observed enantioselectivity has a “reversed order”, and the highest enantioselectivity (49% ee) was recorded with Yb^{3+} complex **9** for the most sterically crowded phenylglycine substrate. Although these rare earth complexes usually have several stereoisomers in solution, the smaller rare earth ions provide closer asymmetric interaction between the chiral β -diketonate ligand and the amino acid substrate, which results in an enhanced enantioselectivity in the extraction processes. Willner et al. (1991) reported the enantiomer-selective transport of cationic amino acid ester salts, in which the negatively charged ternary complexes between chiral europium tris(β -diketonate) and inorganic anions act as carriers.

Since Bednarski and Danishefsky (1983) first reported the promoted hetero-Diels–Alder reactions, several types of chiral rare earth complexes have been shown to exhibit dynamic

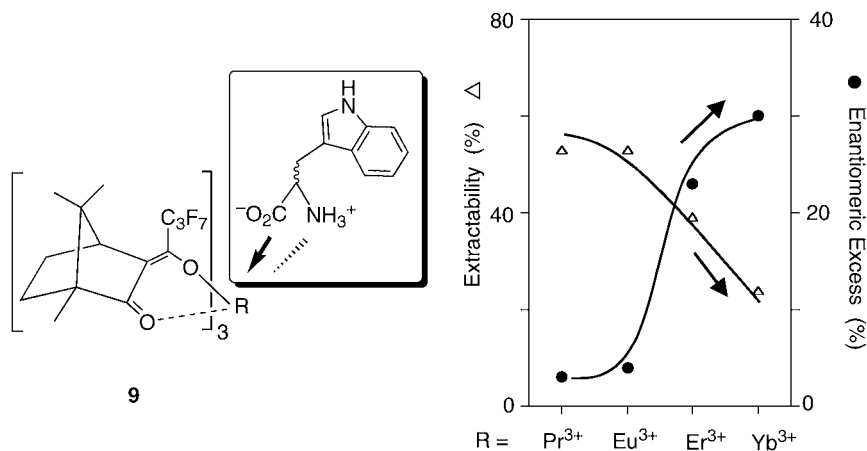
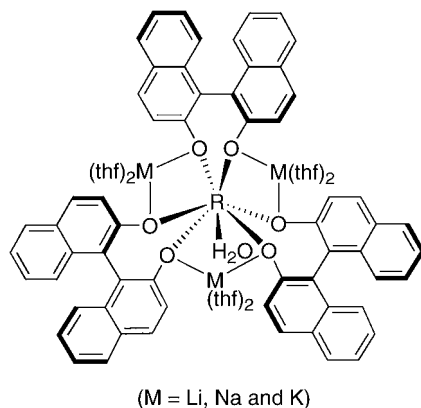


Fig. 9. Enantiomer-selective extraction of amino acids with chiral rare earth tris(β -diketonates) **9**. Redrawn, with permission, after Miyake et al. (2001).



10

Scheme 3.

chiral recognition abilities in enantioselective catalysis such as cycloaddition, hydrogenation, hydrosilylation, hydroamination, polymerization, and aldol reactions (Inanaga et al., 2002; Aspinall, 2002). Shibasaki and Yoshikawa (2002) further developed the rare-earth-containing multifunctional catalysts **10** (scheme 3), which show both Lewis acidity and Brønsted basicity, and catalyze a variety of enantioselective transformations. Therefore, a rational design can add both dynamic and static chiral recognition functions to the rare earth complexes.

3. Optical sensing via rare earth probes

3.1. Rare earth complexes for luminescence sensing

3.1.1. Introduction

Luminescence properties of rare earth complexes provide a useful methodology for detection and sensing of a targeted species. When a luminescent rare earth complex interacts with the targeted guest, it acts as a signaling device responsive to the nature, concentration, and reaction behavior of the guest. In addition to narrow and intense spectral shapes, rare earth complexes generally feature long-lived luminescence signals at room temperature occurring at constant wavelengths in the visible (Sm^{3+} , Eu^{3+} , Tb^{3+} , and Dy^{3+}) or near-IR spectral ranges (Nd^{3+} , Er^{3+} , and Yb^{3+}) (fig. 10). Since common organic fluorophores exhibit short-lived emissions in variable spectral ranges, the rare earth complexes have practical advantages not only as labeling reagents but also as sensing devices.

Since rare earth metals have spin-forbidden f–f transitions with very weak absorptivity, there are two approaches to generate intense luminescence: (1) the use of intense light sources, such as lasers, to directly excite the rare earth center and (2) the attachment of an appropriate antenna chromophore to the ligands coordinated onto the rare earth center. The latter approach

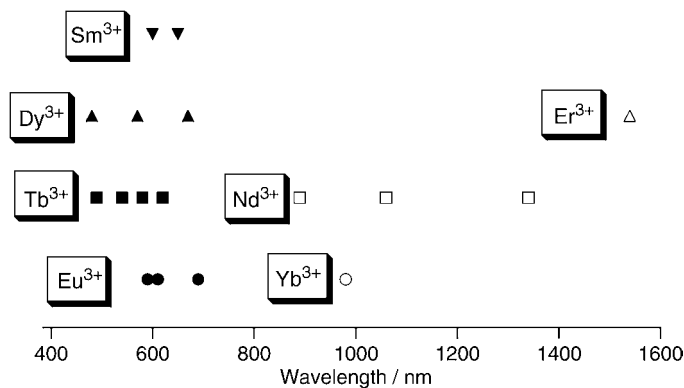


Fig. 10. Intense emission bands of trivalent rare earth ions. Reproduced, with permission, after Shinoda (2004).

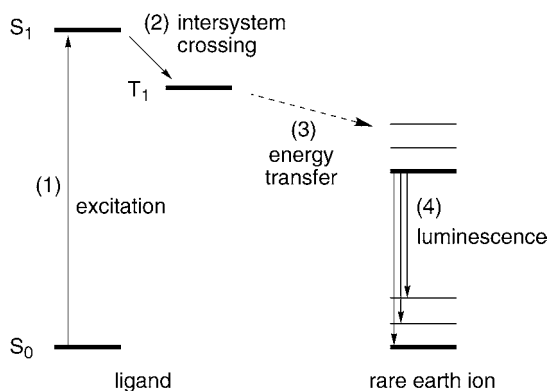


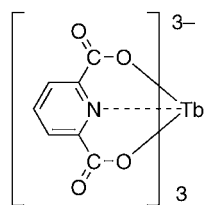
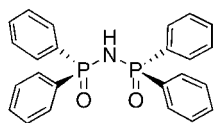
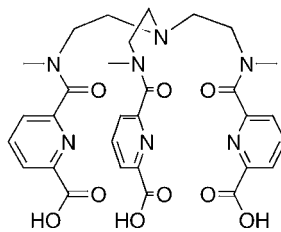
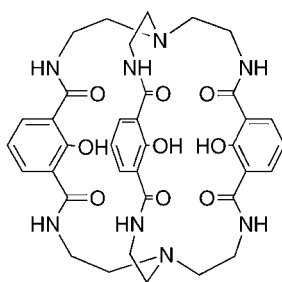
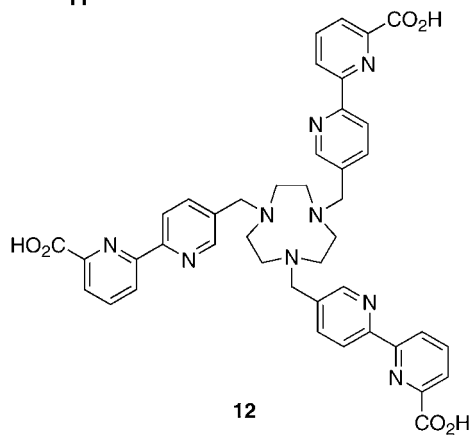
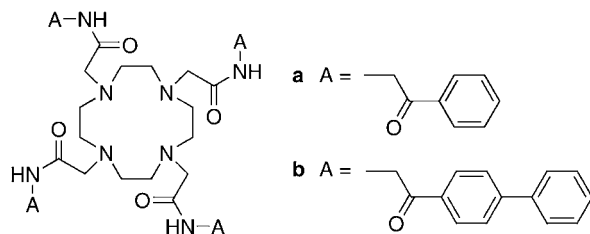
Fig. 11. Luminescence processes in rare earth complexes. (1) excitation; (2) intersystem crossing; (3) energy transfer; and (4) luminescence. Reproduced, with permission, after Shinoda (2004).

has more practical applications, because common fluorimeters can record this type of luminescence spectra. Fig. 11 illustrates the energy migration processes taking place in a rare earth complex: excitation of the ligand chromophore, intersystem crossing, energy transfer, and rare earth luminescence. When an organic ligand plays the role of a photo-antenna, the excitation energy of the organic molecule is transferred from its triplet state to the rare earth center via an electron exchange mechanism or via dipole moment coupling. The luminescence efficiency is thus determined by several factors: (1) the efficiency of triplet state formation of the ligand chromophore from its singlet excited state; (2) the efficiency of energy transfer from the triplet state to the rare earth center; (3) the radiation efficiency of the rare earth complex; and (4) the quenching efficiency by other species located in the environment of the metal ion.

Among these four processes, the non-radiative quenching process from the excited to the ground states of the rare earth ion is the most important factor in determining the luminescence quantum yield. As the 4f electrons of the rare earth ion are shielded, the excited state can live for a long period and return to the ground state by emitting light. Deactivation of the excited state is often caused by energy transfer into the higher levels of vibrational modes that energetically match the excited state of the rare earth ion. High frequency vibrations such as O–H, N–H, and C–H stretchings are dominant in energy dissipation based on overlap with Franck-Condon envelopes. The energy dissipation via molecular vibration competes with the rare earth luminescence process. The lower the excited-state energy of rare earth ion, the more efficient the energy dissipation process due to the larger Franck-Condon overlaps. Since water and solvent molecules directly coordinating the rare earth center effectively quench its excited states, nature of the coordinated species has great influence on the luminescence efficiency and lifetime.

Several multidentate ligands yield thermodynamically stable rare earth complexes, in which the metal centers are completely enclosed and significantly protected from solvation effects. The octadentate cyclen derivatives are typical examples. They form quite stable and structurally well-defined 1:1 complexes with rare earth ions, in which four cyclen nitrogen atoms and four donor atoms on the sidearms cooperatively coordinate. [Zucchi et al. \(2002\)](#) prepared tetraamide cyclens bearing aromatic chromophores **11a** and **11b** (scheme 4), and characterized luminescence properties of their Sm^{3+} , Eu^{3+} , Tb^{3+} , and Dy^{3+} complexes. These rare earth complexes possess high quantum yields in aqueous solutions when phenacyl and 4-phenylphenacyl chromophores are excited: 23.1% for Tb^{3+} -**11a** complex and 24.7% for Eu^{3+} -**11b** complex. The efficient energy conversion results from efficient intersystem crossing in the chromophore as well as fast ligand-to-metal energy transfer. [Charbonnière et al. \(2001\)](#) prepared a nonadentate ligand **12** from 1,4,7-triazacyclononane and three 6-carboxyl-2,2'-bipyridine units for luminescent Eu^{3+} complex. The crystal structure revealed that the Eu^{3+} center is nona-coordinated and has no water nor solvent molecule in its inner coordination sphere. Its luminescence has a 1.85 ms lifetime in H_2O with a quantum yield of 12% at 300 K. Other cage-type ligands give intensely luminescent rare earth complexes via effective protection. [Petoud et al. \(2003\)](#) reported that multidentate ligand H_3L (**13**) forms 2:1 complexes $[\text{R}(\text{H}_2\text{L})_2]^+$ ($\text{R} = \text{Sm}, \text{Eu}, \text{Tb}, \text{and Dy}$) and intense luminescence spectra are observed via ligand sensitization. Other authors prepared nona-coordinated complexes with tripodal ligand H_3L (**14**), but its Eu^{3+} and Tb^{3+} complexes have modest luminescence quantum yields in water (<1%) due to the low efficiency of the intersystem crossing process ([Senegas et al., 2003](#)). [Magennis et al. \(2002\)](#) described highly luminescent Sm^{3+} , Eu^{3+} , Tb^{3+} , and Dy^{3+} complexes with aryl-substituted imidodiphosphinate ligand **15**. The introduction of appropriate chromophoric sidearms in multidentate ligands generally leads to highly luminescent rare earth complexes, and, in addition, such a simple ligand also forms solvent-free rare earth complexes.

Luminescent rare earth complexes have been utilized as labeling agents of proteins and nucleic acids for luminescent immunoassays and hybridization assays. Since Tb^{3+} -dipicolinic acid complex **16** is highly luminescent, its conjugate with immunoglobulin works as a sensitive luminescent probe in the immunoassay. Thanks to their long lifetimes allowing time-



Scheme 4.

resolved detection of the luminescence, rare earth complexes have great advantages of sensitivity and detection limit over common organic fluorophores, thus, they provide practical alternatives to radioisotopes in labeling experiments. Recent examples of luminescent labeling with rare earth complexes have been reviewed (Matsumoto and Yuan, 2003; Turro et al., 2003).

Although Eu^{3+} and Tb^{3+} complexes generally exhibit intense luminescence at 10^{-5} – 10^{-6} M concentration, practical sensory application requires that their luminescence changes occur sensitively and selectively upon interaction with guest species and, also, that other existing species in the system do not perturb the luminescence process. Since the transition probability and degeneracy strongly depend on the fine structure of the highly coordinated complex, ligand-field splitting of the narrow emission bands, relative intensity, and other luminescence properties of the rare earth complexes provide excellent indications of guest recognition. Therefore, they can probe the microenvironments around the active sites of biomolecules as well as the concentration of biologically active species.

3.1.2. Luminescence sensing of neutral and anionic substrates

Recognition and sensing of anionic guests have been a spreading area in molecular recognition chemistry, material science, bioscience and related technology. Various anions including DNAs, RNAs, proteins, and co-factors are significantly involved in biological processes. Several receptors have recently been designed for the recognition of biologically relevant anions, in which quaternary ammonium groups, metal complexes, and neutral hydrogen bond donor groups bind anionic guests via electrostatic interactions. More recently, a series of rare earth complexes have been pointed out as effective receptors for anion recognition (Tsukube and Shinoda, 2002). Rare earth tris(β -diketonate) complexes **7** typically form highly coordinated complexes with anions as well as organic Lewis bases (see section 2.2). NMR and MS spectroscopic characterizations revealed that one guest anion is bound to the rare earth complex and forms a negatively charged ternary complex. When a solution of Eu^{3+} complex **7** in CH_3CN is excited into the β -diketonate absorption band, characteristic red luminescence signals are seen at 593, 613, 652, and 700 nm (Mahajan et al., 2003). Addition of 3 equivalent Cl^- anion to this solution enhances the luminescence intensity at 613 nm by 2.0-fold, while Br^- , I^- , or ClO_4^- anion only slightly increases the luminescence intensity. The observed selectivity on luminescence clearly reflects the stability constants of highly coordinated complexes (table 1), and indicates a hard anion preference of the rare-earth-containing receptor. Since the anion-enhanced luminescence can be detectable by the naked eye (fig. 12), the rare earth complexes are applicable in not only spectroscopic probing but also visual sensing of anions.

The series of neutral tripodal ligands **17**–**22** were reported to form stable cationic complexes with trivalent rare earth ions. Since they cannot wrap around large rare earth ions completely, several coordination sites remain available on the rare earth center. Mazzanti et al. (2002) reported crystal structures of rare earth complexes with tripodal ligands **17** and **18** (fig. 13). Tris(2-pyridylmethyl)amine **17** gives octa-coordinated complexes with La^{3+} and Nd^{3+} ions including three halides and one neutral solvent molecule (Wietzke et al., 1998, 2000). In contrast, this ligand forms hepta-coordinated complexes with Eu^{3+} , Tb^{3+} , and Lu^{3+} ions, in which three chloride anions occupy the remaining sites (Wietzke

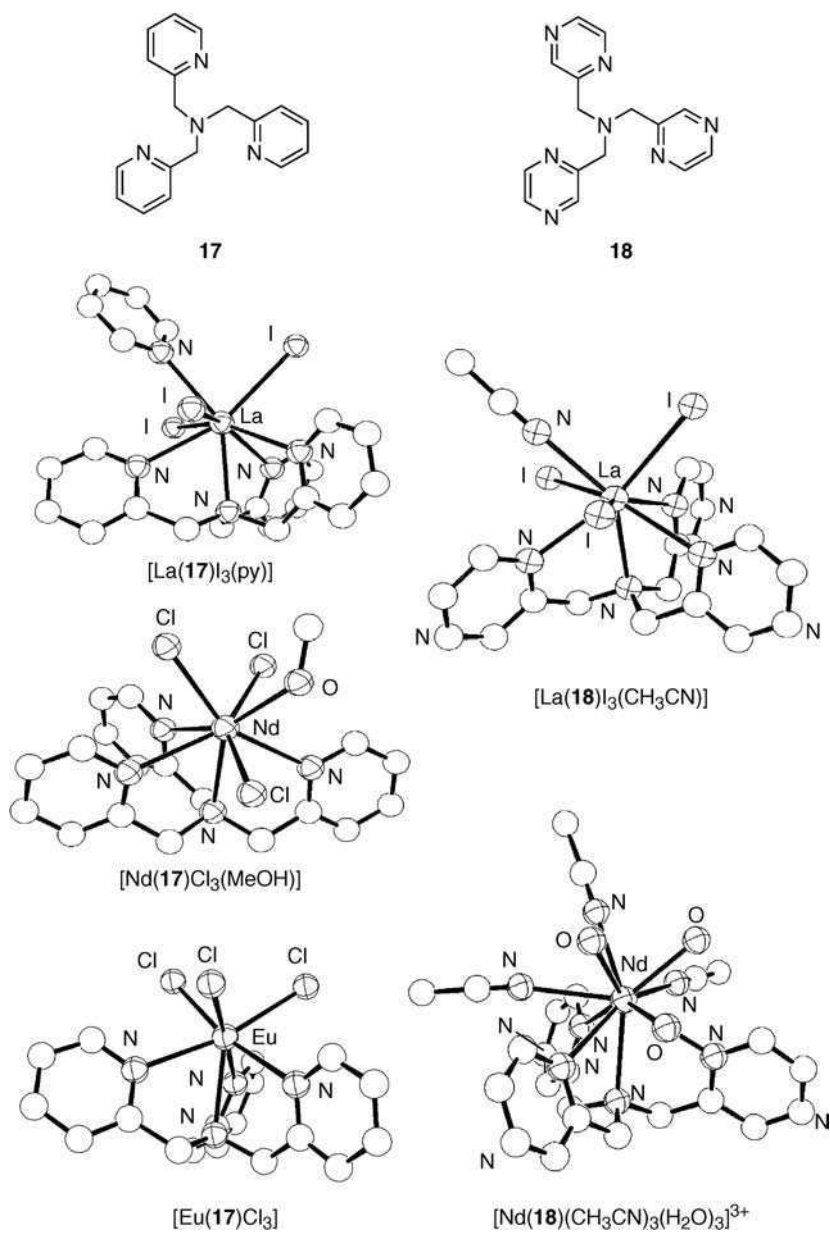
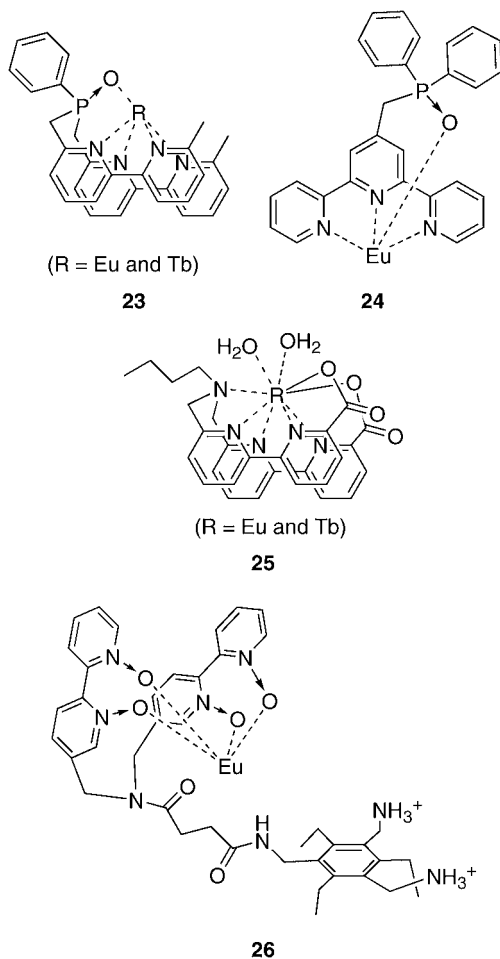


Fig. 13. Crystal structures of 1:1 rare earth complexes with tripodal ligands **17** and **18**. Redrawn, with permission, after Wietzke et al. (1998, 2000) and Mazzanti et al. (2002).

anion give deca-coordinated complexes, $[R(\mathbf{19} \text{ or } \mathbf{20})(\text{NO}_3)_3]$, while monodentate Cl^- anion gives octa-coordinated complexes, $[R(\mathbf{19})\text{Cl}_3(\text{H}_2\text{O})]$. Wietzke et al. (1999) reported that tripodal ligand **21** bearing 2-benzimidazole rings preferentially forms 2:1 (L:M) rare earth complexes with no coordinated anion due to strong intramolecular π - π interactions. Further combinations of tripodal ligands and rare earth cations provide wide variations in the anion recognition and luminescence sensing processes.

When the tripodal $\mathbf{17}\text{-Eu}^{3+}$ and Tb^{3+} complexes are employed as luminescent anion receptors, the coordinative guest anion easily occupies additional coordination site, and modifies the overall shape of the luminescence spectra. Among F^- , Cl^- , Br^- , I^- , SCN^- , NO_3^- , AcO^- , HSO_4^- , H_2PO_4^- , and ClO_4^- anions, only Cl^- and NO_3^- effectively enhanced the intensities of Eu^{3+} and Tb^{3+} luminescence (Yamada et al., 2002, 2003). Formation of the highly coordinated ternary complex between ligand **17**, the rare earth ion, and the external anion was confirmed by ESI MS method. The luminescence lifetimes of the ternary complexes are larger than those of corresponding complexes without the added anions, suggesting that the quenching process is suppressed by ternary complexation. The Eu^{3+} and Tb^{3+} complexes showed different anion selectivities. The former showed the largest enhancement with NO_3^- and the latter with Cl^- . Methyl substituted tripods **5** and **22** enhance the luminescence sensitivity compared with simple tripod **17**, though they exhibit similar anion selectivity. The nature of the ligand wrapped around the rare earth centers had great influence on anion coordination and subsequent luminescence properties.

Charbonnière et al. (2002) prepared a multidentate ligand for luminescent rare earth complexes **23** (scheme 6) which includes bis(bipyridine) and phosphine-oxide units. The soft and hard donors cooperatively coordinate to the rare earth center to form penta-coordinated complexes, while the bipyridines also serves as good photo-antenna. Addition of 2 equivalents of NO_3^- leads to 11-fold enhancement in europium luminescence and 7-fold enhancement in terbium emission, while Cl^- , F^- , and AcO^- generate much smaller effects. The authors pointed out that the coordinative guest anion replaces the bipyridine unit, but the phosphine oxide unit is still bound to the rare earth ion. The tetra-coordinated Eu^{3+} complex **24** including soft terpyridine and hard phosphine-oxide donors shows a 20-fold luminescence enhancement upon addition of 3 equivalent of NO_3^- (Prodi et al., 2003). Therefore, tetra- and penta-dentate ligands are also useful in the design of luminescent rare earth complexes acting as anion-selective sensory devices. A similar strategy can be applied in the design of luminescent anion receptors effective in water. Mameri et al. (2004) prepared a heptadentate ligand leading to rare earth complexes **25**. Since this ligand has enough coordinating atoms to protect the rare earth center from hydration, ATP^{4-} and HPO_4^{2-} anions were well-sensed in the neutral aqueous solution. The formation of a ternary complex between ATP^{4-} and the Eu^{3+} complex **25** increases the luminescence lifetime by replacing the bound water molecules, though the less effective energy transfer process decreases the luminescence intensity to 20% of its initial value. Best and Anslyn (2003) combined an Eu^{3+} complex with quaternary ammonium cation units, and prepared the hybrid anion receptor **26**. Since the Eu^{3+} center and additional cationic sites cooperatively bind 2,3-bisphosphoglycerate anion, this phosphate anion was detected by monitoring the europium luminescence (fig. 14).



Scheme 6.

A series of rare earth complexes with cyclen derivatives fitted pendant arms exhibit effective sensing abilities in water. Fig. 15 illustrates the crystal structure of the **27**-Eu³⁺ complex with an octadentate cyclen, in which one water molecule occupies the ninth coordination site (Zucchi et al., 2001). The lifetime and NMR measurements confirmed that only one water molecule is located in the first coordination sphere even in aqueous solution. In contrast, heptadentate cyclen **28** leaves two vacant sites on the rare earth center, and bidentate guest anions are expected to occupy the two adjacent coordination sites. Therefore, cyclen derivatives can be used to control the number of anion binding sites.

Dickins et al. (1998) reported that Eu³⁺ and Tb³⁺ complexes with heptadentate cyclen **28** sensed bicarbonate anion in neutral aqueous solution. Among F⁻, Cl⁻, Br⁻, I⁻, NO₃⁻,

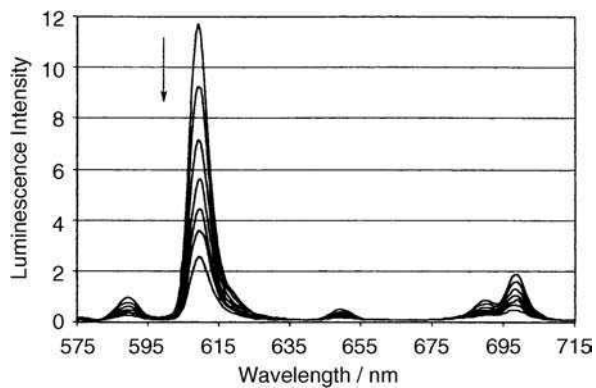


Fig. 14. Europium luminescence changes of hybrid receptor **26** upon addition of 2,3-bis(phosphoglycerate) anion in 50% MeOH/CH₃CN. Reproduced, with permission, after Best and Anslyn (2003).

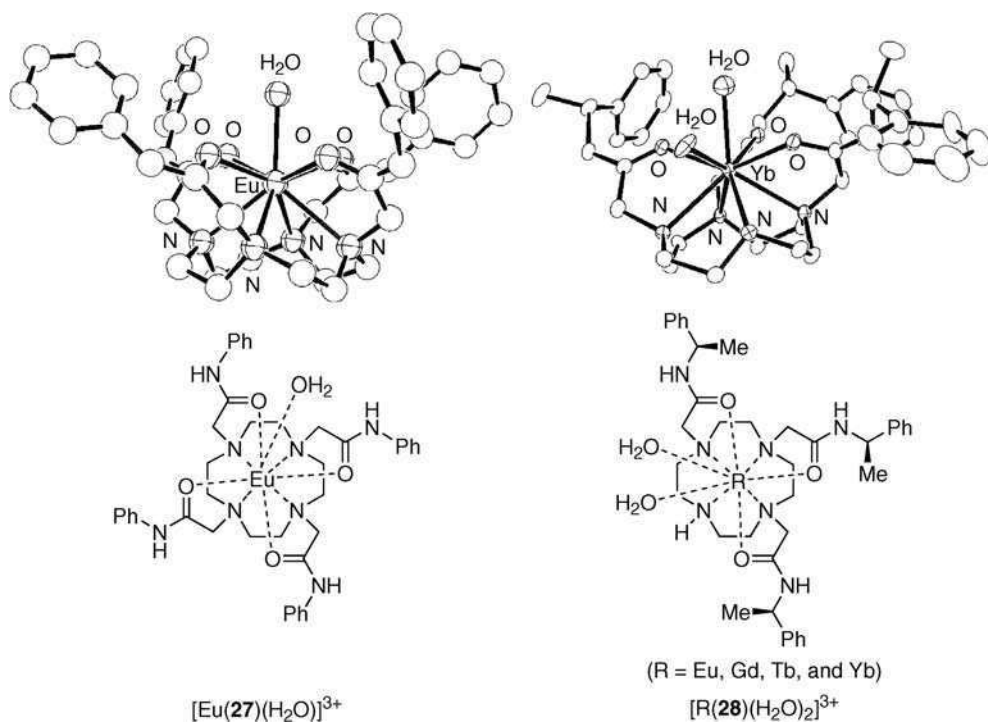


Fig. 15. Rare earth complexes with octadentate cyclen **27** and heptadentate cyclen **28**. Redrawn, with permission, after Zucchi et al. (2001).

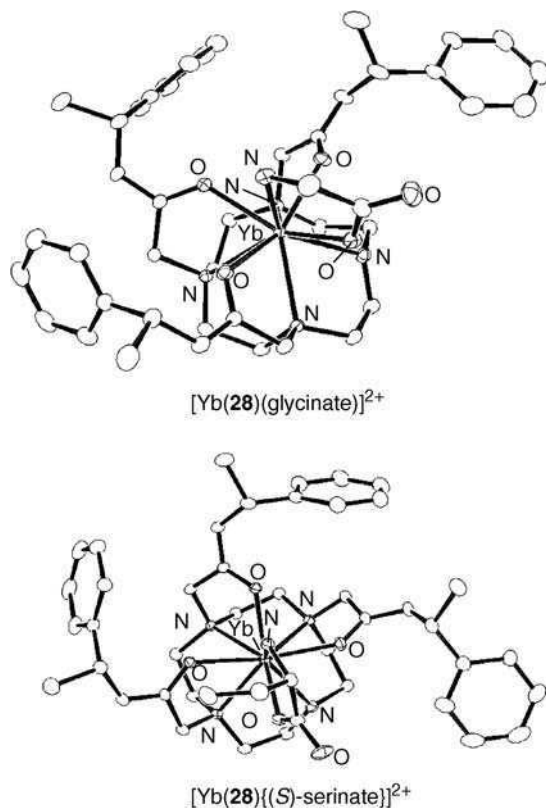
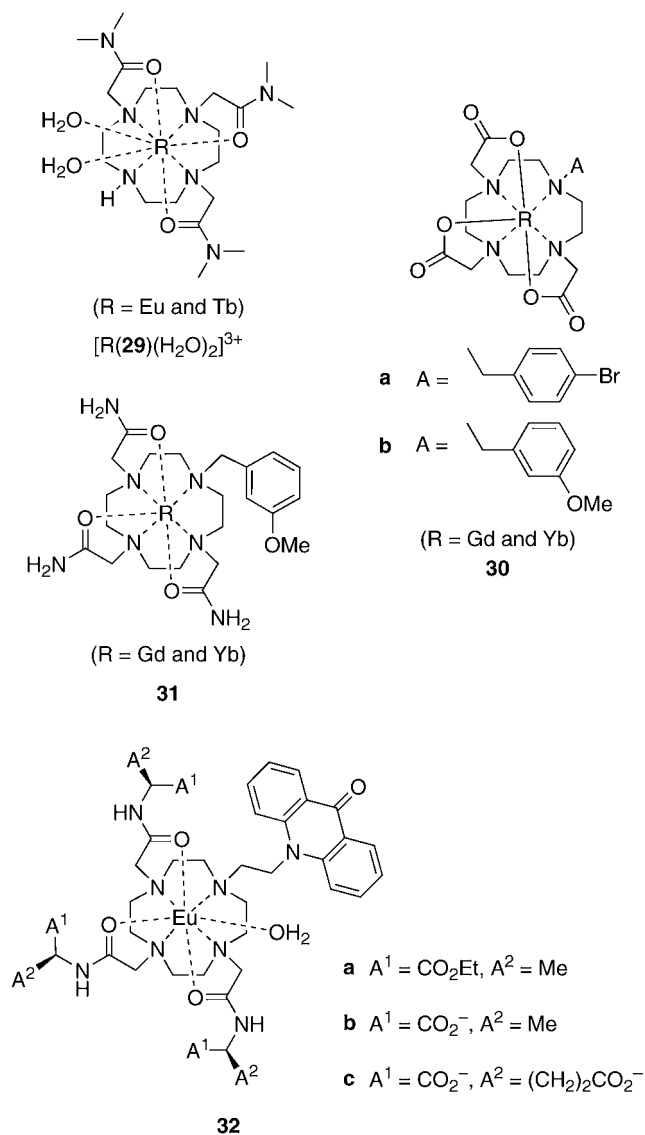


Fig. 16. Crystal structures of highly coordinated ternary complexes between rare earth complexes of heptadentate cyclen **28** and amino acid anions. Redrawn, with permission, after Dickins et al. (2004).

acetate, SO_4^{2-} , H_2PO_4^- , citrate, and HCO_3^- anions, HCO_3^- decreased the hydration number most efficiently and enhanced luminescence intensity, though lactate, citrate, and malonate anions also provided bidentate coordination (Bruce et al., 2000). Since these bidentate guest anions generate different bond lengths and bite angles, they probably provide different steric hindrances and strains in the highly coordinated complexes. Dickins et al. (2002, 2004) further applied Eu^{3+} and Yb^{3+} complexes with chiral cyclen **28** to luminescence sensing of amino acid anions. The crystal structures of ternary adducts between the Yb^{3+} complex and amino acid anions (fig. 16) revealed that $-\text{NH}_2$ and $-\text{CO}_2^-$ groups of the amino acid cooperatively chelate and the two bound water molecules are replaced. Such bidentate coordination effectively results in intense luminescence.

Gunnlaugsson et al. (2002, 2003a) reported effective luminescence sensing of aromatic carboxylate guests using the Tb^{3+} complex with heptadentate cyclen **29** (scheme 7). Replacement of the two coordinated water molecules with bidentate guest anion easily occurred. Although the Tb^{3+} complex does not include intense chromophores, highly coordinated com-



Scheme 7.

plexation promotes efficient energy transfer from the photo-excited guest anion to the Tb³⁺ center, and also suppresses the quenching process of the excited rare earth center by water molecules. The ratio of Tb³⁺ luminescence intensities at several wavelengths significantly depended on the nature of the bound aromatic anions, indicating that the symmetry of the ligand field around the metal center is altered by the guest coordination. Terreno et al. (2003)

prepared the Gd^{3+} and Yb^{3+} complexes **30** and **31** as effective receptors for α -hydroxy-carboxylates, and Atkinson et al. (2004) used the Eu^{3+} complex **32** in the luminescence sensing of phosphorylated glucose, serine, and tyrosine anions. These rare earth complexes have structurally defined binding sites for anion recognition, and work as luminescent receptors effective in water.

Neutral guest species can be similarly sensed by rare earth luminescence. Tsukube et al. (2001) reported that amino alcohol derivatives formed highly coordinated 1:1 complexes with europium tris(β -diketonate) **7** in 1% MeOH/ CH_2Cl_2 solution (fig. 6). The Eu^{3+} luminescence observed at 611 nm was enhanced 2.2-fold upon addition of 10 equivalents of (*S*)- or (*R*)-2-amino-1-ethanol, while corresponding diol, mono-alcohol, and mono-amine derivatives induced no enhancement. A further application for sensing of biogenetic amines and catechol amines can be envisaged.

3.1.3. Luminescence sensing of cationic substrates

Although proton and metal ions do not directly interact with the rare earth ions, they can interact with the ligands in various ways, modifying the absorption bands, redox potentials, energies of excited states, and ligand arrangements. Thus, overall luminescence profiles of the rare earth complex including efficiencies of intersystem crossing, energy transfer, and luminescence quenching processes are often sensitive to the external cationic species (fig. 17).

Rare earth complexes having both Lewis base and chromophoric moieties on the ligands exhibited luminescence spectral changes upon protonation or metal complexation. Fig. 18 illustrates a typical example of a pH-responsive Eu^{3+} complex (**33**), in which the deprotonation of sidearm chromophores modifies the luminescence process (Lowe et al., 2001). When the sulfonamide group on the cyclen sidearm is deprotonated, the resulting amide anion strongly coordinates to the Eu^{3+} center. Since strong coordination from the sidearm anion removes the bound water molecule and also brings the aromatic chromophore closer to the metal center, the quantum yield of the europium luminescence is drastically enhanced. In contrast, the protonated sidearm only weakly coordinated with the rare earth ion, and the luminescence was switched off at acidic pH. When $-\text{CF}_3$, $-\text{Me}$, and $-\text{OMe}$ groups were sub-

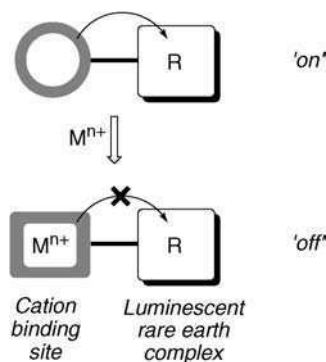


Fig. 17. Cation binding effects on rare earth luminescence.

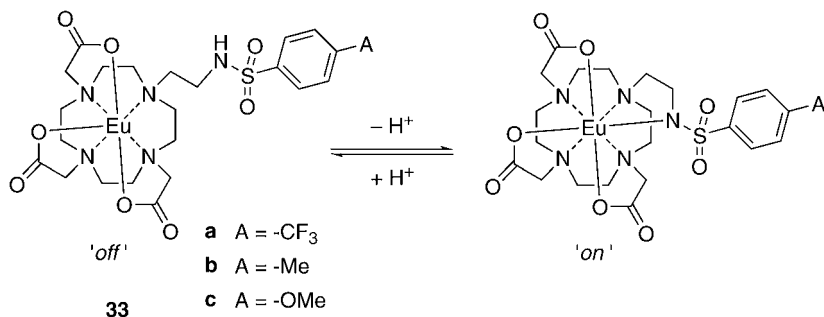
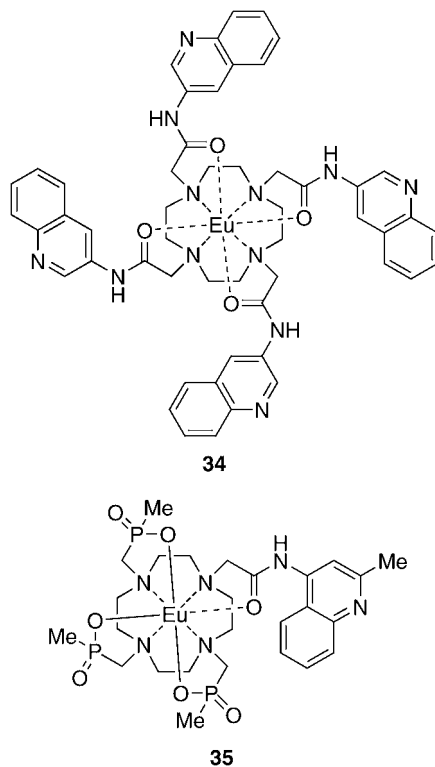


Fig. 18. pH responsive rare earth complexes.



Scheme 8.

stituted at the *para*-position of the phenyl ring, the apparent protonation constants ($\log K_a$) were estimated as 5.7, 6.4, and 6.7, respectively. This means that the pH-responsive ranges of these luminescent probes can be finely tuned by ligand architecture. The Eu³⁺ complexes **34** (Gunnlaugsson, 2001) and **35** (Gunnlaugsson et al., 2001) exhibit pH-responsive luminescence in a different fashion (scheme 8). Since the protonation of quinoline nitro-

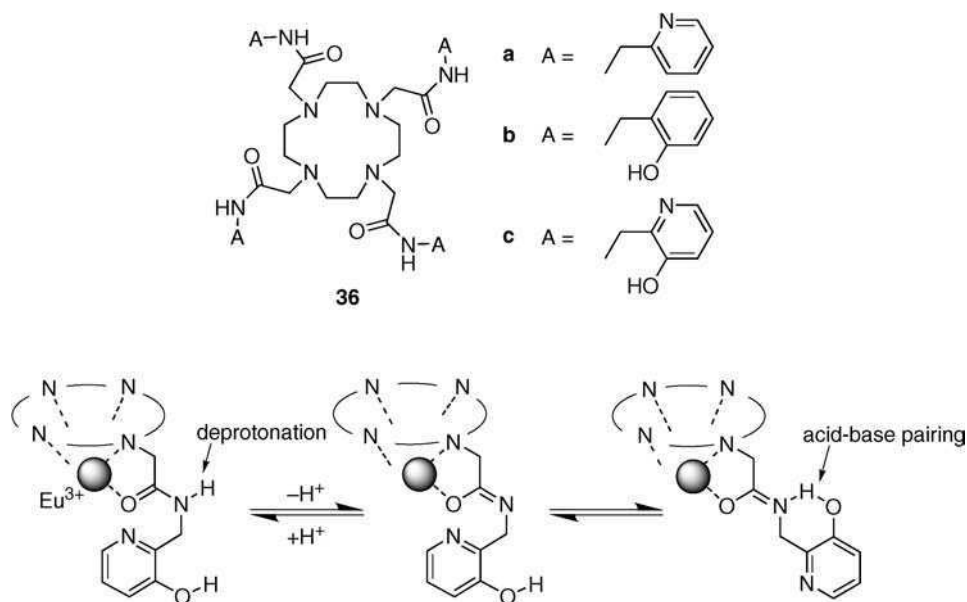


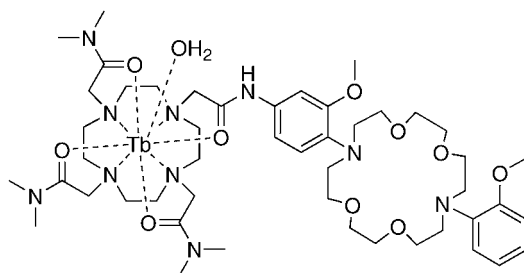
Fig. 19. Deprotonation and intramolecular acid-base pairing in Eu^{3+} -**36c** complex system. Redrawn, with permission, after Woods et al. (2003).

gen atom disturbs energy transfer processes, they act as pH probes. Sherry et al. successfully described another type of pH-responsive rare earth complex **36** (Woods et al., 2003; Woods and Sherry, 2003). When the cyclen **36c** – Eu^{3+} complex is employed, deprotonation of the amide sidearm triggers structural changes and causes significant changes in the europium luminescence patterns as shown in fig. 19.

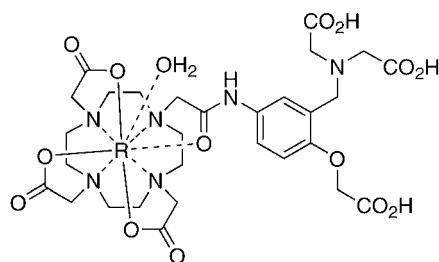
Incorporation of potential metal ion binding sites into the octadentate cyclen ligands results in metal cation-specific luminescent probes. Gunnlaugsson and Leonard (2003) designed the cyclen Tb^{3+} complex **37** (scheme 9), in which a diaza-18-crown-6 ring was introduced on one of the cyclen sidearms. This gave 40-fold enhancement of Tb^{3+} luminescence in the presence of excess K^{+} cations, because the crown-bound K^{+} cation stabilizes the excited state of the Tb^{3+} ion. The Eu^{3+} and Tb^{3+} complexes **38** are effective for sensing transition metal cations. Luminescence intensity increases by 42% and 26% upon Zn^{2+} binding under extracellular conditions (Reany et al., 2000). The Eu^{3+} complex **39** shows reduced Eu^{3+} luminescence intensity in the presence of μM quantity of Cu^{2+} , because this cation is strongly bound to the appended phenanthroline ring and efficiently prevents energy transfer to the Eu^{3+} center (Gunnlaugsson et al., 2003b).

3.1.4. Luminescence sensing of biological substrates

In addition to being luminescent molecular tags, several types of rare earth complexes exhibit elaborate molecular recognition properties for biological substrates. A new class of DNA tar-

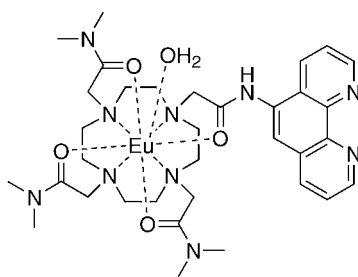


37



(R = Eu and Tb)

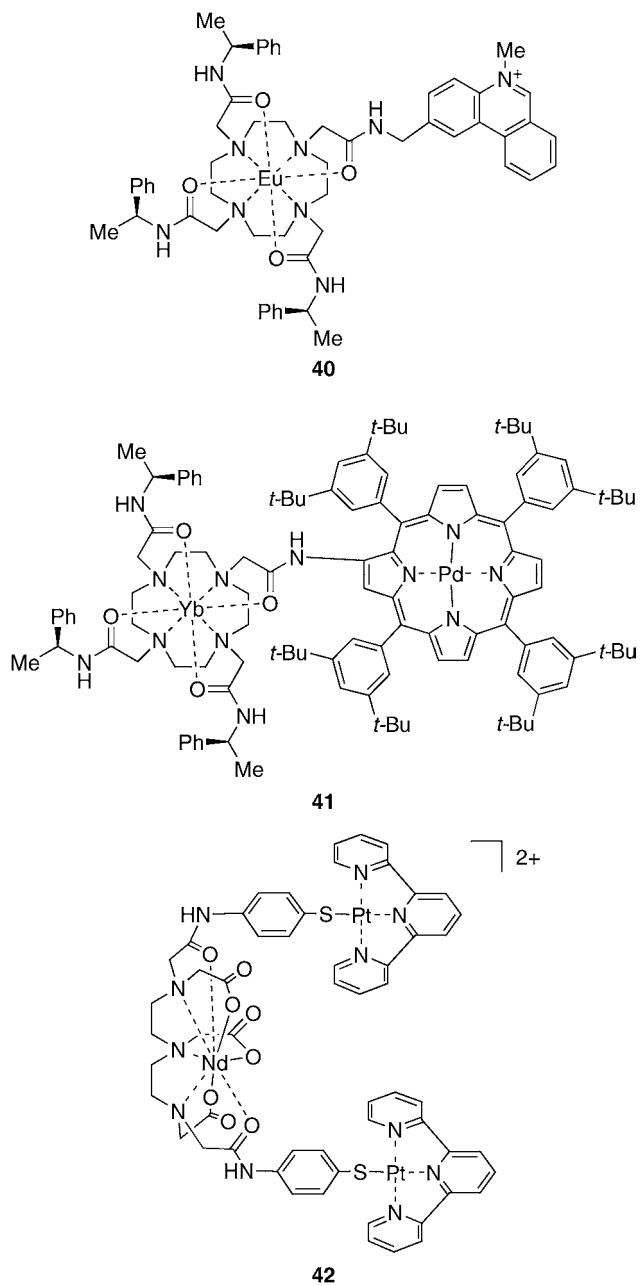
38



39

Scheme 9.

geting reagents has been synthesized by introducing DNA intercalating units into luminescent rare earth complexes. [Govenlock et al. \(1999\)](#) typically combined an octadentate cyclen-Eu³⁺ complex with *N*-methylphenanthridinium moiety (see **40**). Δ - and Λ -isomers of the Eu³⁺ complex **40** ([scheme 10](#)) show different efficiencies in [(CG)₆]₂-phenanthroline intercalation processes, though [(CG)₆]₂ is more strongly bound than [(AT)₆]₂. When Pd²⁺ porphyrinate is linked to an Yb³⁺ cyclen complex ([Beeby et al., 2000](#)), the triplet quenching of the Pd²⁺ porphyrinate by the molecular oxygen is suppressed upon DNA binding. Thus, the Yb³⁺ complex **41** exhibits DNA-responsive NIR luminescence signals. [Glover et al. \(2003\)](#) reported hairpin-shaped Nd³⁺ complex **42**, in which two planar Pt²⁺ complexes act as strong DNA



Scheme 10.

intercalators and also as effective sensitizers of Nd^{3+} NIR luminescence. Since the Nd^{3+} NIR luminescent rare earth complex has a long lifetime (670 ns) and is not perturbed by the photoactive moieties of the targeted biomolecules and their environments, they provide an effective methodology for sensing biological substrates.

3.2. Rare earth complexes for CD sensing

3.2.1. Introduction

Chirality provides crucial information not only in biological systems but also in industrial processes. Several methods have been developed to determine the absolute configuration and to characterize the stereochemical purity of a particular molecule, in which the interactions between the chiral molecule and polarized light are read out. Circular dichroism (CD) spectroscopy is a well-established method, but limited to the measurement of chromophoric chiral molecules. When non-chromophoric molecules are targeted, chromophoric probes should be attached to amplify and transfer the chirality information of the target species. Some rare earth complexes having chromophores were reported as effective CD probes that induced or enhanced the CD signals upon highly coordinated complexation with the chiral targets. As described above, they provide specific molecular recognition for chiral substrates, and the chirality information of the bound species only can be sensed even in the presence of other chiral species. In common chirality probing systems, the chromophores are covalently linked with the chiral substrates. Since the covalent derivatization method usually requires laborious procedures before and after CD measurements, the rare earth complexation method has several advantages of facile procedures and high selectivity.

Rare earth complexes can offer three kinds of CD signals: ligand based CD; metal based CD; and circularly polarized luminescence (CPL) (fig. 4). The two kinds of CD signals are observed as the differences in absorption between left and right circularly polarized lights, and reflect the chirality of the ground state. The CPL signal is an indication of the difference in luminescence intensity between left and right circularly polarized light, and the chirality of the excited state is characterized. When a chromophoric ligand is incorporated into a chiral rare earth complex, intense ligand-based CD signals are often observed. In contrast, metal-based CD or CPL measurements of rare earth complexes require highly concentrated sample solutions, because their $f-f$ transitions are forbidden. The observed signals consist of several transitions arising from the 4f electronic configurations. Thus, the chirality information around the metal center can be precisely analyzed by this method, in the case that one peak comes from only one transition, such as the ${}^5\text{D}_0 \rightarrow {}^7\text{F}$ transition of Eu^{3+} (Riehl and Muller, 2005). We discuss below CD and CPL probing profiles of various rare earth complexes. Based on rare earth coordination chemistry, several strategies are successfully established for the chirality sensing of amino acids, sugars, nucleic acids, and other biological substances.

3.2.2. Chirality sensing with ligand-based CD

Several types of rare earth complexes easily accommodate chiral substrates in their inner-coordination spheres thanks to the high coordination number of the R^{3+} ions. When the rare earth complex includes chromophoric ligands, it can act as an effective CD probe for chirality

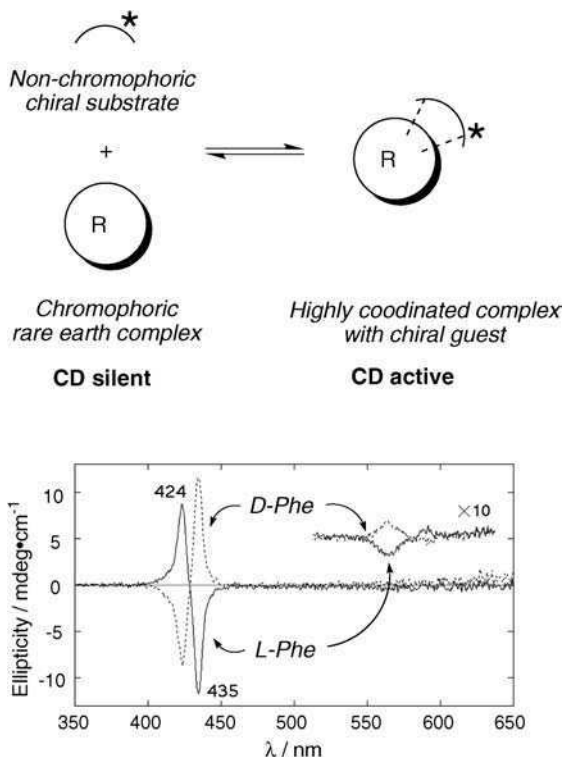
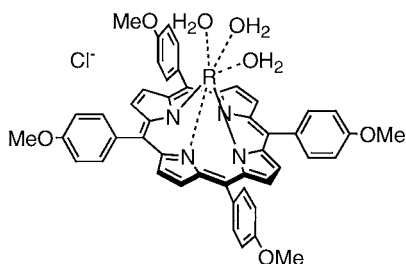
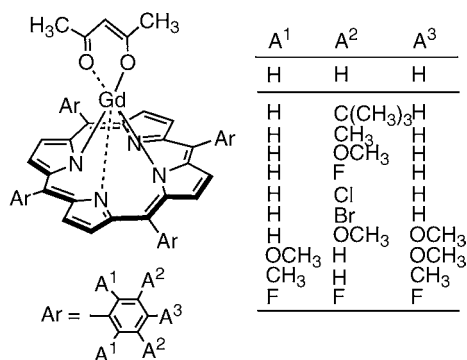


Fig. 20. Formation of CD active species via highly coordinated complexation (above) and CD chirality sensing of phenylalanine with Gd^{3+} complex **44** (below). Reproduced, with permission, after Tsukube and Shinoda (2002).

determination of the substrate (fig. 20). Since the complexation between the rare earth complex and the chiral substrate results in asymmetric arrangements of the chromophoric ligands around the rare earth center, the chiral substrate induces CD signals at the ligand absorption bands, the sign of which is dependent on the substrate chirality.

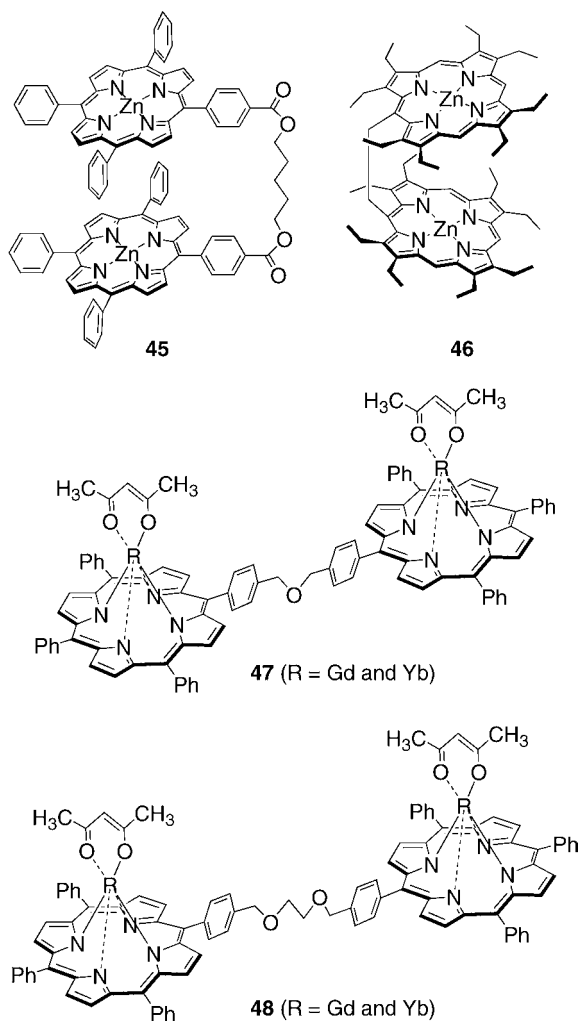
Rare earth tris(β -diketonates) such as **7** were used as effective CD probes for chiral biological substrates, even if they are CD silent. When they form highly coordinated complexes with amino alcohols, the chiral bidentate amino alcohols are bound onto the metal center and organize the diketonate ligands in an asymmetric fashion (fig. 6). Nakanishi and Dillon (1971) and Dillon and Nakanishi (1974) first employed rare earth tris(β -diketonate) **6** to determine the chirality of steroidal diols. Since the resulting highly coordinated complexes are too thermodynamically unstable to obtain reproducible and reliable CD signals, the interaction between the β -diketonate ligand and the rare earth center had to be properly optimized. Tsukube et al. (2001) successfully demonstrated that the use of fluorinated β -diketonate ligands increased the stability of highly coordinated complexes and observed reproducible CD spectra with much improved signal-to-noise ratios. The intensity of the CD signals induced

**43** (R = Y, Eu, and Yb)**44**

Scheme 11.

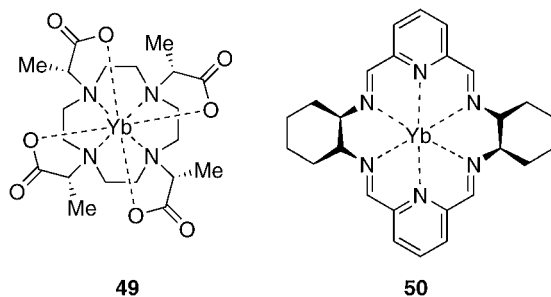
at the β -diketonate absorption bands correlated well with the ionic radius of the rare earth ion: the smallest Yb^{3+} ion gives the most intense CD signals; and the bulky substituent in the β -diketonate ligand also increases the CD intensity. Thus, the geometric match between the β -diketonate and the guest species should be considered in designing CD probes of this type.

Rare earth porphyrinates have been developed as more sensitive CD probes for chiral amino acids. The porphyrinates act as tetradentate ligands for rare earth metal ions and formed 1:1 complexes as well as sandwich-type 2:1 complexes. As the trivalent rare earth ion has larger ionic radius than the cavity size of the porphyrin ring, the rare earth center locates above the porphyrin plane and is coordinated by other anionic ligands and solvent molecules. Wong et al. (1999) reported the crystal structure of cationic rare earth porphyrinates **43** (scheme 11), in which three water molecules directly coordinated to the Yb^{3+} centers while the Cl^- anion located outside the inner coordination sphere. When acetylacetonate was used as co-ligand (see **44**), it coordinated in a bidentate fashion, but further coordination sites were still available for accepting external guests. Since these rare earth porphyrinates exhibit strong absorptions at their B bands (400–450 nm) and Q bands (550–600 nm), as observed with common porphyrin metal complexes, they act as highly sensitive CD probes. Tamiaki et al. (1997) and



Scheme 12.

Tsukube et al. (1999) demonstrated that the series of Gd^{3+} porphyrinate complexes **44** efficiently extract chiral amino acids from neutral aqueous solutions into organic solutions. The resulting organic phases include highly coordinated complexes and display characteristic CD signals at the B and Q bands, though the employed complexes **44** are CD silent in the absence of amino acids (fig. 20). Interestingly, the signs of the observed CD signals correlated well with the configuration of the extracted amino acids, indicating that chirality information is effectively amplified and detected by this type of CD probes. Some of the complexes **44** also extract dipeptides such as Ala–Ala and detect their chirality (Tamiaki et al., 2003). The signs



Scheme 13.

of the CD signals observed at the B band are primarily determined by the stereochemistry of C-terminal side amino acids, suggesting that the carboxylate group of the dipeptide strongly coordinates to the Gd^{3+} center.

When two or more porphyrinate chromophores are bridged in an asymmetric fashion, the chromophore absorption bands display an exciton coupled CD signal, and its sign provides a good indication of the absolute configuration of the bridging chiral substrate. Kurtán et al. (2001a, 2001b) and Borovkov et al. (2001) reported the flexible zinc porphyrin dimers **45** and **46** as CD probes for chiral diamine substrates (scheme 12). The two porphyrins are asymmetrically positioned upon amine coordination and give intense CD signals in their B band spectral ranges. When two rare earth porphyrinates are linked together, the resulting dimers **47** and **48** simultaneously bind cystine and related polyions including two amino acid moieties (Tsukube et al., 2002b). Adjustment of the spacer length of the porphyrinate dimer to fit the binding sites of the targeted polyion allows precise discrimination between cystine and homocystine. The formed ternary complexes give intense CD signals, the sign of which reflects the absolute configuration of the bound polyion. Since their CD intensities were much higher than those observed with the monomeric rare earth porphyrinate, the two rare earth porphyrinates were suitably arranged in the dimer to give intense CD signals reflecting a supramolecular chirality.

3.2.3. Chirality sensing with metal-based CD

The rare earth ions have many excited states and exhibit characteristic absorption bands in the visible and near-infrared regions. Although they generally have low absorptivity and give weak metal-based CD signals, the chiral environments around the metal centers can be sensed. In particular, the f–f transition of the Yb^{3+} ion between the ${}^2F_{7/2}$ and ${}^2F_{5/2}$ levels is magnetically allowed and generates a characteristic NIR luminescence band around 980 nm. Since most organic compounds have no absorption in this spectral range, Yb^{3+} complexes act as unique CD probes. Di Bari et al. (2000) reported the solution NIR CD spectrum of the chiral Yb^{3+} complex **49** (scheme 13). In such a C_4 symmetric complex, the ground state (${}^2F_{7/2}$) and excited state (${}^2F_{5/2}$) split into 4 and 3 doubly degenerated levels, respectively (fig. 21). The energy differences between sub-levels in the ground state are so small that the higher levels are sufficiently populated according to Boltzman distribution at room temperature, and thus

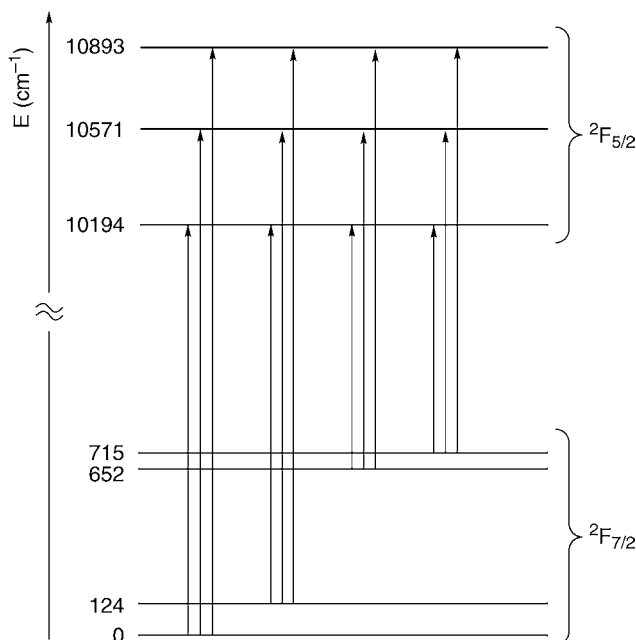


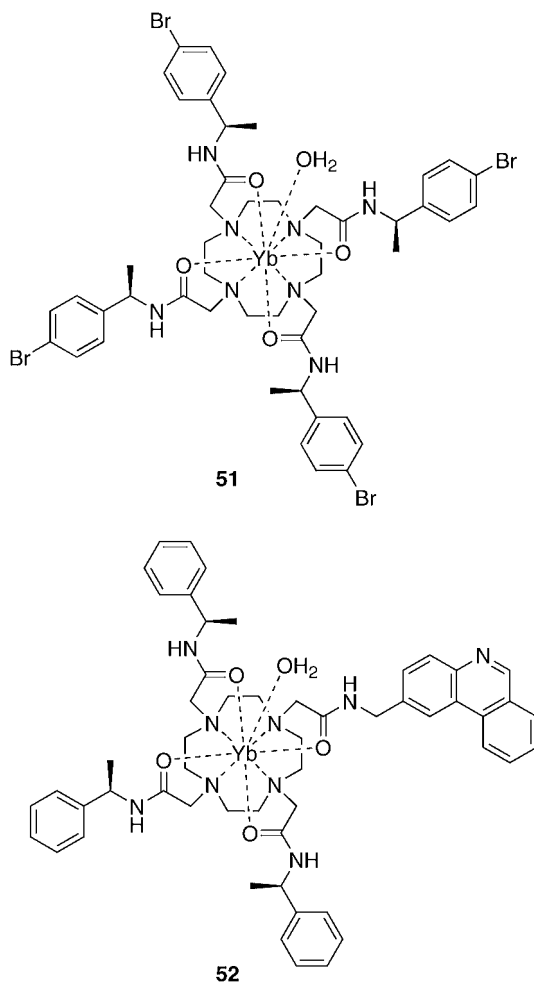
Fig. 21. Electronic transitions of Yb^{3+} in a C_4 symmetric complex. Redrawn, with permission, after Di Bari et al. (2000).

12 transitions take place around 980 nm. Indeed, complex **49** exhibited several well-resolved metal-based CD signals with different signs and amplitudes, which were good indications of the fine complex structures. Di Bari et al. (2003) further discovered that the NIR CD spectra of $\text{M}_3[\text{Yb}\{(S)\text{-binol}\}_3]$ complexes **10** are very sensitive to the chiral coordination environments.

Lisowski et al. (2004) characterized macrocyclic Yb^{3+} complex **50**, in which two external substrates locate on both sides of the macrocyclic plane. Since the intensity and shape of its NIR CD signals were determined by the nature of axially coordinating anion, this complex was appropriate for anion sensing. The order of anion effects on the NIR CD signals was confirmed to be $\text{PhSO}_3^- < \text{Cl}^- < \text{NO}_3^- < \text{AcO}^- < \text{phenylphosphate}^{2-}$, $\text{diphenylphosphate}^-$. Because of the uncommon wavelength of the magnetically allowed f-f transition, the structurally defined Yb^{3+} complexes are particularly promising NIR CD probes for chemical and biological targets.

3.2.4. Chirality sensing with metal-based CPL

Metal-centered circularly polarized luminescence (CPL) can also be observed for rare earth complex. Since the luminescence from a chiral rare earth complex is circularly polarized, the chirality of the excited states can be determined. Most reported CPL studies have dealt with luminescent Eu^{3+} and Tb^{3+} complexes. Racemic Tb^{3+} complex **16** generates non-racemic excited states upon interaction with chiral species. Its CPL signals are enantioselectively quenched by biological vitamin B_{12} derivatives (Meskers and Dekkers, 2001), cytochrome *c*



Scheme 14.

(Meskers et al., 1998a), and blue copper proteins (Meskers et al., 1998b). The employed Tb^{3+} complex is trianionic, and the electrostatic interaction with positively charged protein surface is significantly involved in their quenching processes. Since the replacement of amino acid residues of the metalloproteins greatly modifies the quenching efficiency and enantioselectivity, local structures of the metalloprotein can be sensed by this type of CPL probes.

Maupin et al. (1998, 2000) applied chiral cyclen Yb^{3+} complexes **51** and **52** (scheme 14) as CPL probes. As described above (see section 3.1.2), the nona-coordinated complex **51** has a helically twisted ligand arrangement, and shows high emission dissymmetry factors. Since its helical twist angle is sensitively modified by the nature of the axially coordinated ligand, the

guest-induced transition is monitored by CPL spectroscopy. A similar cyclen Yb³⁺ complex based on the DNA intercalating unit **52** gives an intense CPL spectrum and acts as a chirality probe of DNA strands.

Rare earth complexes form highly coordinated ternary complexes with rapid ligand exchange, flexible conformation, and versatile stoichiometry. Since their CPL spectra give unique information about their chirality, further advances in instrument technology and rare earth complex chemistry will create more intelligent rare earth probes effective in life sciences and materials technology.

4. Magnetic sensing via rare earth probes

4.1. Rare earth complexes for NMR sensing

4.1.1. Introduction

Since the trivalent rare earth metal cations have strong ionic characters and, except for La³⁺ and Lu³⁺, are paramagnetic, their complexes induce two types of “lanthanide-induced shifts” (LIS) in NMR spectra: a “contact shift” resulting from the presence of unpaired electron spin density at the resonating nucleus; and a “dipolar shift” caused by a dipolar interaction between the electronic magnetic moment and the nuclear spin (Horrocks, 1970). Since the anisotropic dipolar shift generally has a larger contribution than the isotropic shift, the dipolar shift observed is proportional to the magnetic susceptibility anisotropy including two independent tensors, χ_{\parallel} and χ_{\perp} . Fig. 22 shows the observed induced shifts for α -methylene proton resonance of *n*-hexanol (0.8 M) in the presence of rare earth tris(2,2,6,6-tetramethyl-3,5-heptanedionate) complex **6** (0.1 M) in CDCl₃ (Horrocks and Sipe, 1971). Among the early rare earth metals, Pr³⁺ complexes give the largest upfield shifts and Eu³⁺ complexes provide the largest downfield shifts. Among the later rare earth metal complexes, the Dy³⁺ complexes cause the largest upfield shifts and Tm³⁺ complexes the largest downfield shifts. Similar trends were confirmed for 4-picoline-*N*-oxide and 4-vinylpyridine. In the isostructural series R(C₂H₅SO₄)₃·9H₂O, the Pr³⁺, Nd³⁺, Sm³⁺, Dy³⁺, and Ho³⁺ salts have $\chi_{\parallel} > \chi_{\perp}$, while the Er³⁺ and Yb³⁺ salts exhibit a reverse trend $\chi_{\parallel} < \chi_{\perp}$. Thus, the relative tensor size of the rare earth complex is important in determining the direction and amplitude of the dipolar shift. Pr³⁺, Eu³⁺, and Yb³⁺ complexes have often been used as NMR shift reagents because they induce large shifts without signal broadening (Forsberg, 1996). Although Gd³⁺ complexes severely broaden the signals due to seven singly occupied 4f-orbitals, some of them were successfully employed in the MRI technique as described below.

Chiral NMR shift reagents (CSRs) have many practical applications in chemistry, biology, medicine, and related fields. A pair of enantiomers exhibit markedly different biological properties but provide the same chemical shifts in NMR measurements. Since the diastereomers have different chemical shifts (Wenzel and Wilcox, 2003; Jacobus and Raban, 1969; Viswanathan and Toland, 1995; Parker, 1991), the chiral anions and cations have often been mixed with pairs of enantiomers for signal separation (Jodry and Lacour, 2000). The effective CSRs of rare earth metal complexes should have high stability in the presence of interfering

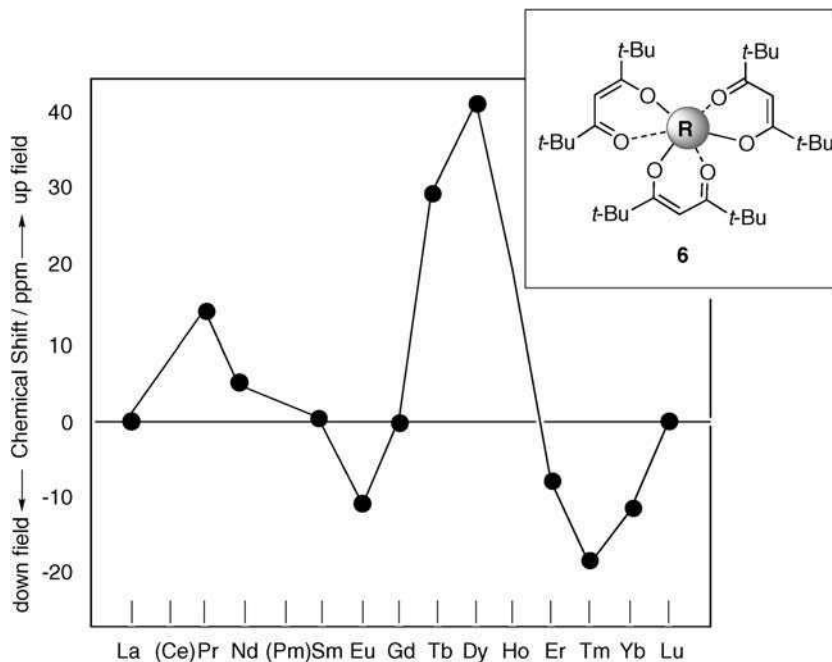
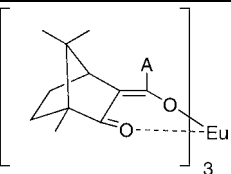
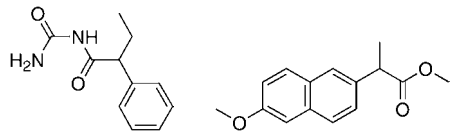
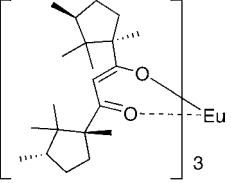
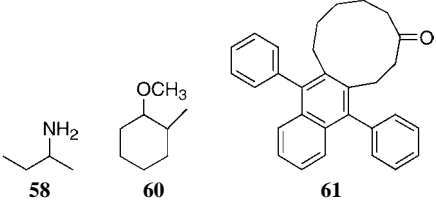
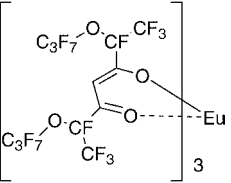
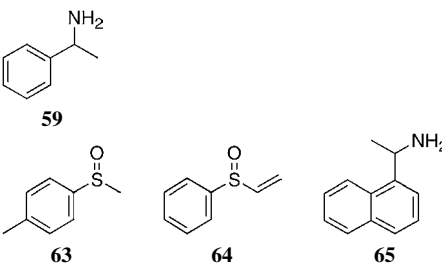
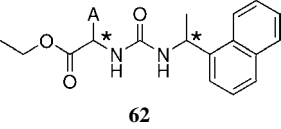
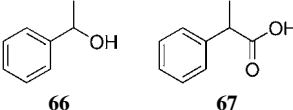


Fig. 22. Shifts of the $^1\text{H-NMR}$ signal for the α -methylene proton of *n*-hexanol induced by rare earth tris(β -diketonates) **6**. Redrawn, with permission, after Horrocks and Sipe (1971).

species and also binding sites available for coordination of external target substrate. When the chiral rare earth complex forms a highly coordinated complex with a chiral substrate, the resulting diastereomeric complex exhibits different chemical shifts from those of the stereoisomers. This phenomenon has been widely applied in the determination of enantiomer excess and/or assignment of absolute configuration of chiral substrates (Wenzel, 1987). Since complexation of the chiral substrate does not involve any covalent bond, the substrate can be easily recovered by column chromatographic or other separation techniques.

Table 2 lists typical CSR reagents with Eu^{3+} ions which were used for the determination of enantiomeric purity of several chiral organic substrates. Europium tris(β -diketonates) **9**, **53–55** preferred oxygen- and nitrogen-containing biological substrates such as pheneturide **56** (anticonvulsant) (Byrne and Rothchild, 1999), naproxen methyl ester **57** (anti-inflammatory agent) (Hanna and Lau-Cam, 1992), and chiral amines **58** and **59** (McCreary et al., 1974; Kawa et al., 1982). The Eu^{3+} complex **54** allows to distinguish the pairs of chiral ether **60** and helical naphtho[9]annulene **61**, the $^1\text{H-NMR}$ signals being well separated (McCreary et al., 1974; Anastassiou and Hasan, 1982). Eu^{3+} complexes with chiral 1-(1-naphthyl)ethylureas **62** are effective for NMR measurements of the chiral sulfoxides **63** and **64** as well as amine **65**, alcohol **66**, and carboxylic acid **67** (Wenzel et al., 1997). Since most of rare earth CSRs operate only in organic solvents, they are severely limited for targeting water-soluble substrates.

Table 2
 Typical chiral shift reagents containing Eu³⁺ ions and the substrates they resolve best

Complex/ligand	Substrate	Solvent
 <p>9: A = C₃F₇ 53: A = CF₃</p>	 <p>56 57</p>	CDCl ₃
 <p>54</p>	 <p>58 60 61</p>	C ₆ D ₆ CDCl ₃ CCl ₄
 <p>55</p>	 <p>59 63 64 65</p>	CCl ₄
 <p>62</p> <p>A = CH(CH₃)₂, CH₂CH(CH₃)₂, C(CH₃)₃</p>	 <p>66 67</p>	CDCl ₃

This section focuses on recent advances in rare earth CSRs which allow chirality sensing in aqueous solutions. Various substrates of biological and pharmaceutical importance are known to exhibit chirality-dependent activities and functionalities in aqueous solutions. Because water and hydroxide provide particularly strong coordination with the rare earth center in water, the targeted substrates should compete with the environmental water molecules in the formation of highly coordinated ternary complexes with rare earth CSRs.

When the rare earth metal cation is unsaturatedly coordinated by the initial ligands, the additional neutral or anionic substrate occupies the vacant sites of the metal ion to

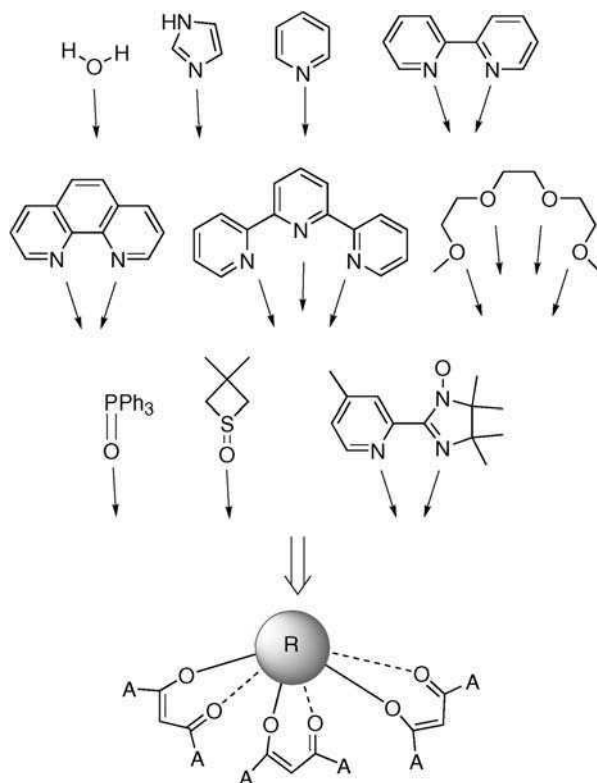


Fig. 23. External guest species yielding highly coordinated ternary complexes with rare earth tris(β -diketonates).

form a highly coordinated ternary complex, though water molecule and hydroxide anion are particularly competing in aqueous media. Fig. 23 illustrates typical examples of the external guest species for tris(β -diketonates) such as **6**, **7**, and **9**. These include two water molecules (Phillips et al., 1968; Kooijman et al., 2000), imidazole (Wayda et al., 1990), pyridine (Cramer and Seff, 1972), 2,2'-bipyridine (van Staveren et al., 2001; Batista et al., 1998), 1,10-phenanthroline (Watson et al., 1972; Christidis et al., 1998), 2,2':6',2''-terpyridine (Holz and Thompson, 1988), polyether (Evans et al., 2002; Baxter et al., 1995), phosphate (Petrov et al., 2002; Brittain, 1983), aliphatic amines (Brittain, 1979), alcohols (Brittain and Richardson, 1976), acetone (Plakatouras et al., 1994), acetamide (Brittain, 1982), dimethylformamide (Cunningham and Sievers, 1980), and others (Wing et al., 1973; Tsukuda et al., 2002). Some of the highly coordinated ternary complexes are stable and can be isolated as crystals. The rare earth complexes with edta ligand have been also characterized. Fig. 24 compares two rare earth metal complexes, in which the metal cations are coordinated by four carboxylate anions and two amine nitrogens of the edta ligand. Interestingly, the complex with the larger Dy^{3+} ion has three additional water molecules (Nassimbeni et al., 1979)

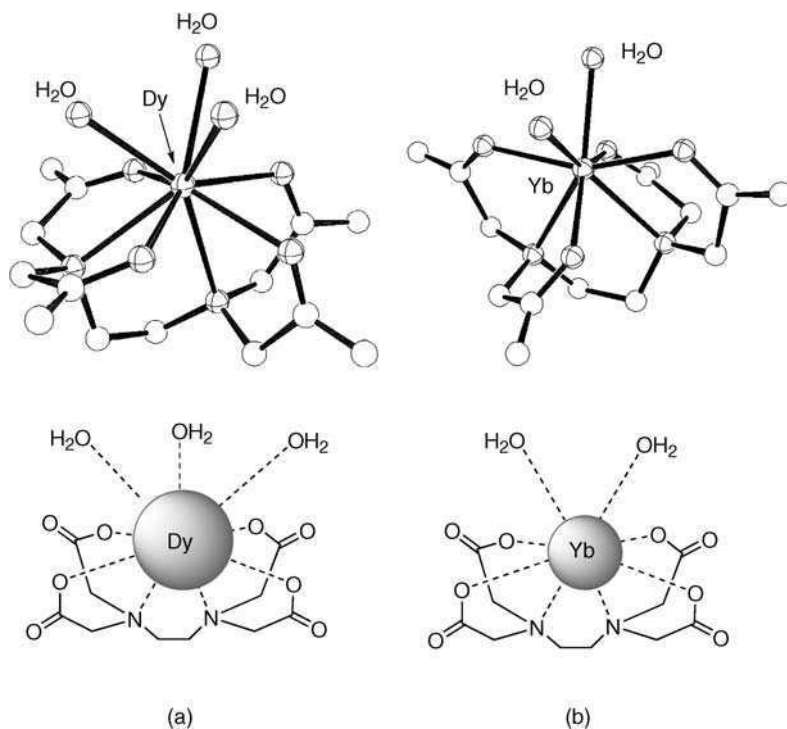
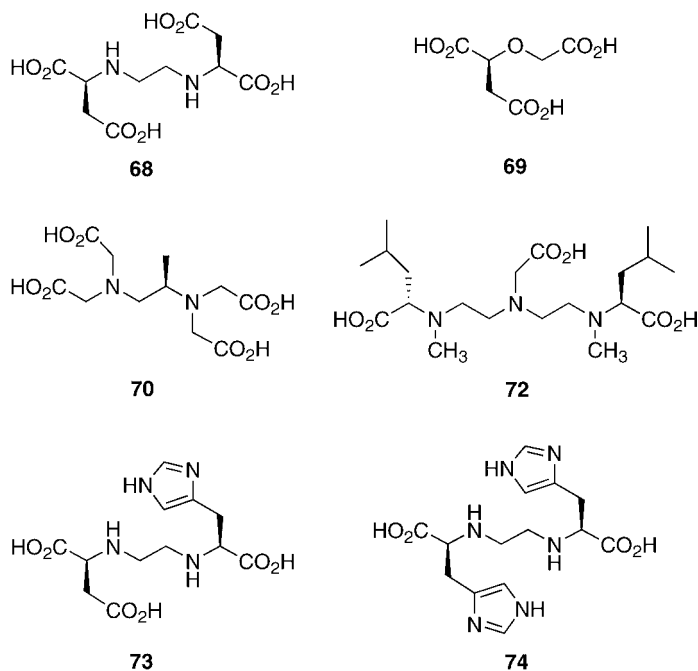


Fig. 24. Crystal structures of (a) $[\text{Dy}(\text{edta})(\text{H}_2\text{O})_3]^-$ and (b) $[\text{Yb}(\text{edta})(\text{H}_2\text{O})_2]^-$ complexes. Redrawn, with permission, after Nassimbeni et al. (1979) and Sakagami et al. (1997).

and the complex with the smaller Yb^{3+} ion incorporates two water molecules (Sakagami et al., 1997). Thus, a proper combination of primary ligand and rare earth ion allows the design of effective CSRs having predetermined coordination numbers.

4.1.2. Chirality sensing in aqueous solutions

Reuben (1979, 1980) reported the first example of CSRs operating in aqueous media. The enantiomeric methyl proton signals of the non-racemic mixture of lactate are separated in the presence of EuCl_3 , indicating that the Eu^{3+} complex with the chiral lactate is formed in situ and acts as an effective CSR. Since this pioneer work, several types of water-soluble CSRs have been developed for detection of chiral, unprotected α -amino acids without signal broadening. Kido et al. (1991) have successfully showed that an Eu^{3+} complex with chiral polyaminocarboxylic acid **68** (scheme 15) separates the α -proton signals of L- or D-phenylglycine. The stability constants of its highly coordinated ternary complexes were estimated as 6.1 for the D-isomer and as 3.7 for the L-isomer at pH = 9.5. Their detailed structures have not been determined, but the enantiomer-selective complexation resulted in a useful CSR phenomenon. The cationic Yb^{3+} complex with chiral heptadentate ligand **28** was recently re-



Scheme 15.

ported to resolve a pair of enantiomeric CH and CH₃ resonances of lactate with large induced shifts ($\Delta\Delta\delta \sim 10$ ppm) (Dickins et al., 2001). As shown in fig. 13, this type of cyclen-rare earth complexes bind lactate and other bidentate substrates. Since the formation constants of the highly coordinated ternary complexes with the two lactate enantiomers are almost the same ($\log K = 3.7$ in water for Eu³⁺-**28** complex) (Bruce et al., 2000), enantiomer-selectivity in the thermodynamic sense is not always necessary for NMR chirality sensing.

Other rare earth metal complexes proved to be effective CSRs. The Eu³⁺ complexes with chiral polyaminocarboxylic acid ligands **69** (Peters et al., 1983) and **70** (Kabuto and Sasaki, 1984, 1987, 1989, 1990; Kabuto et al., 1992) induce excellent separation of the α -H signals of α -amino acids under weak acidic or weak alkaline aqueous conditions. The Eu³⁺ complex with ligand **70** was further used in enantiomer purity determination of α -hydroxy carboxylic acids, α -methyl- α -amino acids, and aldonic acids. Although these Eu³⁺ complexes with polyaminocarboxylic acid ligands **68–70** work under acidic (pH = 3–5) or alkaline (pH = 9–10) conditions, the Eu³⁺ complex with neutral polypyridine ligand **71** is also efficient in the case of unprotected α -amino acids at neutral pH (Hazama et al., 1996). Its crystal structure clearly indicates that it accommodates two chloride anions (fig. 25), which can be easily replaced by bidentate substrates to give highly coordinated ternary complexes. This resulted in the α -H signals of (*S*)-amino acids appearing at higher magnetic field than those of the (*R*)-isomers. The Eu³⁺ complex with chiral diethylenetriamine-based ligand **72** also

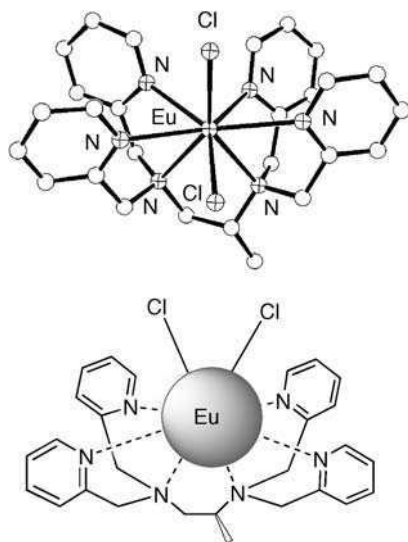


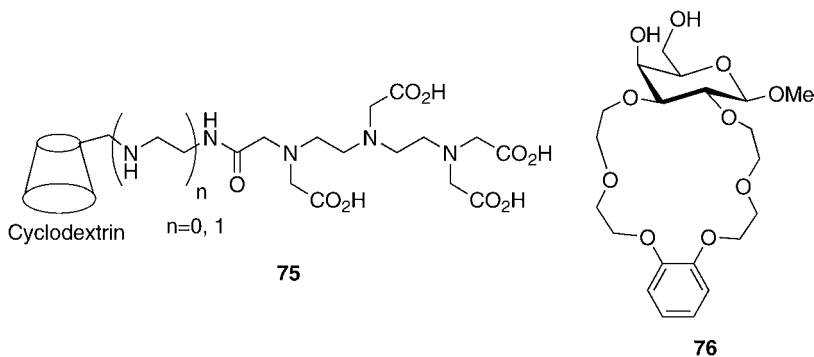
Fig. 25. Crystal structure of $[\text{Eu}(\mathbf{71})\text{Cl}_2]^+$. Redrawn, with permission, after Hazama et al. (1996).

works as a CSR for α -amino acids and N-protected oligopeptide at neutral pH (Watanabe et al., 2001).

The total charge of the rare earth metal complexes largely influences their CSR ability. When Eu^{3+} complexes with polyaminocarboxylic acids **68**, **73**, and **74** are compared under neutral pH conditions, the signal separation of isoleucine protons is apparently dependent on the total charge of the CSRs: ligand **68** having four COOH groups results in a broadening of the signals of most protons; the complex with ligand **73** having three COOH groups gives slightly separated α -CH and γ -CH₃ proton signals; and the complex with ligand **74** having two COOH groups provided clearly separated signals for all protons. Since these three Eu^{3+} complexes have the same ligand chirality and high stability in water, both the structure and charge of the employed rare earth metal complex should be considered in the design of CSRs (Takemura et al., 2001).

4.1.3. Chirality sensing with hybrid probes

Grafting a receptor moiety onto rare earth metal complexes led to a new series of CSRs operating in water. Dy^{3+} complexes with cyclodextrin derivatives **75** (scheme 16) were synthesized as hybrid-type CSRs in which the triaminotetracarboxylic acid moiety chelates the rare earth ion while the chiral cyclodextrin accommodates aromatic compounds in its hydrophobic pocket (Wenzel et al., 1994, 2000). Wenzel et al. (2003) demonstrated that the commercially available sulfonated and carboxymethylated cyclodextrins are effective CSRs for water-soluble aromatic cations in the presence of Dy^{3+} or Yb^{3+} . A crown ether derivative, which accommodates primary ammonium cations, also forms chelates with rare earth



Scheme 16.

metal cations through its β -diol unit (see **76**). Its Yb^{3+} complex enhances the separation of enantiomeric proton signals of several protonated primary amines (Wenzel et al., 2001).

4.1.4. Chirality sensing with dynamic probes

As mentioned above, some rare earth metal complexes with achiral ligands exist as racemic mixtures in solution. Rare earth complexes such as **30** and **31** with heptadentate cyclens are typically present as an equimolar mixture of Δ - and Λ -isomers according to the orientation of the coordinating arms (fig. 26) (Terreno et al., 2003). When Yb^{3+} complex **30b** interacted with (*S*)- α -hydroxylcarboxylate, each diastereomer exhibited different NMR chemical shifts, and the absolute configuration of the substrate as well as the enantiomeric purity were determined. The stability constants K of the ternary adducts were determined for the Gd^{3+} complex **30b**. (*S*)-Tartrate $[(\text{HO})\text{CH}\{\text{CH}(\text{OH})\text{CO}_2^-\}\text{CO}_2^-]$ exhibited larger K value (3000) than (*S*)-lactate $[(\text{HO})\text{CH}(\text{CH}_3)\text{CO}_2^-]$ (1500), (*S*)-malate $[(\text{HO})\text{CH}(\text{CH}_2\text{CO}_2^-)\text{CO}_2^-]$ (500), and (*S*)-trifluorolactate $[(\text{HO})\text{CH}(\text{CF}_3)\text{CO}_2^-]$ anions (90) at neutral pH. In the ^1H -NMR experiments with **30b**, the more efficient tartrate anion preferred one predominant isomer to the other, while lactate gave a mixture of two diastereomeric ternary complexes.

4.1.5. Chirality sensing with high resolution NMR spectrometers

High resolution NMR spectrometers often cause serious line broadening with common Pr^{3+} -, Eu^{3+} -, and Yb^{3+} -containing CSRs. To overcome this problem, other rare earth ions have been incorporated in CSRs, which are less paramagnetic. Kabuto et al. reported that Sm^{3+} and La^{3+} complexes with ligands **70** and **71** separate the enantiomer resonances of α -amino acids without signal broadening (Sato et al., 1999; Inamoto et al., 2000). As shown in fig. 27, the Sm^{3+} complex with **70** completely separates a pair of enantiomer signals of asparagine with sharp line shapes, though its Eu^{3+} complex causes serious signal broadening. This Sm^{3+} complex induces well-separated ^1H -NMR signals for 15 kinds of α -amino acids, though shifts are inverted compared with those induced by the corresponding Eu^{3+} complex (see fig. 22).

Kabuto et al. successfully modified Mosher's method to determine the absolute configuration of chiral organic compounds with diamagnetic lanthanum tris(β -diketonate) **77** (Omata

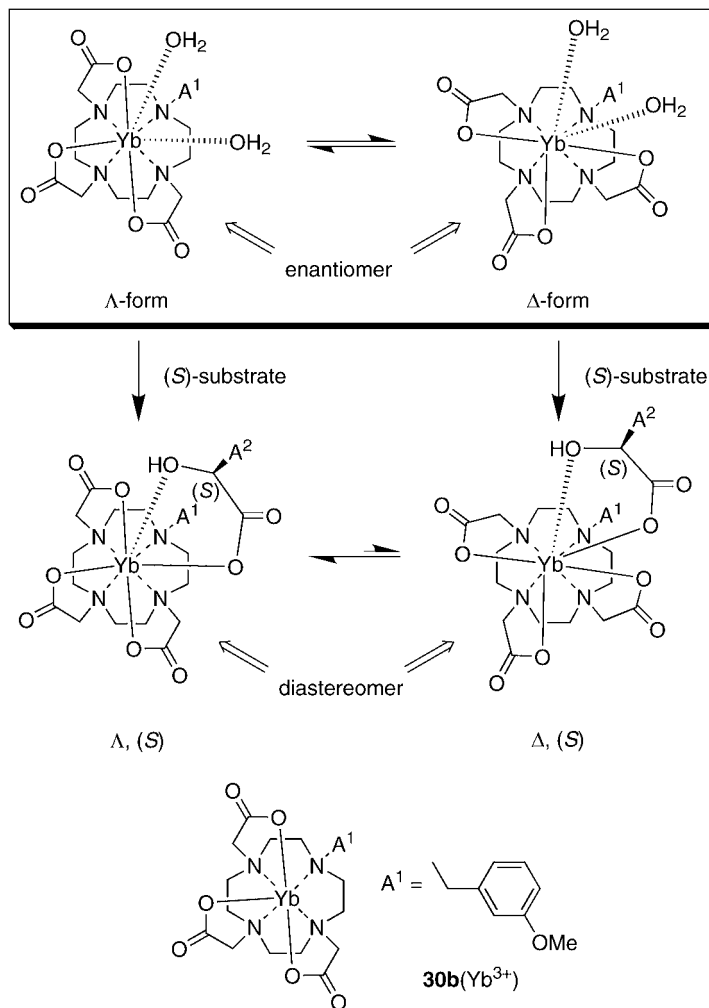


Fig. 26. Diastereomeric complexes between (S) - α -hydroxycarboxylate with **30b**(Yb^{3+}) complex.

et al., 2002). To determine the configuration of secondary alcohols or primary amines, (R)- and (S)-MTPA chloride (MTPA = α -methoxy- α -(trifluoromethyl)phenylacetic acid) were reacted with substrates to yield pairs of diastereomers. Since the proton of the L^1 or L^2 group is shielded by the phenyl ring (see fig. 28), the chemical shift difference ($\Delta\delta = \delta_S - \delta_R$) of L^1 between (R)- and (S)-derivatives is positive and that of L^2 is negative (Dale and Mosher, 1973). When La^{3+} complex **77** was added, the bidentate chelation of methoxy oxygen and carbonyl oxygen to the La^{3+} center inverted the relative position of L^1 and L^2 groups with respect to the phenyl ring. As a result, the relative positions of diastereomeric signals of MTPA derivatives became inverted, compared with those obtained by the common Mosher's method.

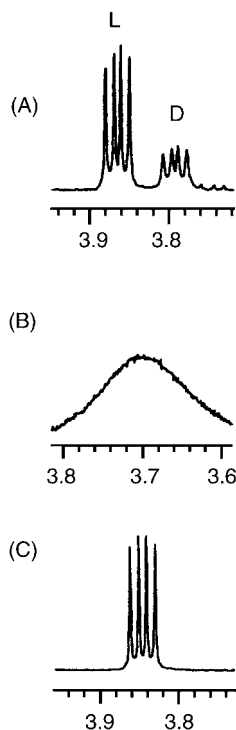


Fig. 27. $^1\text{H-NMR}$ (400 MHz) signals for $\alpha\text{-CH}$ group of asparagine (D/L = 1/2) in D_2O : (A) $[\text{Sm-70}]/[\text{asparagine}] = 0.10$, pH = 9.3; (B) $[\text{Eu-70}]/[\text{asparagine}] = 0.02$, pH = 8.9; (C) no shift reagent, pH = 9.3. Reproduced, with permission, after Inamoto et al. (2000).

Several types of CSRs effective in aqueous or other polar media have been successfully developed. Since their coordination chemistry was often not investigated in detail, further characterization of their host-guest behavior with CD, CPL, luminescence and other spectroscopic methods would be useful to help more accurate design of new CSRs for biological substrates.

4.2. Rare earth complexes for MRI sensing

4.2.1. Introduction

Magnetic resonance imaging (MRI) is one of the most effective NMR techniques in the clinical field (Caravan et al., 1999; Tóth et al., 2004), which provides important information on damaged tissues in the living body. The resonance of water proton exhibits spin-lattice (longitudinal) relaxation time (T_1) and spin-spin (transverse) relaxation time (T_2) which depend on pH, temperature, and properties of their microenvironments (Lauffer, 1987). Many kinds of Gd^{3+} complexes have already been employed as effective MRI contrast agents, because the

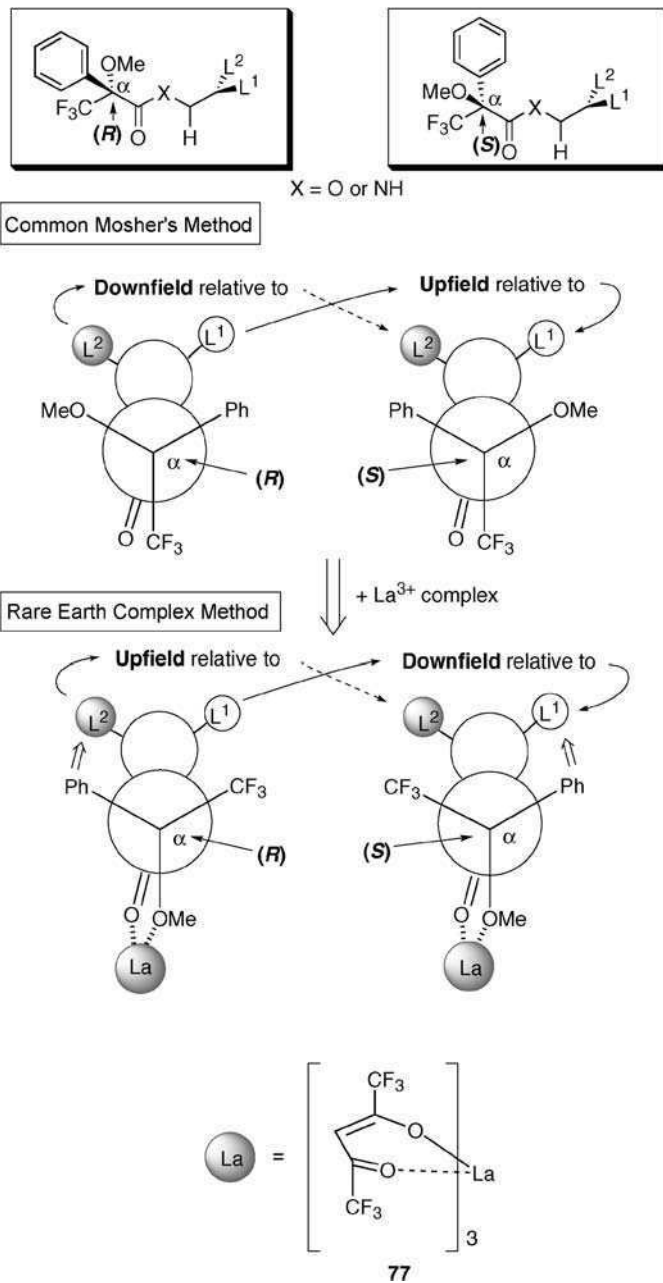


Fig. 28. Configurational correlation models for (*R*)- and (*S*)-MTPA derivatives. Redrawn, with permission, after Dale and Mosher (1973).

Gd^{3+} center contains seven unpaired electrons, binds a considerable number of water molecules, and rapidly exchanges them with bulk water molecules. Practical MRI contrast agents should have (1) high solubility in neutral aqueous media, (2) high thermodynamic and kinetic stability under physiological conditions, (3) non-toxicity, (4) fast excretion, and (5) tissue selectivity.

Gd^{3+} complexes with macrocyclic and acyclic polyaminocarboxylic acid ligands **78–80**, **8** are typical MRI contrast agents (Caravan et al., 1999). Although they effectively encapsulate the Gd^{3+} cation and form stable complexes in water ($\log K = 16\text{--}25$), their metal centers have free coordination sites for water molecules and their unpaired electrons reduce the relaxation times T_1 and T_2 (fig. 29) (Ruloff et al., 1998; Aukrust et al., 2001; Dubost et al., 1991; Kumar et al., 1994). The exchange processes of the coordinated water molecules (inner-sphere water) and hydrogen-bonded water molecules (2nd-sphere water) with bulk water molecules have a significant influence on the reduction of the relaxation times (fig. 30). Therefore, the structural and electronic factors of the Gd^{3+} complex should be controlled to attain dynamic water exchange.

When polyaminocarboxylic acid ligands **81a** and **81b** (scheme 17) form Gd^{3+} complexes, the chiral centers are induced on central nitrogen atoms besides chiral carbon centers. The resulting diastereomeric Gd^{3+} complexes exhibited different water exchange rates: $(1.4 \pm 0.1) \times 10^8 \text{ s}^{-1}$ and $(2.6 \pm 0.2) \times 10^8 \text{ s}^{-1}$ for Gd^{3+} –**81a** complex; $(1.8 \pm 0.1) \times 10^8 \text{ s}^{-1}$ and $(4.4 \pm 0.2) \times 10^8 \text{ s}^{-1}$ for Gd^{3+} –**81b** complex (Burai et al., 2003). In addition to the asymmetry perturbations, other structural factors significantly influence the cation–water binding interaction. Typically, the Gd^{3+} complexes **82** and **83** exhibit markedly different water coordination modes, though both include octadentate cyclen ligands. The Gd^{3+} complex **82** possessing a 7-membered chelate ring binds one water molecule which is easily exchanged with bulk water molecules ($1.1 \times 10^8 \text{ s}^{-1}$). On the other hand, no inner-sphere water molecule coordinates to Gd^{3+} in complex **83** including an 8-membered chelate ring (Congreve et al., 2004). Water exchange phenomena are also controlled by the steric crowding around the Gd^{3+} centers. Comparing macrocyclic ligands **80**, **84**, and **85**, we note that the former two yield monohydrated Gd^{3+} complexes with water exchange rates of $0.04 \times 10^8 \text{ s}^{-1}$ and $2.7 \times 10^8 \text{ s}^{-1}$. In contrast, the Gd^{3+} complex with the latter ligand had no inner-sphere water molecule. Preliminary X-ray structural study of the Gd^{3+} –**84** complex suggested that high steric crowding of the carboxylate side arms destabilizes water coordination and facilitates the water exchange process (Ruloff et al., 2002).

In addition to the common MRI contrast agents, other types of smart Gd^{3+} complexes were recently developed which exhibited new sensing functions. Some of them worked as responsive MRI reagents to pH ($= -\log[\text{H}^+]$), P_{O_2} (partial oxygen pressure), pCa^{2+} ($= -\log[\text{Ca}^{2+}]$), and other environmental factors. This section highlights recent advances in such intelligent Gd^{3+} complexes, although the practical significance of various MRI reagents has already been reviewed (Aime et al., 2003).

4.2.2. pH-sensing

There are several different exchange systems in biological cells such as $\text{H}^+/\text{HCO}_3^-$, $\text{Cl}^-/\text{HCO}_3^-$, and the ATP-dependent H^+ pump. It is particularly noteworthy that pH in tu-

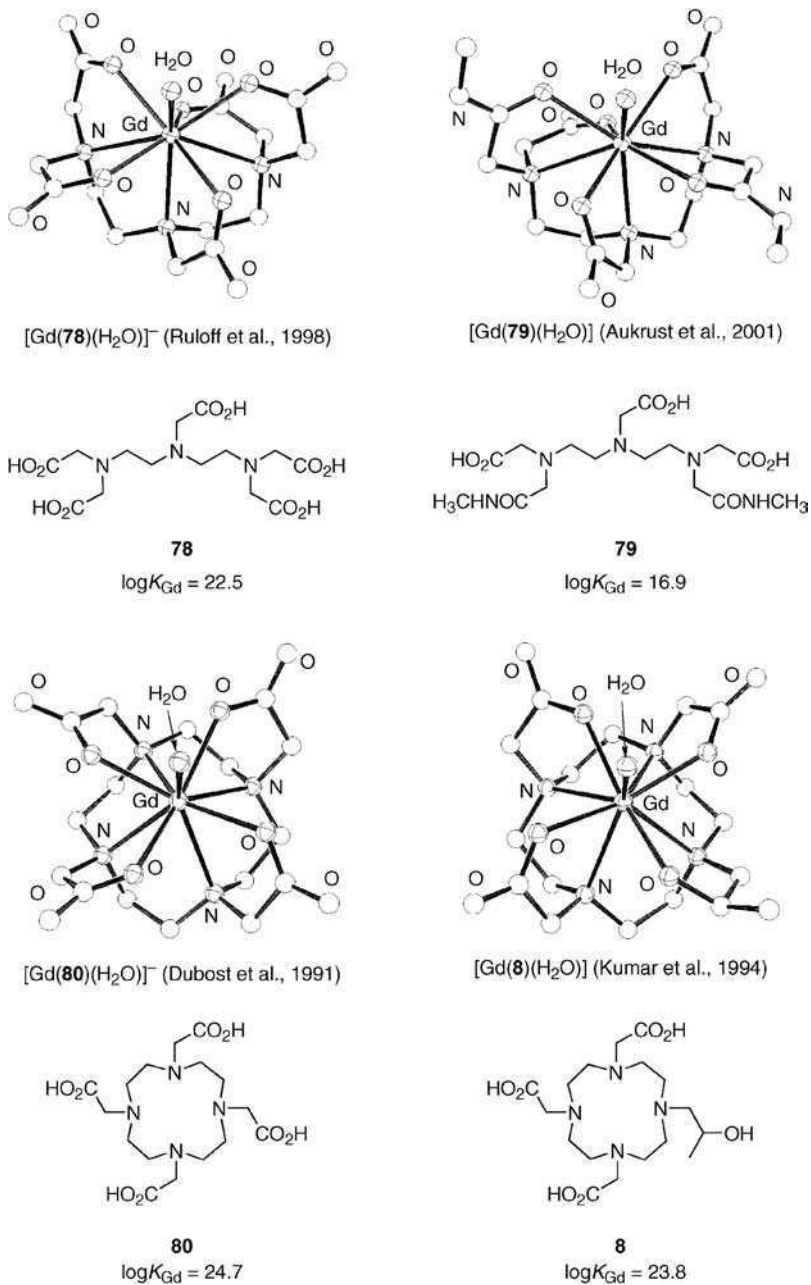


Fig. 29. Crystal structures and thermodynamic stabilities of Gd^{3+} complexes with ligands **8**, **78**–**80**. Redrawn, with permission, after the cited references.

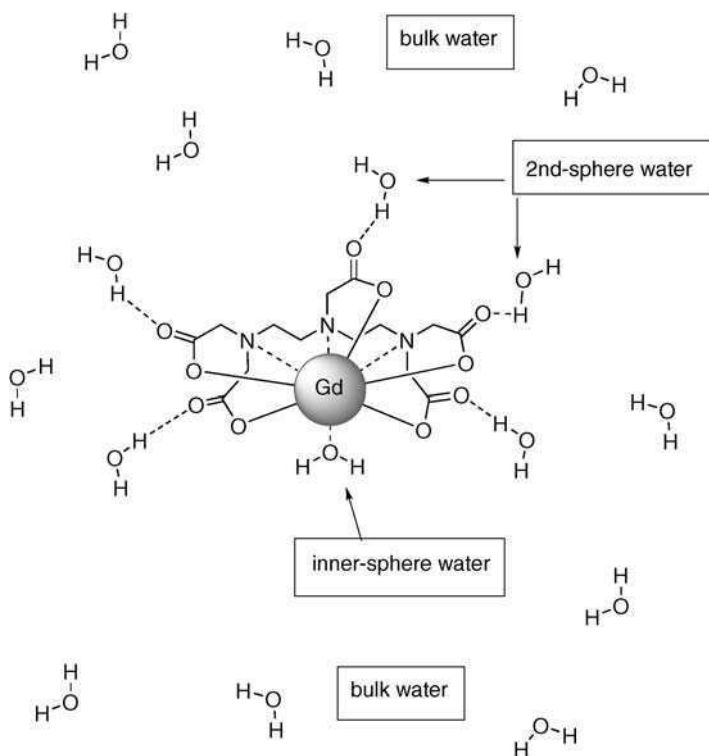
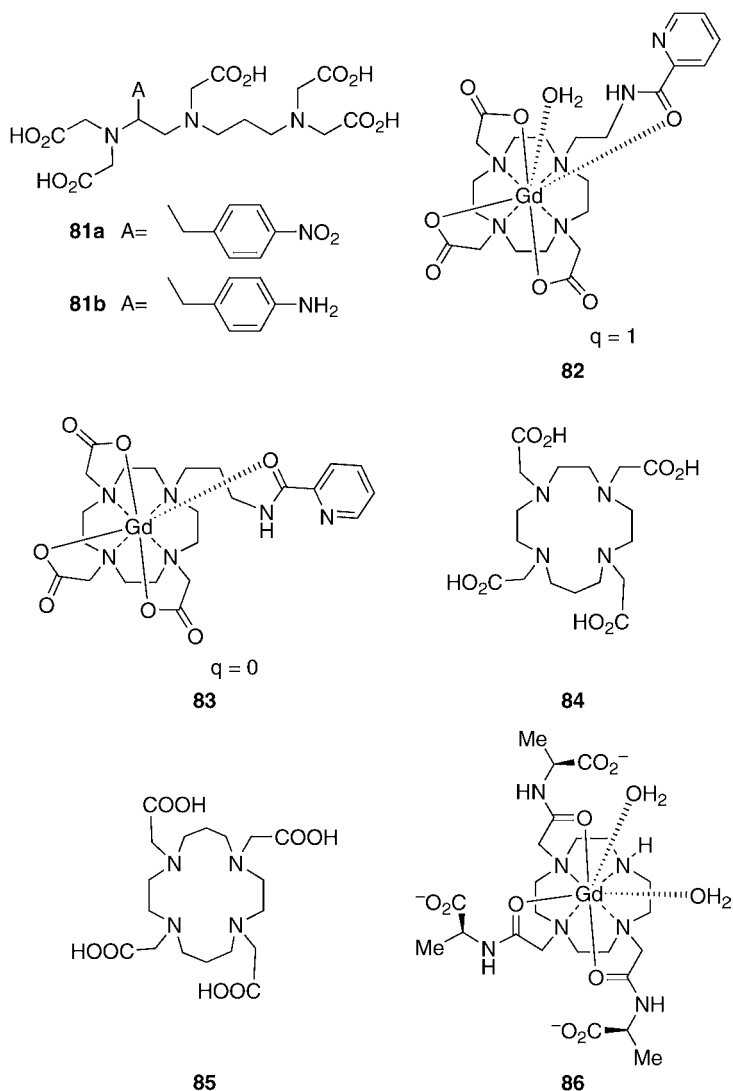


Fig. 30. Water molecules around the Gd^{3+} ion.

mors is generally more acidic than in regular tissues (Tannock and Rotin, 1989), suggesting that the production of lactic acid and the hydrolysis of ATP occurs rapidly in hypoxic regions of tumors. Since microelectrodes are not available for in vivo pH measurements, a new series of MRI reagents sensitive to pH differences is needed.

As described above for complex **28**, rare earth complexes with derivatized cyclen ligands are amenable to binding by hydrogen carbonate and other bidentate anions. When the Gd^{3+} complex with chiral heptadentate cyclen **86** (scheme 17) was used as an MRI probe (Dickins et al., 1998), the two bound water molecules were replaced by bidentate hydrogen carbonate anion (HCO_3^-) at higher pH. Thus, this Gd^{3+} complex has water proton relaxivity which is responsive to the pH of the system (Aime et al., 1999a).

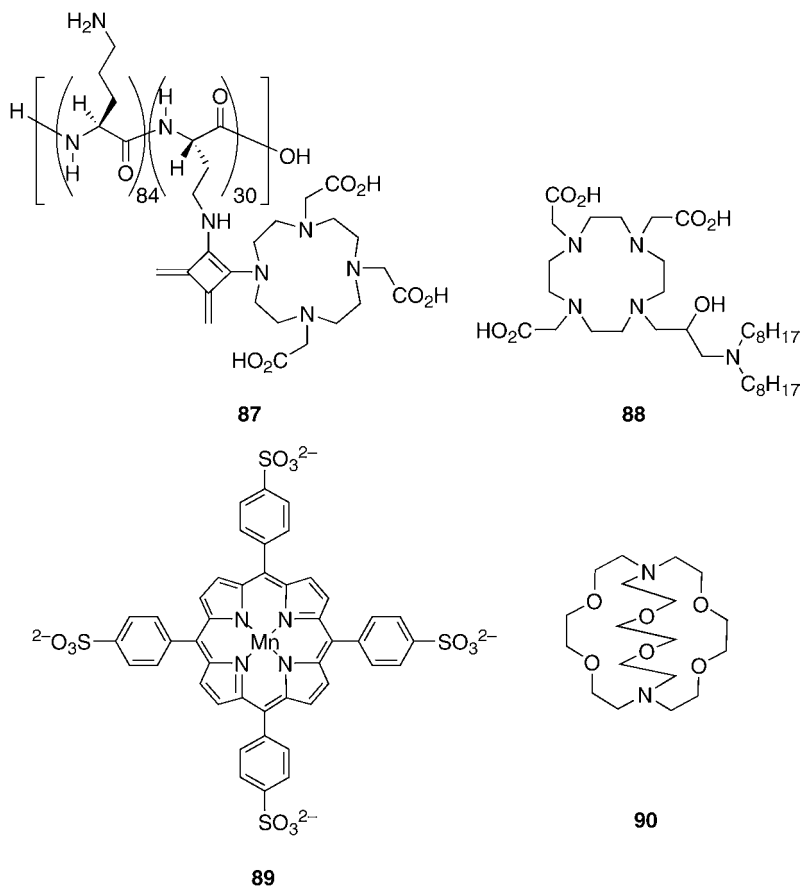
The relaxivity of Gd^{3+} complexes is also determined by the molecular reorientation time, and their pH-dependent mobility can be monitored by MRI. For example, polylysine and polyornithine exhibit pH-dependent conformational changes: highly flexible structures at low pH due to the repulsion among protonated amino groups; and rigid structures at high pH via intramolecular hydrogen bond formation. The relaxivity value of the Gd^{3+} complex with polyornithine-functionalized cyclen **87** (scheme 18) largely changes in the pH range 4–8



Scheme 17.

(Aime et al., 1999b). The Gd^{3+} complex with cyclen-based surfactant **88** also showed pH-responsive relaxivity around pH 6–8, because its deprotonated form aggregated, resulting in an enhancement of the water proton relaxivity (Hovland et al., 2001).

Sherry et al. successfully proposed another type of pH-responsive MRI contrast agent with a Gd^{3+} complex with cyclen **36c** possessing hydroxypyridyl substituents (see fig. 19) (Woods et al., 2003). This complex exhibits a small relaxivity enhancement (25%) at pH 2–4 where



Scheme 18.

prototropic exchange of the coordinated water molecules occurs. On the other hand, deprotonation of the amide sidearm results in the formation of intramolecular acid-base pair interaction and a larger enhancement (84%) is observed at pH 6–9.

4.2.3. O_2 -sensing

Since partial oxygen pressure, P_{O_2} , is one of the important reporters of the biological environments, the P_{O_2} -responsive MRI contrast agents are effective in image separation of arterial and venous blood and the detection of tumors and related pathological states. Some redox-active transition metal complexes have been employed for this purpose, in which the number of unpaired electrons is coupled with the redox state of the metal center. Aime et al. (2000) typically proposed the Mn^{2+}/Mn^{3+} porphyrin complex **89** (scheme 18). Since the Mn^{2+} complex is completely oxidized in presence of over 40 Torr of O_2 , the resulting Mn^{3+} com-

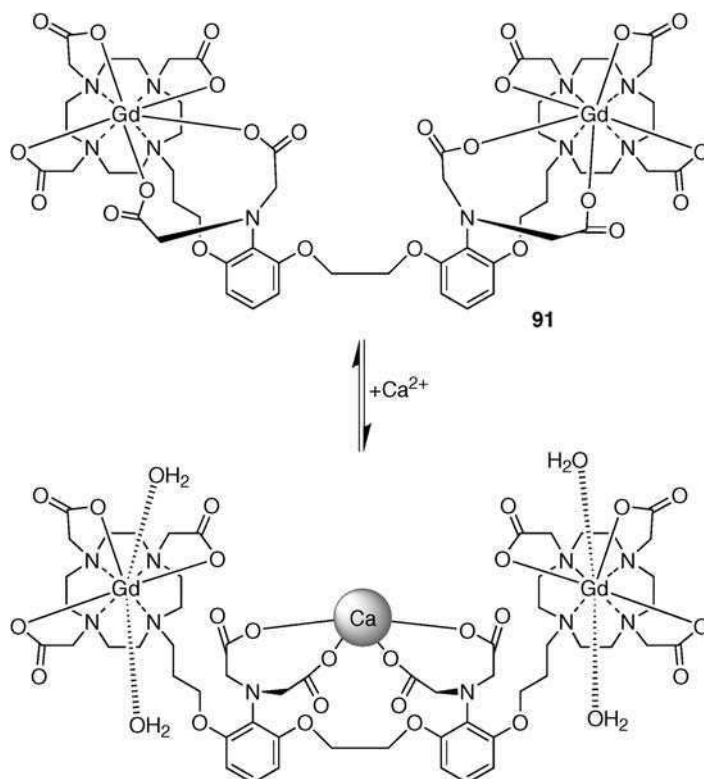


Fig. 31. Ca^{2+} binding of Gd^{3+} -**91** complex. Redrawn, with permission, after Li et al. (1999).

plex dramatically decreases the water proton relaxation rate. $\text{Eu}^{2+}/\text{Eu}^{3+}$ redox systems similarly act as P_{O_2} -responsive MRI contrast agents. The Eu^{2+} (reduced) state, isoelectronic with Gd^{3+} , enhances relaxivity, while the Eu^{3+} (oxidized) state shows poor relaxivity. Cryptand [2.2.2] **90** (scheme 18) forms an Eu^{2+} complex exhibiting several interesting features as a P_{O_2} -responsive MRI contrast agent: (1) relative stability against oxidation; (2) high proton relaxivity due to rapid water exchange; and (3) slow electron spin relaxation (Burai et al., 2002). The rare earth complexes react with O_2 and act as high-contrast MRI agents highly sensitive to partial oxygen pressure.

4.2.4. Sensing of metal cations

Several kinds of metal cations regulate signal transduction, cellular processes, and related biological processes. Since their concentrations and distributions in the living tissues are important indicators of disease states, metal-cation-sensitive MRI contrast agents are currently the focus of attention. Li et al. (1999) reported that Ca^{2+} -sensitive Gd^{3+} complex **91** modulates the relaxivity depending on the Ca^{2+} concentration (fig. 31). When Ca^{2+} is added, a trimetal-

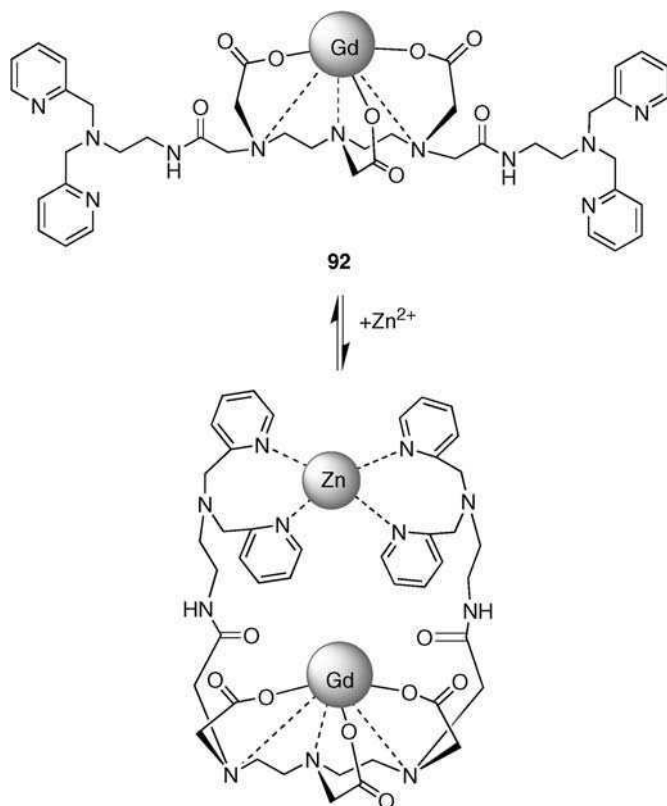
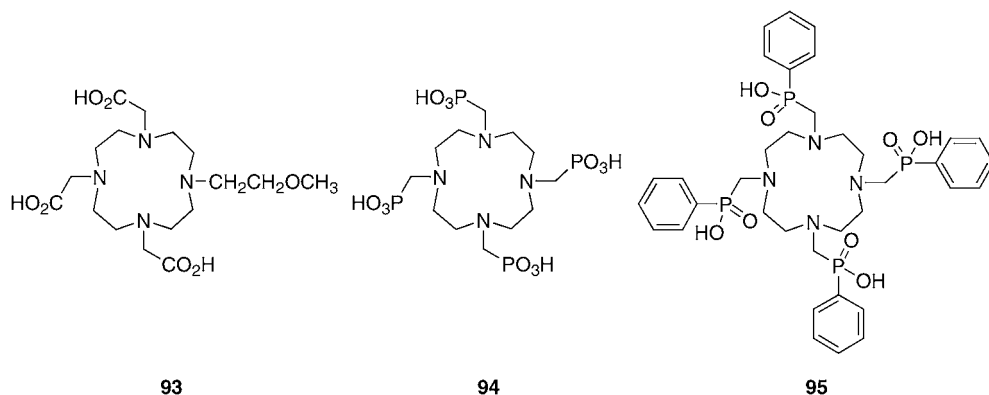


Fig. 32. Zn^{2+} binding of Gd^{3+} -**92** complex. Redrawn, with permission, after Hanaoka et al. (2001).

lic complex forms which exhibits an increased proton relaxation rate of approximately 80%. Nagano and his colleagues designed Gd^{3+} complex **92** as a Zn^{2+} -sensitive MRI contrast agent (Hanaoka et al., 2001, 2002). Because N,N,N',N' -tetrakis(2-pyridylmethyl)ethylenediamine ligand prefers Zn^{2+} to Ca^{2+} and Mg^{2+} cations, the Gd^{3+} complex **92** exhibits Zn^{2+} -sensitive water proton relaxivity (fig. 32).

4.2.5. Temperature sensing

The temperature in the living cell has a large influence on the metabolic activity of an organism. Some rare earth complexes have been developed as *in vivo* thermometers, because both of contact and pseudo-contact shifts vary with the local temperature. The Pr^{3+} complex with cyclen **93** (scheme 19) is the first example of an *in vivo* NMR thermometer based on a rare earth complex (Roth et al., 1996). The methoxy signal of the ligand sidearm did not broaden and sensitively shifted *in vivo*, upon raising the body temperature of a rat by a few degrees. Tm^{3+} complexes with cyclens **94** and **95** also exhib-



Scheme 19.

ited ^1H - and ^{31}P -NMR chemical shifts highly sensitive to temperature (Zuo et al., 1998; Rohovec et al., 1999). Because these two complexes have different hydrophobicity, they possess different biodistributions. Linear correlations between ^1H -/ ^{31}P -NMR chemical shifts and physiological environmental temperatures were consequently established.

4.2.6. MRI sensing with supramolecular probes

Gd^{3+} complexes with dendrimers and other macromolecular ligands are expected to have large water proton relaxivity because of large rotational correlation time. They have long retention times in blood, in contrast to common Gd^{3+} complexes, and allow the recording of high-contrast images of blood vessels. Bryant, Jr. et al. (1999) prepared several generations of dendrimers with octadentate cyclen- Gd^{3+} complexes **96** (fig. 33). Total water proton relaxivity r_1 of the dendrimer complex increases from 2880 to 66 960 $\text{mM}^{-1} \text{s}^{-1}$ from the 5th generation to the 10th generation. However, relaxivity values per Gd^{3+} ion of the high generation dendrimers are saturated at 36 $\text{mM}^{-1} \text{s}^{-1}$. Since lower generation dendrimer- Gd^{3+} complexes are more quickly excreted by the kidneys, MRI agents of smaller dendrimers **97** have been synthesized and their pharmacokinetics, whole-body retention and dynamics have been evaluated in the mice system (Kobayashi et al., 2003).

Some Gd^{3+} complexes display high water proton relaxivity upon non-covalent interaction with poly- β -cyclodextrins. For instance, the relaxivity of the Gd^{3+} -**98** complex increases from 10 $\text{mM}^{-1} \text{s}^{-1}$ to 61 $\text{mM}^{-1} \text{s}^{-1}$ by addition of poly- β -cyclodextrin (15 kDa). Since benzyl groups of the Gd^{3+} complex are included in the β -cyclodextrin cavities, the interlocked polymeric aggregates form in the water. This enhanced the water exchange contribution of the 2nd coordination sphere (Aime et al., 2001b).

Endohedral metallofullerenes were presented as a new family of Gd^{3+} complexes, in which Gd^{3+} cations are nicely encapsulated inside fullerene cages. Since the Gd^{3+} cation is protected from chemical attack, the Gd^{3+} -fullerenes are chemically stable and less toxic (Wilson, 1999). Water-soluble Gd^{3+} endohedral metallofullerene **99** (scheme 20), was characterized as an MRI contrast agent (Kato et al., 2003). Its water proton relaxivity r_1 was estimated as being

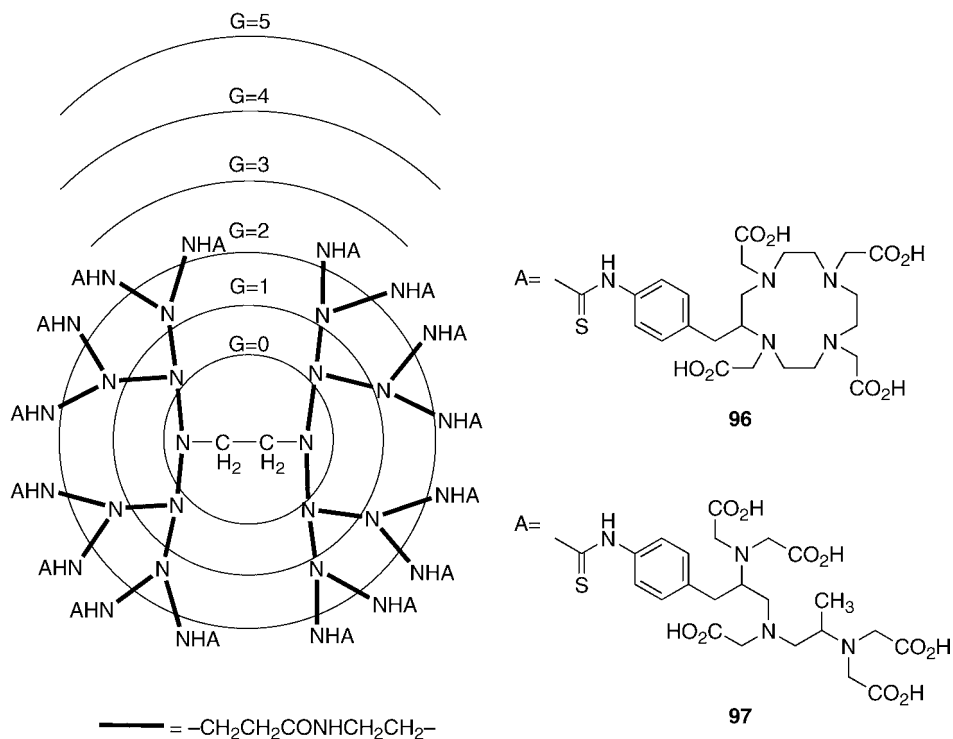
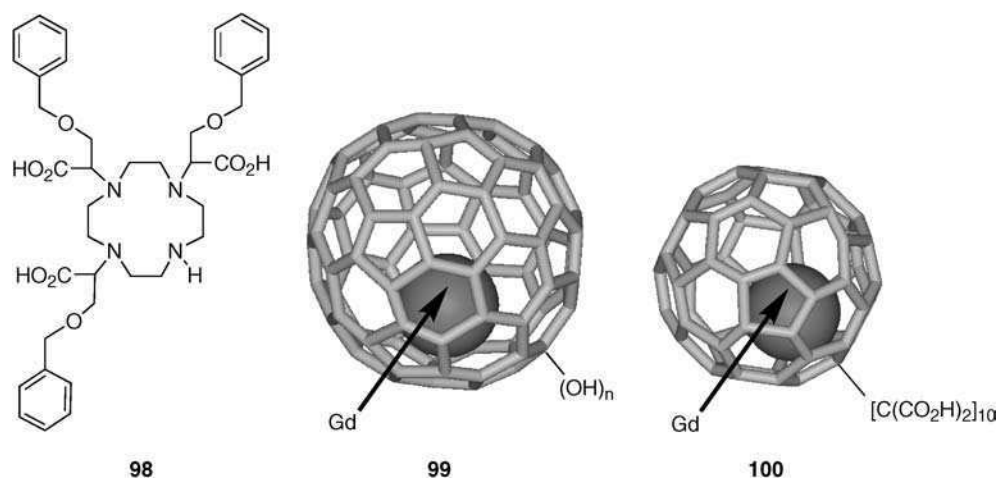
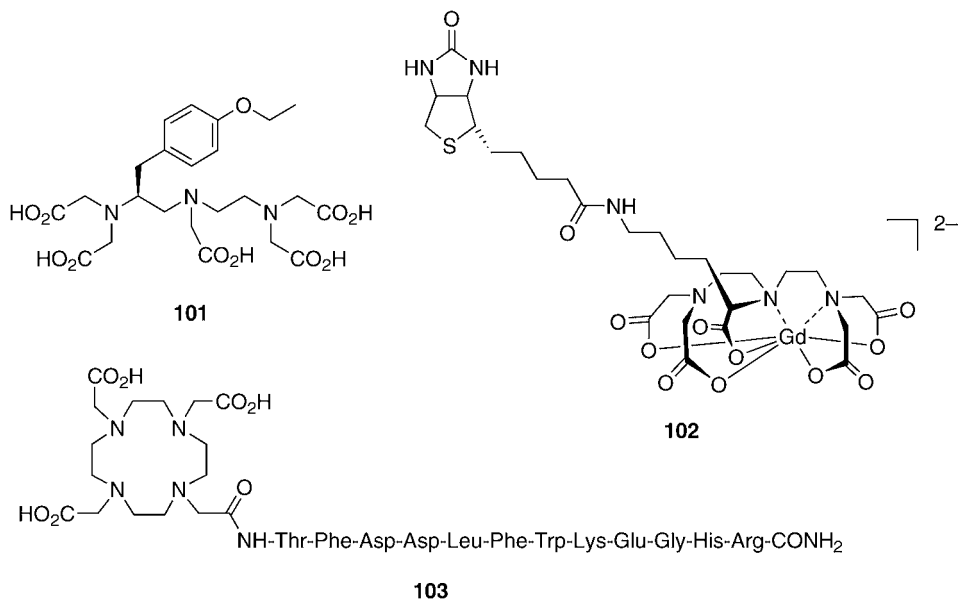


Fig. 33. Ethylenediamine-core polyamidoamine-dendrimers **96** and **97**. Redrawn, with permission, after Kobayashi et al. (2003).



Scheme 20.



Scheme 21.

$73 \text{ mM}^{-1} \text{ s}^{-1}$ (0.47 T, 19°C) which is more than 17-fold longer than that of the common Gd^{3+} complex with polyaminocarboxylic acid **78**. An intense signal was detected in *in vivo* MRI experiments imaging lung, liver, spleen, and kidney of mice after intravenous administration. The water-soluble carboxylated Gd^{3+} -fullerene **100**, $\text{Gd}@C_{60}[\text{C}(\text{CO}_2\text{H})_2]_{10}$, has a comparable water proton relaxivity ($4.6 \text{ mM}^{-1} \text{ s}^{-1}$ at 20 MHz and 40°C) to Gd^{3+} -**78** (Bolskar et al., 2003). Although both Gd^{3+} complexes have similar biodistributions, complex **100** depresses excess reticuloendothelial uptake as seen for other polyhydroxylated fullerenes. In these metallofullerene systems, the bulk water molecules do not directly coordinate to the Gd^{3+} centers shielded by the fullerene cages, but hydrogen bonds with the paramagnetic ($s = 1/2$) metallofullerene surfaces induce short relaxation times of the bulk water protons.

4.2.7. Sensing of natural supramolecules

Since Gd^{3+} -**78** complex is typically distributed in the extracellular water space of the body after intravenous administration, specific binding sites for a given protein were introduced into rare earth complexes to develop tissue-selective MRI reagents (Aime et al., 1998). Meares and Wensel (1984) prepared the bleomycin A₂ conjugated EDTA complex, which is effective for the diagnosis and treatment of cancer. Such a large molecular weight Gd^{3+} complex generally induces a pronounced enhancement of the relaxivity, due to a decrease in the molecular tumbling rate. One successful example is the Gd^{3+} complex with ligand **101** (scheme 21) which includes chiral polyaminocarboxylate and 4-ethoxybenzyl groups. Since this complex is specifically uptaken by the hepatocytes, hepatic tumors can be selectively detected and differentiated (Schmitt-Willich et al., 1999). Meijer et al. reported the biotiny-

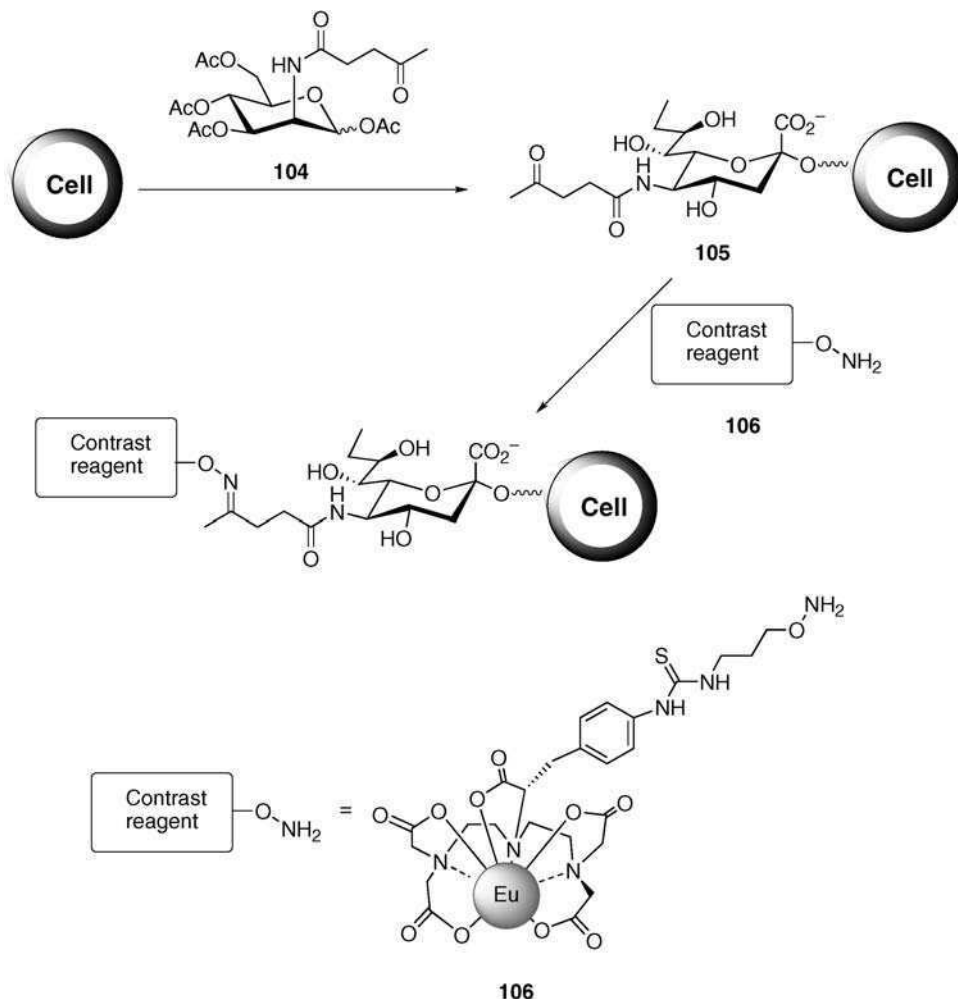


Fig. 34. Selective targeting of MRI contrast agents for sialylated cancer cells. Redrawn, with permission, after Lemieux et al. (1999).

lated Gd^{3+} complex **102**, which strongly binds avidin ($K_a \sim 10^{15} \text{ M}^{-1}$) (Langereis et al., 2004). Its longitudinal relaxivity r_1 was confirmed as $6.1 \text{ mM}^{-1} \text{ s}^{-1}$ (1.5 T and 20°C), which is slightly higher than that of the parent Gd^{3+} -**79** complex ($4.2 \text{ mM}^{-1} \text{ s}^{-1}$). After complexation with avidin, the Gd^{3+} complex **102** exhibits an enhanced longitudinal relaxivity ($17.5 \text{ mM}^{-1} \text{ s}^{-1}$), probably due to a decrease in the molecular tumbling rate. Recently, Kodadek et al. developed Gd^{3+} complex with an octadentate cyclen fitting with an oligopeptide (**103**). This complex specifically binds the yeast transcription repressor protein Gal80

($K_a \sim 5 \times 10^5 \text{ M}^{-1}$) (De León-Rodríguez et al., 2002). Its water proton relaxivity was estimated as being $8.3 \text{ mM}^{-1} \text{ s}^{-1}$ (pH 7.4, 20 MHz, 25 °C), but complexation with Gal80 remarkably increased it to $44.8 \text{ mM}^{-1} \text{ s}^{-1}$. Since addition of bovine serum albumin rarely influences the relaxation rate of water molecules, one may state that Gd^{3+} -**103** complex possesses a specific affinity for Gal80.

Selective delivery of MRI contrast agents to the targeted cells is an effective methodology for early detection and diagnosis of tumors. Bertozzi et al. proposed a new strategy for exploiting differences in sialoside expression. Peracetylated *N*-levulinoylmannosamine **104** was converted to the corresponding *N*-levulinoyl sialic acid **105** in human cells. Since the aminoxy-functionalized contrast agent **106** reacts with the ketone group of **105**, the cell was labeled with the contrast agent (fig. 34) (Lemieux et al., 1999). When the Eu^{3+} complex was attached for facile detection and quantification, luminescence measurements revealed that an adequate amount of Eu^{3+} complex was loaded on the cell surface. Thus, this method is applicable in the design of specific Gd^{3+} contrast agents.

Several biological environments were successfully detected by rare earth complexes. Since their MRI contrast profiles were significantly controlled by the dynamics of the coordinated water molecules and molecular tumbling, several external stimuli such as pH, P_{O_2} , and temperature can be sensitively sensed. Further sophisticated contrast agents specific for certain damaged tissues can be developed by bottom-up synthesis of rare earth complexes.

5. Conclusion

This chapter summarizes recent advances in the chemistry of rare earth complexes used in molecular recognition and sensing technology. Based on their unique coordination chemistry, rare earth cations and their complexes allow specific recognition and sensing of the targeted substrates. Since they have versatile coordination characteristics, the structural, electronic, magnetic, and other properties, the highly coordinated complexes can be finely optimized by careful ligand design. A variety of intelligent sensory devices have been developed, particularly for inorganic anions, amino acids, and other biologically important substrates. Tris(β -diketonates), porphyrinates, and polyaminocarboxylate complexes, as well as complexes with derivatized cyclens were shown to be efficient optical and magnetic probes in practical luminescence, CD, NMR, and MRI sensing techniques. In addition to ligand optimization, further hybridization with functional molecules significantly enhanced the selectivity and sensitivity of rare-earth-containing probes. Since rare earth complexes are widely used as labeling agents in gene- and protein-science and technology, new rare earth compounds are expected to occupy a prominent place as intelligent materials in chemistry, biology, medicine, and related technologies of the next generation.

Acknowledgements

The authors express their thanks to the Ministry of Education, Culture, Sports, Science and Technology of Japan for supporting our research cited here. Permission to use table 1 and

figs. 7, 12, 13, 15, 16, 25, and 32 for Royal Society of Chemistry, figs. 3, 13, 20, 21, 22, 27, 28, 29, 31, 33, and 34 for American Chemical Society, fig. 24 for International Union of Crystallography, fig. 29 for Verlag der Zeitschrift für Naturforschung and Académie des sciences, figs. 14 and 19 for Wiley-VCH and figs. 6, 9, 10, and 11 for The Rare Earth Society of Japan. Crystal structures in figs. 13, 15, 16, 24, 25, and 29 were prepared by ORTEP-3 for windows (Farrugia, 1997) based on Cambridge crystallographic Data (Allen, 2002).

References

- Aime, S., Botta, M., Fasano, M., Terreno, E., 1998. *Chem. Soc. Rev.* **27**, 19.
- Aime, S., Barge, A., Botta, M., Howard, J.A.K., Katak, R., Lowe, M.P., Moloney, J.M., Parker, D., de Sousa, A.S., 1999a. *Chem. Commun.*, 1047.
- Aime, S., Botta, M., Crich, S.G., Giovenzana, G., Palmisano, G., Sisti, M., 1999b. *Chem. Commun.*, 1577.
- Aime, S., Botta, M., Gianolio, E., Terreno, E., 2000. *Angew. Chem., Int. Ed. Engl.* **39**, 747.
- Aime, S., Botta, M., Bruce, J.I., Mainero, V., Parker, D., Terreno, E., 2001a. *Chem. Commun.*, 115.
- Aime, S., Botta, M., Fedeli, F., Gianolio, E., Terreno, E., Anelli, P., 2001b. *Chem.-Eur. J.* **7**, 5262.
- Aime, S., Barge, A., Botta, M., Terreno, E., 2003. *Metal Ions in Biological Systems* **40**, 643.
- Alexander, V., 1995. *Chem. Rev.* **95**, 273.
- Allen, F.M., 2002. *Acta Crystallogr.* **B58**, 380.
- Anastassiou, A., Hasan, M., 1982. *Helv. Chim. Acta* **65**, 2526.
- Aspinall, H.C., 2002. *Chem. Rev.* **102**, 1807.
- Atkinson, P., Bretonniere, Y., Parker, D., 2004. *Chem. Commun.*, 438.
- Aukrust, A., Engebretsen, T., Sydnes, L.K., Sæthre, L.J., Törnroos, K.W., 2001. *Organic Process Research & Development* **5**, 361.
- Batista, H.J., de Andrade, A.V.M., Longo, R.L., Simas, A.M., de Sa, G.F., Ito, N.K., Thompson, L.C., 1998. *Inorg. Chem.* **37**, 3542.
- Baxter, I., Drake, S.R., Hursthouse, M.B., Abdul Malik, K.M., McAleese, J., Otway, D.J., Plakatouras, J.C., 1995. *Inorg. Chem.* **34**, 1384.
- Bednarski, M., Danishefsky, S., 1983. *J. Am. Chem. Soc.* **105**, 3716.
- Beeby, A., Dickins, R.S., FitzGerald, S., Govenlock, L.J., Maupin, C.L., Parker, D., Riehl, J.P., Siligardi, G., Williams, J.A.G., 2000. *Chem. Commun.*, 1183.
- Beer, P.D., Gale, P.A., 2001. *Angew. Chem. Int. Ed. Engl.* **40**, 486.
- Best, M.D., Anslyn, E.V., 2003. *Chem.-Eur. J.* **9**, 51.
- Bolskar, R.D., Benedetto, A.F., Husebo, L.O., Price, R.E., Jackson, E.F., Wallace, S., Wilson, L.J., Alford, J.M., 2003. *J. Am. Chem. Soc.* **125**, 5471.
- Borovkov, V.V., Lintuluoto, J.M., Inoue, Y., 2001. *J. Am. Chem. Soc.* **123**, 2979.
- Brittain, H.G., 1979. *J. Am. Chem. Soc.* **101**, 1733.
- Brittain, H.G., 1982. *J. Chem. Soc., Dalton Trans.*, 2059.
- Brittain, H.G., 1983. *Polyhedron* **2**, 261.
- Brittain, H.G., Richardson, F.S., 1976. *J. Chem. Soc., Dalton Trans.*, 2253.
- Bruce, J.I., Dickins, R.S., Govenlock, L.J., Gunnlaugsson, T., Lopinski, S., Lowe, M.P., Parker, D., Peacock, R.D., Perry, J.J.B., Aime, S., Botta, M., 2000. *J. Am. Chem. Soc.* **122**, 9674.
- Bryant Jr., L.H., Brechbiel, M.W., Wu, C., Bulte, J.W.M., Herynek, V., Frank, J.A., 1999. *J. Magn. Reson. Imaging* **9**, 348.
- Burai, L., Scopelliti, R., Tóth, É., 2002. *Chem. Commun.*, 2366.
- Burai, L., Tóth, É., Merbach, A.E., 2003. *Chem. Commun.*, 2680.
- Byrne, B., Rothchild, R., 1999. *Chirality* **11**, 529.
- Caravan, P., Ellison, J.J., McMurry, T.J., Lauffer, R.B., 1999. *Chem. Rev.* **99**, 2293.
- Charbonnière, L., Ziessel, R., Guardigli, M., Roda, A., Sabbatini, N., Cesario, M., 2001. *J. Am. Chem. Soc.* **123**, 2436.
- Charbonnière, L.J., Ziessel, R., Montalti, M., Prodi, L., Zaccaroni, N., Boehme, C., Wipff, G., 2002. *J. Am. Chem. Soc.* **124**, 7779.
- Christidis, P.C., Tossidis, I.A., Paschalidis, D.G., Tzavelas, L.C., 1998. *Acta Cryst. C* **54**, 1233.
- Congreve, A., Parker, D., Gianolio, E., Botta, M., 2004. *Dalton Trans.*, 1441.
- Cramer, R.E., Seff, K., 1972. *Acta Cryst. B* **28**, 3281.
- Cunningham, J.A., Sievers, R.E., 1980. *Inorg. Chem.* **19**, 595.
- Dale, L.A., Mosher, H.S., 1973. *J. Am. Chem. Soc.* **95**, 512.

- De León-Rodríguez, L.M., Ortiz, A., Weiner, A.L., Zhang, S., Kovacs, Z., Kodadek, T., Sherry, A.D., 2002. *J. Am. Chem. Soc.* **124**, 3514.
- Di Bari, L., Pintacuda, G., Salvadori, P., 2000. *J. Am. Chem. Soc.* **122**, 5557.
- Di Bari, L., Lelli, M., Pintacuda, G., Pescitelli, G., Marchetti, F., Salvadori, P., 2003. *J. Am. Chem. Soc.* **125**, 5549.
- Dickins, R.S., Gunnlaugsson, T., Parker, D., Peacock, R.D., 1998. *Chem. Commun.*, 1643.
- Dickins, R.S., Love, C.S., Puschmann, H., 2001. *Chem. Commun.*, 2308.
- Dickins, R.S., Aime, S., Batsanov, A.S., Beeby, A., Botta, M., Bruce, J.I., Howard, J.A.K., Love, C.S., Parker, D., Peacock, R.D., Puschmann, H., 2002. *J. Am. Chem. Soc.* **124**, 12697.
- Dickins, R.S., Batsanov, A.S., Howard, J.A.K., Parker, D., Puschmann, H., Salamano, S., 2004. *Dalton Trans.*, 70.
- Dillon, J., Nakanishi, K., 1974. *J. Am. Chem. Soc.* **96**, 4057.
- Dubost, J.-P., Leger, J.-M., Langlois, M.-H., Meyer, D., Schaefer, M., 1991. *C. R. Seances Acad. Sci., Ser.* **2** **312**, 349.
- Evans, W.J., Giarikos, D.G., Johnston, M.A., Greci, M.A., Ziller, J.W., 2002. *J. Chem. Soc., Dalton Trans.*, 520.
- Farrugia, L.J., 1997. *J. Appl. Cryst.* **30**, 565.
- Forsberg, J.H., 1996. In: Gschneidner Jr., K.A., Eyring, L. (Eds.), *Handbook on the Physics and Chemistry of Rare Earths*, vol. **23**. Elsevier, Amsterdam. Ch. 153.
- Fukuda, Y., Nakano, A., Hayashi, K., 2002. *Chem. Soc., Dalton Trans.*, 527.
- Glover, P.B., Ashton, P.R., Childs, L.J., Rodger, A., Kercher, M., Williams, R.M., De Cola, L., Pikramenou, Z., 2003. *J. Am. Chem. Soc.* **125**, 9918.
- Govenlock, L.J., Mathieu, C.E., Maupin, C.L., Parker, D., Riehl, J.P., Siligardi, G., Williams, J.A.G., 1999. *Chem. Commun.*, 1699.
- Gunnlaugsson, T., 2001. *Tetrahedron Lett.* **42**, 8901.
- Gunnlaugsson, T., Leonard, J.P., 2003. *Chem. Commun.*, 2424.
- Gunnlaugsson, T., Mac Dónaill, D.A., Parker, D., 2001. *J. Am. Chem. Soc.* **123**, 12866.
- Gunnlaugsson, T., Harte, A.J., Leonard, J.P., Nieuwenhuyzen, M., 2002. *Chem. Commun.*, 2134.
- Gunnlaugsson, T., Harte, A.J., Leonard, J.P., Nieuwenhuyzen, M., 2003a. *Supramol. Chem.* **15**, 505.
- Gunnlaugsson, T., Leonard, J.P., Sénéchal, K., Harte, A.J., 2003b. *J. Am. Chem. Soc.* **125**, 12062.
- Hanaoka, K., Kikuchi, K., Urano, Y., Nagano, T., 2001. *J. Chem. Soc., Perkin Trans.* **2**, 1840.
- Hanaoka, K., Kikuchi, K., Urano, Y., Narazaki, M., Yokawa, T., Sakamoto, S., Yamaguchi, K., Nagano, T., 2002. *Chemistry & Biology* **9**, 1027.
- Hanna, G.H., Lau-Cam, C.A., 1992. *J. AOAC Int.* **75**, 417.
- Hazama, R., Umakoshi, K., Kabuto, C., Kabuto, K., Sasaki, Y., 1996. *Com. Commun.*, 15.
- Holz, R.C., Thompson, L.C., 1988. *Inorg. Chem.* **27**, 4640.
- Horrocks Jr., W.DeW., 1970. *Inorg. Chem.* **9**, 690.
- Horrocks Jr., W.DeW., Sipe III, J.P., 1971. *J. Am. Chem. Soc.* **93**, 6800.
- Hovland, R., Gløggård, C., Aasen, A.J., Klaveness, J., 2001. *J. Chem. Soc., Perkin Trans.* **2**, 929.
- Imamoto, T., 1994. *Lanthanides in Organic Synthesis*. Academic Press, London.
- Inamoto, A., Ogasawara, K., Omata, K., Kabuto, K., Sasaki, Y., 2000. *Org. Lett.* **2**, 3543.
- Inanaga, J., Furuno, H., Hayano, T., 2002. *Chem. Rev.* **102**, 2221.
- Jacobus, J., Raban, M., 1969. *J. Chem. Edu.* **46**, 351.
- Jodry, J.J., Lacour, J., 2000. *Chem.-Eur. J.* **6**, 4297.
- Kabuto, K., Sasaki, Y., 1984. *J. Chem. Soc., Chem. Commun.*, 316.
- Kabuto, K., Sasaki, Y., 1987. *J. Chem. Soc., Chem. Commun.*, 670.
- Kabuto, K., Sasaki, Y., 1989. *Chem. Lett.*, 385.
- Kabuto, K., Sasaki, Y., 1990. *Tetrahedron Lett.* **31**, 1031.
- Kabuto, K., Sasaki, K., Sasaki, Y., 1992. *Tetrahedron: Asymmetry* **3**, 1357.
- Kaltsoyannis, N., 1999. *The F Elements*, Oxford Chemistry Primers 76. Oxford University Press, Oxford.
- Kato, H., Kanazawa, Y., Okumura, M., Taninaka, A., Yokawa, T., Shinohara, H., 2003. *J. Am. Chem. Soc.* **125**, 4391.
- Katzin, L.I., 1968. *Inorg. Chem.* **7**, 1183.
- Katzin, L.I., 1969. *Inorg. Chem.* **8**, 1649.
- Kawa, H., Yamaguchi, F., Ishikawa, N., 1982. *Chem. Lett.*, 153.
- Kido, J., Okamoto, Y., Brittain, H.G., 1991. *J. Org. Chem.* **56**, 1412.
- Kobayashi, H., Kawamoto, S., Jo, S.-K., Bryant Jr., H.L., Brechbiel, M.W., Star, R.A., 2003. *Bioconjugate Chem.* **14**, 388.
- Kobayashi, S., Sugiura, M., Kitagawa, H., Lam, W.W.-L., 2002. *Chem. Rev.* **102**, 2227.
- Komiyama, M., Takeda, N., Shigekawa, H., 1999. *Chem. Commun.*, 1443. (Feature Article).
- Kooijman, H., Nijssen, F., Spek, A.L., Schip, F., 2000. *Acta Cryst. C* **56**, 156.

- Kumar, K., Chang, C.A., Francesconi, I.C., Dischino, D.D., Malley, M.F., Gougoutas, J.Z., Tweedle, M.F., 1994. *Inorg. Chem.* **33**, 3567.
- Kuriki, K., Koike, Y., Okamoto, Y., 2002. *Chem. Rev.* **102**, 2347.
- Kuroda, R., Saito, Y., 2000. In: Berova, N., Nakanishi, K., Woody, R.W. (Eds.), *Circular Dichroism: Principles and Applications*. 2nd edn. Wiley-VCH, New York, pp. 563–599.
- Kurtán, T., Nesnas, N., Li, Y.-Q., Huang, X., Nakanishi, K., Berova, N., 2001a. *J. Am. Chem. Soc.* **123**, 5962.
- Kurtán, T., Nesnas, N., Koehn, F.E., Li, Y.-Q., Nakanishi, K., Berova, N., 2001b. *J. Am. Chem. Soc.* **123**, 5974.
- Langereis, S., Kooistra, H.-A.T., van Genderen, M.H.P., Meijer, E.W., 2004. *Org. Biomol. Chem.* **2**, 1271.
- LaPlanche, L.A., Vanderkooi, G., 1983. *J. Chem. Soc., Perkin Trans. 2*, 1585.
- Lauffer, R.B., 1987. *Chem. Rev.* **87**, 901.
- Lemieux, G.A., Yarema, K.J., Jacobs, C.L., Bertozzi, C.R., 1999. *J. Am. Chem. Soc.* **121**, 4278.
- Li, W.-H., Fraser, S.E., Meade, T.J., 1999. *J. Am. Chem. Soc.* **121**, 1413.
- Lisowski, J., Ripoli, S., Di Bari, L., 2004. *Inorg. Chem.* **43**, 1388.
- Lowe, M.P., Parker, D., Reany, O., Aime, S., Botta, M., Castellano, G., Gianolio, E., Pagliarin, R., 2001. *J. Am. Soc. Chem.* **123**, 7601.
- Magennis, S.W., Parsons, S., Pikramenou, Z., 2002. *Chem.-Eur. J.* **8**, 5761.
- Mahajan, R.K., Kaur, I., Kaur, R., Uchida, S., Onimaru, A., Shinoda, S., Tsukube, H., 2003. *Chem. Commun.*, 2238.
- Mameri, S., Charbonnière, L.J., Ziessel, R.F., 2004. *Inorg. Chem.* **43**, 1819.
- Matsumoto, K., Yuan, J., 2003. In: Sigel, A., Sigel, H. (Eds.), *Metal Ions in Biological Systems*, vol. **40**. Marcel Dekker, New York, pp. 191–232.
- Maupin, C.L., Parker, D., Williams, J.A.G., Riehl, J.P., 1998. *J. Am. Chem. Soc.* **120**, 10563.
- Maupin, C.L., Dickins, R.S., Govenlock, L.G., Mathieu, C.E., Parker, D., Williams, J.A.G., Riehl, J.P., 2000. *J. Phys. Chem. A* **104**, 6709.
- Mazzanti, M., Wietzke, R., Pécaut, J., Latour, J.-M., Maldivi, P., Remy, M., 2002. *Inorg. Chem.* **41**, 2389.
- McCreary, M.D., Lewis, D.W., Wernick, D.L., Whitesides, G.M., 1974. *J. Am. Chem. Soc.* **96**, 1038.
- Meares, C.F., Wensel, T.G., 1984. *Acc. Chem. Res.* **17**, 202.
- Meskers, S.C.J., Dekkers, H.P.J.M., 2001. *J. Phys. Chem. A* **105**, 4589.
- Meskers, S.C.J., Ubbink, M., Canters, G.W., Dekkers, H.P.J.M., 1998a. *J. Biol. Inorg. Chem.* **3**, 463.
- Meskers, S.C.J., Ubbink, M., Canters, G.W., Dekkers, H.P.J.M., 1998b. *J. Biol. Inorg. Chem.* **3**, 663.
- Messori, L., Monnanni, R., Scozzafava, A., 1986. *Inorg. Chim. Acta* **124**, L15.
- Miyake, H., Shinoda, S., Tsukube, H., 2001. *Rare Earths* **39**, 41.
- Molander, G.A., Romero, J.A.C., 2002. *Chem. Rev.* **102**, 2161.
- Montalti, M., Prodi, L., Zaccheroni, N., Charbonnière, L., Douce, L., Ziessel, R., 2001. *J. Am. Chem. Soc.* **123**, 12694.
- Nakanishi, K., Dillon, J., 1971. *J. Am. Chem. Soc.* **93**, 4058.
- Nassimbeni, L.R., Wright, M.R.W., van Niekerk, J.C., McCallum, P.A., 1979. *Acta Cryst. B* **35**, 1341.
- Omata, K., Fujiwara, T., Kabuto, K., 2002. *Tetrahedron: Asymmetry* **13**, 1655.
- Parker, D., 1991. *Chem. Rev.* **91**, 1441.
- Parker, D., 2000. *Coord. Chem. Rev.* **205**, 109.
- Parker, D., Dickins, R.S., Puschmann, H., Crossland, C., Howard, J.A.K., 2002. *Chem. Rev.* **102**, 1977.
- Peters, J.A., Vijverberg, C.A.M., Kieboom, A.P.G., van Bekkum, H., 1983. *Tetrahedron Lett.* **24**, 3141.
- Petoud, S., Cohen, S.M., Bünzli, J.-C.G., Raymond, K.N., 2003. *J. Am. Chem. Soc.* **125**, 13324.
- Petrov, V.A., Marshall, W.J., Grushin, V.V., 2002. *Chem. Commun.*, 520.
- Phillips II, T., Sands, D.E., Wagner, W.F., 1968. *Inorg. Chem.* **7**, 2295.
- Piguet, C., Bünzli, J.-C.G., 1999. *Chem. Soc. Rev.* **28**, 347.
- Plakatouras, J.C., Baxter, I., Hursthouse, M.B., Abdul Malik, K.M., McAleese, J., Drake, S.R., 1994. *J. Chem. Soc., Chem. Commun.*, 2455.
- Prodi, L., Montalti, M., Zaccheroni, N., Pickaert, G., Charbonnière, L., Ziessel, R., 2003. *New J. Chem.* **27**, 134.
- Reany, O., Gunnlaugsson, T., Parker, D., 2000. *J. Chem. Soc., Perkin Trans. 2*, 1819.
- Reuben, J., 1979. *J. Chem. Soc., Chem. Commun.*, 68.
- Reuben, J., 1980. *J. Am. Chem. Soc.* **102**, 2232.
- Richardson, F.S., 1982. *Chem. Rev.* **82**, 541.
- Riehl, J.P., Muller, G., 2005. In: Gschneidner Jr., K.A., Bünzli, J.-C., Pecharsky, V. (Eds.), *Handbook on the Physics and Chemistry of Rare Earths*, vol. **34**. Elsevier, Amsterdam. Ch. 220.
- Rohovec, J., Lukes, I., Hermann, P., 1999. *New J. Chem.* **23**, 1129.
- Roth, K., Bartholomae, G., Bauer, H., Frenzel, T., Kossler, S., Platzek, J., Radüchel, B., Weinmann, H.-J., 1996. *Angew. Chem., Int. Ed. Engl.* **35**, 655.

- Ruloff, R., Gelbrich, T., Hoyer, E., Sieler, J., Beyer, L., 1998. *Z. Naturforsch., B: Chem. Sci.* **53**, 955.
- Ruloff, R., Tóth, É., Scopelliti, R., Tripier, R., Handel, H., Merbach, A.E., 2002. *Chem. Commun.*, 2630.
- Sabbatini, N., Guardigli, M., 1993. *Coord. Chem. Rev.* **123**, 201.
- Sakagami, N., Homma, J.-I., Konno, T., Okamoto, K.-I., 1997. *Acta Cryst. C* **53**, 1376.
- Salvadori, P., Rosini, C., Bertucci, C., 1984. *J. Am. Chem. Soc.* **106**, 2439.
- Sato, J., Jin, H.-Y., Omata, K., Kabuto, K., Sasaki, Y., 1999. *Enantiomer* **4**, 147.
- Schmidtchen, F.P., Berger, M., 1997. *Chem. Rev.* **97**, 1609.
- Schmitt-Willich, H., Brehm, M., Ewers, C.L.J., Michl, G., Müller-Fahnow, A., Petrov, O., Platzek, J., Radüchel, B., Sülzle, D., 1999. *Inorg. Chem.* **38**, 1134.
- Senegas, J.-M., Bernardinelli, G., Imbert, D., Bünzli, J.-C.G., Morgantini, P.-Y., Weber, J., Piguët, C., 2003. *Inorg. Chem.* **42**, 4680.
- Shannon, R.D., 1976. *Acta Cryst. A* **32**, 751.
- Shibasaki, M., Yoshikawa, N., 2002. *Chem. Rev.* **102**, 2187.
- Shinoda, S., 2004. *Kidorui* **45**, 35.
- Takemura, M., Yamato, K., Doe, M., Watanabe, M., Miyake, H., Kikunaga, T., Yanagihara, N., Kojima, Y., 2001. *Bull. Chem. Soc. Jpn.* **74**, 707.
- Tamiaki, H., Matsumoto, N., Tsukube, H., 1997. *Tetrahedron Lett.* **38**, 4239.
- Tamiaki, H., Unno, S., Takeuchi, E., Tameshige, N., Shinoda, S., Tsukube, H., 2003. *Tetrahedron* **59**, 10477.
- Tannock, I.F., Rotin, D., 1989. *Cancer Res.* **49**, 4373.
- Terreno, E., Botta, M., Fedeli, F., Mondino, B., Milone, L., Aime, S., 2003. *Inorg. Chem.* **42**, 4891.
- Tóth, É., Helm, L., Merbach, A.E., 2004. In: Fenton, D.E. (Ed.), *Comprehensive Coordination Chemistry II*, vol. **9**. Elsevier, Oxford, pp. 841–881.
- Tsukube, H., Shinoda, S., 2000. *Enantiomer* **5**, 13.
- Tsukube, H., Shinoda, S., 2002. *Chem. Rev.* **102**, 2389.
- Tsukube, H., Uenishi, J., Kanatani, T., Itoh, H., Yonemitsu, O., 1996a. *J. Chem. Soc., Chem. Commun.*, 477.
- Tsukube, H., Uenishi, J., Shiba, H., Yonemitsu, O., 1996b. *J. Membrane Sci.* **114**, 187.
- Tsukube, H., Shinoda, S., Uenishi, J., Kanatani, T., Itoh, H., Shide, M., Iwachido, T., Yonemitsu, O., 1998. *Inorg. Chem.* **37**, 1585.
- Tsukube, H., Wada, M., Shinoda, S., Tamiaki, H., 1999. *Chem. Commun.*, 1007.
- Tsukube, H., Hosokubo, M., Wada, M., Shinoda, S., Tamiaki, H., 2001. *Inorg. Chem.* **40**, 740.
- Tsukube, H., Shinoda, S., Tamiaki, H., 2002a. *Coord. Chem. Rev.* **226**, 227.
- Tsukube, H., Tameshige, N., Shinoda, S., Unno, S., Tamiaki, H., 2002b. *Chem. Commun.*, 2574.
- Tsukuda, T., Suzuki, T., Kaizaki, S., 2002. *Mol. Cryst. Liq. Cryst. Sci. Technol. A* **379**, 159.
- Turro, C., Fu, P.K.-L., Bradley, P.M., 2003. In: Sigel, A., Sigel, H. (Eds.), *Metal Ions in Biological Systems*, vol. **40**. Marcel Dekker, New York, pp. 323–353.
- van Staveren, D.R., van Albada, G.A., Haasnoot, J.G., Kooijman, H., Lanfredi, A.M.M., Nieuwenhuizen, P.J., Spek, A.L., Ugozzoli, F., Weyhermüller, T., Reedijk, J., 2001. *Inorg. Chim. Acta* **315**, 163.
- Viswanathan, T., Toland, A., 1995. *J. Chem. Edu.* **72**, 945.
- Watanabe, M., Hasegawa, T., Miyake, H., Kojima, Y., 2001. *Chem. Lett.*, 4.
- Watson, W.H., Williams, R.J., Stemple, N.R., 1972. *J. Inorg. Nucl. Chem.* **34**, 501.
- Wayda, A.L., Kaplan, M.L., Lyons, A.M., Rogers, R.D., 1990. *Polyhedron* **9**, 751.
- Wenzel, T.J., 1987. *NMR Shift Reagents*. CRC Press, Boca Raton, Florida.
- Wenzel, T.J., Wilcox, J.D., 2003. *Chirality* **15**, 256.
- Wenzel, T.J., Bogyo, M.S., Lebeau, E.L., 1994. *J. Am. Chem. Soc.* **116**, 4858.
- Wenzel, T.J., Miles, R.D., Weinstein, S.E., 1997. *Chirality* **9**, 1.
- Wenzel, T.J., Miles, R.D., Zomlefer, K., Frederique, D.E., Roan, M.A., Troughton, J.S., Pond, B.V., Colby, A.L., 2000. *Chirality* **12**, 30.
- Wenzel, T.J., Thurston, J.E., Sek, D.C., Joly, J.-P., 2001. *Tetrahedron: Asymmetry* **12**, 1125.
- Wenzel, T.J., Amonoo, E.P., Shariff, S.S., Aniagyei, S.E., 2003. *Tetrahedron: Asymmetry* **14**, 3099.
- Wietzke, R., Mazzanti, M., Latour, J.-M., Pécaut, J., Cordier, P.-Y., Madic, C., 1998. *Inorg. Chem.* **37**, 6690.
- Wietzke, R., Mazzanti, M., Latour, J.-M., Pécaut, J., 1999. *Chem. Commun.*, 209.
- Wietzke, R., Mazzanti, M., Latour, J.-M., Pécaut, J., 2000. *J. Chem. Soc., Dalton Trans.*, 4167.
- Willner, I., Eichen, Y., Sussan, S., Shoham, B., 1991. *New J. Chem.* **15**, 879.
- Wilson, L.J., 1999. *Interface*, 24.
- Wing, R.M., Uebel, J.J., Andersen, K.K., 1973. *J. Am. Chem. Soc.* **95**, 6046.
- Wiskur, S.L., Haddou, H.A., Lavigne, J.J., Anslyn, E.V., 2001. *Acc. Chem. Res.* **34**, 963.
- Wong, W.-K., Zhang, L., Wong, W.-T., Xue, F., Mak, T.C.W., 1999. *J. Chem. Soc., Dalton Trans.*, 615.

- Woods, M., Sherry, A.D., 2003. *Inorg. Chem.* **42**, 4401.
- Woods, M., Zhang, S., von Ebron, H., Sherry, A.D., 2003. *Chem.-Eur. J.* **9**, 4634.
- Yamada, T., Shinoda, S., Tsukube, H., 2002. *Chem. Commun.*, 1218.
- Yamada, T., Shinoda, S., Sugimoto, H., Uenishi, J., Tsukube, H., 2003. *Inorg. Chem.* **42**, 7932.
- Yang, X., Brittain, H.G., 1982. *Inorg. Chim. Acta* **57**, 165.
- Yang, X.-P., Su, C.-Y., Kang, B.-S., Fong, X.-L., Xiao, X.-L., Liu, H.-Q., 2000. *J. Chem. Soc., Dalton Trans.*, 3253.
- Yang, X.-P., Kang, B.-S., Wong, W.-K., Su, C.-Y., Liu, H.-Q., 2003. *Inorg. Chem.* **42**, 169.
- Zucchi, G., Scopelliti, R., Bünzli, J.-C.G., 2001. *J. Chem. Soc., Dalton Trans.*, 1975.
- Zucchi, G., Ferrand, A.-C., Scopelliti, R., Bünzli, J.-C.G., 2002. *Inorg. Chem.* **41**, 2459.
- Zuo, C.S., Metz, K.R., Sun, Y., Sherry, A.D., 1998. *J. Magn. Reson.* **133**, 53.

This page intentionally left blank

AUTHOR INDEX

- Aasen, A.J., see Hovland, R. 322
 Abdul Malik, K.M., see Baxter, I. 311
 Abdul Malik, K.M., see Plakatouras, J.C. 311
 Abe, T., see Itoh, H. 18
 Abe, T., see Mori, M. 29
 Abe, T., see Takeuchi, H. 10
 Ableeva, N.S., see Kazakov, V.P. 185
 Abraham, M.M., see Boatner, L.A. 46
 Abraham, M.M., see Petek, M. 46
 Abramson, E., see Melby, L.R. 121, 122, 148–150, 154–156
 Abramson, E.J., see Mattson, S.M. 122, 126, 149
 Abrutis, A., see Galindo, V. 240
 Abrutis, A., see Weiss, F. 240
 Accorsi, G., see Shavaleev, N.M.M. 168
 Achete, C.A., see Reyes, R. 214
 Acosta, J.J.C., see Berg, E.W. 146–152
 Adachi, C. 215
 Adachi, G.Y., see Jiang, J.Z. 128, 198, 199
 Adachi, G.Y., see Li, H.H. 187
 Adachi, K., see Yamada, T. 14
 Adachi, T. 186
 Adam, W., see Schuster, G.B. 183
 Adolphe, C., see Khodadad, P. 96
 Ahmad, N. 219
 Ahmad, N., see Ansari, M.S. 145–152
 Ahmad, N., see Iftikhar, K. 145–153
 Ahmad, N., see Selbin, J. 146–153
 Ahmed, M.O. 131
 Aihara, M. 228
 Aikawa, S., see Takeuchi, H. 10
 Aiki, H., see Nakanishi, A. 12
 Aikihanyan, A.S. 128
 Aime, S. 274, 278, 281, 319, 321–323, 326, 328
 Aime, S., see Bruce, J.I. 276, 294, 313
 Aime, S., see Dickins, R.S. 294
 Aime, S., see Lowe, M.P. 296
 Aime, S., see Terreno, E. 295, 315
 Ainitdinov, Kh.A. 150
 Airoldi, C. 159
 Airoldi, C., see Santos Jr., L.S. 159
 Aizawa, M., see Nishiyama, H. 40
 Aizawa, M., see Sakai, N. 27
 Ajgaonkar, V.R., see Barfiwala, U.A. 61
 Ajgaonkar, V.R., see Nabar, M.A. 59, 60, 62
 Akashi, T. 39
 Akiba, K., see Nakamura, S. 245
 Akikusa, J., see Yamada, T. 14
 Akimoto, H., see Ohta, K. 119
 Akiyama, Y. 239
 Akiyama, Y., see Taniguchi, S. 17
 Akubay, T., see Yamada, T. 14
 Alberts, J.H., see Peters, J.A. 224, 235
 Albuquerque, R.Q., see Carlos, L.D. 170
 Aldred, A.T., see Karim, D.P. 24
 Alexander, V. 274
 Alford, J.M., see Bolskar, R.D. 328
 Alikhanyan, A., see Gleizes, A. 128, 235, 240
 Alikhanyan, A., see Gleizes, A.N. 240
 Alikhanyan, A., see Kuzmina, N. 240, 241
 Alire, R.M., see Crosby, G.A. 121, 125, 163
 Allan, J.R. 193
 Allard, B. 141
 Allen, F.M. 331
 Almeida, F.V., see Alves Jr., S. 172
 Alstad, J. 244
 Altman, D.E. 205
 Alvaro, M. 196
 Alves, S., see Gonçalves e Silva, F.R. 170, 172
 Alves Jr., S. 172
 Alves Jr., S., see Carlos, L.D. 170
 Alves Jr., S., see de Farias, R.F. 188, 193
 Alves Jr., S., see de Mello Donegá, C. 170, 172
 Alves Jr., S., see Malta, O.L. 172
 Amano, A. 139, 235, 236
 Amao, Y. 232
 Amirkhaniv, W., see Borzechowska, M. 159
 Ammermann, D., see Dirr, S. 211
 Amonoo, E.P., see Wenzel, T.J. 314
 An, Y.Z. 168
 Anastassiou, A. 309
 Andersen, K.K., see Wing, R.M. 311
 Andersen, T.J. 130, 135
 Andersen, W.C. 139, 146, 151, 157
 Anderson, H.U. 19, 24

- Anderson, H.U., see Group, L. 19
 Anderson, H.U., see Koc, R. 20, 34, 35
 Anderson, H.U., see Kuo, J. 23
 Andreev, A.V., see Petrov, A.N. 23
 Andrews, G.W., see Richards, B.C. 240
 Anelli, P., see Aime, S. 326
 Aniagyei, S.E., see Wenzel, T.J. 314
 Ansari, M.S. 145–152
 Anslyn, E.V., see Best, M.D. 291, 293
 Anslyn, E.V., see Wiskur, S.L. 280
 Antipin, V.A. 185
 Antipin, V.A., see Kazakov, V.P. 185
 Antonovich, V.P., see Meshkova, S.B. 173
 Antson, J., see Suntola, T. 241
 Anwander, R., see Gerstberger, G. 249
 Aoki, S., see Yamaguchi, T. 240
 Arai, M., see Aihara, M. 228
 Arakawa, M., see Tobita, S. 165
 Arati, Y., see Yamamoto, O. 34
 Arduini, A. 223
 Aristov, A.V. 205
 Armitage, I. 219
 Armitage, I.M., see Arduini, A. 223
 Armstrong, T.R. 30
 Armstrong, T.R., see Stevenson, J.W. 19
 Arnaud, N. 228
 Artemenko, A.G., see Meshkova, S.B. 173
 Ashton, P.R., see Glover, P.B. 299
 Aslanov, L.A. 50, 52
 Aspinall, H.C. 284
 Astier, R., see Meyer, Y. 205
 Atanassova, M. 244
 Atchison, F.W., see Thompson, L.C. 129, 131
 Atkinson, P. 296
 Audebert, P., see Pagnot, T. 193
 Augustson, L.H., see Alstad, J. 244
 Aukrust, A. 319
 Avalos-Borja, M., see Hirata, G.A. 239

 Babushkina, N.A., see Gorbenco, O.Yu. 239
 Badalyan, A.M., see Polyakov, O.V. 240
 Badcock, R., see Sage, I. 180, 182
 Badwal, S.P.S., see Drennan, J. 30
 Bagger, C., see Marina, O. 14
 Bai, F.L., see Ling, Q.D. 213
 Bai, G.B., see Gao, J.Z. 228
 Bai, J., see Li, H. 204
 Bai, J., see Zhou, D.J. 154, 198
 Baidina, I.A., see Zaitseva, E.G. 130, 135
 Bailey, N.J., see Christou, V. 214
 Balakrishnan, N., see Takeuchi, T. 29

 Balamantsarashvili, G., see Beltyukova, S. 229
 Balasubramanian, C., see Mahalingam, T. 242
 Balasubramanian, N., see Biju, V.M. 228, 229
 Baldo, M.A., see Adachi, C. 215
 Ballon, O. 30
 Bance, P. 14
 Banks, C., see Mitchell, J.W. 150
 Banks, C.V., see Butts, W.C. 238
 Banks, C.V., see Sieck, R.F. 238
 Banks, E., see Ueba, Y. 192
 Banning, S.A., see Dickinson, P.H. 240
 Barash, E.U. 124, 139, 234
 Barbera, J. 119
 Bard, A.J. 48
 Bard, A.J., see Hemingway, R.E. 159
 Bard, A.J., see Richter, M.M. 158
 Barfiwala, U.A. 61
 Barge, A., see Aime, S. 319, 321
 Barkhatova, L.Yu. 32
 Barkley, L.B. 119
 Barrer, R.M. 195
 Bartholomae, G., see Roth, K. 325
 Baskaran, S., see Stevenson, J.W. 19
 Bassett, A.P. 158
 Basson, S.S., see Leipoldt, J.G. 131, 133
 Bastin, L., see Kahr, B. 177
 Batawi, E. 17
 Batista, H.J. 131, 148, 311
 Batista, H.J., see Malta, O.L. 172
 Batsanov, A.S. 132
 Batsanov, A.S., see Dickens, R.S. 294
 Battiston, J., see Kuz'mina, N.P. 128
 Batyaev, I.M. 205
 Bauer, H. 121, 122, 148–151, 154–156
 Bauer, H., see Roth, K. 325
 Bauer, T. 249
 Baxter, I. 132, 139, 311
 Baxter, I., see Plakatouras, J.C. 132, 311
 Bazan, G.C., see McGehee, M.D. 211, 213
 Bazan, G.C., see Robinson, M.R. 212
 Bazan, G.C., see Srdanov, V.I. 177, 194
 Bazan, G.C., see Yang, C.Y. 177, 194
 Bazhulin, P.A. 205
 Beall, G.W., see Boatner, L.A. 46
 Becht, M. 146, 236, 241
 Beck, J.S. 196
 Beck, J.S., see Kresge, C.T. 196
 Becker, E.D. 220
 Bednarski, M. 248, 249, 283
 Bednarski, M., see Danishefsky, S. 247, 249
 Beeby, A. 173, 299

- Beeby, A., see Dickins, R.S. 294
 Beer, P.D. 280
 Behrsing, T. 141, 142, 159
 Bekiari, V. 189
 Bekiari, V., see Moleski, R. 189
 Belanger, P. 221
 Belcher, R. 123, 146
 Belian, M.F., see de Farias, R.F. 188, 193
 Bell, Z.R., see Shavaleev, N.M. 168, 174, 175
 Bellamy, L.J. 161
 Belova, L.M., see Gorbenko, O.Yu. 239
 Belova, N.V. 236
 Belova, N.V., see Girichev, G.V. 235
 Belova, N.V., see Giricheva, N.I. 235, 236
 Beltyukova, S. 229
 Belyi, V.I., see Polyakov, O.V. 240
 Ben Hamida, M. 90, 91, 93
 Ben Hamida, M., see Wickleder, M.S. 90, 91
 Bender, J.L. 194
 Benedetto, A.F., see Bolskar, R.D. 328
 Benelli, C. 141, 159, 160
 Benelli, C., see Malandrino, G. 130, 146, 239
 Bennett, M.J. 133
 Bentsen, L.D., see Hasselman, D.P.H. 30–33
 Berdonosov, P.S. 78, 99
 Berdonosov, P.S., see Oppermann, H. 78, 97
 Berdonosov, P.S., see Schmidt, P. 78, 97
 Berdonosov, P.S., see Shabalin, D.G. 81
 Berg, E.W. 146–152
 Berger, M., see Schmidtchen, F.P. 280
 Bergstedt, T., see McGehee, M.D. 211, 213
 Bernardinelli, G., see Senegas, J.-M. 286
 Berova, N., see Kurtán, T. 305
 Berrigan, R. 85, 90
 Berry, M.T., see An, Y.Z. 168
 Berry, S., see Thompson, L.C. 129, 149, 171
 Bertozzi, C.R., see Lemieux, G.A. 329, 330
 Bertucci, C., see Salvadori, P. 274
 Best, M.D. 291, 293
 Bettes, T.C., see Wenzel, T.J. 220, 225
 Bettinelli, M., see Lo Nigro, R. 239
 Bettinelli, M., see Malandrino, G. 124, 149, 172, 175, 239
 Bex, C., see Binnemans, K. 162, 203
 Beyer, L., see Ruloff, R. 319
 Bhacca, N., see Selbin, J. 146–153
 Bhacca, N.S., see Ahmad, N. 219
 Bhatti, M.S. 244
 Bhaumik, M.L. 149, 156, 165, 171, 205, 233, 237
 Bian, Z.Q. 121
 Bian, Z.Q., see Gao, D.Q. 211
 Biju, V.M. 228, 229
 Billard, A., see Gourba, E. 241
 Bilobran, D., see Morrill, T.C. 224, 247
 Bindu Gopinath, A. 96
 Binnemans, K. 162, 189, 201–203
 Binnemans, K., see Galyametdinov, Yu.G. 202
 Binnemans, K., see Görlner-Walrand, C. 161
 Binnemans, K., see Van Deun, R. 203
 Binnemans, K., see Wostyn, K. 204
 Birnie, J., see Allan, J.R. 193
 Bishop, S., see Sage, I. 182
 Bjorklund, S. 161, 171, 205
 Bjorklund, S., see Hurt, C.R. 179, 180
 Blackborow, J.R. 125
 Blanc, J. 144, 177
 Blanc, J., see Bauer, H. 121, 122, 148–151, 154–156
 Blanc, J., see Ross, D.L. 205, 206
 Blasse, G. 168
 Blasse, G., see de Mello Donegá, C. 170
 Bleaney, B. 221
 Blumental, R.N., see Park, J.-H. 21, 22
 Boatner, L.A. 46
 Boatner, L.A., see Petek, M. 46
 Bock, R. 46
 Bodanowicz, M., see Trost, B.M. 247
 Boehme, C., see Charbonnière, L.J. 291
 Boerner, H. 216
 Boeyens, J.C.A. 132, 135
 Boeyens, J.C.A., see de Villiers, J.P.R. 132, 139
 Boeyens, J.C.A., see Erasmus, C.S. 132, 135, 139, 140, 158
 Bogyo, M.S., see Wenzel, T.J. 314
 Bohatý, L., see Held, P. 46
 Böhler, A., see Dirr, S. 211
 Bohra, R., see Mehrotra, R.C. 112
 Bok, L.D.C., see Leipoldt, J.G. 131, 133
 Bol'shoi, D.B. 173
 Bol'shoi, D.V., see Meshkova, S.B. 173
 Bol'shoi, D.V., see Topilova, Z.M. 173
 Bolskar, R.D. 328
 Bond, A.M., see Behrsing, T. 141, 142, 159
 Bonnet, G. 239, 242
 Borchardt, G., see Chevalier, S. 239
 Borduin, W.G., see Hammond, G.S. 119
 Borisov, A.P., see Zaitseva, I.G. 125
 Borisov, S.V., see Zaitseva, E.G. 130, 135
 Borovkov, V.V. 305
 Borzechowska, M. 159
 Bos, W.G., see Koehler, J.M. 123
 Bos, W.G., see Liss, I.B. 123, 147, 148, 153

- Bos, W.G., see Przystal, J.K. 123
 Bosak, A.A., see Gorbenko, O.Yu. 239
 Botta, M., see Aime, S. 274, 278, 281, 319, 321–323, 326, 328
 Botta, M., see Bruce, J.I. 276, 294, 313
 Botta, M., see Congreve, A. 319
 Botta, M., see Dickins, R.S. 294
 Botta, M., see Lowe, M.P. 296
 Botta, M., see Terreno, E. 295, 315
 Boulon, G., see Boyaval, J. 203
 Bourhill, G. 181
 Bourhill, G., see Clegg, W. 130, 132, 182
 Bourhill, G., see Sage, I. 180–182
 Boursier, D., see Thomas, O. 240
 Bouwnmeester, H.J.M. 28
 Bovée, W.M.M.J., see Peters, J.A. 224, 235
 Boyaval, J. 202, 203
 Boyaval, J., see Hapiot, F. 202
 Bradley, D.D.C., see Burroughes, J.H. 207
 Bradley, P.M., see Turro, C. 288
 Braga, S.S. 127
 Braginski, A.I., see Panson, A.J. 240
 Branch, R.F., see Bellamy, L.J. 161
 Brandon, N.P., see Bance, P. 14
 Brauer, G. 48
 Braun, W.L., see McDevitt, N.T. 242
 Brechbiel, M.W., see Bryant Jr., L.H. 326
 Brechbiel, M.W., see Kobayashi, H. 326, 327
 Brecher, C. 205, 206
 Brecher, C., see Lempicki, A. 205
 Brecher, C., see Samelson, H. 156, 157, 205, 206
 Breck, D.W. 195
 Brehm, M., see Schmitt-Willich, H. 328
 Brennessel, W., see Thompson, L. 131, 135, 169
 Brennetot, R. 228
 Bretonniere, Y., see Atkinson, P. 296
 Brezeanu, M. 46
 Briggs, J. 219
 Bril, A. 170
 Brinen, J.S., see Halverson, F. 126, 149, 150, 156
 Brinker, C.J. 186
 Brito, H.F. 127, 172, 175, 176
 Brito, H.F., see Carlos, L.D. 189
 Brito, H.F., see Gonçalves e Silva, F.R. 170, 172
 Brito, H.F., see Malta, O.L. 170, 172
 Brito, H.F., see Parra, D.F. 193
 Brito, H.F., see Reyes, R. 214, 216
 Brito, H.F., see Sigoli, F.A. 189
 Brittain, H.G. 176, 177, 311
 Brittain, H.G., see Chan, H.K. 177
 Brittain, H.G., see Kido, J. 283, 312
 Brittain, H.G., see Richardson, F.S. 177
 Brittain, H.G., see Yang, X. 280
 Brittain, H.G., see Yang, X.C. 177
 Brix, L.B., see Dickinson, J.T. 179
 Brooks, J.J. 232
 Brooks, J.J., see Dyer, D.S. 224
 Brooks, J.J., see Sievers, R.E. 224
 Brophy, V.A., see Samelson, H. 205
 Brouca-Cabarrecq, C., see Fernandes, A. 197
 Brough, P., see Clegg, W. 130, 132, 182
 Brown, A., see Richards, B.C. 240
 Brown, A.R., see Burroughes, J.H. 207
 Brown, E., see Dujardin, G. 249
 Brown, H.A., see Park, J.D. 119
 Brown, W.B. 244
 Bruce, D.W. 201, 204
 Bruce, D.W., see Binnemans, K. 203
 Bruce, D.W., see Donnio, B. 201
 Bruce, J.I. 276, 294, 313
 Bruce, J.I., see Aime, S. 281
 Bruce, J.I., see Dickins, R.S. 294
 Brück, S. 130, 136
 Bruder, A.H. 158
 Brunel, D., see Fernandes, A. 197
 Bruno, T.J., see Andersen, W.C. 157
 Brüser, W., see Lorenz, V. 135, 136
 Bryant Jr., H.L., see Kobayashi, H. 326, 327
 Bryant Jr., L.H. 326
 Bu, X., see Srdanov, V.I. 177, 194
 Bueno, L.A., see Carlos, L.D. 189
 Bulai, A.K., see Slonim, I.Y. 220
 Bulsing, J.M. 220
 Bulte, J.W.M., see Bryant Jr., L.H. 326
 Bünzli, J.-C.G. 172, 175
 Bünzli, J.-C.G., see Chauvin, A.S. 170
 Bünzli, J.-C.G., see Petoud, S. 286
 Bünzli, J.-C.G., see Piguot, C. 274
 Bünzli, J.-C.G., see Senegas, J.-M. 286
 Bünzli, J.-C.G., see Zucchi, G. 286, 292, 293
 Burai, L. 319, 324
 Burdett, J.L. 118
 Burgett, C.A. 224, 238
 Burggraaf, A.J., see Bouwnmeester, H.J.M. 28
 Burns, J.H. 133, 136, 138
 Burns, P.L., see Burroughes, J.H. 207
 Burova, S.A., see Martynenko, L.I. 132
 Burroughes, J.H. 207
 Busch, H. 240
 Butter, E. 148
 Butts, W.C. 238
 Buzady, A., see Erostyak, J. 228

- Buzady, A., see Hornyak, I. 228
 Byrne, B. 309
- Cai, G.L., see Wang, M.Z. 123, 162
 Caldwell, J.P. 232
 Calefi, P.S., see Nassar, E.J. 189
 Calefi, P.S., see Serra, O.A. 174, 177
 Calvin, M., see Reid, J.C. 119, 244
 Cameron, T.S., see Urs, U.K. 130
 Campbell, J.R. 220
 Campos, R.A. 211
 Caneschi, A., see Benelli, C. 141, 159, 160
 Canters, G.W., see Meskers, S.C.J. 307
 Cao, H., see Gao, X.C. 151, 214
 Cao, Y., see Pei, J. 194, 213
 Capparelli, A.L., see Villata, L.S. 168
 Cappechi, S., see Christou, V. 214
 Caravan, P. 274, 278, 317, 319
 Carducci, M.D., see Wang, J.F. 211, 212
 Carducci, M.D., see Zheng, Z.P. 131, 181
 Carette, P., see Boyaval, J. 202, 203
 Caris, J.C., see Melby, L.R. 121, 122, 148–150, 154–156
 Carlin, R.L., see Benelli, C. 159
 Carlos, L.D. 170, 189
 Carlos, L.D., see Braga, S.S. 127
 Carlos, L.D., see Fernandes, J.A. 121
 Carlos, L.D., see Malta, O.L. 172
 Carlos, L.D., see Sá Ferreira, R.A. 189
 Carp, O., see Brezeanu, M. 46
 Carpy, A., see Delage, C. 69, 70
 Carson, B.R., see Allan, J.R. 193
 Carvalho, C.A.A., see Brito, H.F. 127, 175, 176
 Casanova, A., see George, R. 10
 Cashel, M.L., see Sweeting, L.M. 179
 Cassir, M., see Gourba, E. 241
 Castellano, G., see Lowe, M.P. 296
 Castelli, F., see Malandrino, G. 130, 131, 146, 239
 Castro, A. 72, 75, 94
 Castro, A., see Bindu Gopinath, A. 96
 Castro, A., see de Pedro, M. 72, 74, 94
 Castro, A.M.M., see Ruano, J.L.G. 249
 Cativiela, C., see Barbera, J. 119
 Caulton, K.G., see Barash, E.U. 124, 139, 234
 Cayou, T., see Wang, J.F. 211, 212
 Cazlefi, P.S., see Serra, O.A. 174, 177
 Cesario, M., see Charbonnière, L. 286
 Chadwick, D. 239
 Chalker, P.R., see Jones, A.C. 241
 Chan, H.K. 177
 Chang, C.A., see Kumar, K. 319
 Chang, W.B., see Ci, Y.Y. 230
 Chang, W.B., see Yang, X.D. 166, 167, 230
 Chapuis, C., see Bauer, T. 249
 Charbonnière, L. 286
 Charbonnière, L., see Montalti, M. 276
 Charbonnière, L., see Prodi, L. 291
 Charbonnière, L.J. 291
 Charbonnière, L.J., see Mameri, S. 291
 Charles, R.G. 122, 127, 146–150, 153, 154, 156, 171
 Charles, R.G., see Hirayama, C. 235
 Charles, R.G., see Panson, A.J. 240
 Chauvin, A.S. 170
 Cheetham, A.K., see Morris, R. 74
 Cheetham, A.K., see Morris, R.E. 88, 90, 99
 Chen, B., see Dong, N. 192
 Chen, B.T. 181
 Chen, C.H., see Hung, L.S. 207
 Chen, C.S., see Pan, M. 239
 Chen, G.Q., see Gao, X.C. 151, 214
 Chen, H., see Xu, Z. 239
 Chen, J., see Chour, K.W. 239
 Chen, M., see Yang, W. 228
 Chen, M.Y., see Ciufolini, M.A. 249
 Chen, T.M., see Okada, K. 211, 215
 Chen, W., see Chen, X.F. 133, 182
 Chen, W., see Xiong, R.G. 182
 Chen, X.F. 131, 133, 155, 181, 182
 Chen, X.W., see Ahmed, M.O. 131
 Chen, Y.Q., see Hu, M.L. 131
 Chenevier, B., see Thomas, O. 240
 Cheng, C.H., see Sun, P.P. 211, 215
 Cheng, Y.X., see Liang, F.S. 212, 215
 Cherepanov, V.A., see Petrov, A.N. 23
 Cheung, K.K., see Chen, X.F. 133, 181
 Cheung, K.K., see Zeng, X.R. 133, 181, 182
 Chevalier, S. 239
 Chick, L., see Mukerjee, S. 12
 Childs, L.J., see Glover, P.B. 299
 Chin, U., see Wada, E. 249
 Chippindale, A.M., see Christou, V. 214
 Chitose, N., see Yamada, T. 14
 Cho, S.I., see Jung, Y.S. 130, 141
 Choi, D.S., see Kim, Y.K. 211
 Choi, J.S., see Lee, M.H. 211, 215
 Choppin, G.R., see Hasegawa, Y. 244
 Chou, K.S. 234
 Choudhury, N.S. 22
 Chour, K.W. 239
 Christidis, P.C. 130, 311
 Christie, G.M. 20

- Christou, V. 214
 Christou, V., see Male, N.A.H. 215
 Christou, V., see Moon, D.G. 214
 Chu, B. 214
 Chu, C.T.W., see Beck, J.S. 196
 Chuan, G., see Zheng, Y.X. 211
 Chugarov, N.V., see Kuz'mina, N.P. 130
 Chugarov, N.V., see Kuzmina, N.P. 234, 235
 Chugarov, N.V., see Zharkova, Ya.N. 130
 Ci, Y.X. 228–230
 Ci, Y.Y. 230
 Ci, Y.Y., see Yang, X.D. 166, 167, 230
 Ciacchi, F.T., see Drennan, J. 30
 Ciufolini, M.A. 249
 Ciufolini, M.A., see Deaton, M.V. 249
 Clark, R.A., see Morrill, T.C. 224, 247
 Clarke, S., see Robards, K. 237
 Clarkson, I.M., see Beeby, A. 173
 Claude, C.D., see Kobayashi, T. 218
 Clays, K. 204
 Clays, K., see Verbiest, T. 203
 Clays, K., see Wostyn, K. 204
 Clegg, W. 130, 132, 182
 Clow, J.K., see Kahr, B. 177
 Coan, P.S., see Barash, E.U. 124, 139, 234
 Cockerill, A.F. 220
 Cohen, S.M., see Petoud, S. 286
 Colby, A.L., see Wenzel, T.J. 314
 Colditz, R., see Grummt, U.W. 204
 Collings, P.J. 200
 Collman, J., see Dickinson, P.H. 240
 Colson, J.C., see Bonnet, G. 239, 242
 Condorelli, G.G. 239
 Congreve, A. 319
 Cook, S.L., see Richards, B.C. 240
 Cook, S.L., see Timmer, K. 145, 234
 Corbin, P.S., see Bender, J.L. 194
 Cordier, P.-Y., see Wietzke, R. 288–290
 Cormier, J.M. 183
 Cotton, F.A. 130, 133, 135, 156, 180
 Cotton, F.A., see Bennett, M.J. 133
 Coutable, L., see Dujardin, G. 249
 Couto dos Santos, M.A., see Malta, O.L. 131, 149
 Coutsolelos, A.G., see Spyroulias, G.A. 128
 Cowley, A., see Christou, V. 214
 Craig, G., see Dickinson, P.H. 240
 Cramer, R.E. 131, 279, 311
 Cremona, M., see Reyes, R. 214, 216
 Cresge, C.T., see Beck, J.S. 196
 Criasia, R.T. 133
 Crich, S.G., see Aime, S. 322
 Crisler, L.R. 124
 Crosby, G.A. 121, 125, 163
 Crosby, G.A., see Freeman, J.J. 165
 Crosby, G.A., see Whan, R.E. 121, 163, 205
 Crossland, C., see Parker, D. 280
 Crozet, P. 205
 Crump, D.R. 219
 Cruz, P.M. 62
 Cui, D.F., see Wang, K.Z. 198
 Cunningham, J.A. 130–132, 135, 234, 311
 Cunningham, J.A., see Dyer, D.S. 224
 Cunningham, J.A., see Sievers, R.E. 224
 Cutter, B., see McGoran, E.C. 226
 Cybinska, J., see Thompson, L. 131, 135, 169
 da Costa, M.R., see D'Assunção, L.M. 96
 da Costa, N.B., see Rocha, G.B. 172
 da Costa Jr., N.B., see de Andrade, A.V.M. 172
 da Silva, C.F.B., see Reyes, R. 214
 da Silva Jr., E.F., see de Sá, G.F. 170, 172
 Daga, A., see Xu, Z. 239
 Dahmen, K.-H., see Becht, M. 146, 236, 241
 Dai, J.B., see Wei, A.Z. 133, 181
 Dai, W.M. 249
 Dakubu, S., see Hemmilä, I. 229
 Dale, L.A. 316, 318
 Dallara, J.J. 161
 Dalton, L.R., see Jiang, X.Z. 211, 213
 Dambaska, A. 225
 Damodaran, A.D., see Sita, M. 228, 229
 Danford, M.D., see Burns, J.H. 133, 136, 138
 Daniels, L.M., see Cotton, F.A. 133, 180
 Danishefsky, S. 247, 249
 Danishefsky, S., see Bednarski, M. 248, 249, 283
 Dao, P. 237
 Dao Quoc, H., see Oppermann, H. 78, 97
 Dao Quoc, H., see Schmidt, P. 78, 97
 Darr, J.A. 139, 140, 152
 Das, J.N. 179
 D'Assunção, L.M. 96
 Davalos, M.R., see Sigoli, F.A. 189
 David, V.K., see Han, B. 239
 David, V.P., see Han, B. 239
 Davidenko, N.K., see Yatmirskii, K.B. 157
 Davies, G.L.O., see Cockerill, A.F. 220
 de Andrade, A.V.M. 172
 de Andrade, A.V.M., see Batista, H.J. 131, 148, 311
 de Andrade, A.V.M., see Malta, O.L. 172
 De Ávila Agostini, P.R. 60, 62
 de Castilho Agostini, E., see De Ávila Agostini, P.R. 60, 62

- De Cola, L., see Bassett, A.P. 158
 De Cola, L., see Glover, P.B. 299
 de Farias, R.F. 188, 193
 De Fré, B., see Van Deun, R. 203
 De Horrocks Jr., W., see Frey, S.T. 158
 De Jager-Veenis, W., see Brill, A. 170
 De Jonghe, L.C., see Visco, S. 12
 De Leebeeck, H., see Binnemans, K. 162
 De León-Rodríguez, L.M. 330
 de Mello Donegá, C. 170, 172
 de Mello Donegá, C., see Alves Jr., S. 172
 de Mello Donegá, C., see Carlos, L.D. 170
 de Mello Donegá, C., see de Sá, G.F. 170, 172
 de Mello Donegá, C., see Malta, O.L. 170
 de Pedro, M. 72, 74, 94
 de Pedro, M., see Castro, A. 72, 75, 94
 de Sá, G.F. 170, 172
 de Sá, G.F., see Alves Jr., S. 172
 de Sá, G.F., see Batista, H.J. 131, 148
 de Sa, G.F., see Batista, H.J. 311
 de Sá, G.F., see de Andrade, A.V.M. 172
 de Sá, G.F., see de Farias, R.F. 188, 193
 de Sá, G.F., see de Mello Donegá, C. 170, 172
 de Sá, G.F., see Faustino, W.M. 172
 de Sá, G.F., see Rocha, G.B. 172
 de Sousa, A.S., see Aime, S. 321
 de Sousa, A.S., see Beeby, A. 173
 de Souza, J.M., see de Farias, R.F. 193
 de Villardi, G.C., see Evans, F.D. 225
 de Villiers, J.P.R. 132, 139
 de Villiers, J.P.R., see Boeyens, J.C.A. 132, 135
 de Witte, O. 205
 de Zea Bermudez, V., see Carlos, L.D. 189
 de Zea Bermudez, V., see Sá Ferreira, R.A. 189
 Deacon, G.B., see Behrsing, T. 141, 142, 159
 Deaton, M.V. 249
 Deaton, M.V., see Ciufolini, M.A. 249
 Declercq, J.P., see Vancoppemolle, A. 131
 Dedlovskaya, E., see Gleizes, A.N. 240
 Dedlovskaya, E.M., see Kuz'mina, N.P. 128
 Degnan, J., see Bjorklund, S. 161, 171
 Deibler, J., see Mukerjee, S. 12
 Deka, D.C., see Terada, M. 249
 Dekkers, H.P.J.M., see Meskers, S.C.J. 306, 307
 Delage, C. 69, 70
 Demianets, L.N., see Berdonosov, P.S. 78
 Demus, D. 200
 Deng, A.P., see Huang, C.H. 147
 Denning, R.G., see Bruce, D.W. 204
 Derkacheva, L.D., see Bazhulin, P.A. 205
 Deschenaux, R., see Donnio, B. 201
 DeSisto, W.J., see Rappoli, B.J. 237
 Desreux, J.F. 127, 158, 226, 244
 Desreux, J.F., see Bhatti, M.S. 244
 Devanarayanan, S., see Bindu Gopinath, A. 96
 Devlin, D., see Hirata, G.A. 239
 Dexpert-Ghys, J., see Fernandes, A. 197
 Di Bari, L. 305, 306
 Di Bari, L., see Lisowski, J. 306
 Diamandis, E.P. 229
 Dias, L.C., see Parra, D.F. 193
 Diaz-Garcia, M.A. 213
 Dickins, R.S. 292, 294, 313, 321
 Dickins, R.S., see Beeby, A. 173, 299
 Dickins, R.S., see Bruce, J.I. 276, 294, 313
 Dickins, R.S., see Maupin, C.L. 307
 Dickins, R.S., see Parker, D. 280
 Dickinson, J.T. 179
 Dickinson, P.H. 240
 Diethelm, R., see Batawi, E. 17
 Dietze, F., see Uhlemann, E. 146, 238
 Dilli, S., see Robards, K. 237
 Dillon, J. 302
 Dillon, J., see Nakanishi, K. 278, 302
 Ding, J., see Zhu, G.Y. 228
 Dirr, S. 211
 Dirreen, G.E., see Schreiner, R. 183
 Dischino, D.D., see Kumar, K. 319
 Distanov, B.G., see Bazhulin, P.A. 205
 Dityat'yev, O.A., see Berdonosov, P.S. 99
 Do Rosario Matos, J., see Parra, D.F. 193
 Dobson, P.J., see Moon, D.G. 214
 Doe, M., see Takemura, M. 314
 Doggwiler, B., see Batawi, E. 17
 Dokiya, M., see Horita, T. 39
 Dokiya, M., see Kawada, T. 36
 Dokiya, M., see Mori, M. 20
 Dokiya, M., see Nishiyama, H. 40
 Dokiya, M., see Sakai, N. 17, 19, 20, 27, 29–35, 38, 39
 Dokiya, M., see Van Hassel, B.A. 25, 26
 Dokiya, M., see Yamaji, K. 21, 22
 Dokiya, M., see Yokokawa, H. 19, 36
 Dolgikh, V.A., see Berdonosov, P.S. 78, 99
 Dolgikh, V.A., see Oppermann, H. 78, 97
 Dolgikh, V.A., see Schmidt, P. 78, 97
 Dolgikh, V.A., see Shabalin, D.G. 81
 D'Olieslager, W., see Van Meervelt, L. 131, 148
 Dong, N. 192
 Donnio, B. 201
 Doreshenko, N.A., see Suponitskii, Yu.L. 49
 Douce, L., see Montalti, M. 276

- Dow, W.-P., see Wang, J.B. 14
 Drake, S.R. 139
 Drake, S.R., see Baxter, I. 132, 139, 311
 Drake, S.R., see Leedham, T.J. 145–152, 239
 Drake, S.R., see Plakatouras, J.C. 132, 311
 Dravid, V.P., see Han, B. 239
 Drennan, J. 30
 Driesen, K., see Binnemans, K. 189
 Driesen, K., see Galyametdinov, Yu.G. 202
 Drisque, I., see Van Meervelt, L. 131, 148
 Duan, C.Y., see Chen, X.F. 133, 155, 181
 Duan, J.P., see Sun, P.P. 211, 215
 Dubey, S., see Hasan, M. 124
 Dubois, J.T., see Sicre, J.E. 234–236
 Dubost, J.-P. 319
 Dudeney, A.W.L., see Belcher, R. 146
 Dugue, J., see Khodadad, P. 96
 Duignan, J.P., see Bourhill, G. 181
 Duin, M.A., see Werts, M.H.V. 167, 168
 Dujardin, G. 249
 Dukov, I.L. 244, 245
 Dukov, I.L., see Atanassova, M. 244
 Dukov, I.L., see Genov, L. 244
 Duyckaerts, G., see Bhatti, M.S. 244
 Duyckaerts, G., see Desreux, J.F. 244
 Dyer, D.S. 224
 Dzyubenko, N.G., see Zharkova, Ya.N. 130
- Eaton, D.F. 170
 Edelmann, F.T., see Lorenz, V. 135, 136
 Edy, C.R., see Blackborow, J.R. 125
 Efremov, A.A., see Smolyakova, K.E. 49
 Efremov, V.A., see Ovanisyan, S.M. 58, 59
 Eichen, Y., see Willner, I. 283
 Eikenberry, J.N., see Goering, H.L. 226
 Eisentraut, K.J. 126, 127, 145–153, 157, 233, 234, 237
 Eisentraut, K.J., see Sicre, J.E. 234–236
 El-Sayed, M.A., see Bhaumik, M.L. 165
 Elbanowski, M. 183
 Elbanowski, M., see Kaczmarek, M. 185
 Elbanowski, M., see Lis, S. 168, 176
 Elbanowski, M., see Szyzewski, A. 161
 Elgavish, G.A., see Reuben, J. 112, 220
 Ellison, J.J., see Caravan, P. 274, 278, 317, 319
 Emsley, J. 118
 Engebretsen, T., see Aukrust, A. 319
 Enjalbert, R., see Castro, A. 72, 75, 94
 Enjalbert, R., see de Pedro, M. 72, 74, 94
 Epstein, A.J., see Sun, R.G. 214
 Era, M., see Noto, M. 213
- Erämetsä, O. 96
 Erasmus, C.S. 132, 135, 139, 140, 158
 Ercoli, R., see Sacconi, L. 145–147, 150
 Eremenko, I.L., see Aikihanyan, A.S. 128
 Eriksson, B., see Valkonen, J. 50, 52
 Erostyak, J. 228
 Erostyak, J., see Hornyak, I. 228
 Esaka, T., see Iwahara, H. 14
 Espinet, P. 201
 Espinoza, B.F., see Hubbard, K.M. 239
 Esteruelas, M.A., see Espinet, P. 201
 Etchells, M., see Moon, D.G. 214
 Evans, F.D. 225
 Evans, W.J. 124, 126, 130–132, 147, 149, 150, 311
 Ewers, C.L.J., see Schmitt-Willich, H. 328
 Ezhov, Y.S. 236
- Fabretti, A.C., see Benelli, C. 160
 Faler, G., see Schuster, G.B. 183
 Fan, D., see Chu, B. 214
 Fan, D., see Hong, Z.R. 214
 Fan, P.C. 119
 Fan, X.P. 186, 188
 Fan, X.P., see Hao, X.P. 186
 Fan, Y., see Wang, K.Z. 198
 Fan, Y.G., see Shen, C. 130–132, 143, 144
 Fang, G. 242
 Farag, I.S.A., see Aslanov, L.A. 50, 52
 Farbu, L., see Alstad, J. 244
 Farias Jr., F.S., see Malta, O.L. 172
 Farrugia, L.J. 331
 Fasano, M., see Aime, S. 274, 278, 328
 Faulkner, S., see Beeby, A. 173
 Faulkner, S., see Shavaleev, N.M. 174, 175
 Faustino, W.M. 172
 Fay, R.C., see Steffen, W.L. 141
 Fedeli, F., see Aime, S. 326
 Fedeli, F., see Terreno, E. 295, 315
 Fedorov, V.V., see Suponitskii, Yu.L. 49
 Feibush, B. 145–148, 150, 232
 Feistel, G., see Moeller, T. 244
 Felinto, M.C.F.C., see Brito, H.F. 175, 176
 Féliz, M.R., see Villata, L.S. 168
 Feller, K.H., see Grummt, U.W. 204
 Felsche, J. 46
 Felten, F., see Weiss, F. 240
 Feng, H.Y. 194
 Feng, X.S., see Liu, H.G. 191
 Fenkhua, L. 234
 Feofilov, P.P. 194
 Ferguson, L.N., see Lowe Jr., J.U. 119

- Fernandes, A. 197
 Fernandes, J.A. 121
 Fernandez De Avila, S., see Diaz-Garcia, M.A. 213
 Ferrand, A.-C., see Zucchi, G. 286
 Ferrus, R., see Moeller, T. 244
 Fery-Forgues, S. 169
 Feuerstein, R.J., see Lin, S. 218
 Filipescu, N. 164–166, 205
 Filipescu, N., see Bjorklund, S. 161, 171, 205
 Filipescu, N., see Hurt, C.R. 179, 180
 Filipescu, N., see Sager, W.F. 165
 Finch, C.B., see Boatner, L.A. 46
 Fink, A., see Busch, H. 240
 Fischer, A., see Lorenz, V. 135, 136
 Fischer, R.D., see von Ammon, R. 220
 FitzGerald, S., see Beeby, A. 299
 Fitzsimmons, E.S. 32, 33
 Fjellvåg, H., see Seim, H. 242
 Flanigen, E.M., see van Bekkum, H. 195
 Fldinger, F., see Sammes, N.M. 30
 Fletcher, P.C., see Bhaumik, M.L. 205
 Flockhart, B.D. 220
 Foiret, V., see Bünzli, J.-C.G. 172, 175
 Fong, X.-L., see Yang, X.-P. 289
 Foreman, B.M., see Poskanzer, A.M. 244
 Fomes, V., see Alvaro, M. 196
 Forrest, S.R., see Adachi, C. 215
 Forsberg, J.H. 112, 220, 308
 Forsyth, C.M., see Behrsing, T. 141, 142, 159
 Forsyth, M., see Behrsing, T. 141, 142, 159
 Foster, D.R. 178
 Foulletier, J., see Sauvet, A.-L. 15
 Foulon, J.-D., see Gleizes, A. 124, 130, 135, 141
 Fox, L.E., see Desreux, J.F. 127, 158, 226
 Fragala, I.L., see Condorelli, G.G. 239
 Fragala, I.L., see Lo Nigro, R. 239
 Fragala, I.L., see Malandrino, G. 124, 130, 131, 146, 149, 172, 175, 239
 Francesconi, I.C., see Kumar, K. 319
 Frank, J.A., see Bryant Jr., L.H. 326
 Fraser, C.L., see Bender, J.L. 194
 Fraser, S.E., see Li, W.-H. 324
 Frassica, A., see Malandrino, G. 239
 Frederique, D.E., see Wenzel, T.J. 314
 Freeman, J.J. 165
 Freeman, J.J., see Crosby, G.A. 163
 Freire, R.O., see Rocha, G.B. 172
 Freiser, H., see Sasaki, Y. 245
 Freiser, H., see Umetani, S. 245
 Freltoft, T., see Richards, B.C. 240
 Frenzel, T., see Roth, K. 325
 Freppel, C., see Belanger, P. 221
 Frey, S.T. 158
 Friend, R.H., see Burroughes, J.H. 207
 Fritz, J.S., see Burgett, C.A. 238
 Fröhlich, K., see Weiss, F. 240
 Frost, G.H., see Briggs, J. 219
 Froyen, A., see Van Meervelt, L. 131, 148
 Fry, F.H. 206
 Fu, L.S. 196
 Fu, L.S., see Guo, J.F. 188
 Fu, P.K.-L., see Turro, C. 288
 Fu, Y.J. 148, 150
 Fueki, K., see Horinouchi, K. 32
 Fuji, T., see Sano, T. 211
 Fujii, H. 10
 Fujimoto, T., see Ohta, K. 119
 Fujinaga, T. 147, 237
 Fujita, M., see Sano, T. 211
 Fujiwara, K., see Oka, T. 249
 Fujiwara, T., see Omata, K. 315
 Fukaya, K., see Hayashi, S. 20, 34, 35
 Fukuda, K., see Qian, D.J. 198
 Fukuda, Y. 122, 143, 144, 275
 Fukui, S., see Ishihara, T. 16
 Fukui, T., see Matsuda, M. 19
 Fukui, T., see Zhang, X. 37
 Fukutomi, H., see Hatakeyama, Y. 156
 Fun, H.K., see Chen, X.F. 131, 155, 181
 Funahashi, S., see Matsumoto, M. 159
 Furuno, H., see Inanaga, J. 284
 Gadonas, R., see Grummt, U.W. 204
 Galarneau, A., see Fernandes, A. 197
 Gale, P.A., see Beer, P.D. 280
 Galindo, V. 240
 Galy, J., see de Pedro, M. 72, 74, 94
 Galyametdinov, Yu.G. 202
 Gan, L.B., see Xia, W.S. 198
 Gao, D.Q. 211
 Gao, D.Q., see Huang, L. 211, 214
 Gao, G.Q., see Wang, K.Z. 198
 Gao, J.Z. 228
 Gao, J.Z., see Yang, W. 228
 Gao, L., see Chen, B.T. 181
 Gao, L.H. 162, 198, 204
 Gao, L.H., see Wang, K.Z. 149, 150, 175, 198, 199, 211
 Gao, P.L., see Jiang, J.Z. 128, 198, 199
 Gao, R.Y. 190, 191
 Gao, X. 162, 199

- Gao, X.C. 151, 214
 Gao, X.X., see Xiao, Y.J. 162
 Garcia, H., see Alvaro, M. 196
 Garcia, S., see Alvaro, M. 196
 Garito, A.F., see Gao, R.Y. 190, 191
 Gasanov, Y.M. 58, 60
 Gatehouse, B.M., see Berrigan, R. 85, 90
 Gattaschi, D., see Benelli, C. 141, 160
 Gatteschi, D., see Benelli, C. 159, 160
 Gauckler, L.G., see Joeger, M. 14
 Gaur, D.P., see Mehrotra, R.C. 112
 Geballe, T.H., see Dickinson, P.H. 240
 Geddes, N., see Sage, I. 180, 182
 Geira, E. 159
 Gelbrich, T., see Ruloff, R. 319
 Geller, M., see Altman, D.E. 205
 Gennaro, S., see Condorelli, G.G. 239
 Genov, L. 244
 Genov, L., see Dukov, I.L. 244, 245
 George, R. 10
 Georges, J., see Arnaud, N. 228
 Georges, J., see Brennetot, R. 228
 Geraldès, C.F.G.C. 220
 Gerfin, T., see Becht, M. 146, 236, 241
 Gerrard, D.L., see Allan, J.R. 193
 Gerstberger, G. 249
 Gevaza, Yu.I., see Rusakova, N.V. 173
 Gianolio, E., see Aime, S. 323, 326
 Gianolio, E., see Congreve, A. 319
 Gianolio, E., see Lowe, M.P. 296
 Giarikos, D.G., see Evans, W.J. 124, 126, 130–132, 147, 149, 150, 311
 Giesbrecht, E. 94
 Giesbrecht, E., see Giolito, I. 49, 63, 73, 94
 Gin, Y., see Li, W. 176
 Giolito, I. 49, 62, 63, 73, 94
 Giolito, I., see Cruz, P.M. 62
 Giolito, I., see De Ávila Agostini, P.R. 60, 62
 Giolito, I., see Ionashiro, M. 59, 62
 Giovenzana, G., see Aime, S. 322
 Girichev, G.V. 235
 Girichev, G.V., see Belova, N.V. 236
 Girichev, G.V., see Giricheva, N.I. 235, 236
 Giricheva, N.I. 235, 236
 Giricheva, N.I., see Belova, N.V. 236
 Giricheva, N.I., see Girichev, G.V. 235
 Giroud-Godquin, A.M. 201
 Girvan, B., see Bance, P. 14
 Glatz, W., see Batawi, E. 17
 Gleizes, A. 124, 128, 130, 135, 141, 235, 240
 Gleizes, A., see Aikihyanan, A.S. 128
 Gleizes, A., see Fernandes, A. 197
 Gleizes, A., see Kuz'mina, N.P. 128
 Gleizes, A., see Ryazanov, M. 128
 Gleizes, A.N. 240
 Gleizes, A.N., see Kuzmina, N. 240, 241
 Gleizes, A.N., see Kuz'mina, N.P. 128
 Gløgård, C., see Hovland, R. 322
 Glover, P.B. 299
 Glover, P.B., see Bassett, A.P. 158
 Godlewski, M., see Karpinska, L. 242
 Goedken, V.L., see Luten, H.A. 139
 Goering, H.L. 226
 Göhausen, I. 50, 55, 80, 83, 100, 102
 Golovin, Yu.M., see Petrov, K.I. 73, 94, 96
 Golubtsova, V.I., see Spitsyn, V.I. 238
 Gonçalves, I.S., see Braga, S.S. 127
 Gonçalves, I.S., see Fernandes, J.A. 121
 Gonçalves, R.R., see de Mello Donegá, C. 170
 Gonçalves, R.R., see Sá Ferreira, R.A. 189
 Gonçalves e Silva, F.R. 170, 172
 Gonçalves e Silva, F.R., see Faustino, W.M. 172
 Gonçalves e Silva, F.R., see Malta, O.L. 170, 172
 Gong, M.L., see Frey, S.T. 158
 Gong, M.L., see Yang, Y.S. 166, 167, 230
 Gong, M.L., see Yao, Y.F. 197
 Goodby, J., see Demus, D. 200
 Gorbenko, O., see Wahl, G. 240
 Gorbenko, O.Yu. 239
 Gorbenko, Yu., see Girichev, G.V. 235
 Görrler-Walrand, C. 161
 Görrler-Walrand, C., see Binnemans, K. 162, 189, 201
 Gorte, R.J. 15
 Gospodinov, G.G. 74, 76, 99
 Gotanda, K., see Tamura, O. 249
 Goto, T., see Kimura, T. 239
 Gougoutas, J.Z., see Kumar, K. 319
 Gourba, E. 241
 Goursolle, M., see Delage, C. 69, 70
 Govenlock, L.G., see Maupin, C.L. 307
 Govenlock, L.J. 299
 Govenlock, L.J., see Beeby, A. 299
 Govenlock, L.J., see Bruce, J.I. 276, 294, 313
 Grahn, W., see Dirr, S. 211
 Gray, G.W., see Demus, D. 200
 Grayson, M., see Bruce, D.W. 204
 Grdenić, D., see Matković, B. 141
 Greci, M.A., see Evans, W.J. 124, 126, 130–132, 147, 149, 150, 311
 Grigor'ev, A.N., see Martynenko, L.I. 139
 Grigoriev, A.N., see Kuzmina, N.P. 234, 235

- Grupp, L. 19
 Grummt, U.W. 204
 Grushin, V.V., see Petrov, V.A. 125, 131, 132, 311
 Gu, J.H. 249
 Gu, J.H., see Terada, M. 249
 Gu, Z.N., see Jiang, J.Z. 128, 198, 199
 Guardigli, M., see Charbonnière, L. 286
 Guardigli, M., see Sabbatini, N. 168, 229, 274
 Gudmundson, R.A. 170
 Guery, J., see Jardin, M. 241
 Guillon, D., see Donnio, B. 201
 Gumy, F., see Chauvin, A.S. 170
 Gundermann, K.D. 183
 Gunnlaugsson, T. 276, 294, 297, 298
 Gunnlaugsson, T., see Bruce, J.I. 276, 294, 313
 Gunnlaugsson, T., see Dickins, R.S. 292, 321
 Gunnlaugsson, T., see Reany, O. 298
 Guo, C., see Zheng, Y.X. 211, 214, 215
 Guo, F.W., see Huang, C.H. 181
 Guo, J.F. 188
 Guo, Y., see Campos, R.A. 211
 Gupta, M.K. 49, 63
 Guru Row, T.N., see Urs, U.K. 130
 Guter, G.A., see Hammond, G.S. 119
 Gutiérrez, L.G., see Ruano, J.L.G. 249
 Guyon, J.C., see Williams, D.E. 228
 Guyot, Y., see Boyaval, J. 203

 Ha, Y.K., see Kim, Y.K. 211
 Ha, Y.K., see Pyo, S.W. 216
 Haas, Y. 170
 Haas Jr., J.W. 183
 Haase, W., see Galyametdinov, Yu.G. 202
 Haasnoot, J.G., see Van Staveren, D.R. 125, 130, 132, 136, 138, 139
 Haasnoot, J.G., see van Staveren, D.R. 311
 Haddou, H.A., see Wiskur, S.L. 280
 Hagiwara, H., see Saitoh, T. 249
 Hájek, B. 49, 61, 63
 Hajek, M., see Raber, D.J. 225
 Hall, L.D., see Arduini, A. 223
 Hall, L.D., see Armitage, I. 219
 Hall, L.D., see Bulsing, J.M. 220
 Haltiwanger, R.C., see Wenzel, T.J. 146, 243
 Halverson, F. 126, 149, 150, 156
 Hamada, Y., see Ohmori, Y. 211
 Hamada, Y., see Sano, T. 211
 Hamaguchi, W., see Dai, W.M. 249
 Hammon, G.S., see Johnston, K.E. 127
 Hammond, G.S. 119, 148
 Han, B. 239
 Han, S.Q., see Wu, F.B. 230
 Han, Y.Z., see Huang, C.H. 147
 Hanaoka, K. 325
 Hanaoka, K., see Harima, H. 236
 Handel, H., see Ruloff, R. 319
 Hanna, G.H. 309
 Hao, X.P. 186
 Hapiot, F. 202
 Hapiot, F., see Boyaval, J. 202, 203
 Harada, M., see Hatakeyama, Y. 156
 Harden, R.C., see Cockerill, A.F. 220
 Hardy, G.E., see Zink, J.I. 179, 182
 Harima, H. 236
 Härkönen, G., see Leskelä, T. 235, 236, 239, 242
 Harrison, W.T.A. 67, 70, 90, 91, 100
 Harrison, W.T.A., see Morris, R. 74
 Hart, F.A., see Briggs, J. 219
 Harte, A.J., see Gunnlaugsson, T. 276, 294, 298
 Hartle, R.J. 243
 Hartley, A. 16
 Hasan, M. 124
 Hasan, M., see Anastassiou, A. 309
 Hasegawa, A., see Yamada, T. 14
 Hasegawa, T., see Watanabe, M. 314
 Hasegawa, Y. 173, 244
 Hasegawa, Y., see Kawamura, Y. 214
 Hasegawa, Y., see Matsubayashi, I. 244
 Hasegawa, Y., see Yanagida, S. 173
 Hashimoto, T., see Sakai, N. 37
 Hasselman, D.P.H. 30–33
 Hatakeyama, Y. 156
 Hattori, M., see Nakanishi, A. 12
 Haukka, S. 242
 Haung, C.H., see Gao, L.H. 204
 Hay, D., see Drennan, J. 30
 Hayano, T., see Inanaga, J. 284
 Hayase, H., see Kido, J. 210, 211, 215
 Hayashi, K., see Fukuda, Y. 122, 143, 144, 275
 Hayashi, S. 20, 34, 35
 Hazama, R. 313, 314
 He, J., see Gao, J.Z. 228
 He, Y.F., see Wu, F.B. 230
 He, Z., see Xu, G. 141
 Healy, T.V. 244
 Heeger, A.J., see McGehee, M.D. 211, 213
 Heeger, A.J., see Yang, C.Y. 177, 194
 Heikkinen, H. 242
 Heikkinen, H., see Kukli, K. 242
 Heil, H. 215
 Held, P. 46
 Helliwell, M. 249

- Hellmuth, K.-H. 149
 Hellwig, H., see Held, P. 46
 Helm, L., see Tóth, É. 317
 Hemingway, R.E. 159
 Hemmilä, I. 229
 Hemmilä, I., see Xu, Y.Y. 228
 Hemmilä, I.A., see Xu, Y.Y. 176, 228
 Henderson, W., see Caldwell, J.P. 232
 Hendriksen, P.V., see Larsen, P.H. 20
 Hercules, D.M., see Cormier, J.M. 183
 Hering, E.N., see Reyes, R. 214
 Hermann, P., see Rohovec, J. 326
 Herynek, V., see Bryant Jr., L.H. 326
 Hibbs, D.E., see Darr, J.A. 139, 140, 152
 Hieda, S., see Takada, N. 181, 182
 Higa, S., see Bhaumik, M.L. 205
 Higashi, T., see Sugimoto, H. 142–144
 Higgins, J.B., see Beck, J.S. 196
 Hikada, H., see Tasaki, Y. 145, 147, 239
 Hikita, T., see Yasuda, I. 24, 29
 Hildenbrand, D., see Dickinson, P.H. 240
 Hilder, M., see Brück, S. 130, 136
 Hiltunen, L. 50, 51
 Hinchley, S.L., see Belova, N.V. 236
 Hincley, C.C. 219
 Hinds, B.J., see Han, B. 239
 Hirai, T., see Yamane, H. 240
 Hirano, N., see Yamaguchi, T. 240
 Hirata, G.A. 239
 Hirata, Y., see Sameshima, S. 30, 34
 Hirayama, C. 235
 Hird, M., see Collings, P.J. 200
 Hisatome, N., see Konishi, K. 10, 17
 Hishinuma, M., see Yasuda, I. 34
 Hishinuma, M., see Yasuda, T. 38
 Hitchman, M.L., see Richards, B.C. 240
 Hiuang, C.H., see Zhou, D.J. 204
 Hiwatashi, K., see Sakai, N. 27
 H'Naifi, A., see Delage, C. 69, 70
 Hnatejko, Z., see Lis, S. 168, 176
 Hocking, M.B. 179
 Hoe, H.S., see Pyo, S.W. 211, 214, 216
 Hofer, H.E. 34, 35
 Hofstraat, H., see Werts, M.H.V. 167, 168
 Holbeche, P., see Bance, P. 14
 Holmes, A.B., see Burroughes, J.H. 207
 Hölsä, J., see Leskelä, M. 72
 Holttinen, S., see Xu, Y.Y. 228
 Holz, R.C. 121, 129–132, 134, 311
 Homma, J.-I., see Sakagami, N. 312
 Honda, M., see Ishihara, T. 15
 Hong, S.T., see Lim, J.T. 124, 145, 146
 Hong, X.Z.R., see Zhao, D. 211, 214
 Hong, Z., see Li, W.L. 211, 214
 Hong, Z., see Zhao, D. 214
 Hong, Z., see Zhao, D.X. 213
 Hong, Z.R. 214
 Hong, Z.R., see Chu, B. 214
 Hong, Z.R., see Liang, C.J. 211, 214, 215
 Hong, Z.R., see Liu, L. 211, 215
 Hongawa, K., see Kido, J. 210, 211, 215
 Honjo, T., see Shigematsu, T. 237, 244
 Horinouchi, K. 32
 Horita, T. 39
 Horita, T., see Nishiyama, H. 40
 Horita, T., see Sakai, N. 27, 29, 31–33, 37, 39
 Horita, T., see Xiong, Y. 21, 22
 Horita, T., see Xiong, Y.P. 37
 Horita, T., see Yamaji, K. 21, 22
 Horita, T., see Yokokawa, H. 36
 Horiuchi, H., see Sasaki, M. 127, 159, 160
 Hornyak, I. 228
 Hornyak, I., see Erostyak, J. 228
 Horrocks Jr., W.DeW. 129, 132, 220, 221, 223, 224, 308, 309
 Horrocks Jr., W.DeW., see Wang, C.P. 128
 Hoshi, T., see Saitoh, T. 249
 Hoshino, K., see Yamada, T. 14
 Hoshinouchi, S., see Harima, H. 236
 Hosoi, K., see Yamada, T. 14
 Hosokubo, M., see Tsukube, H. 161, 279, 296, 302
 Houbrechts, S., see Verbiest, T. 203
 Hovland, R. 322
 Hovnanian, N., see Gleizes, A. 124, 130, 135, 141
 Howard, J.A.K., see Aime, S. 321
 Howard, J.A.K., see Dickins, R.S. 294
 Howard, J.A.K., see Parker, D. 280
 Hoyer, E., see Ruloff, R. 319
 Hradilová, J., see Hájek, B. 49, 61, 63
 Hriljac, J.A., see Morris, R.E. 88, 90
 Hu, J.F., see Zhang, R.J. 200
 Hu, L. 228
 Hu, M.L. 131
 Hu, W.P. 211, 215
 Hu, X., see Fu, Y.J. 148, 150
 Hu, Y., see Hu, M.L. 131
 Huang, C.H. 147, 181, 198, 204
 Huang, C.H., see Gao, D.Q. 211
 Huang, C.H., see Gao, L.H. 162, 204
 Huang, C.H., see Gao, X.C. 151, 214
 Huang, C.H., see Huang, L. 211, 214
 Huang, C.H., see Jiang, W. 128, 198, 199

- Huang, C.H., see Li, H. 162, 204
 Huang, C.H., see Pavier, M.A. 200
 Huang, C.H., see Wang, K.Z. 149, 150, 162, 175,
 198, 199, 202, 204, 211
 Huang, C.H., see Xia, W.S. 198
 Huang, C.H., see Xiao, Y.J. 162
 Huang, C.H., see Zhao, X.S. 204
 Huang, C.H., see Zhao, Y.L. 198
 Huang, C.H., see Zhou, D.J. 154, 155, 198
 Huang, D.Y., see Jiang, X.Z. 211, 213
 Huang, H.X. 200
 Huang, J.L., see Wang, M.Z. 123, 162
 Huang, L. 211, 214
 Huang, L., see Wang, K.Z. 149, 199, 211
 Huang, P.L., see Cotton, F.A. 133, 180
 Huang, S.H., see Wang, M.Z. 123, 162
 Huang, T.-J., see Wang, J.B. 14
 Huang, W., see Wang, L.H. 193
 Huang, X., see Kurtán, T. 305
 Huang, Y.Y., see Huang, L. 214
 Huang, Z.Y., see Hu, M.L. 131
 Hubbard, K.M. 239
 Hubert-Pfalzgraf, L.G., see Poncelet, O. 139
 Hubert-Pfalzgraf, L.G. 146
 Hudner, J., see Thomas, O. 240
 Hudson, S.A. 201
 Hue, H.S., see Kim, Y.K. 211
 Huffman, E.H. 205
 Huffmann, E.H. 191, 205
 Humberstone, L., see Sage, I. 180, 182
 Hung, L.S. 207
 Hung, L.S., see Hong, Z.R. 214
 Huray, P.G., see Boatner, L.A. 46
 Hursthouse, M.B., see Baxter, I. 132, 139, 311
 Hursthouse, M.B., see Darr, J.A. 139, 140, 152
 Hursthouse, M.B., see Drake, S.R. 139
 Hursthouse, M.B., see Plakatouras, J.C. 132, 311
 Hurt, C.R. 179, 180
 Hurt, C.R., see Bjorklund, S. 205
 Husebo, L.O., see Bolskar, R.D. 328
 Huskens, J., see Peters, J.A. 220

 Ichiki, S., see Fujinaga, T. 147
 Iftikhar, K. 145–153
 Iguchi, M., see Nagano, H. 249
 Igumenov, I.K., see Zaitseva, E.G. 130, 135
 Iijima, K., see Shibata, S. 235
 Iijima, Y., see Yamaguchi, T. 240
 Ikeda, H., see Miyamoto, Y. 211
 Ikeda, K., see Konishi, K. 10, 17
 Ikeda, W., see Kido, J. 210, 211, 214

 Imai, N., see Kobayashi, T. 218
 Imai, N., see Kuriki, K. 218
 Imaishi, N., see Akiyama, Y. 239
 Imamoto, T. 247, 274
 Imanishi, N., see Yamamoto, O. 34
 Imbert, D., see Chauvin, A.S. 170
 Imbert, D., see Senegas, J.-M. 286
 Immonen, E. 94, 96
 Inagaki, F. 220
 Inagaki, T., see Yamada, T. 14
 Inagaki, T., see Zhang, X. 37
 Inamoto, A. 315, 317
 Inanaga, J. 284
 Incontro, O., see Malandrino, G. 131, 239
 Inoue, H., see Okada, K. 211, 215
 Inoue, S., see Li, H.H. 187
 Inoue, Y., see Borovkov, V.V. 305
 Inuzuka, T., see Shibata, S. 235
 Ionashiro, M. 59, 62
 Ionashiro, M., see Cruz, P.M. 62
 Ionashiro, M., see D'Assunção, L.M. 96
 Ionashiro, M., see De Ávila Agostini, P.R. 60, 62
 Ionashiro, M., see Giolito, I. 62
 Ionashiro, M., see Spirandeli Crespi, M. 62
 Ionov, V.M., see Aslanov, L.A. 50, 52
 Irie, K., see Noto, M. 213
 Iritani, J., see Konishi, K. 10, 17
 Isaert, N., see Boyaval, J. 202, 203
 Ishayek, R., see Serpone, N. 156
 Ishihara, T. 14–16
 Ishihara, T., see Yamada, T. 14
 Ishikawa, M., see Yamaji, K. 21, 22
 Ishikawa, N., see Kawa, H. 227, 249, 309
 Ishikawa, T., see Sameshima, S. 30, 34
 Ishikawa, Y., see Amao, Y. 232
 Ishiwata, E., see Hasegawa, Y. 244
 Iskhakova, L.D. 49, 50, 55–58, 60
 Iskhakova, L.D., see Gasanov, Y.M. 58, 60
 Iskhakova, L.D., see Ovanisyan, S.M. 50, 51,
 57–60
 Ismail, M. 123, 126, 158
 Ito, N.K., see Batista, H.J. 131, 148, 311
 Ito, N.K., see Malta, O.L. 131, 149
 Ito, Y., see Yamaguchi, R. 216
 Itoh, H. 18
 Itoh, H., see Mori, M. 29
 Itoh, H., see Tsukube, H. 246, 247, 282, 283
 Itoh, K.I. 239
 Ivanov, V.I., see Petrov, K.I. 49, 63
 Iwachido, T., see Tsukube, H. 246, 247, 282, 283
 Iwafuji, T., see Kobayashi, T. 218

- Iwahara, H. 14
 Iwamuro, M. 166, 173
 Iwamuro, M., see Kawamura, Y. 214
 Iwasaki, H., see Yamane, H. 240
 Iwasaki, N., see Misumi, S. 161
 Iwata, T., see Sakai, N. 17, 19, 20, 34, 35
- Jabbour, G.E. 211
 Jabbour, G.E., see Wang, J.F. 211, 212
 Jabbourb, G.E., see Zheng, Z.P. 131, 181
 Jackson, E.F., see Bolskar, R.D. 328
 Jackson III, G.F., see Raber, D.J. 223
 Jacob, K., see Lorenz, V. 135, 136
 Jacoboni, C., see Jardin, M. 241
 Jacobs, C.L., see Lemieux, G.A. 329, 330
 Jacobs, R.R. 237
 Jacobson, C.P., see Visco, S. 12
 Jacobus, J. 308
 Jafellici Jr., M., see Sigoli, F.A. 189
 Jang, K.W., see Liu, H.G. 191
 Jang, S.H., see Kahr, B. 177
 Janks, C.M., see Raber, D.J. 223
 Janowski, A., see Dambaska, A. 225
 Jansen, J.C., see van Bekkum, H. 195
 Jaonusek, M., see Batawi, E. 17
 Jarczuk, J. 249
 Jardin, M. 241
 Jeannin, Y., see Ramade, I. 128, 130, 132
 Jen, A.K.Y., see Jiang, X.Z. 211, 213
 Jensen, L.C., see Dickinson, J.T. 179
 Jere, G.V., see Gupta, M.K. 49, 63
 Jezewski, A., see Bauer, T. 249
 Jezewski, A., see Jarczuk, J. 249
 Jian, S.H., see Feng, H.Y. 194
 Jian, Y.P., see Feng, H.Y. 194
 Jiang, J.Z. 128, 198, 199
 Jiang, P., see Gao, X.C. 151, 214
 Jiang, Q., see Zhu, W.G. 211, 215
 Jiang, W. 128, 198, 199
 Jiang, W., see Wang, K.Z. 204
 Jiang, W., see Zhu, G. 229
 Jiang, X.Z. 211, 213
 Jiang, Y.Z., see Song, H.Z. 145, 150, 234, 239
 Jin, H.-Y., see Sato, J. 315
 Jin, J.I., see Zhong, G.L. 211
 Jin, L.P., see Bian, Z.Q. 121
 Jin, L.P., see Bünzli, J.-C.G. 172, 175
 Jin, L.P., see Gao, D.Q. 211
 Jin, L.P., see Hu, W.P. 211, 215
 Jin, L.P., see Huang, L. 211
 Jin, L.P., see Tang, B. 192
 Jin, L.P., see Wang, K.Z. 149, 199, 211
 Jin, L.P., see Wang, M.Z. 123, 162
 Jin, L.P., see Yu, G. 213, 215
 Jing, X.B., see Liang, F.S. 212, 215
 Jo, S.-K., see Kobayashi, H. 326, 327
 Jodry, J.J. 308
 Joeger, M. 14
 Johannes, H.-H., see Dirr, S. 211
 Johansson, L.-S., see Putkonen, M. 241
 Johansson, L.-S., see Heikkinen, H. 242
 Johansson, L.-S., see Putkonen, M. 241
 Johansson, L.-S., see Seim, H. 242
 Johnson, C.R., see Brittain, H.G. 177
 Johnson, L.F., see Hasselman, D.P.H. 30–33
 Johnston, K.E. 127
 Johnston, M.A., see Evans, W.J. 124, 126, 130–132, 147, 149, 150, 311
 Johnston Jr., M.D., see Raber, D.J. 223
 Johnston Jr., M.D., see Shapiro, B.L. 224
 Joly, J.-P., see Wenzel, T.J. 315
 Jones, A.C. 241
 Jordan, J., see Bard, A.J. 48
 Jordanov, V.M., see Atanassova, M. 244
 Jordanov, V.M., see Dukov, I.L. 244
 Ju, S.H., see Lee, M.H. 211, 215
 Judenstein, P., see Bekiari, V. 189
 Julve, M., see Gleizes, A. 128, 235, 240
 Julve, M., see Gleizes, A.N. 240
 Julve, M., see Ryazanov, M. 128
 Julve-Olsina, M., see Aikihanyan, A.S. 128
 Juneau, G.P. 226
 Jung, S.C., see Akiyama, Y. 239
 Jung, W.K., see Mihara, T. 156
 Jung, Y.K., see Kang, S.J. 149, 239
 Jung, Y.S. 130, 141
 Jung, Y.S., see Kang, S.J. 131, 151
 Jung, Y.S., see Lee, J.H. 132, 141, 151
 Junk, P.C., see Brück, S. 130, 136
 Jurczak, J., see Bauer, T. 249
 Jürgensen, H., see Richards, B.C. 240
 Justel, T., see Boerner, H. 216
 Jyothi, A. 245
 Kabata, T., see Konishi, K. 10, 17
 Kabuto, C., see Hazama, R. 313, 314
 Kabuto, K. 313
 Kabuto, K., see Hazama, R. 313, 314
 Kabuto, K., see Inamoto, A. 315, 317
 Kabuto, K., see Omata, K. 315
 Kabuto, K., see Sato, J. 315
 Kaczmarek, M. 185

- Kaczmarek, M., see Elbanowski, M. 183
 Kadowaki, M., see Taniguchi, S. 17
 Kagan, M.R., see Filipescu, N. 205
 Kageyama, H., see Takeuchi, T. 29
 Kahn, O., see Ramade, I. 128, 130, 132
 Kahr, B. 177
 Kaifu, K., see Miyamoto, Y. 211
 Kaizaki, S., see Tsukuda, T. 311
 Kajii, H., see Ohmori, T. 211
 Kakolowicz, W., see Geira, E. 159
 Kaldis, J.H., see Ahmed, M.O. 131
 Kaltsoyannis, N. 274
 Kamble, K.J., see Behrsing, T. 141, 142, 159
 Kamegashira, N., see Kobayashi, H. 30–33
 Kamihara, T., see Yamamoto, O. 14
 Kanatani, T., see Tsukube, H. 246, 247, 282, 283
 Kanazawa, Y., see Kato, H. 326
 Kanemasa, S., see Wada, E. 249
 Kang, B.-S., see Yang, X.-P. 289
 Kang, E.T., see Wang, L.H. 193
 Kang, J.W., see Yang, W. 228
 Kang, S.J. 131, 149, 151, 239
 Kang, S.J., see Jung, Y.S. 130, 141
 Kang, S.J., see Lee, J.H. 132, 141, 151
 Kannan, G., see Biju, V.M. 228, 229
 Kanno, R., see Yamamoto, O. 14
 Kaplan, M.L., see Wayda, A.L. 311
 Kapoor, R.N., see Hasan, M. 124
 Kapoor, R.N., see Sankhla, B.S. 124
 Karapet'yants, M., see Suponitskii, Yu.L. 49
 Karim, D.P. 24
 Karpinska, L. 242
 Karraker, D.E. 157
 Karraker, D.G., see Zalkin, A. 129, 132, 134
 Karvinen, S. 50, 52, 61, 72
 Kassabov, G.I., see Genov, L. 244
 Kaszas, A., see Hornyak, I. 228
 Katagiri, R., see Tamura, O. 249
 Katakya, R., see Aime, S. 321
 Kataoka, H., see Tasaki, Y. 145, 147, 239
 Kato, H. 326
 Katoh, R., see Takada, N. 181, 182
 Katsube, T., see Sakai, N. 37
 Katzin, L.I. 281
 Kaul, A., see Wahl, G. 240
 Kaul', A.R., see Girichev, G.V. 235
 Kaul, A.R., see Gorbenko, O.Yu. 239
 Kaur, I., see Mahajan, R.K. 232, 280, 281, 288, 289
 Kaur, R., see Mahajan, R.K. 232, 280, 281, 288, 289
 Kauranen, M., see Verbiest, T. 203
 Kaushik, S.M., see Gupta, M.K. 49, 63
 Kawa, H. 227, 249, 309
 Kawada, T. 36
 Kawada, T., see Horita, T. 39
 Kawada, T., see Mori, M. 20
 Kawada, T., see Nishiyama, H. 40
 Kawada, T., see Sakai, N. 17, 19, 20, 27, 29, 30, 34, 35, 38, 39
 Kawada, T., see Van Hassel, B.A. 25, 26
 Kawada, T., see Yokokawa, H. 19, 36
 Kawahara, T., see Mori, M. 29
 Kawai, M., see Yamamoto, O. 34
 Kawamoto, S., see Kobayashi, H. 326, 327
 Kawamoto, Y., see Fan, X.P. 186
 Kawamura, H., see Taniguchi, S. 17
 Kawamura, Y. 214
 Kawanami, M., see Sameshima, S. 30, 34
 Kawano, M., see Yamada, T. 14
 Kawasaki, S., see Matsumoto, K. 230
 Kawase, Y., see Umetani, S. 245
 Kazakov, V.P. 172, 173, 183–185
 Kazakov, V.P., see Antipin, V.A. 185
 Kazakov, V.P., see Ostakhov, S.S. 172, 173, 185
 Kazakov, V.P., see Sharipov, G.L. 184
 Kazakov, V.P., see Voloshin, A.I. 172, 173, 183, 184
 Keller, F. 250
 Kellmeyer, G., see Bjorklund, S. 205
 Kelly, M.P., see Kahr, B. 177
 Kemlo, J.A. 158
 Kemp, M., see Sage, I. 180, 182
 Keppeler, F.M., see Sammes, N.M. 30
 Kercher, M., see Glover, P.B. 299
 Ketsko, V.A., see Kuz'mina, N.P. 128
 Ketsko, V.Z., see Kuz'mina, N.P. 128
 Khandekar, V.V., see Nabar, M.A. 62
 Khodadad, P. 96
 Khopkar, P.K. 244
 Khusainiova, I.A., see Ostakhov, S.S. 185
 Khusainova, I.A., see Kazakov, V.P. 185
 Kido, H., see Hatakeyama, Y. 156
 Kido, J. 191, 208–211, 213–215, 283, 312
 Kido, J., see Taniguchi, H. 206
 Kieboom, A.P.G., see Peters, J.A. 313
 Kihara, S., see Miyazaki, S. 245, 246
 Kihara, S., see Mukai, H. 245
 Kikuchi, K., see Hanaoka, K. 325
 Kikunaga, T., see Takemura, M. 314
 Kilo, M., see Chevalier, S. 239
 Kim, C.D., see Liu, H.G. 191

- Kim, H., see Gorte, R.J. 15
 Kim, J.-H. 21, 22
 Kim, J.H., see Hasegawa, Y. 173
 Kim, J.S., see Kim, Y.K. 211
 Kim, J.S., see Lee, M.H. 211, 215
 Kim, J.S., see Pyo, S.W. 211, 214, 216
 Kim, K.K., see Zhong, G.L. 211
 Kim, N.D., see Caldwell, J.P. 232
 Kim, W.Y., see Kim, Y.K. 211
 Kim, W.Y., see Lee, M.H. 211, 215
 Kim, Y.K. 211
 Kim, Y.K., see Lee, M.H. 211, 215
 Kim, Y.K., see Pyo, S.W. 211, 214, 216
 Kimoto, T., see Fujinaga, T. 237
 Kimura, H., see Yuan, J. 230
 Kimura, M., see Kido, J. 210, 211, 214
 Kimura, S., see Shibata, S. 235
 Kimura, T. 239
 King, G.S.D., see Van Meervelt, L. 131, 148
 King, W., see Rheingold, A.M. 133, 179, 180
 Kinoshita, J., see Miyabayashi, T. 127
 Kippelen, B., see Jabbour, G.E. 211
 Kirby, A.F. 129, 130, 144, 161
 Kitagawa, H., see Kobayashi, S. 247, 274
 Kitamura, M., see Okada, K. 211, 215
 Kitamura, T., see Iwamuro, M. 166, 173
 Kitamura, T., see Kawamura, Y. 214
 Klaveness, J., see Hovland, R. 322
 Kleinerman, M. 164
 Klimentko, A.N., see Barkhatova, L.Yu. 32
 Klippe, L., see Weiss, F. 240
 Klotz, P., see Newman, L. 244
 Knobbe, E.T., see Matthews, L.R. 186
 Knol-Kalkman, A.H., see Peters, J.A. 235
 Knyazev, A.A., see Galyametdinov, Yu.G. 202
 Kobayashi, H. 30–33, 326, 327
 Kobayashi, M., see Harima, H. 236
 Kobayashi, N., see Yamane, H. 240
 Kobayashi, S. 247, 274
 Kobayashi, T. 218
 Kobayashi, T., see Kuriki, K. 218
 Kobayashi, T., see Zhang, X.M. 214
 Koc, R. 20, 34, 35
 Kock, W.F., see Hofer, H.E. 34, 35
 Kodadek, T., see De León-Rodríguez, L.M. 330
 Kodaira, C.A., see Serra, O.A. 174, 177
 Kodama, H., see Matsumoto, M. 159
 Koehler, J.M. 123
 Koehn, F.E., see Kurtán, T. 305
 Koeppen, C., see Gao, R.Y. 190, 191
 Koermer, G.S., see Goering, H.L. 226
 Kofstad, P., see Petrov, A.N. 23
 Kohno, K., see Yamamoto, O. 14
 Kohno, O., see Yamaguchi, T. 240
 Koike, Y., see Kobayashi, T. 218
 Koike, Y., see Kuriki, K. 191, 193, 218, 274
 Kojima, I., see Sakai, N. 17, 20
 Kojima, Y., see Takemura, M. 314
 Kojima, Y., see Watanabe, M. 314
 Komada, N., see Yamada, T. 14
 Komarov, S.A., see Ezhov, Y.S. 236
 Komiyama, M. 274
 Komiyama, N., see Konishi, K. 10, 17
 Kondoh, I., see Takeuchi, T. 29
 Konishi, K. 10, 17
 Konno, T., see Sakagami, N. 312
 Konochuk, O.F., see Barkhatova, L.Yu. 32
 Kononchuk, O.F., see Petrov, A.N. 23
 Kononenko, L.I. 145–148, 150–152
 Kononenko, L.I., see Melent'eva, E.V. 126, 150
 Kononenko, L.I., see Topilova, Z.M. 173
 Kooijman, H. 132, 311
 Kooijman, H., see Van Staveren, D.R. 130, 132, 136, 138, 139
 Kooijman, H., see van Staveren, D.R. 311
 Kooistra, H.-A.T., see Langereis, S. 329
 Koreeda, M., see Shull, B.K. 249
 Koshimura, H. 118
 Koskenlinna, M. 74, 76
 Koskenlinna, M., see Immonen, E. 94, 96
 Kossler, S., see Roth, K. 325
 Kotecki, A.M., see Scribner, W.G. 244
 Kougami, K., see Konishi, K. 10, 17
 Kovacs, Z., see De León-Rodríguez, L.M. 330
 Kovalev, I.P., see Campos, R.A. 211
 Kowalski, W.J. 233
 Kowalsky, W., see Dirr, S. 211
 Koyama, T., see Yasuda, I. 30, 34
 Kozak, J., see Bauer, T. 249
 Kozlova, N.P., see Iskhakova, L.D. 49, 50
 Kozma, L., see Erostyak, J. 228
 Kozma, L., see Hornyak, I. 228
 Krasutsky, P.A. 225
 Kraussler, W., see Batawi, E. 17
 Kravchenko, L.Kh., see Suponitskii, Yu.L. 49
 Kreher, K., see Butter, E. 148
 Kresge, C.T. 196
 Krügermann, I. 49–52, 55, 56, 58, 60, 62, 67, 69, 70, 80, 83
 Kruidhof, H., see Bouwnmeester, H.J.M. 28
 Krzyminiwski, R., see Szczyewski, A. 161
 Kudryashova, A.A., see Tsaryuk, V.I. 176

- Kudryashova, V., see Tsaryuk, V. 211
 Kudryatseva, L.S., see Topilova, Z.M. 173
 Kukli, K. 242
 Kumagai, M., see Sasaki, M. 127, 159, 160
 Kumar, K. 319
 Kumar, K., see Hasan, M. 124
 Kume, H., see Matsumoto, K. 230
 Kume, Y., see Ukai, Y. 15
 Kunkely, H. 178
 Kuno, Y., see Nagano, H. 249
 Kuo, H., see Kuo, J. 23
 Kuo, J. 23
 Kuo, S.C., see Thompson, L.C. 176
 Kupriyanova, G.N., see Kuz'mina, N.P. 128
 Kuriki, K. 191, 193, 218, 274
 Kuriki, K., see Kobayashi, T. 218
 Kuroda, R. 277
 Kuroishi, M., see Takeuchi, H. 10
 Kuroki, K., see Sano, T. 211
 Kurosaka, Y., see Ohmori, Y. 211
 Kurosawa, H., see Yamane, H. 240
 Kurtán, T. 305
 Kusabayashi, S., see Ohta, K. 119
 Kuwamoto, T., see Fujinaga, T. 147, 237
 Kuz'min, V.E., see Meshkova, S.B. 173
 Kuzmina, N. 240, 241
 Kuzmina, N., see Gleizes, A. 128, 235, 240
 Kuzmina, N., see Gleizes, A.N. 240
 Kuzmina, N., see Ryazanov, M. 128
 Kuz'mina, N.P. 128, 130, 132
 Kuzmina, N.P. 234, 235
 Kuz'mina, N.P., see Aikihanyan, A.S. 128
 Kuzmina, N.P., see Belova, N.V. 236
 Kuz'mina, N.P., see Belova, N.V. 236
 Kuz'mina, N.P., see Fenkhua, L. 234
 Kuz'mina, N.P., see Girichev, G.V. 235
 Kuzmina, N.P., see Giricheva, N.I. 235, 236
 Kuz'mina, N.P., see Martynenko, L.I. 139
 Kuzmina, N.P., see Zaitseva, I.G. 235
 Kuz'mina, N.P., see Zaitseva, I.G. 125, 235
 Kwon, O.K., see Pyo, S.W. 216
 Kynast, U., see Sendor, D. 195, 196
 Kynast, U.H., see Brück, S. 130, 136
 Kyzuk, M.G., see Diaz-Garcia, M.A. 213

 Labes, M.M. 216
 Labes, M.M., see Yu, L.J. 216
 Lacher, J.R., see Park, J.D. 119
 Lachkar, M., see Bonnet, G. 239, 242
 Lacour, J., see Jodry, J.J. 308
 Lagalante, A.F., see Andersen, W.C. 157

 Lagendijk, A., see Schuurmans, F.J.P. 172
 Lai, C.K., see Fan, P.C. 119
 Lai, K.K., see Bruce, D.W. 204
 Lai, K.W., see Dai, W.M. 249
 Lai, Y.H., see Pei, J. 194, 213
 Lalonde Jr., D.R., see Wenzel, T.J. 225, 227
 Lam, W.W.-L., see Kobayashi, S. 274
 Lam, W.W.L., see Kobayashi, S. 247
 Lan, W.Z., see Liu, H.G. 198
 Lan, Z.H., see Ci, Y.X. 228, 229
 Lanfredi, A.M.M., see van Staveren, D.R. 311
 Langereis, S. 329
 Langlet, M. 239
 Langlois, M.-H., see Dubost, J.-P. 319
 LaPlanche, L.A. 279
 Laprin, J.P., see Bonnet, G. 242
 Larpin, J.P., see Bonnet, G. 239
 Larpin, J.P., see Chevalier, S. 239
 Larrabee, R.D. 216
 Larsen, P.H. 20
 Larsson, L.O., see Valkonen, J. 50, 52
 Laschewesky, A., see Lupo, D. 204
 Latour, J.-M., see Mazzanti, M. 288–290
 Latour, J.-M., see Wietzke, R. 288–291
 Lattimer, C.J., see Goering, H.L. 226
 Lau-Cam, C.A., see Hanna, G.H. 309
 Laubscher, A.E., see Leipoldt, J.G. 131, 133
 Lauffer, R.B. 317
 Lauffer, R.B., see Caravan, P. 274, 278, 317, 319
 Laulicht, I., see Pinchas, S. 161
 Lavabre, D., see Fery-Forgues, S. 169
 Lavigne, J.J., see Wiskur, S.L. 280
 Le, Q.T.H. 244, 245
 Le, Q.T.H., see Umetani, S. 245
 Le Lagadec, R., see Bruce, D.W. 204
 Lebeau, E.L., see Wenzel, T.J. 314
 Lebedev, O.L., see Ainitdinov, Kh.A. 150
 Leconte, S., see Dujardin, G. 249
 Ledoux, I., see Lupo, D. 204
 Lee, C.H., see Lee, M.H. 211, 215
 Lee, C.S., see Liang, C.J. 211, 215
 Lee, C.S., see Zhao, D. 211, 214
 Lee, H.L., see Hasselman, D.P.H. 30–33
 Lee, H.S., see Kim, Y.K. 211
 Lee, H.S., see Lee, M.H. 211, 215
 Lee, H.S., see Pyo, S.W. 211, 214, 216
 Lee, I.K., see Lim, J.T. 124, 145, 146
 Lee, J., see Cormier, J.M. 183
 Lee, J.C., see Lim, J.T. 124, 145, 146
 Lee, J.H. 132, 141, 151
 Lee, J.H., see Jung, Y.S. 130, 141

- Lee, M.H. 211, 215
 Lee, M.H., see Pyo, S.W. 211, 214
 Lee, M.Y.H., see Dai, W.M. 249
 Lee, S.H., see Kim, Y.K. 211
 Lee, S.H., see Lee, M.H. 211, 215
 Lee, S.H., see Pyo, S.W. 211, 214, 216
 Lee, S.M., see Bhaumik, M.L. 205
 Lee, S.P., see Pyo, S.W. 216
 Lee, S.T., see Hong, Z.R. 214
 Lee, S.T., see Liang, C.J. 211, 215
 Lee, S.T., see Zhao, D. 211, 214
 Lee, Y.I., see Liu, H.G. 191
 Leedham, T.J. 145–152, 239
 Legendziewicz, J., see Borzechowska, M. 159
 Legendziewicz, J., see Strek, W. 186
 Legendziewicz, J., see Thompson, L. 131, 135, 169
 Legendziewicz, J., see Tsaryuk, V. 161, 176, 211
 Leger, J.-M., see Dubost, J.-P. 319
 Legzdins, P., see Bennett, M.J. 133
 Legzdins, P., see Cotton, F.A. 130, 135, 156
 Lehmann, F., see Grummt, U.W. 204
 Lehn, J.M., see Sabbatini, N. 168
 Lehto, S., see Nieminen, M. 241, 242
 Lei, H.Y., see Yang, Y.S. 166, 167, 230
 Lei, Z.Q., see Feng, H.Y. 194
 Leigh Jr., J.S., see Reuben, J. 221
 Leipold, M.H., see Nielsen, T.H. 34
 Leipoldt, J.G. 131, 133
 Lelli, M., see Di Bari, L. 306
 Lemieux, G.A. 329, 330
 Lempicki, A. 205
 Lempicki, A., see Brecher, C. 205, 206
 Lempicki, A., see Samelson, H. 156, 157, 205, 206
 Lenaerts, P., see Binnemans, K. 189
 Lengeling, G., see Richards, B.C. 240
 Lenstra, A.T.H., see Van Meervelt, L. 131, 148
 Leonard, J.P., see Gunnaugsson, T. 276, 294, 298
 Leonowicz, M.E., see Beck, J.S. 196
 Leonowitz, M.E., see Kresge, C.T. 196
 Leskelä, M. 46, 72, 234–236, 240, 242
 Leskelä, M., see Karpinska, L. 242
 Leskelä, M., see Koskenlinna, M. 74
 Leskelä, M., see Niinistö, L. 46, 241, 242
 Leskelä, M., see Valkonen, J. 76
 Leskelä, T. 235, 236, 239, 242
 Lessing, P.A., see Tai, L.W. 19
 Leto, J.R., see Halverson, F. 126, 149, 150, 156
 Levine, R., see Barkley, L.B. 119
 Lewinsohn, C.A., see Stevenson, J.W. 19
 Lewis, D., see Whitesides, G.M. 227
 Lewis, D.J., see Bassett, A.P. 158
 Lewis, D.W., see McCreary, M.D. 127, 227, 309
 Lewis, D.W., see Whitesides, G.M. 219, 226
 Li, B., see Xu, Q.H. 196
 Li, C., see Boyaval, J. 202, 203
 Li, C., see Yang, J. 228
 Li, F.Y., see Huang, L. 214
 Li, H. 162, 204
 Li, H., see Pavier, M.A. 200
 Li, H., see Zhao, X.S. 204
 Li, H.H. 187
 Li, H.R. 188
 Li, H.R., see Guo, J.F. 188
 Li, H.Y., see Yu, G. 213, 215
 Li, J., see Hu, L. 228
 Li, J., see Si, Z.K. 228
 Li, J., see Stevenson, J.W. 19
 Li, J., see Zhu, G. 229
 Li, J.B., see Zhang, R.J. 200
 Li, L.J., see Wang, K.Z. 211
 Li, L.S., see Fu, L.S. 196
 Li, L.S., see Xu, Q.H. 196
 Li, R.G., see Chu, B. 214
 Li, R.G., see Hong, Z.R. 214
 Li, T.K., see Gao, L.H. 162, 198, 204
 Li, T.K., see Huang, C.H. 204
 Li, T.K., see Li, H. 162, 204
 Li, T.K., see Wang, K.Z. 204
 Li, T.K., see Zhao, X.S. 204
 Li, T.K., see Zhou, D.J. 154, 155, 198, 204
 Li, W. 176
 Li, W., see Li, W. 176
 Li, W., see Zhao, D. 214
 Li, W., see Zhu, G. 229
 Li, W.-H. 324
 Li, W.L. 211, 214
 Li, W.L., see Chu, B. 214
 Li, W.L., see Hong, Z.R. 214
 Li, W.L., see Liang, C.J. 211, 214, 215
 Li, W.L., see Liu, L. 211, 215
 Li, W.L., see Zhang, X.M. 214
 Li, W.L., see Zhao, D. 211, 214
 Li, W.L., see Zhao, D.X. 213
 Li, X.Y., see Liang, C.J. 211, 215
 Li, Y.-Q., see Kurtán, T. 305
 Li, Y.G. 131, 132
 Li, Y.Y., see Li, Y.G. 131, 132
 Li, Y.Y., see Yang, Y.S. 166, 167, 230
 Liang, C., see Zhao, D. 214
 Liang, C.J. 211, 214, 215
 Liang, C.J., see Hong, Z.R. 214

- Liang, C.J., see Liu, L. 211, 215
 Liang, C.J., see Zhao, D. 211, 214
 Liang, C.J., see Zhao, D.X. 213
 Liang, C.Y. 148, 154, 155, 161
 Liang, D.C., see Wei, A.Z. 133, 181
 Liang, F.S. 212, 215
 Liang, J.Y., see Zheng, Y.X. 211
 Liang, Y.J. 213
 Liang, Y.J., see Zheng, Y.X. 211, 214, 215
 Lianos, P., see Bekiari, V. 189
 Lianos, P., see Moleski, R. 189
 Liao, C.S., see Huang, C.H. 181
 Liao, C.S., see Xu, G. 141
 Liao, J.L., see Ahmed, M.O. 131
 Licata, R., see Malandrino, G. 146
 Liebig, S., see Oppermann, H. 72, 97
 Lightfoot, P., see Berdonosov, P.S. 99
 Lim, J.T. 124, 145, 146
 Lin, H.Z., see Ling, Q.D. 213
 Lin, J., see Li, H.R. 188
 Lin, J., see Zheng, Y.X. 211, 214, 215
 Lin, J.H., see Wang, K.Z. 211
 Lin, J.J., see Hu, M.L. 131
 Lin, Q., see Liang, Y.J. 213
 Lin, Q., see Zheng, Y.X. 211, 214
 Lin, S. 218
 Lin, X.Y., see Huang, C.H. 147
 Lin, Y.H. 157
 Lin, Y.S., see Pan, M. 239
 Lindblad, M., see Haukka, S. 242
 Linden, J.L., see Richards, B.C. 240
 Ling, Q.D. 213
 Lintuluoto, J.M., see Borovkov, V.V. 305
 Lippard, S.J. 234, 235
 Lippard, S.J., see Bennett, M.J. 133
 Lippard, S.J., see Cotton, F.A. 156
 Lis, S. 168, 176
 Lis, S., see Reisfeld, R. 186
 Lis, S., see Szyzewski, A. 161
 Lisowski, J. 306
 Liss, I.B. 123, 147, 148, 153
 Liss, I.B., see Przystal, J.K. 123
 Liu, C., see Fang, G. 242
 Liu, F.G., see Guo, J.F. 188
 Liu, G.F. 128
 Liu, G.F., see Shen, C. 130–132, 143, 144
 Liu, H., see Zheng, Z.P. 131, 181
 Liu, H.-Q., see Yang, X.-P. 289
 Liu, H.G. 191, 198
 Liu, H.G., see Gao, X. 162, 199
 Liu, H.G., see Huang, H.X. 200
 Liu, H.G., see Zhang, R.J. 199, 200
 Liu, J.C., see Schuster, G.B. 183
 Liu, L. 211, 215
 Liu, L., see Liang, C.J. 214
 Liu, L.Y., see Wang, K.Z. 162
 Liu, P., see Zhu, G.Y. 228, 229
 Liu, S.H., see Chen, X.F. 133, 181
 Liu, S.X., see Wang, M.Z. 123, 162
 Liu, W.M., see Wang, K.Z. 211
 Liu, W.S. 130
 Liu, X., see Zhao, D. 214
 Liu, X.L., see Pei, J. 194, 213
 Liu, X.X., see Liu, G.F. 128
 Liu, X.Y., see Hong, Z.R. 214
 Liu, X.Y., see Liang, C.J. 211, 214, 215
 Liu, X.Y., see Liu, L. 211, 215
 Liu, X.Y., see Zhao, D. 211, 214
 Liu, X.Y., see Zhao, D.X. 213
 Liu, Y.Q., see Huang, C.H. 198, 204
 Liu, Y.Q., see Wang, K.Z. 162, 204
 Liu, Y.Q., see Yu, G. 213, 215
 Liu, Z., see Fang, G. 242
 Liu, Z.B., see Liang, C.J. 214
 Liu, Z.B., see Liu, L. 211, 215
 Lloret, F., see Gleizes, A. 128, 235, 240
 Lloret, F., see Ryazanov, M. 128
 Lo Nigro, R. 239
 Lobkovskii, E.B., see Barash, E.U. 124, 139, 234
 Lock, E.R.A. 232
 Lodewyckx, K., see Binnemans, K. 201, 202
 Londergan, T.M., see Jiang, X.Z. 211, 213
 Long, J.R. 112
 Longo, R.L., see Batista, H.J. 131, 148, 311
 Longo, R.L., see de Andrade, A.V.M. 172
 Longo, R.L., see de Sá, G.F. 170, 172
 Longo, R.L., see Gonçalves e Silva, F.R. 170, 172
 Lopinski, S., see Bruce, J.I. 276, 294, 313
 Lorenz, V. 135, 136
 Lounasmaa, M., see Leskelä, T. 235, 236, 239, 242
 Love, C.S., see Dickins, R.S. 294, 313
 Lövgren, T., see Hemmilä, I. 229
 Lovgren, T., see Soini, E. 229
 Lövgren, T., see Xu, Y.Y. 228
 Lövgren, T.N., see Xu, Y.Y. 176
 Lowe, M.P. 296
 Lowe, M.P., see Aime, S. 321
 Lowe, M.P., see Bruce, J.I. 276, 294, 313
 Lowe Jr., J.U. 119
 Lozinskii, M.O., see Bol'shoi, D.B. 173
 Lozinskii, M.O., see Meshkova, S.B. 173
 Lozinskii, M.O., see Rusakova, N.V. 173

- Lozinskii, M.O., see Topilova, Z.M. 173
 Lu, P.Z., see Shen, C. 130–132, 143
 Lu, Z., see Xu, G. 141
 Lu, Z.Y., see Liang, C.J. 214
 Lu, Z.Y., see Zhu, W.G. 211, 215
 Luber, J.R., see Horrocks Jr., W.DeW. 129, 132
 Luchinat, C., see Geraldès, C.F.G.C. 220
 Lukes, I., see Rohovec, J. 326
 Lumme, K., see Karvinen, S. 72
 Luo, C.P., see Xia, W.S. 198
 Lupo, D. 204
 Luten, H.A. 139
 Ly, T.Q., see Christou, V. 214
 Lyer, C.S.P., see Sita, M. 228, 229
 Lyle, S.J. 122, 125–127
 Lyle, S.J., see Ismail, M. 123, 126, 158
 Lyons, A., see Drake, S.R. 139
 Lyons, A.M., see Wayda, A.L. 311
- Ma, D.G., see Liang, F.S. 212, 215
 Ma, J., see Chen, X.F. 131, 133, 181
 Mac Dónaill, D.A., see Gunnlaugsson, T. 297
 Machia, K.I., see Jiang, J.Z. 128, 198, 199
 Machida, K.I., see Li, H.H. 187
 Machiko, G.J., see Panson, A.J. 240
 Macicek, J., see Stancheva, M. 76
 Mackay, K., see Burroughes, J.H. 207
 Madic, C., see Wietzke, R. 288–290
 Maeda, A., see Sugimoto, H. 142–144
 Maeda, N., see Iwahara, H. 14
 Maes, S., see Van Meervelt, L. 131, 148
 Magazeeva, N.V. 238
 Magennis, S.W. 286
 Magennis, S.W., see Bassett, A.P. 158
 Mahajan, R.K. 232, 280, 281, 288, 289
 Mahalingam, T. 242
 Maier, A.I., see Suponitskii, Yu.L. 49
 Mainero, V., see Aime, S. 281
 Maiti, B., see Ramkumar, J. 246
 Maitlis, P.M., see Giroud-Godquin, A.M. 201
 Maitlis, P.M., see Hudson, S.A. 201
 Majer, J., see Belcher, R. 123
 Mak, T.C.W., see Wong, W.-K. 303
 Mak, T.W.C., see Li, Y.G. 131, 132
 Mak, W.L., see Dai, W.M. 249
 Makarevich, L.G., see Iskhakova, L.D. 50, 55
 Makhaev, V.D., see Zaitseva, I.G. 125
 Makowska, B., see Elbanowski, M. 183
 Makowska, M., see Lis, S. 168, 176
 Malandrino, G. 124, 130, 131, 146, 149, 172, 175, 239
 Malandrino, G., see Lo Nigro, R. 239
 Maldivi, P., see Mazzanti, M. 288–290
 Male, N.A.H. 215
 Malik, K.M.A., see Baxter, I. 132, 139
 Malik, K.M.A., see Darr, J.A. 139, 140, 152
 Malik, K.M.A., see Drake, S.R. 139
 Malik, K.M.A., see Plakatouras, J.C. 132
 Malinovskii, Yu.A., see Vigdorichik, A.G. 46
 Malkerova, I., see Gleizes, A. 128, 235, 240
 Malkerova, I., see Gleizes, A.N. 240
 Malkerova, I., see Kuzmina, N. 240, 241
 Malkerova, I.P., see Aikihanyan, A.S. 128
 Malley, M.F., see Kumar, K. 319
 Malta, O.L. 131, 149, 170, 172
 Malta, O.L., see Brito, H.F. 127, 172, 175, 176
 Malta, O.L., see Carlos, L.D. 170
 Malta, O.L., see de Sá, G.F. 170, 172
 Malta, O.L., see Faustina, W.M. 172
 Malta, O.L., see Gonçalves e Silva, F.R. 170, 172
 Malta, O.L., see Reyes, R. 216
 Malykhina, L.V., see Galyametdinov, Yu.G. 202
 Mameri, S. 291
 Manet, I., see Sabbatini, N. 168, 229
 Manschreck, A., see Offermann, W. 225
 Manotti Lanfredi, A.M., see Van Staveren, D.R. 125, 130, 132, 136, 138, 139
 Manseki, K., see Sasaki, M. 127, 159, 160
 Manso, C.M.C.P., see Nassar, E.J. 189
 Mantzavinos, D., see Hartley, A. 16
 Marchetti, F., see Di Bari, L. 306
 Margot, P., see Lock, E.R.A. 232
 Margrave, J.L., see Sathianandan, K. 96
 Maric, R., see Zhang, X. 37
 Marina, O. 14, 15
 Maring, C., see Bednarski, M. 249
 Marks, R.N., see Burroughes, J.H. 207
 Marks, T.J., see Han, B. 239
 Marsh, O.J., see Gudmundson, R.A. 170
 Marshall, A.G., see Arduini, A. 223
 Marshall, W.J., see Petrov, V.A. 125, 131, 132, 311
 Martel, A., see Dujardin, G. 249
 Martell, A.E., see Nakamoto, K. 161
 Martin, D.F., see Moeller, T. 244
 Martynenko, L.I. 132, 139
 Martynenko, L.I., see Batsanov, A.S. 132
 Martynenko, L.I., see Fenkhua, L. 234
 Martynenko, L.I., see Kuz'mina, N.P. 130, 132
 Martynenko, L.I., see Kuzmina, N.P. 234, 235
 Martynenko, L.I., see Magazeeva, N.V. 238
 Martynenko, L.I., see Spitsyn, V.I. 238
 Martynenko, L.I., see Zaitseva, I.G. 125, 235

- Martynenko, L.I., see Zharkova, Ya.N. 130
 Marugin, V.V., see Iskhakova, L.D. 49, 50
 Maruszewski, K., see Strek, W. 186
 Maruyama, T., see Akashi, T. 39
 Maslyukov, Yu.S., see Aristov, A.V. 205
 Massaux, J., see Desreux, J.F. 244
 Masuda, H., see Sugimoto, H. 142–144
 Mathieu, C.E., see Govenlock, L.J. 299
 Mathieu, C.E., see Maupin, C.L. 307
 Mathis, G. 229
 Mathur, J.N. 243
 Mathur, J.N., see Khopkar, P.K. 244
 Mathur, P.K., see Ramkumar, J. 246
 Matković, B. 141
 Matovich, E., see Gudmundson, R.A. 170
 Matsamura, M., see Hu, W.P. 211
 Matsubayashi, I. 244
 Matsuda, H., see Ishihara, T. 14
 Matsuda, M. 19
 Matsui, M., see Le, Q.T.H. 244, 245
 Matsui, M., see Miyazaki, S. 245, 246
 Matsui, M., see Mukai, H. 245
 Matsui, M., see Sasayama, K. 245
 Matsui, M., see Shigematsu, T. 145, 147–153, 237, 244
 Matsui, M., see Umetani, S. 245
 Matsui, M., see Umitani, S. 245
 Matsumoto, H., see Yamane, H. 240
 Matsumoto, K. 230, 288
 Matsumoto, K., see Yuan, J. 230
 Matsumoto, K., see Yuan, J.L. 174
 Matsumoto, M. 159
 Matsumoto, N., see Tamiaki, H. 303
 Matsumoto, O., see Itoh, K.I. 239
 Matsumura, M., see Hu, W.P. 211, 215
 Matsuno, S. 240
 Matsuya, T., see Matsumoto, K. 230
 Matsuzaki, Y. 17
 Matsuzaki, Y., see Yasuda, I. 30, 34
 Matsuzawa, H., see Mikami, K. 249
 Matthews, L.R. 186
 Mattson, S.M. 122, 126, 149
 Maudet, M., see Dujardin, G. 249
 Maupin, C.L. 307
 Maupin, C.L., see Beeby, A. 299
 Maupin, C.L., see Govenlock, L.J. 299
 Maxwell, J.C. 32
 Mazzanti, M. 288–290
 Mazzanti, M., see Wietzke, R. 288–291
 Mazzella, W.D., see Lock, E.R.A. 232
 McAleese, J. 146, 239
 McAleese, J., see Baxter, I. 132, 139, 311
 McAleese, J., see Chadwick, D. 239
 McAleese, J., see Plakatouras, J.C. 132, 311
 McAvoy, N., see Bjorklund, S. 161, 171, 205
 McAvoy, N., see Filipescu, N. 205
 McAvoy, N., see Hurt, C.R. 179, 180
 McCallum, P.A., see Nassimbeni, L.R. 311, 312
 McCarthy, G.J. 46
 McConnell, H.M. 220
 McCory, L.D., see Sathianandan, K. 96
 McCreary, M., see Whitesides, G.M. 227
 McCreary, M.D. 127, 227, 309
 McCullen, S.B., see Beck, J.S. 196
 McDevitt, N.T. 242
 McGehee, M.D. 211, 213
 McGoran, E.C. 226
 McKiernan, J., see Hocking, M.B. 179
 McKittrick, J., see Hirata, G.A. 239
 McMurry, T.J., see Caravan, P. 274, 278, 317, 319
 McPhail, A.T. 133
 Meade, T.J., see Li, W.-H. 324
 Meadowcroft, D.B. 20
 Meares, C.F. 328
 Medeiros, C.L., see Serra, O.A. 198
 Medus, D., see Gleizes, A. 124, 130, 135, 141
 Meek, D.W., see Springer Jr., C.S. 119, 144–153, 172
 Mehrotra, R.C. 112, 124
 Mehrotra, R.C., see Misra, S.N. 124
 Meijer, E.W., see Langereis, S. 329
 Meinhardt, K., see Mukerjee, S. 12
 Melby, L.R. 121, 122, 148–150, 154–156
 Melent'eva, E.V. 126, 150
 Melent'eva, E.V., see Kononenko, L.I. 145–148, 150, 152
 Melson, G.A., see Andersen, T.J. 130, 135
 Menezes, J.F.S., see Brito, H.F. 127, 172, 175, 176
 Menezes, J.F.S., see Carlos, L.D. 170
 Menezes, J.F.S., see Gonçalves e Silva, F.R. 170, 172
 Menezes, J.F.S., see Malta, O.L. 170, 172
 Meng, G.Y. 240
 Meng, G.Y., see Pan, M. 239
 Meng, G.Y., see Song, H.Z. 145, 150, 234, 239
 Meng, G.Y., see Wang, H.B. 214
 Meng, Q.G., see Fu, L.S. 196
 Meng, Q.G., see Guo, J.F. 188
 Menzer, S., see Van Staveren, D.R. 125
 Merbach, A.E., see Burai, L. 319
 Merbach, A.E., see Ruloff, R. 319
 Merbach, A.E., see Tóth, É. 317

- Meshkova, S.B. 173
 Meshkova, S.B., see Bol'shoi, D.B. 173
 Meshkova, S.B., see Rusakova, N.V. 173
 Meshkova, S.B., see Topilova, Z.M. 173
 Meskers, S.C.J. 306, 307
 Messaddeq, Y., see Carlos, L.D. 189
 Messori, L. 274
 Mészáros-Szécscényi, K. 235
 Metcalf, D.H., see Bender, J.L. 194
 Metcarfe, L.S., see Hartley, A. 16
 Metz, K.R., see Zuo, C.S. 326
 Meyer, D., see Dubost, J.-P. 319
 Meyer, S.F. 81
 Meyer, Y. 205
 Meyer, Y., see Crozet, P. 205
 Meyer, Y., see de Witte, O. 205
 Meyer, Y., see Verron, M. 205
 Michl, G., see Schmitt-Willich, H. 328
 Michurina, A.V., see Ainitdinov, Kh.A. 150
 Mickelson, A., see Lin, S. 218
 Middleton, P.H., see Christie, G.M. 20
 Mie, X.M., see Zhou, D.J. 204
 Miele, P., see Gleizes, A. 124, 130, 135, 141
 Mihara, T. 156
 Mikami, K. 249
 Mikami, K., see Gu, J.H. 249
 Mikami, K., see Terada, M. 249
 Mikami, M. 161
 Mikawa, H., see Ohta, K. 119
 Miles, R.D., see Wenzel, T.J. 309, 314
 Miller, S.A.S., see Drake, S.R. 139
 Milone, L., see Terreno, E. 295, 315
 Min, N.B., see Chen, X.F. 133, 181
 Minami, H., see Ishihara, T. 15
 Minami, N., see Takada, N. 181, 182, 211
 Mindru, I., see Brezeanu, M. 46
 Mingos, D.M.P., see Darr, J.A. 139, 140, 152
 Mirzai, H., see Hellmuth, K.-H. 149
 Mishra, A.K., see Biju, V.M. 228, 229
 Misner, A. 231
 Misner, A.H., see Wilkinson, D.A. 232
 Misra, S.N. 124
 Misra, S.N., see Hasan, M. 124
 Misra, S.N., see Mehrotra, R.C. 124
 Misra, T.N., see Mehrotra, R.C. 124
 Misra, T.N., see Misra, S.N. 124
 Misumi, S. 161
 Mita, N., see Tamura, O. 249
 Mitchell, J.W. 150
 Miura, K., see Yamada, T. 14
 Miura, K., see Zhang, X. 37
 Miyabayashi, T. 127
 Miyachi, M. 17
 Miyake, H. 275, 283
 Miyake, H., see Takemura, M. 314
 Miyake, H., see Watanabe, M. 314
 Miyake, M., see Matsuda, M. 19
 Miyake, Y., see Taniguchi, S. 17
 Miyamoto, H., see Nakanishi, A. 12
 Miyamoto, Y. 211
 Miyashita, T., see Amao, Y. 232
 Miyazaki, S. 245, 246
 Miyazaki, S., see Mukai, H. 245
 Miyazawa, T., see Inagaki, F. 220
 Miyazawa, T., see Yamada, T. 14
 Mizutani, Y., see Ukai, Y. 15
 Mizutani, Y., see Yamamoto, O. 34
 Mo, Z.L., see Yang, W. 228
 Moeller, T. 244
 Mogensen, M., see Larsen, P.H. 20
 Mogensen, M., see Marina, O. 14
 Molander, G. 247
 Molander, G.A. 247, 274
 Moleski, R. 189
 Molina, C., see Carlos, L.D. 189
 Moloney, J.M., see Aime, S. 321
 Mölsä, H. 241, 242
 Mölsä, H., see Leskelä, M. 240, 242
 Mondino, B., see Terreno, E. 295, 315
 Monnanni, R., see Messori, L. 274
 Montalti, M. 276
 Montalti, M., see Charbonnière, L.J. 291
 Montalti, M., see Prodi, L. 291
 Moon, D.G. 214
 Moorcraft, L.P., see Shavaleev, N.M. 174
 Moors, D., see Binnemans, K. 203
 Moors, D., see Van Deun, R. 203
 Moret, E., see Bünzli, J.-C.G. 172, 175
 Morgan, G.T. 145
 Morgantini, P.-Y., see Senegas, J.-M. 286
 Mori, M. 20, 29
 Mori, M., see Itoh, H. 18
 Mori, M., see Sugimoto, H. 142–144
 Mori, N., see Itoh, H. 18
 Morishita, T., see Zama, H. 240
 Morrill, T.C. 224, 247
 Morris, M.L. 147
 Morris, R. 74
 Morris, R.E. 88, 90, 99
 Morse, K., see McGoran, E.C. 226
 Moser, D.F. 131, 134, 149, 171
 Mosher, H.S., see Dale, L.A. 316, 318

- Moshier, R.W. 237
 Moshier, R.W., see Morris, M.L. 147
 Moss, G.P., see Briggs, J. 219
 Moss, H.W., see Morgan, G.T. 145
 Mossang, E., see Thomas, O. 240
 Mottram, P., see Hemmilä, I. 229
 Mucciolo, A., see Parra, D.F. 193
 Mukai, H. 245
 Mukai, H., see Miyazaki, S. 245, 246
 Mukai, K., see Zhang, X. 37
 Mukerjee, S. 12
 Mukkala, V., see Hemmilä, I. 229
 Mukkala, V., see Xu, Y.Y. 228
 Müller, A., see Busch, H. 240
 Muller, G., see Riehl, J.P. 301
 Müller-Fahnow, A., see Schmitt-Willich, H. 328
 Murai, A., see Oka, T. 249
 Murai, S., see Fujinaga, T. 237
 Murakami, N., see Nishi, T. 17
 Murakami, N., see Yamada, T. 14
 Murakoshi, K., see Hasegawa, Y. 173
 Murata, K., see Matsuda, M. 19
 Murav'eva, I.A., see Batsanov, A.S. 132
 Muraveva, I.A., see Magazeeva, N.V. 238
 Muraveva, I.A., see Spitsyn, V.I. 238
 Murray, G.M. 171
 Mutikainen, I., see Koskenlinna, M. 74
 Muto, Y., see Yamane, H. 240

 Nabar, M.A. 49, 59–62
 Nafe, H., see Sammes, N.M. 30
 Nag, K., see Roy, A. 245
 Nagai, K., see Kido, J. 209–211, 213–215
 Nagai, K., see Nakamura, M. 130, 134
 Nagano, H. 249
 Nagano, T., see Hanaoka, K. 325
 Nagata, K., see Konishi, K. 10, 17
 Nagaya, S., see Yamaguchi, T. 240
 Naik, V.R., see Nabar, M.A. 62
 Nakabayashi, S., see Matsuno, S. 240
 Nakagawa, I., see Mikami, M. 161
 Nakagawa, M., see Sakai, N. 37
 Nakagome, H., see Whitney, P.S. 239
 Nakahara, H., see Qian, D.J. 198
 Nakai, T., see Gu, J.H. 249
 Nakai, T., see Mikami, K. 249
 Nakai, T., see Terada, M. 249
 Nakamoto, K. 161
 Nakamoto, T., see Kobayashi, T. 218
 Nakamura, K. 170
 Nakamura, M. 130, 134
 Nakamura, R., see Nakamura, M. 130, 134
 Nakamura, S. 244, 245
 Nakamura, Y., see Yamamoto, O. 34
 Nakanishi, A. 12
 Nakanishi, K. 278, 302
 Nakanishi, K., see Dillon, J. 302
 Nakanishi, K., see Kurtán, T. 305
 Nakano, A., see Fukuda, Y. 275
 Nakano, T., see Tamura, O. 249
 Nakao, A., see Fukuda, Y. 122, 143, 144
 Nakashima, N., see Hasegawa, Y. 173
 Nakashima, N., see Iwamuro, M. 166, 173
 Nakatsuka, S., see Kobayashi, T. 218
 Nakaya, T., see Okada, K. 211, 215
 Naki, T., see Terada, M. 249
 Nandi, J. 65
 Nandy, J., see Neogy, D. 65
 Nanko, M., see Akashi, T. 39
 Napier, G.D.R. 168
 Narazaki, M., see Hanaoka, K. 325
 Nassar, E.J. 189
 Nasser, E.J., see Serra, O.A. 174, 177
 Nassimbeni, L.R. 311, 312
 Nazarov, A.M. 185
 Negishi, H., see Sakai, N. 37, 39
 Negishi, H., see Xiong, Y.P. 37
 Nehrich, R.B., see Schimitschek, E.J. 205
 Nehring, R.B. 205
 Nehring, R.B., see Schimitschek, E.J. 205, 206
 Nehring, R.N., see Schimitschek, E.J. 148, 151, 152, 205
 Neilson, J.D. 158
 Neilson, J.D., see Kemlo, J.A. 158
 Neilson, J.D., see Napier, G.D.R. 168
 Neogy, D. 65
 Neogy, D., see Nandi, J. 65
 Neri, C.R., see Nassar, E.J. 189
 Neri, C.R., see Serra, O.A. 174, 177
 Nesnas, N., see Kurtán, T. 305
 Neuman, M.A., see Andersen, T.J. 130, 135
 Neumayer, D., see Han, B. 239
 Neumayer, D.A., see Han, B. 239
 Newbery, J.E., see Ismail, M. 123, 126, 158
 Newman, L. 244
 Ni, J.Z., see Yan, B. 172, 186
 Nielsen, T.H. 34
 Nieminen, M. 241, 242
 Nieminen, M., see Putkonen, M. 241
 Nieminen, M., see Seim, H. 242
 Nieuwenhuizen, P.J., see Van Staveren, D.R. 125, 130, 132, 136, 138, 139, 311

- Nieuwenhuyzen, M., see Gunnlaugsson, T. 276, 294
- Niinistö, J., see Gourba, E. 241
- Niinistö, J., see Putkonen, M. 241
- Niinistö, L. 46, 72, 88, 241, 242
- Niinistö, L., see Erämetsä, O. 96
- Niinistö, L., see Gourba, E. 241
- Niinistö, L., see Heikkinen, H. 242
- Niinistö, L., see Hiltunen, L. 50, 51
- Niinistö, L., see Immonen, E. 94, 96
- Niinistö, L., see Karpinska, L. 242
- Niinistö, L., see Karvinen, S. 50, 52, 61, 72
- Niinistö, L., see Koskenlinna, M. 74
- Niinistö, L., see Kukli, K. 242
- Niinistö, L., see Leskelä, M. 46, 234–236, 240, 242
- Niinistö, L., see Mészáros-Szccsényi, K. 235
- Niinistö, L., see Mölsä, H. 241
- Niinistö, L., see Nieminen, M. 241, 242
- Niinistö, L., see Päiväsääri, A. 241
- Niinistö, L., see Putkonen, M. 241
- Niinistö, L., see Seim, H. 242
- Niinistö, L., see Tiitta, M. 238, 240
- Niinistö, L., see Valkonen, J. 50, 52, 58, 59
- Nijssen, F., see Kooijman, H. 132, 311
- Nikiforov, V., see Ryazanov, M. 128
- Nikol, H., see Boerner, H. 216
- Ning, L.X., see Dong, N. 192
- Nishi, T. 17
- Nishida, Y., see Sasaki, M. 127, 159, 160
- Nishiguchi, H., see Ishihara, T. 15, 16
- Nishihara, S., see Kuriki, K. 193
- Nishimura, M., see Zhang, X. 37
- Nishiura, M., see Nakanishi, A. 12
- Nishiya, M., see Taniguchi, H. 206
- Nishiyama, H. 40
- Nishizawa, Y., see Kuriki, K. 193
- Niu, Y.H., see Pei, J. 194, 213
- Noll, B.C., see Andersen, W.C. 139, 146, 151, 157
- Nomura, K., see Takeuchi, T. 29
- Nonhebel, D.C., see Hammond, G.S. 148
- Noro, J. 244, 246
- Noto, M. 213
- Novotna, N., see Hájek, B. 49, 61, 63
- Nugent, L.J., see Bhaumik, M.L. 205
- Nykänen, E., see Heikkinen, H. 242
- Nykänen, E., see Kukli, K. 242
- Nykänen, E., see Leskelä, M. 234–236
- Obi, B., see Otway, D.J. 240
- O'Dea, S., see Bance, P. 14
- Offermann, W. 225
- Ogasawara, K., see Inamoto, A. 315, 317
- Ogiwara, T., see Yasuda, I. 34–36
- Ohara, O., see Matsuda, M. 19
- Ohara, S., see Matsuda, M. 19
- Ohara, S., see Zhang, X. 37
- Ohashi, Y., see Kido, J. 209, 214
- Ohba, M., see Sasaki, M. 127, 159, 160
- Ohlmann, R.C., see Charles, R.G. 122, 146–150, 153, 156
- Ohmori, T. 211
- Ohmori, Y. 211
- Ohnishi, H., see Harima, H. 236
- Ohnishi, T., see Hasegawa, Y. 244
- Ohta, K. 119
- Oka, T. 249
- Okada, K. 211, 215
- Okamoto, K.-I., see Sakagami, N. 312
- Okamoto, M., see Gu, J.H. 249
- Okamoto, Y., see Kido, J. 191, 208, 210, 213, 215, 283, 312
- Okamoto, Y., see Kuriki, K. 191, 193, 218, 274
- Okamoto, Y., see Ueba, Y. 192
- Okawa, H., see Sasaki, M. 127, 159, 160
- Okumura, M., see Kato, H. 326
- Okuno, T., see Koshimura, H. 118
- Okura, I., see Amao, Y. 232
- Olenev, A.V., see Berdonosov, P.S. 78
- Olson, D.H., see Beck, J.S. 196
- Olson, P.A., see Stolzenberg, G.E. 226
- Omata, K. 315
- Omata, K., see Inamoto, A. 315, 317
- Omata, K., see Sato, J. 315
- Omori, Y., see Nagano, H. 249
- Onimaru, A., see Mahajan, R.K. 232, 280, 281, 288, 289
- Onodera, N., see Saitoh, T. 249
- Onoue, H., see Onuma, S. 132, 139
- Onuma, S. 132, 139
- Oppermann, H. 72, 78, 97
- Oppermann, H., see Schmidt, P. 78, 97
- Oppermann, H., see Shabalin, D.G. 81
- Oppermann, H., see Zhang-Preße, M. 72, 97
- O'Regan, M.B., see McGehee, M.D. 211, 213
- O'Regan, M.B., see Robinson, M.R. 212
- Oro, L.A., see Espinet, P. 201
- Ortiz, A., see De León-Rodríguez, L.M. 330
- Osanaï, H., see Yamaguchi, T. 240
- Ostakhov, S.S. 172, 173, 185
- Ostakhov, S.S., see Antipin, V.A. 185

- Ostakhov, S.S., see Kazakov, V.P. 172, 173, 184, 185
- Östling, M., see Thomas, O. 240
- Oswald, I., see Clegg, W. 130, 132, 182
- Oswald, I.D.H., see Bourhill, G. 181
- Otway, D.J. 240
- Otway, D.J., see Baxter, I. 132, 139, 311
- Otway, D.J., see Drake, S.R. 139
- Ou, Q.Y., see Yang, W. 228
- Ouchi, A., see Nakamura, M. 130, 134
- Ouyang, J., see Shen, Z.Q. 112
- Ovanisyan, S.M. 50, 51, 57–60
- Ovanisyan, S.M., see Iskhakova, L.D. 49, 50, 55, 57, 58
- Ozawa, T. 240
- Öztürk, S., see Chen, X.F. 131, 181
- Pachalidis, D.G., see Christidis, P.C. 130
- Paeterson, M.L., see Kahr, B. 177
- Pagliarin, R., see Lowe, M.P. 296
- Pagnot, T. 193
- Päiväsaari, A. 241
- Päiväsaari, J., see Gourba, E. 241
- Päiväsaari, J., see Mészáros-Szccésényi, K. 235
- Pakkanen, T., see Erämetsä, O. 96
- Pakkanen, T., see Immonen, E. 94, 96
- Palm, C., see Gerstberger, G. 249
- Palmer, R.A., see Kirby, A.F. 130, 161
- Palmisano, G., see Aime, S. 322
- Palsson, L.O., see Bourhill, G. 181
- Pan, L., see Thompson, L. 131, 135, 169
- Pan, M. 239
- Panson, A.J. 240
- Parac-Vogt, T.N., see Binnemans, K. 201, 202
- Paralkar, S.V., see Nabar, M.A. 49, 59, 61, 62
- Pardi, L., see Benelli, C. 141, 159, 160
- Park, J.-H. 21, 22
- Park, J.D. 119
- Park, K., see Jung, Y.S. 130, 141
- Park, S.M., see Hemingway, R.E. 159
- Park, S.T., see Liu, H.G. 191
- Parker, D. 274, 280, 308
- Parker, D., see Aime, S. 281, 321
- Parker, D., see Atkinson, P. 296
- Parker, D., see Beeby, A. 173, 299
- Parker, D., see Bruce, J.I. 276, 294, 313
- Parker, D., see Congreve, A. 319
- Parker, D., see Dickins, R.S. 292, 294, 321
- Parker, D., see Govenlock, L.J. 299
- Parker, D., see Gunnlaugsson, T. 297
- Parker, D., see Lowe, M.P. 296
- Parker, D., see Maupin, C.L. 307
- Parker, D., see Reany, O. 298
- Parlett, H.W., see Sweet, T.R. 244
- Parra, D.F. 193
- Parsons, R., see Bard, A.J. 48
- Parsons, S., see Bassett, A.P. 158
- Parsons, S., see Magennis, S.W. 286
- Paschalidis, D.G., see Christidis, P.C. 311
- Paskevich, K.I. 118, 119
- Passos, J.J., see Brito, H.F. 127
- Patron, L., see Brezeanu, M. 46
- Patsalides, E., see Robards, K. 237
- Pavich, T., see Strek, W. 186
- Pavier, M.A. 200
- Paxton, D., see Mukerjee, S. 12
- Peacock, R.D., see Bruce, J.I. 276, 294, 313
- Peacock, R.D., see Dickens, R.S. 292, 294, 321
- Pearson, R.K., see Jacobs, R.R. 237
- Pécaut, J., see Mazzanti, M. 288–290
- Pécaut, J., see Wietzke, R. 288–291
- Pedersen, L., see Marina, O. 15
- Pederson, L.R., see Armstrong, T.R. 30
- Pederson, L.R., see Stevenson, J.W. 19
- Pedeson, J.W., see Choudhury, N.S. 22
- Pedrosa, G.G., see de Farias, R.F. 193
- Pei, J. 194, 213
- Pei, W., see Wada, E. 249
- Peng, D.K., see Meng, G.Y. 240
- Peng, D.K., see Pan, M. 239
- Peng, D.K., see Song, H.Z. 145, 150, 234, 239
- Peng, D.K., see Wang, H.B. 214
- Peng, J., see Takada, N. 211
- Peng, J.B., see Hong, Z.R. 214
- Peng, J.B., see Li, W.L. 211, 214
- Peng, J.B., see Liang, C.J. 211, 214, 215
- Peng, J.B., see Liu, L. 211, 215
- Peng, J.B., see Zhao, D.X. 213
- Peregudov, G.V., see Bazhulin, P.A. 205
- Perkovskaya, Yu.B. 94
- Perret, R., see Rosso, B. 49
- Perrier, M., see Giesbrecht, E. 94
- Perry, J.J.B., see Bruce, J.I. 276, 294, 313
- Perry, J.W., see Raber, D.J. 223
- Perry, R., see Belcher, R. 123
- Persoons, A., see Clays, K. 204
- Persoons, A., see Verbiest, T. 203
- Persoons, A., see Wostyn, K. 204
- Pescitelli, G., see Di Bari, L. 306
- Pesterfield, L.L., see Murray, G.M. 171
- Petek, M. 46
- Peters, J.A. 220, 224, 235, 313

- Peterson Jr., M.R. 220
 Petoud, S. 286
 Petre, N.L., see Brezeanu, M. 46
 Petrov, A.N. 23
 Petrov, A.N., see Barkhatova, L.Yu. 32
 Petrov, K.I. 49, 63, 73, 94, 96
 Petrov, O., see Schmitt-Willich, H. 328
 Petrov, V.A. 125, 131, 132, 311
 Petrova, R., see Stancheva, M. 76
 Peyghambarian, N., see Jabbour, G.E. 211
 Peyghambarian, N., see Wang, J.F. 211, 212
 Peyghambarian, N., see Zheng, Z.P. 131, 181
 Pfoertsch, D.E., see McCarthy, G.J. 46
 Phelan, G.D., see Jiang, X.Z. 211, 213
 Philippot, E., see Fernandes, A. 197
 Philips, I.M., see Helliwell, M. 249
 Philips, T. 130
 Phillips II, T. 311
 Pickaert, G., see Prodi, L. 291
 Picker, J.E. 232
 Pickup, B.T., see Bruce, D.W. 204
 Pietraszkiewicz, M., see Reisfeld, R. 186
 Pietrzak, J., see Szyzewski, A. 161
 Pignard, S., see Weiss, F. 240
 Piguet, C. 274
 Piguet, C., see Senegas, J.-M. 286
 Pikramenou, Z., see Bassett, A.P. 158
 Pikramenou, Z., see Glover, P.B. 299
 Pikramenou, Z., see Magennis, S.W. 286
 Pillinger, M., see Braga, S.S. 127
 Pillinger, M., see Fernandes, J.A. 121
 Pinch, D.L., see Richards, B.C. 240
 Pinchas, S. 161
 Ping, L., see Zhu, G.Y. 228, 229
 Pintacuda, G., see Di Bari, L. 305, 306
 Pirie, W.R., see Fry, F.H. 206
 Pisarevskii, A.P., see Kuz'mina, N.P. 132
 Pisarevskii, A.P., see Martynenko, L.I. 132
 Pisarevsky, A.P., see Kuz'mina, N.P. 130
 Pisch, A., see Weiss, F. 240
 Plakatouras, J.C. 132, 311
 Plakatouras, J.C., see Baxter, I. 132, 139, 311
 Plakatouras, J.C., see McAleese, J. 146, 239
 Platzek, J., see Roth, K. 325
 Platzek, J., see Schmitt-Willich, H. 328
 Pohl, L. 223, 224
 Pokol, G., see Mészáros-Szecsényi, K. 235
 Poluektov, N.S., see Kononenko, L.I. 145–148, 150–152
 Poluektov, N.S., see Melent'eva, E.V. 126, 150
 Polyakov, O.V. 240
 Poncelet, O. 139
 Poncet, H., see Meyer, Y. 205
 Pond, B.V., see Wenzel, T.J. 314
 Pope, S.J.A., see Shavaleev, N.M. 174, 175
 Popovkin, B.A., see Berdonosov, P.S. 78
 Popovkin, B.A., see Oppermann, H. 78, 97
 Popovkin, B.A., see Schmidt, P. 78, 97
 Popovkin, B.A., see Shabalin, D.G. 81
 Porai-Koshits, M., see Aslanov, L.A. 50, 52
 Poskanzer, A.M. 244
 Postovskii, I.Ya., see Paskevich, K.I. 118, 119
 Prandtl, W. 46
 Prass, W., see Lupo, D. 204
 Pressley, R.J., see Wolff, N.E. 191, 205
 Price, R.E., see Bolskar, R.D. 328
 Primdahl, S., see Marina, O. 14
 Pritchard, R.G., see Helliwell, M. 249
 Prodi, L. 291
 Prodi, L., see Charbonnière, L.J. 291
 Prodi, L., see Montalti, M. 276
 Prokhorov, A.P.M., see Bazhulin, P.A. 205
 Przystal, J.K. 123
 Pugzlys, A., see Grummt, U.W. 204
 Puntus, L., see Tsaryuk, V. 161
 Purushottam, D. 145–148, 150–153
 Puschmann, H., see Dickins, R.S. 294, 313
 Puschmann, H., see Parker, D. 280
 Putkonen, M. 241
 Putkonen, M., see Gourba, E. 241
 Putkonen, M., see Mészáros-Szecsényi, K. 235
 Putkonen, M., see Nieminen, M. 241
 Putkonen, M., see Päiväsääri, A. 241
 Pykhiteeva, E.G., see Meshkova, S.B. 173
 Pyo, S.W. 211, 214, 216
 Pyo, S.W., see Kim, Y.K. 211
 Pyo, S.W., see Lee, M.H. 211, 215
 Qian, D.J. 198
 Qian, D.J., see Huang, H.X. 200
 Qian, G.D. 172, 188
 Qin, P.W., see Wang, M.Z. 123, 162
 Qin, W.P., see Liu, H.G. 191
 Qiu, J.B., see Fan, X.P. 186
 Raban, M., see Jacobus, J. 308
 Raber, D.J. 223, 225
 Raber, D.J., see Peters, J.A. 220
 Rackham, D.M., see Cockerill, A.F. 220
 Radhakrishnan, M., see Mahalingam, T. 242
 Radionov, V.N., see Krasutsky, P.A. 225
 Radüchel, B., see Roth, K. 325

- Radüchel, B., see Schmitt-Willich, H. 328
Raghava Rao, Bh.S.V., see Purushottam, D. 145–148, 150–153
Rainho, J.P., see Carlos, L.D. 189
Raj, S.S.S., see Chen, X.F. 131, 155, 181
Rajendran, S., see Drennan, J. 30
Ramachandra Rao, V., see Purushottam, D. 146–148, 150–153
Ramade, I. 128, 130, 132
Ramkumar, J. 246
Randall, W.J., see Moeller, T. 244
Raney, P.E., see Armstrong, T.R. 30
Rankin, D.W.H., see Belova, N.V. 236
Rao, G.N., see Jyothi, A. 245
Rao, T.P., see Biju, V.M. 228, 229
Rao, T.P., see Sita, M. 228, 229
Rappaz, M., see Boatner, L.A. 46
Rappoli, B.J. 237
Ratnaraj, R., see Sammes, N.M. 30
Ratonaraj, R., see Sammes, N. 30
Raupach, E., see Rikken, G.L.J.A. 178
Raymond, K.N., see Petoud, S. 286
Raymond, K.N., see Xu, J.D. 139
Reany, O. 298
Reany, O., see Lowe, M.P. 296
Reddy, M.L.P., see Biju, V.M. 228, 229
Reedijk, J., see Van Staveren, D.R. 125, 130, 132, 136, 138, 139, 311
Rees Jr., W.S., see Luten, H.A. 139
Rees Jr., W.S., see Otway, D.J. 240
Register, R.A., see Jiang, X.Z. 213
Reid, J.C. 119, 244
Reid, M.F., see Dallara, J.J. 161
Reilley, C.R., see Desreux, J.F. 127, 158, 226
Reisfeld, R. 186
Reisfeld, R., see Strek, W. 186
Remennik, E.M., see Petrov, K.I. 73, 94, 96
Remy, M., see Mazzanti, M. 288–290
Ren, X., see Yang, J. 228
Reuben, J. 112, 220, 221, 312
Rey, D., see Benelli, C. 141
Rey, P., see Benelli, C. 159
Reyes, R. 214, 216
Rheingold, A.L., see Sweeting, L.M. 179, 180
Rheingold, A.M. 133, 179, 180
Rhine, W.E., see Sievers, R.E. 224
Ribeiro, C.A., see Cruz, P.M. 62
Ribeiro, C.A., see Spirandeli Crespi, M. 62
Ribeiro, S.J.L., see Carlos, L.D. 189
Ribeiro, S.J.L., see de Mello Donegá, C. 170
Ribeiro, S.J.L., see Sá Ferreira, R.A. 189
Ribeiro-Claro, P.J.A., see Fernandes, J.A. 121
Ribot, F., see Sanchez, C. 187
Richards, B.C. 240
Richardson, F.S. 177, 274
Richardson, F.S., see Brittain, H.G. 176, 177, 311
Richardson, F.S., see Dallara, J.J. 161
Richardson, F.S., see Foster, D.R. 178
Richardson, F.S., see Kirby, A.F. 129, 144, 161
Richardson, F.S., see Riehl, J.P. 177
Richardson, M.F. 126, 233, 234
Richardson, M.F., see Feibush, B. 145–148, 150, 232
Richardson, M.M. 236
Richardson, M.R., see Cunningham, J.A. 132, 135
Richardson, T., see Pavier, M.A. 200
Richardson, F.S., see Bender, J.L. 194
Richter, J.C., see Belanger, P. 221
Richter, M.M. 158
Riedel, E.P., see Charles, R.G. 127, 148, 154, 171
Riehl, J.P. 177, 301
Riehl, J.P., see Beeby, A. 299
Riehl, J.P., see Govenlock, L.J. 299
Riehl, J.P., see Maupin, C.L. 307
Riehl, J.P., see Richardson, F.S. 177
Rikken, G.L.J.A. 178
Ringsdorf, H., see Lupo, D. 204
Ringuedé, A., see Gourba, E. 241
Ripoli, S., see Lisowski, J. 306
Ritala, M., see Niinistö, L. 241, 242
Roan, M.A., see Wenzel, T.J. 314
Robards, K. 237
Robert, F., see Ramade, I. 128, 130, 132
Robertson, R.E., see McConnell, H.M. 220
Robinson, M.R. 212
Robinson, M.R., see Srdanov, V.I. 177, 194
Robinson, M.R., see Yang, C.Y. 177, 194
Roca, S., see Santos Jr., L.S. 159
Rocha, G.B. 172
Rocha, G.B., see Faustino, W.M. 172
Rocha, G.B., see Gonçalves e Silva, F.R. 170, 172
Rocha, J., see Braga, S.S. 127
Rockefeller, H.A., see Bruder, A.H. 158
Roda, A., see Charbonnière, L. 286
Rodger, A., see Glover, P.B. 299
Rogachev, A., see Gleizes, A.N. 240
Rogachev, A., see Kuzmina, N. 240, 241
Rogachev, A.Y., see Kuz'mina, N.P. 128
Rogers, M.T., see Burdett, J.L. 118
Rogers, R.D., see Wayda, A.L. 311
Rohovec, J. 326
Romero, J.A.C., see Molander, G.A. 274

- Ronda, C., see Boerner, H. 216
 Rondeau, R.E. 219, 223
 Rondeau, R.E., see Dyer, D.S. 224
 Rosa, I.L.V., see Serra, O.A. 174, 177, 198
 Rose, N.J., see Melby, L.R. 121, 122, 148–150, 154–156
 Rosenblatt, M.M., see Sweeting, L.M. 179
 Rosini, C., see Salvadori, P. 274
 Ross, D.L. 205, 206
 Ross, D.L., see Bauer, H. 121, 122, 148–151, 154–156
 Ross, D.L., see Blanc, J. 144, 177
 Rosso, B. 49
 Roth, K. 325
 Roth, W.J., see Beck, J.S. 196
 Roth, W.J., see Kresge, C.T. 196
 Rothchild, R. 226
 Rothchild, R., see Byrne, B. 309
 Rotin, D., see Tannock, I.F. 321
 Roy, A. 245
 Royle, L., see Beeby, A. 173
 Ruano, J.L.G. 249
 Ruck, M. 89, 90, 94
 Ruck, M., see Berdonosov, P.S. 99
 Ruck, M., see Schmidt, P. 78, 97
 Rudman, D.A., see Han, B. 239
 Ruggles, A.C., see Wenzel, T.J. 227
 Rühle, S., see Held, P. 46
 Ruloff, R. 319
 Rusakova, N.V. 173
 Rusakova, N.V., see Meshkova, S.B. 173
 Rusakova, N.V., see Topilova, Z.M. 173
 Russett, M.D., see Wenzel, T.J. 225
 Ryazanov, M. 128
 Ryazanov, M., see Gleizes, A.N. 240
 Ryazanov, M., see Kuzmina, N. 240, 241
 Ryazanov, M.V., see Kuz'mina, N.P. 128
- Sá Ferreira, R.A. 189
 Sá Ferreira, R.A., see Braga, S.S. 127
 Sá Ferreira, R.A., see Carlos, L.D. 189
 Sá Ferreira, R.A., see Fernandes, J.A. 121
 Saab, A.P., see McGehee, M.D. 211, 213
 Sabbatini, N. 168, 229, 274
 Sabbatini, N., see Charbonnière, L. 286
 Sacconi, L. 145–147, 150
 Sadakata, N., see Yamaguchi, T. 240
 Sadaoka, Y., see Sasaki, M. 127, 159, 160
 Sadowski, J.E., see Sievers, R.E. 234, 238, 242, 243
 Sadowski, J.E., see Wenzel, T.J. 220, 225
- Sæthre, L.J., see Aukrust, A. 319
 Sage, I. 180–182
 Sage, I., see Clegg, W. 130, 132, 182
 Sage, I.C., see Bourhill, G. 181
 Sager, W.F. 165
 Sager, W.F., see Filipescu, N. 164–166
 Sahibzada, M., see Hartley, A. 16
 Saito, H., see Hayashi, S. 20, 34, 35
 Saito, J., see Koshimura, H. 118
 Saito, S., see Takada, N. 211
 Saito, Y., see Kuroda, R. 277
 Saitoh, T. 249
 Saitoh, T., see Taniguchi, S. 17
 Sajavaara, T., see Putkonen, M. 241
 Sakagami, N. 312
 Sakai, N. 17, 19, 20, 27, 29–35, 37–39
 Sakai, N., see Horita, T. 39
 Sakai, N., see Kawada, T. 36
 Sakai, N., see Mori, M. 20
 Sakai, N., see Nishiyama, H. 40
 Sakai, N., see Van Hassel, B.A. 25, 26
 Sakai, N., see Xiong, Y. 21, 22
 Sakai, N., see Xiong, Y.P. 37
 Sakai, N., see Yamaji, K. 21, 22
 Sakai, N., see Yokokawa, H. 19, 36
 Sakai, T., see Shull, B.K. 249
 Sakamoto, M., see Sasaki, M. 127, 159, 160
 Sakamoto, M., see Tamura, O. 249
 Sakamoto, S., see Hanaoka, K. 325
 Saki, M., see Sasaki, M. 127, 159, 160
 Sakiyama, H., see Sasaki, M. 127, 159, 160
 Sakka, S., see Adachi, T. 186
 Salamano, S., see Dickins, R.S. 294
 Salata, O.V., see Christou, V. 214
 Salata, O.V., see Male, N.A.H. 215
 Salata, O.V., see Moon, D.G. 214
 Saloutin, V.I., see Paskevich, K.I. 118, 119
 Salvadori, P. 274
 Salvadori, P., see Di Bari, L. 305, 306
 Samelson, H. 156, 157, 205, 206
 Samelson, H., see Brecher, C. 205, 206
 Samelson, H., see Lempicki, A. 205
 Sameshima, S. 30, 34
 Sammes, N. 30
 Sammes, N.M. 30
 Sammes, N.M., see Ballon, O. 30
 Samuel, I.D.W., see Bourhill, G. 181
 Sanchez, C. 187
 Sanders, J.K.M. 219, 223
 Sanders, J.K.M., see Bulsing, J.M. 220
 Sanders, J.K.M., see Crump, D.R. 219

- Sands, D.E., see Cunningham, J.A. 130, 132, 135, 234
- Sands, D.E., see Philips, T. 130
- Sands, D.E., see Phillips II, T. 311
- Sands, D.E., see Richardson, M.M. 236
- Sands, D.E., see Wasson, S.J.C. 132, 135
- Sanjurjo, A., see Dickinson, P.H. 240
- Sankhla, B.S. 124
- Sano, T. 211
- Sans-Lenain, S., see Gleizes, A. 124, 130, 135, 141
- Santa-Cruz, P.A., see de Sá, G.F. 170, 172
- Santos, L.S., see Airoldi, C. 159
- Santos Jr., L.S. 159
- Sanz, J.L., see Aikihanyan, A.S. 128
- Sanz, J.L., see Gleizes, A. 128, 235, 240
- Sanz, J.L., see Gleizes, A.N. 240
- Saraidarov, T., see Reisfeld, R. 186
- Sarkio, P., see Leskelä, T. 235, 236, 239, 242
- Sasaki, K., see Kabuto, K. 313
- Sasaki, K., see Kobayashi, T. 218
- Sasaki, M. 127, 159, 160
- Sasaki, S., see Taniguchi, H. 206
- Sasaki, T., see Yamada, T. 14
- Sasaki, Y. 245
- Sasaki, Y., see Hazama, R. 313, 314
- Sasaki, Y., see Inamoto, A. 315, 317
- Sasaki, Y., see Kabuto, K. 313
- Sasaki, Y., see Nakanishi, A. 12
- Sasaki, Y., see Sato, J. 315
- Sasayama, K. 245
- Sathianandan, K. 96
- Sato, A., see Amano, A. 139, 235, 236
- Sato, A., see Taketatsu, T. 228
- Sato, J. 315
- Sato, S. 165
- Sato, S., see Sato, Y. 216
- Sato, S., see Yamaguchi, R. 216
- Sato, T., see Shibata, S. 235
- Sato, Y. 216
- Sato, Y., see Yamaguchi, R. 216
- Satoh, H., see Kobayashi, H. 30–33
- Satoh, M., see Tasaki, Y. 145, 147, 239
- Sauvet, A.-L. 15
- Savchenko, G.S. 73, 94
- Sawatani, T., see Ohmori, T. 211
- Sayeed, M., see Iftikhar, K. 145–153
- Scaiano, J.C., see Alvaro, M. 196
- Scardi, P., see Malandrino, G. 239
- Schaap, A.P., see Schuster, G.B. 183
- Schaefer, M., see Dubost, J.-P. 319
- Schenk, K.J., see Bünzli, J.-C.G. 172, 175
- Scherer, G.W., see Brinker, C.J. 186
- Scheunemann, U., see Lupo, D. 204
- Schimitschek, E.J. 148, 151, 152, 205, 206
- Schimitschek, E.J., see Liang, C.Y. 148, 154, 155, 161
- Schimitschek, E.J., see Nehring, R.B. 205
- Schip, F., see Kooijman, H. 132, 311
- Schleid, Th., see Meyer, S.F. 81
- Schleid, Th., see Wontcheu, J. 69, 70, 73, 80, 84–86, 88–90
- Schlenker, J.L., see Beck, J.S. 196
- Schmatz, U., see Weiss, F. 240
- Schmechel, R., see Heil, H. 215
- Schmidt, D.N., see Panson, A.J. 240
- Schmidt, P. 78, 97
- Schmidt, P., see Berdonosov, P.S. 99
- Schmidt, P., see Oppermann, H. 78, 97
- Schmidt, P., see Ruck, M. 89, 90, 94
- Schmidt, P., see Shabalin, D.G. 81
- Schmidtchen, F.P. 280
- Schmitt-Willich, H. 328
- Schramm, G.A.E., see An, Y.Z. 168
- Schreeve, W.L., see Evans, W.J. 126, 130, 131
- Schreiner, R. 183
- Schulte, B., see Richards, B.C. 240
- Schultz, D.L., see Han, B. 239
- Schurig, V., see Keller, F. 250
- Schuster, G.B. 183
- Schuermans, F.J.P. 172
- Schuyf, P.J.W., see Peters, J.A. 224, 235
- Schwarz, E.G.K., see Schimitschek, E.J. 205
- Schweitzer, G.K., see Murray, G.M. 171
- Scopelliti, R., see Burai, L. 324
- Scopelliti, R., see Ruloff, R. 319
- Scopelliti, R., see Zucchi, G. 286, 292, 293
- Scozzafava, A., see Messori, L. 274
- Scribner, W.G. 244
- Scrivanti, A., see Blackborow, J.R. 125
- Searle, T.M., see Pavier, M.A. 200
- Seff, K., see Cramer, R.E. 131, 279, 311
- Seim, H. 242
- Seitz, R. 205
- Sek, D.C., see Wenzel, T.J. 315
- Sekiguchi, H., see Saitoh, T. 249
- Sekine, T., see Noro, J. 244, 246
- Selbin, J. 146–153
- Selbin, J., see Ahmad, N. 219
- Selbmann, D., see Weiss, F. 240
- Sellers, S.P., see Andersen, W.C. 139, 146, 151, 157

- Sénateur, J.P., see Galindo, V. 240
 Sénateur, J.P., see Thomas, O. 240
 Sénateur, J.P., see Weiss, F. 240
 Sendor, D. 195, 196
 Sénéchal, K., see Gunnlaugsson, T. 298
 Senegas, J.-M. 286
 Senkiw, K., see Chadwick, D. 239
 Senocq, F., see Gleizes, A. 128, 235, 240
 Senocq, F., see Gleizes, A.N. 240
 Seo, H.J., see Liu, H.G. 191
 Serafin, F.A., see Filipescu, N. 164–166, 205
 Serafin, F.A., see Sager, W.F. 165
 Serebrennikov, V.V., see Smolyakova, K.E. 49
 Sergeev, S.V., see Barkhatova, L.Yu. 32
 Serpone, N. 156
 Serra, O.A. 174, 177, 198
 Serra, O.A., see Nassar, E.J. 189
 Serrano, J.L. 201
 Serrano, J.L., see Barbera, J. 119
 Serrano, J.L., see Espinet, P. 201
 Sessoll, R., see Benelli, C. 160
 Sevast'yanov, V.G., see Ezhov, Y.S. 236
 Sevchenko, A.N. 163
 Shabalin, D.G. 81
 Shabalin, D.G., see Berdonosov, P.S. 78
 Shaffer, S., see Mukerjee, S. 12
 Shalini, K., see Urs, U.K. 130
 Shamlan, S.H., see Richards, B.C. 240
 Shannon, R.D. 274, 280
 Shannon, R.D., see Langlet, M. 239
 Shapiro, B.L. 224
 Shapiro, Yu.E., see Bol'shoi, D.B. 173
 Shapiro, Yu.E., see Meshkova, S.B. 173
 Shapiro, Yu.E., see Topilova, Z.M. 173
 Shariff, S.S., see Wenzel, T.J. 314
 Sharipov, G.L. 184
 Shavaleev, N.M. 168, 174, 175
 Shavaleev, N.M., see Kazakov, V.P. 172, 173, 183, 184
 Shavaleev, N.M., see Ostakhov, S.S. 172, 173
 Shavaleev, N.M., see Voloshin, A.I. 172, 173, 183, 184
 Shen, C. 130–132, 143, 144
 Shen, F.L., see Huang, C.H. 147
 Shen, S.A., see Ahmed, M.O. 131
 Shen, Y.Q., see Richards, B.C. 240
 Shen, Z.Q. 112
 Shepherd, T.M. 157, 159, 171
 Shepherd, T.M., see Kemlo, J.A. 158
 Shepherd, T.M., see Napier, G.D.R. 168
 Shepherd, T.M., see Neilson, J.D. 158
 Sheppard, E.W., see Beck, J.S. 196
 Sherry, A.D., see De León-Rodríguez, L.M. 330
 Sherry, A.D., see Woods, M. 298, 322
 Sherry, A.D., see Zuo, C.S. 326
 Shi, J.X., see Yao, Y.F. 197
 Shi, R., see Yang, J. 228
 Shi, T.S., see Liu, G.F. 128
 Shiba, H., see Tsukube, H. 246, 282
 Shibasaki, M. 284
 Shibata, K., see Sano, T. 211
 Shibata, S. 235
 Shibata, S., see Onuma, S. 132, 139
 Shibayama, T., see Ishihara, T. 15
 Shigekawa, H., see Komiyama, M. 274
 Shigematsu, T. 145, 147–153, 237, 244
 Shigematsu, T., see Utsunomiya, K. 147, 150, 152
 Shigorin, D.N., see Bazhulin, P.A. 205
 Shih, H.T., see Sun, P.P. 211, 215
 Shillady, D., see Foster, D.R. 178
 Shimada, M., see Tsukuma, K. 29
 Shimanouchi, T., see Mikami, M. 161
 Shimoi, M., see Nakamura, M. 130, 134
 Shin, Y.K., see Akiyama, Y. 239
 Shinoda, S. 285
 Shinoda, S., see Mahajan, R.K. 232, 280, 281, 288, 289
 Shinoda, S., see Miyake, H. 275, 283
 Shinoda, S., see Tamiaki, H. 304
 Shinoda, S., see Tsukube, H. 161, 246, 247, 275, 276, 278–280, 282, 283, 288, 296, 302, 304, 305
 Shinoda, S., see Yamada, T. 277, 291
 Shinohara, H., see Kato, H. 326
 Shiode, M., see Tsukube, H. 246, 247, 282, 283
 Shiraishi, Y., see Akashi, T. 39
 Shivashankar, S.A., see Urs, U.K. 130
 Shlykov, S.A., see Belova, N.V. 236
 Shlykov, S.A., see Giricheva, N.I. 235, 236
 Shoham, B., see Willner, I. 283
 Shull, B.K. 249
 Shum, D.P., see Benelli, C. 159
 Si, Z., see Zhu, G. 229
 Si, Z.K. 228
 Si, Z.K., see Zhang, R.J. 199
 Si, Z.K., see Zhu, G.Y. 228, 229
 Sicre, J.E. 234–236
 Sieck, R.F. 238
 Sieler, J., see Ruloff, R. 319
 Sievers, R.E. 146, 147, 220, 223, 224, 234, 238, 242, 243
 Sievers, R.E., see Andersen, W.C. 139, 146, 151, 157

- Sievers, R.E., see Brooks, J.J. 232
 Sievers, R.E., see Cunningham, J.A. 131, 311
 Sievers, R.E., see Dickinson, P.H. 240
 Sievers, R.E., see Dyer, D.S. 224
 Sievers, R.E., see Eisentraut, K.J. 126, 127,
 145–153, 157, 233, 234, 237
 Sievers, R.E., see Feibush, B. 145–148, 150, 232
 Sievers, R.E., see Morris, M.L. 147
 Sievers, R.E., see Moshier, R.W. 237
 Sievers, R.E., see Picker, J.E. 232
 Sievers, R.E., see Richardson, M.F. 126, 233, 234
 Sievers, R.E., see Rondeau, R.E. 219, 223
 Sievers, R.E., see Sicre, J.E. 234–236
 Sievers, R.E., see Springer Jr., C.S. 119, 144–153,
 172
 Sievers, R.E., see Wenzel, T.J. 119, 146, 220, 225,
 227, 243
 Sigoli, F.A. 189
 Siitari, H., see Hemmilä, I. 229
 Siligardi, G., see Beeby, A. 299
 Siligardi, G., see Govenlock, L.J. 299
 Sillanpää, R., see Leskelä, M. 235, 242
 Silva, C.F.B., see Brito, H.F. 175, 176
 Silver, B.L., see Pinchas, S. 161
 Simas, A.M., see Batista, H.J. 131, 148, 311
 Simas, A.M., see de Andrade, A.V.M. 172
 Simas, A.M., see de Sá, G.F. 170, 172
 Simas, A.M., see Faustino, W.M. 172
 Simas, A.M., see Rocha, G.B. 172
 Simon, J., see Meyer, Y. 205
 Sinisterra, R.D., see Brito, H.F. 127
 Sioubara, M.P., see Spyroulias, G.A. 128
 Sipe III, J.P., see Horrocks Jr., W.DeW. 129, 132,
 221, 223, 224, 308, 309
 Siqueiros, J.M., see Hirata, G.A. 239
 Sisk, P.J., see Wahid, P.F. 242
 Sisti, M., see Aime, S. 322
 Sita, M. 228, 229
 Skelton, B.W., see Behrsing, T. 141, 142, 159
 Skhashiri, B.Z., see Schreiner, R. 183
 Skoglund, U., see Valkonen, J. 50, 52
 Skotheim, T., see Campos, R.A. 211
 Skotheim, T., see Kido, J. 210, 213, 215
 Slawin, A.M.Z., see Drake, S.R. 139
 Slonim, I.Y. 220
 Smart, N., see Lin, Y.H. 157
 Smith, K.D., see Beck, J.S. 196
 Smith, W.B. 225
 Smolyakova, K.E. 49
 Sohn, Y.S., see Kang, S.J. 131, 149, 151, 239
 Sohn, Y.S., see Lee, J.H. 132, 141, 151
 Soini, E. 229
 Soiminen, P., see Leskelä, M. 234–236
 Sokolnicki, J., see Strek, W. 186
 Sokolnicki, J., see Tsaryuk, V. 161, 211
 Sokolov, D.N. 237
 Sokolov, D.N., see Magazeeva, N.V. 238
 Sokolov, D.N., see Spitsyn, V.I. 238
 Sola, E., see Espinet, P. 201
 Sololovskaya, A.I., see Bazhulin, P.A. 205
 Song, G., see Hu, L. 228
 Song, H.Y., see Yu, X.J. 166
 Song, H.Z. 145, 150, 234, 239
 Song, H.Z., see Meng, G.Y. 240
 Song, H.Z., see Wang, H.B. 214
 Song, J.Q., see Huang, C.H. 181
 Sparlin, D.M., see Anderson, H.U. 24
 Sparlin, D.M., see Kuo, J. 23
 Spee, C., see Timmer, K. 145, 234
 Spee, C.I.M.A., see Richards, B.C. 240
 Speghini, A., see Lo Nigro, R. 239
 Speghini, A., see Malandrino, G. 124, 149, 172,
 175, 239
 Spek, A.L., see Kooijman, H. 132, 311
 Spek, A.L., see Van Staveren, D.R. 125, 130, 132,
 136, 138, 139
 Spek, A.L., see van Staveren, D.R. 311
 Spencer, N., see Bassett, A.P. 158
 Spiess, H., see Demus, D. 200
 Spirandeli Crespi, M. 62
 Spirandeli Crespi, M., see Cruz, P.M. 62
 Spiridonov, F.M., see Kuz'mina, N.P. 128
 Spitsin, V.I., see Batsanov, A.S. 132
 Spitsyn, V.I. 238
 Spitsyn, V.I., see Magazeeva, N.V. 238
 Sprengle, V., see Mukerjee, S. 12
 Springer Jr., C.S. 119, 144–153, 172
 Springer Jr., C.S., see Bruder, A.H. 158
 Springer Jr., C.S., see Feibush, B. 145–148, 150,
 232
 Spyroulias, G.A. 128
 Srdanov, V., see Yang, C.Y. 177, 194
 Srdanov, V.I. 177, 194
 Srdanov, V.I., see McGehee, M.D. 211, 213
 Stabnikov, P.A., see Zaitseva, E.G. 130, 135
 Stadel, O., see Wahl, G. 240
 Ståhlberg, T., see Hemmilä, I. 229
 Stancheva, M. 76
 Stancheva, M.G., see Gospodinov, G.G. 74, 76, 99
 Staniforth, J., see Ballon, O. 30
 Staniforth, M.L., see Briggs, J. 219
 Staninski, K., see Elbanowski, M. 183

- Staninski, K., see Kaczmarek, M. 185
 Star, R.A., see Kobayashi, H. 326, 327
 Stathatos, E., see Moleski, R. 189
 Steele, B.C.H. 14
 Steele, B.C.H., see Bance, P. 14
 Steele, B.C.H., see Chadwick, D. 239
 Steele, B.C.H., see Christie, G.M. 20
 Steele, B.C.H., see McAleese, J. 146, 239
 Steffen, W.L. 141
 Steiger, J., see Heil, H. 215
 Stein, G., see Haas, Y. 170
 Steinbach, J.F., see Brown, W.B. 244
 Steinmetzer, H.-C., see Schuster, G.B. 183
 Stemple, N.R., see Watson, W.H. 131, 136, 137, 311
 Stephen, W.I., see Belcher, R. 123, 146
 Stevenson, J.W. 19
 Stevenson, J.W., see Armstrong, T.R. 30
 Stølen, S., see Sakai, N. 31
 Stolzenberg, G.E. 226
 Stoodley, R.J., see Helliwell, M. 249
 Strakey, J.P., see Williams, M.C. 3
 Straw, R.D., see Hirayama, C. 235
 Streib, W.E., see Barash, E.U. 124, 139, 234
 Streck, W. 186
 Struchkov, Yu.T., see Batsanov, A.S. 132
 Struchkov, Yu.T., see Kuz'mina, N.P. 132
 Stucky, G.D., see Morris, R. 74
 Stucky, G.D., see Watson, M.M. 171
 Stump, N.A., see Murray, G.M. 171
 Su, C.-Y., see Yang, X.-P. 289
 Su, Q.D., see Wu, R.H. 166
 Su, Q.D., see Yang, Y.T. 166
 Su, Q.D., see Yu, X.J. 166
 Subramony, J.A., see Kahr, B. 177
 Sugimoto, H. 142–144
 Sugimoto, H., see Yamada, T. 277, 291
 Sugimoto, M., see Saitoh, T. 249
 Sugiura, K., see Fujinaga, T. 147
 Sugiura, M., see Kobayashi, S. 247, 274
 Sugiyama, J., see Takada, N. 181, 182
 Sullivan, G.R. 220
 Sullivan, P.G., see Hirayama, C. 235
 Sülzle, D., see Schmitt-Willich, H. 328
 Sun, G., see Li, W.L. 211, 214
 Sun, J.B., see Wei, A.Z. 133
 Sun, P.P. 211, 215
 Sun, R.G. 214
 Sun, R.G., see Zhang, X.M. 214
 Sun, Y., see Zuo, C.S. 326
 Sundaram, K.B., see Wahid, P.F. 242
 Suntola, T. 241
 Suntola, T., see Haukka, S. 242
 Suponitskii, Yu.L. 49
 Surendra, L., see Gupta, M.K. 49, 63
 Sussan, S., see Willner, I. 283
 Sutton, J.E., see Zink, J.I. 179, 182
 Suzuki, M., see Le, Q.T.H. 244
 Suzuki, N., see Nakamura, S. 244
 Suzuki, S., see Amano, A. 139, 235, 236
 Suzuki, T., see Saitoh, T. 249
 Suzuki, T., see Tsukuda, T. 311
 Swager, T.M., see Trzaska, S.T. 201
 Swain, M.V., see Hasselman, D.P.H. 30–33
 Sweet, T.R. 244
 Sweeting, L.M. 179, 180, 182
 Sydnos, L.K., see Aukrust, A. 319
 Syed, R., see Hasselman, D.P.H. 30–33
 Szedon, J.R., see Panson, A.J. 240
 Szejtli, J. 127
 Szycczewski, A. 161
 Tabushi, M., see Shigematsu, T. 237, 244
 Tachibana, K., see Harima, H. 236
 Tadano, J., see Matsumoto, K. 230
 Taga, T., see Sugimoto, H. 142–144
 Tagaya, A., see Kuriki, K. 193, 218
 Tai, L.W. 19
 Tai, Y.R., see Wang, J.B. 14
 Taira, H., see Zhou, H.B. 20
 Takada, N. 181, 182, 211
 Takagi, H., see Zhou, H.B. 20
 Takagi, H.D., see Matsumoto, M. 159
 Takahara, H., see Le, Q.T.H. 245
 Takahashi, N., see Sato, Y. 216
 Takahashi, Y., see Horinouchi, K. 32
 Takahashi, Y., see Sakai, N. 37
 Takahei, K., see Whitney, P.S. 239
 Takeda, N., see Komiyama, M. 274
 Takeda, T., see Mori, M. 29
 Takeda, Y., see Takeuchi, T. 29
 Takeda, Y., see Yamamoto, O. 14, 34
 Takei, S., see Nakamura, S. 245
 Takeishi, H., see Tsukube, H. 247
 Takemura, M. 314
 Takenobu, K., see Nakanishi, A. 12
 Taketatsu, T. 228
 Taketatsu, T., see Aihara, M. 228
 Takeuchi, E., see Tamiaki, H. 304
 Takeuchi, H. 10
 Takeuchi, T. 29
 Takeuchi, Y., see Nakamura, M. 130, 134

- Takita, Y., see Ishihara, T. 14–16
 Takita, Y., see Yamada, T. 14
 Tamakawa, T., see Yasuda, I. 30, 34
 Tamari, N., see Takeuchi, T. 29
 Tameshige, N., see Tamiaki, H. 304
 Tameshige, N., see Tsukube, H. 305
 Tamiaka, H., see Tsukube, H. 246
 Tamiaki, H. 303, 304
 Tamiaki, H., see Tsukube, H. 161, 276, 279, 296,
 302, 304, 305
 Tamura, O. 249
 Tamura, T., see Kuriki, K. 218
 Tan, G.K., see Chen, X.F. 133, 182
 Tan, M.Y., see Liu, W.S. 130
 Tanabe, J., see Akashi, T. 39
 Tanaka, I., see Tobita, S. 165
 Tanaka, N., see Zama, H. 240
 Tananaev, I.V., see Savchenko, G.S. 73, 94
 Tang, B. 192
 Tang, C.W. 207
 Taniguchi, H. 206
 Taniguchi, S. 17
 Taninaka, A., see Kato, H. 326
 Tannock, I.F. 321
 Tanny, S.R., see Bruder, A.H. 158
 Tasaki, Y. 145, 147, 239
 Teiserskis, A., see Galindo, V. 240
 Teixeira-Dias, J.J.C., see Braga, S.S. 127
 Telk, C.L., see Bhaumik, M.L. 205
 Templeton, D.H., see Zalkin, A. 129, 132, 134
 Teng, M.K., see Wei, A.Z. 133, 181
 Teng, X.L., see Yang, W. 228
 Teotonio, E.E.S., see Brito, H.F. 175, 176
 Teotonio, E.E.S., see Reyes, R. 216
 Terada, M. 249
 Terada, M., see Gu, J.H. 249
 Terada, M., see Mikami, K. 249
 Terreno, E. 295, 315
 Terreno, E., see Aime, S. 274, 278, 281, 319, 323,
 326, 328
 Testen, M.E., see Schreiner, R. 183
 Thomas, E.L., see Bender, J.L. 194
 Thomas, O. 240
 Thompson, L. 131, 135, 169
 Thompson, L.C. 46, 112, 129, 131, 149, 171, 176
 Thompson, L.C., see Batista, H.J. 131, 148, 311
 Thompson, L.C., see Holz, R.C. 121, 129–132,
 134, 311
 Thompson, L.C., see Malta, O.L. 131, 149
 Thompson, L.C., see Mattson, S.M. 122, 126, 149
 Thompson, L.C., see Moeller, T. 244
 Thompson, L.C., see Moser, D.F. 131, 134, 149,
 171
 Thornton, A., see Bruce, D.W. 204
 Thurston, J.E., see Wenzel, T.J. 315
 Tian, H., see Huang, L. 214
 Tiitta, M. 238, 240
 Tiitta, M., see Leskelä, M. 234–236, 242
 Timmer, K. 145, 234
 Timoyasu, H., see Hatakeyama, Y. 156
 Tinant, B., see Binnemans, K. 201, 202
 Tischenko, M.A., see Kononenko, L.I. 145–148,
 150, 151
 Titzte, H. 141, 142
 Tizane, D., see Belanger, P. 221
 Tobita, S. 165
 Toei, J., see Umitani, S. 245
 Toland, A., see Viswanathan, T. 308
 Tolstikov, G.A., see Sharipov, G.L. 184
 Tomada, S., see Nakamura, M. 130, 134
 Tomisawa, H., see Taniguchi, H. 206
 Tomitsugu, T., see Aihara, M. 228
 Tomiyama, C.S., see Brito, H.F. 175, 176
 Tomiyasu, H., see Mihara, T. 156
 Tomono, K., see Zhou, H.B. 20
 Topilova, Z.M. 173
 Topilova, Z.M., see Bol'shoi, D.B. 173
 Topilova, Z.M., see Meshkova, S.B. 173
 Topilova, Z.M., see Rusakova, N.V. 173
 Törnroos, K.W., see Aukrust, A. 319
 Toro, R., see Lo Nigro, R. 239
 Tossidis, I.A., see Christidis, P.C. 130, 311
 Tóth, É. 317
 Tóth, É., see Burai, L. 319, 324
 Tóth, É., see Ruloff, R. 319
 Trembovetskii, G.V., see Batsanov, A.S. 132
 Trias, J.A., see Liang, C.Y. 148, 154, 155, 161
 Trias, J.A., see Nehring, R.B. 205
 Trias, J.A., see Schimitschek, E.J. 148, 151, 152,
 205, 206
 Tribillon, G., see Pagnot, T. 193
 Trifimov, A.K., see Sevchenko, A.N. 163
 Tripier, R., see Ruloff, R. 319
 Trombe, J.C., see Castro, A. 72, 75, 94
 Trombe, J.C., see de Pedro, M. 72, 74, 94
 Trost, B.M. 247
 Troughton, J.S., see Wenzel, T.J. 314
 Troyanov, S., see Gleizes, A.N. 240
 Troyanov, S.I., see Kuz'mina, N.P. 128
 Troyanov, S.I., see Zharkova, Ya.N. 130
 Trunov, V.K., see Gasanov, Y.M. 58, 60
 Trunov, V.K., see Iskhakova, L.D. 50, 55, 57, 58

- Trunov, V.K., see Ovanisyan, S.M. 50, 51, 58–60
 Trush, V., see Borzechowska, M. 159
 Trzaska, S.T. 201
 Tsaplev, Yu.B. 185
 Tsaryuk, V. 161, 176, 211
 Tschang, P.S.W., see McPhail, A.T. 133
 Tsukahara, Y., see Matsumoto, K. 230
 Tsukube, H. 161, 246, 247, 275, 276, 278–280, 282, 283, 288, 296, 302, 304, 305
 Tsukube, H., see Mahajan, R.K. 232, 280, 281, 288, 289
 Tsukube, H., see Miyake, H. 275, 283
 Tsukube, H., see Tamiaki, H. 303, 304
 Tsukube, H., see Yamada, T. 277, 291
 Tsukuda, T. 311
 Tsukuma, K. 29
 Tsunenobu, T., see Umitani, S. 245
 Tsunoda, K., see Matsumoto, K. 230
 Tsuru, Y., see Miyachi, M. 17
 Tsutsui, T., see Li, W.L. 211, 214
 Tsutsui, T., see Takada, N. 211
 Tsutsui, T., see Zhu, W.G. 211, 215
 Tucker, J.N., see Evans, F.D. 225
 Turanova, O.A., see Galyametdinov, Yu.G. 202
 Turowska-Tyrk, I., see Borzechowska, M. 159
 Turro, C. 288
 Turro, N.J., see Schuster, G.B. 183
 Tursina, A.I., see Iskhakova, L.D. 50, 56
 Tverdova, N.V., see Belova, N.V. 236
 Tverdova, N.V., see Giricheva, N.I. 235, 236
 Twarowski, A.J., see Dao, P. 237
 Tweedle, M.F., see Kumar, K. 319
 Tzavellas, L.C., see Christidis, P.C. 130, 311

 Ubbink, M., see Meskers, S.C.J. 307
 Uchida, H., see Iwahara, H. 14
 Uchida, S., see Mahajan, R.K. 232, 280, 281, 288, 289
 Uchikawa, F., see Matsuno, S. 240
 Ueba, Y. 192
 Uebel, J.J., see Wing, R.M. 311
 Uekawa, M., see Miyamoto, Y. 211
 Uemara, T., see Matsumoto, K. 230
 Uenishi, J., see Tsukube, H. 246, 247, 282, 283
 Uenishi, J., see Yamada, T. 277, 291
 Ueno, A., see Sakai, N. 27
 Ueno, A., see Takeuchi, H. 10
 Ueta, H., see Ohmori, T. 211
 Ueta, H., see Ohmori, Y. 211
 Ugozzoli, F., see Van Staveren, D.R. 125, 130, 132, 136, 138, 139
 Ugozzoli, F., see van Staveren, D.R. 311
 Uhlemann, E. 146, 238
 Ukai, Y. 15
 Umakoshi, K., see Hazama, R. 313, 314
 Umetani, S. 245
 Umetani, S., see Le, Q.T.H. 244, 245
 Umetani, S., see Miyazaki, S. 245, 246
 Umetani, S., see Mukai, H. 245
 Umetani, S., see Sasayama, K. 245
 Umitami, S., see Gao, X.C. 151, 214
 Umitani, S. 245
 Unnikrishnan, E.K., see Ramkumar, J. 246
 Unno, S., see Tamiaki, H. 304
 Unno, S., see Tsukube, H. 305
 Urano, Y., see Hanaoka, K. 325
 Urbain, G. 111
 Urbas, A.M., see Bender, J.L. 194
 Urs, U.K. 130
 Utriainen, M., see Mölsä, H. 241
 Utsinomiya, S., see Matsuno, S. 240
 Utsunomiya, K. 145, 147, 148, 150–153
 Utsunomiya, K., see Shigematsu, T. 145, 147–153, 237
 Uwai, K., see Whitney, P.S. 239

 Valkonen, J. 49, 50, 52, 56, 58, 59, 76, 80, 88
 Valkonen, J., see Koskenlinna, M. 76
 Valkonen, J., see Niinistö, L. 72, 88
 Vallarino, L.M. 230
 Vallarino, L.M., see Foster, D.R. 178
 Van, V., see Galyametdinov, Yu.G. 202
 van Albada, G.A., see Van Staveren, D.R. 130, 132, 136, 138, 139, 311
 van Bekkum, H. 195
 Van Bekkum, H., see Peters, J.A. 224, 235, 313
 Van Deun, R. 203
 Van Deun, R., see Binnemans, K. 201–203
 van Genderen, M.H.P., see Langereis, S. 329
 Van Hassel, B.A. 25, 26
 Van Hecke, K., see Binnemans, K. 201, 202
 Van Meerssche, M., see Vancoppemolle, A. 131
 Van Meervelt, L. 131, 148
 Van Meervelt, L., see Binnemans, K. 201, 202
 van Niekerk, J.C., see Nassimbeni, L.R. 311, 312
 van Seggern, H., see Heil, H. 215
 Van Slyke, S.A., see Tang, C.W. 207
 Van Staveren, D.R. 125, 130, 132, 136, 138, 139, 311
 Van Vollenhoven, J.S., see Leipoldt, J.G. 133
 Vancoppemolle, A. 131
 Vanderkooi, G., see LaPlanche, L.A. 279

- Vandervoort-Maarschalk, F.W., see Hocking, M.B. 179
 Vaquer, E., see Arnaud, N. 228
 Varfolomeev, M.B., see Petrov, K.I. 73, 94, 96
 Vartuli, J.C., see Beck, J.S. 196
 Vartuli, J.C., see Kresge, C.T. 196
 Vasama, K., see Leskelä, T. 235, 236, 239, 242
 Vase, P., see Richards, B.C. 240
 Venard, A., see Binnemans, K. 162
 Venteicher, R.F., see Wang, C.P. 128
 Verbiest, T. 203
 Verhoeven, J.W., see Werts, M.H.V. 167, 168
 Verron, M. 205
 Verron, M., see Meyer, Y. 205
 Vieira, M.P.R.S., see de Farias, R.F. 193
 Vigdorchik, A.G. 46
 Vijverberg, C.A.M., see Peters, J.A. 313
 Viktkun, R.A., see Kononenko, L.I. 145–148, 150, 151
 Vill, V., see Demus, D. 200
 Villata, L.S. 168
 Visco, S. 12
 Viswanathan, T. 308
 Vitkun, R.A., see Kononenko, L.I. 145–148, 150, 152
 Vittal, J.J., see Chen, X.F. 133, 182
 Vogler, A., see Kunkely, H. 178
 Vogt, J., see Giricheva, N.I. 236
 Vogt, N., see Giricheva, N.I. 236
 Vohs, J.M., see Gorte, R.J. 15
 Volodina, A.N., see Savchenko, G.S. 73, 94
 Voloshin, A.I. 172, 173, 183, 184
 Voloshin, A.I., see Antipin, V.A. 185
 Voloshin, A.I., see Kazakov, V.P. 172, 173, 183–185
 Voloshin, A.I., see Ostakhov, S.S. 172, 173, 185
 Voloshin, A.I., see Sharipov, G.L. 184
 von Ammon, R. 220
 von Ebron, H., see Woods, M. 298, 322
 von Gustorf, E.A.K., see Blackborow, J.R. 125
 Voronov, V.K. 220
 Voronskaya, G.N., see Petrov, K.I. 49, 63

 Wada, E. 249
 Wada, M., see Sato, S. 165
 Wada, M., see Tsukube, H. 161, 279, 296, 302, 304
 Wada, Y., see Hasegawa, Y. 173
 Wada, Y., see Iwamuro, M. 166, 173
 Wada, Y., see Kawamura, Y. 214
 Wada, Y., see Yanagida, S. 173
 Wagner, W.F., see Brown, W.B. 244
 Wagner, W.F., see Cunningham, J.A. 132, 135
 Wagner, W.F., see Phillips, T. 130
 Wagner, W.F., see Phillips II, T. 311
 Wagner, W.F., see Richardson, M.M. 236
 Wagner, W.F., see Wasson, S.J.C. 132, 135
 Wahid, P.F. 242
 Wahl, G. 240
 Wahl Jr., H.W., see Peterson Jr., M.R. 220
 Wai, C.M., see Lin, Y.H. 157
 Wakili, N., see Campos, R.A. 211
 Wallace, S., see Bolskar, R.D. 328
 Walrand-Görller, C., see Van Meervelt, L. 131, 148
 Walton, A.J. 179
 Wander, J.D., see Ahmad, N. 219
 Wang, C.K., see Zhong, G.L. 200
 Wang, C.P. 128
 Wang, F.S., see Liang, F.S. 212, 215
 Wang, H., see Yang, J. 228, 229
 Wang, H.B. 214
 Wang, H.B., see Meng, G.Y. 240
 Wang, H.B., see Song, H.Z. 239
 Wang, J.B. 14
 Wang, J.F. 211, 212
 Wang, J.F., see Jabbour, G.E. 211
 Wang, J.F., see Zheng, Z.P. 131, 181
 Wang, K.Z. 149, 150, 162, 175, 198, 199, 202, 204, 211
 Wang, K.Z., see Bian, Z.Q. 121
 Wang, K.Z., see Gao, D.Q. 211
 Wang, K.Z., see Gao, L.H. 162, 198, 204
 Wang, K.Z., see Huang, C.H. 198, 204
 Wang, K.Z., see Huang, L. 211
 Wang, K.Z., see Jiang, W. 128, 198, 199
 Wang, K.Z., see Xia, W.S. 198
 Wang, K.Z., see Xiao, Y.J. 162
 Wang, K.Z., see Zhao, X.S. 204
 Wang, K.Z., see Zhou, D.J. 155, 204
 Wang, L.H. 193
 Wang, L.X., see Liang, F.S. 212, 215
 Wang, M.Q., see Fan, X.P. 186, 188
 Wang, M.Q., see Hao, X.P. 186
 Wang, M.Q., see Qian, G.D. 172, 188
 Wang, M.Q., see Zhang, R.J. 200
 Wang, M.Z. 123, 162
 Wang, M.Z., see Bünzli, J.-C.G. 172, 175
 Wang, M.Z., see Chen, B.T. 181
 Wang, M.Z., see Hu, W.P. 211, 215
 Wang, M.Z., see Yu, G. 213, 215
 Wang, Q., see Li, W. 176
 Wang, R.J., see Wang, K.Z. 204

- Wang, R.M., see Feng, H.Y. 194
Wang, R.Y., see Wang, J.F. 211, 212
Wang, S., see Hu, M.L. 131
Wang, S.B., see Guo, J.F. 188
Wang, S.B., see Li, H.R. 188
Wang, S.B., see Yan, B. 172, 186
Wang, S.B., see Zheng, Y.X. 211, 214, 215
Wang, W., see Wang, L.H. 193
Wang, W.C., see Wang, K.Z. 162
Wang, W.M., see Chou, K.S. 234
Wang, X.P., see Huang, C.H. 198
Wang, X.W., see Gao, J.Z. 228
Wang, Y.F., see Okada, K. 211, 215
Wang, Y.H., see Zhong, G.L. 200
Wang, Y.T., see Shen, C. 130–132, 143, 144
Wang, Y.Z., see Sun, R.G. 214
Wang, Z.M., see Xu, G. 141
Wang, Z.Y., see Fan, X.P. 188
Wanger, W.F., see Cunningham, J.A. 130, 234
Ward, M.D., see Shavaleev, N.M. 174, 175
Ward, M.D., see Shavaleev, N.M.M. 168
Warenghem, M., see Boyalud, J. 202, 203
Warner, P., see Burgett, C.A. 224
Wasson, S.J.C. 132, 135
Watanabe, K., see Yamane, H. 240
Watanabe, M. 314
Watanabe, M., see Takemura, M. 314
Watkin, J., see Misner, A. 231
Watkin, J.E., see Wilkinson, D.A. 232
Watson, M.M. 171
Watson, W.H. 131, 136, 137, 311
Wayda, A.L. 311
Weber, J., see Senegas, J.-M. 286
Weber, M.J. 112
Weber, M.J., see Jacobs, R.R. 237
Weck, S., see Oppermann, H. 72, 97
Wei, A.Z. 133, 181
Wei, J., see Zhu, G.Y. 228, 229
Wei, L.L., see Jiang, J.Z. 128, 198, 199
Wei, X.Q., see Zhu, W.G. 211, 215
Weil, S., see Mukerjee, S. 12
Weinberg, M., see Bhaumik, M.L. 205
Weiner, A.L., see De León-Rodríguez, L.M. 330
Weinmann, H., see Keller, F. 250
Weinmann, H.-J., see Roth, K. 325
Weinstein, S.E., see Wenzel, T.J. 309
Weise, K.H., see Lempicki, A. 205
Weiss, F. 240
Weiss, F., see Galindo, V. 240
Weiss, F., see Thomas, O. 240
Weissman, S.I. 163, 165
Wendtlandt, W.W., see Giesbrecht, E. 94
Weng, G.F., see Shen, C. 144
Wensel, T.G., see Meares, C.F. 328
Wenzel, T.J. 112, 119, 146, 220, 221, 223–227, 243, 308, 309, 314, 315
Wenzel, T.J., see Sievers, R.E. 146, 147, 243
Wernick, D.L., see McCreary, M.D. 127, 227, 309
Werts, M.H.V. 167, 168
Wessels, B.W., see Williams, D.M. 239
Weston, M., see Hartley, A. 16
Weyhermüller, T., see Van Staveren, D.R. 125, 130, 132, 136, 138, 139
Weyhermüller, T., see van Staveren, D.R. 311
Whan, R.E. 121, 163, 205
Whan, R.E., see Crosby, G.A. 121, 125, 163
Whidesides, G.M. 219, 226
Whildin, L.L., see Andersen, W.C. 139, 146, 151, 157
White, A.H., see Behrsing, T. 141, 142, 159
White, E.H., see Wildes, P.D. 185
White, J.G. 131, 136, 137
White, W.B., see McCarthy, G.J. 46
Whitesides, G.M. 227
Whitesides, G.M., see McCreary, M.D. 127, 227, 309
Whitney, P.S. 239
Whittaker, B. 205
Wickleder, M. 46
Wickleder, M.S. 49, 50, 55, 67, 70, 72, 80–83, 88, 90, 91
Wickleder, M.S., see Ben Hamida, M. 90, 93
Wickleder, M.S., see Göhhausen, I. 50, 55, 80, 83, 100, 102
Wickleder, M.S., see Krügermann, I. 49–51, 62, 67, 69, 70, 80, 83
Wiese, S., see Dirr, S. 211
Wietzke, R. 288–291
Wietzke, R., see Mazzanti, M. 288–290
Wilcox, J.D., see Wenzel, T.J. 308
Wildes, P.D. 185
Wildner, M. 72
Wilkinson, A.P., see Morris, R.E. 99
Wilkinson, D., see Misner, A. 231
Wilkinson, D.A. 232
Williams, D.E. 228
Williams, D.H. 220
Williams, D.H., see Crump, D.R. 219
Williams, D.H., see Sanders, J.K.M. 219, 223
Williams, D.M. 239
Williams, E.J., see Wenzel, T.J. 119, 146, 243
Williams, G., see Beeby, A. 173

- Williams, J.A.G., see Beeby, A. 299
 Williams, J.A.G., see Govenlock, L.J. 299
 Williams, J.A.G., see Maupin, C.L. 307
 Williams, L.G., see Schreiner, R. 183
 Williams, M.C. 3
 Williams, R.J., see Watson, W.H. 131, 136, 137, 311
 Williams, R.M., see Bassett, A.P. 158
 Williams, R.M., see Glover, P.B. 299
 Willimas, D.J., see Drake, S.R. 139
 Willner, I. 283
 Wilson, L.J. 326
 Wilson, L.J., see Bolskar, R.D. 328
 Wing, R.M. 311
 Wipff, G., see Charbonnière, L.J. 291
 Wiskur, S.L. 280
 Witts, A.D., see Lyle, S.J. 122, 125–127
 Wolcan, E., see Villata, L.S. 168
 Wolfbeis, O., see Blackborow, J.R. 125
 Wolff, N.E. 191, 205
 Wong, T.K.S., see Fu, Y.J. 148, 150
 Wong, W.-K. 303
 Wong, W.-K., see Yang, X.-P. 289
 Wong, W.-T., see Wong, W.-K. 303
 Wontcheu, J. 67, 69, 70, 73, 80, 84–86, 88–90
 Woods, M. 298, 322
 Woods, M., see Beeby, A. 173
 Wostyn, K. 204
 Wright, M.R.W., see Nassimbeni, L.R. 311, 312
 Wu, A., see Dai, W.M. 249
 Wu, A.X., see Dai, W.M. 249
 Wu, C., see Bryant Jr., L.H. 326
 Wu, C.H.S., see Hammond, G.S. 148
 Wu, F.B. 230
 Wu, H., see Lin, Y.H. 157
 Wu, J., see Chen, X.F. 133, 155, 181, 182
 Wu, N.Z., see Wang, K.Z. 162, 204
 Wu, R.H. 166
 Wu, S.L. 166
 Wu, S.L., see Yang, Y.S. 166, 167, 230
 Wu, W.L., see Wu, S.L. 166
 Wu, X., see Yu, G. 213, 215
 Wu, X.P., see Fan, X.P. 186
 Wu, Y.L., see Wu, S.L. 166

 Xia, C.G., see Song, H.Z. 145, 150, 234, 239
 Xia, C.R., see Meng, G.Y. 240
 Xia, C.R., see Wang, H.B. 214
 Xia, S.D., see Dong, N. 192
 Xia, W.S. 198
 Xia, X.H., see Gao, L.H. 162, 198, 204
 Xia, X.H., see Li, H. 204
 Xia, X.H., see Zhao, X.S. 204
 Xiao, X.-L., see Yang, X.-P. 289
 Xiao, Y.J. 162
 Xie, M.G., see Zhu, W.G. 211, 215
 Xie, M.Q., see Liang, C.J. 214
 Xie, X., see Li, H. 162, 204
 Xie, X.M., see Huang, C.H. 204
 Xie, X.M., see Wang, K.Z. 204
 Xie, X.M., see Zhao, X.S. 204
 Xin, H.W., see Pan, M. 239
 Xiong, R.G. 133, 180, 182
 Xiong, R.G., see Zeng, X.R. 133, 181, 182
 Xiong, Y. 21, 22
 Xiong, Y.P. 37
 Xiong, Y.P., see Sakai, N. 37
 Xu, D.J., see Hu, M.L. 131
 Xu, G. 141
 Xu, G.X., see Huang, C.H. 147, 198, 204
 Xu, G.X., see Jiang, W. 128, 198, 199
 Xu, G.X., see Wang, K.Z. 162, 198, 202, 204
 Xu, G.X., see Zhou, D.J. 155, 204
 Xu, J.D. 139
 Xu, J.M., see Gao, L.H. 162, 198, 204
 Xu, L., see Li, H. 162, 204
 Xu, L.G., see Huang, C.H. 204
 Xu, L.G., see Wang, K.Z. 204
 Xu, L.G., see Zhao, X.S. 204
 Xu, L.G., see Zhou, D.J. 155, 204
 Xu, Q.H. 196
 Xu, Q.H., see Fu, L.S. 196
 Xu, R., see Chour, K.W. 239
 Xu, R.R., see Fu, L.S. 196
 Xu, R.R., see Xu, Q.H. 196
 Xu, Y., see Huang, C.H. 198, 204
 Xu, Y., see Wang, K.Z. 162, 204
 Xu, Y.H., see Chen, X.F. 131, 133, 181
 Xu, Y.Y. 176, 228
 Xu, Y.Z., see Hu, M.L. 131
 Xu, Z. 239
 Xu, Z.H., see Huang, C.H. 181
 Xue, F., see Wong, W.-K. 303
 Xue, Q.B., see Huang, H.X. 200
 Xue, Z.Q., see Wang, K.Z. 211

 Yakabe, T., see Yasuda, I. 34–36
 Yakushevich, A.N., see Kuzmina, N.P. 234, 235
 Yamada, K., see Tamura, O. 249
 Yamada, M., see Yamada, T. 14
 Yamada, T. 14, 277, 291
 Yamaguchi, F., see Kawa, H. 227, 249, 309

- Yamaguchi, K., see Hanaoka, K. 325
 Yamaguchi, R. 216
 Yamaguchi, T. 240
 Yamaji, K. 21, 22
 Yamaji, K., see Sakai, N. 27, 29, 37, 39
 Yamaji, K., see Xiong, Y. 21, 22
 Yamaji, K., see Xiong, Y.P. 37
 Yamamoto, H. 247
 Yamamoto, H., see Miyachi, M. 17
 Yamamoto, H., see Nishi, T. 17
 Yamamoto, I., see Ohta, K. 119
 Yamamoto, O. 14, 34
 Yamamoto, O., see Mori, M. 29
 Yamamoto, O., see Ukai, Y. 15
 Yamanaka, T., see Hasegawa, Y. 173
 Yamane, H. 240
 Yamato, K., see Takemura, M. 314
 Yan, B. 172, 186, 188
 Yan, C.H., see Xu, G. 141
 Yan, Y.K., see Fu, Y.J. 148, 150
 Yanagida, S. 173
 Yanagida, S., see Hasegawa, Y. 173
 Yanagida, S., see Iwamuro, M. 166, 173
 Yanagida, S., see Kawamura, Y. 214
 Yanagihara, N., see Takemura, M. 314
 Yang, C.Y. 177, 194
 Yang, J. 228, 229
 Yang, J., see Wang, J.F. 211, 212
 Yang, J.G., see Zhu, G.Y. 228
 Yang, K.Y., see Li, H.R. 188
 Yang, K.Z., see Gao, X. 162, 199
 Yang, K.Z., see Liu, H.G. 198
 Yang, K.Z., see Qian, D.J. 198
 Yang, K.Z., see Zhang, R.J. 199, 200
 Yang, K.Z., see Zhong, G.L. 200
 Yang, M.J., see Ling, Q.D. 213
 Yang, M.S., see Tang, B. 192
 Yang, W. 228
 Yang, X. 280
 Yang, X.-P. 289
 Yang, X.A., see Ci, Y.Y. 230
 Yang, X.C. 177
 Yang, X.D. 166, 167, 230
 Yang, X.D., see Ci, Y.X. 230
 Yang, Y.S. 166, 167, 230
 Yang, Y.S., see Li, Y.G. 131, 132
 Yang, Y.S., see Wu, S.L. 166
 Yang, Y.S., see Yao, Y.F. 197
 Yang, Y.T. 166
 Yang, Z., see Qian, G.D. 172, 188
 Yao, G.Q., see Zhao, Y.L. 198
 Yao, G.Q., see Zhou, D.J. 154, 198
 Yao, K.L., see Fang, G. 242
 Yao, Y.F. 197
 Yardley, J.T., see Watson, M.M. 171
 Yarema, K.J., see Lemieux, G.A. 329, 330
 Yasuda, I. 24, 29, 30, 34–36
 Yasuda, I., see Matsuzaki, Y. 17
 Yasuda, T. 38
 Yasuo, T., see Taniguchi, S. 17
 Yasuoka, H., see Wada, E. 249
 Yatmirskii, K.B. 157
 Ye, X.Z., see Xia, W.S. 198
 Yin, M., see Dong, N. 192
 Ylinen, P., see Niinistö, L. 72, 88
 Ylinen, P., see Valkonen, J. 80, 88
 Yokawa, T., see Hanaoka, K. 325
 Yokawa, T., see Kato, H. 326
 Yokokawa, H. 19, 36
 Yokokawa, H., see Horita, T. 39
 Yokokawa, H., see Kawada, T. 36
 Yokokawa, H., see Mori, M. 20
 Yokokawa, H., see Nishiyama, H. 40
 Yokokawa, H., see Sakai, N. 17, 19, 20, 27, 29–35, 37–39
 Yokokawa, H., see Van Hassel, B.A. 25, 26
 Yokokawa, H., see Xiong, Y. 21, 22
 Yokokawa, H., see Xiong, Y.P. 37
 Yokokawa, H., see Yamaji, K. 21, 22
 Yokoyama, M., see Ohta, K. 119
 Yonemitsu, O., see Tsukube, H. 246, 247, 282, 283
 Yoo, H.I., see Kim, J.-H. 21, 22
 Yoshida, H. 244
 Yoshida, H., see Yamada, T. 14
 Yoshida, H., see Zhang, X. 37
 Yoshida, Z., see Tsukube, H. 247
 Yoshikawa, N., see Shibasaki, M. 284
 Yoshino, K., see Ohmori, T. 211
 Yoshino, K., see Ohmori, Y. 211
 Yoshizawa, S., see Tasaki, Y. 145, 147, 239
 You, J.Y., see Yan, B. 188
 You, X.Z., see Chen, X.F. 131, 133, 155, 181, 182
 You, X.Z., see Xiong, R.G. 133, 180, 182
 You, X.Z., see Zeng, X.R. 133, 181, 182
 You, Y.Z., see Chen, X.F. 182
 Young Jr., V.G., see Moser, D.F. 131, 134, 149, 171
 Young Jr., V.G., see Thompson, L.C. 129, 131
 Youngs, D.S., see Morrill, T.C. 224, 247
 Yu, G. 213, 215
 Yu, G., see Li, W. 176
 Yu, G., see Ling, Q.D. 213

- Yu, J.H., see Xu, Q.H. 196
 Yu, J.Q., see Li, W.L. 211, 214
 Yu, J.Q., see Liang, C.J. 211, 214, 215
 Yu, J.Q., see Liu, L. 211, 215
 Yu, L.J. 216
 Yu, W.L., see Pei, J. 194, 213
 Yu, X.J. 166
 Yu, Y., see Li, W.L. 211, 214
 Yu, Y.N., see Zheng, Y.X. 211, 214
 Yu, Z., see Chen, X.F. 133, 181
 Yu, Z., see Xiong, R.G. 182
 Yuan, J. 230
 Yuan, J., see Matsumoto, K. 288
 Yuan, J.C., see Matsumoto, K. 230
 Yuan, J.L. 174
 Yuan, L., see Yang, W. 228
 Yudanova, I.V., see Meshkova, S.B. 173
 Yurchenko, A.G., see Krasutsky, P.A. 225
 Yuste, F., see Ruano, J.L.G. 249

 Zaccheroni, N., see Charbonnière, L.J. 291
 Zaccheroni, N., see Montalti, M. 276
 Zaccheroni, N., see Prodi, L. 291
 Zaia, J., see Wenzel, T.J. 226
 Zaitseva, E.G. 130, 135
 Zaitseva, I.G. 125, 235
 Zaitseva, I.G., see Belova, N.V. 236
 Zaitseva, I.G., see Giricheva, N.I. 235, 236
 Zaitseva, I.G., see Kuzmina, N.P. 234, 235
 Zaitzeva, I.G., see Belova, N.V. 236
 Zalkin, A. 129, 132, 134
 Zama, H. 240
 Zang, F.X., see Hong, Z.R. 214
 Zaniquelli, M.E.D., see Serra, O.A. 198
 Zayskie, R.G., see Stolzenberg, G.E. 226
 Zeizko, V., see Drennan, J. 30
 Zeng, X.R. 133, 181, 182
 Zerger, R.P., see Watson, M.M. 171
 Zha, S.W., see Song, H.Z. 239
 Zhang, C., see McGehee, M.D. 211, 213
 Zhang, C., see Wu, F.B. 230
 Zhang, C.R., see Zhang, R.J. 200
 Zhang, H., see Han, B. 239
 Zhang, H.J., see Fu, L.S. 196
 Zhang, H.J., see Guo, J.F. 188
 Zhang, H.J., see Li, H.R. 188
 Zhang, H.J., see Liang, Y.J. 213
 Zhang, H.J., see Sun, R.G. 214
 Zhang, H.J., see Yan, B. 172, 186
 Zhang, H.J., see Yao, Y.F. 197
 Zhang, H.J., see Zheng, Y.X. 211, 214, 215
 Zhang, H.W., see Liu, H.G. 198
 Zhang, H.W., see Zhang, R.J. 199, 200
 Zhang, J., see Song, H.Z. 239
 Zhang, L., see Wong, W.-K. 303
 Zhang, M.S., see Yao, Y.F. 197
 Zhang, P., see Huang, C.H. 198
 Zhang, Q.J., see Dong, N. 192
 Zhang, R.J. 199, 200
 Zhang, R.J., see Gao, X. 162, 199
 Zhang, S., see De León-Rodríguez, L.M. 330
 Zhang, S., see Woods, M. 298, 322
 Zhang, S.D., see Huang, C.H. 147
 Zhang, W.G., see Ling, Q.D. 213
 Zhang, W.G., see Wang, L.H. 193
 Zhang, W.S., see Liu, H.G. 191
 Zhang, X. 37
 Zhang, X.M. 214
 Zhang, Y.G., see Chen, B.T. 181
 Zhang, Y.X., see Liang, Y.J. 213
 Zhang, Z., see Harrison, W.T.A. 90, 91, 100
 Zhang-Preße, M. 72, 97
 Zhang-Preße, M., see Oppermann, H. 72, 78, 97
 Zhao, D. 211, 214
 Zhao, D., see Hong, Z.R. 214
 Zhao, D., see Liang, C.J. 211, 215
 Zhao, D., see Zhao, D. 211, 214
 Zhao, D., see Zhao, D.X. 213
 Zhao, D.Q., see Liang, C.J. 214
 Zhao, D.X. 213
 Zhao, D.X., see Hong, Z.R. 214
 Zhao, D.X., see Liang, C.J. 211, 215
 Zhao, D.X., see Liu, L. 211, 215
 Zhao, G.W., see Yang, Y.T. 166
 Zhao, X.S. 204
 Zhao, X.S., see Gao, L.H. 162, 198, 204
 Zhao, X.S., see Huang, C.H. 204
 Zhao, X.S., see Li, H. 162, 204
 Zhao, X.S., see Wang, K.Z. 204
 Zhao, X.S., see Zhou, D.J. 204
 Zhao, Y., see Li, W.L. 211, 214
 Zhao, Y.L. 198
 Zhao, Y.L., see Li, H. 204
 Zharinova, E.V., see Kazakov, V.P. 184
 Zharkova, Ya.N. 130
 Zheng, G.Q., see Gao, R.Y. 190, 191
 Zheng, H.X., see Trzaska, S.T. 201
 Zheng, Q.B., see Sun, R.G. 214
 Zheng, Q.B., see Zhang, X.M. 214
 Zheng, Q.T., see Huang, C.H. 147
 Zheng, S.P., see Zhang, R.J. 200
 Zheng, X.J., see Tang, B. 192

- Zheng, Y.X. 211, 214, 215
Zheng, Y.X., see Guo, J.F. 188
Zheng, Z.P. 131, 181
Zheng, Z.P., see Wang, J.F. 211, 212
Zhong, G.L. 200, 211
Zhou, D., see Li, H. 162, 204
Zhou, D., see Pavier, M.A. 200
Zhou, D.J. 154, 155, 198, 204
Zhou, D.J., see Zhao, Y.L. 198
Zhou, H., see Yang, J. 228
Zhou, H.B. 20
Zhou, J.G., see Zhu, W.X. 122, 181
Zhou, Q.F., see Wang, K.Z. 202
Zhou, Q.G., see Liang, F.S. 212, 215
Zhou, Y.F., see Gao, L.H. 162, 204
Zhou, Y.H., see Zheng, Y.X. 211, 215
Zhu, D.B., see Wang, K.Z. 162, 204
Zhu, D.B., see Yu, G. 213, 215
Zhu, G. 229
Zhu, G., see Yang, J. 228, 229
Zhu, G.Y. 228, 229
Zhu, G.Y., see Liu, H.G. 198
Zhu, G.Y., see Si, Z.K. 228
Zhu, G.Y., see Zhang, R.J. 199, 200
Zhu, L.Y., see Tang, B. 192
Zhu, N.J., see Zhu, W.X. 122, 181
Zhu, S.R., see Ciufolini, M.A. 249
Zhu, W.G. 211, 215
Zhu, W.X. 122, 181
Zhu, X.H., see Chen, X.F. 131, 133, 155, 181, 182
Zhu, X.Y., see Huang, C.H. 181, 198
Zhu, Y., see Liu, W.S. 130
Ziessel, R., see Charbonnière, L. 286
Ziessel, R., see Charbonnière, L.J. 291
Ziessel, R., see Montalti, M. 276
Ziessel, R., see Prodi, L. 291
Ziessel, R.F., see Mameri, S. 291
Ziller, J.W., see Evans, W.J. 124, 126, 130–132,
147, 149, 150, 311
Ziller, W.J., see Evans, W.J. 126, 130, 131
Zink, J.I. 179, 182
Zink, J.I., see Hocking, M.B. 179
Zisk, M., see Dickinson, P.H. 240
Zizelman, J., see Mukerjee, S. 12
Zolin, V., see Tsaryuk, V. 161, 176, 211
Zomlefer, K., see Wenzel, T.J. 314
Zou, D.C., see Zhu, W.G. 211, 215
Zou, H., see Yang, J. 228
Zucchi, G. 286, 292, 293
Zuo, C.S. 326
Zuo, J.L., see Xiong, R.G. 182
Zurbano, M., see Barbera, J. 119

SUBJECT INDEX

- 1,4,7-triazacyclononane 286
2-thenoyltrifluoroacetone 244
2nd coordination sphere 326
2nd-sphere water 319
- α -[Ce(acac)₄] 141
absolute quantum yields 169
acetylacetonate 275
achiral shift reagents 221
acidic oxo-selenates
– mixed valent acidic selenates 56
acidic oxo-selenates(IV) 73
acidic oxo-selenates(VI)
– hydrogen selenate-diselenates 55
– hydrogen selenates 55
– hydroselenate-selenates 55
– ternary selenate-hydroselenate 60
acylpyrazoles 245
adamantylideneadamantane-1,2-dioxetane 183
adducts of [R(dbm)₃] 122
[Ag(fod)] 225
aggregation behavior in solution 158
aggregation state 144
[Ag(tfac)] 225
amino alcohol 279
aminostyrylpyridinium 203
anhydrous oxo-selenates(VI) 48
anhydrous tris acetylacetonate complexes 123, 124
anion carriers 246
anion sensing 232
anion-selective electrode 281
antenna effect 163
antiferromagnetic coupling 159
atomic layer deposition 241
- β -diketonates in polymer matrices 190
 β -diketonates in zeolites 195
 β -diketone ligands 113
 β -[Ce(acac)₄] 141
 β -diketones
– acidity 119
– keto–enol tautomerism 118
– synthesis 119
(Ba, La)CoO₃ 15
Ba(Ce,M)O_{3- δ} 14
back transfer 165
benzoylacetone 244
bicapped trigonal prism 129
binary oxo-selenates(IV) 65
binary rare earth oxo-selenates
– syntheses 66
bridging ligands 139
- Ca_{1-x}Sr_xMnO₃ 34
catalytic properties 247
CD 277
Ce_{0.8}Sm_{0.2}O_{1.9}
– mechanical strength 30
Ce_{1-x}Gd_xO_{2-x/2} 239
Ce₂(SeO₃)₃ 67, 70
Ce₂(SeO₄)₃·5H₂O 50
[Ce(acac)₃(H₂O)₂] 141
[Ce(acac)₃(phen)] 130
[Ce(acac)₄] 141, 157, 159
[Ce(acac)₄]·10H₂O 142
CeF₃ 239
[Ce(fdh)₄] 146, 236
[Ce(fdh)₄(phen)] 146, 236
[Ce(fod)₄] 146
[Ce(hfac)₃(diglyme)] 130
CeO₂ 15, 239, 241
{(CeO₂)_x(ZrO₂)_{1-x}}_{0.8}(YO_{1.5})_{0.2} 37
Ce(SeO₃)₂ 69, 70
Ce(SeO₄)₂ 48–50
[Ce(thd)₃] 238, 243
[Ce(thd)₃(dme)] 146
[Ce(thd)₃(phen)] 236
[Ce(thd)₃(tmeda)] 146
[Ce(thd)₃(triglyme)] 146
[Ce(thd)₄] 146, 157, 235, 236, 239
[Ce(tmp)₃] 146, 236
[Ce(tod)₄] 146, 157
[Ce(tta)₃(H₂O)₂] 146
[Ce(tta)₄]⁻(isoquinolinium) 133

- chelates for lasers 205
 chemical sensors 232
 chemical vapor deposition 238
 chemiluminescence 163, 183
 chiral NMR shift reagents 226, 308
 chiral recognition 283
 chirality sensing 161, 301, 302, 305, 306, 312
 chloride-selenites 81
 circular dichroism 161, 277, 301
 circularly polarized emission 177
 circularly polarized luminescence 177, 277, 306
 co-luminescence 176
 CoLaCl(SeO₃)₂ 90
 CoNd₁₀Cl₁₂(SeO₃)₈ 90
 CoNd₁₀Cl₈(SeO₃)₁₂ 93
 contact shift 308
 CoRCl(SeO₃)₂ 92
 CoSmCl(SeO₃)₁ 90
 CoTbCl(SeO₃)₂ 90
 CPL 177, 277, 306
 crown ether 314
 crystal-field splittings 160
 crystallographic data of anionic oxo-selenate(IV) derivatives 80
 crystallographic data of binary oxo-selenates(VI) 50
 crystallographic data of cationic oxo-selenate(IV) derivatives 90
 crystallographic data of oxo-selenites in the systems R₂O₃/SeO₂ 70
 crystallographic data of ternary oxo-selenates(VI) 58
 CsEu₄O₃Cl₃(SeO₃)₂ 89, 90
 Cs[Eu(hfac)₄] 136
 CsNd(SeO₄)₂·4H₂O 58, 60
 CsSm₂₁Br₁₆(SeO₃)₂₄ 89, 90
 CsTmCl₂(SeO₃) 89, 90
 Cs[Y(hfac)₄] 234
 Cu₃ErO₂Cl(SeO₃)₂ 85, 90
 CuEu₂(SeO₃)₄ 90
 CuGd₂(SeO₃)₄ 90
 CuGdCl(SeO₃)₂ 90, 93
 CuLa₂(SeO₃)₄ 90
 CuNd₂(SeO₃)₄ 90
 CuR₂(SeO₃)₄ 91
 CuSm₂(SeO₃)₄ 90
 cyclodextrins 127, 314, 326
 CYTOP 190
 decomposition of binary selenate-hydrates 62
 decomposition of selenite hydrates 94
 decomposition of ternary selenate-hydrates 62
 DELFIA 229
 dendrimers 326, 327
 derivatives of oxo-selenates(IV) 77
 – cationic derivatives 88
 – derivatives with complex anions 88
 – halide-oxo-selenates 81
 – oxide-halide oxo-selenates 84
 determination of enantiomer excess 309, 313
 di-ureasil gels 189
 diaza-18-crown-6 298
 dipicolinic acid 286
 dipolar shift 308
 diselenite-nitrates 88
 Dy₂O₃ 239
 Dy₂O(SeO₃)₂ 70
 Dy₂(SeO₃)₃ 70
 Dy₃F(SeO₃)₄ 80
 Dy₃O₂Cl(SeO₃)₂ 80
 [Dy(acac)₃] 123
 [Dy(fod)₃] 151
 [Dy(fod)₃(bipy)]·2H₂O 151
 [Dy(fod)₃(H₂O)] 151
 [Dy(hfac)₄][−](triethylammonium) 156
 [Dy(pta)₃] 151
 [Dy(thd)₃] 151, 236
 [{Dy(thd)₃}₂(heptaglyme)] 151
 [{Dy(thd)₃}₂(triglyme)] 151
 [Dy(thd)₃(H₂O)] 132, 135
 [Dy(thd)₃(phtthalazine)] 151
 [Dy(thd)₃(py)] 151
 [Dy(thd)₃(pyr)] 151
 [Dy(trimh)₃] 151
 [Dy(tta)₃] 151
 [Dy(tta)₃(phen)] 151
 eight-coordinate complexes 128, 135
 electrical conductivity 24
 electrochemical properties 158
 electroluminescence 163, 178
 emission anisotropy factor 177
 enantioselective extraction 283
 energy transfer 163, 285, 291, 295, 298
 EPA solution 165
 Er₂O₃ 239
 Er₂O(SeO₃)₂ 70
 Er₂(SeO₃)₂(SeO₄)·2H₂O 99
 Er₂(SeO₃)₃ 70
 Er₂(SeO₄)₃ 49
 Er₂(SeO₄)₃·8H₂O-II 50
 Er₃O₂Cl(SeO₃)₂ 80, 85
 Er₄O₃Cl₂(SeO₃)₂ 80

- [Er(acac)₃] 123
 [Er(acac)₃(H₂O)₂] 132
 [Er(acac)₃(phen)] 152, 214
 ErCl(SeO₃) 80, 81
 [Er(fod)₃] 152, 153
 [Er(fod)₃(bipy)]·2H₂O 152
 [Er(fod)₃(H₂O)] 152
 [Er(hfac)₂(μ-OCH₃)(bipy)]₂ 125
 [Er(hfac)₂(μ-OCH₃)(phen)]₂ 125
 [Er(hfac)₃(bipy)] 125, 137
 [Er(hfac)₃(phen)] 125, 132
 [Er(hfac)₄]⁻(triethylammonium) 156
 [Er(pta)₃] 152
 [Er(thd)₃] 132, 139, 152, 236, 237
 [{Er(thd)₃]₂(tetraglyme)] 139, 152
 [{Er(thd)₃]₂(triglyme)] 152
 [Er(thd)₃(diglyme)₂] 152
 [Er(thd)₃(dme)] 152
 [Er(thd)₃(dmf)] 152
 [Er(thd)₃(H₂O)]_n 152
 [Er(thd)₃(phthalazine)] 152
 [Er(thd)₃(pivalic acid)] 132
 [Er(thd)₃(py)] 152
 [Er(thd)₃(pyr)] 152
 [Er(trimh)₃] 152
 [Er(tta)₃] 152
 (Et₃NH)⁺[Eu(dbm)₄]⁻ 179
 (Et₄N)[Eu(dbm)₄] 161
 [Eu₂(acac-F₇)₄(OAc)₂]²⁻[bipyH]₂⁺ 125
 Eu₂O₃ 239
 Eu₂O₃-doped Y₂O₃ 239
 Eu₂O(SeO₃)₂ 70
 [Eu₂(phen)₂(acac-F₇)₂(μ-OCOCF₃)₄] 125
 Eu₂(SeO₃)₃ 70
 Eu₂(SeO₄)₃·8H₂O-I 50
 [Eu₄(phen)₄(acac-F₇)₄(μ³-F)₄(μ-F)₂(μ-OCOCF₃)₂] 125
 [Eu(acac-F₇)₃(HOAc)₃] 125
 [Eu(acac-F₇)₃(tppo)₂] 125, 131
 [Eu(acac)₃] 123, 153, 156
 [Eu(acac)₃] (amorphous) 148
 [Eu(acac)₃] (crystalline) 148
 [Eu(acac)₃(bipy)] 148
 [Eu(acac)₃(distyphen)] 148
 [Eu(acac)₃(H₂O)₂] 148, 161, 186
 [Eu(acac)₃(phen)] 131, 136, 148, 186, 213
 [Eu(acac)₄]⁻K⁺ 154
 [Eu(acac)₄]⁻Na⁺ 154
 [Eu(btfac)₃(bipy)] 131, 148
 [Eu(btfac)₃(H₂O)₂] 126, 131, 148, 172, 188
 [Eu(btfac)₃(phen)] 148
 [Eu(btfac)₃(phenNO)] 172
 [Eu(btfac)₃(tppo)₂] 131, 148
 [Eu(btfac)₄]⁻(2-hydroxyethylammonium) 154
 [Eu(btfac)₄]⁻(benzylammonium) 154
 [Eu(btfac)₄]⁻(dibenzylammonium) 154
 [Eu(btfac)₄]⁻(diethylammonium) 154
 [Eu(btfac)₄]⁻(isoquinolinium) 154
 [Eu(btfac)₄]⁻(*n*-butylammonium) 154
 [Eu(btfac)₄]⁻(piperidinium) 154
 [Eu(btfac)₄]⁻(pyridinium) 154
 [Eu(btfac)₄]⁻(quinolinium) 154
 [Eu(btfac)₄]⁻(tetra-*n*-butylammonium) 154
 [Eu(btfac)₄]⁻(tetra-*n*-propylammonium) 154
 [Eu(btfac)₄]⁻(tetraethylammonium) 154
 [Eu(btfac)₄]⁻(tetramethylammonium) 154
 [Eu(btfac)₄]⁻(tetramethylguanidium) 154
 [Eu(btfac)₄]⁻(triethylammonium) 154
 [Eu(bzac)₃(bipy)] 134, 148
 [Eu(bzac)₃(H₂O)₂] 148, 172, 186
 [Eu(bzac)₃(phen)] 148, 172, 175, 186, 213
 [Eu(bzac)₃(phenNO)] 172
 [Eu(bzac)₄]⁻Na⁺ 154
 [Eu(bzac)₄]⁻(piperidinium) 133, 154
 [Eu(bzac)₄]⁻(tetrapropylammonium) 154
 [Eu(dbm)₃] 126, 191
 [Eu(dbm)₃(1,4-dioxane)₂] 148
 [Eu(dbm)₃(4,7-dimethylphenanthroline)] 148
 [Eu(dbm)₃(aniline)] 148
 [Eu(dbm)₃(bath)] 148
 [Eu(dbm)₃(bipy)] 148
 [Eu(dbm)₃(bipy)](Hdbm) 123
 [Eu(dbm)₃(dmbp)](H₂O) 131
 [Eu(dbm)₃(dmf)] 148
 [Eu(dbm)₃(dmop)] 131
 [Eu(dbm)₃(dmsO)₃] 148
 [Eu(dbm)₃(H₂O)] 161
 [Eu(dbm)₃(*n*-butylamine)₂] 148
 [Eu(dbm)₃(opb)] 149, 211
 [Eu(dbm)₃(phen)] 131, 148, 149, 172, 175, 186, 191, 206, 210, 213
 [Eu(dbm)₃(pip)] 159
 [Eu(dbm)₃(piperidine)₂] 149
 [Eu(dbm)₃(piphen)] 211
 [Eu(dbm)₃(py)₂] 149
 [Eu(dbm)₃(pyO)] 149
 [Eu(dbm)₃(quinoline)₂] 149
 [Eu(dbm)₃(terpy)] 131
 [Eu(dbm)₃(topo)] 129
 [Eu(dbm)₄]⁻(azabicyclononane ion) 155
 [Eu(dbm)₄]⁻Cs⁺ 154

- [Eu(dbm)₄]⁻ (diethylammonium) 154
 [Eu(dbm)₄]⁻ (dimethylbenzylammonium) 133
 [Eu(dbm)₄]⁻ (hexadecyltrimethylammonium) 154
 [Eu(dbm)₄]⁻ (imidazolium) 133
 [Eu(dbm)₄]⁻ K⁺ 154
 [Eu(dbm)₄]⁻ (morpholinium) 133
 [Eu(dbm)₄]⁻ (*N*-hexadecylpyridinium) 155
 [Eu(dbm)₄]⁻ Na⁺ 154
 [Eu(dbm)₄]⁻ (octadecyltriethylammonium) 154
 [Eu(dbm)₄]⁻ (piperidinium) 155
 [Eu(dbm)₄]⁻ Rb⁺ 154
 [Eu(dbm)₄]⁻ (tetraethylammonium) 154
 [Eu(dbm)₄]⁻ (tetrahexylammonium) 155
 [Eu(dbm)₄]⁻ (tetramethylammonium) 154
 [Eu(dbm)₄]⁻ (tetrapropylammonium) 154
 [Eu(dbm)₄]⁻ (triethylammonium) 133, 154
 [Eu(dbp)₄]⁻ (tetraethylammonium) 155
 [Eu(dbp)₄]⁻ (triethylammonium) 155
 [Eu(dmbm)₃(phen)] 172, 175
 [Eu(dmh)₃(bipy)] 131, 149
 [Eu(dmh)₃(phen)] 131
 [Eu(dnm)₃(phen)] 149, 177, 194, 213
 [Eu(dnm)₃(pip)] 159
 [Eu(dppm)₃] 249
 [Eu(dtp)₄]⁻ (piperidinium) 155
 [Eu(facam)₃] 177
 [EuF(hfac)₃K(diglyme)]₂ 126
 [Eu(fod)₃] 122, 149, 158, 184, 220, 232, 233, 247, 248
 [Eu(fod)₃(4-picO)] 149
 [Eu(fod)₃(bipy)] 122, 149
 [Eu(fod)₃(bipy)]·2H₂O 149
 [Eu(fod)₃(dmsO)] 122, 149
 [Eu(fod)₃(H₂O)] 149
 [Eu(fod)₃(H₂O)₂] 131, 188
 [Eu(fod)₃(phen)] 122, 149
 [Eu(fod)₃(py)₂] 149
 [Eu(fod)₃(tppo)₂] 149
 [Eu(hfac)₃] 149, 156, 218
 [Eu(hfac)₃]·2H₂O 149
 [Eu(hfac)₃(bipy)(H₂O)] 131, 135
 [Eu(hfac)₃(dhso)₂] 149
 [Eu(hfac)₃(diglyme)] 126, 131, 149, 172, 175, 239
 [Eu(hfac)₃(dme)] 149
 [Eu(hfac)₃(monoglyme)] 172, 175
 [Eu(hfac)₃(phen)] 149
 [Eu(hfac)₃(terpy)] 149
 [Eu(hfac)₃(topo)₂] 149
 [Eu(hfac)₃(tppo)₂] 131
 [Eu(hfac)₄]⁻ (2,4,6-collidinium) 155
 [Eu(hfac)₄]⁻ (2,6-lutidinium) 155
 [Eu(hfac)₄]⁻ Cs⁺ 133
 [Eu(hfac)₄]⁻ (*N*-methylphenazinium) 155
 [Eu(hfac)₄]⁻ (*N*-methylquinolinium) 155
 [Eu(hfac)₄]⁻ (piperazinium) 155
 [Eu(hfac)₄]⁻ (pyridinium) 155
 [Eu(hfac)₄]⁻ (tetraethylammonium) 155
 [Eu(hfac)₄]⁻ (tetramethylammonium) 155
 [Eu(hfac)₄]⁻ (triethylammonium) 155
 Eu(HSeO₄)(SeO₄) 50, 55
 [Eu(mdbm)₃(phen)] 172, 175
 [Eu(mfa)₃(phen)] 172, 175
 [Eu(mhd)₃(phen)] 149
 [Eu(NO₃)(tta)₂(tppo)₂] 122
 [Eu(nta)₄]⁻ (*N*-hexadecylpyridinium) 155
 [Eu(ntac)₃(bipy)] 129, 131
 [Eu(ntac)₃(bipy)]·0.5(2-propanol) 131
 [Eu(pta)₃] 149
 [Eu(ptp)₄]⁻ (tetrapropylammonium) 155
 europium tris(β -diketonate) 279, 296, 309
 europium(III) β -diketonate complexes in OLEDs 215
 [Eu(tbp)₄]⁻ (2,4,6-trimethylpyridinium) 155
 [Eu(tbp)₄]⁻ (isoquinolinium) 155
 [Eu(tfa)₄]⁻ (isoquinolinium) 155
 [Eu(tfac)₃(dhso)₂] 149
 [Eu(tfac)₃(tbp)₂] 149
 [Eu(tfac)₃(topo)₂] 149
 [Eu(thd)₂(dme)₂] 126
 [Eu(thd)₃] 149, 219, 236
 [{Eu(thd)₃}₂(tetraglyme)] 149
 [{Eu(thd)₃}₂(triglyme)] 139, 150
 [Eu(thd)₃(bipy)] 131
 [Eu(thd)₃(dme)] 149
 [Eu(thd)₃(dmf)₂] 131
 [Eu(thd)₃(monoglyme)] 131
 [Eu(thd)₃(phen)] 131, 149
 [Eu(thd)₃(py)] 149
 [Eu(thd)₃(py)₂] 131
 [Eu(thd)₃(pyr)] 149
 [Eu(thd)₃(terpy)] 129
 [Eu(thd)₃(topo)₂] 150
 [Eu(tnb)₄]⁻ (isoquinolinium) 155
 [Eu(tpb)₃(phen)] 149
 [Eu(trimh)₃] 150
 [Eu(tta)₂(tppo)₂(NO₃)] 122
 [Eu(tta)₃] 150, 210, 218
 [Eu(tta)₃] 228
 [Eu(tta)₃(4-picO)₂] 150
 [Eu(tta)₃(5-phenyl-phen)] 181
 [Eu(tta)₃(bath)] 181
 [Eu(tta)₃(bipy)] 131, 150, 188, 189

- [Eu(tta)₃(bmbp)] 131
 [Eu(tta)₃(dbzso)₂] 172, 175
 [Eu(tta)₃(dmsO)₂] 172
 [Eu(tta)₃(dppz)] 211
 [Eu(tta)₃(H₂O)₂] 131, 136, 172, 175, 186, 216
 [Eu(tta)₃(opb)] 150, 175
 [Eu(tta)₃(pha)₂] 175
 [Eu(tta)₃(phen)] 126, 131, 150, 172, 181, 185, 188, 189, 199, 203, 216, 229, 232
 [Eu(tta)₃(ptso)₂] 172, 175
 [Eu(tta)₃(terpy)] 150
 [Eu(tta)₃(topo)₂] 200
 [Eu(tta)₃(topo)₂] 228
 [Eu(tta)₃(tppo)₂] 122, 131, 150, 175, 188
 [Eu(tta)₄][−](1,2-dimethylpyridinium) 155
 [Eu(tta)₄][−](1,4-dimethylpyridinium) 133
 [Eu(tta)₄][−](2,4,6-collidinium) 155
 [Eu(tta)₄][−](2,4,6-trimethylpyridinium) 155
 [Eu(tta)₄][−](4-aminopyridinium) 155
 [Eu(tta)₄][−](isoquinolinium) 155
 [Eu(tta)₄][−](*N*-methylisoquinolinium) 155
 [Eu(tta)₄][−](tetrahexylammonium) 155
 [Eu(tta)₄][−](tetrapropylammonium) 155
 [Eu(tta)₄][−](triethylammonium) 155
 exciton coupled CD 305
 extraction 283, 304
 – enantioselective 283

 f–f intensities 161
 ferromagnetic coupling 159
 fluorescence 162
 [(fod)₃R(OH₂)R(fod)₃] 158
 fractoluminescence 179
 Franck–Condon 286
 fuel additives 242

 gadolinium doped ceria
 – mechanical strength 30
 gadolinium doped ceria (Ce_{1−x}Gd_xO_{2−δ}) 14
 gadolinium doped ceria (GDC)
 – oxide ion conductivity 21
 gas chromatographic separation of the rare earths 237
 gas-phase electron-diffraction 235
 Gd₂O₃ 239
 Gd₂O₃-doped CeO₂ 239
 Gd₂O(SeO₃)₂ 70
 Gd₂(SeO₃)₃ 70
 Gd₂(SeO₄)₃·4H₂O 55
 Gd₂(SeO₄)₃·4H₂O-II 50
 Gd₂(SeO₄)₃·8H₂O-I 50

 Gd₃F(SeO₃)₄ 80
 Gd₅O₄Br₃(SeO₃)₂ 80
 Gd₉O₈Cl₃(SeO₃)₄ 80
 [Gd(acac)₃] 123
 [Gd(acac)₃(dme)] 150
 [Gd(acac)₃(H₂O)₂] 131
 [Gd(acac)₃(phen)] 150
 [Gd(bzac)₃(H₂O)₂] 150
 GDC 22
 [Gd(dbm)₄][−](piperidinium) 155
 GdF₃ 239
 [Gd(fod)₃] 150
 [Gd(fod)₃(bipy)]·2H₂O 150
 [Gd(fod)₃(H₂O)] 150
 [Gd(hfac)₃{Cu(salen)}] 132
 [Gd(hfac)₃(diglyme)] 131
 [Gd(hfac)₃(H₂O)(acetone)] 132
 [Gd(hfac)₄][−](triethylammonium) 155
 Gd(HSeO₄)(SeO₄) 50, 55
 [Gd(pta)₃] 150
 [Gd(thd)₃] 150, 235, 236
 [{Gd(thd)₃]₂(heptaglyme)] 139, 150
 [{Gd(thd)₃]₂(hmteta)] 150
 [{Gd(thd)₃]₂(tetraglyme)] 139, 150
 [{Gd(thd)₃]₂(triglyme)] 150
 [Gd(thd)₃(diglyme)₂] 150
 [Gd(thd)₃(monoglyme)] 132
 [Gd(thd)₃(phthalazine)] 150
 [Gd(thd)₃(py)] 150
 [Gd(thd)₃(pyr)] 150
 [Gd(trimh)₃] 150
 [Gd(tta)₃] 150
 [Gd(tta)₃·2H₂O] 150
 [Gd(tta)₃(tppo)₂] 132
 geometrical isomers 129
 glass-forming solvents 171, 206

 (H₃O)Ce₂(SeO₄)₄ 56
 H₃OCe^{III}Ce^{IV}(SeO₄)₄ 50
 (H₃O)Nd(SeO₃)(HSeO₃)(ClO₄) 80, 88
 (H₅O₂)Sc(SeO₄)₂ 50, 56
 heat capacity 31, 32
 helicates 158
 hemicyanine 203
 hemicyanine dyes with β-diketonate counter ions 162
 heptadentate cyclen
 – Eu³⁺ complexes 294
 – Gd³⁺ complex 315, 321
 – Tb³⁺ complex 294
 – Yb³⁺ complex 293, 294, 315
 heptafluoroacetylacetone 125

- heterodinuclear d-f complexes 174
 heteropolynuclear d-f complexes 127
 hexafluoroacetylacetone 244
 highly-symmetric complexes 129
 $\text{Ho}_2\text{O}(\text{SeO}_3)_2$ 70
 $\text{Ho}_2(\text{SeO}_3)_3$ 70
 $\text{Ho}_2(\text{SeO}_4)_3 \cdot 8\text{H}_2\text{O}$ -II 50
 $[\text{Ho}(\text{acac})_3]$ 123
 $[\text{Ho}(\text{acac})_3(\text{H}_2\text{O})_2] \cdot \text{H}_2\text{O}$ 132
 $[\text{Ho}(\text{acac})_3(\text{H}_2\text{O})_2] \cdot \text{H}_2\text{O} \cdot (\text{Hacac})$ 132
 $\text{HoCl}(\text{SeO}_3)$ 80, 81
 $[\text{Ho}(\text{dbm})_3(\text{dmop})]$ 132
 $[\text{Ho}(\text{dbm})_3(\text{H}_2\text{O})]$ 129, 132
 $[\text{Ho}(\text{fod})_3]$ 151
 $[\text{Ho}(\text{fod})_3(\text{bipy})] \cdot 2\text{H}_2\text{O}$ 151
 $[\text{Ho}(\text{fod})_3(\text{H}_2\text{O})]$ 151
 $[\{\text{Ho}(\text{hfac})_3\}_2(\text{tetraglyme})]$ 151
 $[\text{Ho}(\text{hfac})_3(\text{H}_2\text{O})_2]$ 132, 141, 151
 $[\text{Ho}(\text{hfac})_3(\text{H}_2\text{O})_2] \cdot \text{triglyme}$ 151
 $[\text{Ho}(\text{hfac})_3(\text{H}_2\text{O})_2](\text{triglyme})$ 132, 141
 $[\text{Ho}(\text{hfac})_3(\text{phen})]$ 137
 $[\text{Ho}(\text{hfac})_4]^-$ (triethylammonium) 156
 hole and oxide ion conductivity 26
 $[\{\text{Ho}(\text{tfac})_3\}_2(\text{hmteta})]$ 151
 $[\text{Ho}(\text{thd})_3]$ 151, 159, 236, 237
 $[\{\text{Ho}(\text{thd})_3\}_2(\text{triglyme})]$ 151
 $[\text{Ho}(\text{thd})_3(4\text{-pic})_2]$ 132
 $[\text{Ho}(\text{thd})_3(\text{dmf})]$ 151
 $[\text{Ho}(\text{thd})_3(\text{phthalazine})]$ 151
 $[\text{Ho}(\text{thd})_3(\text{pivalic acid})]$ 132
 $[\text{Ho}(\text{thd})_3(\text{py})]$ 151
 $[\text{Ho}(\text{thd})_3(\text{pyr})]$ 151
 $[\text{Ho}(\text{trimh})_3]$ 152
 $[\text{Ho}(\text{tta})_3]$ 152
 hydrolysis products 153
 hyper-Rayleigh scattering 204
 hyperpolarizability 203
 hypersensitive transitions 157

 inclusion compounds 127
 indium tin oxide 207
 infrared spectra 161
 inner coordination sphere 286
 inner-sphere water 319
 intensity ratios 175, 176
 internal conversion 163
 intersystem crossing 163
 intramolecular energy transfer 163
 ion-selective electrode 281
 ionic radius 276, 279, 280, 283, 289, 303

 $\text{KDy}(\text{SeO}_4)_2$ 57, 58
 $\text{KER}(\text{SeO}_4)_2 \cdot \text{H}_2\text{O}$ 58, 59
 $\text{K}[\text{Eu}(\text{tta})_4]$ 213
 kinetic stability 156
 $\text{KPr}(\text{SeO}_4)_2$ 58

 $(\text{La}, \text{Ca})(\text{Cr}, \text{Co})\text{O}_3$ 20
 $(\text{La}, \text{Ca})(\text{Cr}, \text{Ni})\text{O}_3$ 20
 $(\text{La}, \text{Ca})\text{CrO}_3$ 19
 – diffusivity 39
 $(\text{La}, \text{Ca})\text{MnO}_3$ 15
 $(\text{La}, \text{Sr})(\text{Co}, \text{Fe})\text{O}_3$ 7
 $(\text{La}, \text{Sr})\text{CoO}_3$ 15
 $(\text{La}, \text{Sr})(\text{Fe}, \text{Co})\text{O}_3$ 16
 $(\text{La}, \text{Sr})(\text{Ga}, \text{Mg}, \text{Co})\text{O}_{3-\delta}$ (LSGMC) 19
 $(\text{La}, \text{Sr})(\text{Ga}, \text{Mg})_3$ (LSGM)
 – oxide ion conductivity 21
 $(\text{La}, \text{Sr})(\text{Ga}, \text{Mg})\text{O}_{3-\delta}$ (LSGM) 19
 $(\text{La}, \text{Sr})\text{MnO}_3$ 7, 15
 – thermal expansion coefficients 34
 $(\text{La}, \text{Pr})_{0.7}(\text{Ca}, \text{Sr})_{0.3}\text{MnO}_3$ 239
 $(\text{La}, \text{Sr})(\text{Ga}, \text{Mg}, \text{Co})\text{O}_3$ 13
 $(\text{La}, \text{Sr})(\text{Ga}, \text{Mg})\text{O}_3$ 13
 $(\text{La}, \text{Sr})(\text{Ti}, \text{Ce})\text{O}_3$ 15
 $\text{La}_{0.5}\text{Sr}_{0.5}\text{CoO}_3$
 – electrical conductivity 23
 $\text{La}_{0.75}\text{Ca}_{0.25}\text{CrO}_3$
 – oxygen permeation flux 27–29
 $\text{La}_{0.75}\text{Ca}_{0.25}\text{CrO}_{3-\delta}$ 29
 $\text{La}_{0.7}\text{Ca}_{0.3}\text{CrO}_3$ 25
 – mechanical strength 30
 $\text{La}_{0.7}\text{Ca}_{0.3}\text{CrO}_{3-6}$
 – hole and oxide ion conductivity 25
 $\text{La}_{0.7}\text{Sr}_{0.3}\text{CrO}_3$
 – mechanical strength 30
 $\text{La}_{0.8}\text{Ca}_{0.25}\text{CrO}_{3-\delta}$ 27
 $\text{La}_{0.8}\text{Sr}_{0.2}\text{MnO}_3$
 – electrical conductivity 23
 $\text{La}_{0.9}\text{Ca}_{0.1}\text{CrO}_3$ 25
 – oxygen permeation flux 27, 29
 $\text{La}_{0.9}\text{Ca}_{0.1}\text{CrO}_{3-\delta}$
 – hole and oxide ion conductivity 25, 26
 $\text{La}_{1-x}\text{Ca}_x\text{CrO}_3$
 – electrical conductivity 24
 – heat capacity 31
 – mean free path of phonon 33
 – thermal conductivity 32, 33
 – thermal diffusivity 30, 31
 $\text{La}_{1-x}\text{Ca}_x\text{CrO}_{3-\delta}$ 26, 39
 $\text{La}_{1-x}\text{Sr}_x\text{CoO}_3$
 – heat capacity 32
 $\text{La}_{1-x}\text{Sr}_x\text{Cr}_{1-y}\text{Co}_y\text{O}_3$

- mechanical strength 30
- $\text{La}_{1-x}\text{Sr}_x\text{Cr}_{1-y}\text{RuO}_{3-\delta}$ 15
- $\text{La}_{1-x}\text{Sr}_x\text{CrO}_3$
 - electrical conductivity 24
- La_2O_3 20, 239, 241
- La_2S_3 242
- $\text{La}_2(\text{SeO}_3)_3$ 67, 70
- $\text{La}_2(\text{SeO}_4)_3 \cdot 12\text{H}_2\text{O}$ 50, 52
- $\text{La}_2(\text{SeO}_4)_3 \cdot 5\text{H}_2\text{O}$ 50
- $\text{La}_2\text{Zr}_2\text{O}_7$ 15, 24, 36
- $\text{La}_6\text{O}_8\text{Br}_3(\text{SeO}_3)_4$ 80
- $[\text{La}(\text{acac})_3]$ 123, 145, 159
- $[\text{La}(\text{acac})_3(\text{H}_2\text{O})_2]$ 130
- $[\text{La}(\text{acac})_3(\text{phen})]$ 130, 145
- $[\text{La}(\text{acac})_3(\text{tetraglyme})]$ 145
- LaAlO_3 239
- $[\text{La}(\text{bzac})_3]$ 159
- $[\text{La}(\text{bzac})_3(\text{H}_2\text{O})_2]$ 145
- LaCoO_3 242
 - heat capacity 32
- $\text{LaCr}_{1-x}\text{Mg}_x\text{O}_3$
 - electrical conductivity 24
- (LaCrO_3) 16
- LaCrO_3 31
 - electric conductivity 25
 - thermal expansion coefficients 34
- $[\text{La}(\text{dbm})_3]$ 146
- $[\text{La}(\text{dbm})_3(\text{dmop})]$ 130
- $[\text{La}(\text{dbp})_4]^-$ (triethylammonium) 154
- $[\text{La}(\text{dipydike})_3]_2$ 130, 136
- LaF_3 239
- $[\text{La}(\text{facam})_3]$ 146
- $[\text{La}(\text{fod})_3]$ 146
- $[\text{La}(\text{fod})_3(\text{bipy})] \cdot 2\text{H}_2\text{O}$ 146
- $[\text{La}(\text{fod})_3(\text{H}_2\text{O})]$ 146
- $[\text{La}(\text{fod})_3(\text{phen})]$ 146
- $\text{LaF}(\text{SeO}_3)$ 80, 83
- LaGaO_3 242
- $[\text{La}(\text{hfac})_3]$ 146
- $[\{\text{La}(\text{hfac})_3\}_2(\text{heptaglyme})]$ 146
- $[\text{La}(\text{hfac})_3] \cdot 2\text{H}_2\text{O}$ 146
- $[\text{La}(\text{hfac})_3(\text{bipy})_2]$ 130, 136
- $[\text{La}(\text{hfac})_3(\text{diglyme})]$ 130, 146
- $[\text{La}(\text{hfac})_3(\text{H}_2\text{O})\{\text{Cu}(\text{salen})\}]$ 130
- $[\text{La}(\text{hfac})_3(\text{monoglyme})]$ 130
- $[\text{La}(\text{hfac})_3(\text{phen})_2]$ 136
- $[\text{La}(\text{hfac})_3(\text{triglyme})]$ 130, 146
- $[\text{La}(\text{hfac})_4]^-$ (2,6-lutidinium) 154
- $[\text{La}(\text{hfac})_4]^-$ (triethylammonium) 154
- $\text{La}(\text{HSeO}_3)(\text{SeO}_4) \cdot 2\text{H}_2\text{O}$ 100
- $\text{La}(\text{HSeO}_4)_3$ 50, 55
- LaMnO_3
 - heat capacity 32
 - thermal conductivity 32, 33
 - thermal diffusivity 30, 31
- Langmuir-Blodgett films 197
- LaNiO_3 239, 240
- lanthanide shift reagents 219
- lanthanide-induced shifts 308
- lanthanum gallate based oxides (LSGM) 13
 - thermal expansion coefficients 34
- $\text{La}(\text{OH})_3$ 20
- LaSrGaO_4 19
- $[\text{La}(\text{tfac})_3]$ 146
- $[\text{La}(\text{tfac})_3] \cdot 2\text{H}_2\text{O}$ 146
- $[\text{La}(\text{thd})_3]$ 146, 159, 236, 237, 241, 242
- $[\text{La}(\text{thd})_3(\text{phthalazine})]$ 146
- $[\text{La}(\text{thd})_3(\text{pyr})]$ 146
- $[\text{La}(\text{thd})_3(\text{tetraglyme})]$ 146
- $[\text{La}(\text{thd})_3(\text{triglyme})]$ 146
- $[\text{La}(\text{tod})_3]$ 146
- $[\text{La}(\text{tod})_3] \cdot 2\text{H}_2\text{O}$ 146
- $[\text{La}(\text{tta})_3]$ 146
- $[\text{La}(\text{tta})_3] \cdot 2\text{H}_2\text{O}$ 146
- $[\text{La}(\text{tta})_3(\text{phen})]$ 146
- $[\text{La}(\text{tta})_4]^-$ (quinolinium) 133
- $[\text{La}(\text{tta})_4]^-$ (triethylammonium) 154
- Lewis bases 119
- $\text{Li}_3\text{Lu}_5(\text{SeO}_3)_9$ 89, 90
- $\text{Li}[\text{Eu}(\text{tta})_4]$ 213
- ligand exchange 156
- ligand-to-metal charge-transfer state 168
- liquid crystal displays 216
- liquid crystals 200
- $[\text{Ln}(\text{bfac})_3] \cdot n\text{H}_2\text{O}$ 184
- $[\text{Ln}(\text{tta})_3] \cdot n\text{H}_2\text{O}$ 184
- LSGM 30
- LSGM9 22
- LSGMCo 6
- Lu_2SeO_3 70
- $[\text{Lu}(\text{fod})_3]$ 153
- $[\text{Lu}(\text{fod})_3(\text{H}_2\text{O})]$ 132, 135, 153
- $[\text{Lu}(\text{fod})_3(\text{phen})]$ 153
- luminescence 162
 - decay times 171
 - enhancement 288, 291, 294, 296, 298
 - in vapor phase 236, 237
 - intensity 166, 167
 - lifetime 172, 291, 301
 - NIR (near infrared) 299, 305
 - polarized 177, 194
 - quantum yield 169, 170, 286

- sensing 284, 288
- standards for quantum yields 170
- luminescent hourglass inclusions 177
- luminescent visualization of latent fingerprints 230
- [Lu(pta)₃] 153
- [Lu(thd)₃] 132, 153
- [Lu(thd)₃(3-pic)] 132, 135
- [Lu(thd)₃(py)] 153
- [Lu(trimh)₃] 153
- [Lu(tta)₃].2H₂O 153

- (M, M')TiO₃ (M = Ca, Sr, Ba) (M' = La, Sm, Pr, Gd, Nd, Y, Er, etc.) 17
- magnetic anisotropy 160
- magnetic circularly polarized luminescence 177
- magnetic properties 159
- magnetic resonance imaging 317
- magneto-chiral anisotropy 178
- magneto-chiral dichroism 178
- magneto-chiral luminescence anisotropy 178
- MCM-41 196
- mean free path of phonon 33
- mechanoluminescence 179
- melting point 144, 145
- metal-organic chemical vapor deposition 238
- metallofullerene 326
- metallomesogens 201
- Michler's ketone 167
- mixed-valent oxo-selenates(VI/IV) 99
- MnNdCl(SeO₃)₂ 90
- MnRCl(SeO₃)₂ 92
- MnSmCl(SeO₃)₂ 90
- modifications of Er₂(SeO₄)₃ 51
- modifications of Sc₂(SeO₄)₃.5H₂O
 - crystal structures of 54
- modifications of Sc₂(SeO₄)₃.5H₂O 52
- molar magnetic susceptibility 159
- monocapped square antiprism 139
- mordenite 196
- Mosher's method 315
- M[Pr(acac)₄] (M = Li, Na) 124
- MRI contrast agent 278, 317, 329
- MTPA 318

- Na_{3.68}Dy_{1.44}(SeO₄)₄ 58, 59
- NaCe(SeO₄)₂.2H₂O 58
- NaEr(HSeO₄)₂(SeO₄).5H₂O 58, 60
- Na[Eu(tta)₄] 213
- naked-eye detection 277, 288, 289
- NaLa(SeO₃)₂ 90
- NaLa(SeO₄)₂.2H₂O 58, 59
- NaPr(SeO₄)₂ 57, 58
- NaR(SeO₃)₂ 88
- NaSm(SeO₃)(SeO₄) 101
- NaSm(SeO₄)₂.2H₂O 58
- NaY(SeO₃)₂ 90
- Nd₂O₃ 239
- Nd₂(Se₂O₅)₃(H₂SeO₃).2H₂O 76
- Nd₂(SeO₃)₂(SeO₄).2H₂O 99
- Nd₂(SeO₃)₃ 70
- Nd₂(SeO₄)₃.8H₂O-I 50
- Nd₃F(SeO₃)₄ 80
- [Nd₄(acac)₁₀(OH)₂] 139
- Nd₉O₈Cl₃(SeO₃)₄ 80
- [Nd(acac)₃] 123, 153
- [Nd(acac)₃] (crystalline) 147
- [Nd(acac)₃(H₂O)₂](acetone) 130
- [Nd(acac)₃(phen)] 147
- [Nd(bzac)₂(OH)(H₂O)] 127
- [Nd(bzac)₃] 127
- [Nd(bzac)₃(H₂O)₂] 147
- [Nd(bzac)(OH)₂(H₂O)₂] 127
- NdCl(SeO₃) 80, 81
- [Nd(dbm)₃(bath)] 214
- [Nd(dbm)₃(H₂O)] 130
- [Nd(dbp)₄]⁻ (triethylammonium) 154
- [Nd(fod)₃] 147
- [Nd(fod)₃(bipy)].2H₂O 147
- [Nd(fod)₃(H₂O)] 147
- NdGaO₃ 239
- [Nd(hfac)₃] 218
- [Nd(hfac)₃].H₂O 147
- [Nd(hfac)₃(diglyme)] 130, 147
- [Nd(hfac)₄]⁻ (2,6-lutidinium) 154
- [Nd(hfac)₄]⁻ (pyridinium) 154
- [Nd(hfac)₄]⁻ (triethylammonium) 154
- Nd(HSeO₃)₃ 76
- Nd(HSeO₄)(Se₂O₇) 50, 55
- [Nd(pmtfp)₃(dmsO)₂] 147
- [Nd(pta)₃] 147
- [Nd(tfac)₃(H₂O)₂] 134
- [Nd(thd)₃] 147, 236, 237
- [{Nd(thd)₃}₂(triglyme)] 147
- [Nd(thd)₃(diglyme)₂] 147
- [Nd(thd)₃(phthalazine)] 147
- [Nd(thd)₃(pyr)] 147
- [Nd(mod)₃] 147
- [Nd(tod)₃] 147
- [Nd(trimh)₃] 147
- [Nd(tta)₃] 147
- [Nd(tta)₃].2H₂O 147
- [Nd(tta)₃(bipy)] 131

- [Nd(tta)₃(phen)] 147
 [Nd(tta)₃(tppo)₂] 131
 [Nd(tta)₄]⁻ (pyridinium) 133
 [Nd(tta)₄]⁻ (triethylammonium) 154
 nematic liquid crystals 203, 216
 (NH₄)₃Sc(SeO₄)₃ 58, 59
 (NH₄)Pr(SeO₄)₂·5H₂O 58
 nine-coordinate complexes 139
 nitrile solvent 206
 nitronyl nitroxides 159
 NMR shift reagents 218, 278
 NMR solvents 223
 non-coordinated polydentate ligand 135
 non-stoichiometric selenate 59
 nonanuclear rare-earth oxo-hydroxo clusters 141
 nonlinear optical materials 203

 O₂-sensing 323
 octadentate cyclen 286, 298
 – Eu³⁺ complex 293
 – Eu³⁺ complex 292, 298, 299
 – Gd³⁺ complex 282, 319, 322, 329
 – Yb³⁺ complexes 307
 organic light-emitting diodes (OLEDs) 206
 – three-layer 207
 ormosils 186
 oxo-selenate(IV)-hydrates 73
 oxo-selenates R₂(SeO₃)₃
 – structure types 67
 oxo-selenates(IV) R₂(SeO₃)₃ 67
 oxo-selenate(VI)-hydrates 49
 oxygen permeation flux 27, 28

 paramagnetic effect 165
 Pd²⁺ porphyrinate 299
 pH-response 296, 298
 pH-responsive 297
 pH-sensing 319
 [(Ph₂SiO)₂O]₂Sc₃(acac)₅] 135
 phase diagram of the system Nd₂O₃/SeO₂ 99
 phase transition of Nd₂(SeO₃)₃ 97
 phosphorescence 162
 photoacoustic spectroscopy 166
 photoluminescence 162, 163
 photostability 206
 piezoluminescence 179
 piperidine method 121, 125
 (pipH)[Eu(tta)₄] 186
 pivaloyltrifluoroacetone 244
 PMMA 190
 polarizability 203
 polarized absorption spectra 144
 polarized luminescence 177, 194
 polymeric optical amplifiers 217
 polymeric optical waveguides 217
 Pr₂O₃ 239
 Pr₂(SeO₃)₃ 70
 Pr₂(SeO₄)₃·4H₂O 55
 Pr₂(SeO₄)₃·4H₂O-I 50
 Pr₂(SeO₄)₃·5H₂O 50
 Pr₄(SeO₃)₂(SeO₄)F₆ 100
 Pr₉O₈Br₃(SeO₃)₄ 80
 Pr₉O₈Cl₃(SeO₃)₄ 80
 [Pr(acac)₃] 124
 [Pr(acac)₃(H₂O)₂] 130, 173
 [Pr(acac)₃(phen)] 130, 146
 [Pr(bzac)₃(H₂O)₂] 146
 [Pr(dbm)₃(bath)] 214
 [Pr(dbm)₃(H₂O)₂] 173
 [Pr(facam)₃] 147
 [Pr(fod)₃] 146, 158, 184, 220, 233
 [Pr(fod)₃(bipy)]·2H₂O 147
 [Pr(fod)₃(H₂O)] 146
 PrGaO₃ 239
 [Pr(hfac)₃] 147
 [Pr(hfac)₃(diglyme)₂] 147
 [Pr(hfac)₃(pmdeta)] 147
 [Pr(hfac)₄]⁻ (triethylammonium) 154
 properties of oxo-selenates(IV)
 – thermal behaviour 94
 properties of oxo-selenates(VI) 61
 – thermal behaviour 61
 – vibrational spectra 63
 Pr(Se₂O₅)(HSeO₃)(H₂SeO₃) 76
 [Pr(thd)₃] 147, 159, 184, 219, 236
 [Pr(thd)₃(phthalazine)] 147
 [Pr(thd)₃(pyr)] 147
 [Pr(thd)₃(tetraglyme)] 147
 [Pr(tod)₃] 147
 [Pr(trimh)₃] 147
 [Pr(tta)₃] 147
 [Pr(tta)₃(H₂O)₂] 173
 [Pr(tta)₄]⁻ (tetrabutylammonium) 133
 purification
 – liquid chromatography 127
 – recrystallization 126
 – vacuum sublimation 126
 purification of β-diketonates 126
 PVA 190
 (pyH)⁺[Eu(tta)₄]⁻ 214
 quenching 285, 291, 295, 307

- $[R_2(\text{fod})_6]$ 158
 $R_2\text{Se}_{1.5}\text{O}_6$ 72
 $R_2\text{Se}_2\text{O}_7$ 72
 $R_2\text{Se}_{3.5}\text{O}_{10}$ 72
 $R_2\text{Se}_4\text{O}_{11}$ 72
 $R_2\text{Se}_5\text{O}_{13}$ 72
 $R_2(\text{SeO}_4)_3 \cdot 8\text{H}_2\text{O-I}$ 51
 $R_2(\text{SeO}_4)_3 \cdot 8\text{H}_2\text{O-II}$ 51
 $R_2\text{SeO}_5$ 72
 $[R_3(\text{fod})_9]$ 158
 $R_3\text{F}(\text{SeO}_3)_4$ 83
 $R_3\text{O}_2\text{Cl}(\text{SeO}_3)_2$ 85
 $R_4\text{O}_3\text{Cl}_2(\text{SeO}_3)_2$ 85
 $R_5\text{O}_4\text{X}_3(\text{SeO}_3)_2$ 86
 $R_5\text{O}(\text{O}^i\text{Pr})_{13}$ 124
 $R_9\text{O}_8\text{X}_3(\text{SeO}_3)_4$ 86
 $[\text{R}(\beta\text{-diketonate})_2(\text{OH})(\text{H}_2\text{O})]$ 127
 $[\text{R}(\text{acac})_3]$ 234
 $[\text{R}(\text{acac})(\text{terpy})(\text{NO}_3)_2(\text{H}_2\text{O})_n]$ 122
radiationless deactivation 164
rare earth doped ceria (RDC) 13, 19
– thermal expansion coefficients 34
rare earth porphyrinates 303
rare earth tris(β -diketonates) 280, 281
– as CD probe 302
– as CSR reagent 309
– binding with amino acids 282
– binding with amino alcohols 279, 296
– binding with anions 280, 281, 288, 289
– coordination chemistry 278, 311
– extraction of amino acids 283
– for NMR sensing 308, 309
– tetrakis complexes 121, 154, 157, 158
rare-earth bis(trimethylsilyl)amides 124
rare-earth isopropoxides 124
rare-earth porphyrin complexes 128
 $\text{RbCe}(\text{SeO}_4)_2 \cdot 5\text{H}_2\text{O}$ 58, 60
 $\text{RbNd}(\text{SeO}_4)_2 \cdot 3\text{H}_2\text{O}$ 58, 60
 $\text{RCl}(\text{SeO}_3)$ 81
 $[\text{R}(\text{dbm})_2(\text{OH})]$ 123
 $[\text{R}(\text{dbm})_3]$ 126
 $[\text{R}(\text{dbm})_3] \cdot \text{H}_2\text{O}$ 123
 $[\text{R}(\text{dbm})_3(\text{H}_2\text{O})]$ 129, 161
RDC 6
recrystallization 126
relaxivity 321, 322
resonance levels 164
 $[\text{R}(\text{facam})_3]$ 226
 $[\text{R}(\text{fod})_3]$ 126, 127, 153, 158, 234, 239, 246
 $[\text{R}(\text{hfac})_3]$ 234, 238, 239
 $[\text{R}(\text{hfac})_3(\text{diglyme})]$ 124
 $[\text{R}(\text{hfbc})_3]$ 226
 $\text{R}(\text{HSeO}_3)(\text{SeO}_3)$ 74
 $\text{R}(\text{HSeO}_3)(\text{SeO}_3) \cdot 2\text{H}_2\text{O}$ 74
rifamycin 274
 $\text{R}(\text{O}^i\text{Pr})_3$ 124
 $\text{R}(\text{Se}_2\text{O}_5)(\text{NO}_3) \cdot 3\text{H}_2\text{O}$ 88
 $[\text{R}(\text{tfac})_3]$ 234, 237
 $[\text{R}(\text{thd})_3]$ 126, 127, 139, 158, 237, 243
 $[\text{R}(\text{tod})_3]$ 243

 Sc_2O_3 239, 241
 $\text{Sc}_2(\text{SeO}_3)_3$ 70
 $\text{Sc}_2(\text{SeO}_4)_3$ 48, 50
 $\text{Sc}_2(\text{SeO}_4)_3 \cdot 5\text{H}_2\text{O-I}$ 50
 $\text{Sc}_2(\text{SeO}_4)_3 \cdot 5\text{H}_2\text{O-II}$ 50
 $[\text{Sc}(\text{acac})_3]$ 130, 135, 145
scandium doped zirconia (ScSZ) 13
– oxide ion conductivity 21
– thermal expansion coefficients 34
scanning near-field optical microscopy (SNOM)
193
 $[\text{Sc}(\text{dbm})_3]$ 130, 135
 $[\text{Sc}(\text{facam})_3]$ 145
Schiff base 201
 $\text{Sc}(\text{HSeO}_3)_3$ 76
 $\text{ScH}(\text{SeO}_4)_2 \cdot 2\text{H}_2\text{O}$ 50
 $[\text{Sc}(\text{pta})_3]$ 145
ScSZ 6, 19
 $[\text{Sc}(\text{thd})_3]$ 145, 159, 235, 237
 $[\text{Sc}(\text{trimh})_3]$ 145
 $[\text{Sc}(\text{tta})_3]$ 145
 $[\text{Sc}(\text{tta})_3(\text{bipy})]$ 145
 $[\text{Sc}(\text{tta})_3(\text{phen})]$ 145
second harmonic generation 203
selectivity coefficient 281
self-association 158
sensitized chemiluminescence 183
 SeO_2 -poor oxo-selenates(IV) 72
 SeO_2 -rich oxo-selenates(IV) 72
seven-coordinate complexes 129, 135
silica glasses 185
single-layer OLED 207
six-coordinate complexes 128
(Sm, Sr) CoO_3 15
 Sm_2O_3 239
 $\text{Sm}_2\text{O}(\text{SeO}_3)_2$ 70
 $\text{Sm}_2(\text{Se}_2\text{O}_5)_2(\text{SeO}_3)$ 70
 $\text{Sm}_2\text{Se}_5\text{O}_{13}$ 72
 $\text{Sm}_2(\text{SeO}_3)_3$ 70
 $\text{Sm}_2(\text{SeO}_4)_3 \cdot 8\text{H}_2\text{O-I}$ 50
 $[\text{Sm}_2(\text{thd})_4(\text{Pc})]$ 144
 $\text{Sm}_3\text{F}(\text{SeO}_3)_4$ 80

- $\text{Sm}_9\text{O}_8\text{Cl}_3(\text{SeO}_3)_4$ 80
 $[\text{Sm}(\text{acac})_3]$ 123, 124
 $[\{\text{Sm}(\text{acac})_3\}_2(\text{heptaglyme})]$ 147
 $[\text{Sm}(\text{acac})_3(\text{bipy})]$ 147
 $[\text{Sm}(\text{acac})_3(\text{H}_2\text{O})_2]$ 130
 $[\text{Sm}(\text{acac})_3(\text{phen})]$ 130, 147
 smart sensors for structural damage monitoring
 182
 $[\text{Sm}(\text{bzac})_3(\text{H}_2\text{O})_2]$ 147
 $[\text{Sm}(\text{facam})_3]$ 148
 $[\text{Sm}(\text{fod})_3]$ 148
 $[\text{Sm}(\text{fod})_3(\text{bipy})] \cdot 2\text{H}_2\text{O}$ 148
 $[\text{Sm}(\text{fod})_3(\text{H}_2\text{O})]$ 148
 $[\{\text{Sm}(\text{hfac})_3\}_2(\text{tetraglyme})]$ 148
 $[\text{Sm}(\text{hfac})_3(\text{bipy})_2]$ 137
 $[\text{Sm}(\text{hfac})_3(\text{bipy})] \cdot (\text{bipy})$ 130
 $[\text{Sm}(\text{hfac})_3(\text{bipy})(\text{H}_2\text{O})] \cdot (\text{bipy})$ 137
 $[\text{Sm}(\text{hfac})_3(\text{diglyme})]$ 130, 147
 $[\text{Sm}(\text{hfac})_4]^-$ (triethylammonium) 154
 $[\text{Sm}(\text{pta})_3]$ 148
 $[\text{Sm}(\text{thd})_2(\text{dme})_2]$ 126
 $[\text{Sm}(\text{thd})_3]$ 148, 236
 $[\text{Sm}(\text{thd})_3(\text{dmap})]$ 130
 $[\text{Sm}(\text{thd})_3(\text{dme})]$ 148
 $[\text{Sm}(\text{thd})_3(\text{dmf})]$ 148
 $[\text{Sm}(\text{thd})_3(\text{monoglyme})]$ 130
 $[\text{Sm}(\text{thd})_3(\text{phthalazine})]$ 148
 $[\text{Sm}(\text{thd})_3(\text{py})]$ 148
 $[\text{Sm}(\text{thd})_3(\text{pyr})]$ 148
 $[\text{Sm}(\text{trimh})_3]$ 148
 $[\text{Sm}(\text{tta})_3]$ 148
 $[\text{Sm}(\text{tta})_3(\text{phen})]$ 148, 199
 $[\text{Sm}(\text{tta})_3(\text{tppo})_2]$ 214
 $[\text{Sm}(\text{tta})_3(\text{tppo})_2(\text{NO}_3)]$ 148
 $[\text{Sm}(\text{tta})_4]^-$ (1,2,6-trimethylpyridinium) 133
 $[\text{Sm}(\text{tta})_4]^-$ (1,2-dimethylpyridinium) 133
 $[\text{Sm}(\text{tta})_4]^-$ (tetrabutylammonium) 133
 SOFC electrolytes
 – oxide ion conductivity 10
 sol-gel glasses 185
 solubility 157
 – in organic solvents 157, 223
 – in supercritical CO_2 157
 – in water 157
 solution structure 157
 solvent extraction 243
 sparkle model 172
 spin-lattice relaxation time 317
 spin-spin relaxation time 317
 square antiprism 128
 SrCeO_3 239
 $\text{SrLaGa}_3\text{O}_7$ 19
 stability constant of ternary complex
 – difference between diastereomers 283
 – with amino acid 312
 – with amino alcohol 279
 – with carboxylate 315
 – with inorganic anion 280, 288
 stability in aqueous solution 158
 standard molar enthalpies of formation 159
 standard molar enthalpies of sublimation 159
 stationary phases in gas chromatography 232
 stretched polyethylene films 177
 stretched polymer 195
 structural isomers 129
 structural properties 128
 structure of the oxide-selenites $\text{R}_2\text{O}(\text{SeO}_3)_2$ 74
 sublimation behavior 236
 super cages 195
 synergistic effect 243
 synthesis by extraction 126
 synthetic strategies 121
 system $\text{Nd}_2\text{O}_3\text{-SeO}_2\text{-H}_2\text{O}$ 76
 systems $\text{R}_2\text{O}_3/\text{RX}_3/\text{SeO}_2$ 78
 systems $\text{R}_2\text{O}_3/\text{SeO}_2$ 73
 systems $\text{R}_2\text{O}_3/\text{SeO}_2/\text{H}_2\text{O}$ 76
 systems $\text{R}_2\text{O}_3\text{-RF}_3\text{-SeO}_2$ 82
 systems $\text{R}_2(\text{SeO}_3)_3\text{-A}_2\text{SeO}_3$ 88
 $\text{Tb}_2\text{O}(\text{SeO}_3)_2$ 70
 $\text{Tb}_2\text{Se}_2\text{O}_7$ 73
 $\text{Tb}_2(\text{SeO}_3)_3$ 70
 $\text{Tb}_2(\text{SeO}_4)_3 \cdot 8\text{H}_2\text{O-I}$ 50
 $[\text{Tb}_2(\text{thd})_6]$ 139
 $[\text{Tb}_2(\text{tod})_6]$ 139, 151
 $\text{Tb}_3\text{O}_2\text{Cl}(\text{SeO}_3)_2$ 80, 84, 85
 $\text{Tb}_5\text{O}_4\text{Cl}_3(\text{SeO}_3)_2$ 80
 $[\text{Tb}(\text{acac-F}_7)_3(\text{tppo})_2]$ 132
 $[\text{Tb}(\text{acac})_3]$ 123, 156, 157, 209
 $[\text{Tb}(\text{acac})_3(\text{bipy})]$ 150
 $[\text{Tb}(\text{acac})_3(\text{Cl-phen})]$ 216
 $[\text{Tb}(\text{acac})_3(\text{dam})]$ 188
 $[\text{Tb}(\text{acac})_3(\text{phen})]$ 150, 186, 188, 200, 210
 $[\text{Tb}(\text{dbm})_3(\text{dmop})]$ 132
 $[\text{Tb}(\text{dbm})_3(\text{phen})]$ 214
 $[\text{Tb}(\text{dbp})_4]^-$ (triethylammonium) 155
 $[\text{Tb}(\text{dtp})_4]^-$ (piperidinium) 155
 $[\text{Tb}(\text{facam})_3]$ 150
 $[\text{Tb}(\text{fod})_3]$ 150
 $[\text{Tb}(\text{fod})_3(\text{bipy})] \cdot 2\text{H}_2\text{O}$ 151
 $[\text{Tb}(\text{fod})_3(\text{H}_2\text{O})]$ 151
 $[\text{Tb}(\text{hfac})_3]$ 156
 $[\text{Tb}(\text{hfac})_3(\text{diglyme})]$ 132, 150

- [Tb(hfac)₃(phen)] 200
 [Tb(hfac)₃(tppo)₂] 132
 [Tb(hfac)₄][−](2,4,6-collidinium) 155
 [Tb(hfac)₄][−](2,6-lutidinium) 155
 [Tb(hfac)₄][−](pyridinium) 155
 [Tb(hfac)₄][−](triethylammonium) 155
 [Tb(pmip)₃(tppo)₂] 151
 [Tb(pta)₃] 151
 [{Tb(tfac)₃}₂(tetraglyme)₂] 151
 [Tb(tfac)₃(phen)] 188, 200
 [Tb(thd)₃] 151, 157, 235, 236
 [{Tb(thd)₃}₂(triglyme)] 139, 151
 [Tb(thd)₃(dmap)] 132
 [Tb(thd)₃(phthalazine)] 151
 [Tb(thd)₃(py)] 151
 [Tb(thd)₃(pyr)] 151
 [Tb(thd)₃(tmeda)] 151
 [Tb(tod)₃] 157
 [Tb(trimh)₃] 151
 [Tb(tta)₃] 151
 [Tb(tta)₃(phen)] 122, 151, 200
 [Tb(tta)₄][−](2,4,6-trimethylpyridinium) 156
 [Tb(tta)₄][−](pyridinium) 155
 [Tb(tta)₄][−](triethylammonium) 155
 temperature sensing 325
 ten-coordinate complexes 136
 TEOS 186
 ternary oxo-selenates(VI) 57
 ternary rare-earth β-diketonates 119
 terpyridine 275
 tetraethyl orthosilicate 186
 tetrakis β-diketonates
 – adduct formation 157
 – dissociation 157
 – electrochemical properties 158
 – melting points 154
 – synthesis 121
 tetramethoxy orthosilicate 186
 the electronic and hole conductivity 22
 thermal behaviours of the acidic selenites 94
 thermal conductivity 32, 33
 thermal decomposition schemes of
 oxo-selenites(IV) 95
 thermal diffusivity 30, 31
 thermal expansion coefficient 34
 thermochemical investigations of oxo-selenates(IV)
 97
 thermodynamic properties 159
 thermodynamical data of compounds in the systems
 R₂O₃/RX₃/SeO₂ 98
 thermodynamical data of compounds in the systems
 R₂O₃/SeO₂ 98
 time-resolved luminescent immunoassay 229
 Tm₂O(SeO₃)₂ 70
 Tm₂(SeO₃)₃ 70
 [Tm(acac-F7)₃(tppo)₂] 132
 [{Tm(acac)₃}₂(heptaglyme)] 152
 [Tm(acac)₃(H₂O)₂·H₂O] 132
 [Tm(acac)₃(phen)] 214
 [Tm(fod)₃] 152
 [Tm(fod)₃(bipy)]·2H₂O 152
 [Tm(fod)₃(H₂O)] 152
 TMOS 186
 [Tm(ppa)₃(H₂O)₂] 174
 [Tm(thd)₃] 152, 236
 [{Tm(thd)₃}₂(tetraglyme)] 152
 [{Tm(thd)₃}₂(triglyme)] 152
 [Tm(thd)₃(phthalazine)] 152
 [Tm(thd)₃(py)] 152
 [Tm(thd)₃(pyr)] 152
 [Tm(tta)₃] 152
 trace analysis of lanthanide ions 227
 transport 282
 triboluminescence 163, 179
 tricapped trigonal prism 141
 triplet state energy 164
 tripodal ligand 288
 – nonadentate 286
 – tetradentate 290, 291
 tris(2-pyridylmethyl)amine 276, 288
 tris(methyl)lanthanum 124
Triton X-100 227
 two-layer OLED 207

 vibrational spectra of oxo-selenates(IV) 96
 vibronic coupling 164
 vibronic spectra 176
 volatile β-diketonate complexes 233

 water exchange rate 319
 water proton relaxivity 326

 xerogel 186

 Y₂BaCu₃O₇ 240
 Y₂O₃ 241
 Y₂(SeO₃)₃ 70
 Y₂(SeO₄)₃·8H₂O-II 50
 [Y₂(tod)₆] 139
 [Y₄(acac)₁₀(OH)₂] 139
 [Y(acac)₃] 123

- [Y(acac)₃(dmsO)(H₂O)]·(dmsO) 130
 [Y(acac)₃(H₂O)₂]·(H₂O) 130
 [Y(acac)₃(phen)] 130, 145, 214
 YAlO₃ 239
 Yb₂(SeO₃)₃ 70
 Yb₂(SeO₄)₃ 48, 50
 Yb₂(SeO₄)₃·8H₂O-II 50
 Yb₄O₃Cl₂(SeO₃)₂ 80
 [Yb(acac)₃] 132
 [Yb(acac)₃(H₂O)] 132, 135
 [Yb(acac)₃(H₂O)₂] 132
 [Yb(dbm)₃(bath)] 214
 [Yb(fod)₃] 152, 220, 249
 [Yb(fod)₃(bipy)]·2H₂O 152
 [Yb(fod)₃(H₂O)] 152
 [Yb(hfac)₄]⁻(triethylammonium) 156
 [Yb(pta)₃] 152
 [Yb(thd)₃] 152, 157, 236
 [Yb(thd)₃(diglyme)] 152
 [Yb(thd)₃(phthalazine)] 152
 [Yb(thd)₃(py)] 152
 [Yb(thd)₃(pyr)] 152
 [Yb(thd)₃(triglyme)] 152
 [Yb(trimh)₃] 153
 [Yb(tta)₃] 153
 [Y(bzac)₃(H₂O)] 130, 135
 [Y(facam)₃] 145
 [Y(fod)₃] 145, 240
 [Y(fod)₃(bipy)]·2H₂O 145, 153
 [Y(fod)₃(H₂O)] 145
 [Y(fod)₃(phen)] 145
 [Y(hfac)₃(H₂O)₂Cu(acac)₂] 128
 [Y(hfac)₃(H₂O)₂][Cu(acac)₂] 130, 141
 [Y(hfac)₃(tetraglyme)] 145
 [Y(hfac)₃(triglyme)] 145
 [Y(hfac)₄]⁻Cs⁺ 133
 [Y(pta)₃] 145
 Y(Se₂O₅)NO₃·3H₂O 80
 YSZ 6, 19, 21
 [Y(thd)₃] 124, 130, 145, 159, 235–237, 240
 [{Y(thd)₃}₂(triglyme)] 139
 [Y(thd)₃(4-Et-pyO)] 145
 [Y(thd)₃(4-tert-But-pyO)] 145
 [Y(thd)₃(bipy)] 145
 [Y(thd)₃((CH₃)₃NO)] 145
 [Y(thd)₃(diglyme)] 145
 [Y(thd)₃(dmf)] 145
 [Y(thd)₃(dmsO)] 145
 [Y(thd)₃(Et₃PO)] 145
 [Y(thd)₃(H₂O)] 130, 135, 141
 [Y(thd)₃(hmteta)] 145
 [Y(thd)₃(Ph₃PO)] 145
 [Y(thd)₃(phen)] 145
 [Y(thd)₃(pyO)] 145
 [Y(thd)₃(pyr)] 145
 [Y(thd)₃(tmeda)] 145
 [Y(thd)₃(triglyme)] 145
 [Y(tmod)₃] 145
 yttria stabilized zirconia (YSZ) 9
 – ionic conductivity 21
 – mechanical strength 29
 – the electronic and hole conductivity 22
 – thermal conductivity 32, 33
 – thermal diffusivity 30, 31
 – thermal expansion coefficients 34
 [Y(trimh)₃] 145
 [Y(tta)₃] 145
 [Y(tta)₃(phen)] 145, 200
 zeolite-X 195
 zeolite-Y 196
 zirconia glasses 186

This page intentionally left blank